Catalytic Upgrading of Bio-oil Produced from Fast Pyrolysis of Pinewood Sawdust

By: Ravinder Kumar

Supervisor: Professor Vladimir Strezov

A thesis in fulfilment of the requirements for the degree of

Doctor of Philosophy

MACQUARIE University

Department of Earth and Environmental Sciences

Macquarie University

Australia

March 2021

MACQUARIE
University

STUDENT'S DECLARATION

I hereby declare that the work in this thesis is based on my original work except for quotations and citation, which have been duly acknowledged. I also declare that it has not been previously or concurrently submitted for any other degree at other institutions.

_____

(Author's Signature)

Full Name: RAVINDER KUMAR

Student ID Number:

Date: 10/03/2021

Abstract

Catalytic biomass pyrolysis (CBP) is considered an effective approach to convert the oxygenated compounds into various hydrocarbons and improve bio-oil quality. The introduction of a catalyst generally decreases the temperature of the pyrolysis process and removes the oxygen, and converts the oxygenated compounds like phenols, ketones, alcohols, esters into various hydrocarbons through a variety of catalytic reactions such as dehydration (removing oxygen as H_2O), decarboxylation (removing oxygen as CO_2) and decarbonylation (removing oxygen as CO), hydrogenation, condensation, aromatization and polymerization. There are different modes of CBP in a fixed-bed reactor, primarily used *in-situ* and *ex-situ,* and less studied combined *in-situ* and *ex-situ* mode. *In-situ* pyrolysis involves the addition of a catalyst mixed with biomass. In contrast, in *ex-situ* pyrolysis, the catalyst is separately placed downstream to the biomass, and the produced pyrolytic vapours are passed through the catalyst bed. The combined *in-situ* and *ex-situ* mode utilizes a catalyst mixed with biomass and a similar or different catalyst placed downstream to convert the unreacted pyrolytic vapours. This thesis examines the application of microporous and mesoporous solid acid catalysts like zeolites, Al_2O_3 and basic catalysts such as CaO in three modes of CBP for bio-oil upgrading. *Radiata pine* sawdust was selected as the feedstock for pyrolysis to produce bio-oil.

The first key chapter of the thesis examines the comparative catalytic activity of zeolite catalysts (Zeolite, Cu/zeolite and Ni/zeolite) on bio-oil upgrading in three modes of pyrolysis: *in-situ, ex-situ,* and combined *in-situ* and *ex-situ*. Though noticeable bio-oil deoxygenation was achieved in ex-situ and combined pyrolysis mode, the study concludes that *ex-situ* pyrolysis mode is economically beneficial compared to either *in-situ* or combined since the catalyst can be easily retrieved from the process, oxidized to remove the coke and reused in the pyrolysis. Therefore, considering the importance of *ex-situ* pyrolysis mode, bio-oil upgrading was further investigated using various catalysts.

In the next chapters, the catalytic activity of monometallic catalysts Cu/zeolite and Ni/zeolite was compared with a bimetallic catalyst NiCu/zeolite in one-stage *ex-situ* pyrolysis. The catalysts were used in *ex-situ* pyrolysis with three different C/B ratios of 1, 2, and 3. CuNi/zeolite showed better deoxygenation efficiency than monometallic catalysts and produced a comparatively higher percentage of aromatic hydrocarbons at 14.3% and aliphatic hydrocarbons at 39.9%. The main deoxygenation pathway during monometallic catalytic pyrolysis was found to be dehydration and decarboxylation because a higher CO_2 yield was observed during the reaction. The CuNi/zeolite converted the oxygenated compounds into hydrocarbons via dehydration, decarboxylation, and decarbonylation because higher yields of both CO_2 and CO were observed. Overall, CuNi/zeolite catalytic pyrolysis of biomass resulted in improved bio-oil quality when compared to the monometallic counterparts. The activity of CuNi/zeolite was further compared

with combined mono-metallic catalysts in two-stage *ex-situ* pyrolysis mode. The results demonstrated that in comparison to the combined mono-metallic catalysts, the sole bi-metallic catalyst showed better deoxygenation for all the oxygenated compounds and favoured the production of aliphatic hydrocarbons, whereas the combination of monometallic catalysts generated higher proportion of aromatic hydrocarbons in the bio-oil. Considering the significance of bimetallic catalysts over monometallic catalysts, more bimetallic catalysts with combinations of Ni, Cu, Fe, and Mo on ZSM-5 support were prepared and examined for bio-oil upgrading. It was observed that the synergistic effect of Ni-Cu and Ni-Fe showed higher hydrocarbon production compared to Cu-Fe, Ni-Mo, Cu-Mo, and Fe-Mo, which can be attributed to their higher surface area that probably resulted in better metal dispersion on ZSM-5 surface and synergistic catalytic sites that favoured selective deoxygenation reactions. *Ex-situ* CBP could be either one-stage (a single catalyst is used) or two-stage (two catalysts are used). Though one-stage *ex-situ* CBP has been widely explored with different types of catalysts, the effect of catalyst type on bio-oil upgrading during two-stage ex-situ CBP was not investigated. Thus, to understand the impact of the nature of catalyst support in two-stage *ex-situ* CBP, different catalytic supports, from strongly acidic to basic such as ZSM-5, Al_2O_3, Al_2O_3/CaO/MgO, and CaO with and without Ni loading were demonstrated in both modes of *ex-situ* CBP. It was found that in one-stage *ex-situ* CBP, microporous acidic catalysts like ZSM-5 and Ni/ZSM-5 promoted the formation of naphthalenes and other polycyclic aromatics, mesoporous Al_2O_3, and Al_2O_3/CaO/MgO or Ni-modified counterparts also favoured the formation of benzene derivatives and cycloalkanes, while CaO or Ni/CaO generated aliphatic hydrocarbons. It was further noticed that the combination of mesoporous and microporous catalysts in two-stage *ex-situ* CBP provided varying catalytic properties and improved mass transfer kinetics which was advantageous to produce a variety of hydrocarbons.

Acknowledgements

I would like to thank many people for their help, motivation and support. Without their guidance, this PhD journey would not have been possible.

Firstly, I would be grateful to my chief supervisor Professor Vladimir Strezov whose generous efforts allowed me to join his research group. It would not be possible for me to even come to Australia if he didn't arrange the health insurance for a sick prone person like me. He has been a great motivation for me, and his guidance has been incredibly influential in achieving my goals throughout this PhD. Every meeting with him worked like boosting energy, and his final words, "*excellent, go ahead*" after the meeting, gave me more enthusiasm to work.

Secondly, I would be highly thankful to my co-supervisor, Dr. Tao Kan. It was he who gave direction to my work. I had insightful meetings and discussions with him on catalytic pyrolysis during the initial days of my PhD. He was always available in any need of the hour and keen to share his knowledge with me. He solved all the instrumental problems I ever had throughout this PhD journey.

I would like to thank all members of our research group. I would start with Dr. Haftom Weldekidan. There would not be a day I did not visit his desk. We always have insightful discussions on pyrolysis. I enjoyed working with him in the lab, and lunch or coffee breaks were always cheerful. Jing and I started our PhD journey almost together. She has been a very helpful colleague in the last three years. Her hard-working nature is always motivational. My first trip with her to the Sydney Opera house and a field trip near Newcastle to collect plant samples will be memorable. Behnam Dastjerdi is always there to help me. Insightful discussions about waste to energy technologies and his advice were constructive. Dr. Sayka was also very helpful. It was great working with her, and learned lots of valuable experiences.

I would like to acknowledge the support of other friends, including Armin, Sam, and Mehrnoush. I have enjoyed their company a lot on the university campus and unforgettable trips around Sydney. I feel blessed to have them all in my life.

I am thankful to all the department's technical staff for their immense help in handling the instruments. Thank you, Late Russell Field and Sean Murray, for helping me with X-ray diffraction equipment. In our department's admin staff, Phil Dartnell and Aida Pujol were helpful for arranging the finance of essential chemicals.

Macquarie Research Training Scholarship and annual budget for research from the university is fully acknowledged.

I dedicate this PhD to my parents, brother and family. I am grateful for their unconditional support, encouragement and love throughout my life.

Table of contents

Chapter 1

Introduction

1. Lignocellulose biomass as a feedstock for renewable energy

The most pressing challenges facing humankind in the 21st century is increasing energy demand and irregular climate change, which altered the scientific community to search for alternative energy sources to fossil fuels. It is predicted that the share of fossil fuels, i.e. coal, crude oil, and natural gas, accounting for the highest use at the moment, would slowly decrease. In contrast, the share of renewable energy would significantly increase from the current 4% to 15% by 2040 [1]. Figure 1 shows the historical and predicted consumption of different types of energy sources across the world [1]. Currently, wind and solar are the primary sources of renewable energy, which are also expected to hold a significant share of the energy supply by 2040. The production of biofuels is also expected to grow steadily [1]. Although the energy or the power produced from wind and solar can be utilized in industry and building sectors, most transport vehicles (aeroplanes, ships, automobiles, and long-haul trucks) are still dependent on high energy-density liquid fuels. Therefore, finding feasible renewable energy sources for the production of high-density liquid fuels is inevitably required to meet the increasing energy demand since conventional liquid fuels like petrol and diesel are rapidly diminishing. In this regard, biomass, especially lignocellulose, has been considered the most suitable renewable energy source for liquid fuel production [2–5]. Lignocellulose biomass is rich in carbon and contains negligible content of other undesirable elements, such as nitrogen and sulphur. Hence, the combustion of lignocellulose biomass does not release toxic NO_x and SO_x emissions. Carbon emissions (CO_2) released during the consumption of biomass, including lignocellulose is captured by plants to produce biomass via photosynthesis, causing no net addition of CO_2 to the atmosphere. Hence, biomass energy is considered carbon-neutral [6]. Therefore, the efficient use of lignocellulose biomass-derived fuels could help mitigate greenhouse gas (GHG) emissions and reduce our dependency on fossil fuels.

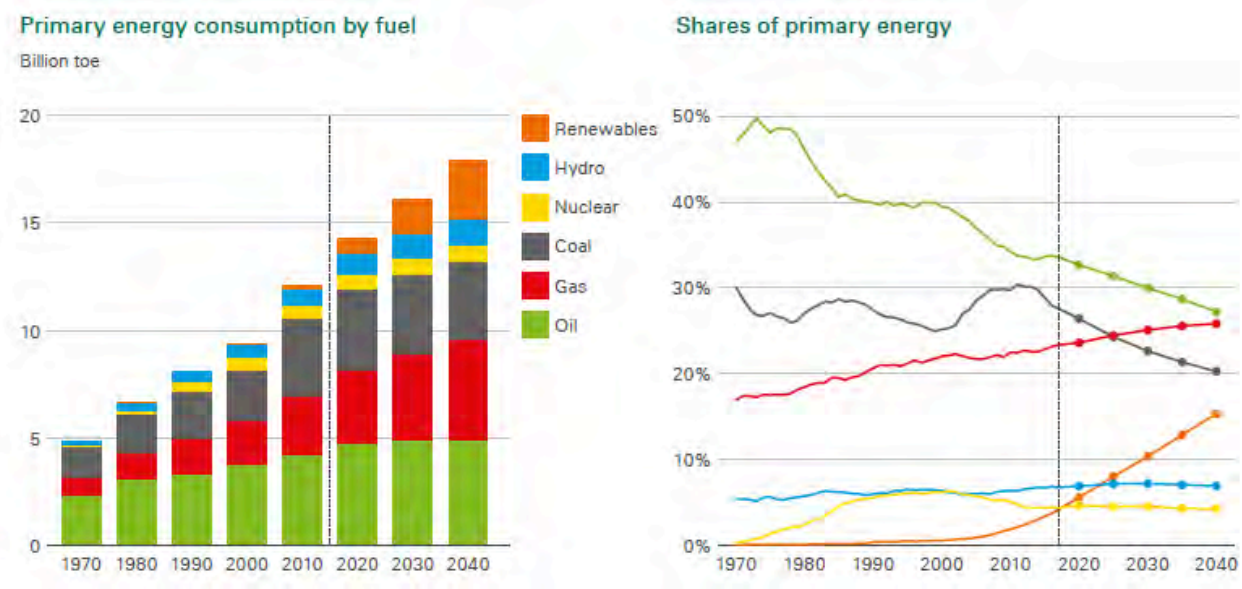

Figure 1. Historical and predicted consumption of different energy sources and their usage share across the world [1].

2. Pyrolysis technology to convert biomass into bio-oil

There are several developed promising thermochemical and biochemical technologies, including pyrolysis, hydrothermal liquefaction, esterification and fermentation for the conversion of lignocellulose biomass to a variety of energy-rich liquid fuels [2,7–9]. Among these, thermochemical techniques, particularly pyrolysis, have been significantly used for bioenergy production, primarily for liquid bio-oil production. Generally, pyrolysis is termed as biomass processing at high temperatures (>350°C) in an oxygen-free environment, resulting in the generation of three types of products, such as solid-char, gaseous mixture (CO_2, CO, H_2, CH_4) and liquid bio-oil or also termed as pyrolytic oil [10–12]. The yield of all pyrolytic products mainly depends on the biomass composition and the operating parameters [13]. It is well understood that a higher content of cellulose in lignocellulose biomass and pyrolysis temperature of around 500-550°C usually results in a higher yield of bio-oil at approximately 55-70% [13,14].

The bio-oil produced from biomass pyrolysis contains a complex composition of more than 200 different organic compounds, dominated by oxygenated compounds, such as phenols, alcohols, esters, aldehydes, ketones, acids, furans, as well as nitrogen and sulfur-containing compounds [15]. The higher content of the oxygenated compounds in the bio-oil accounts for its total oxygen content, which is responsible for several poor characteristics. Table 1 compares the physicochemical properties of bio-oil and heavy fuel oil. As shown in the table, bio-oil comprises the oxygen content of around 35-55 wt% while the heavy fuel oil has an oxygen content of merely 1 wt% and contains predominantly the carbon content of 85 wt%. The presence of highly reactive oxygen species results in high acidic character, which is the reason for its low stability and easy corrosiveness, making it unsuitable for turbines or combustion engines [16]. In addition, the other undesirable properties of pyrolysis bio-oil, such as low calorific value, high viscosity, and low

carbon/hydrogen ratio, hamper the commercialization of bio-oil. The ash content in bio-oil is also slightly higher than the desired value. The ash contains some alkali metals such as sodium and potassium, responsible for its corrosive nature. The metals and other inorganic particles may agglomerate, subsequently, may lead to the formation of a sludge layer on the base of the container. The water content in bio-oil is between 15 and 30%, which is also very high compared to heavy fuel oil. The high-water content affects the heating and ignition properties of the bio-oil, decreases adiabatic flame temperature (the temperature in the combustion process if no heat is lost) and combustion temperature, and reduces the combustion reaction rates. Besides, it delays the ignition of bio-oil by reducing the droplet's vaporization rate, which may pose severe concerns if used in compression ignition engines.

Table 1. Comparative properties of bio-oil and heavy fuel oil. Data were taken from reference [17] with permission. Copyright © 2004, American Chemical Society

Physical properties	**Value**	
	Bio-oil	**Heavy fuel oil**
pH	2.5	
Specific gravity	1.2	0.94
Moisture content (wt%)	15-30	0.1
Carbon (wt%)	54-58	85
Hydrogen (wt%)	5.5-7.0	11
Oxygen (wt%)	35-55	1.0
Nitrogen (wt%)	0-0.2	0.3
Ash (wt%)	0-0.2	0.1
HHV (MJ/kg)	16-19	40
Viscosity, at 500 °C (cP*)	40-100	180
Solids (wt%)	0.2-1.0	1
Distillation residue (wt%)	Up to 50	1

*cP: centipoise

Hence, it is imperative to remove the oxygen content and improve other properties of the bio-oil. The resulting deoxygenated high energy-density biofuel can be used as the transportation fuel or used as a drop-in fuel for heat or power generation applications. To achieve this, various techniques have been successfully applied for bio-oil upgrading, mainly based on biomass pretreatment (torrefaction, wet-torrefaction, steam explosion, densification) [18–21], downstream bio-oil upgrading (solvent addition, emulsification, microfiltration) [22–27] and catalytic bio-oil upgrading [28–33]. Catalysts have been widely used for bio-oil upgrading and have shown a significant role in the conversion of oxygenated compounds in bio-oil into useful hydrocarbons, and consequently increasing the calorific value and improving other physicochemical properties of bio-oil. The pyrolysis process that involves the application of catalysts is often termed as catalytic biomass pyrolysis (CBP).

3. Catalytic biomass pyrolysis for bio-oil upgrading

Over the past two decades, a number of studies have been carried out on catalytic bio-oil upgrading, employing various types of catalysts in different modes of pyrolysis [34–39]. Especially, the solid acid catalysts are highly preferred for bio-oil upgrading because of their unique catalytic properties, such as high BET surface area, strong chemical and hydrothermal stability, high acidity, suitable porosity, high selectivity, and high resistance to the deposition of carbonaceous species [40–42]. The most commonly used solid acid catalysts are typically composed of zeolites, mordenites, aluminosilicates, or metal oxides, such as TiO_2, Al_2O_3, ZnO and their modification with different active metals, like Ni, Cu, Pd, and Fe to obtain either supported monometallic or bimetallic catalysts [43–45]. These catalysts can be applied for bio-oil upgrading, mainly using two approaches, hydrodeoxygenation (HDO) [46] and catalytic cracking [47]. HDO route involves utilization of hydrogen under high pressures, which could increase the overall cost of bio-oil upgrading and will show safety concerns. In contrast, the catalytic cracking involves the direct cracking of oxygenated compounds present in the bio-oil using heterogeneous solid catalysts and avoids the use of flammable, high pressure bottled molecular hydrogen [46,47]. Since HDO requires highly expensive hydrogen and other issues faced in transportation and storage of hydrogen make the bio-oil upgrading uneconomical. On the other hand, catalytic cracking may prove cost-effective compared to HDO as it does not require hydrogen and hence can be preferred over HDO for efficient bio-oil upgrading. Catalytic cracking during biomass pyrolysis may involve an array of different reactions, such as dehydration, decarboxylation, decarbonylation, condensation, isomerization, aromatization, hydrogenation, dehydrogenation, and many other steps [48,49]. It can be carried out primarily in two configurations based on incorporating the catalyst, i.e. *in-situ* and *ex-situ* [50]. In *in-situ* catalytic pyrolysis, the biomass is mixed with the catalyst and simultaneously heated at a certain temperature, resulting in the upgraded bio-oil [34,51]. On the other hand, in *ex-situ* catalytic pyrolysis, the biomass and the catalyst bed are placed separately in the reactor at a certain distance or in separate reactors. The produced pyrolytic vapours are passed through the catalyst bed [28,52]. The two-stage *ex-situ* pyrolysis route allows the thermal degradation of biomass and catalytic process at different favorable temperatures, resulting in the enhanced yield of bio-oil with high quality [52]. Different types of catalysts have been applied in both modes of catalytic pyrolysis for bio-oil upgrading and showed significant results for improving the properties of bio-oil and its utilization. For instance, Paysepar *et al.* [53] demonstrated the application of various zeolite catalysts (zeolite X, zeolite Y and ZSM-5) in the *ex-situ* pyrolysis of hydrolysis lignin to examine the cracking of oxygenated compounds into hydrocarbon-rich compounds. The authors reported that ZSM-5 showed the best cracking activity than zeolite X and Y and achieved the maximum amount of monomeric hydrocarbons in the bio-oil, which was 0.11 g/g of feedstock. In addition, other properties of bio-

oil were also improved with catalytic pyrolysis. For example, ZSM-5 catalyzed pyrolysis route provided the bio-oil with enhanced HHV (higher heating value) of 23.7 MJ/kg and increased carbon content of 62.6 wt%. In contrast, bio-oil obtained in the absence of a catalyst showed HHV of only 17.4 MJ/kg and a carbon content of 47.1 wt% [53]. The substantial cracking activity of ZSM-5 was attributed to the presence of higher Brønsted acid sites, which promote different deoxygenation reactions to convert oxygenated compounds into hydrocarbons and hence improved properties of bio-oil [54]. However, strong acidic catalysts are easily deactivated due to the coke formation resulted from the enhanced production of polycyclic aromatic hydrocarbons (PAHs) [55]. Therefore, it is essential to maintain the catalyst's acidity to improve its reusability and stability, which can be maintained by introducing the basic metal oxides to the solid acid catalysts. The basic catalyst can promote additional reactions like ketonization and de-acidification that may increase the total amount of hydrocarbons [56]. To understand this, a study was reported based on the *ex-situ* pyrolysis of bamboo sawdust over HZSM-5 and mixed HZSM-5 + CaO in a two-step bench-scale bubbling fluidized bed/fixed-bed reactor [57]. The results suggested that the *ex-situ* pyrolysis with the mixed HZSM-5+CaO catalyst provided a higher percentage of aromatic hydrocarbons (31.34%) in the bio-oil to the sole catalyst of either HZSM-5 or CaO. The enhanced selectivity of aromatic hydrocarbons in the presence of a mixed catalyst could be attributed to the synergistic catalytic activity of CaO and HZSM-5 [57]. Similarly, various catalysts have been examined for *in-situ* catalytic bio-oil upgrading. For example, Karnjanakom et al. [58] reported the *in-situ* catalytic pyrolysis of various feedstocks (cellulose, lignin, and sunflower stalk) using Mg/Al-MCM-41 catalyst. The study concluded that the proportion of aromatic hydrocarbons increased up to ~80% in the bio-oils obtained from all the feedstocks in the presence of Mg/Al-MCM-41 catalyst. Particularly, the content of monocyclic aromatic hydrocarbons (MAHs) like benzene, toluene and xylenes were significantly increased in the catalytic pyrolysis [58]. Therefore, the optimization of acid and base active sites in solid catalysts is crucial for achieving promising results in terms of the high percentage of hydrocarbons with high quality during bio-oil catalytic cracking.

4. Aims of the Thesis

It is evident from previous studies that the application of catalysts has shown remarkable results for bio-oil upgrading in different pyrolysis modes. Hence, this thesis proposes preparing different catalysts using a facile and cost-effective method and investigating their potential for bio-oil upgrading. The thesis' primary aim was to examine the role of mono and bimetallic catalysts for bio-oil upgrading and identify key favoured pathways to convert the dominant oxygenated compounds, such as phenols, acids, ketones and alcohols, into different types of hydrocarbons. To achieve this, mesoporous zeolite and microporous zeolite (ZSM-5) were impregnated with

different transition metals. Their catalytic activity was examined for selectivity of hydrocarbon formation, bio-oil deoxygenation, yields of pyrolysis products and energy distribution in pyrolytic products.

Two-stage *ex-situ* pyrolysis has not been explored so far for CBP. Therefore, in the second part of the thesis, we aimed to demonstrate the effect of different types of catalysts for bio-oil upgrading. To achieve this, diverse nature of catalytic supports like ZSM-5, Al_2O_3, Al_2O_3/CaO/MgO, and CaO were impregnated with nickel metal and explored their activity for bio-oil deoxygenation, hydrocarbon production and energy distribution in pyrolytic products. Later, nickel modified catalysts were tested for their stability, and the effect of deactivation on their physicochemical properties and, consequently, on yields of pyrolytic products and bio-oil deoxygenation were thoroughly studied. We believe that the findings obtained in the thesis may play an important role to enhance the fundamental understandings of *ex-situ* CBP and designing catalysts for two-stage *ex-situ* CBP for efficient bio-oil deoxygenation or production of other sustainable chemicals.

5. Thesis Outline

Overall, this thesis contains 10 chapters, with chapters 2 to 4 reviewing the types of primary methods (catalytic, biomass pretreatment and downstream bio-oil upgrading) employed for potential bio-oil upgrading. The original research work of the thesis is presented in chapters 5 to 9, followed by chapter 10 which summarizes the conclusions and future perspectives.

Chapter 2 reviews vital reaction pathways that take place during noncatalytic pyrolysis and possible routes to the formation of organic compounds from their primary substrates. The chapter also discusses the types of catalytic biomass pyrolysis (CBP) in a fixed-bed pyrolysis reactor, and possible routes carried out by the catalysts to convert the oxygenated compounds into various hydrocarbons.

Chapter 3 reviews different physicochemical biomass pretreatment methods used to improve the bio-oils' physicochemical properties produced from pyrolysis of treated biomass. Biomass pretreatment was classified as physical, thermal, chemical and biological methods, their effect on the bio-oil composition and other properties was discussed in detail. Chapter 4 focusses on the widely used methods for downstream bio-oil upgrading, such as hydrotreatment, solvent addition, emulsification, microfiltration and electrocatalytic hydrogenation. Basic principles of the processes and effects of different parameters on bio-oil upgrading are thoroughly discussed. In addition, techno-economic analysis, policy analysis, challenges related to downstream processes are provided in the chapter.

Chapter 5 compares the potential of Cu/zeolite and Ni/zeolite catalysts for bio-oil deoxygenation in *in-situ*, *ex-situ* and combined *in-situ* and *ex-situ* pyrolysis using pinewood

sawdust as the feedstock. Though combined catalytic pyrolysis process could be advantageous to obtain higher deoxygenation of bio-oil compared to either *in-situ* or *ex-situ* catalytic pyrolysis, *ex-situ* pyrolysis proved economically more viable since the catalyst can be easily retrieved from the reactor and can be used multiple times in further pyrolysis experiments. For this reason, *ex-situ* pyrolysis was further explored for bio-oil upgrading using different types of catalysts.

Chapter 6 examines the effect of mono and bimetallic catalysts on different product yields and the selectivity of hydrocarbons from biomass pyrolysis. Three catalyst to biomass ratios of 1, 2 and 3 were used in *ex-situ* pyrolysis mode to demonstrate the effect on hydrocarbon selectivity and the overall bio-oil upgrading. The possible pathways for bio-oil deoxygenation are also discussed. Chapter 7 presents a comparative investigation of the difference between the combined mono-metallic and bi-metallic catalysts for upgrading the bio-oils produced during biomass pyrolysis. The study was carried out using Cu/zeolite and Ni/zeolite as mono-metallic catalysts and CuNi/zeolite as the bimetallic catalyst. The study suggested that Cu and Ni synergistic effect produced better results for hydrocarbon formation and bio-oil deoxygenation. Therefore, in Chapter 8, we prepared additional bimetallic catalysts and investigated the synergistic effect of different transition metals for bio-oil deoxygenation, the selectivity of hydrocarbons and energy distribution in pyrolytic products.

After exploring the one-stage *ex-situ* catalytic pyrolysis, further catalysts were examined in a two-stage *ex-situ* catalytic pyrolysis. Chapter 9 details the effect of catalytic supports ZSM-5, Al_2O_3, Al_2O_3/CaO/MgO, and CaO impregnated with nickel-metal for bio-oil deoxygenation, hydrocarbon production and energy distribution in pyrolytic products.

Chapter 10 concludes the main findings of the thesis and identifies key limitations, and recommends possible solutions to address them in the future.

6. List of publications

Each chapter of the thesis is written as a separate manuscript except for chapters 1 and 10. The articles resulted from the thesis are following:

Chapter 2: Ravinder Kumar, Vladimir Strezov. Role of heterogeneous catalysts for upgrading pyrolysis bio-oil into viable hydrocarbon fuels (to be submitted).

Chapter 3: Ravinder Kumar, Vladimir Strezov, Haftom Weldekidan, Jing He, Sharanjit Singh, Tao Kan, Behnam Dastjerdi. Lignocellulose biomass pyrolysis for bio-oil production: A review of biomass pretreatment methods for production of drop-in fuels. *Renewable & Sustainable Energy Reviews* 123: 109763, 2020.

Chapter 4: Ravinder Kumar, Vladimir Strezov. Thermochemical production of bio-oil: A review of downstream processing technologies for bio-oil upgrading, production of hydrogen and high value-added products. *Renewable & Sustainable Energy Reviews* 135:110152, 2020.

Chapter 5: Ravinder Kumar, Vladimir Strezov, Emma Lovell, Tao Kan, Haftom Weldekidan, Jing He, Behnam Dastjerdi, Jason Scott. Enhanced bio-oil deoxygenation activity by Cu/zeolite and Ni/zeolite catalysts in combined in-situ and ex-situ biomass pyrolysis. *Journal of Analytical and Applied Pyrolysis* 140: 148-160, 2019.

Chapter 6: Ravinder Kumar, Vladimir Strezov, Tao Kan, Haftom Weldekidan, Jing He, Sayka Jahan. Investigating the effect of mono/bi-metallic-zeolite catalysts on the selectivity of hydrocarbons during bio-oil upgrading from ex-situ pyrolysis of biomass. *Energy & Fuels*, 34(1), 389-400, 2020.

Chapter 7: Ravinder Kumar, Vladimir Strezov, Emma Lovell, Tao Kan, Haftom Weldekidan, Jing He, Behnam Dastjerdi, Jason Scott. Bio-oil upgrading with catalytic pyrolysis of biomass using Copper/zeolite-Nickel/zeolite and Copper-Nickel/zeolite catalysts. *Bioresource Technology* 279: 404-409, 2019.

Chapter 8: Ravinder Kumar, Vladimir Strezov, Jing He, Yutong Zhao, Behnam Dastjerdi, Tao Kan, Haimei Xu, Yijiao Jiang. Synergistic effect of transition metals on ZSM-5 supported catalysts for *ex-situ* bio-oil upgrading (to be submitted).

Chapter 9: Ravinder Kumar, Vladimir Strezov, Jing He, Yutong Zhao, Behnam Dastjerdi, Tao Kan, Haimei Xu, Yijiao Jiang. Effect of catalyst supports with and without nickel on bio-oil upgrading and energy distribution in pyrolytic products during one and two-stage *ex-situ* pyrolysis (to be submitted).

References

[1] Capuano DL. International Energy Outlook 2018 (IEO2018) 2000:21.

[2] Adams P, Bridgwater T, Lea-Langton A, Ross A, Watson I. Biomass Conversion Technologies. Greenhouse Gases Balances of Bioenergy Systems, Elsevier; 2018, p. 107–39. https://doi.org/10.1016/B978-0-08-101036-5.00008-2.

[3] Cunha JA, Pereira MM, Valente LMM, de la Piscina PR, Homs N, Santos MRL. Waste biomass to liquids: Low temperature conversion of sugarcane bagasse to bio-oil. The effect of combined hydrolysis treatments. Biomass and Bioenergy 2011;35:2106–16. https://doi.org/10.1016/j.biombioe.2011.02.019.

[4] Liu Q, Chmely SC, Abdoulmoumine N. Biomass Treatment Strategies for Thermochemical Conversion. Energy & Fuels 2017;31:3525–36. https://doi.org/10.1021/acs.energyfuels.7b00258.
[5] Weldekidan H, Strezov V, He J, Kumar R, Asumadu-Sarkodie S, Doyi INY, et al. Energy Conversion Efficiency of Pyrolysis of Chicken Litter and Rice Husk Biomass. Energy Fuels 2019:acs.energyfuels.9b01264. https://doi.org/10.1021/acs.energyfuels.9b01264.
[6] Staples MD, Malina R, Barrett SRH. The limits of bioenergy for mitigating global life-cycle greenhouse gas emissions from fossil fuels. Nature Energy 2017;2:16202. https://doi.org/10.1038/nenergy.2016.202.
[7] Dhyani V, Bhaskar T. A comprehensive review on the pyrolysis of lignocellulosic biomass. Renewable Energy 2018;129:695–716. https://doi.org/10.1016/j.renene.2017.04.035.
[8] de Caprariis B, De Filippis P, Petrullo A, Scarsella M. Hydrothermal liquefaction of biomass: Influence of temperature and biomass composition on the bio-oil production. Fuel 2017;208:618–25. https://doi.org/10.1016/j.fuel.2017.07.054.
[9] Gollakota ARK, Kishore N, Gu S. A review on hydrothermal liquefaction of biomass. Renewable and Sustainable Energy Reviews 2018;81:1378–92. https://doi.org/10.1016/j.rser.2017.05.178.
[10] Dai L, Wang Y, Liu Y, Ruan R, He C, Yu Z, et al. Integrated process of lignocellulosic biomass torrefaction and pyrolysis for upgrading bio-oil production: A state-of-the-art review. Renewable and Sustainable Energy Reviews 2019;107:20–36. https://doi.org/10.1016/j.rser.2019.02.015.
[11] Kumar R, Strezov V, Kan T, Weldekidan H, He J. Investigating the effect of Cu/zeolite on deoxygenation of bio-oil from pyrolysis of pine wood. Energy Procedia 2019;160:186–93. https://doi.org/10.1016/j.egypro.2019.02.135.
[12] He J, Strezov V, Kan T, Weldekidan H, Kumar R. Slow pyrolysis of metal(loid)-rich biomass from phytoextraction: characterization of biomass, biochar and bio-oil. Energy Procedia 2019;160:178–85. https://doi.org/10.1016/j.egypro.2019.02.134.
[13] Guedes RE, Luna AS, Torres AR. Operating parameters for bio-oil production in biomass pyrolysis: A review. Journal of Analytical and Applied Pyrolysis 2018;129:134–49. https://doi.org/10.1016/j.jaap.2017.11.019.
[14] Kan T, Strezov V, Evans TJ. Lignocellulosic biomass pyrolysis: A review of product properties and effects of pyrolysis parameters. Renewable and Sustainable Energy Reviews 2016;57:1126–40. https://doi.org/10.1016/j.rser.2015.12.185.
[15] Zhao C, Jiang E, Chen A. Volatile production from pyrolysis of cellulose, hemicellulose and lignin. Journal of the Energy Institute 2017;90:902–13. https://doi.org/10.1016/j.joei.2016.08.004.
[16] Zhu L, Li K, Ding H, Zhu X. Studying on properties of bio-oil by adding blended additive during aging. Fuel 2018;211:704–11. https://doi.org/10.1016/j.fuel.2017.09.106.
[17] Czernik S, Bridgwater AV. Overview of Applications of Biomass Fast Pyrolysis Oil. Energy & Fuels 2004;18:590–8. https://doi.org/10.1021/ef034067u.
[18] Acharya B, Dutta A, Minaret J. Review on comparative study of dry and wet torrefaction. Sustainable Energy Technologies and Assessments 2015;12:26–37. https://doi.org/10.1016/j.seta.2015.08.003.
[19] He C, Tang C, Li C, Yuan J, Tran K-Q, Bach Q-V, et al. Wet torrefaction of biomass for high quality solid fuel production: A review. Renewable and Sustainable Energy Reviews 2018;91:259–71. https://doi.org/10.1016/j.rser.2018.03.097.
[20] Jacquet N, Maniet G, Vanderghem C, Delvigne F, Richel A. Application of Steam Explosion as Pretreatment on Lignocellulosic Material: A Review. Industrial & Engineering Chemistry Research 2015;54:2593–8. https://doi.org/10.1021/ie503151g.
[21] Abdul PM, Jahim JMd, Harun S, Markom M, Lutpi NA, Hassan O, et al. Effects of changes in chemical and structural characteristic of ammonia fibre expansion (AFEX) pretreated oil palm empty fruit bunch fibre on enzymatic saccharification and fermentability for biohydrogen. Bioresource Technology 2016;211:200–8. https://doi.org/10.1016/j.biortech.2016.02.135.

[22] Xu X, Li Z, Sun Y, Jiang E, Huang L. High-Quality Fuel from the Upgrading of Heavy Bio-oil by the Combination of Ultrasonic Treatment and Mutual Solvent. Energy & Fuels 2018;32:3477–87. https://doi.org/10.1021/acs.energyfuels.7b03483.
[23] Li H, Xia S, Ma P. Upgrading fast pyrolysis oil: Solvent–anti-solvent extraction and blending with diesel. Energy Conversion and Management 2016;110:378–85. https://doi.org/10.1016/j.enconman.2015.11.043.
[24] Leng L, Li H, Yuan X, Zhou W, Huang H. Bio-oil upgrading by emulsification/microemulsification: A review. Energy 2018;161:214–32. https://doi.org/10.1016/j.energy.2018.07.117.
[25] Zhang M, Yewe-Siang Lee Shee We M, Wu H. Direct emulsification of crude glycerol and bio-oil without addition of surfactant via ultrasound and mechanical agitation. Fuel 2018;227:183–9. https://doi.org/10.1016/j.fuel.2018.04.099.
[26] Ruiz M, Martin E, Blin J, Van de Steene L, Broust F. Understanding the Secondary Reactions of Flash Pyrolysis Vapors inside a Hot Gas Filtration Unit. Energy & Fuels 2017;31:13785–95. https://doi.org/10.1021/acs.energyfuels.7b02923.
[27] Baldwin RM, Feik CJ. Bio-oil Stabilization and Upgrading by Hot Gas Filtration. Energy & Fuels 2013;27:3224–38. https://doi.org/10.1021/ef400177t.
[28] Kumar R, Strezov V, Lovell E, Kan T, Weldekidan H, He J, et al. Bio-oil upgrading with catalytic pyrolysis of biomass using Copper/zeolite-Nickel/zeolite and Copper-Nickel/zeolite catalysts. Bioresource Technology 2019;279:404–9. https://doi.org/10.1016/j.biortech.2019.01.067.
[29] Budhi S, Mukarakate C, Iisa K, Pylypenko S, Ciesielski PN, Yung MM, et al. Molybdenum incorporated mesoporous silica catalyst for production of biofuels and value-added chemicals via catalytic fast pyrolysis. Green Chemistry 2015;17:3035–46. https://doi.org/10.1039/C4GC02477J.
[30] Sudarsanam P, Peeters E, Makshina EV, Parvulescu VI, Sels BF. Advances in porous and nanoscale catalysts for viable biomass conversion. Chemical Society Reviews 2019;48:2366–421. https://doi.org/10.1039/C8CS00452H.
[31] Sudarsanam P, Zhong R, Van den Bosch S, Coman SM, Parvulescu VI, Sels BF. Functionalized heterogeneous catalysts for sustainable biomass valorization. Chemical Society Reviews 2018;47:8349–402. https://doi.org/10.1039/C8CS00410B.
[32] Lin Y-C, Huber GW. The critical role of heterogeneous catalysis in lignocellulosic biomass conversion. Energy Environ Sci 2009;2:68–80. https://doi.org/10.1039/B814955K.
[33] Ruddy DA, Schaidle JA, Ferrell III JR, Wang J, Moens L, Hensley JE. Recent advances in heterogeneous catalysts for bio-oil upgrading via "ex situ catalytic fast pyrolysis": catalyst development through the study of model compounds. Green Chem 2014;16:454–90. https://doi.org/10.1039/C3GC41354C.
[34] Kumar R, Strezov V, Lovell E, Kan T, Weldekidan H, He J, et al. Enhanced bio-oil deoxygenation activity by Cu/zeolite and Ni/zeolite catalysts in combined in-situ and ex-situ biomass pyrolysis. Journal of Analytical and Applied Pyrolysis 2019. https://doi.org/10.1016/j.jaap.2019.03.008.
[35] Chen H, Shi X, Zhou F, Ma H, Qiao K, Lu X, et al. Catalytic fast pyrolysis of cellulose to aromatics over hierarchical nanocrystalline ZSM-5 zeolites prepared using sucrose as a template. Catalysis Communications 2018;110:102–5. https://doi.org/10.1016/j.catcom.2018.03.016.
[36] Araújo A, Queiroz G, Maia D, Gondim A, Souza L, Fernandes V, et al. Fast Pyrolysis of Sunflower Oil in the Presence of Microporous and Mesoporous Materials for Production of Bio-Oil. Catalysts 2018;8:261. https://doi.org/10.3390/catal8070261.
[37] Alekseeva (Bykova) MV, Otyuskaya DS, Rekhtina MA, Bulavchenko OA, Stonkus OA, Kaichev VV, et al. NiCuMo-SiO2 catalyst for pyrolysis oil upgrading: Model acidic treatment study. Applied Catalysis A: General 2019;573:1–12. https://doi.org/10.1016/j.apcata.2019.01.003.
[38] Jaroenkhasemmeesuk C, Diego ME, Tippayawong N, Ingham DB, Pourkashanian M. Simulation analysis of the catalytic cracking process of biomass pyrolysis oil with mixed

catalysts: Optimization using the simplex lattice design. International Journal of Energy Research 2018;42:2983–96. https://doi.org/10.1002/er.4023.
[39] Nguyen TS, Zabeti M, Lefferts L, Brem G, Seshan K. Catalytic upgrading of biomass pyrolysis vapours using faujasite zeolite catalysts. Biomass and Bioenergy 2013;48:100–10. https://doi.org/10.1016/j.biombioe.2012.10.024.
[40] Gamliel DP, Wilcox L, Valla JA. The Effects of Catalyst Properties on the Conversion of Biomass via Catalytic Fast Hydropyrolysis. Energy & Fuels 2017;31:679–87. https://doi.org/10.1021/acs.energyfuels.6b02781.
[41] Veses A, Puértolas B, Callén MS, García T. Catalytic upgrading of biomass derived pyrolysis vapors over metal-loaded ZSM-5 zeolites: Effect of different metal cations on the bio-oil final properties. Microporous and Mesoporous Materials 2015;209:189–96. https://doi.org/10.1016/j.micromeso.2015.01.012.
[42] Serrano DP, Melero JA, Morales G, Iglesias J, Pizarro P. Progress in the design of zeolite catalysts for biomass conversion into biofuels and bio-based chemicals. Catalysis Reviews 2018;60:1–70. https://doi.org/10.1080/01614940.2017.1389109.
[43] Bizkarra K, Bermudez JM, Arcelus-Arrillaga P, Barrio VL, Cambra JF, Millan M. Nickel based monometallic and bimetallic catalysts for synthetic and real bio-oil steam reforming. International Journal of Hydrogen Energy 2018;43:11706–18. https://doi.org/10.1016/j.ijhydene.2018.03.049.
[44] Alonso DM, Wettstein SG, Dumesic JA. Bimetallic catalysts for upgrading of biomass to fuels and chemicals. Chemical Society Reviews 2012;41:8075. https://doi.org/10.1039/c2cs35188a.
[45] Chen J, Wang S, Lu L, Zhang X, Liu Y. Improved catalytic upgrading of simulated bio-oil via mild hydrogenation over bimetallic catalysts. Fuel Processing Technology 2018;179:135–42. https://doi.org/10.1016/j.fuproc.2018.06.022.
[46] Kim S, Kwon EE, Kim YT, Jung S, Kim HJ, Huber GW, et al. Recent advances in hydrodeoxygenation of biomass-derived oxygenates over heterogeneous catalysts. Green Chem 2019:10.1039.C9GC01210A. https://doi.org/10.1039/C9GC01210A.
[47] Li C, Ma J, Xiao Z, Hector SB, Liu R, Zuo S, et al. Catalytic cracking of Swida wilsoniana oil for hydrocarbon biofuel over Cu-modified ZSM-5 zeolite. Fuel 2018;218:59–66. https://doi.org/10.1016/j.fuel.2018.01.026.
[48] Liu W-J, Li W-W, Jiang H, Yu H-Q. Fates of Chemical Elements in Biomass during Its Pyrolysis. Chemical Reviews 2017;117:6367–98. https://doi.org/10.1021/acs.chemrev.6b00647.
[49] Saraeian A, Nolte MW, Shanks BH. Deoxygenation of biomass pyrolysis vapors: Improving clarity on the fate of carbon. Renewable and Sustainable Energy Reviews 2019;104:262–80. https://doi.org/10.1016/j.rser.2019.01.037.
[50] Huo X, Xiao J, Song M, Zhu L. Comparison between in-situ and ex-situ catalytic pyrolysis of sawdust for gas production. Journal of Analytical and Applied Pyrolysis 2018;135:189–98. https://doi.org/10.1016/j.jaap.2018.09.003.
[51] Kurnia I, Karnjanakom S, Bayu A, Yoshida A, Rizkiana J, Prakoso T, et al. In-situ catalytic upgrading of bio-oil derived from fast pyrolysis of lignin over high aluminum zeolites. Fuel Processing Technology 2017;167:730–7. https://doi.org/10.1016/j.fuproc.2017.08.026.
[52] Ratnasari DK, Yang W, Jönsson PG. Two-stage ex-situ catalytic pyrolysis of lignocellulose for the production of gasoline-range chemicals. Journal of Analytical and Applied Pyrolysis 2018;134:454–64. https://doi.org/10.1016/j.jaap.2018.07.012.
[53] Paysepar H, Rao KTV, Yuan Z, Nazari L, Shui H, Xu C (Charles). Zeolite catalysts screening for production of phenolic bio-oils with high contents of monomeric aromatics/phenolics from hydrolysis lignin via catalytic fast pyrolysis. Fuel Processing Technology 2018;178:362–70. https://doi.org/10.1016/j.fuproc.2018.07.013.
[54] Puértolas B, Veses A, Callén MS, Mitchell S, García T, Pérez-Ramírez J. Porosity-Acidity Interplay in Hierarchical ZSM-5 Zeolites for Pyrolysis Oil Valorization to Aromatics. ChemSusChem 2015;8:3283–93. https://doi.org/10.1002/cssc.201500685.

[55] Mullen CA, Dorado C, Boateng AA. Catalytic co-pyrolysis of switchgrass and polyethylene over HZSM-5: Catalyst deactivation and coke formation. Journal of Analytical and Applied Pyrolysis 2018;129:195–203. https://doi.org/10.1016/j.jaap.2017.11.012.
[56] Kalogiannis KG, Stefanidis SD, Karakoulia SA, Triantafyllidis KS, Yiannoulakis H, Michailof C, et al. First pilot scale study of basic vs acidic catalysts in biomass pyrolysis: Deoxygenation mechanisms and catalyst deactivation. Applied Catalysis B: Environmental 2018;238:346–57. https://doi.org/10.1016/j.apcatb.2018.07.016.
[57] Wang J, Zhong Z, Ding K, Deng A, Hao N, Meng X, et al. Catalytic fast pyrolysis of bamboo sawdust via a two-step bench scale bubbling fluidized bed/fixed bed reactor: Study on synergistic effect of alkali metal oxides and HZSM-5. Energy Conversion and Management 2018;176:287–98. https://doi.org/10.1016/j.enconman.2018.09.029.
[58] Karnjanakom S, Suriya-umporn T, Bayu A, Kongparakul S, Samart C, Fushimi C, et al. High selectivity and stability of Mg-doped Al-MCM-41 for in-situ catalytic upgrading fast pyrolysis bio-oil. Energy Conversion and Management 2017;142:272–85. https://doi.org/10.1016/j.enconman.2017.03.049.

Chapter 2

Catalytic Biomass Pyrolysis: formation of hydrocarbons and improved bio-oil properties

This chapter reviews the key reaction pathways taking place during noncatalytic pyrolysis and possible routes to the formation of organic compounds from their primary substrates. The chapter also discusses the types of catalytic biomass pyrolysis (CBP) in a fixed-bed pyrolysis reactor and possible routes carried out by the catalysts to convert the oxygenated compounds into various hydrocarbons. Kinetic of the reactions involved in CBP are also discussed. Effect of catalysts on physicochemical properties of bio-oil and pyrolytic products has been overviewed.

1. Bio-oil composition

Lignocellulose biomass is generally made up of three biopolymers i.e. cellulose (40-50 wt%, a linear polymer of glucose), hemicellulose (25-35 wt%, a branched polymer of C5 and C6 sugars) and lignin (16-33 wt%, aromatic polymer) [1]. Biomass pyrolysis usually results in three types of products, liquid bio-oil, solid biochar and pyrolytic gases [2]. The yield of pyrolytic products mainly depends on the composition of biomass and the distribution of biopolymers in the biomass, which is further governed by different pyrolysis parameters [3]. Generally, at 500 °C, pyrolysis of cellulose results in approximately 85 wt% bio-oil, 8 wt% char and 7 wt% of gases, while the pyrolysis of hemicellulose (xylan) produces around 55 wt% bio-oil, 16 wt% char and 4 wt% gases and the thermal degradation of lignin generates the least amount of bio-oil (44 wt%), maximum char (30 wt%) and gases of ~4 wt% [4]. A number of studies suggest that biomass with a higher amount of cellulose produces greater bio-oil yield [4–6], while the composition of bio-oil highly depends on the decomposition of individual biomass component, which undergoes many primary and secondary reactions, such as depolymerization, fragmentation, dehydration, repolymerization and reforming [4,7]. Table 1 shows the bio-oil composition obtained from the pyrolysis of model compounds like cellulose, hemicellulose and lignin and Table 2 presents a selection of bio-oil properties and yields of pyrolytic products from pyrolysis of lignocellulose feedstocks. Numerous studies have attempted to understand the biomass pyrolysis using model compounds of cellulose, hemicellulose and lignin, which will be discussed in the following sections.

Table 1. Bio-oil composition obtained from pyrolysis of cellulose, hemicellulose and lignin at 500 °C. Data taken from reference [8].

Groups	Compound	Formula	Cellulose (area %)	Hemicellulose (area %)	Lignin (area %)
Saccharides	Levoglucosan	$C_6H_{10}O_5$	34.13	/	/
	1,4,3,6-Dianhydro-. alpha. -D-glucopyranose	$C_6H_8O_4$	6.02	/	/
Furans	Furfural	$C_5H_4O_2$	5.87	1.32	/
	2,3-Dihydrobenzofuran	C_8H_8O	/	/	6.22
	3-Furaldehyde	$C_5H_4O_2$	1.35	/	/
	2,2-Dimethyl-3(2H)-furanone	$C_6H_8O_2$	1.25	/	/
	2(5H)-Furanone	$C_4H_4O_2$	1.58	/	/
	5-Methyl-2(5H) furanone	$C_5H_6O_2$	1.38	/	/
	5-Methyl-2-furaldehyde	$C_6H_6O_2$	0.71	/	/
	2-Furanmethanol	$C_5H_6O_2$	5.09	/	/
	2-Ethyl-furan	C_6H_8O	/	2.12	/
	5-Methyl-2-furancarboxaldehyde	$C_6H_6O_2$	/	3.36	/
Ketones	1-Hydroxy-2-propanone	$C_3H_6O_2$	1.84	/	/
	1-Hydroxy-2-butanone	$C_4H_8O_2$	1.16	/	/

	2-Methylcyclopentanone	$C_6H_{10}O$	0.41	/	/
	3-Methyl-1,2-cyclopentenodione	$C_6H_8O_2$	1.56	/	/
	3-Methyl-2-cyclopenten-1-one	C_6H_8O	0.22	2.60	/
	1,2-Cyclopentanedione	$C_5H_6O_2$	1.38	/	/
	3-Hydroxy-2-butanone	$C_4H_8O_2$	/	2.60	/
	4-Hydroxy-3-hexanone	$C_6H_{12}O_2$	/	1.83	/
	2-Cyclopenten-1-one	C_5H_6O	/	6.47	/
	2-Cyclohexen-1-one	C_6H_8O	/	1.23	/
	2,3-Dimethyl-2-cyclopenten-1-one	$C_7H_{10}O$	/	8.12	/
	2-Hydroxy-3-methyl-2-cyclopenten-1-one	$C_6H_8O_2$	/	3.96	/
	2,3,4,5-Tetramethyl-2-cyclopenten-1-one	$C_9H_{14}O$	/	0.25	/
	Acetovanillone	$C_9H_{10}O_3$			0.93
	4-O-Methylphloracetophenone	$C_9H_{10}O_4$			1.24
	Acetosyringone	$C_{10}H_{12}O_4$			4.31
Phenols	Phenol	C_6H_5OH	0.44	4.07	9.00
	4-Methyl-phenol	C_7H_8O	0.43	2.33	5.12
	Maltol	$C_6H_6O_3$	0.65	/	/
	2-Methyl-phenol	C_7H_8O	/	4.65	1.60
	4-Ethyl-2-methoxy-phenol	$C_9H_{12}O_2$	/	1.55	10.07
	3-Methoxyphenol	$C_7H_8O_2$	/	/	5.71
	3,4-Dimethylphenol	$C_8H_{10}O$	/	/	1.15
	4-Ethylphenol	$C_8H_{10}O$	/	/	12.57
	3-Methoxy-2-benzenediol	$C_7H_8O_3$	/	/	1.02
	O-Methylorcinol	$C_8H_{10}O_2$	/	/	1.08
	2,6-Dimethoxyphenol	$C_8H_{10}O_3$	/	/	5.47
	3,4-Dimethoxyphenol	$C_8H_{10}O_3$	/	/	1.58
	4-Ethylresorcinol	$C_8H_{10}O_2$	/	/	1.99
Alcohols	4-Methyl-1-hepten-4-ol	$C_8H_{16}O$	0.54	/	/
	1-Methylcycloheptanol	$C_8H_{16}O$	0.25	/	/
	cis-1,2-Cyclohexanediol	$C_6H_{12}O_2$	0.52	/	/
	(E)-3-Methyl-2-penten-4-yn-1-ol	C_6H_8O	/	1.34	/
	4-Methyl-cyclohexanol	$C_7H_{14}O$	/	0.87	/
Acids	Palmitic acid	$C_{16}H_{32}O_2$	/	/	2.93
	Linoleic acid	$C_{18}H_{32}O_2$	/	/	2.04
	Petroselic acid	$C_{18}H_{34}O_2$	/	/	6.79
	Stearic acid	$C_{18}H_{36}O_2$	/	/	0.37
	Acetic acid	CH_3COOH	/	22.86	/
	Propanoic acid	CH_3CH_2COOH	6.30	8.80	/
	3,4-Dihydroxy-3-cyclobutene-1,2-dione	$C_4H_2O_4$	2.44	/	/
	Heptanoic acid	$C_7H_{14}O_2$	1.20	/	/
Esters	5-Methyl-2(3H)-furanone	$C_5H_6O_2$	1.20	/	/
	Methyl 2-furoate	$C_6H_6O_3$	0.93	/	/
	Methyl-4-methyl-2-pentenoate	$C_7H_{12}O_2$	1.58	/	
	2-Hexenoic acid, methyl ester	$C_7H_{12}O_2$	2.55	/	/
	Ethyl homovanillate	$C_{11}H_{14}O_4$	/	/	0.57
	Methyl petroselinate	$C_{19}H_{36}O_2$	/	/	1.27

Aldehydes	2-Methylcrotonaldehyde	C_5H_8O	0.16	/	/
	Heptanal	$C_7H_{14}O$	3.53	/	/
	Formaldehyde di-isopropyl acetal	$C_7H_{16}O_2$	3.81	/	/

Cellulose is the major component of dry wood, comprising approximately 40-50 wt% [1]. Cellulose is a polysaccharide of $\beta(1 \rightarrow 4)$ linked D-glucose units. Glucose anhydride is formed after the release of a water molecule from a glucose unit and two glucose anhydride units combined to form a cellobiose unit, which acts as the repeating unit of cellulose [9]. A cellulose molecule may contain several hundred to thousands of units in linear chains. While two glucose units are connected through the glycosidic bonds $\beta(1 \rightarrow 4)$. The glucose units of one chain forms intramolecular hydrogen bonds ($O3 - H \rightarrow O5' and\ O6 \rightarrow H - O2'$) to connect with the similar chain and form intrastand hydrogen bonds ($O6 - H \rightarrow O3'$) to connect with the neighboring chain [10]. The pyrolysis of cellulose occurs between 240 and 350 °C, leading to generation of different organic compounds. At 300 °C, the dominant compounds are anhydrosugars e.g., levoglucosan (LGA), levoglucosenone (LGO), pyrans and furans, while at the higher temperature of around 500 °C, anhydrosugars start converting into light oxygenates, like formic acid, methyl glyoxal and hydroxyacetone [4]. Figure 1a shows the possible pathways for the generation of different organic compounds during the pyrolysis of cellulose. As shown in the figure, the initial degradation of cellulose could result into different anhydrosugars, such as LGA and LGO, and furans, such as hydroxymethyl furfural (HMF) and pyrans like dianhydroglucopyranose (DAGP) [4]. Cellulose could be converted into LGA possible via three pathways, including ionic pathway, free-radical pathway or concerted mechanism where all bond breaking and bond making reactions occur in a single step [11–13]. The latter is the most favorable pathway for LGA formation due to the low energy barrier, which involves the cleavage of glycosidic bond ($C1' - O$), and hydrogen-oxygen bond ($O6' - H6'$) and formation of two other bonds simultaneously i.e. ($C1' - O6'$) and ($O6' - H6'$) [11]. On the other hand, LGO could be formed via two pathways, the first includes its formation from direct cellulose through the concerted mechanism and, secondly, from LGA through a dehydration reaction [14].

Table 2. Effect of lignocellulose biomass composition on the yield of pyrolytic products and bio-oil properties.

Lignocellulose biomass	**Biomass constituents (%)**			**Pyrolysis**		**Product yield (wt%)**			**Bio-oil properties**								**Reference**
	C	HC	L	Reactor	T (°C)	Bio-oil	Gas	Char	Elemental composition (wt%)			HHV (MJ/kg)	Viscosity (cP)	Water content (wt%)	pH	Density (g/cm^3)	
									C	H	O						
Walnut shells	32.19	26.20	36.89	Fixed-bed	500	20.67	26.78	29.83	63.10	6.91	29.42	24.38	/	/	/	/	[15]
Peach stones	29.50	25.10	39.26	Fixed-bed	500	18.98	25.09	32.88	62.00	6.39	30.60	24.67	/	/	/	/	[15]
Sugarcane leaves	/	/	/	Fixed-bed	550	32.45	43.32	24.23	42.70	7.40	33.32	29.57	7.9	/	/	0.01	[16]
Wheat straw	33.30	24.00	15.10	Fluidized-bed	509	34.97	26.99	28.05	60.33	8.61	30.01	22.0	/	22.10	4.10	/	[17–19]
Switch grass	36.00	31.60	6.10	Fluidized-bed	500	57.90	16.57	20.03	63.15	7.97	28.15	22.3	/	21.60	3.39	/	[17–19]
Miscanthus	54.00	23.90	14.94	Fluidized-bed	500	46.61	9.13	31.37	54.90	7.40	36.07	18.8	/	22.00	3.78	/	[17–19]
Beech wood	43.30	31.80	21.40	Fluidized-bed	498	51.34	13.03	14.43	54.24	6.90	38.86	20.1	/	12.80	2.86	/	[17–19]
Willow SRC	49.30	14.10	20.00	Fluidized-bed	500	40.51	19.89	19.28	62.94	5.86	31.09	21.8	/	15.00	3.42	/	[17–19]
Wheat straw	38.00	36.00	22.00	Fixed-bed	500	47.00	20.00	33.00	/	/	/	/	/	/	/	/	[18]
Rape straw	36.00	37.00	24.00	Fixed-bed	500	48.00	20.00	32.00	/	/	/	/	/	/	/	/	[18]
Spruce + bark	42.00	27.00	26.00	Fixed-bed	500	41.00	16.00	43.00	/	/	/	/	/	/	/	/	[18]
Eucalyptus wood	46.25	13.49	34.00	Fluidized-bed	450	50.80	29.40	19.70	/	/	/	/	/	31.00	/	/	[20]
Sweet sorghum	34.20	24.30	6.50	Fluidized-bed	500	43.50	32.80	23.80	22.08	0.21	71.20	12.39	2.48	56.29	2.84	1.08	[21]
Sugarcane bagasse	43.55	32.99	21.76	Fluidized-bed	500	72.00	4.00	24.00	/	/	/	/	/	/	/	/	[22]
Napier grass	38.75	19.76	26.99	Vertical fixed-bed	600	49.34	29.28	21.89	50.89	6.02	41.98	26.77	/	/	2.65	/	[23]
Anchusa azurea	40.67	24.23	18.11	Tubular fixed-bed	550	30.84	33.23	35.93	45.59	7.11	45.72	17.43	/	/	/	/	[24]
Corn straw	37.60	21.60	18.40	Fluidized-bed	500	41.34	44.92	12.98	/	/	/	9.47	9.58	/	/	1.12	[25]
Pine wood	33.55	27.34	39.90	Auger reactor	450	54.00	/	19.00	/	/	/	16.10	6.49	20.83	2.65	1.17	[26]
Sweetgum	39.70	12.20	34.00	Auger reactor	450	51	/	/	/	/	/	/	8.26	38.30	2.65	1.16	[27]
Switch grass	29.60	9.80	19.90	Auger reactor	450	31	/	/	/	/	/	/	1.51	61.70	2.98	1.08	[27]
Corn stover	31.10	10.80	22.60	Auger reactor	450	35	/	/	/	/	/	/	1.60	54.70	2.66	1.08	[27]

C: cellulose, HC: hemicellulose, L: lignin, T: temperature, HR: heating rate

Cellulose could also be converted into furans like HMF via a concerted mechanism which includes four main steps at the same time i.e. breaking of $C4-O4$, transfer of hydrogen from $O2'H$ to $O4$, cleavage of $C2'-C3'$, and lastly, the formation of $C1'-C3'$ bond [10]. However, it has been also reported that this mechanism is kinetically not favoured due to the high energy barrier (53.9 kcal/mol). HMF can be further converted into furfural via deformylation reactions or other furans like 5-methylfurfural and 2-furan methanol via decarboxylation and other deoxygenation reactions [28,29]. The formation of pyrans like 1,5-anhydro-4-deoxy-D-glycerohex-1-en-3-ulose (ADGH) from cellulose is generally carried out via a mechanism involving glycosylation, ring-opening/closing and dehydration reactions [10,30]. Above 500 °C, anhydrosugars could undergo various secondary degradation reactions, such as retro-Diels−Alder, decarbonylation, and dehydration to produce different light oxygenates, including formic acid, methyl glyoxal and hydroxyacetone, while LGO can be further converted into furans like furfural or 5-methylfurfural and light oxygenates like formaldehyde [10,13].

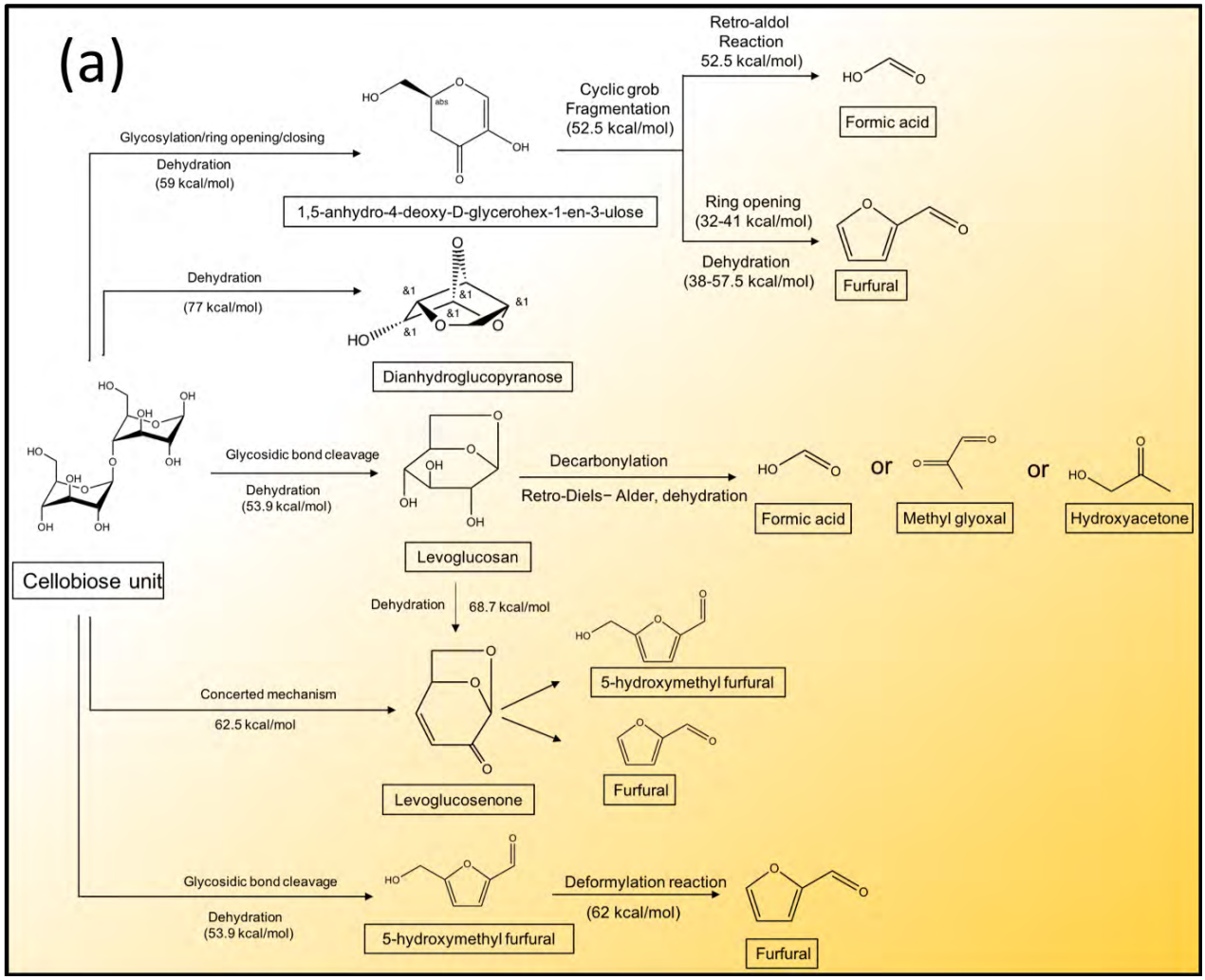

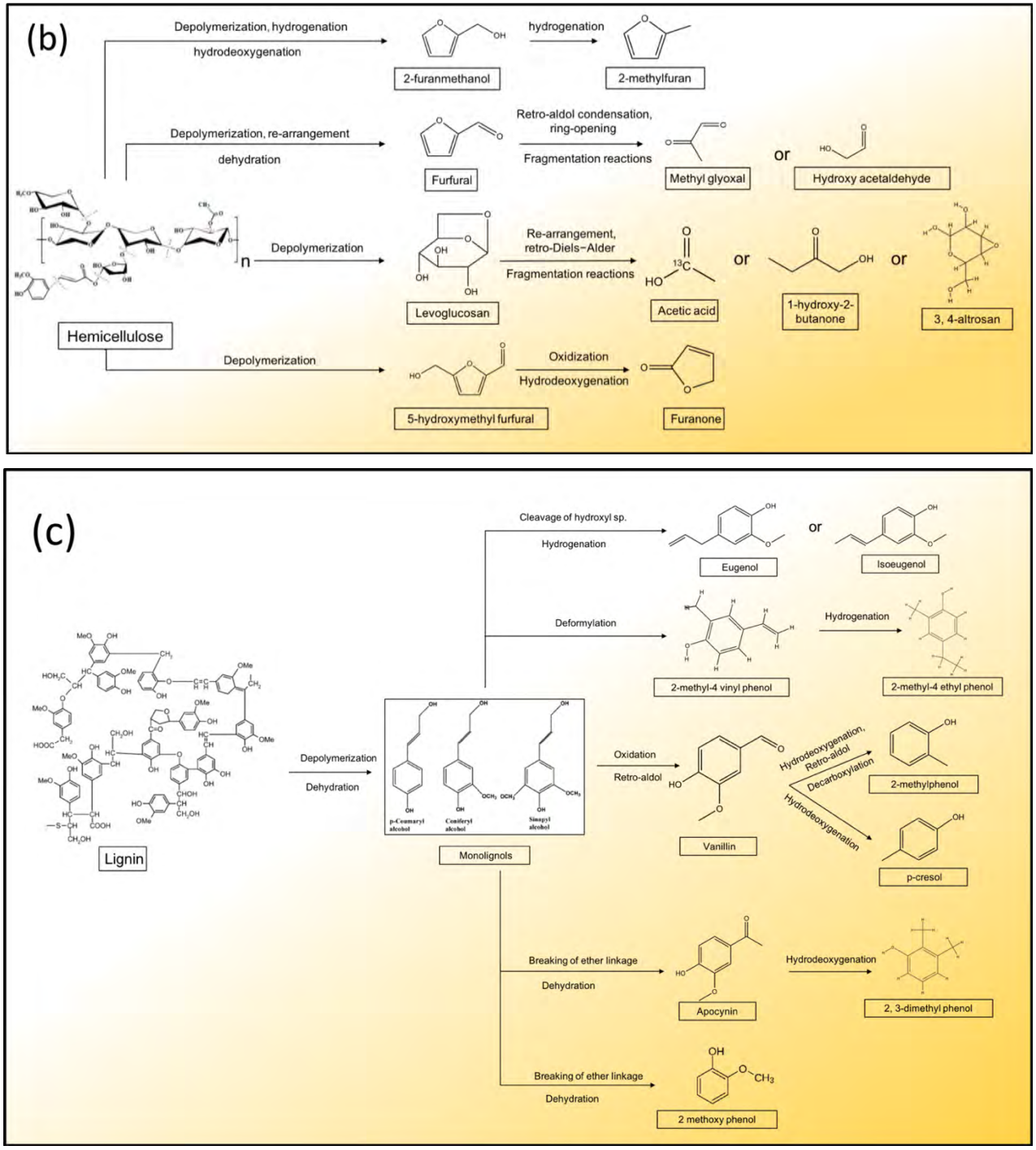

Figure 1. Possible pathways for the generation of different organic compounds during the pyrolysis of (a) cellulose, (b) hemicellulose, and (c) lignin at a temperature range of 350-550 °C.

After cellulose, hemicellulose is considered as the second-largest component of dry wood, comprising 25-35 wt% of the total biomass. Hemicellulose is a heteropolymer of different pentose and hexose sugars, such as glucose, xylose, mannose, galactose, and arabinose. Hemicellulose contains short branched chains of sugar units, of approximately 150 compared to cellulose that contains 5000-10000 glucose units in unbranched chains [1]. Hemicellulose starts decomposing above the pyrolytic temperature of 200 °C and completely degrades up to 350 °C [31]. The pyrolysis of hemicellulose mainly produces volatiles and less char and gases compared to cellulose

[8]. At 300 °C, the bio-oil produced from the pyrolysis of hemicellulose (usually represented by xylan) generally contains more furans (37.75 wt%), light oxygenates (29.20 wt%), anhydrosugars (27.31 wt%), and a few phenolic compounds (5.75 wt%) [4]. Figure 1b shows the possible pathways for the generation of different organic compounds during the pyrolysis of hemicellulose. Above 200 °C, xylan could be depolymerized to produce the primary products, mainly furans, anhydrosugars or it could also undergo a mechanism of depolymerization, re-arrangement and dehydration reactions to yield furfural. During cellulose pyrolysis, the cleavage of glycosidic bond between the two pyranose rings results in the formation of a glucosyl cation, further stabilized by the formation of 1,6-anhydride [6]. However, in hemicellulose pyrolysis, cleavage of glycosidic bond produces a xylosyl cation, however, a stable anhydride could not be formed due to the absence of the sixth carbon and substituted oxygen at the fourth number [32]. In this condition, xylosyl cation could undergo further glycosidic bond breaking and dehydration reactions, followed by the addition of OH^- and H^+ to yield xylose [32]. The C_5 intermediate compounds generated during xylan pyrolysis usually requires a carbon atom to form C_6 compounds like HMF and LGA. Ansari et al. [4] suggest that this required carbon atom could be provided *in-situ* during the xylan pyrolysis to form C_6 compounds. It has been also reported that xylan could undergo depolymerization, hydrogenation and hydrodeoxygenation reactions to yield 2-furanmethanol. A further increase in pyrolysis temperature can convert the primary pyrolysis products into secondary products through various reactions. For instance, above 300 °C, LGA could be further converted into acetic acid and 1-hydroxy-butanone possibly via fragmentation and retro-Diels-Alder reactions. HMF could be decomposed into furanone via oxidization and hydrodeoxygenation reactions [33]. This conversion could take place in three steps. In the first step, an anhydride could be formed which immediately undergoes hydrolysis reaction to produce an alcohol compound (5-(hydroxymethyl) furan-2-ol), releasing a formic acid molecule. 5-(hydroxymethyl) furan-2-ol could undergo rearrangement reaction in the last step to form 5-hydroxymethyl-2(5H)-furanone [33]. Similarly, 2-furanmethanol could be hydrogenated to form 2-methylfuran, which involves the scission of $C-O$ bond of the side chain and furan ring activation by the addition of a hydrogen atom [34].

Lignin is the third most abundant and complex biopolymer found in the lignocellulose biomass, constitutes nearly 16-33 wt% of dry wood [1]. Lignin is an amorphous, high branched polymer of phenolic compounds that is made up of an irregular array of variously bonded “hydroxy-” and “methoxy-” substituted phenylpropane units. The main monomeric phenylpropanoid units found in lignin structure are *p*-hydroxyphenyl, guaiacyl, and syringyl units which are derived from *p*-coumaryl, coniferyl, and sinapyl alcohols, respectively [35]. The pyrolysis of lignin requires comparatively higher temperature compared to cellulose and hemicellulose. Thermal degradation of lignin starts above 350 °C and at this temperature the main

pyrolytic product is char (~53 wt%) and bio-oil (27 wt%), while no gases are observed [4]. However, increasing the temperature >550 °C enhances the bio-oil yield and decreases the char yield. The bio-oil produced from the pyrolysis of lignin mainly contains different phenolic compounds. For example, Ansari et al. [4] showed that pyrolysis of lignin at 550 °C produces bio-oil with ~45 wt% of low molecular weight phenols, ~25 wt% phenolic aldehydes/ketones, ~20 wt% methoxyphenols and 9.5 wt% light phenols. Figure 1c shows the possible pathways for the generation of different organic compounds during pyrolysis of lignin. Lignin generally starts depolymerizing above 350 °C and produces monolignols that are *p*-coumaryl, coniferyl, and sinapyl alcohols which act as intermediate compounds in formation of various phenolic compounds like vanillin, apocynin, eugenol, 2-methyl-4-vinylphenol, creosol [8,36,37]. It has been reported that coniferyl alcohol could be converted to 2-methyl-4-vinylphenol via deformylation reaction and vanillin via oxidation and retro-aldol reactions [4,37]. The produced 2-methyl-4-vinylphenol could further undergo hydrogenation reaction to generate 2-methyl-4-ethylphenol, where vanillin acts as the intermediate product for formation of *p*-cresol via hydrodeoxygenation reaction and 2-methylphneol through a mechanism of multiple reactions like hydrodeoxygenation, decarboxylation and retro-aldol reactions [38,39]. In addition, coniferyl alcohol undergoes a scission of its -OH group and hydrogenation reaction to form eugenol or isoeugenol [40]. On the other hand, the lignin compound could undergo dehydration reactions, followed by cleavage of the ether linkage $(\beta - O - 4)$ and rearrangement reactions to produce apocynin and 2-methoxyphenol [37]. Apocynin can be further converted into 2, 3-dimethylphenol via hydrodeoxygenation reaction [4].

Together, these studies outline that the bio-oil produced from pyrolysis of the individual component of lignocellulose biomass contains a variety of organic compounds (anhydrosugars, furans, pyrans, phenols), which are produced through a number of different reactions involving glycosidic bond cleavage, dehydration, hydrogenation, hydrodeoxygenation, ring-opening/closing, rearrangement, retro-Diels-Alder, oxidization, reduction, retro-aldol reaction, the breaking of ether linkage, decarboxylation. Therefore, it can be assumed that the pyrolysis of lignocellulose biomass also results in the bio-oil composition containing almost similar types of organic compounds that are produced from the pyrolysis of each biomass component. The bio-oil obtained from a general pyrolysis process contains a variety of oxygenated compounds, such as alcohols, phenols, acids, ketones and aldehydes while a negligible proportion of aromatic or aliphatic hydrocarbons is produced. The dominant presence of oxygenated compounds results in its acidic character, water content and high instability, lower calorific value, high viscosity, low carbon/hydrogen ratio that is impeding the commercialization of the bio-oil [41]. The application of catalysts can successfully convert the oxygenated compounds into desirable aromatic or aliphatic hydrocarbons by carrying out various catalytic reactions, such as hydrogenation,

dehydration, decarboxylation, decarbonylation, aromatization, condensation, ketonization, Diels-Alder reaction [42–46]. Consequently, it could increase the total content of carbon and hydrogen in the bio-oil and enhance the calorific value. The role of a catalyst in converting the oxygenated compounds into hydrocarbons and the possible mechanisms involved, and the influence of the catalyst properties on bio-oil upgrading is discussed in successive sections of the chapter.

2. Catalytic biomass pyrolysis

A catalyst is generally defined as a substance that increases the rate of a chemical reaction without being itself consumed [47,48]. The catalyst could be made of various materials that contains the desirable physical or chemical properties for the required applications. However, for bio-oil upgrading, solid catalysts have been utilized which are usually made up of either sole support of high surface area like ZSM-5, Al_2O_3, TiO_2 or metal-impregnated catalysts like Ni/ZSM-5, Cu/Al_2O_3, NiCu/ZSM-5, CuMo/ZSM-5 [48,49]. For bio-oil upgrading, the highly desirable catalysts should promote cleavage of the $C-O$ bond to remove oxygen and formation of $C-C$ bond to generate hydrocarbons [50]. The catalysts usually promote various deoxygenation reactions like dehydration, decarboxylation, decarbonylation and remove the oxygen in the form of non-condensable gases like CO_2, CO and H_2O and solid coke that is deposited on the catalyst surface. Majority of deoxygenation reactions are believed to occur inside the pores of the catalyst, however, some of the reactions can be catalyzed outside of the pores or on the external surface of the catalyst when the reactant molecules could not pass through the pores, suggesting the importance of size of pores in the catalyst for bio-oil upgrading. Kinetically, a catalyst reduces the potential energy barrier of a reaction by decreasing the activation energy between reactants and products. Thus, it could be suggested that the reactions in noncatalytic pyrolysis that could not take place due to high potential energy barrier can be carried out in the presence of a catalyst.

Based on the incorporation of the catalyst, the catalytic upgrading of bio-oil can be carried out primarily in two widely used configurations i.e. *in-situ* and *ex-situ* and two other less explored modes i.e. two stage *ex-situ* and combined *in-situ* and *ex-situ* pyrolysis [51–54]. Figure 2 shows the different pyrolysis modes which can be used in a fixed-bed reactor. In *in-situ* catalytic pyrolysis, the biomass is mixed with the catalyst and simultaneously heated at a certain temperature, resulting in the upgraded bio-oil [55,56]. This pyrolysis mode favors the higher biomass conversion to pyrolytic products as the catalyst remains in direct contact with produced pyrolytic vapours. As a result, a higher bio-oil yield could be obtained [57]. Moreover, the catalyst exhibits greater vapour residence time, allowing more oxygenated compounds to react with the active sites inside or on the catalyst surface and leading to higher conversion rate of oxygenated compounds into hydrocarbons [58]. However, it has been noticed that the *in-situ* pyrolysis mode requires higher amount of catalyst compared to *ex-situ* mode as the in-situ produced pyrolytic

vapours could not contact the sufficient amount of the catalyst [51,55]. Another challenge for *in-situ* process is the rapid deactivation of the catalyst as the catalyst remains in direct contact with the biomass. On the other hand, in *ex-situ* catalytic pyrolysis, the biomass and the catalyst bed are placed separately in the reactor at a certain distance or in the separate reactors and the produced pyrolytic vapours are passed through the catalyst bed [50,59]. *Ex-situ* pyrolysis allows carrying out the thermal degradation of biomass and catalytic process at different optimal temperatures to obtain the enhanced bio-oil yield and upgraded bio-oil [56,59]. According to the previous studies, *ex-situ* pyrolysis produces better quality of bio-oil, by favoring the production of higher proportion of aromatic hydrocarbons in the bio-oil compared to *in-situ* mode [52,60]. It has been reported that *ex-situ* pyrolysis results in less coke formation, however, it also results in lower bio-oil yield in comparison to the *in-situ* mode [57].

In two-stage *ex-situ* pyrolysis, two different catalyst beds are used, where the pyrolytic vapours are firstly passed through catalyst 1 and the reacted vapours are further passed through catalyst 2 [53]. This type of mode allows the use of two catalysts with different catalytic properties and carry out enhanced number of deoxygenation reactions. For example, a catalyst that exhibits $C - C$ formation can be used as catalyst 1 and a catalyst that shows high activity for aromatization and cyclization reactions can be used at catalyst 2, leading to enhanced formation of aromatics. Therefore, this process could prove highly advantageous to produce more variety of hydrocarbons in the bio-oil and consequently increase its quality [59]. For instance, Ratnasari et al. [53] applied HZSM-5 and Al-MCM-41 in two-stage *ex-situ* pyrolysis of beech wood at varying HZSM-5: Al-MCM-41 ratios (7:1, 3:1, 1:1, 1:3). The results revealed that the 3:1 and 7:1 ratio achieved 90.55 and 90.76% of aromatics, while decreasing the HZSM-5 content in the catalytic ratio at 1:1 and 1:3 reduced the proportion of aromatics in the bio-oil samples, which suggested that higher amount of HZSM-5 participated dominantly in the aromatization reactions and Al-MCM-41 was less responsible for the production of aromatics [53]. Three-stage *ex-situ* pyrolysis has been also adopted for bio-oil upgrading. In three stage *ex-situ* pyrolysis, three separate catalyst beds are placed and the produced pyrolytic vapours are passed through. For example, Asadieraghi and Daud [61] examined the effect of HZSM-5, Ga/HZSM-5 and Cu/ HZSM-5 for fast pyrolysis of palm kernel shell and achieved the highest proportion of hydrocarbons compared to two-stage and single-stage pyrolysis carried out with similar catalysts.

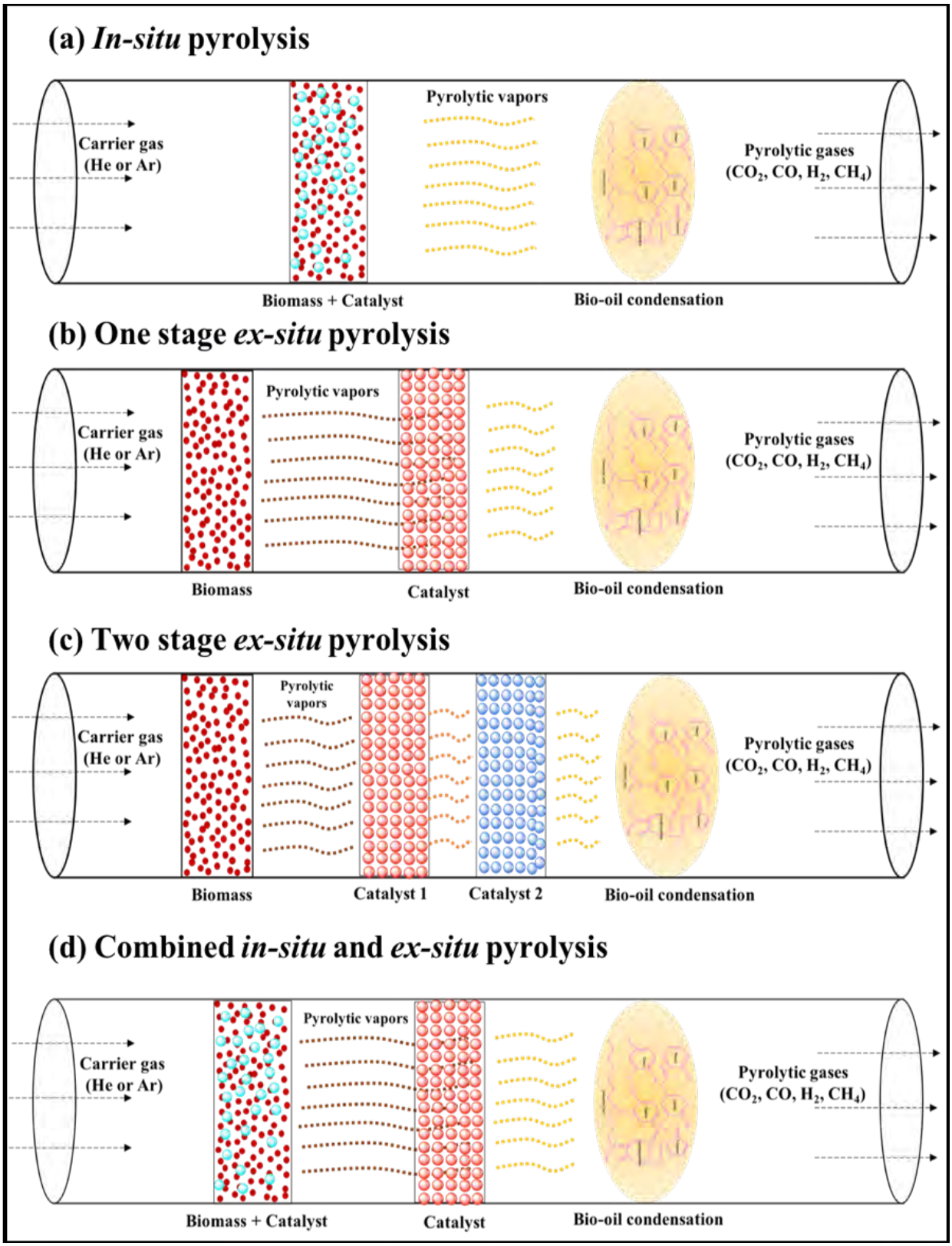

Figure 2. Types of pyrolysis modes in a fixed-bed pyrolysis reactor.

In combined *in-situ* and *ex-situ* catalytic pyrolysis mode, a catalyst is mixed with the biomass and the produced pyrolytic vapours are passed through the similar catalyst or a different catalyst bed, as shown in Figure 2d [51,62,63]. This pyrolysis mode could prove significant to achieve enhanced deoxygenation of bio-oil in which the *in-situ* mode could help to convert the oxygenated compounds into hydrocarbons while the unreacted oxygenated compounds can be successfully converted in the *ex-situ* catalysis. Evidently, Kumar et al. [51] applied Cu/zeolite and Ni/zeolite in a combined *in-situ* and *ex-situ* catalytic pyrolysis mode that achieved the deoxygenation activity of approximately 98% and obtained ~72% hydrocarbons in the bio-oil. In another combined catalytic pyrolysis study, natural zeolite and HZSM-5 were used *in-situ* and *ex-situ*, respectively [62]. The results demonstrated that the combined pyrolysis process produced nearly 8.7% BTEX (benzene, toluene, ethylbenzene, xylenes), while the sole *ex-situ* pyrolysis mode using HZSM-5 could only produce 5.6% BTEX in the bio-oil [62]. However, this process is not completely understood and thus requires more research to explore the distribution of pyrolytic products, total bio-oil yield and catalyst deactivation.

3. Catalytic routes for the conversion of oxygenates into hydrocarbons

The bio-oil produced from a noncatalytic pyrolysis process is typically enriched with low energy density oxygenated compounds, mainly phenols, alcohols, acids, esters, furans and a very low amount of high energy density hydrocarbons. The incorporation of a heterogenous catalysts carries out enhanced number of deoxygenation reactions and converts the oxygen containing compounds into more energy rich aromatic and aliphatic hydrocarbons, consequently, increasing the carbon content and calorific value of the bio-oil. A large number of studies have already demonstrated the catalytic pyrolysis of model compounds, such as 5-HMF, furfural, acetic acid, propanoic acid, *o*-cresol and guaiacol, to understand the reaction pathways involved in their conversion to hydrocarbons and other high value-added compounds [64–70]. This section introduces some chemical routes that are possibly favoured by the catalysts to convert the low energy density oxygenated compounds produced during the primary and secondary pyrolytic reactions into high energy density aliphatic and aromatic hydrocarbons.

Furanic compounds, such as furan, 5-HMF, furfural and 2,5-dimethylfuran (DMF), are generally produced from thermal degradation of cellulose and hemicellulose components of the lignocellulose biomass. HMF and furfural could be produced directly from cellulose via a concerted mechanism which includes four main steps at the same time i.e. breaking of $C4-O4$, transfer of hydrogen from $O2'H$ to $O4$, cleavage of $C2'-C3'$, and lastly, the formation $C1'-C3'$ bond, followed by the dehydration reactions [10]. Also, 5-HMF could be formed via the glycosidic cleavage of cellobiose unit, followed by the dehydration reactions, and subsequently, 5-HMF could undergo deformylation reactions to produce furfural. Similarly, the pyrolysis of

hemicellulose produces 2-methylmethanol via a series of reactions including depolymerization, hydrogenation, hydrodeoxygenation, which further undergoes hydrogenation reaction to produce 2-methylfuran. In the presence of an acid catalyst like H-ZSM-5, these furanic compounds can be converted into short and long straight chain alkanes, monocyclic aromatic hydrocarbons (MAH), and polycyclic aromatic hydrocarbons (PAH) via dehydration, decarboxylation, decarbonylation and oligomerization reactions [71]. DMF could be converted into aromatics like *p*-xylene and 1-methyl-4-propylbenzene (MPB) via Diels-Alder cycloaddition and subsequent dehydration reactions, as shown in Figure 3. It has been reported that Lewis acid sites containing catalysts catalyse the Diels-Alder reaction of DMF and ethylene resulting in a cycloadduct intermediate product [65,71]. This intermediate product could undergo dehydration reaction to form *p*-xylene by either Lewis acids or Brønsted acids. In a side reaction, *p*-xylene could also undergo alkylation reaction to form 1-methyl-4-propylbenzene [68]. The production of *p*-xylene from DMF has been reported to follow pseudo-first order kinetics [72]. Moreover, the conversion efficiency of DMF to *p*-xylene significantly depends on the amount of acidic sites of the catalyst. Evidently, Yin et al. [73] showed that the conversion of DMF increased from 19.9% to 87.2% when the acidity of the catalyst was increased from 0.094 to 0.376 mmol. On the other hand, catalytic fast pyrolysis of furan could produce a variety of hydrocarbons, such as olefins (ethylene, propylene), MAH (benzene, toluene) and PAH (Indene, Naphthalene) via Diels-Alder condensation, decarboxylation, decarbonylation, oligomerization and aromatization reactions. Possible reaction pathways involved in the conversion of furan to hydrocarbons are shown in Figure 4. Noticeably, Gou et al. [69] carried out catalytic fast pyrolysis of furan at 600 °C using zeolite catalysts and showed that mesoporous ZSM-5 achieved approximately 27% furan conversion to produce nearly 41% aromatics (benzene, toluene, xylenes, indenes, naphthalenes) and 29% olefins (ethylene, propylene, allene and C_4, C_5 and C_6 olefins). Similarly, furfural could undergo decarbonylation reaction to generate furan which can follow similar pathways shown in Figure 6 to produce various olefins and aromatics. Alternatively, furfural can also be converted to tetrahydrofurfural by selective hydrogenation of $C = C$ bonds in the furan ring, followed by dehydrogenation of the primary $-C - OH$ to form an aldehyde. Subsequently, tetrahydrofurfural can undergo Aldol self-condensation, hydrogenation and dehydration reactions to form C_{12} and C_{10} alkanes.

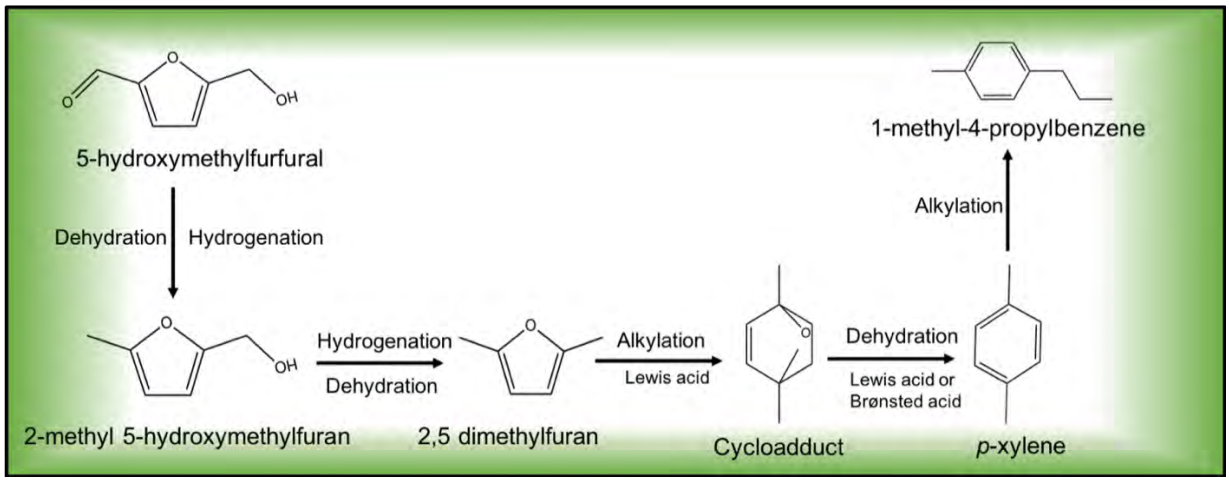

Figure 3. Reaction pathways to convert HMF to DMF and further conversion to *p*-xylene.

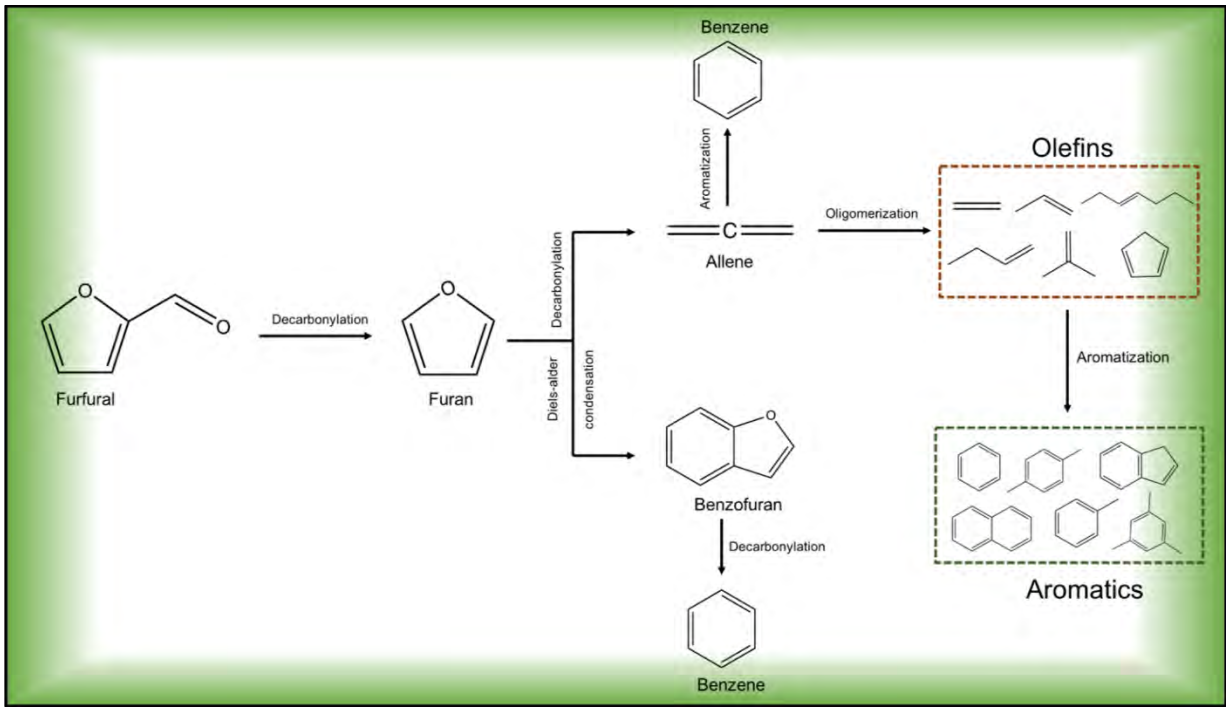

Figure 4. Possible reaction pathways for the conversion of furfural and furan to olefins and aromatics.

Catalytic pyrolysis of 5-HMF produces a variety of aliphatic and aromatic hydrocarbons. Zhao et al. [74] demonstrated the catalytic pyrolysis of 5-HMF at 600 °C on a fixed bed reactor at atmospheric pressure using zeolite-based catalysts. The results showed that HZSM-5 achieved the production of MAH, such as benzene (1.76%), toluene (20.90%), xylene (2.86%), naphthalene (4.81%), while the other aromatics contributed approximately 18.66% of the total hydrocarbon content. The possible route to produce aromatic hydrocarbons from HMF could take place via hydrogenation and dehydration reactions in the presence of a metal-acid catalyst, where zeolite can carry out dehydration reaction and the metal can favor hydrogenation reaction [71]. Hydrogen required for the reaction could be supplied *in-situ* produced during the biomass pyrolysis. However, the production of high concentration of H_2 during pyrolysis of 5-HMF in the presence

of a bifunctional catalyst can lead to a series of Aldol self-condensation, Aldol-crossed condensation, hydrogenation and dehydration reactions to produce C_9-C_{15} alkanes [75].

Bio-oil is usually enriched of different carboxylic acids (acetic acid, propanoic acid, palmitic acid, heptanoic acid), esters and ketones, which are formed by the pyrolysis of all three components of lignocellulose biomass. The presence of these acids makes the bio-oil acidic and consequently highly unstable. The application of acid catalysts can successfully convert the acids into high energy density hydrocarbons and thus enhance the bio-oil properties. The cracking of carboxylic acids over acidic catalysts could be carried out in two pathways [67,76,77]. In the first pathway, -COOH could undergo decarbonylation reaction to produce -CO and -OH and decarboxylation reactions to generate CO_2 and H^- [67]. The further cracking of carboxylic acids can produce light chain hydrocarbons and free -CH_2-CH_3, -CH_2 and CH_3 radicals. In the next step, carbon chain elongation could take place to form short or long chain olefins, which could further undergo aromatization reactions to produce aromatics like benzene, toluene and xylene [78,79]. In the alternative pathway, during the first step of acid-catalysed pyrolysis, carboxylic acids transform into symmetrical ketones, which would further undergo γ-hydrogen transfer rearrangement mechanism to form methyl ketones and a terminated alkene [76,77], as shown in Figure 5. For instance, the pyrolysis of carboxylic acid, like dodecanoic acid, would transform into the ketonic form, that is diundecyl ketone, which would undergo γ-hydrogen transfer mechanism to form 2-tridecanone and 1-decene. It has been reported that γ-hydrogen transfer is favoured by the binding of the carbonyl group to Lewis acid sites of the catalysts and leaving the oxygen atom with a partial positive charge [76]. This mechanism leads to scission between α and β carbon of the symmetrical ketone to generate an enolic product and a terminated alkene. The enolic product is highly unstable, thus could undergo keto-enol tautomerism to form methyl ketone [76].

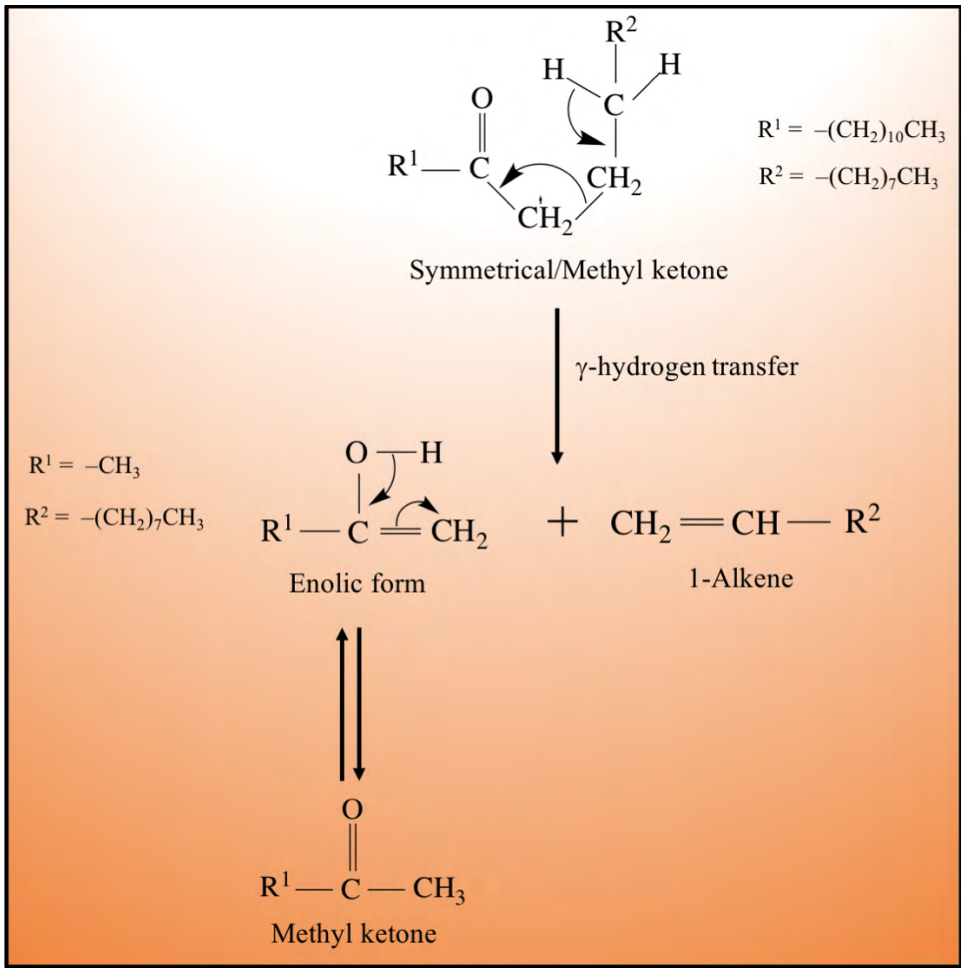

Figure 5. γ-hydrogen transfer mechanism on symmetrical ketone/methyl ketone. Adapted from reference [76].

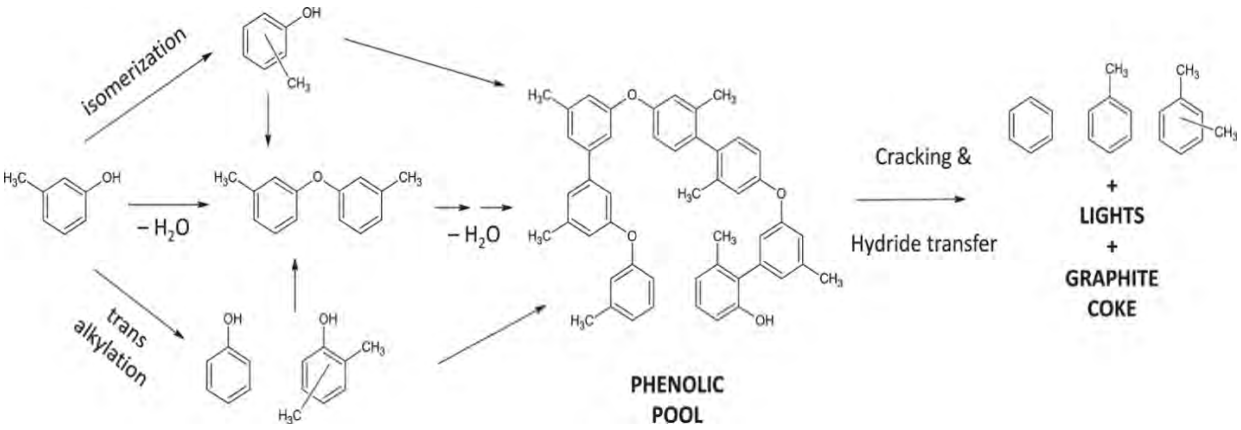

Figure 6. Proposed reaction pathway for *m*-cresol conversion over zeolites. Reproduced with permission from [80].

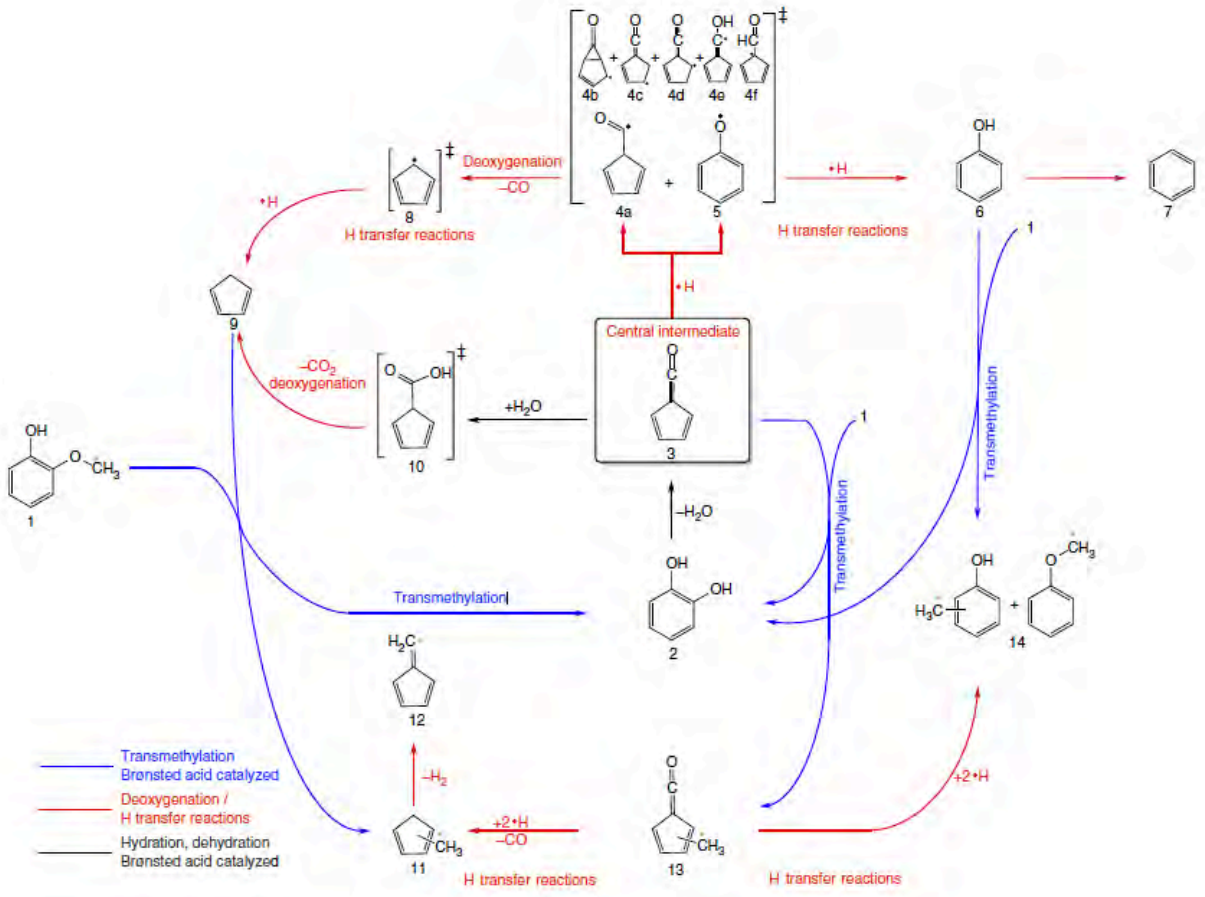

Figure 7. Overview of the whole reaction mechanism of H-USY zeolite-catalysed pyrolysis of guaiacol. Reproduced with permission from [81].

Phenols are the dominant organic compounds found in the bio-oil, mainly produced from the pyrolysis of lignin component of the lignocellulose biomass. A number of studies have carried out the catalytic cracking activity of various phenolic model compounds to understand their transformation reaction pathways to hydrocarbons [80,82–86]. For instance, To and Resasco [80] demonstrated the pyrolysis of *m*-cresol using acidic zeolites, HZSM-5 and HY. The possible reaction pathway for *m*-cresol conversion to aromatics over zeolite catalysts is shown in Figure 6, which suggests that cracking of *m*-cresol to aromatics firstly involves three main reactions that are isomerization, transalkylation and condensation to convert *m*-cresol into a phenolic pool that acts as the precursor for the generation of different aromatics. Later this phenolic pool undergoes cracking and hydrogen transfer reactions to produce mainly aromatic hydrocarbons, such as benzene, toluene, xylenes and naphthalenes, while no aliphatics were reported [80]. The phenolic compounds have been also reported to undergo direct deoxygenation and dehydration reactions to form aromatics [85]. Guaiacol is another major phenolic compound present in the bio-oil and the acid-catalyzed pyrolysis can successfully convert into various MAH and PAH. Figure 7 shows the possible mechanism of H-USY zeolite-catalysed pyrolysis of guaiacol. Jiang et al. [87] suggested that Brønsted acid sites in HZSM-5 catalyst promote the demethoxylation, dehydroxylation and methyl substitution reactions to produce MAH, like benzene and toluene, which further undergo

secondary polymerization reactions to form PAH, like naphthalene and methylnaphthalene. However, several intermediate compounds are also formed during the conversion of guaiacol to aromatics [87]. For example, the homolytic cleavage of O-CH_3 group of guaiacol leads to the formation of catechol that can further undergo intramolecular hydrogen transfer and decomposition reactions to produce 1,3-butadiene and 3-hexene-1,6-dione. o-hydroxyphenoxy is also formed during the pyrolysis of guaiacol which undergoes decarbonylation reaction to produce hydroxycyclopentadienyl [88]. Liu et al. [89] suggest that hydroxycyclopentadienyl can undergo intramolecular hydrogen transfer reaction to generate cyclopentadienyl radical and its further ring opening can form pentadienone radicals, which undergoes decarbonylation reaction to form C_4 hydrocarbons. Cyclopentadienyl can also combine with indenyl and undergo rearrangement to form phenanthrene [90].

4. Kinetics of catalytic biomass pyrolysis

Generally, the catalytic pyrolysis of lignocellulose biomass is considered as a heterogeneous chemical reaction. During the catalytic biomass pyrolysis, the chemical kinetics depends on several key processes involved, such as adsorption and desorption of reactants and products on the catalyst surface, breaking and formation of chemical bonds and the changing reaction geometry. Therefore, each process can affect the reaction dynamics and kinetics of the pyrolysis. The kinetics also depends on biomass composition, heating rate, particle size, and heat and mass transport. The application of a catalyst usually reduces the potential energy barrier of a reaction by decreasing the activation energy between reactants and products, thereby increasing the feasibility of the formation of a product that could not form in the absence of a catalyst. It could be inferred from Arrhenius equation (eq. 1) that lower the activation the faster the rate of reaction.

$$k(T) = Ae^{-E_a/RT} \quad (1)$$

where *k(T)* is reaction rate constant, *A* is pre-exponential factor (min^{-1}), *R* is gas constant (8.314 × 10 kJ mol^{-1}), *T* is temperature (K) and E_a is activation energy (kJ mol^{-1}). The kinetics of the catalytic pyrolysis process can be studied using thermogravimetric analysis (TGA), while the activation energies for the decomposition of biomass components can be evaluated by employing various kinetic models, such as distributed activation energy model (DAEM) [92], Coats−Redfern [92,93], Flynn-Wall-Ozawa (FWO) [94,95], Kissinger-Akahira-Sunose (KAS) [94] and Starink method [94]. A number of studies have demonstrated the kinetics of biomass pyrolysis and suggest that each biomass component (cellulose, hemicellulose and lignin) exhibits a varying range of activation energies. For example, the pyrolysis of cellulose requires approximately 141 kJ mol^{-1} of activation energy, which is higher compared to hemicellulose (124.51 kJ mol^{-1}) and lower compared to lignin that requires nearly 166.68 kJ mol^{-1} of activation energy [95]. Table 4

summarizes few studies and provides the values of activation energy required for pyrolysis of biomass with and without the presence of a catalyst.

Coat-Redfern method is a global kinetic isoconversional model widely used to study the kinetics of biomass pyrolysis using thermogravimetric (TG) data obtained under varying heating rates [92,93,95]. It divides the pyrolysis process into different stages based on temperature and weight loss and provides the activation energy and reaction order for each stage of the pyrolysis process [94]. This method does not require prior assumption of the reaction model and provides accurate kinetic parameters compared to the other kinetic models. The following formula (eq. 2) can be used to calculate the kinetic parameters of the first-order reactions:

$$\ln\left[\frac{-\ln(1-\alpha)}{T^2}\right] = \ln\left[\frac{AR}{\beta E}\left(1-\frac{2RT}{E}\right)\right] - \frac{E}{RT} \quad (2)$$

where α is the thermal conversion of the substance, A is pre-exponential factor, β is the heating rate dT/dt, T is temperature, R is gas constant. According to Coat-Redfern method, the pyrolysis of biomass with and without catalyst follows a two or three-step reaction mechanism [92,93]. For instance, Lu et al. [93] examined the kinetics of sole wheat straw pyrolysis using various zeolite and Al_2O_3-based catalysts. The results suggested that both non-catalytic and catalytic biomass pyrolysis exhibited multistep reaction characteristics, mainly divided into a two-step reaction mechanism, as shown in Figure 8. Noticeably, during the first step for biomass pyrolysis, the activation energy was 83.6 kJ mol^{-1}, which significantly decreased with the application of catalysts. For example, 41.8 kJ mol^{-1} of activation energy was obtained when HZSM-5/γ-Al_2O_3 was used as catalyst, while 47.6 kJ mol^{-1} for Ni-Mo-HUSY/γ-Al_2O_3. Similarly, during the second step, the sole biomass pyrolysis showed the activation energy of 3.74 kJ $mol^{-1,}$ while the bifunctional catalysts, like Ni-Mo-HUSY/γ-Al_2O_3 and Ni-Mo-HZSM-5/γ-Al_2O_3 showed activation energy values of 1.64 and 2.95 kJ mol^{-1}, respectively [93]. The higher activation energy could result because of their rapid deactivation, probably due to coke deposition in the internal pore passage or pore mouth of the catalyst. In addition, the authors reported that in the temperature range of 200-350 °C, biomass pyrolysis followed first-order reaction kinetics, while the catalytic pyrolysis did not follow the first-order reaction kinetics. Although, in the range of 350-500 °C, both noncatalytic and catalytic biomass pyrolysis followed nearly first-order reaction kinetics but could not continue to follow at the higher temperature of up to 700 °C [93].

Table 4. Summary of the values of activation energy required for noncatalytic and catalytic pyrolysis of biomass samples.

Feedstock	Instrument	Temperature range (°C)	Heating rate (°C/min)	Sample mass (mg)	(E_a) kJ mol^{-1}	Model used	Reference
		Noncatalytic pyrolysis					
Wheat straw	NETZSCH 449 C (TG-DSC)	110-900	30	10	87.34	Coats–Redfern	[93]
Beech wood	TGA*	110-900	10	60	136.64	Coats–Redfern	[92]
Cellulose	SDT Q600 (TA)- HPR20 (MS)	100-800	20-50	5	147.84	FWO	[94]
Straw	SDT Q600 (TA)- HPR20 (MS)	100-800	20-50	5	245.44	FWO	[94]
Hemicellulose	EXSTAR TG/DTA6300	25-800	10-40	10	124.51	FWO	[95]
Lignin	EXSTAR TG/DTA6300	25-800	10-40	10	166.68	FWO	[95]
Cotton stalk	SDT Q600 (TA)	110-800	5	10	239.46	DAEM	[96]
Sugar cane bagasse	SDT Q600 (TA)	110-800	5	10	234.75	DAEM	[96]
Switch grass	SDT Q600 (TA)	110-800	5	10	260.95	DAEM	[96]
Wheat straw	SDT Q600 (TA)	110-800	5	10	240.61	DAEM	[96]
Ground fir wood	STA 409 PC Luxx TG-DSC	25-1300	10	20	90.7	Coats–Redfern	[97]
Elephant grass	Perkin Elmer 2400	25-900	10-30	10	227.20	/	[98]
Date palm seed	METTLER TGA/SDTA 851E	25-900	20	5	20.24	/	[99]
		Catalytic pyrolysis					
HUSY/γ-Al_2O_3 + wheat straw	NETZSCH 449 C (TG-DSC)	110-900	30	10	47.81	Coats–Redfern	[93]
HZSM-5/γ-Al_2O_3+ wheat straw	NETZSCH 449 C (TG-DSC)	110-900	30	10	47.21	Coats–Redfern	[93]
Ni–Mo–REY/γ- Al_2O_3 + wheat straw	NETZSCH 449 C (TG-DSC)	110-900	30	10	57.95	Coats–Redfern	[93]
Ni-CaO-Ca_2SiO_4+ cellulose	SDT Q600 (TA)- HPR20 (MS)	100-800	20-50	7	37.65	FWO	[94]
Ni-CaO-Ca_2SiO_4+ cellulose	SDT Q600 (TA)- HPR20 (MS)	100-800	20-50	7	26.38	DAEM	[94]
Ni-Ca_2SiO_4+ pine sawdust	SDT Q600 (TA)- HPR20 (MS)	100-800	20-50	7	115.14	DAEM	[94]
Ni-CaO-Ca_2SiO_4+ straw	SDT Q600 (TA)- HPR20 (MS)	100-800	20-50	7	165.59	KAS	[94]
Ni-Ca_2SiO_4+ straw	SDT Q600 (TA)- HPR20 (MS)	100-800	20-50	7	188.05	Starnik	[94]
Ni-Ca_2SiO_4+ straw	SDT Q600 (TA)- HPR20 (MS)	100-800	20-50	7	187.64	DAEM	[94]
Cu_2O + ground fir wood	STA 409 PC Luxx TG-DSC	25-1300	10	20	84.80	Coats–Redfern	[97]
CuO + ground fir wood	STA 409 PC Luxx TG-DSC	25-1300	10	20	89.10	Coats–Redfern	[97]

FWO: Flynn-Wall-Ozawa; KAS: Kissinger-Akahira-Sunose; DAEM: Distributed Activation Energy Model; E_a: Activation energy

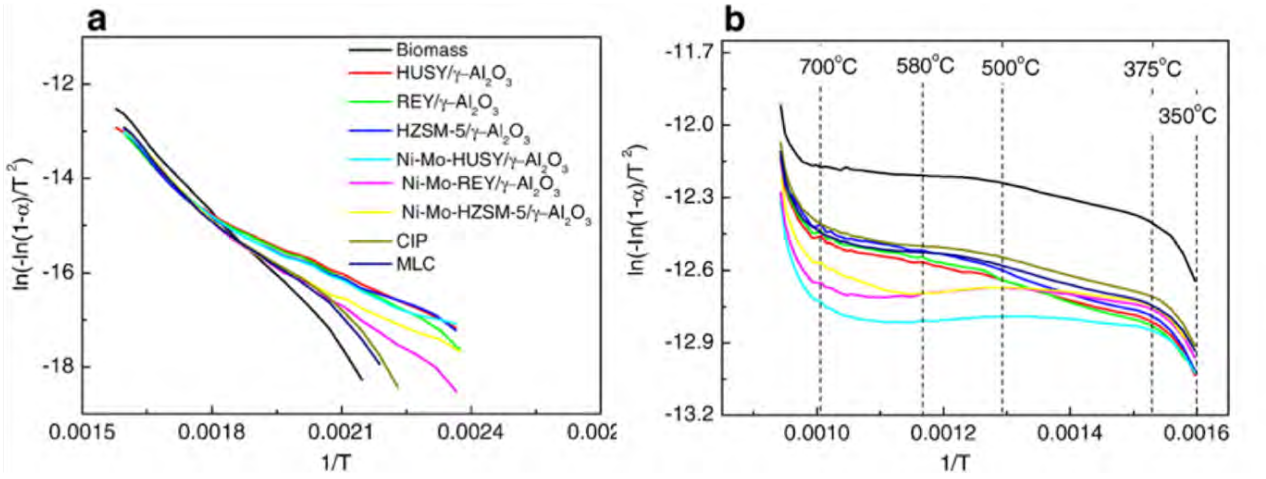

Figure 8. Coats–Redfern curves for biomass catalytic pyrolysis, (a) First stage from 200–350 °C; (b) second stage from 350–700 °C. Reproduced with permission from [93].

In a separate study, Ratnasari et al. [92] adopted Coat-Redfern method to investigate the effect of HZSM-5 and Al-MCM-41 on the kinetics of beech wood biomass pyrolysis between the temperature of 180 and 360 °C at varying heating rates (10-50 °C/min). The study reported that the pyrolysis of beech wood biomass with and without the catalysts followed first-order reaction kinetics during the studied temperature range and the activation energy for non-catalytic and catalytic pyrolysis samples decreased with increase in the heating rate [53]. Interestingly, the results revealed that at lower heating rates of 10 and 20 °C/min, the catalytic pyrolysis showed the reduction of up to 13% for the activation energy compared to the non-catalytic pyrolysis but exhibited comparatively higher activation energy values of up to 66% at the higher heating rates of 30 and 50 °C/min [92]. A study by Belyi et al. [97] also showed that the addition of certain catalysts instead of decreasing can increase the activation energy of the pyrolysis process. The exceptional rise in the activation energy could be due to the competing reactions of the carbonization and chemisorption of the primary pyrolysis products taking place on the catalyst surface during the pyrolysis process [97]. Although Coat-Redfern method is accurate it could only be applied to understand the kinetics of whole pyrolysis process by dividing into two or three stages and could not be adopted to examine the kinetic parameters of independent or parallel reactions involved in the pyrolysis process.

DAEM is a widely known kinetic model to obtain the kinetic parameters of biomass pyrolysis [91,96,100,101]. This model is usually considered more complicated compared to other kinetic models since it covers a wide range of experimental parameters like temperature and heating rate and their effects on different reactions involved in the distribution of char, volatiles and pyrolytic gases [96]. The model is applied based on the assumption that the mechanism of biomass pyrolysis consists of a number of independent and parallel reactions of varying orders of reaction of 1, 2 or 3 [102]. Therefore, it could be further assumed that different activation energies would result from the various reactions involved in the decomposition process, indicating

significant transformations in the bond cleavage and consequently, in the reactant structures [103,104]. DAEM provides the differences in the activation energies and represents them as a continuous distribution function which is usually assumed to be a Gaussian distribution represented with *f(E)* further in the text [105]. The following expression can be used to obtain the distribution of activation energies:

$$\frac{V^*-V}{V^*} = \frac{1}{\sigma\sqrt{2\pi}}\int_{-\infty}^{\infty} exp\left[-A\int_0^t exp\left(\frac{-E}{RT(t)}\right)dt\right]\left[\frac{(E-E_o)^2}{2\sigma^2}\right]dE \quad (3)$$

where *V** and *V* are the maximum amount of volatile or a chemical group present in the gas or vapor phase produced at a time *t*, *E* is activation energy, *A* is rate constant, σ is the variance and E_0 is the mean of the statistical distribution of activation energies. Further, distribution free methods, like Miura differential method and Miura–Maki integral method and distribution fitting methods could be used to solve the exponential integral and obtain the kinetic parameters [91,105]. Distribution free methods are the methods which are independent of the previous assumptions for *f(E),* while the distribution fitting methods need the previous assumptions for *f(E).* More detailed information for derivation and numerical calculation of DAEM could be found elsewhere [91,103]. A number of researchers have utilized a three-parallel-DAEM-reaction model to calculate the kinetic parameters of biomass pyrolysis, assuming three independent parallel reactions for the decomposition of each component of the lignocellulose biomass since it contains the three components cellulose, hemicellulose and lignin, and each component exhibits a Gaussian distribution for activation energies [102,104,106–109]. For instance, Cai et al. [96] conducted a study to understand the chemical kinetics of different lignocellulosic biomass using DAEM and the results suggested that each biomass component shows a range of activation energies depending on the type of biomass. Noticeably, the activation energies for cellulose, hemicellulose and lignin were found in the ranges of 169.7-186.8, 204.2-212.5, and 237.1-266.6 kJ mol^{-1}, respectively. The study also suggested that cellulose had narrowest and lignin the widest distribution of activation energies as the standard deviations for the activation energies were found least and highest for cellulose and lignin, respectively, which could indicate the complexity of chemical reactions during thermal degradation of the latter biomass component [96]. On the other hand, very limited studies have applied DAEM for catalytic pyrolysis so far. Recently, Yang et al. [94] studied the kinetics of nickel-based catalytic pyrolysis of various biomass feedstocks. The study showed that all the biomass feedstocks showed higher activation energies which considerably decreased with the addition of catalysts. For example, the activation energy for pine wood was 231.71 kJ mol^{-1}, which reduced to 163.11 and 115.14 kJ mol^{-1} using Ni-CaO/Ca_2SiO_4 and Ni/Ca_2SiO_4, respectively.

It could be suggested that the addition of catalysts decreases the activation energy of the chemical reactions for thermal degradation of each biomass component and makes the pyrolysis process more complex by deviating the kinetics of the chemical reactions. In addition, sole biomass pyrolysis follows nearly first-order reaction kinetics while catalytic biomass pyrolysis could not

follow first-order reaction kinetics at specific range of temperature, indicating the latter process highly complex compared to the former.

5. Types of catalysts

A number of studies have been carried out on catalytic bio-oil upgrading, employing various types of catalysts in different modes of pyrolysis [51,110–114]. Especially, the solid acid catalysts are highly preferred for bio-oil upgrading because of their unique catalytic properties, such as high BET surface area, strong chemical and hydrothermal stability, high acidity, suitable porosity, high selectivity, and high resistance to the deposition of carbonaceous species [115–117]. The most commonly used solid acid catalysts are typically composed of zeolites, mordenites, aluminosilicates or metal oxides, such as TiO_2, Al_2O_3, ZnO and their modification with different active metals to obtain either supported monometallic or bimetallic catalysts [118–120].

Zeolites have been commonly used in petrochemical and refinery industries for cracking activity for many decades. The main properties include shape selectivity, high strong Brønsted acidity, high stability and porous nature which makes zeolites a highly valuable choice for heterogeneous catalysis for bio-oil upgrading and other value-added product generation [110,121–126]. Zeolites are porous, crystalline aluminosilicate materials that exhibit proton donating (Brønsted) as well as electron accepting (Lewis) properties [127–129]. The zeolite lattice is usually comprised of a three-dimensional network of tetrahedra of metals (TO_4, where T is most commonly Si and Al) having either four or three valency and each metal is connected with four neighboring oxygen atoms [127,130–132]. Two tetrahedra of each metal in the zeolite framework are connected via the common oxygen atom, as shown in Figure 9. It could be stated that one oxygen atom has two neighboring metal cations. In case when Si ions occupy all the lattice, zeolite has SiO_2 composition and exhibits an overall neutral charge [128]. Si, which is a tetra valent metal, is substituted by the metal of a lower valency, mainly trivalent metals and most commonly Al due to the similar value of ionic radii, T-O bond length and T-O-T bond angles. Consequently, this leads to generation of a Brønsted acid site in the zeolite framework [127], which ultimately acts as the active site for acid-catalysed transformations of organic molecules or, in this case, the Brønsted acid site acts as the active site to catalyse the deoxygenation reactions to convert the low energy oxygenated compounds into high energy rich hydrocarbons. The substitution of Si^{4+} by Al^{3+} in the zeolite framework results in the negative charge, which is usually compensated by cations to maintain the charge balance [117,129]. If the cation is H^+, it is attached to the oxygen atom that connects the neighbouring Si and Al atom and the oxygen atom becomes three coordinated, consequently, resulting in a strong Brønsted acid site [133]. Generally, the trivalent metals, like Al, Fe and Ga, are incorporated into the zeolite lattice to generate bridging -OH groups (known to have weaker bonding), with high probability to donate or transfer the attached proton

when interacting with basic molecules and therefore show high acidic character [134]. Noticeably, the higher Al/Si ratios in the zeolite framework show relatively higher number of Brønsted acid sites [135]. However, the excessive loading of Al could also generate weak Brønsted acid sites due to the high accumulation of protons in the zeolite framework. Alternatively, the substitution of Si with tetravalent elements, like Sn or Ti, can generate Lewis acid sites in the resultant zeolite [127,128]. The Lewis acid character generally arises due to the generation of positive charge on the metal atom when the valence electrons of the metal create covalent bond with the oxygen atom of the adjacent tetrahedron. In addition, dehydroxylation of bridging OH groups can lead to the generation of extra-framework species which can act as Lewis acid site [136]. The extra-framework species could also be formed due the difference in the ionic radius between Si^{4+} and other metals present in the zeolite lattice, and forcing the larger metal atom to migrate outside the lattice, consequently, resulting in the lattice instability [125,127].

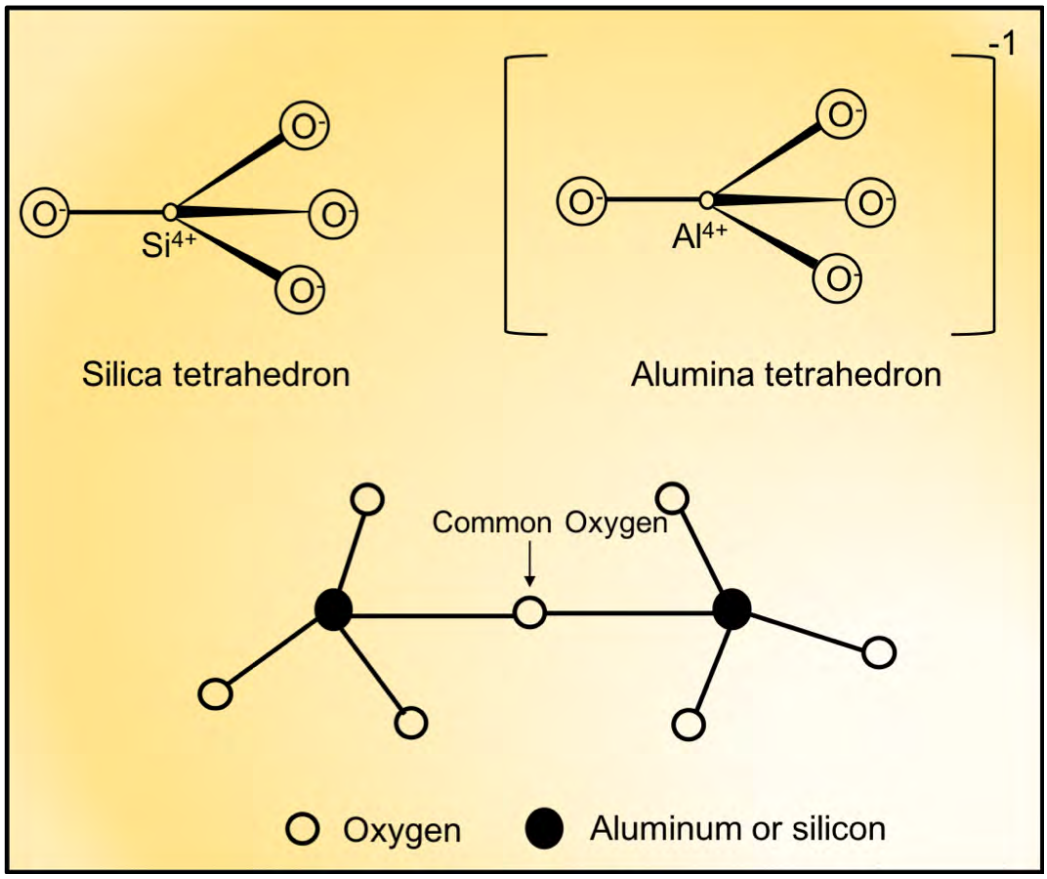

Figure 9. Building blocks of zeolites.

Another primary property of the zeolites that makes them efficient and most desirable catalysts for bio-oil upgrading is their shape and size selectivity, which are mainly ascribed to their varying pore structures and dimensions [121,137–139]. The shape and size selectivity could consist of mainly three types, as shown in Figure 10. The first is reactant shape selectivity where the reactant molecules are sterically restricted to enter the pores due to their larger structure. For instance, the pore aperture of ZSM-5 of nearly 0.5 nm allows the diffusion of linear or nearly linear molecules through it, while the larger molecules could not pass through the pore. The second type

is the product selectivity where the larger organic molecules produced inside the pore structure are sterically restricted to leave the pore structure [132]. For example, the monomolecular isomerization reaction of alkylaromatics in ZSM-5 results in the formation of *p*-xylene, *o*-xylene and *m*-xylene, however, *p*-xylene exhibits substantially higher diffusion co-efficient compared to either *o*-xylene or *m*-xylene and hence leaves the zeolite and appears as the product [137]. On the other hand, the restricted products could further undergo secondary reactions to form smaller compounds or could also block the micropores, subsequently leading to the catalyst deactivation [123]. The third type is transition state selectivity in which the generation of transition state molecules is constrained due to the limited space in zeolite channels or intersections but allows the diffusion of reactant and product molecules. Transalkylation of dialkylbenzenes in mordenite zeolite is a good example of transition state selectivity. For instance, transalkylation of *m*-xylene could produce either 1,3,5- or 1,2,4-trialkylbenzene, however, the dimensions of 1,3,5-trialkylbenzene are too large to fit inside the pore structure of mordenite, therefore, selectively favoring the formation of 1,2,4-trialkylbenzene [137]. There is another type of shape selectivity called secondary shape selectivity, which is caused by the presence of certain molecules other than the reactant molecules. For example, hydrocracking of *n*-hexane is inhibited in the presence of benzene over Pt-H mordenite catalyst [140].

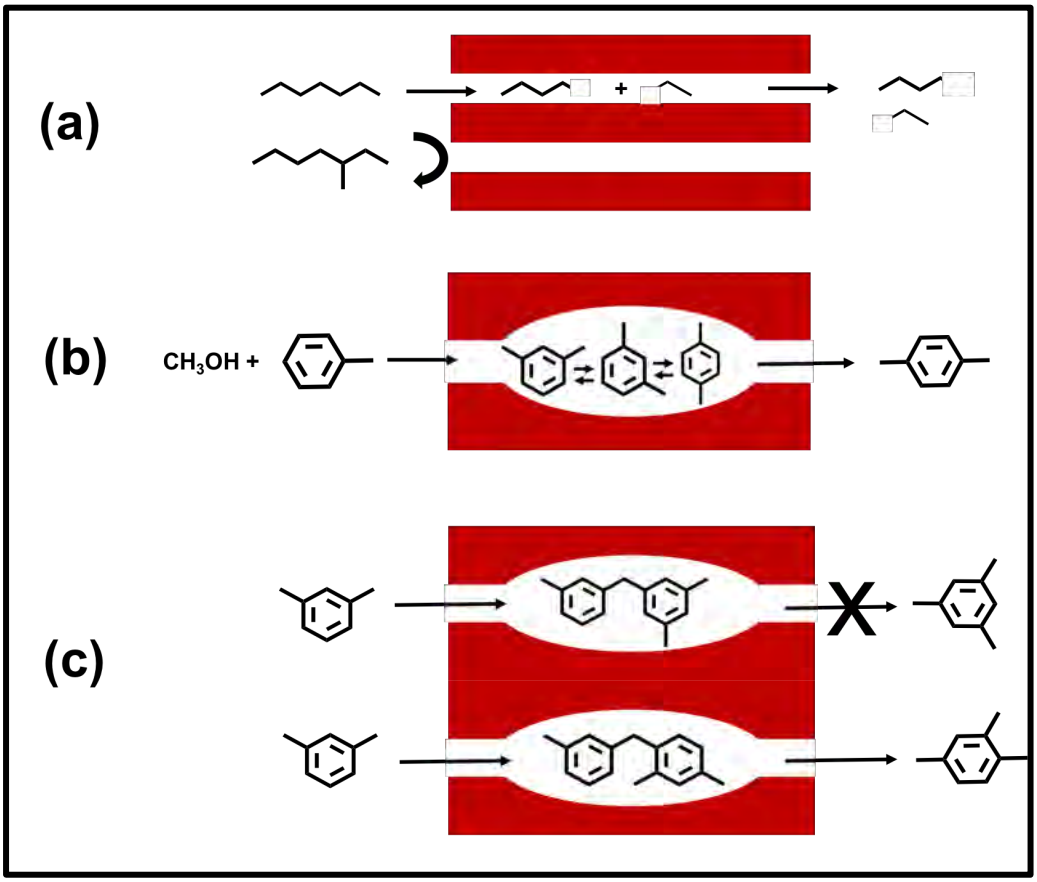

Figure 10. Schematic representation of the types of shape selectivity exhibited by zeolites. (a) reactant selectivity, (b) product selectivity and (c) transition state selectivity. Adapted from reference [137].

In zeolite catalysts, Brønsted acid sites, which act as the main active sites to catalyse a specific chemical reaction, could be present on the external surface as well as on internal surface of the pores [69,141]. However, it is believed that the chemical reactions catalysed by the zeolite catalysts take place primarily at the internal surface of the pores, while the larger molecules that are hindered to enter the pores could be catalysed at external surface of the pores [141]. Therefore, it could be inferred that the pore dimension and structure play a pivotal role in the selection of reactants (oxygenated compounds in the pyrolytic vapours) and distribution of products (hydrocarbons or other organic compounds in the bio-oil composition). Different zeolites exhibit varying micropore systems and dimensions, ranging from 0.3 nm to 2 nm. The micropore systems and dimensions of some zeolites are shown in Figure 11. Depending on the size of pore diameters, zeolites could be regarded as microporous (<2 nm), mesoporous (2-50 nm) and macroporous (>50 nm). A catalyst with micropores and mesopores is generally desirable for bio-oil upgrading to obtain bio-oil composition with olefins, paraffins, naphthenes, MAH and PAH, as these hydrocarbons are necessary to upgrade the bio-oil to a gasoline like fuel. The multiporous catalysts could provide optimum number of active and Brønsted acid sites and increase the mass transfer kinetics to enhance the conversion of oxygenated compounds into hydrocarbons. The pore dimensions of zeolites can be tailored using different post-synthesis modification techniques [127]. In addition, different active metals may also be incorporated into zeolite to enhance their selectivity and catalytic activity to obtain the desirable products. Owing to the effective cracking activity and shape selectivity properties, different zeolites, such as ZSM-5, Y zeolite, Mordenite and Beta zeolite have been modified using various techniques and have been excessively demonstrated for catalytic bio-oil upgrading.

ZSM-5 is the most widely used catalyst or catalyst support for bio-oil upgrading obtained from various types of biomass feedstocks or biomass model compounds. ZSM-5, mainly in its protonated form that is HZSM-5 has been used in different types of pyrolysis reactors and pyrolysis modes and has demonstrated successful conversion of oxygenated compounds into hydrocarbons, hence, improving the physicochemical properties of the bio-oil [63,69,82,84,130,130,142–145]. Table 5, 6 and 7 conclude several studies that utilized various zeolite catalysts in different pyrolysis modes for bio-oil upgrading. Although, HZSM-5 exhibits higher Brønsted acid sites, it has been often modified with the addition of one or two metals to increase its catalytic activity for enhanced bio-oil upgrading. Different methods like ion-exchange, impregnation, chemical vapour deposition could be adopted to load the metals into zeolite framework. It has been observed that the addition of metals could increase the total acidity of the catalyst but decrease strong Brønsted acid sites and the total increase in the acidic character mainly arises due to the increase in Lewis acid sites or the accumulation of extra-framework species.

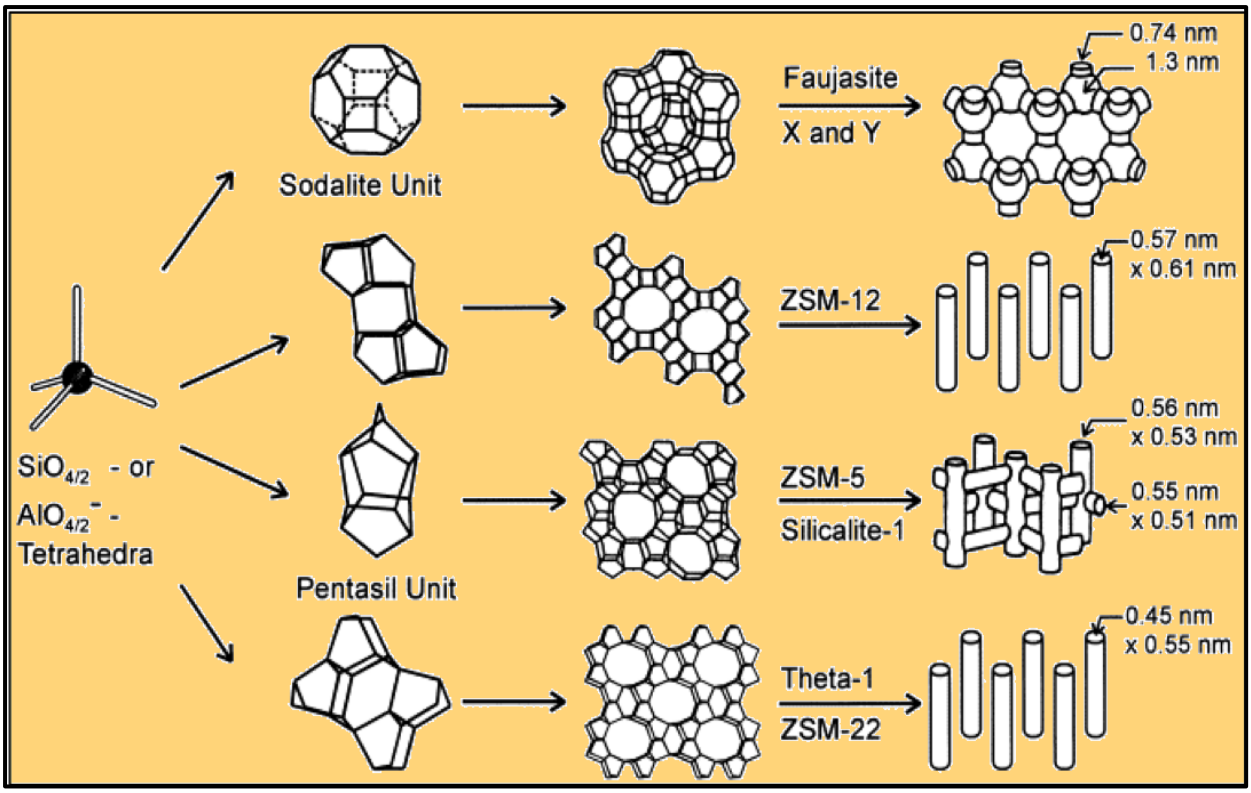

Figure 11. Structures of four zeolites: Faujasite or zeolites X, Y; zeolite ZSM-12; zeolite ZSM-5 or silicalite-1; zeolite Theta-1 or ZSM-22) and their micropore systems and dimensions. Reproduced with permission from reference [132].

Other than ZSM-5, many other metal oxides-based catalysts with varying structural and physicochemical characteristics have been employed for bio-oil upgrading. Table 7 presents the results of some studies for bio-oil upgrading and yields of pyrolytic products achieved after applying different types of catalysts.

Table 5. Zeolite-based catalysts used for bio-oil upgrading.

Catalyst properties					Pyrolysis parameters						Bio-oil composition ([a]yield %, [b]peak area %)						Reference
Catalyst	BET (m^2/g)	Total acidity (mmol/g)	Brønsted (mmol/g)	Lewis (mmol/g)	Feedstock	Reactor	Mode	T (°C)	HR (°C/min/s /ms)	C/B or FR	Aromatics				Aliphatics	Oxygenates	
											Total yield	B	T	X			
Beta zeolite	589	0.68	0.53	0.15	Pine wood	Fluidized bed	In-situ	450	10/min	20g/h	[a]2.14	/	/	/	/	[a]21.69	[146]
Y zeolite	884	0.83	0.58	0.25	Pine wood	Fluidized bed	In-situ	450	10/min	20g/h	[a]1.31	/	/	/	/	[a]20.01	[146]
ZSM-5	443	1.13	1.09	0.04	Pine wood	Fluidized bed	In-situ	450	10/min	20g/h	[a]3.09	/	/	/	/	[a]20.57	[146]
Mordenite	522	0.87	0.83	0.04	Pine wood	Fluidized bed	In-situ	450	10/min	20g/h	[a]0.08	/	/	/	/	[a]19.76	[146]
Zeolite	412	0.06	/	/	Pine wood	Fixed bed	In-situ	700	100/min	5	[b]11.66	/	/	/	[b]0.31	[b]47.14	[51]
Zeolite/Cu10%	212	0.07	/	/	Pine wood	Fixed bed	In-situ	700	100/min	5	[b]20.97	/	/	/	[b]7.51	[b]42.59	[51]
Zeolite/Ni10%	295	0.09	/	/	Pine wood	Fixed bed	In-situ	700	100/min	5	[b]6.12	/	/	/	[b]37.6	[b]15.77	[51]
Zeolite	412	0.06	/	/	Pine wood	Fixed bed	Ex-situ	700	100/min	3	[b]14.20	/	/	/	[b]3.02	[b]25.69	[51]
Zeolite/Cu10%	212	0.07	/	/	Pine wood	Fixed bed	Ex-situ	700	100/min	3	[b]41.64	/	/	/	[b]4.46	[b]17.68	[51]
Zeolite/Ni10%	295	0.09	/	/	Pine wood	Fixed bed	Ex-situ	700	100/min	3	[b]20.54	/	/	/	[b]21.85	[b]9.48	[51]
ZSM-5	416	0.99	/	/	Cellulose	Pyroprobe	In-situ	600	20000/s	9	[a]38.4	[a]14.3	[a]11.9	[a]10.1		[a]1.3	[147]
ZSM-5	416	0.99	/	/	Hemicellulose	Pyroprobe	In-situ	600	20000/s	9	[a]29.8	[a]13.4	[a]18.2	[a]16.8		[a]1.8	[147]
ZSM-5	416	0.99	/	/	Lignin	Pyroprobe	In-situ	600	20000/s	9	[a]10.2	[a]12.1	[a]25.6	[a]27.2		[a]0.4	[147]
ZSM-5	416	0.99	/	/	Pine wood	Pyroprobe	In-situ	600	20000/s	9	[a]25.4	[a]11.6	[a]14.5	[a]14.2		[a]1.2	[147]
ZSM-5	416	0.99	/	/	Corncob	Pyroprobe	In-situ	600	20000/s	9	[a]26.1	[a]11.1	[a]14.3	[a]14.5		[a]1.4	[147]
ZSM-5	416	0.99	/	/	Straw	Pyroprobe	In-situ	600	20000/s	9	[a]28.0	[a]11.9	[a]15.8	[a]15.6		[a]1.8	[147]
HZSM-5	322	/	/	/	Oily Sludge	Fixed bed	Ex-situ	500	10/min	1	[b]58.7	/	/	/	[b]12.3	[b]26.7	[142]
HZSM-5/Zn 3%	199	/	/	/	Sludge	Fixed bed	Ex-situ	500	10/min	1	[b]81.0	/	/	/	[b]7.0	[b]6.4	[142]
HZSM-5/Zn 6%	165	/	/	/	Sludge	Fixed bed	Ex-situ	500	10/min	1	[b]81.8	/	/	/	[b]8.8	[b]3.3	[142]
ZSM-5	138	0.54	0.36	0.18	Beech wood	Fixed bed	In-situ	500	/	0.46	[b]5.72	/	/	/	[b]0.52	[b]59.78	[148]
ZSM-5/Ni1%	138	0.76	0.21	0.54	Beech wood	Fixed bed	In-situ	500	/	0.46	[b]5.96	/	/	/	[b]0	[b]70.95	[148]
ZSM-5/Ni5%	132	0.76	0.21	0.54	Beech wood	Fixed bed	In-situ	500	/	0.46	[b]8.29	/	/	/	[b]0.15	[b]69.28	[148]
ZSM-5/Ni10%	117	0.62	0.19	0.43	Beech wood	Fixed bed	In-situ	500	/	0.46	[b]7.48	/	/	/	[b]0.23	[b]68.19	[148]
ZSM-5/Co1%	138	0.65	0.25	0.39	Beech wood	Fixed bed	In-situ	500	/	0.46	[b]8.12	/	/	/	[b]0.15	[b]67.88	[148]
ZSM-5/Co5%	131	0.63	0.17	0.45	Beech wood	Fixed bed	In-situ	500	/	0.46	[b]7.6	/	/	/	[b]0	[b]67.78	[148]
ZSM-5/Co10%	100	0.48	0.13	0.35	Beech wood	Fixed bed	In-situ	500	/	0.46	[b]7.32	/	/	/	[b]0.56	[b]63.87	[148]
HZSM-5	/	2.3	/	/	[C]Raw bio-oil	Fixed bed	Ex-situ	450	/	5 ml/h	[b]25	/	/	/	[b]3.8	[b]69.5	[116]
HZSM-5/Mg1%	/	2.0	/	/	[C]Raw bio-oil	Fixed bed	Ex-situ	450	/	5 ml/h	[b]26	/	/	/	[b]3.8	[b]69.2	[116]
HZSM-5/Ni1%	/	2.3	/	/	[C]Raw bio-oil	Fixed bed	Ex-situ	450	/	5 ml/h	[b]31	/	/	/	[b]4.7	[b]63	[116]
HZSM-5/Cu1%	/	1.3	/	/	[C]Raw bio-oil	Fixed bed	Ex-situ	450	/	5 ml/h	[b]26	/	/	/	[b]4.7	[b]66.8	[116]
HZSM-5/Ga1%	/	1.8	/	/	[C]Raw bio-oil	Fixed bed	Ex-situ	450	/	5 ml/h	[b]29	/	/	/	[b]4.6	[b]64.5	[116]

HZSM-5/Sn1%	/	2.0	/	/	[C]Raw bio-oil	Fixed bed	Ex-situ	450	/	5 ml/h	[b]28	/	/	/	[b]4.6	[b]65.9	[116]
HZSM-5	425	/	/	/	Algal biomass	Pyroprobe	In-situ	650	2000/s	1	[a]23	[a]0.1	[a]1.9	[a]4.0	[a]4.2	[a]30.7	[149]
HZSM-5	425	/	/	/	Algal biomass	Pyroprobe	In-situ	650	2000/s	4	[a]44.9	[a]0.6	[a]2.0	[a]4.2	[a]0.4	[a]10.4	[149]
HZSM-5	425	/	/	/	Algal biomass	Pyroprobe	In-situ	650	2000/s	9	[a]50.8	[a]0.5	[a]3.4	[a]7.7	[a]0.2	[a]8.4	[149]
HZSM-5	425	/	/	/	Algal biomass	Fixed bed	In-situ	5000	~48/min	1	[a]2.7	/	/	/	[a]7.8	[a]44.8	[149]
HZSM-5	332.34	/	/	/	Waste cardboard	Pyroprobe	Ex-situ	600	20000/s	2	[b] 24.43	[b] 0	[b]6.47	[b]1.25	/	[b]88.18	[124]
ZSM-5	138	/	/	/	Beech wood	Fixed bed	In-situ	500	/	0.46	[b]5.7	/	/	/	[b]0.5	[b]48.8	[150]
HZSM-5	338.44	0.67	/	/	Pine wood	Fixed bed	Ex-situ	500	250/min	2	[a] 86.99	[a]10.83	[a]1.3	[a]25.35	/	/	[151]
HZSM-5/Ga1%	/	/	/	/	Pine wood	Fixed bed	Ex-situ	500	250/min	2	[a] 80.01	[a]4.37	[a]14.62	[a]32.78	/	/	[151]
HZSM-5/Ga5%	293.48	0.39	/	/	Pine wood	Fixed bed	Ex-situ	500	250/min	2	[a] 85.37	[a]7.22	[a]15.16	[a]28.72	/	/	[151]
HZSM-5/Ga10%	/	/	/	/	Pine wood	Fixed bed	Ex-situ	500	250/min	2	[a] 84.65	[a]8.01	[a]18.04	[a]30.73	/	/	[151]
HZSM-5/Co1%	/	/	/	/	Pine wood	Fixed bed	Ex-situ	500	250/min	2	[a] 82.77	[a]6.17	[a]19.53	[a]28.11	/	/	[151]
HZSM-5/Co5%	288.94	0.36	/	/	Pine wood	Fixed bed	Ex-situ	500	250/min	2	[a] 70.67	[a]5.84	[a]14.12	[a]24.7	/	/	[151]
HZSM-5/Co10%	/	/	/	/	Pine wood	Fixed bed	Ex-situ	500	250/min	2	[a] 74.12	[a]4.16	[a]12.89	[a]27.26	/	/	[151]
HZSM-5/Zn1%	/	/	/	/	Pine wood	Fixed bed	Ex-situ	500	250/min	2	[a] 86.32	[a]5.58	[a]23.25	[a]41.83	/	/	[151]
HZSM-5/Zn5%	288.15	0.44	/	/	Pine wood	Fixed bed	Ex-situ	500	250/min	2	[a] 94.36	[a]7.83	[a]21.85	[a]35.32	/	/	[151]
HZSM-5/Zn10%	/	/	/	/	Pine wood	Fixed bed	Ex-situ	500	250/min	2	[a] 90.74	[a]8.16	[a]17.12	[a]30.03	/	/	[151]
HZSM-5/Zn5%-Ni5%	/	/	/	/	Pine wood	Fixed bed	Ex-situ	500	250/min	2	[a] 82.19	[a]10.79	[a]26.04	[a]28.24	/	/	[151]
HZSM-5/Zn5%-Ga5%	/	/	/	/	Pine wood	Fixed bed	Ex-situ	500	250/min	2	[a] 82.92	[a]8.84	[a]30.85	[a]29.64	/	/	[151]
HZSM-5/Zn5%-Co5%	/	/	/	/	Pine wood	Fixed bed	Ex-situ	500	250/min	2	[a]92.76	[a]14.98	[a]40.79	[a]20.37	/	/	[151]
HZSM-5	384.8	0.50	0.42	0.08	Oak wood	Fixed bed	Ex-situ	500	/	0.3	[a]6.84	/	/	/	/	[a]12.68	[143]
HZSM-5/Co4.3%	377.1	0.50	0.25	0.24	Oak wood	Fixed bed	Ex-situ	500	/	0.3	[a]7.48	/	/	/	/	[a]10.10	[143]
HZSM-5	/	0.04	0.03	0.01	Rape straw	Fixed bed	Ex-situ	500	20/min	0.2	[b]25.80	/	/	/	/	[b]74.20	[145]
ZSM-5	406.8	0.48	0.42	0.068	Beech wood	Pyroprobe	In-situ	650	20/ms	10	[a]23.7	/	/	/	[a]3.11	[a]0.32	[152]

C/B: catalyst/biomass ratio; FR: feeding rate; B: Benzene; T: Toluene; X: xylene; [C]Raw bio-oil: bio-oil was obtained from pyrolysis of woody biomass at 450 °C

Table 6. Application of hierarchical zeolite-based catalysts used for bio-oil upgrading.

Catalyst properties					Pyrolysis parameters						Bio-oil composition ([a]wt %, [b]peak area %)						Reference
Catalyst	Method	Chemical	BET (m^2/g)	Total acidity (mmol/g)	Feedstock	Reactor	Mode	T (°C)	HR (°C/min/s /ms)	C/B or FR	Aromatics Total yield	B	T	X	Aliphatics	Oxygenates	
HZSM-5	Desilication	0.1 M NaOH	331.79	/	Waste cardboard	Pyroprobe	Ex-situ	600	20000/s	2	[b] 6.22	[b]2.34	[b]7.18	[b]3.74	/	[b]40.36	[124]
HZSM-5	Desilication	0.3 M NaOH	338.46	/	Waste cardboard	Pyroprobe	Ex-situ	600	20000/s	2	[b]28.48	[b]2.40	[b]7.42	[b]3.05	/	[b]32.22	[124]
HZSM-5	Desilication	0.5 M NaOH	344.06	/	Waste cardboard	Pyroprobe	Ex-situ	600	20000/s	2	[b]29.81	[b]1.50	[b]7.34	[b]3.34	/	[b]27.86	[124]
HZSM-5	Desilication	0.7 M NaOH	337.82	/	Waste cardboard	Pyroprobe	Ex-situ	600	20000/s	2	[b]30.54	[b]1.60	[b]8.42	[b]4.55	/	[b]30.18	[124]
HZSM-5	Desilication	0.2 M NaOH	405.70	0.40	Oak wood	Fixed bed	Ex-situ	500	/	0.3	[a]11.14	/	/	/	/	[a]6.96	[143]
HZSM-5/4.1%Co	Desilication	0.2 M NaOH	397.20	0.57	Oak wood	Fixed bed	Ex-situ	500	/	0.3	[a]7.36	/	/	/	/	[a]8.00	[143]
HZSM-5	Desilication	0.2 M NaOH	/	0.11	Rape straw	Fixed bed	Ex-situ	500	20/min	0.2	/	/	/	/	/	[b]53.72	[145]
HZSM-5/5% La	Desilication	0.2 M NaOH	/	0.12	Rape straw	Fixed bed	Ex-situ	500	20/min	0.2	[b]49.80	/	/	/	/	[b]50.13	[145]
HZSM-5	Desilication	0.1 M NaOH	400.50	0.39	Beech wood	Pyroprobe	In-situ	650	20/ms	10	[a]26.9	/	/	/	[a]2.78	[a]0.32	[152]
HZSM-5	Desilication	0.2 M NaOH	376.90	0.35	Beech wood	Pyroprobe	In-situ	650	20/ms	10	[a]29.0	/	/	/	[a]2.52	[a]0.36	[152]
HZSM-5	Desilication	0.3 M NaOH	363.10	0.32	Beech wood	Pyroprobe	In-situ	650	20/ms	10	[a]30.1	/	/	/	[a]2.59	[a]0.35	[152]
HZSM-5	Desilication	0.4 M NaOH	361.10	0.33	Beech wood	Pyroprobe	In-situ	650	20/ms	10	[a]28.6	/	/	/	[a]3.43	[a]0.50	[152]
HZSM-5	Desilication	0.5 M NaOH	37.70	0.32	Beech wood	Pyroprobe	In-situ	650	20/ms	10	[a]26.2	/	/	/	[a]4.15	[a]0.38	[152]
HZSM-5	Desilication	0.3 M NaOH	363.10	0.32	Cellulose	Pyroprobe	In-situ	650	20/ms	10	[a]32.1	/	/	/	[a]1.88	[a]0	[152]
HZSM-5	Desilication	0.3 M NaOH	363.10	0.32	Lignin	Pyroprobe	In-situ	650	20/ms	10	[a]13.2	/	/	/	[a]1.55	[a]1.17	[152]
HZSM-5	Desilication	0.3 M NaOH	396.20	5.10	Lignin	Pyroprobe	Ex-situ	600	1000/s	1	[c]79.91	/	/	/	/	[a]20.17	[153]
HZSM-5	Desilication	0.3 M $NaAlO_2$	394.20	5.42	Lignin	Pyroprobe	Ex-situ	600	1000/s	1	[c]71.87	/	/	/	/	[a]27.87	[153]
HZSM-5	Desilication	0.3 M Na_2CO_3	396.60	5.93	Lignin	Pyroprobe	Ex-situ	600	1000/s	1	[c]65.14	/	/	/	/	[a]34.77	[153]
HZSM-5	Desilication	0.3 M TPAOH	390.20	5.53	Lignin	Pyroprobe	Ex-situ	600	1000/s	1	[c]62.51	/	/	/	/	[a]37.23	[153]
HZSM-5	Desilication	TPAOH	378.00	/	Glucose	Pyroprobe	In-situ	600	1000/s	9	[a]65.1	7.1	40.4	10.4	/	[a]35.00	[154]
HZSM-5/1.92% Ce	Desilication	TPAOH	351.00	/	Glucose	Pyroprobe	In-situ	600	1000/s	9	[a]47.8	6.9	17.3	15.2	/	[a]52.40	[154]
HZSM-5	Desilication	0.2 M NaOH	369.43	3.00	Napier grass	Fixed bed	In-situ	600	50/min	3	[a]14.16	/	/	/	[a]12.18	[a]73.66	[23]
HZSM-5	Desilication	0.3 M NaOH	374.88	2.96	Napier grass	Fixed bed	In-situ	600	50/min	3	[a]24.72	/	/	/	[a]7.19	[a]68.09	[23]
Z5	Dealumination	0.5 M HF	355.00	0.44	Cellulose	Drop tube	Ex-situ	500	/	2.75	[a]26.68	5.60	10.45	5.80	/	/	[155]
Z5	Dealumination	1 M HF	326.00	0.23	Cellulose	Drop tube	Ex-situ	500	/	2.75	[a]22.61	4.51	10.07	4.28	/	/	[155]
Z5	Dealumination	2 M HF	325.00	0.06	Cellulose	Drop tube	Ex-situ	500	/	2.75	[a]11.94	2.10	3.83	2.89	/	/	[155]
Z5/2% Ni	Dealumination	0.5 M HF	312.00	0.46	Cellulose	Drop tube	Ex-situ	500	/	2.75	[a]22.79	6.20	10.30	3.91	/	/	[155]

Z5/3% Ni	Dealumination	0.5 M HF	297.00	0.46	Cellulose	Drop tube	Ex-situ	500	/	2.75	[a]20.76	5.15	9.23	4.38	/	/	[155]
Z5/4% Ni	Dealumination	0.5 M HF	264.00	0.46	Cellulose	Drop tube	Ex-situ	500	/	2.75	[a]16.80	4.38	6.92	2.73	/	/	[155]
ZSM-5	Desilication	0.2 M NaOH	296.30	1.00	Corncob	DSP	In-situ	550	/	2	[a]46.42	3.40	12.97	12.19	/	/	[156]
ZSM-5/5% Ni	Desilication	0.2 M NaOH	188.95	0.85	Corncob	DSP	In-situ	550	/	2	[a]49.45	3.69	12.98	11.41	/	/	[156]
ZSM-5/ 8% Ni	Desilication	0.2 M NaOH	180.78	0.81	Corncob	DSP	In-situ	550	/	2	[a]54.42	2.87	13.75	13.21	/	/	[156]
ZSM-5/11% Ni	Desilication	0.2 M NaOH	170.43	0.73	Corncob	DSP	In-situ	550	/	2	[a]53.75	2.33	14.10	12.35	/	/	[156]
HZSM-5	Desilication	0.6 M NaOH	147.00	/	Cellulose	TMR	In-situ	/	/	20	2.37	[d]18.23	[d]27.93	[d]18.48	[a]2.93	/	[157]
HZSM-5	Desilication	0.8 M NaOH	80.00	/	Cellulose	TMR	In-situ	/	/	20	[a]1.27	[d]14.66	[d]36.21	[d]23.84	[a]1.83	/	[157]
HZSM-5	Desilication	0.6 M TPAOH	336.00	/	Cellulose	TMR	In-situ	/	/	20	[a]37.59	[d]14.24	[d]24.42	[d]12.97	[a]2.55	/	[157]
HZSM-5	Desilication	0.8 M TPAOH	331.00	/	Cellulose	TMR	In-situ	/	/	20	[a]36.86	[d]14.12	[d]24.55	[d]13.35	[a]2.73	/	[157]
HZSM-5	Desilication	0.6 M Na_2CO_3	321.00	/	Cellulose	TMR	In-situ	/	/	20	[a]38.07	[d]14.96	[d]25.19	[d]14.32	[a]3.33	/	[157]
HZSM-5	Desilication	0.8 M Na_2CO_3	321.00	/	Cellulose	TMR	In-situ	/	/	20	[a]36.96	[d]14.70	[d]25.44	[d]14.19	[a]3.15	/	[157]
HZSM-5	Desilication	0.2 M HCl	354.00	1.03	Rice straw	TMR	In-situ	600	/	20	[a]27.37	[d]9.95	[d]25.00	[d]18.93	[a]9.09	/	[46]
HZSM-5	Desilication	0.4 M HCl	384.00	0.99	Rice straw	TMR	In-situ	600	/	20	[a]26.25	[d]10.92	[d]24.03	[d]20.87	[a]10.12	/	[46]
HZSM-5	Desilication	0.6 M HCl	352.00	0.99	Rice straw	TMR	In-situ	600	/	20	[a]26.15	[d]9.70	[d]23.79	[d]20.87	[a]8.15	/	[46]
HZSM-5	Desilication	0.8 M HCl	404.00	0.89	Rice straw	TMR	In-situ	600	/	20	[a]25.12	[d]9.70	[d]23.06	[d]20.39	[a]8.25	/	[46]
HZSM-5	Desilication	1 M HCl	433.00	0.84	Rice straw	TMR	In-situ	600	/	20	[a]23.34	[d]10.67	[d]24.03	[d]19.42	[a]8.15	/	[46]
HZSM-5/1% Ni	Desilication	0.2 M HCl	/	/	Rice straw	TMR	In-situ	600	/	20	[a]25.93	[d]14.30	[d]27.80	[d]17.80	/	/	[46]
HZSM-5/1 % Cu	Desilication	0.2 M HCl	/	/	Rice straw	TMR	In-situ	600	/	20	[a]26.73	[d]13.40	[d]27.00	[d]18.40	/	/	[46]
HZSM-5/1% Zn	Desilication	0.2 M HCl	/	/	Rice straw	TMR	In-situ	600	/	20	[a]21.74	[d]16.40	[d]29.40	[d]17.80	/	/	[46]
HZSM-5/1% Ga	Desilication	0.2 M HCl	/	/	Rice straw	TMR	In-situ	600	/	20	[a]24.03	[d]17.60	[d]29.10	[d]17.80	/	/	[46]
HZSM-5	Desilication	0.1 M NaOH	425.37	0.44	Beech wood	Fixed bed	In-situ	/	25/min	0.4	[a]30.90	/	/	/	/	[a]69.13	[158]
HZSM-5	Desilication	0.2 M NaOH	434.10	0.45	Beech wood	Fixed bed	In-situ	/	25/min	0.4	[a]33.32	/	/	/	/	[a]66.69	[158]
HZSM-5	Desilication	0.5 M NaOH	438.94	0.45	Beech wood	Fixed bed	In-situ	/	25/min	0.4	[a]38.33	/	/	/	/	[a]63.13	[158]
HZSM-5/Ga	Desilication	0.2 M NaOH	404.00	0.22	Beech wood	Pyroprobe	In-situ	550	20/ms	15	[a]15.66	[a]1.92	[a]4.55	[a]5.48	[a]5.38	/	[159]

C: represents the total selectivity of all hydrocarbons (aromatics + aliphatics); D: represents selectivity of hydrocarbons; DSP: Double shot pyrolyzer; TMR: Tandem micro reactor; C/B: catalyst/biomass ratio; FR: feeding rate; B: Benzene; T: Toluene; X: xylene; TPAOH: tetrapropylammonium hydroxide; Z5: zeolite with SiO_2/Al_2O_3=25; HF: hydrogen fluoride

Table 7. Effect of catalysts on the distribution of pyrolytic products and bio-oil properties.

Catalyst properties			**Pyrolysis parameters**						**Product yield**			**Bio-oil properties**							**Reference**
Catalyst	BET (m^2/g)	Acidity (mmol/g)	Feedstock	Reactor	Mode	T (°C)	HR (°C/min)/WHSV	C/B or FR	Bio-oil (wt%)	Gas (wt%)	Char (wt%)	Elemental composition (wt%) C	H	O	HHV (MJ/kg)	Viscosity (cP)	Water (wt%)	pH	Density g/cm^3	
ZSM-5	380	/	Hydrolysis lignin	Fixed bed	Ex-situ	450	10-20	1	57.50	13.32	28.75	62.6	5.7	31.20	23.7	9.6	32.3	5.6	/	[144]
ZSM-5/Ni5%	305	/	Hydrolysis lignin	Fixed bed	Ex-situ	450	10-20	1	53.48	13.53	30.24	52.74	5.96	40.74	19.08	4.56	7.17	5.2	/	[144]
HZSM-5	384.8	0.50	Oak wood	Fixed bed	Ex-situ	500	/	0.3	20.62	17.79	24.01	57.39	7.13	35.48	/	/	/	/	/	[143]
[a]Ds-HZSM-5	405.7	0.40	Oak wood	Fixed bed	Ex-situ	500	/	0.3	24.33	18.26	23.22	58.81	7.04	31.58	/	/	/	/	/	[143]
HZSM-5/Co4.3%	377.1	0.50	Oak wood	Fixed bed	Ex-situ	500	/	0.3	24.17	18.18	20.31	57.76	7.27	34.97	/	/	/	/	/	[143]
[a]Ds-HZSM 5/Co4.1%	397.2	0.57	Oak wood	Fixed bed	Ex-situ	500	/	0.3	28.11	16.92	22.12	61.63	7.56	30.80	/	/	/	/	/	[143]
HZSM-5	/	0.04	Rape straw	Fixed bed	Ex-situ	500	20	0.2	23.23	39.61	29.07	70.65	8.51	20.82	31.52	6.01	/	5.17	0.93	[145]
[a]Ds-HZSM-5	/	0.11	Rape straw	Fixed bed	Ex-situ	500	20	0.2	17.52	45.17	27.22	77.59	8.03	14.37	35.30	5.81	/	5.94	0.95	[145]
[a]Ds-HZSM-5/La5%	/	0.12	Rape straw	Fixed bed	Ex-situ	500	20	0.2	17.38	46.74	28.07	78.52	8.01	13.47	37.70	5.64	/	6.01	0.94	[145]
[b]MCM-1	972	/	Lignocel	Fixed bed	Ex-situ	500	/	0.4	35.30	15.58	40.96	/	/	/	/	/	/	/	/	[160]
[c]MCM-2	866	/	Lignocel	Fixed bed	Ex-situ	500	/	0.4	31.94	15.51	49.99	/	/	/	/	/	/	/	/	[160]
[d]MCM-3	914	/	Lignocel	Fixed bed	Ex-situ	500	/	0.4	31.74	13.99	44.66	/	/	/	/	/	/	/	/	[160]
MCM/Cu10.7%	879	/	Lignocel	Fixed bed	Ex-situ	500	/	0.4	44.99	9.67	36.48	/	/	/	/	/	/	/	/	[160]
MCM/Fe4.3%	651	/	Lignocel	Fixed bed	Ex-situ	500	/	0.4	35.34	8.55	52.00	/	/	/	/	/	/	/	/	[160]
MCM/Zn2.6%	1298	/	Lignocel	Fixed bed	Ex-situ	500	/	0.4	47.80	8.28	35.04	/	/	/	/	/	/	/	/	[160]
[b]MCM-1	972	/	Miscanthus	Fixed bed	Ex-situ	500	/	0.4	47.93	14.24	29.72	/	/	/	/	/	/	/	/	[160]
[c]MCM-2	866	/	Miscanthus	Fixed bed	Ex-situ	500	/	0.4	39.61	10.58	40.90	/	/	/	/	/	/	/	/	[160]
[d]MCM-3	914	/	Miscanthus	Fixed bed	Ex-situ	500	/	0.4	38.50	13.41	40.69	/	/	/	/	/	/	/	/	[160]
MCM/Cu10.7%	879	/	Miscanthus	Fixed bed	Ex-situ	500	/	0.4	53.29	14035	28.95	/	/	/	/	/	/	/	/	[160]
MCM/Fe4.3%	651	/	Miscanthus	Fixed bed	Ex-situ	500	/	0.4	47.50	17013	34.76	/	/	/	/	/	/	/	/	[160]
MCM/Zn2.6%	1298	/	Miscanthus	Fixed bed	Ex-situ	500	/	0.4	51.15	5.83	39.72	/	/	/	/	/	/	/	/	[160]
HZSM-5	/	/	Beech wood	Fluidized bed	In-situ	520	/	11	18	35	16	73.3	7.2	19.5	32.3	64	6.7	/	1.12	[161]
HZSM-5	/	/	Beech wood	Fluidized bed	In-situ	520	/	14	18	35	16	74.9	7.4	17.7	32.7	42	5.7	/	1.10	[161]
HZSM-5	/	/	Beech wood	Fluidized bed	In-situ	520	/	17	17	36	17	74.2	7.2	18.6	32.6	60	5.7	/	1.12	[161]
HZSM-5	/	/	Beech wood	Fluidized bed	In-situ	520	/	21	15	37	18	75.1	7.4	17.5	34.4	81	5.5	/	1.12	[161]
SO_4^{2-}-ZrO_2	130	/	Pine wood	Auger reactor	Ex-situ	450	14/h	/	39.5	17.0	42.2	66.2	7.2	26.3	34.3	/	11.2	/	1.1	[162]
WO_x-ZrO_2	130	/	Pine wood	Auger reactor	Ex-situ	450	14/h	/	38.4	16.5	43.8	65.6	7.4	27.1	34.3	/	12.3	/	1.1	[162]
ZrO_2-TiO_2	80	/	Pine wood	Auger reactor	Ex-situ	450	14/h	/	38.4	16.2	44.3	61.5	7.1	31.4	32.9	/	10.9	/	1.13	[162]

TiO_2-rutile	3	/	Pine wood	Auger reactor	Ex-situ	450	14/h	/	43.0	16.9	39.9	57.57	7.1	35.5	32.1	/	13.3	/	1.1	[162]
TiO_2-anatase	150	/	Pine wood	Auger reactor	Ex-situ	450	14/h	/	45.2	15.6	37.7	59.8	7.3	32.8	32.8	/	11.5	/	1.12	[162]
γ-Al_2O_3	114.60	0.40	Loblolly pine	Pilot scale plant	Ex-situ	520	0.33/h	/	42.3	25.0	32.7	69.2	6.6	24.2	/	154	11.4	/	1.16	[163]
CaO	2.25	/	Palm fruit bunch	Fixed bed	In-situ	~500	~25	/	39.9	30.7	29.4	/	/	/	/	/	47.5	3.9	/	[164]
MgO	19.84	/	Palm fruit bunch	Fixed bed	In-situ	~500	~25	/	39.3	31.6	29.0	/	/	/	/	/	55.7	3.5	/	[164]
ZnO	0.86	/	Palm fruit bunch	Fixed bed	In-situ	~500	~25	/	44.7	28.2	27.0	/	/	/	/	/	53.9	3.5	/	[164]
ZSM-5	/	/	Rice husk	Fixed bed	Ex-situ	450	25	/	38.29	19.45	42.27	19.99	11.38	68.13	30.01	1.55	55.56	2.74	1.05	[165]
Al-MCM	/	/	Rice husk	Fixed bed	Ex-situ	450	25	/	39.98	18.80	43.15	22.51	11.34	65.71	31.79	1.65	54.66	2.83	1.05	[165]
AL-MSU-F	/	/	Rice husk	Fixed bed	Ex-situ	450	25	/	39.59	19.18	43.31	25.63	10.67	63.12	33.02	1.49	54.64	2.69	1.05	[165]
CeO_2	/	/	*Isochrysis*	Fixed bed	In-situ	550	40	0.11	19.91	51.61	28.48	68.34	8.82	15.74	33.00	/	/	/	/	[166]
TiO_2	/	/	*Isochrysis*	Fixed bed	In-situ	550	40	0.11	21.10	52.51	26.39	69.74	9.14	14.31	34.20	/	/	/	/	[166]
AL_2O_3	/	/	*Isochrysis*	Fixed bed	In-situ	550	40	0.11	20.03	48.17	31.80	67.33	8.15	17.22	31.43	/	/	/	/	[166]
$ZnCl_2$	/	/	*Anchusa azurea*	Fixed bed	In-situ	550	100	0.25	31.40	33.83	34.77	47.41	7.21	43.24	18.64	/	/	/	/	[24]
Na_2CO_3	/	/	*Anchusa azurea*	Fixed bed	In-situ	550	100	0.25	32.10	35.35	32.55	57.06	7.48	32.75	24.18	/	/	/	/	[24]
$Ca(OH)_2$	/	/	*Anchusa azurea*	Fixed bed	In-situ	550	100	0.25	29.28	32.36	38.36	57.01	7.05	33.05	23.49	/	/	/	/	[24]
Al_2O_3	/	/	*Anchusa azurea*	Fixed bed	In-situ	550	100	0.25	31.88	33.95	34.17	49.90	7.43	41.23	20.16	/	/	/	/	[24]
ZnO	/	/	Rice husk	Fixed bed	In-situ	550	25	0.11	45.20	24.81	31.17	49.73	12.57	35.62	26.45	/	14.64	4.35	1.10	[167]
ZSM-5	/	/	Rice husk	Fixed bed	In-situ	450	/	1	28.90	23.83	48.23	18.8	10.55	9.99	10.15	1.52	60.45	2.65	1.04	[168]
ZnO	/	/	*Ferula orientalis L*	Fixed bed	In-situ	500	50	0.17	45.22	30.46	24.32	54.61	6.97	37.18	21.82	/	/	/	/	[169]
Al_2O_3	/	/	*Ferula orientalis L*	Fixed bed	In-situ	500	50	0.17	41.64	36.43	21.93	52.44	6.83	39.38	20.49	/	/	/	/	[169]

[a]Ds-HZSM-5: desilicated HZSM-5; [b]MCM-Si/Al=20.5; [c]MCM: Si/Al=34.2; [d]MCM: Si/Al=51.3; C/B: catalyst/biomass ratio; HR: heating rate; FR: feeding rate; WHSV: weight hourly space velocity

Al_2O_3-based catalysts are mesoporous and mild acidic solid catalysts with high Lewis and low Brønsted acid sites, considerable surface area (>200 m^2/g) considered suitable alternatives for zeolites for bio-oil upgrading [170,171]. These catalysts with larger pore sizes show better mass transfer kinetics and significant cracking activity, and effectively catalyse deoxygenation reactions, like dehydration, decarboxylation and decarbonylation [163]. Consequently, Al_2O_3-based catalysts have been used in *ex-situ* CBP for hydrocarbon production. For example, Che et al. [172] demonstrated the upgrading of pinewood pyrolysis vapours into aromatics using Al_2O_3 catalysts. The results reported that Lewis acid sites of Al_2O_3 promoted cleavage of $C-O$ bonds and showed significant deoxygenation activity [172]. Especially, the proportion of heavy molecular weight compounds derived from lignin pyrolysis were noticeably reduced and monocyclic aromatics like toluene were significantly increased [172]. Another study also confirmed the outstanding deoxygenation activity of Al_2O_3 catalyst, showing higher production of C_5-C_{11} hydrocarbons, like 1-heptene, 1,3,5-cycloheptatriene and 1-Octene, from *ex-situ* CBP of Jatropha wastes [173]. Mante et al. [163] demonstrated catalytic fast pyrolysis of loblolly pine in the presence of γ-Al_2O_3 in a lab scale (450 g/h) and a pilot scale (1 ton/day) pyrolysis reactor. γ-Al_2O_3 exhibited significant aromatic production in both types of reactors. The results showed that the bio-oil produced from the lab scale had 77 wt% carbon content and 15.8 wt% of oxygen, while the pilot scale reactor produced the bio-oil with 70.2 wt% of carbon and 23.1 wt% of oxygen. It was further concluded that γ-Al_2O_3 catalyzed the deoxygenation reactions like decarbonylation, decarboxylation, and dehydration to remove carbonyl, carboxyl and hydroxyl containing compounds. Also, the complex phenolic compounds were converted to light phenolic compounds aromatics through demethoxylation, hydrolysis, cyclization and aldol condensation reactions. All these deoxygenation reactions are carried out by the acidic sites (mainly Lewis acid sites) of γ-Al_2O_3 [163]. Payormhorm et al. [174] investigated the catalytic of Pt/Al_2O_3 on bio-oil deoxygenation in a fixed-bed reactor at 450 °C using *Leucaena leucocephala* trunks as the feedstock. The catalyst showed remarkable ability to reduce the oxygenated compounds through various reactions as mentioned previously. Ozbay et al. [175] also applied Cu/Al_2O_3 to upgrade the bio-oil quality in slow and fast pyrolysis modes from tomato waste in a fixed bed reactor at 500 °C. The resulted revealed that fast pyrolysis produced a better-quality bio-oil compared to the slow pyrolysis. Noticeably, Cu/Al_2O_3 in fast pyrolysis mode produced the bio-oil with an higher heating value (HHV) of 35.47 MJ/kg, while slow pyrolysis could produce the bio-oil with an HHV of 25.19 MJ/kg [175].

Metal oxides such as CaO, MgO, ZnO, and Fe_2O_3 as sole catalysts or impregnated with other catalyst supports like zeolites and Al_2O_3 have also been investigated for bio-oil upgrading in *ex-situ* CBP of biomass [176–178]. On one hand, oxides like CaO can be used to lower the strong acid sites of zeolites to obtain the overall optimal acidity of the catalyst. On the other hand, the

catalytic activity of oxides can also help to improve the yield of aromatics. CaO is known to decrease the concentration of oxygenated compounds through dehydration reactions and directly fixing the active quasi-CO_2 intermediates [178,179]. For instance, Lin et al. [178] investigated the potential of CaO for bio-oil upgrading and showed that CaO catalyzed dehydration reactions of cellulose and hemicellulose. As a result, the proportions of furfuryl and furfuryl alcohol were also increased. In addition, CaO at higher concentrations may promote phenol formation via demethoxylation reactions of lignin components. Another study demonstrated the comparative effect of four metal oxides (CaO, MgO, ZnO, and Fe_2O_3) on bio-oil composition obtained from the pyrolysis of a mixture of poplar wood-polypropylene composite [180]. The results revealed that CaO promoted the formation of cyclopentanones and alkenes, and reduced the content of acids and phenols in the bio-oil. MgO enhanced alkene's yield but had lower deoxygenation activity compared to CaO [180]. ZnO produced the maximum alkenes among all the catalysts, suggesting ZnO's cracking activity to break long-chain aliphatics into shorter-chain alkenes. But ZnO also increased ketone and phenols in the bio-oil. In contrast, Fe_2O_3 favored the formation of p-xylene and 2-methyl-1-butenylbenzene, but also promoted the reaction pathways to form ketones, acids, furans and phenols [180].

MgO catalysts are reported to deoxygenate the bio-oil primarily via decarboxylation, ketonization, and aldol condensation reactions [181,182], and can also reduce the formation of H_2O, thus conserving more hydrogen in the bio-oil and increasing its energy density [183]. Yuan et al. [184] carried out catalytic pyrolysis of rice husk for bio-oil upgrading in the presence of MgO and $MgCO_3$. The study revealed that MgO was more effective than $MgCO_3$ to convert the oxygenated compounds into aromatic hydrocarbons, suggesting the ability of MgO to catalyze deoxygenation reactions [184]. Kalogiannis et al. [183] demonstrated the application of MgO catalysts in a circulating fluidized bed pilot scale unit. It was noticed that MgO favored the formation of cyclo-pentenones and ketones, suggesting MgO's ability to catalyze ketonization and aldol condensation reactions [183]. Another study by Fan et al. [185] employed MgO to upgrade the pyrolytic vapors generated from microwave-assisted pyrolysis of low-density polyethylene. The results showed that MgO catalyzed the reactions to convert oxygenated compounds primarily into monoaromatics and alkenes [185].

6. Conclusion

This chapter discussed key reaction pathways involved in the formation of oxygenated compounds from thermal degradation of lignocellulose biomass, and their conversion into hydrocarbons over catalysts. The furanic compounds generated from cellulose and hemicellulose can be converted over acidic catalysts into short and long straight-chain alkanes, monocyclic and polycyclic aromatic hydrocarbons via dehydration, decarboxylation, decarbonylation and

oligomerization reactions. Phenols are another dominant group of compounds formed from the thermal degradation of the lignin component. The conversion of phenols (e.g., *m*-cresol) into aromatics firstly involves three main reactions that are isomerization, transalkylation and condensation to transform phenol into a phenolic for the pool that acts as the precursor generation of different aromatics. Later this phenolic pool undergoes cracking and hydrogen transfer reactions to produce mainly aromatic hydrocarbons, such as benzene, toluene, xylenes and naphthalenes. On the other hand, basic catalysts also carry out key deoxygenation reactions such as dehydration, decarboxylation, ketonization, and aldol condensation to convert the oxygenated compounds into hydrocarbons. Though catalytic fast pyrolysis is a significant approach and widely used for bio-oil upgrading, other techniques such as biomass pretreatment and downstream techniques can also be applied for bio-oil upgrading. Such techniques are thoroughly discussed in chapters 3 and 4.

References

[1] Mohan D, Pittman, CU, Steele PH. Pyrolysis of Wood/Biomass for Bio-oil: A Critical Review. Energy & Fuels 2006;20:848–89. https://doi.org/10.1021/ef0502397.

[2] Dhyani V, Bhaskar T. A comprehensive review on the pyrolysis of lignocellulosic biomass. Renewable Energy 2018;129:695–716. https://doi.org/10.1016/j.renene.2017.04.035.

[3] Guedes RE, Luna AS, Torres AR. Operating parameters for bio-oil production in biomass pyrolysis: A review. Journal of Analytical and Applied Pyrolysis 2018;129:134–49. https://doi.org/10.1016/j.jaap.2017.11.019.

[4] Ansari KB, Arora JS, Chew JW, Dauenhauer PJ, Mushrif SH. Fast Pyrolysis of Cellulose, Hemicellulose, and Lignin: Effect of Operating Temperature on Bio-oil Yield and Composition and Insights into the Intrinsic Pyrolysis Chemistry. Ind Eng Chem Res 2019:acs.iecr.9b00920. https://doi.org/10.1021/acs.iecr.9b00920.

[5] Chen D, Gao A, Cen K, Zhang J, Cao X, Ma Z. Investigation of biomass torrefaction based on three major components: Hemicellulose, cellulose, and lignin. Energy Conversion and Management 2018;169:228–37. https://doi.org/10.1016/j.enconman.2018.05.063.

[6] Lin Y-C, Cho J, Tompsett GA, Westmoreland PR, Huber GW. Kinetics and Mechanism of Cellulose Pyrolysis. J Phys Chem C 2009;113:20097–107. https://doi.org/10.1021/jp906702p.

[7] Qu T, Guo W, Shen L, Xiao J, Zhao K. Experimental Study of Biomass Pyrolysis Based on Three Major Components: Hemicellulose, Cellulose, and Lignin. Ind Eng Chem Res 2011;50:10424–33. https://doi.org/10.1021/ie1025453.

[8] Zhao C, Jiang E, Chen A. Volatile production from pyrolysis of cellulose, hemicellulose and lignin. Journal of the Energy Institute 2017;90:902–13. https://doi.org/10.1016/j.joei.2016.08.004.

[9] Yu J, Paterson N, Blamey J, Millan M. Cellulose, xylan and lignin interactions during pyrolysis of lignocellulosic biomass. Fuel 2017;191:140–9. https://doi.org/10.1016/j.fuel.2016.11.057.

[10] Zhang Y, Liu C, Chen X. Unveiling the initial pyrolytic mechanisms of cellulose by DFT study. Journal of Analytical and Applied Pyrolysis 2015:9.

[11] Mayes HB, Broadbelt LJ. Unraveling the Reactions that Unravel Cellulose. J Phys Chem A 2012;116:7098–106. https://doi.org/10.1021/jp300405x.

[12] Lu Q. The mechanism for the formation of levoglucosenone during pyrolysis of β-d-glucopyranose and cellobiose: A density functional theory study. Journal of Analytical and Applied Pyrolysis 2014:10.

[13] Shen DK, Gu S. The mechanism for thermal decomposition of cellulose and its main products. Bioresource Technology 2009;100:6496–504. https://doi.org/10.1016/j.biortech.2009.06.095.
[14] Assary RS, Curtiss LA. Thermochemistry and Reaction Barriers for the Formation of Levoglucosenone from Cellobiose 2012:6.
[15] Özsin G, Pütün AE. A comparative study on co-pyrolysis of lignocellulosic biomass with polyethylene terephthalate, polystyrene, and polyvinyl chloride: Synergistic effects and product characteristics. Journal of Cleaner Production 2018;205:1127–38. https://doi.org/10.1016/j.jclepro.2018.09.134.
[16] Charusiri W, Vitidsant T. Biofuel production via the pyrolysis of sugarcane (Saccharum officinarum L.) leaves: Characterization of the optimal conditions. Sustainable Chemistry and Pharmacy 2018;10:71–8. https://doi.org/10.1016/j.scp.2018.09.005.
[17] Greenhalf CE, Nowakowski DJ, Harms AB, Titiloye JO, Bridgwater AV. A comparative study of straw, perennial grasses and hardwoods in terms of fast pyrolysis products. Fuel 2013;108:216–30. https://doi.org/10.1016/j.fuel.2013.01.075.
[18] Burhenne L, Messmer J, Aicher T, Laborie M-P. The effect of the biomass components lignin, cellulose and hemicellulose on TGA and fixed bed pyrolysis. Journal of Analytical and Applied Pyrolysis 2013;101:177–84. https://doi.org/10.1016/j.jaap.2013.01.012.
[19] Greenhalf CE, Nowakowski DJ, Harms AB, Titiloye JO, Bridgwater AV. Sequential pyrolysis of willow SRC at low and high heating rates – Implications for selective pyrolysis. Fuel 2012;93:692–702. https://doi.org/10.1016/j.fuel.2011.11.050.
[20] Heidari A, Stahl R, Younesi H, Rashidi A, Troeger N, Ghoreyshi AA. Effect of process conditions on product yield and composition of fast pyrolysis of Eucalyptus grandis in fluidized bed reactor. Journal of Industrial and Engineering Chemistry 2014;20:2594–602. https://doi.org/10.1016/j.jiec.2013.10.046.
[21] Yin R, Liu R, Mei Y, Fei W, Sun X. Characterization of bio-oil and bio-char obtained from sweet sorghum bagasse fast pyrolysis with fractional condensers. Fuel 2013;112:96–104. https://doi.org/10.1016/j.fuel.2013.04.090.
[22] Montoya JI, Valdés C, Chejne F, Gómez CA, Blanco A, Marrugo G, et al. Bio-oil production from Colombian bagasse by fast pyrolysis in a fluidized bed: An experimental study. Journal of Analytical and Applied Pyrolysis 2015;112:379–87. https://doi.org/10.1016/j.jaap.2014.11.007.
[23] Mohammed IY, Abakr YA, Kazi FK. In-situ Upgrading of Napier Grass Pyrolysis Vapour Over Microporous and Hierarchical Mesoporous Zeolites. Waste Biomass Valor 2018;9:1415–28. https://doi.org/10.1007/s12649-017-9925-x.
[24] Aysu T, Durak H, Güner S, Bengü AŞ, Esim N. Bio-oil production via catalytic pyrolysis of Anchusa azurea: Effects of operating conditions on product yields and chromatographic characterization. Bioresource Technology 2016;205:7–14. https://doi.org/10.1016/j.biortech.2016.01.015.
[25] Liu R, Deng C, Wang J. Fast Pyrolysis of Corn Straw for Bio-oil Production in a Bench-scale Fluidized Bed Reactor. Energy Sources, Part A: Recovery, Utilization, and Environmental Effects 2009;32:10–9. https://doi.org/10.1080/15567030802094037.
[26] Wang H, Srinivasan R, Yu F, Steele P, Li Q, Mitchell B. Effect of Acid, Alkali, and Steam Explosion Pretreatments on Characteristics of Bio-Oil Produced from Pinewood. Energy & Fuels 2011;25:3758–64. https://doi.org/10.1021/ef2004909.
[27] Wang H, Srinivasan R, Yu F, Steele P, Li Q, Mitchell B, et al. Effect of Acid, Steam Explosion, and Size Reduction Pretreatments on Bio-oil Production from Sweetgum, Switchgrass, and Corn Stover. Applied Biochemistry and Biotechnology 2012;167:285–97. https://doi.org/10.1007/s12010-012-9678-8.
[28] Zhou X, Nolte MW, Shanks BH, Broadbelt LJ. Experimental and Mechanistic Modeling of Fast Pyrolysis of Neat Glucose-Based Carbohydrates. 2. Validation and Evaluation of the Mechanistic Model. Ind Eng Chem Res 2014:12.

[29] Arora JS, Chew JW, Mushrif SH. Influence of Alkali and Alkaline-Earth Metals on the Cleavage of Glycosidic Bond in Biomass Pyrolysis: A DFT Study Using Cellobiose as a Model Compound. The Journal of Physical Chemistry n.d.:32.
[30] Zhu C, Krumm C, Facas GG, Neurock M, Dauenhauer PJ. Energetics of cellulose and cyclodextrin glycosidic bond cleavage 2017:14.
[31] Kan T, Strezov V, Evans TJ. Lignocellulosic biomass pyrolysis: A review of product properties and effects of pyrolysis parameters. Renewable and Sustainable Energy Reviews 2016;57:1126–40. https://doi.org/10.1016/j.rser.2015.12.185.
[32] Patwardhan PR, Brown RC, Shanks BH. Product Distribution from the Fast Pyrolysis of Hemicellulose. ChemSusChem 2011;4:636–43. https://doi.org/10.1002/cssc.201000425.
[33] Mliki K, Trabelsi M. Efficient mild oxidation of 5-hydroxymethylfurfural to 5-hydroxymethyl-2(5H)-furanone, a versatile chemical intermediate. Res Chem Intermed 2016;42:8253–60. https://doi.org/10.1007/s11164-016-2593-9.
[34] Jenness GR, Vlachos DG. DFT Study of the Conversion of Furfuryl Alcohol to 2-Methylfuran on RuO_2 (110). J Phys Chem C 2015;119:5938–45. https://doi.org/10.1021/jp5109015.
[35] Lu Y, Lu Y-C, Hu H-Q, Xie F-J, Wei X-Y, Fan X. Structural Characterization of Lignin and Its Degradation Products with Spectroscopic Methods. Journal of Spectroscopy 2017;2017:1–15. https://doi.org/10.1155/2017/8951658.
[36] Kurnia I, Karnjanakom S, Bayu A, Yoshida A, Rizkiana J, Prakoso T, et al. In-situ catalytic upgrading of bio-oil derived from fast pyrolysis of lignin over high aluminum zeolites. Fuel Processing Technology 2017;167:730–7. https://doi.org/10.1016/j.fuproc.2017.08.026.
[37] Patwardhan PR, Brown RC, Shanks BH. Understanding the Fast Pyrolysis of Lignin. ChemSusChem 2011;4:1629–36. https://doi.org/10.1002/cssc.201100133.
[38] Fache M, Boutevin B, Caillol S. Vanillin Production from Lignin and Its Use as a Renewable Chemical. ACS Sustainable Chem Eng 2016;4:35–46. https://doi.org/10.1021/acssuschemeng.5b01344.
[39] He L, Qin Y, Lou H, Chen P. Highly dispersed molybdenum carbide nanoparticles supported on activated carbon as an efficient catalyst for the hydrodeoxygenation of vanillin. RSC Adv 2015;5:43141–7. https://doi.org/10.1039/C5RA00866B.
[40] Kotake T, Kawamoto H, Saka S. Pyrolysis reactions of coniferyl alcohol as a model of the primary structure formed during lignin pyrolysis. Journal of Analytical and Applied Pyrolysis 2013;104:573–84. https://doi.org/10.1016/j.jaap.2013.05.011.
[41] Zhu L, Li K, Ding H, Zhu X. Studying on properties of bio-oil by adding blended additive during aging. Fuel 2018;211:704–11. https://doi.org/10.1016/j.fuel.2017.09.106.
[42] Li C, Ma J, Xiao Z, Hector SB, Liu R, Zuo S, et al. Catalytic cracking of Swida wilsoniana oil for hydrocarbon biofuel over Cu-modified ZSM-5 zeolite. Fuel 2018;218:59–66. https://doi.org/10.1016/j.fuel.2018.01.026.
[43] Dabros TMH, Stummann MZ, Høj M, Jensen PA, Grunwaldt J-D, Gabrielsen J, et al. Transportation fuels from biomass fast pyrolysis, catalytic hydrodeoxygenation, and catalytic fast hydropyrolysis. Progress in Energy and Combustion Science 2018;68:268–309. https://doi.org/10.1016/j.pecs.2018.05.002.
[44] Paysepar H, Rao KTV, Yuan Z, Nazari L, Shui H, Xu C (Charles). Zeolite catalysts screening for production of phenolic bio-oils with high contents of monomeric aromatics/phenolics from hydrolysis lignin via catalytic fast pyrolysis. Fuel Processing Technology 2018;178:362–70. https://doi.org/10.1016/j.fuproc.2018.07.013.
[45] Lu Q, Guo H, Zhou M, Zhang Z, Cui M, Zhang Y, et al. Monocyclic aromatic hydrocarbons production from catalytic cracking of pine wood-derived pyrolytic vapors over Ce-Mo 2 N/HZSM-5 catalyst. Science of The Total Environment 2018;634:141–9. https://doi.org/10.1016/j.scitotenv.2018.03.351.
[46] Chen H, Cheng H, Zhou F, Chen K, Qiao K, Lu X, et al. Catalytic fast pyrolysis of rice straw to aromatic compounds over hierarchical HZSM-5 produced by alkali treatment and metal-modification. Journal of Analytical and Applied Pyrolysis 2018;131:76–84. https://doi.org/10.1016/j.jaap.2018.02.009.

[47] Lin Y-C, Huber GW. The critical role of heterogeneous catalysis in lignocellulosic biomass conversion. Energy Environ Sci 2009;2:68–80. https://doi.org/10.1039/B814955K.
[48] Kim S, Kwon EE, Kim YT, Jung S, Kim HJ, Huber GW, et al. Recent advances in hydrodeoxygenation of biomass-derived oxygenates over heterogeneous catalysts. Green Chem 2019:10.1039.C9GC01210A. https://doi.org/10.1039/C9GC01210A.
[49] Baloch HA, Nizamuddin S, Siddiqui MTH, Riaz S, Jatoi AS, Dumbre DK, et al. Recent advances in production and upgrading of bio-oil from biomass: A critical overview. Journal of Environmental Chemical Engineering 2018;6:5101–18. https://doi.org/10.1016/j.jece.2018.07.050.
[50] Ruddy DA, Schaidle JA, Ferrell III JR, Wang J, Moens L, Hensley JE. Recent advances in heterogeneous catalysts for bio-oil upgrading via "ex situ catalytic fast pyrolysis": catalyst development through the study of model compounds. Green Chem 2014;16:454–90. https://doi.org/10.1039/C3GC41354C.
[51] Kumar R, Strezov V, Lovell E, Kan T, Weldekidan H, He J, et al. Enhanced bio-oil deoxygenation activity by Cu/zeolite and Ni/zeolite catalysts in combined in-situ and ex-situ biomass pyrolysis. Journal of Analytical and Applied Pyrolysis 2019. https://doi.org/10.1016/j.jaap.2019.03.008.
[52] Huo X, Xiao J, Song M, Zhu L. Comparison between in-situ and ex-situ catalytic pyrolysis of sawdust for gas production. Journal of Analytical and Applied Pyrolysis 2018;135:189–98. https://doi.org/10.1016/j.jaap.2018.09.003.
[53] Ratnasari DK, Yang W, Jönsson PG. Two-stage ex-situ catalytic pyrolysis of lignocellulose for the production of gasoline-range chemicals. Journal of Analytical and Applied Pyrolysis 2018;134:454–64. https://doi.org/10.1016/j.jaap.2018.07.012.
[54] Hu C, Xiao R, Zhang H. Ex-situ catalytic fast pyrolysis of biomass over HZSM-5 in a two-stage fluidized-bed/fixed-bed combination reactor. Bioresource Technology 2017;243:1133–40. https://doi.org/10.1016/j.biortech.2017.07.011.
[55] Kumar R, Strezov V, Kan T, Weldekidan H, He J. Investigating the effect of Cu/zeolite on deoxygenation of bio-oil from pyrolysis of pine wood. Energy Procedia 2019;160:186–93. https://doi.org/10.1016/j.egypro.2019.02.135.
[56] Weldekidan H, Strezov V, Kan T, Kumar R, He J, Town G. Solar assisted catalytic pyrolysis of chicken-litter waste with in-situ and ex-situ loading of CaO and char. Fuel 2019;246:408–16. https://doi.org/10.1016/j.fuel.2019.02.135.
[57] Iisa K, French RJ, Orton KA, Yung MM, Johnson DK, ten Dam J, et al. In Situ and ex Situ Catalytic Pyrolysis of Pine in a Bench-Scale Fluidized Bed Reactor System. Energy & Fuels 2016;30:2144–57. https://doi.org/10.1021/acs.energyfuels.5b02165.
[58] Galadima A, Muraza O. In situ fast pyrolysis of biomass with zeolite catalysts for bioaromatics/gasoline production: A review. Energy Conversion and Management 2015;105:338–54. https://doi.org/10.1016/j.enconman.2015.07.078.
[59] Kumar R, Strezov V, Lovell E, Kan T, Weldekidan H, He J, et al. Bio-oil upgrading with catalytic pyrolysis of biomass using Copper/zeolite-Nickel/zeolite and Copper-Nickel/zeolite catalysts. Bioresource Technology 2019;279:404–9. https://doi.org/10.1016/j.biortech.2019.01.067.
[60] Wang K, Johnston PA, Brown RC. Comparison of in-situ and ex-situ catalytic pyrolysis in a micro-reactor system. Bioresource Technology 2014;173:124–31. https://doi.org/10.1016/j.biortech.2014.09.097.
[61] Asadieraghi M, Wan Daud WMA. In-situ catalytic upgrading of biomass pyrolysis vapor: Using a cascade system of various catalysts in a multi-zone fixed bed reactor. Energy Conversion and Management 2015;101:151–63. https://doi.org/10.1016/j.enconman.2015.05.008.
[62] Lee HW, Kim Y-M, Jae J, Sung BH, Jung S-C, Kim SC, et al. Catalytic pyrolysis of lignin using a two-stage fixed bed reactor comprised of in-situ natural zeolite and ex-situ HZSM-5. Journal of Analytical and Applied Pyrolysis 2016;122:282–8. https://doi.org/10.1016/j.jaap.2016.09.015.

[63] Wang S, Li Z, Bai X, Yi W, Fu P. Catalytic pyrolysis of lignin in a cascade dual-catalyst system of modified red mud and HZSM-5 for aromatic hydrocarbon production. Bioresource Technology 2019;278:66–72. https://doi.org/10.1016/j.biortech.2019.01.037.
[64] Serrano-Ruiz JC, Dumesic JA. Catalytic routes for the conversion of biomass into liquid hydrocarbon transportation fuels. Energy Environ Sci 2011;4:83–99. https://doi.org/10.1039/C0EE00436G.
[65] Cheng Y-T, Wang Z, Gilbert CJ, Fan W, Huber GW. Production of *p* -Xylene from Biomass by Catalytic Fast Pyrolysis Using ZSM-5 Catalysts with Reduced Pore Openings. Angew Chem Int Ed 2012;51:11097–100. https://doi.org/10.1002/anie.201205230.
[66] Wang S, Cai Q, Chen J, Zhang L, Wang X, Yu C. Green Aromatic Hydrocarbon Production from Cocracking of a Bio-Oil Model Compound Mixture and Ethanol over Ga_2O_3/HZSM-5. Ind Eng Chem Res 2014;53:13935–44. https://doi.org/10.1021/ie5024029.
[67] Wang S, Guo Z, Cai Q, Guo L. Catalytic conversion of carboxylic acids in bio-oil for liquid hydrocarbons production. Biomass and Bioenergy 2012;45:138–43. https://doi.org/10.1016/j.biombioe.2012.05.023.
[68] Chang C-C, Je Cho H, Yu J, Gorte RJ, Gulbinski J, Dauenhauer P, et al. Lewis acid zeolites for tandem Diels–Alder cycloaddition and dehydration of biomass-derived dimethylfuran and ethylene to renewable p-xylene. Green Chem 2016;18:1368–76. https://doi.org/10.1039/C5GC02164B.
[69] Gou J, Wang Z, Li C, Qi X, Vattipalli V, Cheng Y-T, et al. The effects of ZSM-5 mesoporosity and morphology on the catalytic fast pyrolysis of furan. Green Chem 2017;19:3549–57. https://doi.org/10.1039/C7GC01395G.
[70] Shafaghat H, Rezaei PS, Daud WMAW. Catalytic hydrodeoxygenation of simulated phenolic bio-oil to cycloalkanes and aromatic hydrocarbons over bifunctional metal/acid catalysts of Ni/HBeta, Fe/HBeta and NiFe/HBeta. Journal of Industrial and Engineering Chemistry 2016;35:268–76. https://doi.org/10.1016/j.jiec.2016.01.001.
[71] Maneffa A, Priecel P, Lopez-Sanchez JA. Biomass-Derived Renewable Aromatics: Selective Routes and Outlook for *p* -Xylene Commercialisation. ChemSusChem 2016;9:2736–48. https://doi.org/10.1002/cssc.201600605.
[72] Yu J, Zhu S, Dauenhauer PJ, Cho HJ, Fan W, Gorte RJ. Adsorption and reaction properties of SnBEA, ZrBEA and H-BEA for the formation of p-xylene from DMF and ethylene. Catal Sci Technol 2016;6:5729–36. https://doi.org/10.1039/C6CY00501B.
[73] Yin J, Shen C, Feng X, Ji K, Du L. Highly Selective Production of *p* -Xylene from 2,5-Dimethylfuran over Hierarchical NbO_x -Based Catalyst. ACS Sustainable Chem Eng 2018;6:1891–9. https://doi.org/10.1021/acssuschemeng.7b03297.
[74] Zhao Y, Pan T, Zuo Y, Guo Q-X, Fu Y. Production of aromatic hydrocarbons through catalytic pyrolysis of 5-Hydroxymethylfurfural from biomass. Bioresource Technology 2013;147:37–42. https://doi.org/10.1016/j.biortech.2013.07.068.
[75] Chheda JN, Huber GW, Dumesic JA. Liquid-Phase Catalytic Processing of Biomass-Derived Oxygenated Hydrocarbons to Fuels and Chemicals. Angew Chem Int Ed 2007;46:7164–83. https://doi.org/10.1002/anie.200604274.
[76] Leung A, Boocock DGB, Konar SK. Pathway for the Catalytic Conversion of Carboxylic Acids to Hydrocarbons over Activated Alumina. Energy Fuels 1995;9:913–20. https://doi.org/10.1021/ef00053a026.
[77] Psarras AC, Michailof CM, Iliopoulou EF, Kalogiannis KG, Lappas AA, Heracleous E, et al. Acetic acid conversion reactions on basic and acidic catalysts under biomass fast pyrolysis conditions. Molecular Catalysis 2019;465:33–42. https://doi.org/10.1016/j.mcat.2018.12.012.
[78] Gayubo AG, Aguayo AT, Atutxa A, Aguado R, Olazar M, Bilbao J. Transformation of Oxygenate Components of Biomass Pyrolysis Oil on a HZSM-5 Zeolite. II. Aldehydes, Ketones, and Acids. Industrial & Engineering Chemistry Research 2004;43:2619–26. https://doi.org/10.1021/ie030792g.

[79] Adjaye JD, Bakhshi NN. CATALYTIC CONVERSION OF A BIOMASS-DERIVED OIL TO FUELS AND CHEMICALS I: MODEL COMPOUND STUDIES AND REACTION PATHWAYS n.d.:19.
[80] To AT, Resasco DE. Role of a phenolic pool in the conversion of m-cresol to aromatics over HY and HZSM-5 zeolites. Applied Catalysis A: General 2014;487:62–71. https://doi.org/10.1016/j.apcata.2014.09.006.
[81] Hemberger P, Custodis VBF, Bodi A, Gerber T, van Bokhoven JA. Understanding the mechanism of catalytic fast pyrolysis by unveiling reactive intermediates in heterogeneous catalysis. Nature Communications 2017;8:15946. https://doi.org/10.1038/ncomms15946.
[82] Lu Q, Guo H, Zhou M, Cui M, Dong C, Yang Y. Selective preparation of monocyclic aromatic hydrocarbons from catalytic cracking of biomass fast pyrolysis vapors over Mo 2 N/HZSM-5 catalyst. Fuel Processing Technology 2018;173:134–42. https://doi.org/10.1016/j.fuproc.2018.01.017.
[83] Mullen CA, Boateng AA. Catalytic pyrolysis-GC/MS of lignin from several sources. Fuel Processing Technology 2010;91:1446–58. https://doi.org/10.1016/j.fuproc.2010.05.022.
[84] Chen G, Zhang R, Ma W, Liu B, Li X, Yan B, et al. Catalytic cracking of model compounds of bio-oil over HZSM-5 and the catalyst deactivation. Science of The Total Environment 2018;631–632:1611–22. https://doi.org/10.1016/j.scitotenv.2018.03.147.
[85] Zheng Y, Chen D, Zhu X. Aromatic hydrocarbon production by the online catalytic cracking of lignin fast pyrolysis vapors using Mo2N/γ-Al2O3. Journal of Analytical and Applied Pyrolysis 2013;104:514–20. https://doi.org/10.1016/j.jaap.2013.05.018.
[86] Chen Y-X, Zheng Y, Li M, Zhu X-F. Arene production by W 2 C/MCM-41-catalyzed upgrading of vapors from fast pyrolysis of lignin. Fuel Processing Technology 2015;134:46–51. https://doi.org/10.1016/j.fuproc.2014.12.017.
[87] Jiang X, Zhou J, Zhao J, Shen D. Catalytic conversion of guaiacol as a model compound for aromatic hydrocarbon production. Biomass and Bioenergy 2018;111:343–51. https://doi.org/10.1016/j.biombioe.2017.06.026.
[88] Scheer AM, Mukarakate C, Robichaud DJ, Nimlos MR, Ellison GB. Thermal Decomposition Mechanisms of the Methoxyphenols: Formation of Phenol, Cyclopentadienone, Vinylacetylene, and Acetylene. J Phys Chem A 2011;115:13381–9. https://doi.org/10.1021/jp2068073.
[89] Liu C, Ye L, Yuan W, Zhang Y, Zou J, Yang J, et al. Investigation on pyrolysis mechanism of guaiacol as lignin model compound at atmospheric pressure. Fuel 2018;232:632–8. https://doi.org/10.1016/j.fuel.2018.05.162.
[90] Wang Z, Li Y, Zhang F, Zhang L, Yuan W, Wang Y, et al. An experimental and kinetic modeling investigation on a rich premixed n-propylbenzene flame at low pressure. Proceedings of the Combustion Institute 2013;34:1785–93. https://doi.org/10.1016/j.proci.2012.05.006.
[91] Cai J, Wu W, Liu R. An overview of distributed activation energy model and its application in the pyrolysis of lignocellulosic biomass. Renewable and Sustainable Energy Reviews 2014;36:236–46. https://doi.org/10.1016/j.rser.2014.04.052.
[92] Ratnasari DK, Yang W, Jönsson PG. Kinetic Study of an H-ZSM-5/Al–MCM-41 Catalyst Mixture and Its Application in Lignocellulose Biomass Pyrolysis. Energy Fuels 2019;33:5360–7. https://doi.org/10.1021/acs.energyfuels.9b00866.
[93] Lu C, Song W, Lin W. Kinetics of biomass catalytic pyrolysis. Biotechnology Advances 2009;27:583–7. https://doi.org/10.1016/j.biotechadv.2009.04.014.
[94] Yang H, Ji G, Clough PT, Xu X, Zhao M. Kinetics of catalytic biomass pyrolysis using Ni-based functional materials. Fuel Processing Technology 2019;195:106145. https://doi.org/10.1016/j.fuproc.2019.106145.
[95] Quan C, Gao N, Song Q. Pyrolysis of biomass components in a TGA and a fixed-bed reactor: Thermochemical behaviors, kinetics, and product characterization. Journal of Analytical and Applied Pyrolysis 2016;121:84–92. https://doi.org/10.1016/j.jaap.2016.07.005.

[96] Cai J, Wu W, Liu R, Huber GW. A distributed activation energy model for the pyrolysis of lignocellulosic biomass. Green Chemistry 2013;15:1331. https://doi.org/10.1039/c3gc36958g.
[97] Belyi VA, Udoratina EV, Kuchin AV. Kinetics of the thermocatalytic conversion of lignocellulose. Kinet Catal 2015;56:663–9. https://doi.org/10.1134/S002315841505002X.
[98] Braga RM, Costa TR, Freitas JCO, Barros JMF, Melo DMA, Melo MAF. Pyrolysis kinetics of elephant grass pretreated biomasses. J Therm Anal Calorim 2014;117:1341–8. https://doi.org/10.1007/s10973-014-3884-2.
[99] Sait HH, Hussain A, Salema AA, Ani FN. Pyrolysis and combustion kinetics of date palm biomass using thermogravimetric analysis. Bioresource Technology 2012;118:382–9. https://doi.org/10.1016/j.biortech.2012.04.081.
[100] Pecha MB, Arbelaez JIM, Garcia-Perez M, Chejne F, Ciesielski PN. Progress in understanding the four dominant intra-particle phenomena of lignocellulose pyrolysis: chemical reactions, heat transfer, mass transfer, and phase change. Green Chem 2019;21:2868–98. https://doi.org/10.1039/C9GC00585D.
[101] Wu W, Mei Y, Zhang L, Liu R, Cai J. Effective Activation Energies of Lignocellulosic Biomass Pyrolysis. Energy Fuels 2014;28:3916–23. https://doi.org/10.1021/ef5005896.
[102] Várhegyi G, Bobály B, Jakab E, Chen H. Thermogravimetric Study of Biomass Pyrolysis Kinetics. A Distributed Activation Energy Model with Prediction Tests. Energy Fuels 2011;25:24–32. https://doi.org/10.1021/ef101079r.
[103] Sonobe T, Worasuwannarak N. Kinetic analyses of biomass pyrolysis using the distributed activation energy model. Fuel 2008;87:414–21. https://doi.org/10.1016/j.fuel.2007.05.004.
[104] Arenas CN, Navarro MV, Martínez JD. Pyrolysis kinetics of biomass wastes using isoconversional methods and the distributed activation energy model. Bioresource Technology 2019;288:121485. https://doi.org/10.1016/j.biortech.2019.121485.
[105] Miura K, Maki T. A Simple Method for Estimating $f(E)$ and $k_0(E)$ in the Distributed Activation Energy Model. Energy Fuels 1998;12:864–9. https://doi.org/10.1021/ef970212q.
[106] Cai J, Yang S, Li T. Logistic distributed activation energy model – Part 2: Application to cellulose pyrolysis. Bioresource Technology 2011;102:3642–4. https://doi.org/10.1016/j.biortech.2010.11.073.
[107] Mani T, Murugan P, Mahinpey N. Determination of Distributed Activation Energy Model Kinetic Parameters Using Simulated Annealing Optimization Method for Nonisothermal Pyrolysis of Lignin. Ind Eng Chem Res 2009;48:1464–7. https://doi.org/10.1021/ie8013605.
[108] Xu D, Chai M, Dong Z, Rahman MdM, Yu X, Cai J. Kinetic compensation effect in logistic distributed activation energy model for lignocellulosic biomass pyrolysis. Bioresource Technology 2018;265:139–45. https://doi.org/10.1016/j.biortech.2018.05.092.
[109] Zhou B, Zhou J, Zhang Q. Research on pyrolysis behavior of Camellia sinensis branches via the Discrete Distributed Activation Energy Model. Bioresource Technology 2017;241:113–9. https://doi.org/10.1016/j.biortech.2017.05.083.
[110] Chen H, Shi X, Zhou F, Ma H, Qiao K, Lu X, et al. Catalytic fast pyrolysis of cellulose to aromatics over hierarchical nanocrystalline ZSM-5 zeolites prepared using sucrose as a template. Catalysis Communications 2018;110:102–5. https://doi.org/10.1016/j.catcom.2018.03.016.
[111] Araújo A, Queiroz G, Maia D, Gondim A, Souza L, Fernandes V, et al. Fast Pyrolysis of Sunflower Oil in the Presence of Microporous and Mesoporous Materials for Production of Bio-Oil. Catalysts 2018;8:261. https://doi.org/10.3390/catal8070261.
[112] Alekseeva (Bykova) MV, Otyuskaya DS, Rekhtina MA, Bulavchenko OA, Stonkus OA, Kaichev VV, et al. NiCuMo-SiO2 catalyst for pyrolysis oil upgrading: Model acidic treatment study. Applied Catalysis A: General 2019;573:1–12. https://doi.org/10.1016/j.apcata.2019.01.003.
[113] Jaroenkhasemmeesuk C, Diego ME, Tippayawong N, Ingham DB, Pourkashanian M. Simulation analysis of the catalytic cracking process of biomass pyrolysis oil with mixed

catalysts: Optimization using the simplex lattice design. International Journal of Energy Research 2018;42:2983–96. https://doi.org/10.1002/er.4023.
[114] Nguyen TS, Zabeti M, Lefferts L, Brem G, Seshan K. Catalytic upgrading of biomass pyrolysis vapours using faujasite zeolite catalysts. Biomass and Bioenergy 2013;48:100–10. https://doi.org/10.1016/j.biombioe.2012.10.024.
[115] Gamliel DP, Wilcox L, Valla JA. The Effects of Catalyst Properties on the Conversion of Biomass via Catalytic Fast Hydropyrolysis. Energy & Fuels 2017;31:679–87. https://doi.org/10.1021/acs.energyfuels.6b02781.
[116] Veses A, Puértolas B, Callén MS, García T. Catalytic upgrading of biomass derived pyrolysis vapors over metal-loaded ZSM-5 zeolites: Effect of different metal cations on the bio-oil final properties. Microporous and Mesoporous Materials 2015;209:189–96. https://doi.org/10.1016/j.micromeso.2015.01.012.
[117] Serrano DP, Melero JA, Morales G, Iglesias J, Pizarro P. Progress in the design of zeolite catalysts for biomass conversion into biofuels and bio-based chemicals. Catalysis Reviews 2018;60:1–70. https://doi.org/10.1080/01614940.2017.1389109.
[118] Bizkarra K, Bermudez JM, Arcelus-Arrillaga P, Barrio VL, Cambra JF, Millan M. Nickel based monometallic and bimetallic catalysts for synthetic and real bio-oil steam reforming. International Journal of Hydrogen Energy 2018;43:11706–18. https://doi.org/10.1016/j.ijhydene.2018.03.049.
[119] Alonso DM, Wettstein SG, Dumesic JA. Bimetallic catalysts for upgrading of biomass to fuels and chemicals. Chemical Society Reviews 2012;41:8075. https://doi.org/10.1039/c2cs35188a.
[120] Chen J, Wang S, Lu L, Zhang X, Liu Y. Improved catalytic upgrading of simulated bio-oil via mild hydrogenation over bimetallic catalysts. Fuel Processing Technology 2018;179:135–42. https://doi.org/10.1016/j.fuproc.2018.06.022.
[121] Yu Y, Li X, Su L, Zhang Y, Wang Y, Zhang H. The role of shape selectivity in catalytic fast pyrolysis of lignin with zeolite catalysts. Applied Catalysis A: General 2012;447–448:115–23. https://doi.org/10.1016/j.apcata.2012.09.012.
[122] Widayatno WB, Guan G, Rizkiana J, Yang J, Hao X, Tsutsumi A, et al. Upgrading of bio-oil from biomass pyrolysis over Cu-modified β-zeolite catalyst with high selectivity and stability. Applied Catalysis B: Environmental 2016;186:166–72. https://doi.org/10.1016/j.apcatb.2016.01.006.
[123] Primo A, Garcia H. Zeolites as catalysts in oil refining. Chem Soc Rev 2014;43:7548–61. https://doi.org/10.1039/C3CS60394F.
[124] Ding K, Zhong Z, Wang J, Zhang B, Addy M, Ruan R. Effects of alkali-treated hierarchical HZSM-5 zeolites on the production of aromatic hydrocarbons from catalytic fast pyrolysis of waste cardboard. Journal of Analytical and Applied Pyrolysis 2017;125:153–61. https://doi.org/10.1016/j.jaap.2017.04.006.
[125] Rahman MdM, Liu R, Cai J. Catalytic fast pyrolysis of biomass over zeolites for high quality bio-oil – A review. Fuel Processing Technology 2018;180:32–46. https://doi.org/10.1016/j.fuproc.2018.08.002.
[126] Du Z, Ma X, Li Y, Chen P, Liu Y, Lin X, et al. Production of aromatic hydrocarbons by catalytic pyrolysis of microalgae with zeolites: Catalyst screening in a pyroprobe. Bioresource Technology 2013;139:397–401. https://doi.org/10.1016/j.biortech.2013.04.053.
[127] Shamzhy M, Opanasenko M, Concepción P, Martínez A. New trends in tailoring active sites in zeolite-based catalysts. Chemical Society Reviews 2019;48:1095–149. https://doi.org/10.1039/C8CS00887F.
[128] Busca G. Acidity and basicity of zeolites: A fundamental approach. Microporous and Mesoporous Materials 2017;254:3–16. https://doi.org/10.1016/j.micromeso.2017.04.007.
[129] Huang J, van Vegten N, Jiang Y, Hunger M, Baiker A. Increasing the Brønsted Acidity of Flame-Derived Silica/Alumina up to Zeolitic Strength. Angewandte Chemie International Edition 2010;49:7776–81. https://doi.org/10.1002/anie.201003391.

[130] Engtrakul C, Mukarakate C, Starace AK, Magrini KA, Rogers AK, Yung MM. Effect of ZSM-5 acidity on aromatic product selectivity during upgrading of pine pyrolysis vapors. Catalysis Today 2016;269:175–81. https://doi.org/10.1016/j.cattod.2015.10.032.
[131] Du S, Gamliel DP, Valla JA, Bollas GM. The effect of ZSM-5 catalyst support in catalytic pyrolysis of biomass and compounds abundant in pyrolysis bio-oils. Journal of Analytical and Applied Pyrolysis 2016;122:7–12. https://doi.org/10.1016/j.jaap.2016.11.002.
[132] Weitkamp J. Zeolites and catalysis. Solid State Ionics 2000;131:175–88. https://doi.org/10.1016/S0167-2738(00)00632-9.
[133] Xu B, Sievers C, Lercher JA, van Veen JAR, Giltay P, Prins R, et al. Strong Brønsted Acidity in Amorphous Silica−Aluminas. J Phys Chem C 2007;111:12075–9. https://doi.org/10.1021/jp073677i.
[134] Feng R, Liu S, Bai P, Qiao K, Wang Y, Al-Megren HA, et al. Preparation and Characterization of γ-Al_2O_3 with Rich Brønsted Acid Sites and Its Application in the Fluid Catalytic Cracking Process. J Phys Chem C 2014;118:6226–34. https://doi.org/10.1021/jp411405r.
[135] Mukarakate C, Watson MJ, ten Dam J, Baucherel X, Budhi S, Yung MM, et al. Upgrading biomass pyrolysis vapors over β-zeolites: role of silica-to-alumina ratio. Green Chem 2014;16:4891–905. https://doi.org/10.1039/C4GC01425A.
[136] Hernando H, Hernández-Giménez AM, Ochoa-Hernández C, Bruijnincx PCA, Houben K, Baldus M, et al. Engineering the acidity and accessibility of the zeolite ZSM-5 for efficient bio-oil upgrading in catalytic pyrolysis of lignocellulose. Green Chemistry 2018. https://doi.org/10.1039/C8GC01722K.
[137] Khouw CB, Davis ME. Shape-Selective Catalysis with Zeolites and Molecular Sieves. In: Davis ME, Suib SL, editors. Selectivity in Catalysis, vol. 517, Washington, DC: American Chemical Society; 1993, p. 206–21. https://doi.org/10.1021/bk-1993-0517.ch014.
[138] Jae J, Tompsett GA, Foster AJ, Hammond KD, Auerbach SM, Lobo RF, et al. Investigation into the shape selectivity of zeolite catalysts for biomass conversion. Journal of Catalysis 2011;279:257–68. https://doi.org/10.1016/j.jcat.2011.01.019.
[139] Teketel S, Skistad W, Benard S, Olsbye U, Lillerud KP, Beato P, et al. Shape Selectivity in the Conversion of Methanol to Hydrocarbons: The Catalytic Performance of One-Dimensional 10-Ring Zeolites: ZSM-22, ZSM-23, ZSM-48, and EU-1. ACS Catal 2012;2:26–37. https://doi.org/10.1021/cs200517u.
[140] Chen J. Modifications of n-hexane hydroisomerization over Pt/mordenite as induced by aromatic cofeeds. Journal of Catalysis 1988;111:425–8. https://doi.org/10.1016/0021-9517(88)90102-9.
[141] Puértolas B, Veses A, Callén MS, Mitchell S, García T, Pérez-Ramírez J. Porosity-Acidity Interplay in Hierarchical ZSM-5 Zeolites for Pyrolysis Oil Valorization to Aromatics. ChemSusChem 2015;8:3283–93. https://doi.org/10.1002/cssc.201500685.
[142] Lin B, Wang J, Huang Q, Ali M, Chi Y. Aromatic recovery from distillate oil of oily sludge through catalytic pyrolysis over Zn modified HZSM-5 zeolites. Journal of Analytical and Applied Pyrolysis 2017;128:291–303. https://doi.org/10.1016/j.jaap.2017.09.021.
[143] Kantarelis E, Javed R, Stefanidis S, Psarras A, Iliopoulou E, Lappas A. Engineering the Catalytic Properties of HZSM5 by Cobalt Modification and Post-synthetic Hierarchical Porosity Development. Top Catal 2019;62:773–85. https://doi.org/10.1007/s11244-019-01179-w.
[144] Paysepar H, Rao KTV, Yuan Z, Shui H, Xu C (Charles). Improving activity of ZSM-5 zeolite catalyst for the production of monomeric aromatics/phenolics from hydrolysis lignin via catalytic fast pyrolysis. Applied Catalysis A: General 2018;563:154–62. https://doi.org/10.1016/j.apcata.2018.07.003.
[145] Li X, Zhang X, Shao S, Dong L, Zhang J, Hu C, et al. Catalytic upgrading of pyrolysis vapor from rape straw in a vacuum pyrolysis system over La/HZSM-5 with hierarchical structure. Bioresource Technology 2018;259:191–7. https://doi.org/10.1016/j.biortech.2018.03.046.

[146] Aho A, Kumar N, Eränen K, Salmi T, Hupa M, Murzin DYu. Catalytic pyrolysis of woody biomass in a fluidized bed reactor: Influence of the zeolite structure. Fuel 2008;87:2493–501. https://doi.org/10.1016/j.fuel.2008.02.015.
[147] Zheng A, Zhao Z, Chang S, Huang Z, Wu H, Wang X, et al. Effect of crystal size of ZSM-5 on the aromatic yield and selectivity from catalytic fast pyrolysis of biomass. Journal of Molecular Catalysis A: Chemical 2014;383–384:23–30. https://doi.org/10.1016/j.molcata.2013.11.005.
[148] Iliopoulou EF, Stefanidis SD, Kalogiannis KG, Delimitis A, Lappas AA, Triantafyllidis KS. Catalytic upgrading of biomass pyrolysis vapors using transition metal-modified ZSM-5 zeolite. Applied Catalysis B: Environmental 2012;127:281–90. https://doi.org/10.1016/j.apcatb.2012.08.030.
[149] Thangalazhy-Gopakumar S, Adhikari S, Chattanathan SA, Gupta RB. Catalytic pyrolysis of green algae for hydrocarbon production using H+ZSM-5 catalyst. Bioresource Technology 2012;118:150–7. https://doi.org/10.1016/j.biortech.2012.05.080.
[150] Stefanidis SD, Kalogiannis KG, Iliopoulou EF, Lappas AA, Pilavachi PA. In-situ upgrading of biomass pyrolysis vapors: Catalyst screening on a fixed bed reactor. Bioresource Technology 2011;102:8261–7. https://doi.org/10.1016/j.biortech.2011.06.032.
[151] Zheng Y, Wang F, Yang X, Huang Y, Liu C, Zheng Z, et al. Study on aromatics production via the catalytic pyrolysis vapor upgrading of biomass using metal-loaded modified H-ZSM-5. Journal of Analytical and Applied Pyrolysis 2017;126:169–79. https://doi.org/10.1016/j.jaap.2017.06.011.
[152] Li J, Li X, Zhou G, Wang W, Wang C, Komarneni S, et al. Catalytic fast pyrolysis of biomass with mesoporous ZSM-5 zeolites prepared by desilication with NaOH solutions. Applied Catalysis A: General 2014;470:115–22. https://doi.org/10.1016/j.apcata.2013.10.040.
[153] Tang S, Zhang C, Xue X, Pan Z, Wang D, Zhang R. Catalytic pyrolysis of lignin over hierarchical HZSM-5 zeolites prepared by post-treatment with alkaline solutions. Journal of Analytical and Applied Pyrolysis 2019;137:86–95. https://doi.org/10.1016/j.jaap.2018.11.013.
[154] Neumann GT, Hicks JC. Novel Hierarchical Cerium-Incorporated MFI Zeolite Catalysts for the Catalytic Fast Pyrolysis of Lignocellulosic Biomass. ACS Catalysis 2012;2:642–6. https://doi.org/10.1021/cs200648q.
[155] Wang J-X, Cao J-P, Zhao X-Y, Liu S-N, Ren X-Y, Zhao M, et al. Enhancement of light aromatics from catalytic fast pyrolysis of cellulose over bifunctional hierarchical HZSM-5 modified by hydrogen fluoride and nickel/hydrogen fluoride. Bioresource Technology 2019;278:116–23. https://doi.org/10.1016/j.biortech.2019.01.059.
[156] Dai L, Wang Y, Liu Y, Ruan R, Duan D, Zhao Y, et al. Catalytic fast pyrolysis of torrefied corn cob to aromatic hydrocarbons over Ni-modified hierarchical ZSM-5 catalyst. Bioresource Technology 2019;272:407–14. https://doi.org/10.1016/j.biortech.2018.10.062.
[157] Qiao K, Shi X, Zhou F, Chen H, Fu J, Ma H, et al. Catalytic fast pyrolysis of cellulose in a microreactor system using hierarchical zsm-5 zeolites treated with various alkalis. Applied Catalysis A: General 2017;547:274–82. https://doi.org/10.1016/j.apcata.2017.07.034.
[158] Palizdar A, Sadrameli SM. Catalytic upgrading of biomass pyrolysis oil over tailored hierarchical MFI zeolite: Effect of porosity enhancement and porosity-acidity interaction on deoxygenation reactions. Renewable Energy 2019:S0960148119316520. https://doi.org/10.1016/j.renene.2019.10.155.
[159] Li J, Li X, Hua D, Lu X, Wang Y. Optimizing the Aromatic Product Distribution from Catalytic Fast Pyrolysis of Biomass Using Hydrothermally Synthesized Ga-MFI Zeolites. Catalysts 2019;9:854. https://doi.org/10.3390/catal9100854.
[160] Antonakou E, Lappas A, Nilsen MH, Bouzga A, Stöcker M. Evaluation of various types of Al-MCM-41 materials as catalysts in biomass pyrolysis for the production of bio-fuels and chemicals. Fuel 2006;85:2202–12. https://doi.org/10.1016/j.fuel.2006.03.021.

[161] Paasikallio V, Kalogiannis K, Lappas A, Lehto J, Lehtonen J. Catalytic Fast Pyrolysis: Influencing Bio-Oil Quality with the Catalyst-to-Biomass Ratio. Energy Technology 2017;5:94–103. https://doi.org/10.1002/ente.201600094.
[162] Guda VK, Toghiani H. Catalytic pyrolysis of pinewood using metal oxide catalysts in an integrated reactor system. Biofuels 2017;8:527–36. https://doi.org/10.1080/17597269.2016.1231960.
[163] Mante OD, Dayton DC, Carpenter JR, Wang K, Peters JE. Pilot-scale catalytic fast pyrolysis of loblolly pine over γ-Al2O3 catalyst. Fuel 2018;214:569–79. https://doi.org/10.1016/j.fuel.2017.11.073.
[164] Chong YY, Thangalazhy-Gopakumar S, Ng HK, Lee LY, Gan S. Effect of oxide catalysts on the properties of bio-oil from in-situ catalytic pyrolysis of palm empty fruit bunch fiber. Journal of Environmental Management 2019;247:38–45. https://doi.org/10.1016/j.jenvman.2019.06.049.
[165] Abu Bakar MS, Titiloye JO. Catalytic pyrolysis of rice husk for bio-oil production. Journal of Analytical and Applied Pyrolysis 2013;103:362–8. https://doi.org/10.1016/j.jaap.2012.09.005.
[166] Aysu T. PYROLYSIS OF ISOCHRYSIS MICROALGAE WITH METAL OXIDE CATALYSTS FOR BIO-OIL PRODUCTION. Journal of the Turkish Chemical Society, Section A: Chemistry 2016;4:395–395. https://doi.org/10.18596/jotcsa.287338.
[167] Zhou L, Yang H, Wu H, Wang M, Cheng D. Catalytic pyrolysis of rice husk by mixing with zinc oxide: Characterization of bio-oil and its rheological behavior. Fuel Processing Technology 2013;106:385–91. https://doi.org/10.1016/j.fuproc.2012.09.003.
[168] Naqvi SR, Uemura Y, Yusup SB. Catalytic pyrolysis of paddy husk in a drop type pyrolyzer for bio-oil production: The role of temperature and catalyst. Journal of Analytical and Applied Pyrolysis 2014;106:57–62. https://doi.org/10.1016/j.jaap.2013.12.009.
[169] Aysu T, Küçük MM. Biomass pyrolysis in a fixed-bed reactor: Effects of pyrolysis parameters on product yields and characterization of products. Energy 2014;64:1002–25. https://doi.org/10.1016/j.energy.2013.11.053.
[170] Abu-Laban M. Ex-situ up-conversion of biomass pyrolysis bio-oil vapors using Pt/Al2O3 nanostructured catalyst synergistically heated with steel balls via induction. Catalysis Today 2017:10.
[171] Eschenbacher A, Saraeian A, Jensen PA, Shanks BH, Li C, Duus JØ, et al. Deoxygenation of wheat straw fast pyrolysis vapors over Na-Al2O3 catalyst for production of bio-oil with low acidity. Chemical Engineering Journal 2020;394:124878. https://doi.org/10.1016/j.cej.2020.124878.
[172] Che Q, Yang M, Wang X, Chen X, Chen W, Yang Q, et al. Aromatics production with metal oxides and ZSM-5 as catalysts in catalytic pyrolysis of wood sawdust. Fuel Processing Technology 2019;188:146–52. https://doi.org/10.1016/j.fuproc.2019.02.016.
[173] Kaewpengkrow P, Atong D, Sricharoenchaikul V. Catalytic upgrading of pyrolysis vapors from Jatropha wastes using alumina, zirconia and titania based catalysts. Bioresource Technology 2014;163:262–9. https://doi.org/10.1016/j.biortech.2014.04.035.
[174] Payormhorm J. Pt/Al2O3-catalytic deoxygenation for upgrading of Leucaena leucocephala-pyrolysis oil. Bioresource Technology 2013:8.
[175] Ozbay N, Yargic AS, Yarbay Sahin RZ. Tailoring Cu/Al 2 O 3 catalysts for the catalytic pyrolysis of tomato waste. Journal of the Energy Institute 2018;91:424–33. https://doi.org/10.1016/j.joei.2017.01.010.
[176] Chen X, Li S, Liu Z, Chen Y, Yang H, Wang X, et al. Pyrolysis characteristics of lignocellulosic biomass components in the presence of CaO. Bioresource Technology 2019;287:121493. https://doi.org/10.1016/j.biortech.2019.121493.
[177] Pütün E. Catalytic pyrolysis of biomass: Effects of pyrolysis temperature, sweeping gas flow rate and MgO catalyst. Energy 2010;35:2761–6. https://doi.org/10.1016/j.energy.2010.02.024.

[178] Lin Y, Zhang C, Zhang M, Zhang J. Deoxygenation of Bio-oil during Pyrolysis of Biomass in the Presence of CaO in a Fluidized-Bed Reactor. Energy & Fuels 2010;24:5686–95. https://doi.org/10.1021/ef1009605.
[179] Veses A, Aznar M, Martínez I, Martínez JD, López JM, Navarro MV, et al. Catalytic pyrolysis of wood biomass in an auger reactor using calcium-based catalysts. Bioresource Technology 2014;162:250–8. https://doi.org/10.1016/j.biortech.2014.03.146.
[180] Lin X, Zhang Z, Zhang Z, Sun J, Wang Q, Pittman CU. Catalytic fast pyrolysis of a wood-plastic composite with metal oxides as catalysts. Waste Management 2018;79:38–47. https://doi.org/10.1016/j.wasman.2018.07.021.
[181] Stefanidis SD, Karakoulia SA, Kalogiannis KG, Iliopoulou EF, Delimitis A, Yiannoulakis H, et al. Natural magnesium oxide (MgO) catalysts: A cost-effective sustainable alternative to acid zeolites for the in situ upgrading of biomass fast pyrolysis oil. Applied Catalysis B: Environmental 2016;196:155–73. https://doi.org/10.1016/j.apcatb.2016.05.031.
[182] Fan L, Chen P, Zhang Y, Liu S, Liu Y, Wang Y, et al. Fast microwave-assisted catalytic co-pyrolysis of lignin and low-density polyethylene with HZSM-5 and MgO for improved bio-oil yield and quality. Bioresource Technology 2017;225:199–205. https://doi.org/10.1016/j.biortech.2016.11.072.
[183] Kalogiannis KG, Stefanidis SD, Karakoulia SA, Triantafyllidis KS, Yiannoulakis H, Michailof C, et al. First pilot scale study of basic vs acidic catalysts in biomass pyrolysis: Deoxygenation mechanisms and catalyst deactivation. Applied Catalysis B: Environmental 2018;238:346–57. https://doi.org/10.1016/j.apcatb.2018.07.016.
[184] Yuan R, Shen Y. Catalytic pyrolysis of biomass-plastic wastes in the presence of MgO and MgCO3 for hydrocarbon-rich oils production. Bioresource Technology 2019;293:122076. https://doi.org/10.1016/j.biortech.2019.122076.
[185] Fan L, Zhang Y, Liu S, Zhou N, Chen P, Liu Y, et al. Ex-situ catalytic upgrading of vapors from microwave-assisted pyrolysis of low-density polyethylene with MgO. Energy Conversion and Management 2017;149:432–41. https://doi.org/10.1016/j.enconman.2017.07.039.

MACQUARIE University

MACQUARIE UNIVERSITY
AUTHORSHIP CONTRIBUTION STATEMENT

In accordance with the *Macquarie University Code for the Responsible Conduct of Research* and the *Authorship Standard*, researchers have a responsibility to their colleagues and the wider community to treat others fairly and with respect, to give credit where appropriate to those who have contributed to research.

Note for HDR students: *Where research papers are being included in a thesis, this template must be used to document the contribution of authors to each of the proposed or published research papers. The contribution of the candidate must be sufficient to justify inclusion of the paper in the thesis.*

1. DETAILS OF PUBLICATION & CORRESPONDING AUTHOR

Title of Publication (can be a holding title)		**Publication Status** Choose an item
Lignocellulose biomass pyrolysis for bio-oil production: A review of biomass pre-treatment methods for production of drop-in fuels		☐ In Progress or Unpublished work for thesis submission ☐ Submitted for Publication ☐ Accepted for Publication ☒ Published
Name of **corresponding author**	Department/Faculty	**Publication details:** indicate the name of the journal/ conference/ publisher/other outlet
Ravinder Kumar	Earth and Environmental Sciences/ Science & Engineering	Renewable & Sustainable Energy Reviews

2. STUDENTS DECLARATION (if applicable)

Name of HDR thesis author (If the same as corresponding author - write "as above")	Department/Faculty	Thesis title
As above	Earth and Environmental Sciences/ Science & Engineering	Catalytic Upgrading of Bio-oil Produced from Fast Pyrolysis of Pinewood Sawdust

Description of HDR thesis author's contribution to planning, execution, and preparation of the work if there are multiple authors

(for example, how much as a percent did you contribute to the conception of the project, the design of methodology or experimental protocol, data collection, analysis, drafting the manuscript, revising it critically for important intellectual content, etc.)

In this article, I designed the work, collected data and contributed to write 65% of the manuscript.

I declare that the above is an accurate description of my contribution to this publication, and the contributions of other authors are as described below.	**Student signature** **Date**	 02/22/2021

3. Description of all other author contributions

Use an Asterisk * to denote if the author is also a current student or HDR candidate.

The HDR candidate or corresponding author must, for each paper, list all authors and provide details of their role in the publication. Where possible, also provide a percentage estimate of the contribution made by each author.

Name and affiliation of author	**Intellectual contribution(s)** (for example to the: conception of the project, design of methodology/experimental protocol, data collection, analysis, drafting the manuscript, revising it critically for important intellectual content etc.)
Vladimir Strezov Macquarie University	conception, supervision, critical revision
Haftom Weldekidan Macquarie University	data collection, drafting manuscript, critical revision
Jing He Macquarie University	data collection, drafting manuscript, critical revision
Sharanjit Singh Tsinghua University	critical revision
Tao Kan Macquarie University	critical revision
*Behnam Dastjerdi Macquarie University	critical revision
	Provide summary for any additional Authors in this cell.

4. Author Declarations

I agree to be named as one of the authors of this work, and confirm:

i. *that I have met the authorship criteria set out in the* Authorship Standard, *accompanying the* Macquarie University Research Code,

ii. *that there are no other authors according to these criteria,*

iii. *that the description in Section 3 or 4 of my contribution(s) to this publication is accurate*

iv. *that I have agreed to the planned authorship order following the* Authorship Standard

Name of author	**Authorised *** By Signature or refer to other written record of approval (eg. pdf of a signed agreement or an email record)	**Date**
Vladimir Strezov		24/02/2021
Haftom Weldekidan		22/02/202
Jing He		22/02/202
Sharanjit Singh		22/02/2021
Tao Kan		22/02/2021
Behnam Dastjerdi		02/22/2021
	Provide other written record of approval for additional authors (eg. pdf of a signed agreement or an email record)	

5. Data storage

The original data for this project are stored in the following location, in accordance with the *Research Data Management Standard* accompanying the *Macquarie University Research Code*.

If the data have been or will be deposited in an online repository, provide the details here with any corresponding DOI.

Data description/format	**Storage Location or DOI**	**Name of custodian** if other than the corresponding author

A copy of this form must be retained by the corresponding author and must accompany the thesis submitted for examination.

Chapter 3

Lignocellulose biomass pyrolysis for bio-oil production: A review of biomass pre-treatment methods for production of drop-in fuels

Kumar, R., Strezov, V., Weldekidan, H., He, J., Singh, S., Kan, T., & Dastjerdi, B. (2020). Lignocellulose biomass pyrolysis for bio-oil production: a review of biomass pre-treatment methods for production of drop-in fuels. Renewable and Sustainable Energy Reviews, 123, 1-31. [109763]. https://doi.org/10.1016/j.rser.2020.109763

Renewable and Sustainable Energy Reviews 123 (2020) 109763

Contents lists available at ScienceDirect

Renewable and Sustainable Energy Reviews

journal homepage: http://www.elsevier.com/locate/rser

Lignocellulose biomass pyrolysis for bio-oil production: A review of biomass pre-treatment methods for production of drop-in fuels

R. Kumar[a,*], V. Strezov[a], H. Weldekidan[a], J. He[a], S. Singh[b], T. Kan[a], B. Dastjerdi[a]

[a] Department of Earth & Environmental Sciences, Faculty of Science & Engineering, Macquarie University, Sydney, NSW, 2109, Australia
[b] Department of Organic and Petrochemical Technology, School of Chemical Engineering, Hanoi University of Science and Technology, 1 Dai Co Viet, Hanoi, 10000, Viet Nam

ARTICLE INFO

Keywords:
Biomass pyrolysis
Bio-oil upgrading
Biomass pre-treatment
Physicochemical methods

ABSTRACT

Bio-oil upgrading can be achieved mainly via three types of methods that are biomass pre-treatment, catalytic upgrading and downstream bio-oil upgrading. The article aim is to review the different physicochemical biomass pre-treatment methods used to improve the physiochemical properties of the bio-oils produced from pyrolysis of treated biomass. Biomass pre-treatment could be classified as physical, thermal, chemical and biological methods. The physical methods, such as grinding and densification improve the biomass particle size and density, affecting the heat flow and mass transfer during pyrolysis, while thermal methods, such as torrefaction, decrease the activation energy of the pyrolysis process and increase the amount of hydrocarbons in the produced bio-oil. The chemical methods generally remove the minerals and alkali metals from the biomass, improve its calorific value and enhance other biomass properties. The biomass pre-treatment methods can be integrated with catalytic pyrolysis to enhance the total carbon yield and aromatic hydrocarbons in the bio-oil. This article provides review of the basic principles of the methods, important parameters that affect biomass properties, highlights the key challenges involved in each treatment method and suggests possible future recommendations to further understand the influence of the pre-treatment methods on bio-oil upgrading. In the last section, the effect of integrated catalytic pyrolysis and pre-treatment methods on bio-oil upgrading is provided.

1. Introduction

The total world energy demand is rising each year and is expected to increase by nearly 28% by 2040, estimated to be approximately 739 quadrillion Btus [1]. Fig. 1 shows historical and predicted energy consumption by non-OECD (Organisation for Economic Co-operation and Development) countries and estimation of world energy consumption by energy source. Most of the energy demand is expected to originate from the countries with strong economic growth. It has been predicted that by 2040, non-OECD countries would account for 64% of the total increase in energy consumption, which has been predicted to amount to approximately 473 quadrillion Btus, while the OPEC countries are assumed to consume about 266 quadrillion Btus of energy by 2040 [1]. Currently, most of the energy is produced by fossils fuels which release greenhouse gases, air toxics and criteria pollutants, consequently leading to environmental pollution and adverse climate change impacts. Therefore, to mitigate the environmental concerns and meet the increasing energy demand it is highly indispensable to find alternative renewable and low emission fuels. In this regard, the developing and developed countries are striving to engineer novel and innovative ways to generate clean and environmentally friendly energy and fuels [2,3]. In this perspective, lignocellulose biomass is considered among the most valuable and sustainable energy resources. Recently, it has been estimated that approximately 550 gigatonnes of biomass carbon are present on the planet, where plants contribute to approximately 450 gigatonnes of carbon [4]. Fig. 2 shows the graphical representation of the global biomass distribution by taxa.

There are a number of technologies that can utilize lignocellulose biomass or biomass waste as the feedstock to produce a variety of energy fuels or energy resources that can be utilized to generate energy. Alternatively, biomass can also be used to produce various high value-added chemicals of great agricultural and industrial importance. In this regard, pyrolysis has been considered an efficient, cost-effective and significant process to convert the organics into energy-rich products [5–7]. Pyrolysis can use various types of lignocellulosic biomass or contaminated biomass to produce bio-oil, bio-char and pyrolytic gases [5,8]. Alternatively, it can also be applied to produce valuable

Nomenclature

AFE	Ammonia Fiber Expansion
Btu	British Thermal Unit
C	Carbon
Ca	Calcium
$Ca(OH)_2$	Calcium Hydroxide
CH_4	methane
CO	Carbon Monoxide
CO_2	Carbon Dioxide
cP	Centipoise
cSt	Centistokes
Cu	Copper
DT	Dry Torrefaction
FTIR	Fourier-Transform Infrared Spectroscopy
g	gram
GC-MS	Gas Chromatography-Mass Spectroscopy
H	Hydrogen
h	hour
HCl	Hydrochloric Acid
HH	Higher Heating Value
HNO_3	Nitric Acid
H_3PO_4	Phosphoric Acid
H_2SO_4	Sulphuric Acid
HWE	Hot Water Extraction
K	Potassium
kg	kilogram
KJ	Kilo Joule
kW	kilo watt
kWth	kilo Watt thermal
l	litre
m	metre
M	Molar
MJ	Mega Joule
mg	milligram
Mg	Magnesium
MPa	Mega Pascal
min	minute
mm	milli metre
ml	milli litre
mPa.s	milli Pascal second
MW	Mega Watt
N	Nitrogen
Na	Sodium
NaOH	Sodium Hydroxide
NH_4OH	Ammonium Hydroxide
nm	nano metre
NO_x	Nitrogen Oxides
O	Oxygen
OECD	Organisation for Economic Co-operation and Development
P	Phosphorous
ppm	parts per million
s	second
S	Sulphur
SO_x	Sulphur Oxides
SE	Steam Explosion
WT	Wet Torrefaction
μm	micro meter
°C	degree Celsius

chemicals, such as levoglucosenone, which is generally produced during thermal degradation of cellulose [9]. The yield of the resultant pyrolytic products mainly depends on the type of biomass used and the variables applied during the pyrolysis process. Generally, the pyrolysis of wood biomass at 500–550 °C results in the bio-oil yield in the range of 60–80 wt%, bio-char-20-30 wt% and pyrolytic gases in the range of 20–25 wt% [5,10]. Among all the pyrolytic products, bio-oil is considered of great importance and foreseen as the future drop-in fuel, while the mixture of pyrolytic gases (CO_2, CO, CH_4, H_2 etc.) can be directly used for energy applications and the produced bio-char can be used as a soil amendment in the agriculture or as a solid fuel [8,11]. Bio-oil can be considered as a clean and renewable fuel when compared to the conventional fossil fuels, since its combustion releases a very low amount of acidic SO_x and NO_x emissions. Bio-oil can be potentially used in turbines and boilers for power and heat generation, and the upgraded bio-oil with enhanced higher heating values (HHV) can also be utilized as transportation fuel. Besides, the pyrolysis bio-oils can be used as a promising resource to produce various chemicals with high-added values. However, currently, the bio-oil is considered an unsuitable drop-in fuel because of its poor properties, such as high oxygen content, low carbon and hydrogen content, acidic pH, high instability and low HHVs. The bio-oil properties can be substantially improved by various physical, thermal, chemical and catalytic strategies. The strategies can be applied at different stages of the pyrolysis, such as pre-pyrolysis, during pyrolysis and post-pyrolysis. For example, different physical methods such as grinding, thermal treatment at mild temperatures (torrefaction), chemical treatment with acidic solution or alkali metals can be utilized for pre-treatment of biomass to remove moisture and impurities in the biomass, increasing H/C ratios and energy content, and can also be ameliorated, thereby, improving the overall fuel property of biomass for pyrolysis application. The bio-oil can be upgraded during pyrolysis using advanced and highly active catalysts. The catalysts can be mixed with the biomass and heated together, known as *in-situ* pyrolysis, or the catalyst bed can be placed downstream of the biomass and the pyrolytic vapours are passed through a catalytic bed, termed as *ex-situ* pyrolysis [10]. The catalytic pyrolysis in the both modes has shown significant improvement in the bio-oil properties and currently, is the most widely accepted and demonstrated approach for bio-oil upgrading.

A number of methods have been developed to improve the bio-oil properties which are applicable to different types of biomass. While a considerable amount of literature has been devoted to review of the catalytic upgrading of bio-oils [12–17], there is a limitation of the reviews of physicochemical methods for biomass upgrading, which have been overviewed only in certain sections of review articles [8,16,18] and some published review articles are focussed on a particular upgrading method, such as dry torrefaction and wet torrefaction [19–22]. Hence, a critical review article focussed on physicochemical methods of biomass upgrading is still lacking in the literature. Therefore, this article comprehensively reviews the various physicochemical methods applicable for biomass pre-treatment and consequently, for bio-oil upgrading, providing comprehensive information of the basic principles of the methods and important parameters that affect biomass properties. This article also highlights the key challenges involved in each treatment method and suggests possible future recommendations of the work that can be carried out to further understand the influence of pre-treatment methods on bio-oil upgrading. In the last section, the effect of integrated catalytic pyrolysis and pre-treatment methods on bio-oil upgrading has been provided.

2. Biomass pyrolysis

Biomass is a renewable source of energy, generally referred to biological organic materials derived from living organisms, which can originate from various sources, such as terrestrial forests, agricultural

crops, aquatic plants, manures and different wastes [6,27]. Photosynthesis is the primary process that makes the biomass energy-rich. In this process, plants convert the radiant energy from the sun into chemical energy in the form of glucose or any other sugar. This chemical energy stored in the biomass is released as heat or can be converted using various technologies to produce liquid and gaseous fuels. Fig. 3 presents the technologies that can be employed to generate various fuels from different types of biomass. The solid biomass can be utilized as a potential feedstock to generate various fuels (bio-oil, gases, char) using thermochemical technologies, such as pyrolysis, liquefaction and gasification, while wet biomass (organic waste, manure etc.) can be converted to renewable fuels through biochemical processes like fermentation and anaerobic digestion [25,26]. Pyrolysis is the most studied thermochemical technology because of the ability to produce gas, liquid and solid biofuels in a process that involves degradation of biomass components in an oxygen-less atmosphere at specific heating conditions [6]. The yields of generated pyrolytic products primarily depend on the structure and complexity of biomass composition (fraction of cellulose, hemicellulose and lignin) and secondly on the pyrolysis variables [6,8]. The complete thermal decomposition of biomass involves a complex array of multiple reactions, such as dehydration, decarboxylation, decarbonylation, hydrogenation, isomerization, aromatization, depolymerization and charring, to results in liquid, solid and gaseous pyrolytic products [5,27]. Mechanism of biomass pyrolysis can be described based on the decomposition of its main three components i.e. cellulose, hemicellulose and lignin into subsequent organic compounds, which has been reviewed in the previously published review articles [28,29], hence is not discussed in this article. Fig. 4 shows main pyrolytic pathways during the fast pyrolysis of cellulose, hemicellulose, and lignin.

The distribution of pyrolysis products depends on the interaction between these components during the pyrolysis process of lignocellulose biomass and other factors. Fig. 5 shows the pyrolytic behaviour of biomass with mixed components. Generally, in the biomass structure, lignin is present in the outer cell wall of the biomass, while cellulose is present within a lignin shell and hemicellulose is either located within the cellulose or present between the cellulose and lignin. All these components, for example, cellulose and lignin, cellulose and hemicellulose are mainly linked via hydrogen bonds, whereas, covalent bonds are also present between cellulose and lignin [31]. Thus, these linkages affect the pyrolytic behaviour of biomass and consequently, the production and distribution of pyrolytic products. A number of studies have demonstrated the influence of the interaction of three components of biomass on the pyrolytic behaviour of the biomass and pyrolytic products [32–35]. For example, a study demonstrated the effect of cellulose-xylan-lignin interactions on the distribution of pyrolytic products during fast pyrolysis at 525 °C, heating rate of 1000 °C/s and holding time of 15s [36]. The experimental and predicted results of thermogravimetric analysis and pyrolysis product yields were compared to estimate the possible interactions between the components, the important results of the study are shown in Table 1. Fig. 6 shows the pyrolysis mechanism of cellulose linked with lignin. The study showed that at 325 °C no interactions between the components were observed, which could be ascribed to the insignificant degradation of cellulose which occurs at this temperature. Above 375 °C, mild interactions were estimated between levoglucosan and the pyrolysis products of xylan and

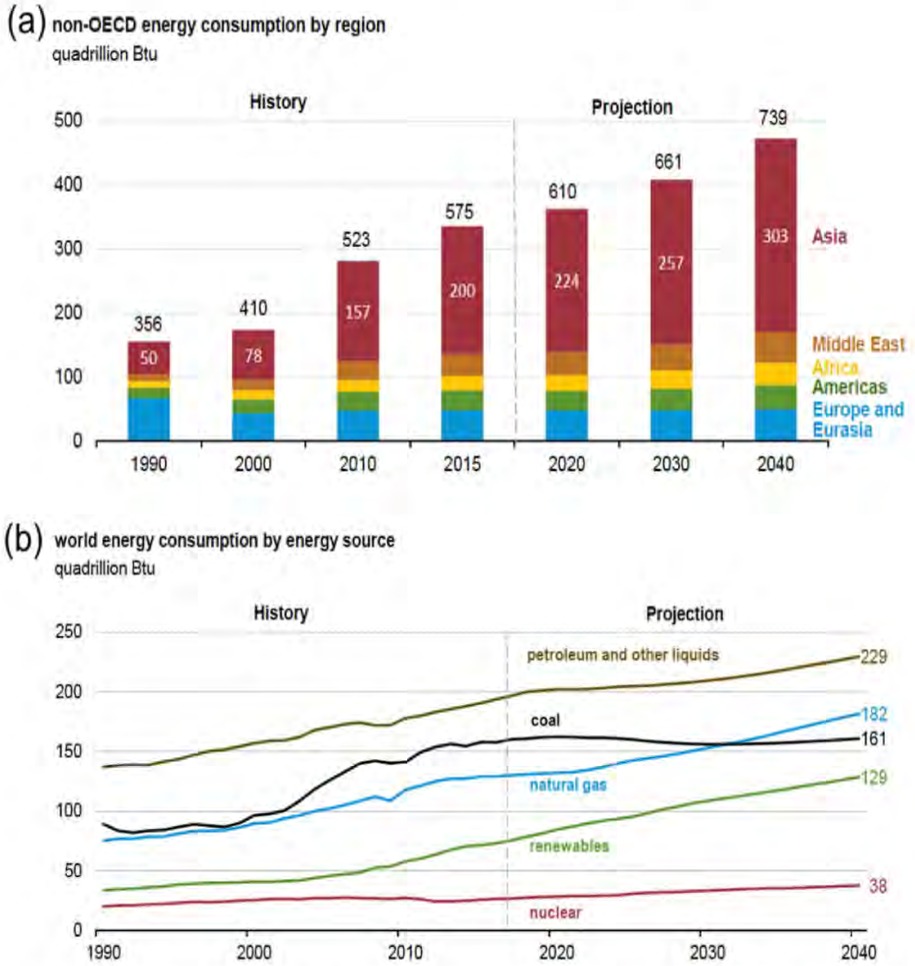

Fig. 1. (a) History and predicted energy consumption by non-OECD (Organisation for Economic Co-operation and Development) countries and (b) estimation of world energy consumption by energy source [1].

lignin, leading to significant changes in product yields. However, at 525 °C, significant interactions were present between cellulose and xylan, cellulose and lignin but no obvious interactions between xylan and lignin were observed [36]. Recently, Volpe et al. [35] demonstrated the synergetic effect between lignin and cellulose during slow pyrolysis at varying temperatures (400–600 °C) with a heating rate of 150 °C/min. The pyrolytic results of the model synthetic mixtures (cellulose/lignin) were compared with real feedstocks, which revealed that the presence of lignin in synthetic mixture behaved differently than the real feedstocks during the pyrolysis process. The results showed that the addition of lignin increased the char yield and decreased the tar yield from the pyrolysis of the synthetic mixture, while it was also responsible for the increased concentration of CO_2 in both synthetic and real biomass samples, attributing to involvement of water molecules released from the pyrolysis of cellulose and lignin to facilitate water gas shift reaction. However, the presence of lignin in the synthetic mixtures inhibited the production of H_2 in the gas, whereas the pyrolysis of real biomass samples showed higher concentration of H_2, ascribed to the presence of higher moisture content in the biomass samples that enhanced the breakdown and degradation of the pyrolysis intermediate molecules and also water gas shift reaction to promote the formation of H_2 [35]. It was also noticed that significant interactions were found between cellulose and lignin during the pyrolysis of herbaceous biomass, estimated by the decreased yield of levoglucosan and increased yield of furans and light weight molecular compounds, while these interactions were not observed for woody biomass [33]. More recently, Zhao et al. [32] studied the interactions of three biomass components during their co-pyrolysis process and the results suggested that considerable interactions existed between the components which influenced the production of pyrolytic products. The study found that increasing the cellulose content in the biomass enhanced the production of levoglucosan, while increasing the hemicellulose content slightly increased the yield of furfural and acetic acid and the presence of higher lignin content promoted the formation of phenolic compounds and inhibited the production of furan substances in the pyrolysis of cellulose and hemicellulose. The presence of cellulose and hemicellulose may promote the pyrolysis of lignin to produce phenolic compounds by favouring the deoxidation of polymer in the lignin structure or by cracking the polymer to produce C_2–C_6 olefins, which may undergo aromatization reactions to produce phenolic compounds [37]. Moreover, it has been noticed that hemicellulose has an inhibitory effect on the formation of carbohydrates, such as levoglucosan from cellulose pyrolysis [32].

Overall, it could be suggested that the presence and the content of each major component in the biomass plays a significant role in production of pyrolytic products. Firstly, the higher content of cellulose is responsible to obtain higher liquid products, while high hemicellulose favours the production of higher gas products and higher lignin content results in more solid residues. Previous studies have shown that cellulose-hemicellulose interactions are less prevalent as compared to cellulose-lignin and hemicellulose-lignin linkages. Moreover, it has been found that the interactions between the biomass components may vary the distribution of pyrolytic products, where the presence of lignin may promote production of phenolic compounds, cellulose and hemicellulose may favour the production of levoglucosan and furfural substances, respectively.

3. Bio-oil properties

Table 2 compares the properties of bio-oil and conventional petroleum fuel (heavy fuel oil) and Table 3 presents physiochemical properties bio-oil produced from different biomass materials without using any upgrading technique. It can be observed from both tables that the bio-oil needs a significant upgrading to compete with petroleum fuels. As shown in Table 2, the water content in bio-oil is generally between 15 and 30%, which affects its heating and ignition properties. The high-water content decreases adiabatic flame temperature (the temperature in the combustion process if no heat is lost) and combustion temperature, and also reduces the combustion reaction rates. Besides, it delays the ignition of bio-oil by reducing the vaporization rate of the droplet, which may pose serious concerns if used in compression ignition engines. The presence of water decreases the heating value but could also help to increase the pH of bio-oil. Higher oxygen content in the bio-oil also has detrimental effect on its applications. The presence of highly reactive oxygen species, such as carboxylic acids and aldehydes are responsible for its acidic pH, and their reaction with other reactive organic compounds affects the stability of the bio-oil, consequently, resulting in more concerns for storage. The acidic pH of bio-oil is responsible for its corrosive nature, making it unsuitable for use in turbines or combustion engines. The ash content in bio-oil is also slightly higher than the desired value. The ash contains some alkali metals such as sodium and potassium which are also responsible for its corrosive nature. The metals along with other inorganic particles may agglomerate, subsequently, may lead to the formation of a sludge layer on the base of the container.

Another major concern is the chemical and thermal stability of bio-oils. Usually, the bio-oil exhibits lower chemical or thermal stability when compared to heavy fuel oil due to the abundance of highly active oxygenated compounds, such as carboxylic acids, aldehydes and phenols, and low boiling point volatiles [60]. Therefore, due to low stability, some chemical reactions continue to occur between the highly active organic compounds with a change in temperature, which fluctuates the physical and chemical properties of the bio-oil. Higher amount of solid

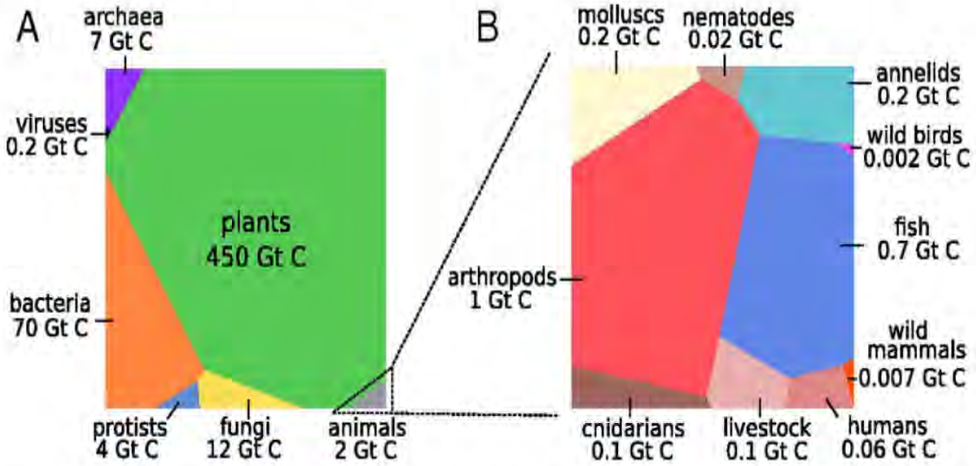

Fig. 2. Graphical representation of the global biomass distribution by taxa. (A) Absolute biomasses of different taxa are represented using a Voronoi diagram, with the area of each cell being proportional to that taxa global biomass. (B) Absolute biomass of different animal taxa. Reproduced from Ref. [4].

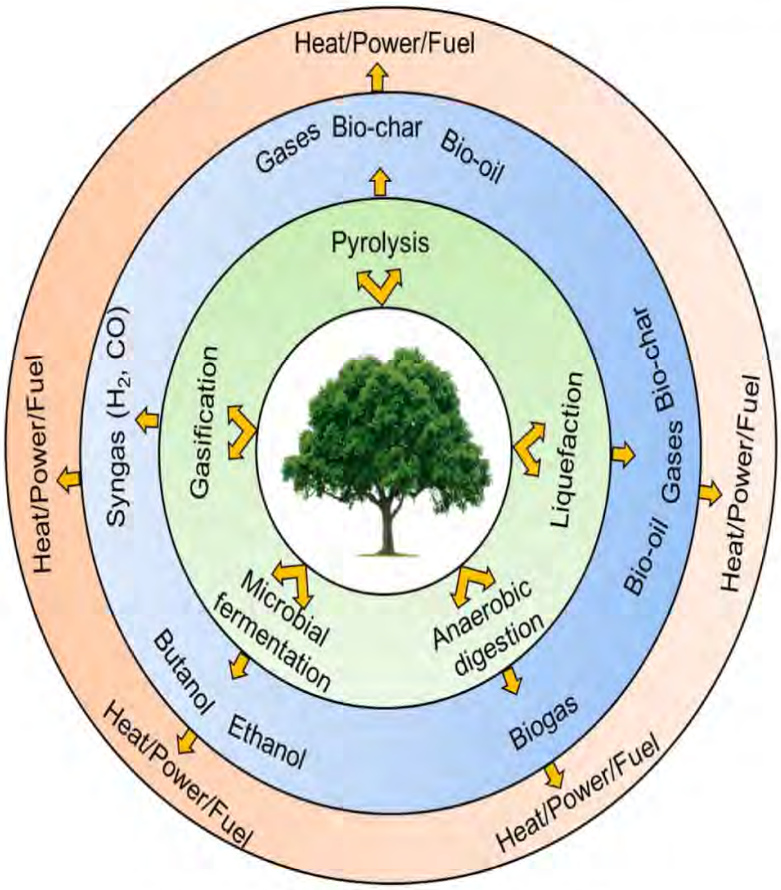

Fig. 3. Technologies that can convert biomass into different fuels.

residues leads to changes in viscosity and molecular weight of bio-oil, which further increases the problems with its storage and transportation. The HHV of the bio-oil produced from the pyrolysis process is very low as compared to the crude oil or heavy fuel oil. This is mainly because the bio-oil contains lower proportion of carbon and hydrogen that possess higher HHVs. The magnitude of HHV of a fuel indicates its heat generation potential after combustion. Therefore, in the current scenario, it could be suggested that bio-oil would produce less heat in the combustion engine comparing to heavy fuel oil. Overall, it can be concluded that bio-oil is a highly unsuitable fuel and require significant upgrading to make it a drop-in fuel, which can be either obtained by biomass pre-treatment methods or downstream bio-oil upgrading. In further sections, this article thoroughly discusses the various physico-chemical methods to improve the bio-oil properties, mainly based on biomass pre-treatment. Physical and thermal methods including grinding, densification, and dry torrefaction (DT) and chemical methods such as acid and alkali pre-treatment, wet torrefaction (WT), ammonia fiber expansion (AFE), steam explosion (SE), hot water extraction (HWE) and biological pre-treatment of lignocellulose biomass have been comprehensively reviewed.

4. Pre-treatment of biomass

4.1. Physical and thermal methods

4.1.1. Grinding

Grinding biomass feedstock is an important process to achieve high yield of quality pyrolysis products, but size reduction is an energy-intensive process and non-trivial operation which requires a considerable amount of cost and resources. The purpose of reducing feedstock size is to improve the heat flow between the substrates and decrease the degree of polymerization and crystallinity of the biomass components during the pyrolysis process which in turn affect the yield and composition of the bio-oil compounds [61]. The effect of biomass particle size on the quality and yield of the bio-oil compounds is more significant for larger particle sizes [62]. For example, the bio-oil yield was observed to decrease as the particle size increased from 0.3 to 1.5 mm in the pyrolysis of mallee wood, which could be attributed to the particle size impact on the heating process and depolymerization of lignin-derived oligomers to bio-oil compounds, however, no change was observed in the yields of bio-oil, biochar and pyrolytic gases when the particle size was increased from 1.5 to 5.2 mm. The change in bio-oil yields with increasing particle size (0.3–1.5 mm) could be attributed to the intra-particle reactions or the pyrolysis factors that influence the intra-particle reactions. In addition, the heating rate remains uniform in the smaller particles compared to the larger particles, which ultimately affects the thermal degradation of biomass constituents and subsequently the yields of pyrolytic products and bio-oil composition. In case of small particles, high heating rates may also favour bond scission reactions that could lead to the formation of volatiles and consequently, the higher bio-oil yield, while in case of larger particles comparatively slower heating rates could favour recombination reactions that could lead to charring instead of volatile formation, thereby decreasing the bio-oil yield. Another reason for lower bio-oil yield with larger particle size could be the enhanced mass resistance of bio-oil precursors to diffuse out of the larger particles that is greatly affected by the cellular structure of the biomass [63].

Particle size of the feedstock plays a pivotal role in the pyrolysis behaviour of the biomass and, consequently, affects the energy content, physical properties and organic composition of the bio-oil. It has been observed that the bio-oil composition is significantly changed with smaller biomass particles. Shen et al. [63] demonstrated decreasing yields of heavy bio-oil compounds with increasing particle sizes from 0.3 to 1.5 mm. In the same study, the yield of light weight bio-oil

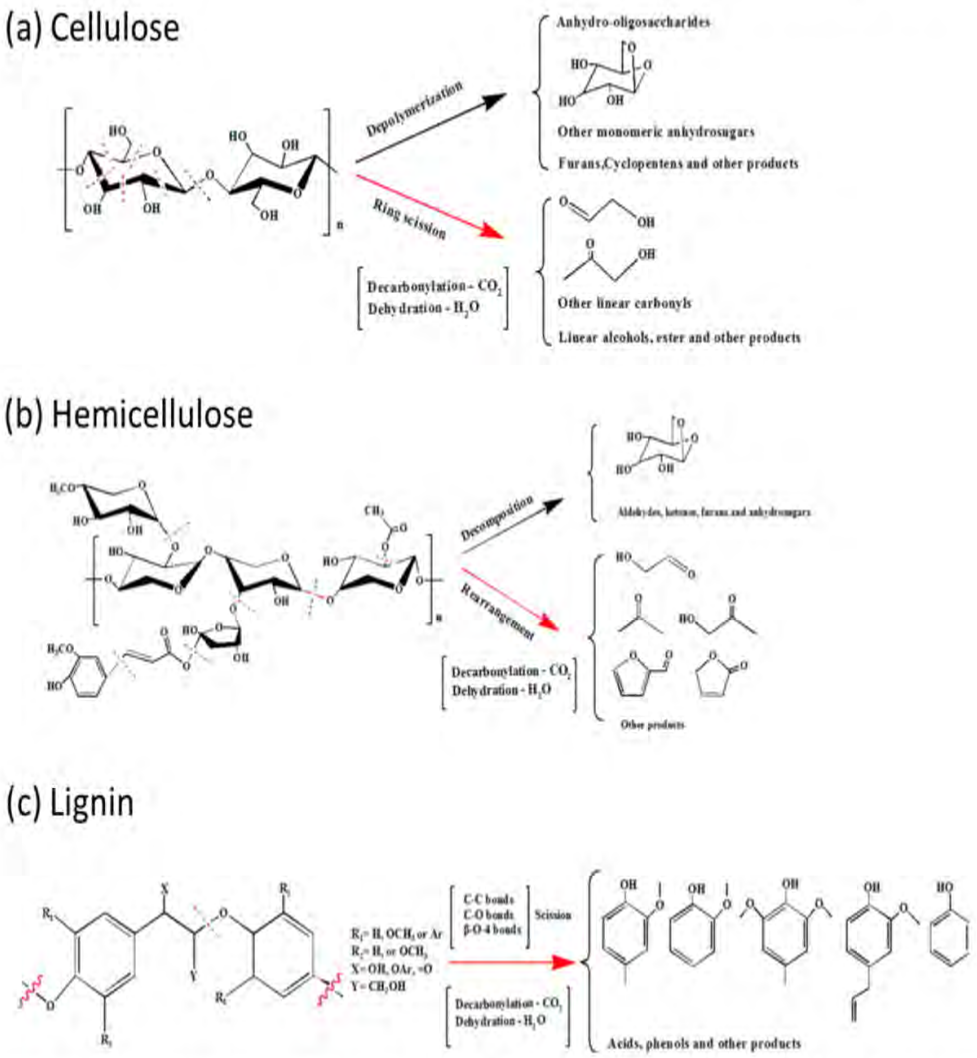

Fig. 4. Pyrolytic pathways during the fast pyrolysis of cellulose, hemicellulose, and lignin. Reproduced with permission from Ref. [30]. Copyright © 2018, American Chemical Society.

compounds was observed to increase with increasing the biomass particle size. This could be attributed to the high heating rates in the smaller particles that promoted the bond breaking reactions at the higher temperatures and favoured the diffusion of organic compounds due to the increased mass transport, while in case of larger particles, bond breaking reactions occur at a slower rate and the simultaneous bond formation reactions could take place, leading to the decrease in the mass transport. Fig. 7 shows the composition of mallee oil expressed as percent of the initial weight of biomass (on dry basis) as a function of average particle size, pyrolysis temperature of 500 °C. The impact of particle size on the yield and composition of bio-oil compounds was further demonstrated in a separate study during fast pyrolysis of different types of biomass materials consisting herbaceous, waste, residue and different blends of feedstocks with a particle size range of 2–6 mm treated at 600 °C and 14.2 °C/s. The study showed slight increments on the yield of the bio-oil compounds, indicating that pyrolysis reactions are slightly affected by samples size in these ranges of particle sizes [64]. Similar bio-oil yields were obtained from the pyrolysis of different sizes of corn stove ranging from 1 to 4 mm. On the other hand, Abnisa et al. [64] observed a decrease in the liquid yield as the particle size increased from 0.5 to 2 mm during pyrolysis of palm shell, which was attributed to the improved heating and mass transfers in the smaller particles while the heat and mass transfer restrictions greatly affect the bio-oil yield for larger particles. Kang et al. [65] also observed increasing yield of bio-oil yields with decreasing particle sizes in the pyrolysis of pine wood and babool seeds at 500 °C, respectively. The highest bio-oil yield was 24.2% but significantly increased to 54% as the particle size decreased from 2 mm to 1 mm. Similarly, the bio-oil yield was observed to increase to 32% with decreasing the babool seed diameter from 1 to 0.4 mm. The bio-oils produced from the pyrolysis of babool seed at 500 °C and particle sizes >0.4 mm had heating value of 36.45 MJ/kg which is close to the transportation grade diesel or kerosene fuels [65]. The decrease in bio-oil yield with increasing particle size is mostly associated with the non-uniform heating of particles during the heating process. It has been demonstrated that smaller particles allow an efficient heat flow between the particles and have shown positive results to increase the bio-oil yield, while the larger particles may result in non-uniform heating of the particles and could result in decreased bio-oil yield and low-quality bio-oil. Moreover, the interactions between the produced volatiles and other particles during the pyrolysis process could enhance the secondary pyrolytic reactions, resulting in enhanced gas yield and decreased bio-oil yield [66]. However, one should be careful to compare the effect of particle size of different biomass samples reported by different researchers in their studies, because the particle sizes of varying biomass samples could possess dissimilar fibrous nature and elongated shapes. In addition to this, the studies might have used different milling and sieving methods that could result in the particle sizes of different diameter and length ratios. Therefore, the fair comparison of effects of particle size on biomass pyrolysis could only be made when the biomass particles are prepared using the same milling and sieving methods for

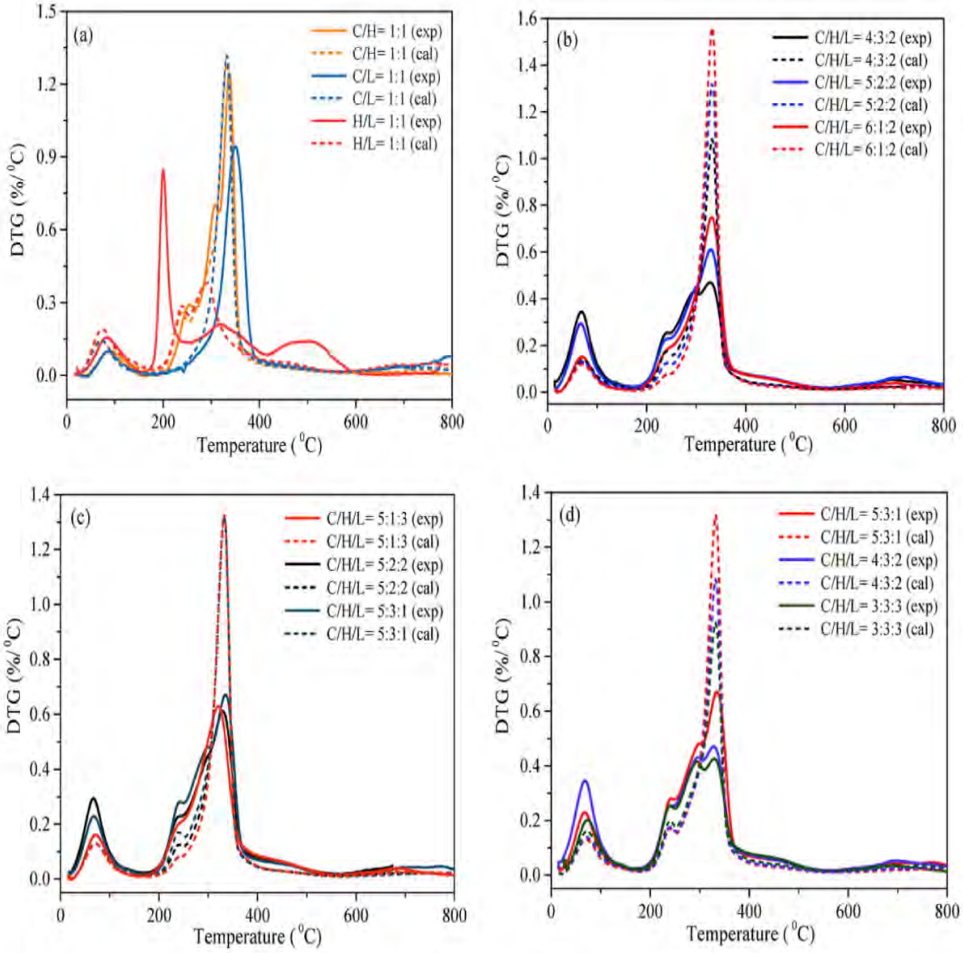

Fig. 5. Pyrolytic behaviour of biomass with mixed components, showing the expected and calculated DTG curves. Reproduced with permission from Ref. [30]. Copyright © 2018, American Chemical Society.

Table 1
Solid, liquid and gas yields from pyrolysis of individual cellulose, xylan, lignin, and mixture of these three components and real biomass samples at 525 °C, heating rate of 1000 °C/s and holding time of 15 s. Data has been taken from Ref. [42].

Sample	Pyrolysis products (wt%)		
	Solid residue	Liquid	Gas
Cellulose	2	82.3	15.7
Xylan	20.5	24.2	55.3
Lignin	34.8	46.3	18.9
Cellulose/xylan (1:1)	16.2	39.7	44.1
Cellulose/lignin (1:1)	17.5	54.1	28.4
Xylan/lignin (1:1)	27.9	35.4	36.7
Cellulose/xylan/lignin (1:1:1)	21.6	43.6	34.8
Oak[a]	9.6	65.6	24.8
Spruce[b]	7.8	62.5	29.7
Pine[c]	7.7	67.5	28.4

[a] Oak (Cellulose-43 wt%, Hemicellulose-22 wt%, Lignin-35 wt%).
[b] Pine (Cellulose-46 wt%, Hemicellulose-24 wt%, Lignin −27 wt%).
[c] Spruce (Cellulose −47 wt%, Hemicellulose −22 wt%, Lignin-29 wt%).

the same type of biomass sample.

The effect of particle size on the yield and quality of the pyrolysis oil may vary depending on the type of biomass, heating rate, temperature and other conditions. Thus, all parameters should be evaluated to identify optimum particle size at each operating condition for higher yield and quality of the pyrolysis oil. In addition to this, the requirement of biomass particle size could vary depending on the type of the reactor used in the pyrolysis process. For instance, the particle size of <200 μm,

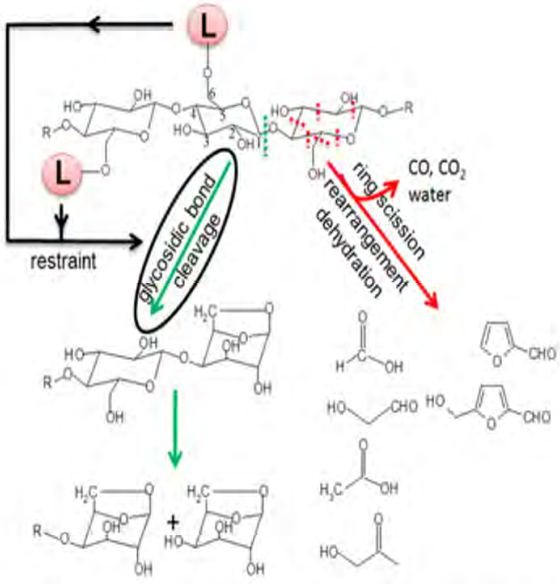

Fig. 6. Postulated pyrolysis mechanisms of cellulose covalently linked with lignin. L in picture means lignin. Reproduced with permission from Ref. [30]. Copyright © 2015, American Chemical Society.

<2 mm and <6 mm is suitable to achieve higher heating rates in rotating cone reactor, fluidised bed reactor and circulating fluidised bed reactor, respectively [67]. Although grinding could be a useful technique to

Table 2
Comparative properties of bio-oil and heavy fuel oil. Data taken from Ref. [38] with permission. Copyright © 2004, American Chemical Society.

Physical properties	Value	
	Bio-oil	Heavy fuel oil
pH	2.5	
Specific gravity	1.2	0.94
Moisture content (wt%)	15–30	0.1
Carbon (wt%)	54–58	85
Hydrogen (wt%)	5.5–7.0	11
Oxygen (wt%)	35–55	1.0
Nitrogen (wt%)	0–0.2	0.3
Ash (wt%)	0–0.2	0.1
HHV (MJ/kg)	16–19	40
Viscosity, at 500 °C (cP[a])	40–100	180
Solids (wt%)	0.2–1.0	1
Distillation residue (wt%)	Up to 50	1

[a] cP: centipoise.

prepare favourable particle sizes for biomass pyrolysis, the process requires energy input adds to the cost of processing. It has been estimated that grinding of biomass could cost around $11/t, and requires approximately 50 kWh of energy to grind 1 tonne of biomass [68]. However, the energy requirement and subsequently the total cost for the process may vary depending on the type of feedstock and the equipment used in the process.

4.1.2. Densification

One of the major limitations of using biomass as feedstock for biofuel production is its low density, which is typically around 40–200 kg/m^3 for agricultural straws and 150–250 kg/m^3 for woody biomass [22,70]. The low density could make the biomass slightly difficult to store, transport and could lead to slow heat transfer through the particles during pyrolysis. The low density of biomass could be improved through densification technique to increase the density up to 10 times and make the biomass more suitable for pyrolysis. Biomass densification is generally referred to the compaction process of biomass by applying mechanical force to produce uniformly sized solid pellets (or briquettes). The compaction mechanism could vary depending on the type of feedstock and machine used for densification. Compaction using a screw extruder generally contains the following three steps: 1) removal of air from void spaces increases the contacts between the particles, which results in the heat generation. 2) as a result of heat generation, the compact biomass becomes soft and further application of high-pressure results in the formation of local bridges and interlocking of particles. 3) Compression in tapered die forms the briquettes with uniform density. Densification changes the bulk density (generally increases), moisture content, durability index and energy contents of the biomass which can also affect the pyrolysis product distribution, heating and mass transfer efficiencies of the pyrolysis process [71]. However, the quality of the densified biomass greatly depends on various process parameters, such as pre-heating of the biomass, diameter of the die used to make pellets, pressure and binders. In addition, the energy required for the densification process also depends on the biomass properties, such as the moisture content, particle size and distribution, biomass composition (content of cellulose, hemicellulose, lignin, protein, fat) and the process parameters [22]. All these factors play an important role to the quality of densified biomass.

The effect of biomass density on the yields of pyrolysis products and bio-oil composition has been studied by several researchers. A study on

Table 3
Physiochemical properties bio-oil produced from different biomasses without using any upgrading technique.

Biomass	Reactor type	T (°C)	Bio-oil elemental analysis (wt%)				Bio-oil fuel properties						Reference
			C	H	N	O	Viscosity	Water content (wt %)	HHV (MJ/kg)	pH	Density (g/ml)	Acid value (mg of KOH/g)	
Softwood	–	600	39.96	7.74	0.11	52.19	67.39[a]	28.05	15.27	–	1.20	79.23	[39]
Oak wood	–	600	59.99	7.18	0.92	31.91	173.35[a]	15.15	24.87	–	–	–	[40]
Pine wood	–	500	42.60	8.47	0.08	48.85	175[a]	–	19.5	–	–	–	[41]
Hardwood	Fluidized bed	500	61.35	6.34	0.24	32.07	715[b]	8.93	23.5	–	–	–	[42]
Saccharina japonica	Fluidized bed	300	60.15	7.74	5.77	16.48	–	1.76	28.63	5.9	–	–	[43]
Pine wood	Auger reactor	450	–	–	–	–	55.2[c]	16.9	22.49	3.08	1.18	69.5	[44]
Pine wood	Auger reactor	450	–	–	–	–	6.49[c]	20.83	16.1	2.65	1.17	90.06	[45]
Sweetgum	Auger reactor	450	–	–	–	–	8.26[c]	38.3	2.65	2.65	1.16	119.2	[46]
Switchgrass	Auger reactor	450	–	–	–	–	1.51[c]	61.7	2.98	2.98	1.08	88.4	
Corn stover	Auger reactor	450	–	–	–	–	1.60[c]	54.7	2.66	2.66	1.08	85.8	
Saccharina japonica	Fixed bed batch	470	69.2	8.3	3.7	15.4	–	34.7	35.0	–	1.13	43	[47]
Pine nuts	Continuous fixed bed	550	58	8.2	0.3	33.5	1244[d]	9.36	19.31	4.84	1.09	–	[48]
Eucalyptus bark	Free-fall pyrolysis unit	550	–	–	–	–	–	26.07	12.45	2.78	1.13	–	[49]
Rice husk	Fluidized bed	600	–	–	–	–	58.16[d]	15.82	22.99	3.59	1.15	–	[50]
Pine wood	Pilot-scale reactor	500	42.64	7.55	0.22	49.59	178.2[c]	23.5	18.9	–	1.21	–	[51]
Walnut shell	–	550	–	–	–	–	7.98[d]	18.87	–	4.38	0.94	–	[52]
Loblolly pine chips	Fluidized bed	500	50.1	6.65	0.53	42.7	16.4[b]	19.8	–	–	–	–	[53]
Rice straw	Fluidized bed	–	34.53	6.17	1.01	57.63	–	27.20	15.62	–	–	–	[54]
Walnut shell	Spouted bed	550	37.91	8.78	1.19	25.02	3.29[d]	23.29	–	4.28	0.95	–	[55]
Pine sawdust	Fluidized bed	500	57.82	7.13	0.04	32.33	–	–	23.83	3.57	1.23	–	[56]
Oak	Fluidized bed	500	54.9	6.28	0.07	38.7	57[d]	20.3	–	–	1.24	110	[57]
Switchgrass	Fluidized bed	500	60.9	5.73	1.07	32.3	9[d]	37.6	–	–	1.15	98	
Corn stover	Fixed bed	400	–	–	–	–	2.6[b]	–	15.3	2.67	1.25	–	[58]
Prairie cord grass	Fixed bed	400	–	–	–	–	2.5[b]	–	15.2	2.59	1.25	–	
Switchgrass	Fixed bed	400	–	–	–	–	2.1[b]	–	14.9	2.77	1.25	–	
Napier grass	Fixed bed	600	45.32	7.17	0.81	46.60	2.71[b]	26.01	20.97	2.95	1.05	–	[59]

Units of viscosity, a-mPa.s; b-cP; c-cSt; d-mm^2/s.

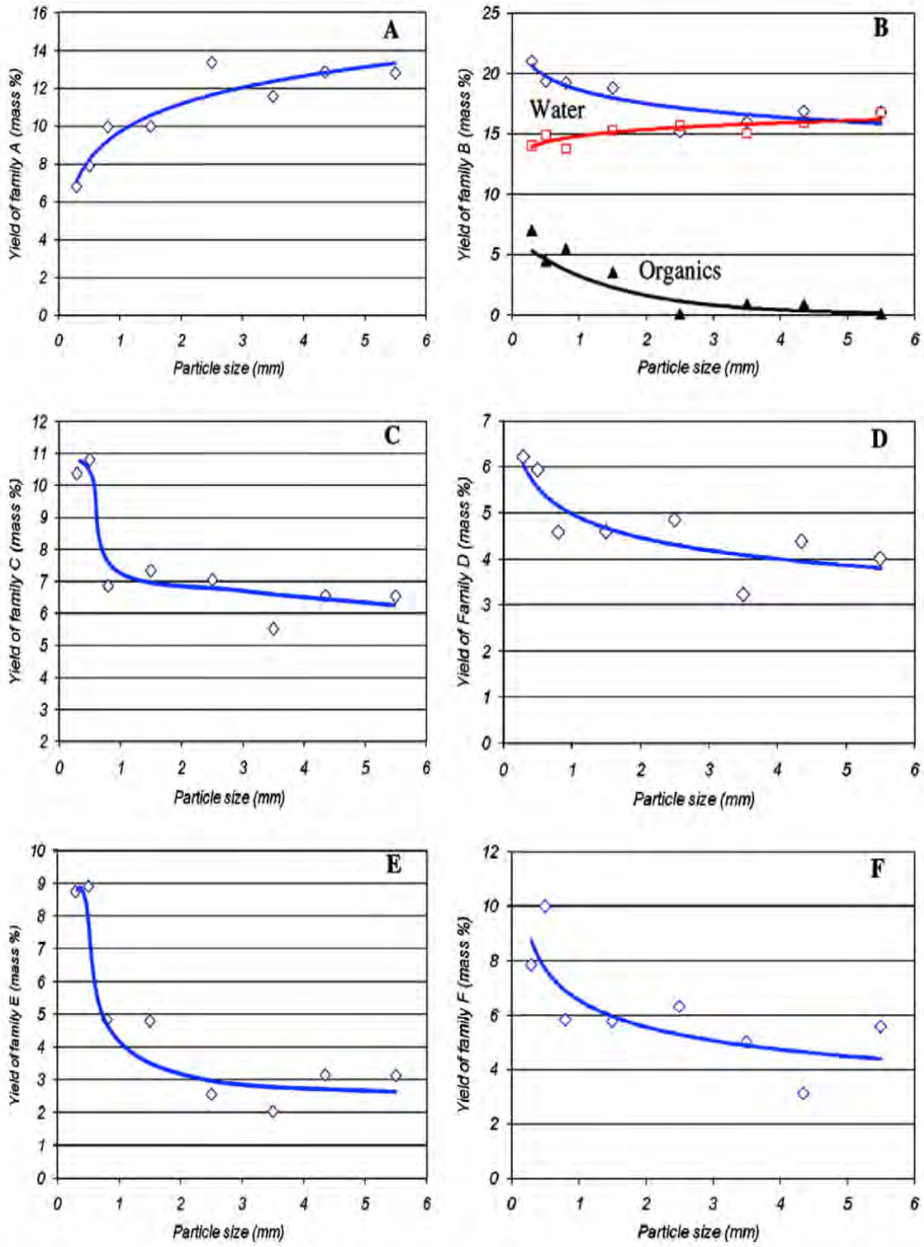

Fig. 7. Composition of mallee oil (A, B, C, D, E, F) expressed as percent of the initial biomass mass (on dry basis) as a function of average particle size, at pyrolysis temperature of 500 °C. A-F shows six families/groups of chemical compounds in the bio-oil. Peak A represents highly volatile organic compounds, mainly hydroxyacetaldehyde, formic acid and methanol. Peak B represents water but also contains other organic compounds with boiling points close to water, e.g. acetic acid, acetol and propionic acid. Peak C shows phenols and furans. Peak D is mainly due to sugars with a thermal behaviour similar to levoglucosan and some polyaromatics. Peak E represents the oligomeric compounds insoluble in water but soluble in CH_2Cl_2. Peak F is assigned to oligomeric compounds (e.g., oligosugars) soluble in water. Reproduced from Ref. [63] with permission from Elsevier.

the pyrolysis of beech wood of different sizes of pellets and particles with varying densities (290–640 kg/m^3) performed in external heat flux of 36.5 kW/m^2 and 26.5 kW/m^2 showed subtle changes in the yields of pyrolytic products and bio-oil composition [72]. However, the results showed that heat flux had significant effect on pyrolytic product yields and bio-oil composition. Noticeably, the bio-oil yields using external heat flux of 26.5 and 36.5 kW/m^2 of nearly 56 and 60 wt% were obtained using the biomass pellets or particles with bulk density of 290–640 kg/m^3. However, small changes were observed in the yields of individual organic compounds in bio-oil composition when the bulk density of the biomass was varied from 290 to 640 kg/m^3. For example, hydroxyacetaldehyde, acetic acid and hydroxypropane were the most abundant bio-oil compounds with yields of 6.6, 18.5 and 4.3 wt%, respectively. As the packing density decreased to 290 kg/m^3, the yields slightly decreased to 5.3, 17.1 and 4.2 wt%, respectively [72]. In a separate study, Rezaei et al. [69] investigated the pyrolysis of pine chip and a pine pellet which was 3–4 times denser than the pine chip and found that the rate of heat transfer in the pellets was low compared to the pine chip. The results are shown in Fig. 8. It has been suggested that heat transfer in central parts of larger particles is slow compared to the peripheral part of the particles and subsequently, show larger conductive heat resistance [73]. Besides, the larger particles show longer diffusion path and exhibit lower specific surface area. In another study, a solar-assisted pyrolysis experiment performed on beech wood demonstrated that pelletizing the feedstock can increase tar residence time which enhanced the formation of gaseous products at the expense of the tar secondary reactions [74].

In summary, densification could be highly advantageous to decrease the moisture content from the biomass, increase the durability index and energy content of the biomass, which could affect the pyrolysis kinetics

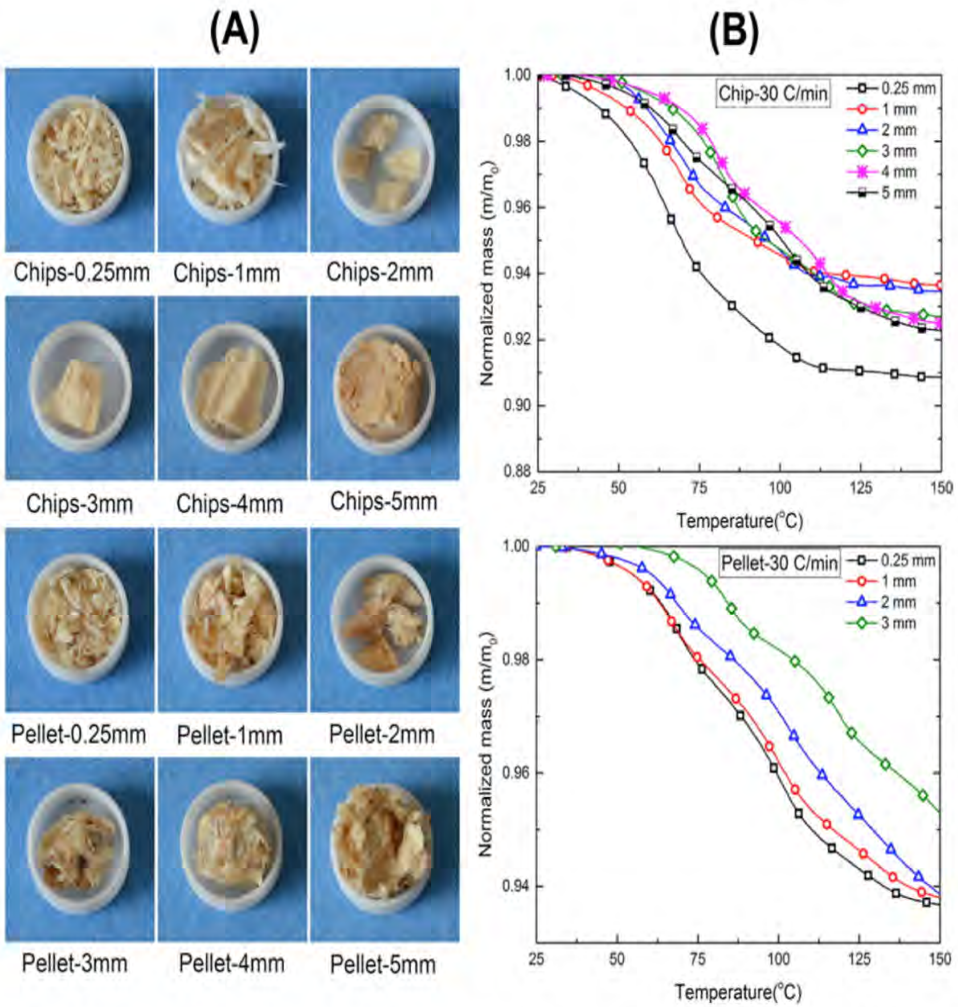

Fig. 8. (A) Different particle sizes of pine chip and pellet particles. (B) Drying mass loss curve for chip and pellet particles; heating rate of 30 °C/min and temperature of up to 150 °C. Reproduced from Ref. [69] with permission from Wiley.

but does not show any significant change in bio-oil composition. However, densification technique uses expensive instruments for compaction process and their further maintenance may increase the overall cost for bio-oil upgrading.

4.1.3. Dry torrefaction

Dry torrefaction (DT) is a thermal pre-treatment process of biomass performed at 200–300 °C and low heating rates under inert atmospheric conditions, which advances the biomass structure to produce better quality biofuels and improves economic feasibility of the pyrolysis process. During the torrefaction process, the fibrous structure and tenacity of the biomass is changed, which could help in decreasing the activation energy for the pyrolysis process [75]. Based on the temperature selection for this biomass pre-treatment process, DT can be further classified into three categories, light, mild and severe torrefaction performed at 200–235 °C, 235–275 °C and 275–300 °C, respectively [76,77]. The light torrefaction (200–235 °C) mainly affects the degradation of hemicellulose component in the biomass, which might constitute an array of reactions. For example, it may result in the breakdown of methenyl groups from the side chains and aldose groups from the main chain of the hemicellulose structure, breaking the glycosidic bonds and causing the dehydration of hydroxyl groups of the monosaccharides [78,79]. The mild torrefaction (235–275 °C) depolymerizes the hemicellulose to a large extent, while several bonds of the cellulose structure are also degraded. Torrefaction of cellulose mainly breaks the glycosidic bonds, hydrogen bonds and depolymerizes free hydroxyl groups on the glucose ring of cellulose structure [78,80]. On the other hand, the severe torrefaction (275–300 °C) degrades hemicellulose almost completely and cellulose to a large extent, while the lignin part starts degrading at this temperature. Torrefaction of lignin generally results in the breakdown of ether bonds (β-O-4 type) and promotes demethoxylation reaction in a benzene ring structure [78,81].

Oxygen migration and carbon migration are two important pathways that affect the oxygen removal and carbon content of the biomass during DT process. Both pathways could significantly affect the energy content of the biomass, where the removal of oxygen could improve the energy content, while the carbon migration could result in energy loss [103]. Torrefaction temperature and content of biomass constituents play a pivotal role in oxygen removal and carbon migration. It has been suggested that the increase in torrefaction temperature (200–300 °C) showed higher oxygen removal during torrefaction of hemicellulose compared to cellulose and lignin, while more carbon was retained in cellulose and lignin compared to hemicellulose [78]. The dominant deoxygenation pathway during DT is dehydration, while the generation of gaseous products, such as CO_2 and CO also contribute to the removal of oxygen. On the other hand, torrefaction temperature also influences the structural properties of biomass constituents, which could further affect their pyrolysis behaviour. It has been observed that the temperature of 200–250 °C increases the crystallinity of cellulose, while further increase in torrefaction temperature has shown to decrease the crystallinity of cellulose [80], which could be attributed to recrystallization of amorphous cellulose or conversion of crystalline cellulose to amorphous cellulose at higher temperature. During torrefaction of hemicellulose at lower temperatures, dehydration and degradation of the branches are

dominant reactions, while the higher temperatures promote depolymerization of hemicellulose and fragmentation of the monosaccharide units [79]. In addition, torrefaction of lignin has been shown to favour demethoxylation and polycondensation reactions [103]. The biomass torrefied at different temperatures with improved characteristics has been applied in pyrolysis to obtain the bio-oil with upgraded physiochemical properties. However, it has been noticed that the selection of temperature is a very important parameter that decides the fate of oxygen and carbon content in the biomass, and could vary depending on the composition of the biomass constituents. Overall, torrefaction has been shown to decrease the oxygen and increase the carbon content in the biomass, consequently, increasing its HHV.

DT could be an advantageous approach to improve the biomass properties, it can alter its structural properties and enhance the carbon content. Utilisation of torrefied biomass in the pyrolysis process could help to obtain bio-oil with enhanced aromatics and calorific value. DT has shown to improve the bio-oil quality, reduce the oxygen content, increase the heating value and enhance the content of hydrocarbons in the bio-oil. Table 4 summarizes the effects of DT on the yield and composition of the pyrolytic oils. However, it has been also observed that DT decreases the bio-oil yield, which can be compensated with the increased quality of the bio-oil. The decrease in the bio-oil yield can be attributed to the torrefaction induced cross linking reactions, charring of the biomass and increase in gaseous products during pyrolysis [104]. More importantly, DT increases the amount of atomic carbon and decreases the oxygen content of the biomass which in turn improves the energy conversion capacity of the biomass during pyrolysis [83]. For example, Gogoi et al. [84,87,88] compared the oxygen content of bio-oils obtained from pyrolysis of torrefied and raw arecanut husk (*Areca catechu*), and found lower oxygen content from the pyrolysis of the torrefied arecanut husk. Two studies by Ren et al. [85,86] reported that yields of aromatic hydrocarbons were greatly improved from the pyrolysis of torrefied woody biomass. Compared to the pyrolytic oils from the raw biomass, the bio-oils obtained from pyrolysis of the torrefied feedstock contained 3.21–7.5% more hydrocarbons and reduced concentration of organic acids, guaiacols and furans. The increased production of aromatics could be attributed to the enhanced deoxygenation reactions, such as dehydration, decarboxylation, decarbonylation, aromatization and rearrangement reactions. The increase of hydrocarbons in the bio-oil also improves other physiochemical properties of the bio-oil and the HHV is significantly increased. In addition, the bio-oil properties and organic composition obtained from pyrolysis of biomass are greatly affected by temperature used to pre-treat the biomass during torrefaction. For instance, a study showed that the bio-oil obtained using biomass torrefied at 240 °C had a pH of 2.49 and HHV of 15.61 MJ/kg, which increased to pH 2.69 and HHV of 18.58 MJ/kg with the biomass torrefied at 320 °C. The effect of torrefied biomass on bio-oil composition has been also investigated in several other studies. For example, DT pre-treatment was conducted on Yunnan pine biomass at different temperatures (210–300 °C) [87]. The torrefied biomass was then pyrolyzed at 450 °C and analysed the bio-oil for its yield, energy and production composition. Results showed that with increasing the torrefaction temperature phenol and hydrocarbon contents in the bio-oil markedly increased while aldehydes, acids and ketones were generally observed to decrease. During torrefaction the cellulose and hemicellulose components of the feedstock are cracked, increasing the lignin concentration for pyrolysis which results in increase of the hydrocarbon and phenolic contents of the bio-oil [105]. In a separate study, Zheng at al [106]. performed two-stage pine chips pyrolysis consisting of torrefaction at 240–320 °C and subsequent fast pyrolysis in fluidized bed reactor at 520 °C. The results showed that the total bio-oil yield, water and acetic acid contents in the bio-oil decreased with elevated torrefaction temperature, whereas the total aromaticity, higher heating value and density of the bio-oil increased. The highest bio-oil yield (55 wt%) was obtained at 240 °C and decreased to its lowest yield (23 wt%) at 320 °C (as shown in Fig. 9) whereas the highest aromatic yield and heating value which occurred at the highest temperature were 30 wt% and 19 MJ/kg, respectively.

Besides bio-oil upgrading, DT effectively enhances the contents of high value chemicals in the bio-oils. For example, all the phenolic and ketone derived bio-oil compounds obtained from the pyrolysis of a torrefied cotton stalk at 500 °C were substantially increased from 0.53 to 8.25% peak area; and 0.59–6.41% peak area, respectively; while acetic acid and furans were observed to decrease from 37 to 1.8% peak area; and from 5 to 1% peak area, respectively [75]. A recent study by Dong et al. [90] compared the bio-oil chemical composition from the pyrolysis of raw and torrefied rice straw samples. The sample was torrefied at 240 °C for 1 h in a tubular furnace reactor and pyrolyzed at 550 °C in a vertical drop fixed bead reactor. Relative contents of oxygenated compounds, such as acids, aldehydes, and ketones decreased while the relative contents of phenols increased from 28 to 42 area% in the bio-oils from the pyrolysis of the torrefied sample which could be associated to the enriched concentration of lignin after torrefaction which favours production of phenols and low weight hydrocarbon compounds [104].

The above discussion suggests that DT is a useful technique to improve the quality of biomass as well as bio-oil composition. On one hand, it can increase the amount of atomic carbon in the biomass and decrease the activation energy for pyrolysis. On the other hand, it can increase the amount of aromatic hydrocarbons in the bio-oil and its heating value. However, it has been also noticed that the pyrolysis of torrefied biomass may result in a decreased bio-oil yield and increased content of ash in the bio-oil, while the biomass with poor pelletability could be obtained after the DT process. Therefore, it is important to apply suitable temperature and residence time conditions to obtain torrefied biomass with desirable properties for the pyrolysis process. Moreover, the pyrolysis parameters and reactor configurations also play an important role in the pyrolysis behaviour of torrefied biomass and subsequently on the bio-oil upgrading.

4.2. Chemical methods

Due to the recalcitrance of lignocellulose, chemical pre-treatment is one of the most important methods for achieving desirable pyrolytic products. To destruct the lignocellulosic structure, decrease the thermal stability and alter the components in the biomass, a variety of chemical treatments have been developed prior to pyrolysis, including acid and alkali pre-treatments, hydrothermal pre-treatment, ammonia fibre expansion and steam explosion, which are discussed in the following sections.

4.2.1. Acid treatment of biomass

Lignocellulose biomass used as the feedstock in pyrolysis process generally contains inorganic minerals, which may be present in the form of phosphates, carbonates, sulphates or chlorides. These minerals exhibit some catalytic activity and hence may influence the pyrolysis behaviour of the biomass and consequently, a certain change in the pyrolytic products could be observed. In addition, some soluble inorganic species may be retained in the produced bio-oil, which would have negative effect on the physical properties of the bio-oil. For example, if present in the bio-oil the inorganics can initiate polymerization or condensation reactions that are highly unfavourable for bio-oil stability, aging and viscosity and they can also increase the corrosion activity, which may limit its application as a transportation fuel. Therefore, it is important to eliminate the inorganic minerals to avoid their further influence on the pyrolysis behaviour and bio-oil quality. In this regard, biomass pre-treatment with dilute acidic chemicals have been considered an advantageous approach to eliminate the inorganic species and simultaneously improve the bio-oil quality. In addition, the acidic pre-treatment of biomass also causes significant changes in its structure and increases its average pore diameter. Generally, the acid treatment with H_2SO_4 favours the cleavage of C–O bonds in the biomass structure, which are present in all the connections between cellulose,

Table 4
Summary of effect of torrefaction on the composition of pyrolytic oils.

Feedstock	Torrefaction temperature	Time	Pyrolysis temperature	Reactor type	Key results	Reference
Fruit bunches	493–573 K; 10 K/min	30 min		Electric furnace	-bio-oil yield decreased from 92 to 81%; calorific value increased by 18%	[83]
Loblolly pine	273–330 °C	2.5 min	500 °C; feeding rate 150 g/h	Fluidised-bed reactor	oxygen-to-carbon ratio of bio-oil decreased from 0.63 to 0.31; heating value increased from 20 to 26.3 MJ/kg	[76]
Arecanut husk	200–300 °C; 10 °C/min	30 min	300–600 °C; 40 °C/min	Fixed bed reactor	bio-oil yield decreased from 21 to 32 wt%; reduced O/C ratio of bio-oil from 0.36 to 0.28	[84]
Douglas Fir Sawdust Pellets	250–300 °C	20 min		Microwave	bio-oil with: Yield of hydrocarbon increased (3.21–7.5 area%), phenols; reduced concentration of acids, guaiacols, furans	[85] [86]
Cotton stalk	220–280 °C	30	500 °C	Fixed-bed	-phenolic (0.53–8.25 peak area%) and ketone (0.59–6.41 peak area%) derived bio-oils increased from 0.53 to 8.25 peak area%; and from 0.59 to 6.41 peak area% respectively. -acids and furnace decreased	[75]
Yunnan pine	210–300 °C	30 min	500 °C	Fixed bed reactor	- bio-oil yield decreased from 37 to 20 wt% -Phenols and hydrocarbons in bio-oil increased -aldehydes, acids and ketones decreased	[87]
Rice straw	225–275 °C	30 min	450–500 °C and 1000 °C/s	Micro pyrolysis reactor	-water, acid and oxygenated species of the bio-oil decreased -acids, aldehydes, ketones, furans and sugar contents also decreased	[88]
Corncobs feedstock	210–300 °C	20–60 min	600 °C; 20000 K/s	Semi-batch pyroprobe reactor	-bio-oil yield increased from 51 to 82% -Aromatic yield increased decreased from 29 to 16% with torrefaction temperature	[89]
Rice straw	240 °C	1 h	550 °C	Vertical drop fixed-be	-phenols increased from 28 to 42 area% -acids, aldehydes, ketones and furans decreased	[90]
Animal waste; Sewage sludge	220 and 300 °C	100–160 min	300 °C, 10 °C/min	/	- torrefaction improved hygroscopicity and heating value of the products -Bio-oil yield increased with temperature from 2.2 to 20.4 for the animal waste and 12.6 to 23.3 wt% for the sludge	[91]
Oak and scrublands	200–300 °C; at 3 °C/min		300 °C for 30 min	/	- acids, furans, alcohols, aldehydes and phenols were the main bio-oil compounds which were observed to increase with torrefaction temperature	[92]
Empty fruit bunch and mesocarp fibers	220–270 °C	60 min	300 °C	Standard retort	- liquid fraction, composed of alcohols, acids and phenols, were in the range of 6–26 wt% and contained 26 to 42 wt% of water and LHV up to 11 MJ/kg	[93]
Pigeon peak stalk	225–275 °C at 15 °C/min	15–45 min	Up to 275 °C	Split tube furnace with quartz tube reactor	- liquid yield increased from 8.84 to 35.44 wt% with torrefaction temperature and residence time	[94]
Douglas fir sawdust	250 °C	10 min	300 °C for 20 min	Microwave	-bio-oil yields increased with torrefaction temperature from 21.73 to 37.77 wt% -produced bio-oils were phenols, cyclooctene, furan, furfural, levoglucosan and others	[95]
Agricultural residues (rice straw, cotton stalk)	200–300 °C at 10 °C/min	60 min	300 °C	Fixed-bed reactor	- the highest bio-oil yields, (19.4%) for the rice straw and 15% for the cotton stalk, were obtained for the biomasses torrefied at 250 °C and 275 °C respectively	[96]
Corn stalk (wet torrefaction)	160–220 °C	30 min	550 °C	Fixed-bed reactor	- bio-oil yield from the torrefied sample increased by 3–5 wt% from the un-torrefied (raw) sample -main bio-oil components were acids (up to 40 area%), phenols (up to 20 area%), sugars (up to 75 area%), cyclopentanes (5 area %), furans (up to 8 area%) and ketones (16 area%)	[97]
Corn stalk (dry torrefaction)	200–290 °C	30 min	550 °C	Fixed-bed reactor	- bio-oil yield obtained from the torrefied sample decreased from the un-torrefied biomass -compositional distribution of the dry torrefied bio-oil compounds were similar to the wet torrefied bio-oils except the sugars component which substantially reduced to ~1 area%	[97]
Cotton stalk with Mg-based additives	200–350 °C at 50 °C/min	50 min	550 for 10 min	Fixed-bed reactor	- the bio-oil compounds from pyrolysis decreased with rising torrefaction temperature from ~6 to 10 wt% - the highest yields of aromatic hydrocarbon (~59 area%), phenols (~51 area%) and ketones (~29 area%) were obtained for 350 °C, 260 °C and 230 °C torrefied samples	[98]
Prosopis Julifloar	250 °C	30 min	300–600 W	Microwave	- guaiacols, syringols and other phenols were the major component of the bio-oil making >50%	[99]
Food waste	225–300 °C at 15 °C/min	1–3 h	Up to 300 °C for 3 h	/	- torrefaction at 275 °C was optimal while sever torrefaction at 300 °C was efficient in terms of producing bio-products with high energy contents	[100]
Herbaceous residues	210–280 °C	60 min	600 °C at 50 °C/min	/	- phenols, acids, ketones, esters and furans were the main bio-oil compounds which account for approximately 72.1% of the total detected compounds	[101]
Rubber wood	200–300 °C at 6 °C/min		500 °C for 10 min	/	- aldehydes (coniferyl aldehyde; 3,5-dimethoxy-4-hydroxycinnamaldehyde) phenols (2,6-dimethyxy-4-allylphenol; isoeugenol) and esters (diethyl phthalate) were the most prominent products	[102]

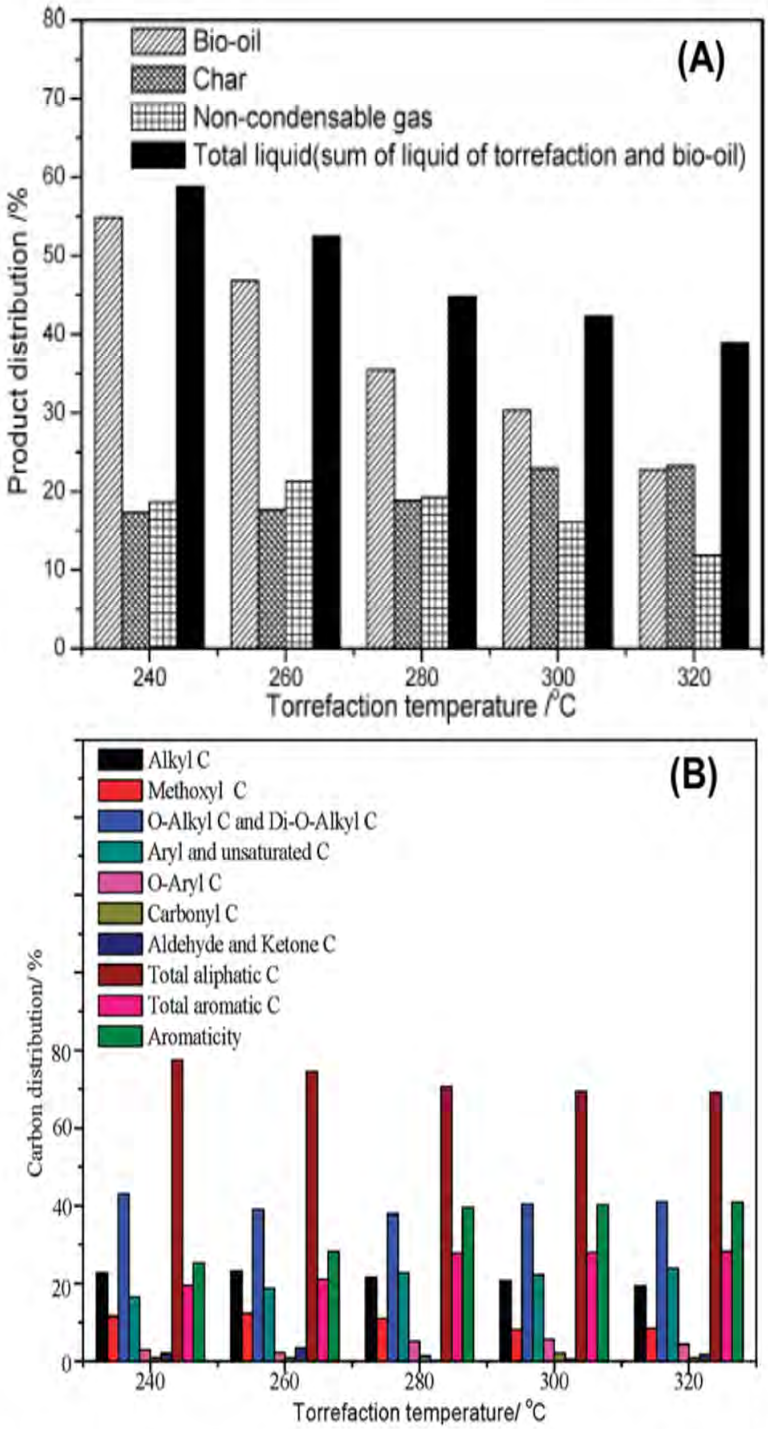

Fig. 9. (A) Effect of torrefaction temperatures on product yields of fast pyrolysis of torrefied pine. (B) Percentage of carbon distribution from ^{13}C NMR spectra of the bio-oil influenced by torrefaction temperature. Reprinted with permission from Ref. [82]. Copyright © 2012, American Chemical Society.

hemicellulose and lignin and the breaking of alkyl-aryl ether bonds in lignin [82]. Consequently, the removal of extractives, and some portions of all three biomass constituents leads to the decrease in the mass yield after the acid treatment. On the other hand, energy density of the treated biomass increases due to the increase in the heating value, mainly attributing to the removal of ash content. It has been indicated that the ash content of even 0.1% in the biomass has significant catalytic effect during pyrolysis, which could lead to decrease in the bio-oil yield [107]. However, the results of acid pre-treatment of biomass have shown to lower the ash content considerably, which could help to obtain higher yield as well as better quality of the bio-oil [59,108]. Certain minerals in the ash, such as silicon, do not affect the pyrolysis process, but alkali metals, including sodium and potassium and alkali earth metals, such as calcium and magnesium, are well known to catalyse the thermal decomposition of biomass [109,110]. The ash content in the biomass could vary depending on the uptake of minerals during plant growth. The acid treatment of biomass generally removes the soluble metals or insoluble minerals that are physiologically not attached to the plant tissue and the leaching of the minerals and metals has been observed to be improved with increase in the concentration of the acidic solvent [59, 107].

Table 5 summarizes various studies that investigated the effect of acid and alkali pre-treatments on physiochemical properties of pyrolytic bio-oil. Among the acids, H_2SO_4 is most widely used acid for biomass

Table 5
Effect of acid and alkali pre-treatment on physio-chemical properties of bio-oil.

Feedstock	Pre-treatment (concentration in wt.% to dry biomass)	Reactor configuration	T (°C)	Biomass composition (%)			Properties of pyrolytic bio-oil				Reference
				lignin	cellulose	hemi-cellulose	Yield (%)	HHV (MJ/kg)	Water content (%)	pH	
Loblolly Pine	untreated	Auger	450	39.9	33.55	27.34	54	16.10	20.83	2.65	[121]
	0.5% H_2SO_4			45.23	34.6	24.25	63	15.00	29.51	2.52	
	1% H_2SO_4			44.26	32.1	24.58	63	16.53	27.45	2.77	
	0.5% NaOH			38.26	31.62	24.80	49	/	55.57	3.15	
Loblolly Pine	untreated	Auger	450	/	/	/	/	22.49	16.9	3.08	[122]
	14% H_3PO_4			/	/	/	/	22.70	17.8	2.92	
	10.4% H_2SO_4			/	/	/	/	23.83	18.9	2.81	
	10.6% NaOH			/	/	/	/	24.4	17.6	3.76	
	10.0% $Ca(OH)_2$			/	/	/	/	21.9	17.9	3.55	
	34.4% NH_4OH			/	/	/	/	19.66	19.4	3.49	
	14.3% H_2O_2			/	/	/	/	7.28	24.0	3.62	
sweetgum	untreated	Auger	450	37.8	/	/	51	/	38.3	2.65	[123]
	1% H_2SO_4			40.6	/	/	56	/	52.2	1.99	
switchgrass	untreated			20.4	/	/	31	/	61.7	2.98	
	1% H_2SO_4			25.1	/	/	46	/	46.2	2.38	
corn stover	untreated			22.6	/	/	35	/	54.7	2.66	
	1% H_2SO_4			28.4	/	/	51	/	41.6	1.87	
Coir pith	untreated	Packed bed	500	31.2	28.6	15.3	29.4	18.66	/	/	[124]
	10% HCl + 5% NaOH			/	/	/	36.2	22.33	/	/	
Corn cob	untreated			16.6	40.3	28.7	37.4	23.81	/	/	
	10% HCl + 5% NaOH			/	/	/	43.4	24.19	/	/	
Ground nut shell	untreated			30.2	35.7	18.7	40.5	23.62	/	/	
	10% HCl + 5% NaOH			/	/	/	45.9	26.15	/	/	
Rice husk	untreated			14.3	31.3	24.3	41.2	22.45	/	/	
	10% HCl + 5% NaOH			/	/	/	57.4	23.72	/	/	
Subabul wood	untreated			24.7	39.8	24.0	22.6	24.94	/	/	
	10% HCl + 5% NaOH			/	/	/	40.1	28.54	/	/	
mallee wood	untreated	Fluidized bed	500	24.7	42.4	23.8	~61	/	~22	/	[110]
	water wash for 1 h			/	/	/	~61	/	~21	/	
	water wash for 24 h			/	/	/	~61	/	~20	/	
	water wash for 48 h			/	/	/	~61	/	~20	/	
	0.1% HNO_3 wash			/	/	/	~61	/	~16	/	
red maple wood	untreated	Pyro-probe	600	24.9	/	/	66.7	/	/	/	[125]
	hot water wash			/	/	/	45.9	/	/	/	
	hot water wash + enzymatic hydrolysis			/	/	/	10.2	/	/	/	
Empty palm fruit bunches	untreated	Semi-batch	300	18.1	59.7	22.1	30	/	/	/	[126]
	80% $Ca(OH)_2$			~16.5	/	/	/	/	/	/	
	80% NaOH			~6.5	/	/	/	/	/	/	
	80% $Ca(OH)_2$ + H_2O_2 simultaneously			~12.5	/	/	/	/	/	/	
	80% NaOH + H_2O_2 simultaneously			~5	/	/	/	/	/	/	
	80% $Ca(OH)_2$, H_2O_2 consecutively			~10	/	/	/	/	/	/	
	80% NaOH, H_2O_2 consecutively			~1	/	/	/	/	/	/	
Corn stalks	untreated (water added)	Auger	450	/	/	/	35	/	27.3	3.29	[127]
	2% H_2SO_4 (water added)			/	/	/	46	/	21	3.09	
	untreated (fed dry)	Auger	400	18.1	/	/	35	/	54.7	2.66	
	2% H_2SO_4 (fed dry)				/	/	51	/	41.6	2.87	
switchgrass	untreated	Fluidized bed	500	8.6	/	/	63.8	16.4	24.7	0.69	[128]
	water wash			8.6	/	/	67.1	16	17.2	2.8	
Festuca arundinacea	untreated			3.6	/	/	47.2	16.7	34.1	0.18	
	water wash			3.6	/	/	50.4	21.7	29.2	3	
Sugarcane bagasse	untreated	Packed bed	500	21.8	31	23.3	19.5	23.3	12	2.6	[129]
	water wash			21.2	43.4	22.2	25.6	22.2	11.2	2.5	
	50% HCl			19.9	61.8	4.4	21	21.6	8.3	2.3	
	3% HF			23.3	40.4	16.2	33.0	23.2	2.4	2.4	
Pinus radiate wood	untreated	Fluidized bed	500	28	43	26	~47	/	24	/	[130]
	1% acetic acid			28	43	26	54.6	/	17.4	/	
	torrefaction at 270 °C			44	44	10	~38	/	6.1	/	
	1% acetic acid + torrefaction at 270 °C			40	46	12	58.7	/	7.1	/	
Cotton stalk	untreated	Downdraft fixed bed	500	/	/	/	41.53	11.34	58.19	2.95	[131]
	washing with torrefaction liquid			/	/	/	41.97	12.57	55.22	3.04	
	torrefaction at 150 °C			/	/	/	27.09	14.83	41.39	3.23	
	washing + torrefaction			/	/	/	24.40	15.56	37.08	3.34	
rick husk	untreated	Vertical drop fixed-bed	550	/	/	/	~40	~12.3	~44	~2.4	[132]
	torrefaction at 210 °C			/	/	/	~36	~13	~42	~2.5	
	torrefaction at 240 °C			/	/	/	~31	~13.5	~39	~2.8	

(continued on next page)

Table 5 (*continued*)

Feedstock	Pre-treatment (concentration in wt.% to dry biomass)	Reactor configuration	T (°C)	Biomass composition (%)			Properties of pyrolytic bio-oil				Reference
				lignin	cellulose	hemi-cellulose	Yield (%)	HHV (MJ/kg)	Water content (%)	pH	
	torrefaction at 270 °C			/	/	/	~15	~15.2	~35	~3.1	
	raw biomass + organic acid leaching			/	/	/	~45	~14	~37	~3	
	torrefaction at 210 °C + organic acid leaching			/	/	/	~41	~14.5	~36	~3.1	
	torrefaction at 240 °C + organic acid leaching			/	/	/	~33	~15.3	~33	~3.3	
	torrefaction at 270 °C + organic acid leaching			/	/	/	~17	~16.2	~32	~3.5	
Napier grass	untreated	Fixed bed	600	/	/	/	~32	20.97	26.01	2.95	[59]
	water wash			/	/	/	~33	22.22	20.52	2.92	
	5% H_2SO_4			/	/	/	~38	27.96	17.36	2.68	
	5% NaOH			/	/	/	~29	21.94	27.47	3.26	

pre-treatment [59,111–113]. For instance, Mohammed et al. [59] investigated the application of different proportion of H_2SO_4 on the removal of alkali metals and bio-oil properties. They treated Napier grass feedstock with 0.5–2.5 wt% of H_2SO_4 at 70 °C for 1 h and the pyrolysis of the pre-treated biomass samples was carried out in a fixed bed reactor at 600 °C at a heating rate of 30 °C/min. The acid pre-treatment results revealed that H_2SO_4 decreased the concentration of all inorganic species in the biomass and this decrease was found proportional to the increase in the concentration of H_2SO_4. For example, treatment with 0.5 wt% of H_2SO_4 resulted in 4.10 mg/kg of Na (12.85 mg/kg in raw biomass) and 988.2 mg/kg of K (3079.5 mg/kg in raw biomass) in the biomass, which further decreased to 0.47 and 142.88 mg/kg for Na and K, respectively. Consequently, the pyrolysis results showed that the acid-treated biomass produced bio-oil with enhanced quality as compared to the untreated biomass, producing bio-oil with a higher HHV of 27.96 MJ/kg and increased carbon content of 48.95 wt%, while the bio-oil produced from untreated biomass had a HHV of 20.97 MJ/kg and C content of 45.32 wt% [59]. Similarly, other acids have also been explored for biomass pre-treatment that have shown promising results for bio-oil upgrading. For example, recently, Cao et al. [113] treated *Enteromorpha clathrate* (microalga biomass) with different acids, such as 7% H_2SO_4 7% HCl and 7% H_3PO_4 for 12 h, and these treated biomass samples were pyrolyzed in a fixed bed reactor at 550 °C. Acid-washing resulted in the significant increase in bio-oil yield. Reportedly, pyrolysis of H_2SO_4, H_3PO_4 and HCl treated biomass increased the bio-oil yield by 11.5% and 9.7% and 9.6% when compared with the untreated biomass. On the other hand, the char yield was significantly reduced, attributing to the removal of inorganic minerals that otherwise could have promoted the char formation. Further, the gas chromatography-mass spectroscopy (GC-MS) results suggested that the acid-washing resulted in reduction in acids and other oxygenated species, while a substantial increase in aliphatic hydrocarbons was observed in the bio-oil samples. For instance, HCl pre-treatment decreased approximately 37% acids and 52.6% other oxygenated compounds in the bio-oil, attributing to the disruption of hydroxyl bonds as indicated by Fourier Transform Infrared (FT-IR) spectroscopic results that showed significant reduction in O–H stretching vibration, while the content of aromatic hydrocarbons was increased by 1.5 times, mainly producing toluene (15.5%), styrene (2.5%) and ethylbenzene (1.4%) [113]. In a separate study, Hassan et al. [44] treated pine wood biomass with dilute H_2SO_4 and H_3PO_4 at 100 °C for 1 h and investigated its influence on the physiochemical properties of the bio-oil produced at 450 °C in a stainless steel auger reactor. The results showed positive effect of the acid pre-treatment on HHV of the bio-oil, which increased to 23.83 MJ/kg with H_2SO_4 and 22.70 MJ/kg with H_3PO_4 compared to untreated pine wood of 22.49 MJ/kg. However, a slight decrease in the pH values and an increase in the acidic values of the bio-oils was observed, attributing to the removal of inorganic minerals and alkali metals from the biomass post acid pre-treatments [44]. Furthermore, Tan and Wang [114] demonstrated the effect of acid pre-treatments of pine wood and rice husk biomass on the removal of inorganic species and subsequently on the bio-oil properties. The results revealed that the acid pre-treatments significantly decreased the concentration of metals ions in the biomass and increased the bio-oil yield during the pyrolysis process. For example, HCl pre-treatment of pine wood decreased the K content to ~116 ppm and increased the bio-oil yield to 52.8 wt% in comparison to the untreated biomass that showed the K content of ~984 ppm and bio-oil yield of 41.74 wt%, respectively [114]. In addition to bio-oil upgrading, acid pre-treatments can also be used to enhance the production of certain chemicals and anhydrosugars (e.g., levoglucosan) by suppressing or eliminating the effect of alkali and alkaline earth metals from biomass pyrolysis. Evidently, David et al. [115] showed a significant increase of about seven times in the formation of anhydrosugars from the pyrolysis of combined acid treatment (0.1 wt% of HNO_3 and 0.2 wt% of H_2SO_4) of sugarcane bagasse biomass pyrolyzed at 350 °C. This increase in concentration of sugars was attributed to the alkali and alkaline earth metal passivation after acid pre-treatment [115]. Acid treatment of lignocellulose biomass has also been shown to promote the formation of certain organic compounds such as 4-vinyl guaiacol and 2,3-dihydrobenzofuran that are mainly derived from thermal degradation of lignin component, indicating the breaking of $\alpha C - \beta C$ bonds and $\beta - 5$ bonds in the lignin structure post acidic treatment [116]. It should be noted that the yield of organic compounds in the pyrolytic bio-oil is greatly influenced by the concentration of acidic solvent and its ratio with biomass used in the pre-treatment process.

Overall, it can be suggested that the treatment of biomass with dilute acid solutions could be highly beneficial to improve the biomass structure and, consequently physiochemical properties of the bio-oil. It can effectively remove the inorganic species from the biomass, solubilize hemicellulose, improve cellulose digestibility and increase the amount of atomic carbon and energy conversion capacity of the biomass. The acid treatment of biomass could also prove useful to achieve the higher bio-oil yield in the pyrolysis process. The main challenge of this process could be disposal of the leachate that is highly acidic and may contain hazardous heavy metals. However, the acidic leachate might contain a higher proportion of sugars which can be subjected to biochemical conversion process to produce some value-added products or bioethanol that can be used as a liquid fuel [59]. Alternatively, the ethanol produced from the biochemical process could also be used for bio-oil stabilization during its storage as ethanol addition to the bio-oil has shown to increase the bio-oil stability [117]. Another challenge of acid pre-treatment is it causes corrosion to the reactor used for the pre-treatment process, which necessitates the use of non-corrosive construction materials that are usually expensive, thus increasing the overall operational and maintenance cost of the process. Less information is available about the possible reactions between the acid chemicals and biomass constituents (cellulose, hemicellulose, lignin) and

inorganic species (Na, K, Ca etc.) present in the biomass. Therefore, more studies should be conducted in the future to examine the chemical reactions and kinetics during the process, which could help to understand the removal mechanism of inorganic species and effect of chemicals on biomass structure.

4.2.2. Alkali treatment of biomass

Similar to acid pre-treatments, alkaline pre-treatments (such as NaOH, Ca $(OH)_2$, NH_4OH) of biomass have also been carried out to improve the biomass structure, especially to remove the lignin component and improve cellulose digestibility. The alkali treatment of lignocellulose biomass has been found to disrupt the ester and glycosidic bonds between lignin and hemicellulose, which consequently leads to solubilization of lignin and hemicellulose, keeping most part of the cellulose intact [59]. The alkali treatment of lignocellulose biomass could also result in cellulose swelling, leading to its partial decrystallization and decrease in degree of polymerization, which helps to improve the internal surface area of the treated biomass [118].

Several alkali reagents, such as NaOH, KOH, $Ca(OH)_2$, and NH_4OH have been extensively used for biomass pre-treatment and subsequently the treated biomass pyrolyzed to investigate the effect on different pyrolytic products, bio-oil composition and its physiochemical properties. Generally, during the alkali pre-treatment, the hydroxide ion and metal ion (e.g., Na^+) dissociate and the increase in concentration of hydroxide ion is directly proportional to the rate of hydrolysis reaction [119]. It has been observed that unlike acid pre-treatments, during the alkaline pre-treatment some of the alkali may convert into salts or may incorporate into the biomass as salts which in turn can inhibit the bio-oil production and increase the char formation. In addition, the alkaline treatments have been also shown to reduce the mass yield as well as energy density of the treated biomass, attributing to the removal of higher amount of lignin, while the increase in ash content could lower the heating value of the biomass [59,107]. As a result, the alkaline pre-treatment decreases the bio-oil yield as well as the concentration of anhydrosugars in the bio-oil where the acid pre-treatment usually increases the bio-oil yield and promotes the formation of anhydrosugars. Noticeably, a study by Wang et al. [45] demonstrated the pre-treatment of pinewood biomass with 0.5% NaOH and its pyrolysis in an auger reactor at 450 °C. The authors reported approximately 5% decrease in the bio-oil with treated biomass compared to the untreated biomass, while some other physical properties were also observed to be altered after NaOH treatment. For example, the higher ash and moisture contents in the bio-oil of 2.49% and 55.57%, respectively were obtained, while a lower viscosity of 1.49 cSt was observed compared to the untreated biomass (6.49 cSt). It was also noticed that the bio-oil produced from the alkaline pre-treatment had a lower concentration of levoglucosan and other anhydrosugars. This could be because the pre-treatment resulted in the attachment of the alkali metals in pinewood biomass and their catalytic effect changed the bio-oil composition, leading to the lower concentration of levoglucosan [108]. The results also revealed that NaOH treatment decreased the amount of hemicellulose and lignin pyrolyzed compounds in the bio-oil, indicating the removal of hemicellulose and lignin in the biomass following the pre-treatment [45]. This study concluded that NaOH was not advantageous for the treatment of pine wood biomass as it could not show noticeable improvement in the bio-oil yield and removal of ash content. However, other studies suggested that NaOH could be useful for pine wood treatment. The difference in the results could be due to the different pre-treatment methods and dissimilar pyrolysis operating conditions. For example, Hassan et al. [44] demonstrated alkaline pre-treatment of pine wood with NaOH, $Ca(OH)_2$, and NH_4OH and its pyrolysis at 450 °C in a stainless steel auger reactor. The bio-oil produced from all the pre-treatments showed improved physical properties, such as the pH and HHV was increased with NaOH, while $Ca(OH)_2$, and NH_4OH exhibited lower viscosities in the produced bio-oils. The higher pH of the bio-oil could be attributed to the removal of acidic groups from hemicellulose structure. In addition, GC-MS results revealed that NaOH and NH_4OH pre-treated biomass produced a lower content of levoglucosan in the bio-oil, while it increased with $Ca(OH)_2$ and the concentration of hydrocarbons improved with all the alkaline treatments, also confirmed by more pronounced C–H stretching vibrations in FTIR results [44]. The treatment with $Ca(OH)_2$ was found to depolymerize the lignin into phenolic monomers and dimers and prevents its agglomeration during the pyrolysis process, hence improving the pyrolytic behaviour of lignin and the biomass containing large proportion of lignin component [120]. Usually, the presence of phenolic hydroxyl, aldehyde and carboxylic acid groups in lignin results in the agglomeration behaviour of lignin, while the pre-treatment with $Ca(OH)_2$ reduces these phenolic hydroxyl and carbonyl containing groups by forming phenolic alcohols, hydroxylcalcium phenoxides, and phenolic carboxylate salts [120]. A possible reaction mechanism of $Ca(OH)_2$ with lignin during pre-treatment and pyrolysis has been depicted in Fig. 10.

The alkali pre-treatment has shown positive results for certain lignocellulose biomass, while few studies suggested that the alkali pre-treated biomass could not prove a suitable feedstock for pyrolysis as the resultant treated biomass is obtained with lower mass yield and higher ash content. Consequently, a lower bio-oil yield is obtained from the pyrolysis process with the treated biomass. However, alkali pre-treatment improves the biomass structure by promoting breaking of the ester and glycosidic linkages in the lignin structure. In addition, the pre-treatment method could be highly advantageous to produce specific high value-added products through pyrolysis. Noticeably, NaOH has shown to increase the yield of methanol and benzene using corncob as the biomass [116]. On the other hand, post-treatment requires washing and drying of the biomass that requires energy input, making the process more uneconomical. Similar to acidic leachate, alkaline leachate also contains small amount of sugars, probably resulted from solubilization of hemicellulose part of the biomass. Subsequently, the downstream biochemical processing of the alkaline leachate could be used to produce valuable fuels like bioethanol. Less attention has been paid to understand the possible reactions between the alkali solvents, such as NaOH and biomass constituents and reactions involved in the removal of minerals, alkali and alkali earth metals. Therefore, more studies should be conducted to examine the chemical reactions and mechanism involved in the removal of inorganic species.

4.2.3. Wet-torrefaction

Wet torrefaction (WT) (sometimes also termed as hydrothermal carbonization or hot compressed water pre-treatment) is usually defined as the biomass treatment in hydrothermal media/hot-compressed water or subcritical water at a mild temperature range of 180–260 °C [97,133–135]. A pressure higher than the saturated vapour pressure of water is applied to keep the water in the liquid phase and the heat of vaporization could increase the required energy for the process [136]. Very high pressures are usually not preferred for WT process as they do not improve the reaction rate. WT process itself results in three types of main products that are hydrochar (the solid product), a mixture of gases, and a liquid product [136,137]. In WT, hydrochar is considered as the primary product, which contains approximately 89.1% of the energy and 88.3% of the mass of the raw biomass, while in gas mixture, CO_2 is the main gas, constituting nearly 95% of the total volume. The liquid product is usually rich in phenolic compounds, organic acids, furans, furfurals and sugars [136,137]. The hydrochar which is considered as the treated biomass could be further subjected to pyrolysis process to produce quality bio-oil. Table 6 shows some of the studies that examined the effect of WT on physiochemical properties of pyrolytic bio-oil.

A number of studies reported the biomass pre-treatment in WT using varying operating conditions (temperature, pressure and residence time) and their effect on the fuel properties and consequently, on the bio-oil production in the pyrolysis process [144–147]. WT of lignocellulose biomass generally solubilizes the hemicellulose part almost completely, breaks the lignin linking interactions and leaves the cellulose part nearly

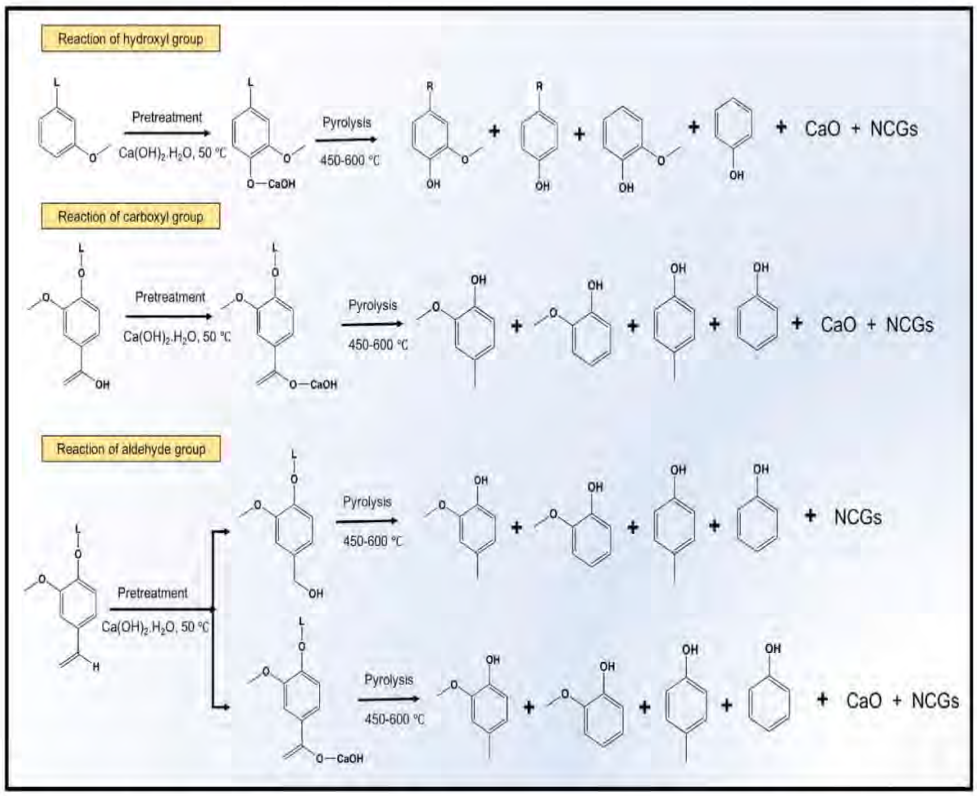

Fig. 10. Proposed reaction mechanism of lignin and calcium hydroxide during pretreatment and pyrolysis. Adapted from Ref. [120] with permission from The Royal Society of Chemistry.

retained in the solid product. Therefore, it could be predicted that WT decreases the formation of water and light compounds in the bio-oil that is mainly produced from the pyrolysis of hemicellulose, while increases the concentration of compounds derived from cellulose and lignin. Zheng et al. [143] demonstrated the application of WT of corncobs in a high pressure reactor at three different temperature of 175, 185, and 195 °C. The results showed that the concentration of hemicellulose significantly decreased from 26.71% at 175 °C and 4.52 at 195 °C, while the content of cellulose increased with rising temperature from 47.51% to 64.72% at 175 and 195 °C, respectively. Subsequently, the pyrolysis results were consistent with the composition of biomass, which revealed that the bio-oil had a higher proportion of compounds derived from the pyrolysis of cellulose. For instance, the yields of hydroxyacetaldehyde and levoglucosan were found maximum with the biomass torrefied at 195 °C, producing 1.89% and 12.13%, respectively. The enhanced production of levoglucosan was also attributed to the removal of undesirable inorganic species, which were significantly reduced after the WT process [143]. Similarly, Bach et al. [148] investigated the effect of temperature (175, 200, and 225 °C) and residence time (10, 30, and 60 min) on Norway spruce and birch woods during the WT and subsequently their effect on the pyrolysis kinetics. The results showed that WT for all the biomass samples decreased the pyrolysis temperature. However, the kinetic analysis further revealed that activation energy decreased for hemicellulose for both types of biomass, for spruce biomass it reduced from 95.67 to 26.63 kJ/mol and for birch wood it decreased from 106.80 to 34.18 kJ/mol. It is known that WT promotes the degradation and cracking of hemicellulose into simpler or smaller molecules, which exhibit a lower degree of polymerization and thus lower activation energy is observed for hemicellulose [149]. However, WT increased the activation energy of cellulose and lignin. Actually, cellulose is a semi-crystal polymer and WT increases its crystallinity [150]. During WT treatment, the number of intermolecular crosslinks increases and the crystalline region is widened [150]. The resultant higher crystallinity shows more thermal resistance and hence higher activation energy is obtained for cellulose after WT. Similarly, lignin is an amorphous and highly complex polymer and its hydrothermal treatment promotes condensation and re-polymerization reactions between the decomposed products of hemicellulose and lignin [149], resulting in higher activation energy after WT. The temperature of 200 °C and residence time of 30 min (70 bar) was found optimum for WT to achieve the maximum pyrolysis rate. Further increase in the temperature and residence time decreased the pyrolysis rate [148]. A recent study by Zhang et al. [134] also suggested that temperature higher than 200 °C is not suitable for WT, as higher contents of ash were observed in the solid char at the higher temperatures of WT.

Apart from water, some other media, such as HCl [151], acetic acid [152] and aqueous ammonia [153], have also been utilized for WT of biomass, which showed significant enhancement in the fuel properties of the produced solid char. For example, Lynam et al. [152] studied the effect of acetic acid of various concentrations (0.25–0.75 g/g of biomass) on WT of loblolly pine biomass in a Parr Series 4560 bench-top reactor using varying temperatures. The results revealed that the increasing concentration of acetic acid decreased the mass yield of the resultant char, while 200 °C was the optimum temperature to obtain the maximum mass yield which was 88.7%. During WT, acetic acid acts as a catalyst for decomposition of the biomass components, resulting in lower activation energy. However, the addition of acetic acid increased the biomass calorific value. 0.4 g of acetic acid with 1 g of the biomass was found the suitable ratio to achieve the maximum HHV of 22.09 MJ/kg, which was nearly 30% higher than the raw biomass. The increase in HHV with the addition of acetic acid was correlated with the removal of cellulose and the presence of higher lignin content in the solid char [152]. In a separate study, Li et al. [151] carried out microwave assisted WT of bamboo biomass with varying concentration of HCl at 180 °C at different residence times of 5–30 min. The results revealed that WT with 0.4 M HCl and a residence time of 30 min produced solid char with the highest carbon content of 67.03%, while 0.2 M HCl resulted in the highest HHV of 24.86 MJ/kg [151]. It was further

Table 6
Effect of wet torrefaction and steam explosion on physio-chemical properties of bio-oil.

Feedstock	Pre-treatment	Reactor configuration	T (°C)	Biomass composition (%)			Properties of pyrolytic bio-oil				Reference
				lignin	cellulose	hemi-cellulose	Bio-oil yield (%)	HHV (MJ/kg)	Water content (%)	pH	
Eucalyptus wood	untreated	Fluidized bed	500	28.25	44.08	24.02	~59	16.62	26	3.13	[138]
	wet torrefaction 160 °C			27.74	45.28	21.85	~62	17.68	21	3.15	
	wet torrefaction 170 °C			28.07	47.90	18.02	~64	17.91	19	3.14	
	wet torrefaction 180 °C			30.60	50.39	8.82	~67	18.35	18	3.17	
	wet torrefaction 190 °C			31.86	52.59	3.47	~68	18.42	18	3.15	
Sweetgum	untreated	Auger	450	37.8	/	/	51	/	38.3	2.65	[123]
	steam explosion			39.0	/	/	33	/	55.4	2.65	
Switchgrass	untreated			20.4	/	/	31	/	61.7	2.98	
	steam explosion			27.8	/	/	28	/	64.8	3.07	
Corn stover	untreated			22.6	/	/	35	/	54.7	2.66	
	steam explosion			41.0	/	/	34	/	58.7	2.47	
Loblolly Pine	untreated	Auger	450	39.9	33.55	27.34	54	16.10	20.83	2.65	[45]
	steam explosion			45.16	46.21	0	44	/	29.32	2.78	
Rice husk	untreated	Vertical drop fixed-bed	550	/	/	/	38.2	~12.2	~41	2.3	[139]
	wet torrefaction 150 °C			/	/	/	45.4	~12.9	~35	~2.4	
	wet torrefaction 180 °C			/	/	/	~44	~13.2	~33	~2.5	
	wet torrefaction 210 °C			/	/	/	42.7	~13.6	~31	~2.5	
	wet torrefaction 240 °C			/	/	/	30.2	~14	~27	2.7	
Cultivar willow	untreated	Microwave	460	~25	~41.6	~19.3	40.1	29.5	47.4	/	[140]
	wet torrefaction 160 °C		580	/	/	/	22.1	31.1	46.6	/	
Beech wood	untreated	Fixed bed	500	/	/	/	60.23	/	21.40	/	[141]
	wet torrefaction 190 °C			/	/	/	68.28	/	16.51	/	
Trembling aspen	untreated	Auger	450	24.4	52.2	23.4	56.1	13.10	41.0	2.3	[142]
	wet torrefaction 195 °C			20.0	72.0	8.0	56.2	15.33	32.0	2.2	
Corncob	untreated	Pyro-probe	500	14.34	38.49	35.36	/	/	/	/	[143]
	wet torrefaction 175 °C			18.09	47.51	26.71	/	/	/	/	
	wet torrefaction 185 °C			20.92	54.11	20.05	/	/	/	/	
	wet torrefaction 195 °C			24.39	64.72	4.52	/	/	/	/	
Corn stalk	untreated	Fixed bed	550	/	/	/	41.45	/	/	/	[144]
	wet torrefaction 230 °C			/	/	/	~38	/	/	/	
	wet torrefaction 260 °C			/	/	/	~33	/	/	/	
	wet torrefaction 290 °C			/	/	/	18.7	/	/	/	
Rice husk	untreated	Vertical drop fixed bed	500	/	/	/	40.78	/	/	/	[145]
	wet torrefaction 170 °C			/	/	/	47.70	/	/	/	

reported that the addition of HCl with a higher concentration removed almost completely the hemicellulose part and the content of cellulose was also decreased, while the lignin was increased with the residence time. The solid residue was found rich in complex condensed aromatic substance, including aromatic, carbonyl and methoxy groups, as FTIR confirmed the signals for C–H, C═C, C═O and C–O–C stretching vibrations [151]. More recently, Hu et al. [146] examined microwave assisted WT of corn stalk in aqueous ammonia (15 wt%) at 180 °C for 30 min and a pressure of up to 2 MPa, which substantially improved the fuel properties of the biomass. Noticeably, the addition of ammonia reduced the ash content from 9.87 wt% (of untreated corn stalk) to 2.19 wt%, while the carbon content and HHV values increased from 41.93 wt% to 48.15 and 14.85 MJ/kg to 17.05 MJ/kg, respectively. The surface area and porosity of the biomass were also increased after pre-treatment with ammonia. The pyrolysis of the pre-treated biomass was carried out at 800 °C and the results showed that the concentration of acids and phenols was reduced in the liquid product, while the proportion of furans, esters and ketones increased after the treatment [146]. WT of biomass with ammonia is believed to disrupt the O-acetyl groups and uronic acid on hemicellulose, consequently produces acetic acids which further promotes cracking of the ester bonds in oligosaccharides and other molecules of hemicellulose and lignin [112].

WT can be considered an effective approach to improve the fuel properties of the biomass, especially to remove the inorganic species present in the biomass and increase the calorific value of the biomass. WT can be applied to the diverse types of lignocellulosic biomass including wet or dry biomass. However, WT could be a complex process when compared to DT, which needs specific reactor materials to maintain the required temperature and pressure for the process. DT has been commercialized, while WT has been used only at the laboratory scale, mainly because of the unsuitable reactor design that requires fast heating and rapid cooling. Therefore, an advanced WT reactor is

required to improve the reaction efficiency and address the challenges related to reactor fouling. Moreover, compared to DT, WT of biomass results in wastewater that might contain toxic metals removed from the biomass during the treatment. Therefore, a proper solubilization of the toxic metals using specific solvents is pivotal before the final disposal of the wastewater. In addition, the downstream recovery of biomass further requires drying process prior to pyrolysis which is an energy-intensive step and would increase the overall cost for the WT process.

4.2.4. Ammonia fibre expansion

Ammonia fibre expansion (AFE) is another effective pre-treatment technique to improve the biomass structure and its fuel properties. This approach has been widely used for biomass pre-treatment and its conversion for biofuel production using various techniques [154–156]. AFE process is usually carried out in a special reactor, equipped with a temperature and pressure controller and an inflow for liquid ammonia. Fig. 11 shows the AFE set up. The process can be applied to a variety of biomass. Generally, the biomass is mixed with liquid ammonia in a ratio of 1:1 or 1:2 at temperature of 60–120 °C and pressure of ~2 MPa for 10–60 min in a closed vessel. The mixture of biomass and ammonia is heated to the required temperature with a holding time of approximately 5 min and then the pressure is rapidly released by opening the vent valve. This rapid release of pressure results in the evaporation of ammonia and the temperature of the system starts decreasing. AFE pre-treatment promotes the removal of acetyl groups on hemicellulose, cleavage of C–O–C bonds and lignin–carbohydrate complex linkages in lignin and decrystallization of cellulose molecules in the lignocellulose biomass. Consequently, it affects the biomass structure considerably, which may result in enhanced thermal stability, pellet durability, and bulk and particle density [58]. It has been also suggested that AFE is not very effective for pre-treatment of biomass with higher content of lignin. Several studies have been conducted to determine the optimum operating conditions, such as temperature or pressure for the pre-treatment of biomass in AFE process but the resultant pre-treated biomass has been utilized for other biofuel production, such as ethanol instead of pyrolysis, for bio-oil production. Since AFE pre-treated biomass has shown positive results for other biofuel production, it could also be used for the pyrolysis process. However, scarce information is available in the literature about the effect of AFE pre-treatment on the pyrolysis process or bio-oil composition. Sundaram et al. [58] demonstrated the effect of AFE pre-treatment on different biomass (corn stover, prairie cord grass, and switchgrass) and their effect on the composition of bio-oil during pyrolysis. The pre-treatment was carried out at 100 °C at varying loadings of ammonia and residence time, while the pyrolysis of the pre-treated biomass was carried out in a cylindrical stainless-steel reactor (batch mode) at 400 °C with a heating rate of 30 °C/min. The results revealed that AFE pre-treatment has a significant effect on physical properties of all biomass samples used in the study but it did not affect the properties of bio-oil produced after their pyrolysis. Noticeably, the pre-treated biomass showed enhanced pellet durability, thermal stability and bulk and particle density. On the other hand, the yields of pyrolytic products, such as bio-oil, biochar and pyrolytic gases were almost similar to the untreated biomass, as well as the bio-oil properties, such as pH, viscosity and heating value which did not show any noticeable changes after the AFE treatment [58]. Therefore, it can be indicated that AFE pre-treatment has less effect on biomass pyrolysis mechanism or kinetics, however, more studies should be conducted to understand its effect on the pyrolysis process and bio-oil upgrading.

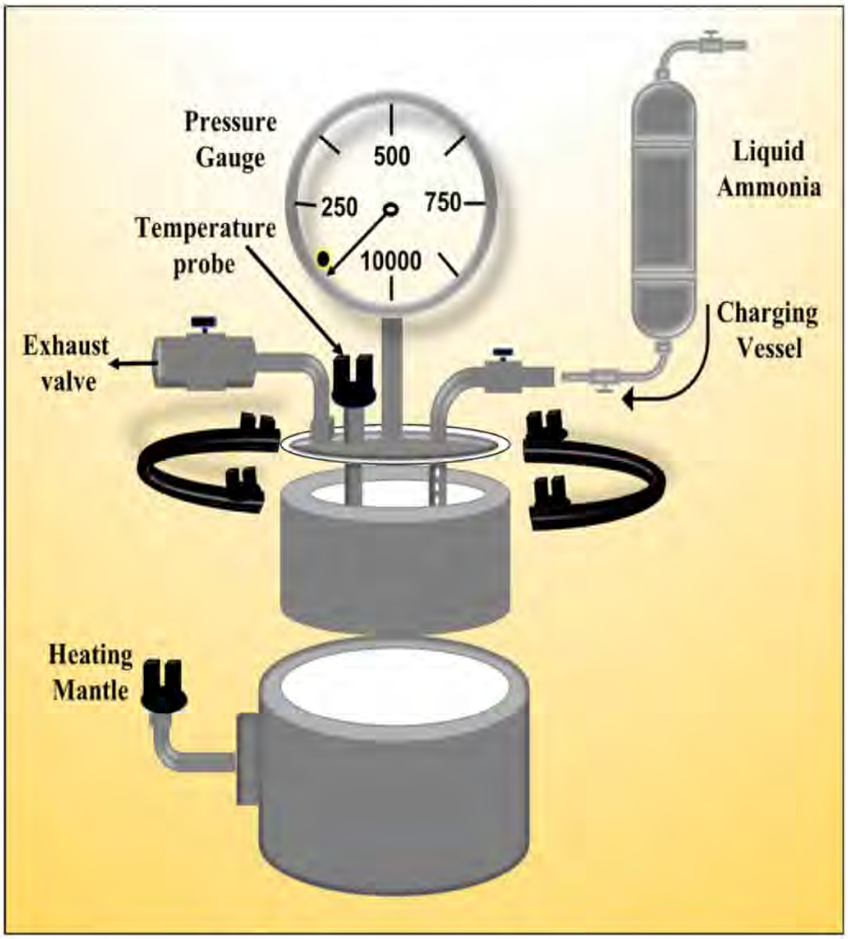

Fig. 11. Picture showing AFEX reactor setup and heating system. Adapted from Ref. [157].

4.2.5. Steam explosion

Steam explosion (SE) is a commonly used biomass pre-treatment technique to improve the biomass structure for its further applications in various processes to generate biofuels. SE could be preferred over AFE due to its low energy consumption and could prove more cost-effective or economical as it does not require any chemical addition. In the first step of the SE process, the biomass is loaded in a steam explosion vessel and water is added, at a range of different water to biomass ratios [123,158]. The vessel is then heated to obtain temperature nearly in the range of 160–260 °C and the pressure in the range of 0.69–4.83 MPa. The mixture of biomass and steam is held for a certain period of time to stimulate the hydrolysis of hemicellulose component of the biomass, followed by reduction in the pressure that allows mixture to undergo an explosive decompression. The resultant biomass or SE treated biomass is then collected through the discharge valve and dried in the oven at nearly 105–110 °C for 10–12 h, which can be further used in the pyrolysis process for bio-oil production [154]. Fig. 12 shows the schematic diagram of a steam explosive vessel. This technique also works in the similar way to WT and AFE, resulting in degradation of mainly hemicellulose and lignin components of the biomass by promoting the removal of acetyl group on hemicellulose, which produces acetic acids that further promote cracking of the ester bonds in oligosaccharides and other molecules of hemicellulose and lignin. The reduction of hemicellulose part results in creation of large pores in the biomass structure which enhances accessibility of the cellulose part [134,150]. Evidently, a study showed that after SE treatment of banana fibres, the cellulose content significantly increased from 64% to 95% and the content of hemicellulose and lignin considerably decreased to 0.4% and 1.9%, respectively [159]. SE can also lead to higher crystallinity of the cellulose and higher thermal stability due to the removal of hemicellulose and lignin [158,159]. In addition, SE pre-treatment has shown a significant decrease in the concentration of alkali and alkaline earth metals [154].

The pyrolysis of SE pre-treated biomass could show noticeable changes in the pyrolysis kinetics and also in the bio-oil composition and bio-oil physical properties. Biswas et al. [149] demonstrated the SE pre-treatment of Salix wood chips at different temperatures (approximately 205, 220, and 228 °C) and residence time of 6–12 min, and further examined their pyrolysis behaviour in a thermogravimetric analyzer, heating the biomass sample from 100 to 750 °C at a heating rate of 10 °C/min. The results reported that SE had a significant effect on the biomass structure, decreased the content of hemicellulose in the biomass, while the crystallinity of cellulose was increased as X-ray diffraction analysis revealed the narrowing of peaks at 2θ of 15 and 22° that represent the crystalline cellulose in the biomass. It was further noticed that the pyrolysis of the pre-treated biomass initiated at a lower temperature compared to the untreated biomass, attributing to the removal of hemicellulose and lignin content after the SE treatment. In a separate study, Wang et al. [45] investigated the influence of SE pre-treated pine wood biomass on the composition and physical properties of the bio-oil. SE process of the biomass was carried out in a vertical stainless-steel reactor at a temperature of 173–193 °C, pressure of 1.3 MPa and residence time of 10 min, while the pyrolysis of the pre-treated biomass was conducted in an auger reactor at a temperature of 450 °C. The results indicated the considerable changes in the bio-oil properties after SE pre-treatment. For example, the viscosity and acid value of the bio-oil decreased from 6.49 to 3.93 cSt and 90.06 to 64.16, respectively, however, the water content increased from 20.83% to 29.32%. GC-MS analysis further revealed that the pre-treated biomass produced the bio-oil with enhanced concentration of phenols that were mainly produced from the pyrolysis of lignin and cellulose and reduced the concentration of hemicellulose derived compounds, suggesting the removal of hemicellulose component during the SE process. Wang et al. [46] conducted another study demonstrating the SE pre-treatment of

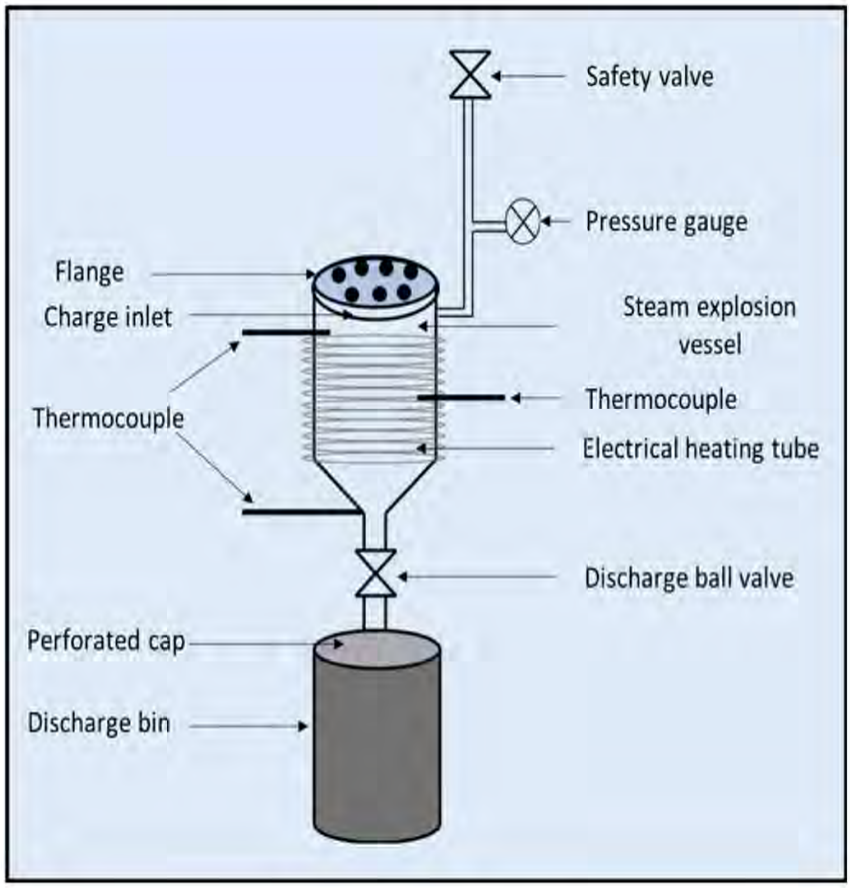

Fig. 12. Schematic of steam explosion equipment. Adapted with permission from Ref. [45]. Copyright © 2011, American Chemical Society.

three biomass samples (sweetgum, switchgrass and corn stover) using almost similar operating conditions for SE and pyrolysis and the trend of the results was also similar to the previous study. The authors reported that some of the bio-oil properties, such as viscosity and acid value, decreased and the bio-oil was enriched with phenols after the SE pre-treatment. Although SE pre-treated biomass could not produce high-quality oil during pyrolysis, certain undesirable oxygenated compounds can be removed and more valuable compounds can be produced.

Overall, it can be suggested that SE is an efficient technique to improve the biomass structure. It can result in the formation of large pores in the biomass and increase the accessibility of the cellulose component. SE has shown a remarkable decrease in the concentration of alkali and alkaline earth metals in the biomass, and decrease in viscosity and acid value of the resultant bio-oil. Besides, the technique requires low energy input. However, the process requires expensive reactor materials and higher temperature to generate the steam, which can make the process slightly expensive compared to the other techniques. Another disadvantage of SE could be the incomplete dissociation of lignin-cellulose or lignin-hemicellulose matrix, which may result in precipitation of soluble lignin constituents.

4.2.6. Hot-water extraction

Hot-water extraction (HWE) is one of the simplest and most cost-effective routes for biomass pre-treatment. It does not require any special reactor and severe temperature and pressure conditions like WT. HWE could be carried out at a temperature range of 160–230 °C. In the pre-treatment process, the biomass and water are kept in contact for nearly 15 min around 200 °C, which usually results in the breaking of hemiacetal linkages which further promotes the cleavage of ether linkages in the biomass. Consequently, HWE is useful for removing a large extent of the hemicellulose part and small part of lignin, therefore, leaving a water-resistant solid residue with higher content of lignin and cellulose. HWE is considered highly useful to improve the biomass structure to obtain a better-quality bio-oil [160]. HWE has shown substantial removal of inorganic metal species from the biomass that could have a negative effect on the pyrolysis chemistry, and their catalytic reactions may enhance the formation of char and gas and result in low bio-oil yield [44,161]. HWE technique has shown to promote the production of high-value added chemicals, such as levoglucosan [161,162].

Several studies have reported the application of hot water pre-treatment of different biomass types to improve the biomass composition and its subsequent use in pyrolysis process to ameliorate the quality of bio-oil or produce some high-value added chemicals [59,162,163]. For instance, a study demonstrated the significant reduction in the concentration of alkali and alkaline earth metals in the biomass after treating with water at different retention times from 30 min to 6 h and pyrolysis at 600 °C, producing bio-oils with varying composition and physical properties [59]. Noticeably, the concentrations of Na, K and Ca significantly reduced, while an increase in HHV of the bio-oil was noticed with the treated biomass. In a separate study, Le Roux et al. [162] carried out fast pyrolysis of hot water pre-treated (at 175–215 °C) trembling aspen (*Populus tremuloides*) and white spruce (*Picea glauca*) and the results revealed that the pre-treated biomass produced higher bio-oil yield, while the concentration of anhydrosugars was also higher compared to the untreated biomass. Furthermore, Tarves et al. [140] demonstrated the HWE of shrub willow and examined its effect on the pyrolysis product distribution. HWE was carried out using 0.5 kg oven dried biomass with a water to biomass ratio of 4:1 at 160 °C for 2 h and the pyrolysis process was performed at 500 °C. The results showed that the pre-treatment affected physical properties of the biomass and altered its elemental composition. There was a significant reduction in the concentration of inorganic minerals, such as Ca, K, Mg, P and S, while the mass fraction of hemicellulose remarkably decreased from 20.1% to 8.4% for Owasco shrub willow and the mass fraction of cellulose increased significantly from 40.2% to 54.7%. The pre-treatment also improved the surface area of the biomass by approximately twice compared to the untreated biomass. The pyrolysis results suggested some variations in the product yields, where the bio-oil yield was slightly affected, the gas yield decreased from 7.8 wt% to 5.6 wt%, mainly attributing to the decrease in CO_2 yield that suggests the removal of carbonyl functional groups in the biomass following the hot water pre-treatment. The authors further reported that the concentration of acetic acid and phenols significantly decreased in the bio-oil, while the content of levoglucosan increased approximately 4 times with the pre-treated biomass [161]. HWE technique could be more effective for biomass pre-treatment in combination with other techniques, such as ultrasonication. A combined process could be highly advantageous to increase the bio-oil yield and can reduce the residence time for HWE. Evidently, Shi et al. [160] demonstrated the application of HWE with ultrasonic pre-treatment of cellulose (at a temperature range of 240–340 °C and pressure of 12–20 MPa) and the results showed an increase of nearly 22% in the bio-oil yield, while the residence time of the process was also reduced.

Overall, it can be suggested that HWE is an efficient and cost-effective technique for biomass pre-treatment and can be applied to improve the biomass structure and remove the inorganic minerals or alkali metals in the biomass. Consequently, a higher bio-oil yield and better bio-oil quality could be obtained. However, the downstream processing of the treated biomass and its subsequent drying process requires high energy input to convert into a suitable feedstock for pyrolysis, which ultimately could increase the overall cost for bio-oil upgrading.

4.3. Biological pre-treatment of lignocellulose biomass

Biological pre-treatment of lignocellulose biomass is considered as one of the most economical and eco-friendly treatment methods since it is carried out under ambient temperature and pressure and requires no energy or chemical inputs, making the process more cost-effective as compared to the physical or chemical methods and improving the biomass composition for the production of high-value-added chemicals and energy-rich pyrolytic products [164,165]. The ultimate goal of biological treatment of lignocellulose biomass is to degrade or depolymerize complex compounds, such as lignin, into their monomer units. Biological treatment of biomass can also decompose the main linkages between lignin and hemicellulose or lignin and cellulose, consequently decreasing the activation energy and increasing the rate of reaction during thermochemical conversion of biomass at lower temperatures [165]. The microorganisms are used for the biomass pre-treatments that exhibit the ligninolytic enzyme system, mainly comprising laccases and peroxidases with a high reduction potential that oxidize the lignin polymer structure [166]. Some low molecular weight organic compounds acting as mediators (for example, 2,4,6-tri-tert -butylphenol, 4-tert -butyl-2,6-dimethylphenol, and 3-hydroxyanthranilic acid) can be used to enhance the oxidation of lignin [167]. These small sized mediators can diffuse through the cell wall pores and help the enzymes, such as laccases, to oxidize the bonds in the lignin structure, which otherwise could not be accessed by the enzymes due to their large size and selectivity. There are several microorganisms including bacteria and fungi that have shown the remarkable ability to degrade the lignocellulose biomass, but only fungi, mainly white rot fungi [166,168] and brown rot fungi [169], have been utilized for biomass pre-treatment, which has been further applied for pyrolysis process.

White rot fungi are considered the most effective microorganisms for lignin degradation due to their ability to produce adequate amount of laccases and peroxidases that effectively help in lignin oxidation, thereby, have been widely used for biomass pre-treatment [166,168]. For example, Yang et al. [168] demonstrated the application of white rot fungus *Echinodontium taxodii* for the pre-treatment of corn stover biomass and analysed its effect on the distribution of pyrolytic products. Approximately 10 g of dry biomass was pre-treated with 10 ml of the fungus seed culture at 28 °C and cultivated for 30 days. Subsequently,

the biomass was pyrolyzed at 340 °C for 1 min. The results revealed that the fungal treatment of biomass improved the pyrolysis of cellulose, hemicellulose and lignin, demonstrating its degrading effect on all the components. Noticeably, the production of pyrolytic products from cellulose and hemicellulose was greatly enhanced. The treated biomass produced enhanced number of polycyclic aromatic hydrocarbons and long chain hydrocarbons as compared to untreated biomass, indicating the effect of white rot fungus on lignin degradation. In addition, the kinetic analysis in the study showed that the biological treatment decreased the activation energy and increased the reaction rate during low temperature pyrolysis [168]. More recently, a combination of white rot fungus (*Trametes orientalis*) and brown rot fungus (*Fomitopsis pinicola*) was applied for corncob lignin treatment at 28 °C for 25 days and the pyrolysis was carried out at 600 °C for 1 min [169]. The study showed that the white rot fungus performed efficient degradation of lignin into its constituent compounds, while the brown rot fungus further promoted the breakdown of guaiacyl units. It was also noticed that in the case of treated biomass, the proportions of phenols and alkyl phenols were significantly increased. These compounds are mainly produced from the pyrolysis of lignin, indicating synergetic effect of the fungi in lignin degradation [169]. In a separate study, lignin pre-treated with *E. taxodii* (at 28 °C for 30 days) was investigated for the generation of pyrolytic products at 600 °C [170]. FTIR results confirmed that the fungus had a significant effect on lignin degradation, especially the aromatic skeletal carbon and side chain of lignin was distorted after the treatment, while the pyrolysis results showed that the formation of lignin-derived pyrolytic compounds increased using the treated biomass as compared to the untreated biomass [170]. The above discussion specifies that the biological treatment of biomass improves the pyrolysis process and kinetics of all the biomass components. The enhanced production of pyrolytic products derived from cellulose, hemicellulose and lignin indicates the degrading effect of biological treatment on all these constituents. Therefore, it could be suggested that an increased number of organic compounds and consequently, a higher liquid yield can be obtained with the treated biomass under favourable pyrolysis variables. However, the process could be time-consuming as microorganisms take longer time to decompose the biomass. Another challenge of this approach is the requirement of large amount of space to carry out the microbial pre-treatment at the pilot scale application. Some part of the carbohydrate could also be consumed by microorganisms for their growth, which could lead to decrease in mass yield of the treated biomass [171]. Since limited microorganisms have been used for biomass pre-treatment and its subsequent thermal degradation process, there is a need to further explore the application of microorganisms for biomass pre-treatment and its effect on pyrolytic behaviour as well as bio-oil upgrading.

5. Catalytic pyrolysis of pre-treated biomass

The different biomass pre-treatment methods discussed in the previous sections suggest that certain pre-treatment methods improve the biomass properties which consequently have significant impact on the distribution of pyrolysis products and bio-oil properties. However, it has been also noticed that biomass pre-treatment methods, except DT, have very less or negligible effect on improving the selectivity of hydrocarbons in the bio-oil, making the bio-oil highly rich with oxygenated compounds and hence resulting in the bio-oil with low energy density. For instance, torrefaction of biomass could increase the content of phenols in the bio-oil composition [172], while the acid treatment of biomass could increase the amount of anhydrosugars, such as levoglucosan, in the bio-oil [173]. Therefore, the conversion of different low energy density oxygenated compounds into high energy density hydrocarbons is very important to transform the bio-oil into a gasoline like liquid fuel. This can be achieved by coupling the biomass-treatment methods and catalytic pyrolysis approach. The application of different catalysts, such as zeolites, metal-zeolite based catalysts and metal oxides can successfully convert the oxygenated compounds (phenols, alcohols, acids, ketones, furans) into various desirable hydrocarbons (olefins, paraffins, monocyclic aromatic hydrocarbons and polycyclic aromatic hydrocarbons) [174–178]. The catalytic pyrolysis of pre-treated biomass samples could be carried out mainly *via* two pyrolysis modes, *in-situ* (catalyst is mixed with biomass) and *ex-situ* catalytic pyrolysis (catalyst is placed separately downstream of the biomass and the produced pyrolytic vapours are passed through the catalyst bed) [179,180]. However, more pyrolysis configurations, like two-stage or three stage *ex-situ* pyrolysis and combined *in-situ* and *ex-situ* pyrolysis, could also be applied for bio-oil upgrading [179,181,182]. The catalytic pyrolysis in all modes could significantly improve the quality of bio-oil by converting the oxygenated compounds into hydrocarbons but it also decreases the bio-oil yield and increases the gaseous products. Generally, the application of catalysts promotes the various deoxygenation reactions, such as dehydration, decarboxylation, decarbonylation, hydrogen transfer, aldol condensation, Diels-Alder reaction, aromatization and rearrangement reactions to convert the oxygen containing compounds into different hydrocarbons [183–186]. These deoxygenation reactions are believed to be catalysed primarily by the Brønsted (proton donating species) and Lewis acid (electron accepting species) sites present inside the pores as well as on the surface of the catalysts [187–189]. More critical information about the role of catalysts and pathways involved in the conversion of oxygenated compounds to hydrocarbons could be found elsewhere [185,190,191].

A number of studies have demonstrated the application of coupled biomass pre-treatment and catalytic pyrolysis, which have shown considerably enhanced bio-oil upgrading. Table 7 summarizes a few studies that utilized catalytic pyrolysis of pre-treated biomass for bio-oil upgrading. Generally, the acidic catalysts that show high number of strong Brønsted acid sites, shape selectivity, and micro and mesoporous properties are highly desirable for bio-oil upgrading. It has been found that the catalysts with a greater number of Brønsted acid sites have achieved higher proportion of aromatic hydrocarbons in the bio-oil and subsequently higher carbon yield [192,193]. Although various thermal and chemical methods can be used to pre-treat the biomass, only few methods, such as dry torrefaction, wet torrefaction and acid treatment have been coupled with catalytic pyrolysis to investigate their effect on bio-oil upgrading. For example, catalytic pyrolysis of torrefied biomass has been extensively demonstrated using zeolite-based catalysts like ZSM-5 [192,194,195]. On one hand, sole pyrolysis of torrefied biomass could generate small amount of aromatics, while considerably increasing the content of phenolics in the bio-oil. The increase in phenolic compounds could be attributed to the significant changes in the lignin structure post torrefaction process [78,103] and the subsequent thermal degradation could result into the phenolic compounds *via* cleavage of ether linkages and demethoxylation reactions [196]. The incorporation of an acidic catalyst could convert the phenolic compounds into various aromatic hydrocarbons *via* dehydration, hydrogen transfer and cracking reactions, thereby increasing the total carbon yield [172,197]. Neupane et al. [193] carried out *in-situ* catalytic pyrolysis of torrefied pine wood using HZSM-5 catalyst at 550 °C with a catalyst to biomass ratio of 9. The results showed that the noncatalytic pyrolysis of pine wood torrefied at 250 °C (for 15 min) resulted in the bio-oil with approximately 0.18% aromatics and 2.67% phenolics, while the catalytic pyrolysis of the torrefied biomass substantially increased the aromatic yield to 37.34% and reduced the phenolic yield to 0.43%. Besides the selection of a particular catalyst, there are several other factors, such as pyrolysis reactors, pyrolysis temperature, heating rate, catalyst to biomass ratio, residence time, biomass composition that affect the selectivity of hydrocarbons and other organic compounds in the bio-oil. It has been found that higher pyrolysis temperatures of 600 °C compared to 450 °C produce greater concentration of aromatic hydrocarbons, however, they also promote formation of phenolic compounds, which could be attributed to the cleavage of ether bonds in lignin structure at higher temperatures [192]. Similarly, the higher catalyst to biomass

Table 7
Effect of catalytic pyrolysis of pre-treated biomass on selectivity of aromatic hydrocarbons in bio-oil samples.

No.	Biomass	Pre-treatment		Non-catalytic pyrolysis				Catalytic pyrolysis				Reference
		Technique	Conditions	Reactor	T (°C)	HR (°C/s)	Bio-oil composition	Catalyst	Mode	C/B or FR	Bio-oil composition	
1.	Loblolly pine	DT	225 °C, 15 min	Pyroprobe	550	2000	AR-0.13%, PH-1.44%	ZSM-5	In-situ	9	AR-27.05%, PH-0.17%, BTX-14.44%	[193]
2.	Loblolly pine	DT	225 °C, 30 min	Pyroprobe	550	2000	AR-0.15%, PH-2.64	ZSM-5	In-situ	9	AR-38.25%, PH-0.26%, BTX-17.82%	[193]
3.	Loblolly pine	DT	225 °C, 45 min	Pyroprobe	550	2000	AR-0.18%, PH-2.57	ZSM-5	In-situ	9	AR-26.68%, PH-0.28%, BTX-13.13%	[193]
4.	Loblolly pine	DT	250 °C, 15 min	Pyroprobe	550	2000	AR-0.18%, PH-2.67	ZSM-5	In-situ	9	AR-37.34%, PH-0.43%, BTX-16.97%	[193]
5.	Loblolly pine	DT	250 °C, 30 min	Pyroprobe	550	2000	AR-0.20%, PH-3.26	ZSM-5	In-situ	9	AR-35.51%, PH-0.61%, BTX-16.33%	[193]
6.	Loblolly pine	DT	250 °C, 45 min	Pyroprobe	550	2000	AR-0.20%, PH-3.16	ZSM-5	In-situ	9	AR-22.05%, PH-0.14%, BTX-11.65%	[193]
7.	Loblolly pine	DT	275 °C, 15 min	Pyroprobe	550	2000	AR-0.19%, PH-3.22	ZSM-5	In-situ	9	AR-29.81%, PH-0.3%, BTX-15.72%	[193]
8.	Loblolly pine	DT	275 °C, 30 min	Pyroprobe	550	2000	AR-0.32%, PH-3.45	ZSM-5	In-situ	9	AR-19.30%, PH-0.21%, BTX-9.61%	[193]
9.	Loblolly pine	DT	275 °C, 45 min	Pyroprobe	550	2000	AR-0.32%, PH-2.94	ZSM-5	In-situ	9	AR-8.57%, PH-0.04%, BTX-4.30%	[193]
10	Corncobs	DT	210 °C, 40 min	Pyroprobe	600	20,000	AR-27.14%	HZSM-5	In-situ	9	PAH-32.7%, BTX-40.0%	[89]
11.	Corncobs	DT	240 °C, 40 min	Pyroprobe	600	20,000	AR-25.35%	HZSM-5	In-situ	9	PAH-30.1%, BTX-43.9%	[89]
12.	Corncobs	DT	270 °C, 40 min	Pyroprobe	600	20,000	AR-20.0%	HZSM-5	In-situ	9	PAH-31.4%, BTX-45.7%	[89]
13.	Corncobs	DT	300 °C, 40 min	Pyroprobe	600	20,000	AR-12.67%	HZSM-5	In-situ	9	PAH-26.0%, BTX-51.1%	[89]
14.	Corncobs	DT	270 °C, 20 min	Pyroprobe	600	20,000	AR-22.18%	HZSM-5	In-situ	9	PAH-28.2%, BTX-47.8%	[89]
15.	Corncobs	DT	270 °C, 40 min	Pyroprobe	600	20,000	AR-20.18%	HZSM-5	In-situ	9	PAH-31.4%, BTX-45.7%	[89]
16.	Corncobs	DT	270 °C, 60 min	Pyroprobe	600	20,000	AR-16.72%	HZSM-5	In-situ	9	PAH-25.5%, BTX-49.0%	[89]
17.	Pine wood	DT	225 °C, 30 min	Pyroprobe	650	2000	AR-8.64%, TCY-18.15%	ZSM-5	In-situ	9	[a]AR-9.57%, PH-1.18%	[192]
18.	Pine wood	DT	225 °C, 30 min	Pyroprobe	650	2000	AR-8.64%, TCY-18.15%	ZSM-5	In-situ	9	[b]AR-15.27%, PH-2.45%	[192]
19.	Pine wood	DT	225 °C, 30 min	Pyroprobe	650	2000	AR-8.64%, TCY-18.15%	ZSM-5	In-situ	9	[c]AR-18.68%, PH-6.17%	[192]
20.	Pine wood	DT	225 °C, 30 min	Pyroprobe	650	2000	AR-8.64%, TCY-18.15%	ZSM-5	In-situ	9	[d]AR-24.22%, 7.67%	[192]
21.	*E. globulus*	DT	304 °C, 15 min	Micropyrolysis unit	500	2000	AR-9.21%, PH-22.48%	HZSM-5	In-situ	5	BTX-26%, PAH-29%, PH-8%	[201]
22.	*E. globulus*	DT	304 °C, 15 min	Micropyrolysis unit	500	2000	AR-9.21%, PH-22.48%	Ni/CAG	In-situ	5	BTX-6.7%, PAH-0%, PH-10%	[201]
23.	*E. globulus*	DT	304 °C, 15 min	Micropyrolysis unit	500	2000	AR-9.21%, PH-22.48%	Fe/CAG	In-situ	5	BTX-5.6%, PAH-0%, PH-8%	[201]
24.	Rice husk	Acid + DT	Acetic acid-30 °C, 4 h DT-210 °C, 1 h	Fixed bed	550	/	PH-23.9%, AC-4.24%	ZSM-5	Ex-situ	5	BTX-45.79%, PAH-3.01%	[195]
25.	Rice husk	Acid + DT	Acetic acid-30 °C, 4 h DT-240 °C, 1 h	Fixed bed	550	/	PH-24.51%, AC-3.15%	ZSM-5	Ex-situ	5	BTX-48.88%, PAH-2.59%	[195]
26.	Rice husk	Acid + DT	Acetic acid-30 °C, 4 h DT-270 °C, 1 h	Fixed bed	550	/	PH-29.00%, AC-1.94%	ZSM-5	Ex-situ	5	BTX-53.99%, PAH-1.75%	[195]
27.	Rice husk	Acid	Acetic acid-30 °C, 4 h	Fixed bed	550	/	PH-23.17%, AC-5.33%	ZSM-5	Ex-situ	5	BTX-43.86%, PAH-3.34%	[195]
28.	Lignin pine	DT	150 °C, 15 min	Tandem microreactor	500	/	PH-11.2%, TCY-82.2%	HZSM-5	In-situ	4	BTX-51.4%, TCY-91.8%	[202]
29.	Lignin pine	DT			500	/		HZSM-5		4		[202]

(continued on next page)

Table 7 (*continued*)

No.	Biomass	Pre-treatment		Non-catalytic pyrolysis				Catalytic pyrolysis				Reference
		Technique	Conditions	Reactor	T (°C)	HR (°C/s)	Bio-oil composition	Catalyst	Mode	C/B or FR	Bio-oil composition	
			175 °C, 15 min	Tandem microreactor			PH-13.1%, TCY-77.2%		In-situ		BTX-56.3%, TCY-91.7%	
30.	Lignin pine	DT	200 °C, 15 min	Tandem microreactor	500	/	PH-15.7%, TCY-77.91%	HZSM-5	In-situ	4	BTX-58.9%, TCY-92.2%	[202]
31.	Lignin pine	DT	225 °C, 15 min	Tandem microreactor	500	/	PH-18.1%, TCY-76.9%	HZSM-5	In-situ	4	BTX-61.4%, TCY-93.4%	[202]
32.	Lignin switchgrass	DT	150 °C, 15 min	Tandem microreactor	500	/	PH-13.5%, TCY-78.3%	HZSM-5	In-situ	4	BTX-50.2%, TCY-89.5%	[202]
33.	Lignin switchgrass	DT	175 °C, 15 min	Tandem microreactor	500	/	PH-15.1%, TCY-78.2%	HZSM-5	In-situ	4	BTX-52.9%, TCY-91.5%	[202]
34.	Lignin switchgrass	DT	200 °C, 15 min	Tandem microreactor	500	/	PH-16.2%, TCY-76.7%	HZSM-5	In-situ	4	BTX-56.8%, TCY-92.2%	[202]
35.	Lignin switchgrass	DT	225 °C, 15 min	Tandem microreactor	500	/	PH-16.8%, TCY-76.0%	HZSM-5	In-situ	4	BTX-59.4%, TCY-91.9%	[202]
36.	Pine wood	DR	220 °C, 30 min	Fixed bed	550	/	AR-24.38%, PH-40.17%	HZSM-5	Ex-situ	0.5	AR-21.29%, PH-32.51%	[203]
37.	Pine wood	DR	250 °C, 30 min	Fixed bed	550	/	AR-29.33%, PH-42.29%	HZSM-5	Ex-situ	0.5	AR-23.06%, PH-35.84%	[203]
38.	Pine wood	DR	280 °C, 30 min	Fixed bed	550	/	AR-30.15%, PH-44.76%	HZSM-5	Ex-situ	0.5	AR-26.18%, PH-37.71%	[203]
39.	Lignocel HBS	WT	190 °C, 8 min, water	Fixed bed	500	/	PH-20.51%, AC-5.76%	HZSM-5	Ex-situ	0.46	AR-41.31%, PAH-22.56%, PH-17.93%	[200]
40.	Lignocel HBS	WT	190 °C, 8 min, water	Fixed bed	500	/	PH-20.51%, AC-5.76%	Al-MCM-41	Ex-situ	0.46	AR-7.77%, PAH-11.73%, PH-32.82%	[200]
41.	Lignocellulose biomass	Acid	Acetic acid-85 °C, 30 min	Fixed bed	600	/	High acids and sugars	HZSM-5	Ex-situ	1	High BTX yield	[204]

C/B-catalyst to biomass; FR-feed rate; DT-dry torrefaction; WT-wet torrefaction; AC-acids; AR-aromatics; PH-phenols; BTX-benzene, toluene, xylene; PAH-polycyclic aromatic hydrocarbons; Oxy-oxygenates; TCY-total carbon yield; CAG-cellulose derived carbon aerogels.

[a] catalytic pyrolysis was carried out at 450 °C.

[b] catalytic pyrolysis was carried out at 500 °C.

[c] catalytic pyrolysis was carried out at 550 °C.

[d] catalytic pyrolysis was carried out at 600 °C.

ratios favour production of monocyclic as well polycyclic aromatic hydrocarbons but decrease the bio-oil yield and increase the gas yield [198]. Higher amount of the catalyst could provide increased number of active sites to carry out the different deoxygenation reactions, thereby increasing the kinetics of pyrolysis process and conversion of oxygenated compounds into hydrocarbons at the expense of the bio-oil yield. It has been observed that *in-situ* catalytic pyrolysis mode requires higher catalyst to biomass ratios compared to the *ex-situ* mode as the biomass and catalyst are heated together during the *in-situ* mode and the produced pyrolytic vapours could not access the required amount of active sites of the catalyst due to less interaction time between the pyrolytic vapours and the catalyst [179]. Although the higher catalyst to biomass ratios could increase the overall yield of aromatic hydrocarbons, this could result into the selectivity of different hydrocarbons. For example, Srinivasan et al. [192] carried out the catalytic pyrolysis of torrefied biomass using ZSM-5 at different catalyst to biomass ratios (4, 9, 14) and suggested that the overall yield of aromatic hydrocarbons increased with increase in catalyst to biomass ratio. However, it was noticed that the increase in catalyst to biomass ratio slightly increased the selectivity of toluene and xylenes, while the selectivity of benzene and naphthalene decreased [192]. Collectively, it could be inferred that the integration of catalytic pyrolysis with torrefaction has proved to improve the quality of bio-oil, particularly, increasing the content of monocyclic hydrocarbons like benzene, toluene and xylenes and improving the overall carbon yield in the bio-oil.

Catalytic pyrolysis of torrefied biomass has been widely explored, however, limited studies have been conducted on catalytic pyrolysis of biomass pre-treated with other thermal, chemical and biological methods. The pre-treatment of biomass with WT mainly causes the hydrolysis of hemicellulose component of the biomass and breaks the lignin linking interactions and leaves the cellulose part nearly retained in the solid product. Subsequently, the pyrolysis increases the formation of organic compounds (mainly oxygenated compounds like phenols, sugars, furans) that are primarily derived from the thermal degradation of lignin and cellulose [135,199]. These oxygen containing compounds can be successfully converted to energy rich hydrocarbons using acidic catalysts. For example, a study demonstrated the catalytic pyrolysis of biomass pre-treated with WT approach, using HZSM-5 and Al-MCM-41 catalysts [200]. The results showed that the catalytic pyrolysis of the pre-treated biomass using both catalysts produced better quality of bio-oil compared to the non-catalytic pyrolysis, with bio-oil rich in monocyclic and polycyclic hydrocarbons, while the bio-oil produced by the non-catalytic pyrolysis of the pre-treated biomass contained higher proportions of furans, sugars and phenols [200]. Similarly, the integration of catalytic pyrolysis using acidic catalysts and acid or alkali biomass pre-treatment approaches can substantially improve the content of aromatic and aliphatic hydrocarbons and remove the oxygenated compounds, owing to the improved pyrolysis kinetics and deoxygenation reactions (like dehydration, decarboxylation, decarbonylation, aromatization, oligomerization and cracking reactions) carried out by the Brønsted acid sites on the catalysts.

Biological pre-treatment of biomass could be highly useful to decompose the main linkages between lignin and hemicellulose, or lignin and cellulose and hence decreasing the activation energy while increasing the rate of reaction during the pyrolysis process. It has shown that biological pre-treatment increases the bio-oil yield and enhances the content of hydrocarbons in the bio-oil. The application of catalytic fast pyrolysis of biologically treated biomass could help to convert these compounds into different valuable hydrocarbons with improved quality of the bio-oil. Yu et al. [166] investigated the effect of ZSM-5 catalyst on

the conversion of pyrolytic vapours generated from corn stover pre-treated with *Irpex lacteus*. Firstly, it was observed that the fungal treatment increased the production of volatile products that mainly contained oxygenated compounds, compared to non-treated corn stover and secondly, the use of ZSM-5 converted the oxygenated compounds into aromatic hydrocarbons, with a maximum percentage of 11.49 wt% obtained in the bio-oil. In addition, a decrease in the char yield was observed with the treated biomass, indicating degradation of the lignin component and its successful conversion to volatile products [166].

It can be suggested that the coupling of catalytic pyrolysis and other pre-treatment methods is a highly advantageous approach to enhance the bio-oil quality. The application of catalysts improves the kinetics of pyrolysis by decreasing the activation energy. The active sites on the catalysts (mainly inside the pores) carry out various deoxygenation reactions to convert the low energy density oxygenated compounds into high energy density aromatic and aliphatic hydrocarbons, hence improving the calorific value of the bio-oil. However, the use of catalysts decreases the bio-oil yield considerably and enhances the gaseous products compared to the non-catalytic pyrolysis of pre-treated biomass feedstocks. Moreover, the catalysts are highly prone to deactivation due to the deposition of coke/carbonaceous species produced during the catalytic pyrolysis. Therefore, the development of advanced catalysts that reduce coke deposition would be required to make the catalytic pyrolysis more efficient and cost-effective. On the other hand, negligible research has been conducted using the catalytic pyrolysis of biomass pre-treated with SE, AFE, and HWE and limited studies have demonstrated the application of catalytic pyrolysis of biologically pre-treated biomass.

6. Current status, challenges and future recommendations

The physicochemical pre-treatment of lignocellulosic biomass has shown significant advantages to improve the biomass properties, which converts the biomass into a more suitable feedstock for pyrolysis, especially for improved pyrolysis kinetics, generation of a better-quality bio-oil and production of desirable high value-added products. The pre-treatment methods, such as DT, acid and alkali treatment, could help to disrupt recalcitrant structure of lignocellulosic biomass, by breaking different chemical bonds or linkages present between three biomass components (cellulose, hemicellulose, and lignin) and also reducing the crystallinity of cellulose and degree of polymerization. As a result, the treated biomass shows lower activation energy for its thermal degradation compared to the untreated biomass. The other methods, SE, HWE and WT, are highly effective to remove undesirable minerals, alkali metals and alkali earth metals that if present in the biomass could significantly affect the pyrolysis process. Overall, all the pre-treatment methods have certain advantages to improve the biomass properties which affect the pyrolysis process and consequently, the bio-oil composition. However, among all the pre-treatment methods, only a few techniques, such as DT, have been used on a pilot scale so far, while most of them are still in the development stages. It is difficult to estimate and compare the efficacy of pre-treatment methods due to the noticeable differences in total capital investment, operating and maintenance costs. Therefore, the economic analysis of each pre-treatment process using a particular biomass feedstock could be carried out to provide a better understanding of the efficacy of the pre-treatment methods. A number of studies have demonstrated techno-economic analysis of different biomass pre-treatment techniques for different fuel production, and separate economic analyses of biomass pyrolysis for bio-oil production as well as catalytic biomass pyrolysis for bio-oil upgrading [68, 205–208], but very limited studies have been conducted to determine the economic analysis of integrated biomass pre-treatment techniques and their effect on bio-oil upgrading. Recently, Chai et al. [209] estimated the cost of integrated torrefaction of spent coffee grounds and its catalytic pyrolysis for bio-oil upgrading, mainly focusing on BTEX (benzene, toluene, ethyl benzene, xylenes) yield. The study applied a range of torrefaction temperatures of 200–300 °C and residence time of 15–50 min, while the cost for BTEX production was predicted using a surface response model. The authors suggested that a temperature of 239 °C and a residence time of 34 min was economical, producing approximately 9.65 wt% BTEX per tonne of biomass which would cost $1246 [209]. It was further indicated that increasing torrefaction temperature as well as residence time or decreasing both parameters increases the overall cost for BTEX production, which could be attributed to the severe mass loss at higher torrefaction temperatures with high residence time and lower BTEX yield at lower torrefaction temperatures with low residence time, thereby making the process expensive for BTEX production.

Although biomass pre-treatment techniques could be useful to improve the physiochemical properties of the bio-oil, there are several challenges related to each technique. Table 8 summarizes the advantages and challenges of each method used for biomass pre-treatment. The major challenge for the physical methods of biomass pre-treatment is that they are energy-intensive which makes the pre-treatment methods expensive. This can be alleviated by supplying the heat form a renewable energy source, which could make the overall process less expensive and self-sustainable. DT could lead to decrease in bio-oil yield and increase in ash content in the bio-oil while the biomass with poor pelletability could be obtained after the DT process. Optimization of different operating parameters during torrefaction, such as temperature, residence time and heating rate, is highly important to obtain the biomass with improved properties. DT of biomass has been used on a pilot scale but more studies are required to transform the technology into a commercial scale, especially, to obtain the torrefied biomass suitable for pyrolysis to achieve better-quality bio-oil. Commercialization of DT could also require the development of new reactors. On the other hand, WT is still in developmental stage and several challenges have been associated with this technology. The first challenge is the requirement of high-pressure slurry pump for feeding the biomass feedstock. During WT process, inorganic precipitates could be formed that can cause clogging in the reactor, which ultimately could increase the maintenance cost. Furthermore, the development of reactors requires non-corrosive materials, which are usually expensive and makes the process highly uneconomical. Similarly, SE and AFE also need expensive reactor materials that can increase the overall cost for bio-oil upgrading. The treated biomass further requires drying of the biomass prior to pyrolysis, which is an energy-intensive step and increases the overall operating costs.

For chemical treatments, including acid and alkali treatments, the disposal of the leachate is a great challenge since it contains toxic metals. Therefore, further treatment of the leachate to remove toxic metals would increase the cost of the process. Alternatively, the leachate also contains small amount of sugars, which could be converted into value-added chemicals or bioethanol using biochemical processes. In this regard, various microorganisms could be potentially applied for the conversion of sugars into bioethanol or other value-added chemicals. The acid and alkali treatment of biomass have shown significant changes in the biomass structure and removal of inorganic minerals, alkali and alkali earth metals but no studies have provided sufficient evidences to understand the reaction mechanisms between the acidic or alkaline chemical and different linkages present between the biomass constituents. Therefore, more studies should be conducted to examine the chemical reactions and kinetics during the process, which could help understand the removal mechanism of inorganic species and effect of chemicals on the biomass structure. On the other hand, the biological pre-treatment of biomass could be time consuming as microorganisms take longer time to decompose the biomass. In addition, very less microorganisms have been known for pre-treatment of biomass, hence, more studies are required to explore the application of microorganisms for biomass treatment and its effect on bio-oil upgrading.

To obtain the bio-oil with higher carbon and hydrogen content and higher calorific value, biomass pre-treatment methods have been

Table 8
Advantages and challenges of methods used for bio-oil upgrading.

No.	Method	Advantages	Challenges
1	Grinding	- improves heat flow between feedstock particles - decreases the degree of polymerization and crystallinity of the biomass components during the pyrolysis process - a higher bio-oil yield and enhanced calorific value bio-oil could be achieved with smaller size particles	- it is an energy-intensive process - increases cost
2	Densification	- decreases moisture content of biomass - increases durability index and energy content of biomass	- requires energy input, e. g., in screw extruder-60 kWh/ton. - high maintenance cost for the instrument used in compaction.
3	Dry-torrefaction	- lowers the activation energy for pyrolysis process - increases the amount of atomic carbon in biomass and hence the energy conversion capacity - improves the quality of bio-oil by decreasing the oxygenated compounds - increases the content of hydrocarbons and heating value of bio-oil	- decreases bio-oil yield - higher ash content - results in the biomass with poor pelletability - it is an energy-intensive process - increases overall cost
4	Acid and Alkali treatment	- removes undesirable inorganic species from the biomass - decreases viscosity of bio-oil - enhances heating value of bio-oil - improves carbon content in the biomass - acid treatment can increase the bio-oil yield - decreases the content of acids and increases the amount of hydrocarbons in the bio-oil -improves cellulose digestibility - acid treatment can enhance the production of certain chemicals and anhydrosugars, such as levoglucosan	- alkali treatment can decrease the bio-oil yield - alkali treatment can decrease the production of levoglucosan - post-treatment requires washing and drying of the biomass, which requires energy input for the process -use of expensive chemicals can make the process costly -leachate contains toxic metals - possible reaction of chemicals and inorganic species needs more investigation
5	Wet-torrefaction	- can be applied to wet biomasses or biomass wastes - removal of minerals and alkali metals - increases calorific value, grindability, and pelletability of biomass - requires less severe operating conditions, such as lower temperature and pressure - decreases activation energy for hemicellulose, while increases for cellulose and lignin - decreases the amount of light compounds in bio-oil - increases the yield of levoglucosan	- requires expensive reactor materials that can increase the overall cost for bio-oil upgrading - inorganic precipitates produced during the process can cause clogging in the reactor - requires a high-pressure slurry pump for feeding the biomass feedstock - requires post-treatment of wastewater for resource recovery - after the downstream recovery of biomass, it further requires drying process prior to use in pyrolysis process
6	Ammonia fibre expansion	- requires less severe temperature and pressure operating conditions (temperature of 60–120 °C and pressure of ~2 MPa) - improves biomass thermal stability - improves pellet durability, and bulk and particle density of biomass	- not very effective for pre-treatment of biomass with higher content of lignin - requires expensive reactor materials that can increase the overall cost for bio-oil upgrading - has less effect on bio-oil properties - requires more investigations to understand its effect on the pyrolysis process and bio-oil upgrading
7	Steam explosion	- improves the biomass structure by creating large pores and increasing the accessibility of the cellulose part - leads to higher crystallinity of the cellulose and higher thermal stability - decreases the concentration of alkali and alkaline earth metals - decreases viscosity and acid value of the bio-oil - can increase the formation of high value-added chemicals	- can increase the moisture content - requires higher temperature - requires expensive reactor materials - after the downstream recovery of biomass, it further requires drying of the biomass prior to use in pyrolysis process
8	Hot-water extraction	- very simple and cost-effective method - improves surface area of biomass - improves the bio-oil quality - removes minerals and inorganic species - enhances the production of high value-added chemicals - increases bio-oil yield	-drying process can make the process an energy intensive
9	Biological pre-treatment	- economical and eco-friendly treatment method - no energy or chemical inputs - decomposes the main linkages between lignin and hemicellulose or lignin and cellulose - decreases activation energy and increases the rate of reaction during pyrolysis process - enhances the content of hydrocarbons in the bio-oil - increases bio-oil yield and decreases char yield	- the process could be time consuming as microorganisms take longer time to decompose biomass - selection of a certain microorganism could be a challenge for specific biomass due to difference in the biomass composition - very less microorganisms have been explored so far, hence, more studies need to carry out to explore the application of microorganism for biomass treatment

combined with catalytic pyrolysis producing substantial increase in the amount of aliphatic and aromatic hydrocarbons in the bio-oil and consequently in the total carbon yield. However, catalytic pyrolysis has been coupled with mainly DT and WT, while limited studies have been carried out using catalytic pyrolysis combined with SE and AFE, HWE, and biologically pre-treated biomass. Thus, more studies should be carried out using an integrated process to optimise the process parameters on bio-oil upgrading.

A number of approaches, as discussed in this article, and some other downstream upgrading methods, like emulsification and solvent addition, have been used for bio-oil upgrading [20,41,45]. Subsequently, the upgraded bio-oil has been tested for different applications and the

demonstrations suggest that the bio-oil has a great potential to serve as a fuel in turbines, boilers and diesel engines for heat and power generation [38,210,211]. However, some modifications are still required either in the combustion units or mixing the bio-oil with solvents, like ethanol, methanol or diesel fuel, to avoid the ignition time delay. On the other hand, application of bio-oil as a transport fuel needs further investigations. Currently, the lower heating values, chemical instability and other poor physical properties restrict its use in internal combustion engines. The bio-oil upgrading to a suitable transport fuel needs complete removal of oxygenated compounds and presence of naphthenes, paraffins and aromatic hydrocarbons and the other physical properties should also be improved to make it a realistic drop-in fuel. Besides, the production of bio-oil at a large scale similar to the cost of conventional fuels is one of the key challenges to overcome in order to make the bio-oil economical and affordable to the consumers.

7. Conclusions

This review article comprehensively discussed the various physico-chemical methods to improve the bio-oil properties, mainly based on biomass pre-treatment. The physical and thermal methods are mainly employed to improve the biomass structure and increase the amount of atomic carbon, which consequently play the significant role in the pyrolysis kinetics, bio-oil yield and bio-oil quality. For, example, grinding is used to reduce the feedstock size to improve the heat flow between the substrates and decrease the degree of polymerization and crystallinity of the biomass components during the pyrolysis process which in turn affects the yield and composition of the bio-oil compounds. Densification changes the density, moisture content, durability index and energy contents of the biomass which can also affect the pyrolysis product distribution, heating and mass transfer efficiencies of the pyrolysis process. Torrefaction improves the biomass structure to produce better quality biofuels and improves economic feasibility of the pyrolysis process. During the torrefaction process, the fibrous structure and tenacity of the biomass is changed, which could help in decreasing the activation energy for the pyrolysis process and has shown positive results to improve the bio-oil quality, such as reduction in oxygen content, and increase in the heating value and amount of hydrocarbons in the bio-oil. Biomass pre-treatment with dilute acidic and alkaline chemicals, and hot water extraction has shown advantageous results to eliminate the inorganic minerals and simultaneously improve the bio-oil quality. In addition, the acid pre-treatment of the biomass also causes significant changes in its structure, and increases its average pore diameter and energy density. On the other hand, biological treatment with white rot fungi can improve the overall biomass conversion efficiency of the pyrolysis process and has shown to enhance the number of hydrocarbons in the bio-oil compared to the untreated biomass.

The integration of catalytic pyrolysis with pre-treatment techniques has proved to be highly significant approach to convert the low energy density oxygenated compounds into high energy density aliphatic and aromatic hydrocarbons, thereby considerably increasing the bio-oil quality. Although biomass pre-treatment methods could prove advantageous for bio-oil upgrading there are also certain challenges related to their applications. For example, the physical methods are energy-intensive and chemical methods, such as SE and AFE require expensive reactor materials, making the bio-oil upgrading an uneconomical approach. The chemical methods of acid and alkali biomass treatment result in the toxic leachate and require another step in the process, while the biological methods are time consuming. Therefore, more research should be carried out to overcome the key challenges related to the pre-treatment methods and make the bio-oil upgrading technique more efficient and cost-effective. Particularly, novel designs of reactors with less expensive materials should be invented for WT, SE and AFE and different approaches should be adopted to convert the low energy density oxygenated compounds into high energy density hydrocarbons and make the bio-oil a realistic drop-in fuel.

Acknowledgments

This research did not receive any specific grant from funding agencies in the public, commercial, or not-for-profit sectors. Some figures included in the article have been reproduced from the given references and copyrights have been taken from the respective publishers.

References

[1] Capuano DL. International energy outlook. 2018 (IEO2018) 2000:21.
[2] Kumar R, Kumar P. Future microbial applications for bioenergy production: a perspective. Front Microbiol 2017;8. https://doi.org/10.3389/fmicb.2017.00450.
[3] Kumar R, Singh L, Zularisam AW, Hai FI. Microbial fuel cell is emerging as a versatile technology: a review on its possible applications, challenges and strategies to improve the performances: microbial fuel cell is emerging as a versatile technology. Int J Energy Res 2018;42:369–94. https://doi.org/10.1002/er.3780.
[4] Bar-On YM, Phillips R, Milo R. The biomass distribution on Earth. Proc Natl Acad Sci Unit States Am 2018;115:6506–11. https://doi.org/10.1073/pnas.1711842115.
[5] Kumar R, Strezov V, Lovell E, Kan T, Weldekidan H, He J, et al. Bio-oil upgrading with catalytic pyrolysis of biomass using Copper/zeolite-Nickel/zeolite and Copper-Nickel/zeolite catalysts. Bioresour Technol 2019. https://doi.org/10.1016/j.biortech.2019.01.067.
[6] Mohan D, Pittman CU, Steele PH. Pyrolysis of wood/biomass for bio-oil: a critical review. Energy & Fuels 2006;20:848–89. https://doi.org/10.1021/ef0502397.
[7] Yang H, Yan R, Chen H, Lee DH, Zheng C. Characteristics of hemicellulose, cellulose and lignin pyrolysis. Fuel 2007;86:1781–8. https://doi.org/10.1016/j.fuel.2006.12.013.
[8] Kan T, Strezov V, Evans TJ. Lignocellulosic biomass pyrolysis: a review of product properties and effects of pyrolysis parameters. Renew Sustain Energy Rev 2016;57:1126–40. https://doi.org/10.1016/j.rser.2015.12.185.
[9] Luo Wang, Liao Cen. Mechanism study of cellulose rapid pyrolysis. Ind Eng Chem Res 2004;43:5605–10. https://doi.org/10.1021/ie030774z.
[10] Kumar R, Strezov V, Kan T, Weldekidan H, He J. Investigating the effect of Cu/zeolite on deoxygenation of bio-oil from pyrolysis of pine wood. Energy Procedia 2019;160:186–93. https://doi.org/10.1016/j.egypro.2019.02.135.
[11] Weldekidan H, Strezov V, Town G. Review of solar energy for biofuel extraction. Renew Sustain Energy Rev 2018;88:184–92. https://doi.org/10.1016/j.rser.2018.02.027.
[12] Alonso DM, Wettstein SG, Dumesic JA. Bimetallic catalysts for upgrading of biomass to fuels and chemicals. Chem Soc Rev 2012;41:8075. https://doi.org/10.1039/c2cs35188a.
[13] Ennaert T, Van Aelst J, Dijkmans J, De Clercq R, Schutyser W, Dusselier M, et al. Potential and challenges of zeolite chemistry in the catalytic conversion of biomass. Chem Soc Rev 2016;45:584–611. https://doi.org/10.1039/C5CS00859J.
[14] Kabir G, Hameed BH. Recent progress on catalytic pyrolysis of lignocellulosic biomass to high-grade bio-oil and bio-chemicals. Renew Sustain Energy Rev 2017;70:945–67. https://doi.org/10.1016/j.rser.2016.12.001.
[15] Rahman MdM, Liu R, Cai J. Catalytic fast pyrolysis of biomass over zeolites for high quality bio-oil – a review. Fuel Process Technol 2018;180:32–46. https://doi.org/10.1016/j.fuproc.2018.08.002.
[16] Zacher AH, Olarte MV, Santosa DM, Elliott DC, Jones SB. A review and perspective of recent bio-oil hydrotreating research. Green Chem 2014;16:491–515. https://doi.org/10.1039/C3GC41382A.
[17] Wang S, Dai G, Yang H, Luo Z. Lignocellulosic biomass pyrolysis mechanism: a state-of-the-art review. Prog Energy Combust Sci 2017;62:33–86. https://doi.org/10.1016/j.pecs.2017.05.004.
[18] Iliopoulou EF, Triantafyllidis KS, Lappas AA. Overview of catalytic upgrading of biomass pyrolysis vapors toward the production of fuels and high-value chemicals. Wiley Interdisciplinary Reviews: Energy and Environment; 2018. p. e322. https://doi.org/10.1002/wene.322.
[19] Chen D, Zhou J, Zhang Q, Zhu X. Evaluation methods and research progresses in bio-oil storage stability. Renew Sustain Energy Rev 2014;40:69–79. https://doi.org/10.1016/j.rser.2014.07.159.
[20] Leng L, Li H, Yuan X, Zhou W, Huang H. Bio-oil upgrading by emulsification/microemulsification: a review. Energy 2018;161:214–32. https://doi.org/10.1016/j.energy.2018.07.117.
[21] Dai L, Wang Y, Liu Y, Ruan R, He C, Yu Z, et al. Integrated process of lignocellulosic biomass torrefaction and pyrolysis for upgrading bio-oil production: a state-of-the-art review. Renew Sustain Energy Rev 2019;107:20–36. https://doi.org/10.1016/j.rser.2019.02.015.
[22] Tumuluru JS, Wright CT, Hess JR, Kenney KL. A review of biomass densification systems to develop uniform feedstock commodities for bioenergy application. Biofuels, Bioproducts and Biorefining 2011;5:683–707. https://doi.org/10.1002/bbb.324.
[25] Ennaert T, Schutyser W, Dijkmans J, Dusselier M, Sels BF. Conversion of biomass to chemicals. In: Zeolites and zeolite-like materials. Elsevier; 2016. p. 371–431. https://doi.org/10.1016/B978-0-444-63506-8.00010-0.
[26] Neumann J, Meyer J, Ouadi M, Apfelbacher A, Binder S, Hornung A. The conversion of anaerobic digestion waste into biofuels via a novel Thermo-

Catalytic Reforming process. Waste Manag 2016;47:141–8. https://doi.org/10.1016/j.wasman.2015.07.001.
[27] Yao X, Zhang L, Li L, Liu L, Cao Y, Dong X, et al. Investigation of the structure, acidity, and catalytic performance of CuO/Ti0.95Ce0.05O2 catalyst for the selective catalytic reduction of NO by NH3 at low temperature. Appl Catal B Environ 2014;150–151:315–29. https://doi.org/10.1016/j.apcatb.2013.12.007.
[28] Liu W-J, Li W-W, Jiang H, Yu H-Q. Fates of chemical elements in biomass during its pyrolysis. Chem Rev 2017;117:6367–98. https://doi.org/10.1021/acs.chemrev.6b00647.
[29] Dhyani V, Bhaskar T. A comprehensive review on the pyrolysis of lignocellulosic biomass. Renew Energy 2018;129:695–716. https://doi.org/10.1016/j.renene.2017.04.035.
[30] Zhang J, Choi YS, Yoo CG, Kim TH, Brown RC, Shanks BH. Cellulose–hemicellulose and cellulose–lignin interactions during fast pyrolysis. ACS Sustainable Chem Eng 2015;3:293–301. https://doi.org/10.1021/sc500664h.
[31] Jin Z, Katsumata KS, Lam TBT, Iiyama K. Covalent linkages between cellulose and lignin in cell walls of coniferous and nonconiferous woods. Biopolymers 2006;83:103–10. https://doi.org/10.1002/bip.20533.
[32] Zhao S, Liu M, Zhao L, Zhu L. Influence of interactions among three biomass components on the pyrolysis behavior. Ind Eng Chem Res 2018;57:5241–9. https://doi.org/10.1021/acs.iecr.8b00593.
[33] Zhang J, Choi YS, Yoo CG, Kim TH, Brown RC, Shanks BH. Cellulose–hemicellulose and cellulose–lignin interactions during fast pyrolysis. ACS Sustainable Chem Eng 2015;3:293–301. https://doi.org/10.1021/sc500664h.
[34] Wu S, Shen D, Hu J, Zhang H, Xiao R. Cellulose-lignin interactions during fast pyrolysis with different temperatures and mixing methods. Biomass Bioenergy 2016;90:209–17. https://doi.org/10.1016/j.biombioe.2016.04.012.
[35] Volpe R, Zabaniotou AA, Skoulou V. Synergistic effects between lignin and cellulose during pyrolysis of agricultural waste. Energy & Fuels 2018;32:8420–30. https://doi.org/10.1021/acs.energyfuels.8b00767.
[36] Yu J, Paterson N, Blamey J, Millan M. Cellulose, xylan and lignin interactions during pyrolysis of lignocellulosic biomass. Fuel 2017;191:140–9. https://doi.org/10.1016/j.fuel.2016.11.057.
[37] Hosoya T, Kawamoto H, Saka S. Pyrolysis behaviors of wood and its constituent polymers at gasification temperature. J Anal Appl Pyrol 2007;78:328–36. https://doi.org/10.1016/j.jaap.2006.08.008.
[38] Czernik S, Bridgwater AV. Overview of applications of biomass fast pyrolysis oil. Energy & Fuels 2004;18:590–8. https://doi.org/10.1021/ef034067u.
[39] Jiang X, Ellis N. Upgrading bio-oil through emulsification with biodiesel: mixture production. Energy & Fuels 2010;24:1358–64. https://doi.org/10.1021/ef9010669.
[40] Farooq A, Shafaghat H, Jae J, Jung S-C, Park Y-K. Enhanced stability of bio-oil and diesel fuel emulsion using Span 80 and Tween 60 emulsifiers. J Environ Manag 2019;231:694–700. https://doi.org/10.1016/j.jenvman.2018.10.098.
[41] Zhang M, Yewe-Siang Lee Shee We M, Wu H. Direct emulsification of crude glycerol and bio-oil without addition of surfactant via ultrasound and mechanical agitation. Fuel 2018;227:183–9. https://doi.org/10.1016/j.fuel.2018.04.099.
[42] Martin JA, Mullen CA, Boateng AA. Maximizing the stability of pyrolysis oil/diesel fuel emulsions. Energy & Fuels 2014;28:5918–29. https://doi.org/10.1021/ef5015583.
[43] Choi JH, Kim S-S, Ly HV, Kim J, Woo HC. Effects of water-washing Saccharina japonica on fast pyrolysis in a bubbling fluidized-bed reactor. Biomass Bioenergy 2017;98:112–23. https://doi.org/10.1016/j.biombioe.2017.01.006.
[44] Hassan EM, Steele PH, Ingram L. Characterization of fast pyrolysis bio-oils produced from pretreated pine wood. Appl Biochem Biotechnol 2009;154:3–13. https://doi.org/10.1007/s12010-008-8445-3.
[45] Wang H, Srinivasan R, Yu F, Steele P, Li Q, Mitchell B. Effect of acid, alkali, and steam explosion pretreatments on characteristics of bio-oil produced from pinewood. Energy & Fuels 2011;25:3758–64. https://doi.org/10.1021/ef2004909.
[46] Wang H, Srinivasan R, Yu F, Steele P, Li Q, Mitchell B, et al. Effect of acid, steam explosion, and size reduction pretreatments on bio-oil production from sweetgum, switchgrass, and corn stover. Appl Biochem Biotechnol 2012;167:285–97. https://doi.org/10.1007/s12010-012-9678-8.
[47] Choi J, Choi J-W, Suh DJ, Ha J-M, Hwang JW, Jung HW, et al. Production of brown algae pyrolysis oils for liquid biofuels depending on the chemical pretreatment methods. Energy Convers Manag 2014;86:371–8. https://doi.org/10.1016/j.enconman.2014.04.094.
[48] Xu X, Li Z, Sun Y, Jiang E, Huang L. High-quality fuel from the upgrading of heavy bio-oil by the combination of ultrasonic treatment and mutual solvent. Energy & Fuels 2018;32:3477–87. https://doi.org/10.1021/acs.energyfuels.7b03483.
[49] Pidtasang B, Udomsap P, Sukkasi S, Chollacoop N, Pattiya A. Influence of alcohol addition on properties of bio-oil produced from fast pyrolysis of eucalyptus bark in a free-fall reactor. J Ind Eng Chem 2013;19:1851–7. https://doi.org/10.1016/j.jiec.2013.02.031.
[50] Zhang L, Liu R, Yin R, Mei Y, Cai J. Optimization of a mixed additive and its effect on physicochemical properties of bio-oil. Chem Eng Technol 2014;37:1181–90. https://doi.org/10.1002/ceat.201300786.
[51] Zhang M, Wu H. Phase behavior and fuel properties of bio-oil/glycerol/methanol blends. Energy & Fuels 2014;28:4650–6. https://doi.org/10.1021/ef501176z.
[52] Zhu L, Li K, Ding H, Zhu X. Studying on properties of bio-oil by adding blended additive during aging. Fuel 2018;211:704–11. https://doi.org/10.1016/j.fuel.2017.09.106.
[53] Meng J, Moore A, Tilotta D, Kelley S, Park S. Toward understanding of bio-oil aging: accelerated aging of bio-oil fractions. ACS Sustainable Chem Eng 2014;2. https://doi.org/10.1021/sc500223e. 2011–8.
[54] Li H, Xia S, Ma P. Upgrading fast pyrolysis oil: solvent–anti-solvent extraction and blending with diesel. Energy Convers Manag 2016;110:378–85. https://doi.org/10.1016/j.enconman.2015.11.043.
[55] Zhu L, Li K, Zhang Y, Zhu X. Upgrading the storage properties of bio-oil by adding a compound additive. Energy & Fuels 2017;31:6221–7. https://doi.org/10.1021/acs.energyfuels.7b00864.
[56] Mei Y, Liu R, Wu W, Zhang L. Effect of hot vapor filter temperature on mass yield, energy balance, and properties of products of the fast pyrolysis of pine sawdust. Energy & Fuels 2016;30:10458–69. https://doi.org/10.1021/acs.energyfuels.6b01877.
[57] Elliott DC, Wang H, French R, Deutch S, Iisa K. Hydrocarbon liquid production from biomass via hot-vapor-filtered fast pyrolysis and catalytic hydroprocessing of the bio-oil. Energy & Fuels 2014;28:5909–17. https://doi.org/10.1021/ef501536j.
[58] Sundaram V, Muthukumarappan K, Gent S. Understanding the impacts of AFEX™ pretreatment and densification on the fast pyrolysis of corn stover, prairie cord grass, and switchgrass. Appl Biochem Biotechnol 2017;181:1060–79. https://doi.org/10.1007/s12010-016-2269-3.
[59] Mohammed IY, Abakr YA, Kazi FK, Yusuf S. Effects of pretreatments of napier grass with deionized water, sulfuric acid and sodium hydroxide on pyrolysis oil characteristics. Waste and Biomass Valorization 2017;8:755–73. https://doi.org/10.1007/s12649-016-9594-1.
[60] Yang Z, Kumar A, Huhnke RL. Review of recent developments to improve storage and transportation stability of bio-oil. Renew Sustain Energy Rev 2015;50:859–70. https://doi.org/10.1016/j.rser.2015.05.025.
[61] Alvira P, Tomás-Pejó E, Ballesteros M, Negro MJ. Pretreatment technologies for an efficient bioethanol production process based on enzymatic hydrolysis: a review. Bioresour Technol 2010;101:4851–61. https://doi.org/10.1016/j.biortech.2009.11.093.
[62] Kersten SRA, Wang X, Prins W, van Swaaij WPM. Biomass pyrolysis in a fluidized bed reactor. Part 1: literature review and model simulations. Ind Eng Chem Res 2005;44:8773–85. https://doi.org/10.1021/ie0504856.
[63] Shen J, Wang X-S, Garcia-Perez M, Mourant D, Rhodes MJ, Li C-Z. Effects of particle size on the fast pyrolysis of oil mallee woody biomass. Fuel 2009;88:1810–7. https://doi.org/10.1016/j.fuel.2009.05.001.
[64] Abnisa F, Daud WMAW, Husin WNW, Sahu JN. Utilization possibilities of palm shell as a source of biomass energy in Malaysia by producing bio-oil in pyrolysis process. Biomass Bioenergy 2011;35:1863–72. https://doi.org/10.1016/j.biombioe.2011.01.033.
[65] Garg R, Anand N, Kumar D. Pyrolysis of babool seeds (Acacia nilotica) in a fixed bed reactor and bio-oil characterization. Renew Energy 2016;96:167–71. https://doi.org/10.1016/j.renene.2016.04.059.
[66] Raja SA, Kennedy ZR, Pillai BC, Lee CLR. Flash pyrolysis of jatropha oil cake in electrically heated fluidized bed reactor. Energy 2010;35:2819–23. https://doi.org/10.1016/j.energy.2010.03.011.
[67] Yin C. Microwave-assisted pyrolysis of biomass for liquid biofuels production. Bioresour Technol 2012;120:273–84. https://doi.org/10.1016/j.biortech.2012.06.016.
[68] Wright MM, Satrio JA, Brown RC, University IS. Techno-economic analysis of biomass fast pyrolysis to transportation fuels. Renew Energy 2010:73.
[69] Rezaei H, Yazdanpanah F, Lim CJ, Lau A, Sokhansanj S. Pyrolysis of ground pine chip and ground pellet particles. Can J Chem Eng 2016;94:1863–71. https://doi.org/10.1002/cjce.22574.
[70] Mani S, Tabil LG, Sokhansanj S. Effects of compressive force, particle size and moisture content on mechanical properties of biomass pellets from grasses. Biomass Bioenergy 2006;30:648–54. https://doi.org/10.1016/j.biombioe.2005.01.004.
[71] Karkania V, Fanara E, Zabaniotou A. Review of sustainable biomass pellets production – a study for agricultural residues pellets' market in Greece. Renew Sustain Energy Rev 2012;16:1426–36. https://doi.org/10.1016/j.rser.2011.11.028.
[72] Di Blasi C, Branca C, Lombardi V, Ciappa P, Di Giacomo C. Effects of particle size and density on the packed-bed pyrolysis of wood. Energy & Fuels 2013;27:6781–91. https://doi.org/10.1021/ef401481j.
[73] Demirbas A. Effects of temperature and particle size on bio-char yield from pyrolysis of agricultural residues. J Anal Appl Pyrol 2004;72:243–8. https://doi.org/10.1016/j.jaap.2004.07.003.
[74] Zeng K, Soria J, Gauthier D, Mazza G, Flamant G. Modeling of beech wood pellet pyrolysis under concentrated solar radiation. Renew Energy 2016;99:721–9. https://doi.org/10.1016/j.renene.2016.07.051.
[75] Chen D, Zheng Z, Fu K, Zeng Z, Wang J, Lu M. Torrefaction of biomass stalk and its effect on the yield and quality of pyrolysis products. Fuel 2015;159:27–32. https://doi.org/10.1016/j.fuel.2015.06.078.
[76] Meng J, Park J, Tilotta D, Park S. The effect of torrefaction on the chemistry of fast-pyrolysis bio-oil. Bioresour Technol 2012;111:439–46. https://doi.org/10.1016/j.biortech.2012.01.159.
[77] Bert V, Allemon J, Sajet P, Dieu S, Papin A, Collet S, et al. Torrefaction and pyrolysis of metal-enriched poplars from phytotechnologies: effect of temperature and biomass chlorine content on metal distribution in end-products and valorization options. Biomass Bioenergy 2017;96:1–11. https://doi.org/10.1016/j.biombioe.2016.11.003.
[78] Chen D, Gao A, Cen K, Zhang J, Cao X, Ma Z. Investigation of biomass torrefaction based on three major components: hemicellulose, cellulose, and lignin. Energy

Convers Manag 2018;169:228–37. https://doi.org/10.1016/j.enconman.2018.05.063.
[79] Wang S, Dai G, Ru B, Zhao Y, Wang X, Zhou J, et al. Effects of torrefaction on hemicellulose structural characteristics and pyrolysis behaviors. Bioresour Technol 2016;218:1106–14. https://doi.org/10.1016/j.biortech.2016.07.075.
[80] Wang S, Dai G, Ru B, Zhao Y, Wang X, Xiao G, et al. Influence of torrefaction on the characteristics and pyrolysis behavior of cellulose. Energy 2017;120:864–71. https://doi.org/10.1016/j.energy.2016.11.135.
[81] Zheng A, Jiang L, Zhao Z, Huang Z, Zhao K, Wei G, et al. Impact of torrefaction on the chemical structure and catalytic fast pyrolysis behavior of hemicellulose, lignin, and cellulose. Energy & Fuels 2015;29:8027–34. https://doi.org/10.1021/acs.energyfuels.5b01765.
[82] Kumagai S, Matsuno R, Grause G, Kameda T, Yoshioka T. Enhancement of bio-oil production via pyrolysis of wood biomass by pretreatment with H 2 SO 4. Bioresour Technol 2015;178:76–82. https://doi.org/10.1016/j.biortech.2014.09.146.
[83] Uemura Y, Omar W, Othman NA, Yusup S, Tsutsui T. Torrefaction of oil palm EFB in the presence of oxygen. Fuel 2013;103:156–60. https://doi.org/10.1016/j.fuel.2011.11.018.
[84] Gogoi D, Bordoloi N, Goswami R, Narzari R, Saikia R, Sut D, et al. Effect of torrefaction on yield and quality of pyrolytic products of arecanut husk: an agro-processing wastes. Bioresour Technol 2017;242:36–44. https://doi.org/10.1016/j.biortech.2017.03.169.
[85] Ren S, Lei H, Wang L, Bu Q, Wei Y, Liang J, et al. Microwave torrefaction of douglas fir sawdust pellets. Energy & Fuels 2012;26:5936–43. https://doi.org/10.1021/ef300633c.
[86] Ren S, Lei H, Wang L, Bu Q, Chen S, Wu J, et al. The effects of torrefaction on compositions of bio-oil and syngas from biomass pyrolysis by microwave heating. Bioresour Technol 2013;135:659–64. https://doi.org/10.1016/j.biortech.2012.06.091.
[87] Zheng Y, Tao L, Yang X, Huang Y, Liu C, Gu J, et al. Effect of the torrefaction temperature on the structural properties and pyrolysis behavior of biomass. BioResources 2017;12. https://doi.org/10.15376/biores.12.2.3425-3447.
[88] Ukaew S, Schoenborn J, Klemetsrud B, Shonnard DR. Effects of torrefaction temperature and acid pretreatment on the yield and quality of fast pyrolysis bio - oil from rice straw. J Anal Appl Pyrol 2018;129:112–22. https://doi.org/10.1016/j.jaap.2017.11.021.
[89] Zheng A, Zhao Z, Huang Z, Zhao K, Wei G, Wang X, et al. Catalytic fast pyrolysis of biomass pretreated by torrefaction with varying severity. Energy & Fuels 2014;28:5804–11. https://doi.org/10.1021/ef500892k.
[90] Dong Q, Zhang S, Ding K, Zhu S, Zhang H, Liu X. Pyrolysis behavior of raw/torrefied rice straw after different demineralization processes. Biomass Bioenergy 2018;119:229–36. https://doi.org/10.1016/j.biombioe.2018.09.032.
[91] Isemin R, Klimov D, Larina O, Sytchev G, Zaichenko V, Milovanov O. Application of torrefaction for recycling bio-waste formed during anaerobic digestion. Fuel 2019;243:230–9. https://doi.org/10.1016/j.fuel.2019.01.119.
[92] González Martínez M, Dupont C, da Silva Perez D, Míguez-Rodríguez L, Grateau M, Thiéry S, et al. Assessing the suitability of recovering shrub biowaste involved in wildland fires in the South of Europe through torrefaction mobile units. J Environ Manag 2019;236:551–60. https://doi.org/10.1016/j.jenvman.2019.02.019.
[93] Talero G, Rincón S, Gómez A. Biomass torrefaction in a standard retort: a study on oil palm solid residues. Fuel 2019;244:366–78. https://doi.org/10.1016/j.fuel.2019.02.008.
[94] kumar Singh R, Sarkar A, Chakraborty JP. Effect of torrefaction on the physicochemical properties of pigeon pea stalk (Cajanus cajan) and estimation of kinetic parameters. Renew Energy 2019;138:805–19. https://doi.org/10.1016/j.renene.2019.02.022.
[95] Ren S, Lei H, Zhang Y, Wang L, Bu Q, Wei Y, et al. Furfural production from microwave catalytic torrefaction of Douglas fir sawdust. J Anal Appl Pyrol 2019;138:188–95. https://doi.org/10.1016/j.jaap.2018.12.023.
[96] Budde PK, Megha R, Patel R, Pandey J. Investigating effects of temperature on fuel properties of torrefied biomass for bio-energy systems. Energy Sources, Part A Recovery, Util Environ Eff 2019;41:1140–8. https://doi.org/10.1080/15567036.2018.1544992.
[97] Wang X, Wu J, Chen Y, Pattiya A, Yang H, Chen H. Comparative study of wet and dry torrefaction of corn stalk and the effect on biomass pyrolysis polygeneration. Bioresour Technol 2018;258:88–97. https://doi.org/10.1016/j.biortech.2018.02.114.
[98] Zeng K, Yang Q, Zhang Y, Mei Y, Wang X, Yang H, et al. Influence of torrefaction with Mg-based additives on the pyrolysis of cotton stalk. Bioresour Technol 2018;261:62–9. https://doi.org/10.1016/j.biortech.2018.03.094.
[99] Natarajan P, Suriapparao DV, Vinu R. Microwave torrefaction of Prosopis juliflora: experimental and modeling study. Fuel Process Technol 2018;172:86–96. https://doi.org/10.1016/j.fuproc.2017.12.007.
[100] Rago YP, Surroop D, Mohee R. Assessing the potential of biofuel (biochar) production from food wastes through thermal treatment. Bioresour Technol 2018;248:258–64. https://doi.org/10.1016/j.biortech.2017.06.108.
[101] Xin S, Mi T, Liu X, Huang F. Effect of torrefaction on the pyrolysis characteristics of high moisture herbaceous residues. Energy 2018;152:586–93. https://doi.org/10.1016/j.energy.2018.03.104.
[102] Chen W-H, Wang C-W, Kumar G, Rousset P, Hsieh T-H. Effect of torrefaction pretreatment on the pyrolysis of rubber wood sawdust analyzed by Py-GC/MS. Bioresour Technol 2018;259:469–73. https://doi.org/10.1016/j.biortech.2018.03.033.
[103] Zheng A, Jiang L, Zhao Z, Huang Z, Zhao K, Wei G, et al. Impact of torrefaction on the chemical structure and catalytic fast pyrolysis behavior of hemicellulose, lignin, and cellulose. Energy Fuels 2015;29:8027–34. https://doi.org/10.1021/acs.energyfuels.5b01765.
[104] Chen Y, Yang H, Yang Q, Hao H, Zhu B, Chen H. Torrefaction of agriculture straws and its application on biomass pyrolysis poly-generation. Bioresour Technol 2014;156:70–7. https://doi.org/10.1016/j.biortech.2013.12.088.
[105] Branca C, Di Blasi C, Galgano A, Broström M. Effects of the torrefaction conditions on the fixed-bed pyrolysis of Norway spruce. Energy & Fuels 2014;28:5882–91. https://doi.org/10.1021/ef501395b.
[106] Zheng A, Zhao Z, Chang S, Huang Z, He F, Li H. Effect of torrefaction temperature on product distribution from two-staged pyrolysis of biomass. Energy & Fuels 2012;26:2968–74. https://doi.org/10.1021/ef201872y.
[107] Carpenter D, Westover TL, Czernik S, Jablonski W. Biomass feedstocks for renewable fuel production: a review of the impacts of feedstock and pretreatment on the yield and product distribution of fast pyrolysis bio-oils and vapors. Green Chem 2014;16:384–406. https://doi.org/10.1039/C3GC41631C.
[108] Scott DS, Paterson L, Piskorz J, Radlein D. Pretreatment of poplar wood for fast pyrolysis: rate of cation removal. J Anal Appl Pyrol 2001;57:169–76. https://doi.org/10.1016/S0165-2370(00)00108-X.
[109] Arora JS, Chew JW, Mushrif SH. Influence of alkali and alkaline-earth metals on the cleavage of glycosidic bond in biomass pyrolysis: a dft study using cellobiose as a model compound. J Phys Chem 2018;122:7646–58. https://doi.org/10.1021/acs.jpca.8b06083.
[110] Mourant D, Wang Z, He M, Wang XS, Garcia-Perez M, Ling K, et al. Mallee wood fast pyrolysis: effects of alkali and alkaline earth metallic species on the yield and composition of bio-oil. Fuel 2011;90:2915–22. https://doi.org/10.1016/j.fuel.2011.04.033.
[111] Garrido R, Reckamp J, Satrio J. Effects of pretreatments on yields, selectivity and properties of products from pyrolysis of phragmites australis (common reeds). Environments 2017;4:96. https://doi.org/10.3390/environments4040096.
[112] Zhang S, Chen T, Xiong Y. Effect of washing pretreatment with aqueous fraction of bio-oil on pyrolysis characteristic of rice husk and preparation of amorphous silica. Waste and Biomass Valorization 2018;9:861–9. https://doi.org/10.1007/s12649-017-9845-9.
[113] Cao B, Wang S, Hu Y, Abomohra AE-F, Qian L, He Z, et al. Effect of washing with diluted acids on Enteromorpha clathrata pyrolysis products: towards enhanced bio-oil from seaweeds. Renew Energy 2019;138:29–38. https://doi.org/10.1016/j.renene.2019.01.084.
[114] Tan H, Wang S. Experimental study of the effect of acid-washing pretreatment on biomass pyrolysis. J Fuel Chem Technol 2009;37:668–72. https://doi.org/10.1016/S1872-5813(10)60014-X.
[115] David GF, Perez VH, Rodriguez Justo O, Garcia-Perez M. Effect of acid additives on sugarcane bagasse pyrolysis: production of high yields of sugars. Bioresour Technol 2017;223:74–83. https://doi.org/10.1016/j.biortech.2016.10.051.
[116] Wang X, Leng S, Bai J, Zhou H, Zhong X, Zhuang G, et al. Role of pretreatment with acid and base on the distribution of the products obtained via lignocellulosic biomass pyrolysis. RSC Adv 2015;5:24984–9. https://doi.org/10.1039/C4RA15426F.
[117] Mei Y, Chai M, Shen C, Liu B, Liu R. Effect of methanol addition on properties and aging reaction mechanism of bio-oil during storage. Fuel 2019;244:499–507. https://doi.org/10.1016/j.fuel.2019.02.012.
[118] Baruah J, Nath BK, Sharma R, Kumar S, Deka RC, Baruah DC, et al. Recent trends in the pretreatment of lignocellulosic biomass for value-added products. Front Energy Res 2018;6:141. https://doi.org/10.3389/fenrg.2018.00141.
[119] Kim JS, Lee YY, Kim TH. A review on alkaline pretreatment technology for bioconversion of lignocellulosic biomass. Bioresour Technol 2016;199:42–8. https://doi.org/10.1016/j.biortech.2015.08.085.
[120] Zhou S, Brown RC, Bai X. The use of calcium hydroxide pretreatment to overcome agglomeration of technical lignin during fast pyrolysis. Green Chem 2015;17:4748–59. https://doi.org/10.1039/C5GC01611H.
[121] Wang H, Srinivasan R, Yu F, Steele P, Li Q, Mitchell B. Effect of acid, alkali, and steam explosion pretreatments on characteristics of bio-oil produced from pinewood. Energy & Fuels 2011;25:3758–64. https://doi.org/10.1021/ef2004909.
[122] Hassan EM, Steele PH, Ingram L. Characterization of fast pyrolysis bio-oils produced from pretreated pine wood. Appl Biochem Biotechnol 2009;154:3–13. https://doi.org/10.1007/s12010-008-8445-3.
[123] Wang H, Srinivasan R, Yu F, Steele P, Li Q, Mitchell B, et al. Effect of acid, steam explosion, and size reduction pretreatments on bio-oil production from sweetgum, switchgrass, and corn stover. Appl Biochem Biotechnol 2012;167:285–97. https://doi.org/10.1007/s12010-012-9678-8.
[124] Raveendran K, Ganesh A, Khilar KC. Influence of mineral matter on biomass pyrolysis characteristics. Fuel 1995;74:1812–22. https://doi.org/10.1016/0016-2361(95)80013-8.
[125] Jae J, Tompsett GA, Lin Y-C, Carlson TR, Shen J, Zhang T, et al. Depolymerization of lignocellulosic biomass to fuel precursors: maximizing carbon efficiency by combining hydrolysis with pyrolysis. Energy Environ Sci 2010;3:358–65. https://doi.org/10.1039/B924621P.
[126] Misson M, Haron R, Kamaroddin MFA, Amin NAS. Pretreatment of empty palm fruit bunch for production of chemicals via catalytic pyrolysis. Bioresour Technol 2009;100:2867–73. https://doi.org/10.1016/j.biortech.2008.12.060.
[127] Pittman CU, Mohan D, Eseyin A, Li Q, Ingram L, Hassan E-BM, et al. Characterization of bio-oils produced from fast pyrolysis of corn stalks in an auger reactor. Energy Fuels 2012;26:3816–25. https://doi.org/10.1021/ef3003922.

[128] Fahmi R, Bridgwater AV, Donnison I, Yates N, Jones JM. The effect of lignin and inorganic species in biomass on pyrolysis oil yields, quality and stability. Fuel 2008;87:1230–40. https://doi.org/10.1016/j.fuel.2007.07.026.
[129] Das P, Ganesh A, Wangikar P. Influence of pretreatment for deashing of sugarcane bagasse on pyrolysis products. Biomass Bioenergy 2004;27:445–57. https://doi.org/10.1016/j.biombioe.2004.04.002.
[130] Wigley T, Yip ACK, Pang S. Pretreating biomass via demineralisation and torrefaction to improve the quality of crude pyrolysis oil. Energy 2016;109:481–94. https://doi.org/10.1016/j.energy.2016.04.096.
[131] Chen D, Mei J, Li H, Li Y, Lu M, Ma T, et al. Combined pretreatment with torrefaction and washing using torrefaction liquid products to yield upgraded biomass and pyrolysis products. Bioresour Technol 2017;228:62–8. https://doi.org/10.1016/j.biortech.2016.12.088.
[132] Zhang S, Su Y, Xu D, Zhu S, Zhang H, Liu X. Effects of torrefaction and organic-acid leaching pretreatment on the pyrolysis behavior of rice husk. Energy 2018;149:804–13. https://doi.org/10.1016/j.energy.2018.02.110.
[133] Gong S-H, Im H-S, Um M, Lee H-W, Lee J-W. Enhancement of waste biomass fuel properties by sequential leaching and wet torrefaction. Fuel 2019;239:693–700. https://doi.org/10.1016/j.fuel.2018.11.069.
[134] Zhang D, Wang F, Zhang A, Yi W, Li Z, Shen X. Effect of pretreatment on chemical characteristic and thermal degradation behavior of corn stalk digestate: comparison of dry and wet torrefaction. Bioresour Technol 2019;275:239–46. https://doi.org/10.1016/j.biortech.2018.12.044.
[135] He C, Tang C, Li C, Yuan J, Tran K-Q, Bach Q-V, et al. Wet torrefaction of biomass for high quality solid fuel production: a review. Renew Sustain Energy Rev 2018;91:259–71. https://doi.org/10.1016/j.rser.2018.03.097.
[136] Hoekman SK, Broch A, Robbins C, Zielinska B, Felix L. Hydrothermal carbonization (HTC) of selected woody and herbaceous biomass feedstocks. Biomass Conversion and Biorefinery 2013;3:113–26. https://doi.org/10.1007/s13399-012-0066-y.
[137] Hoekman SK, Broch A, Robbins C. Hydrothermal carbonization (HTC) of lignocellulosic biomass. Energy & Fuels 2011;25:1802–10. https://doi.org/10.1021/ef101745n.
[138] Chang S, Zhao Z, Zheng A, Li X, Wang X, Huang Z, et al. Effect of hydrothermal pretreatment on properties of bio-oil produced from fast pyrolysis of eucalyptus wood in a fluidized bed reactor. Bioresour Technol 2013;138:321–8. https://doi.org/10.1016/j.biortech.2013.03.170.
[139] Zhang S, Chen T, Xiong Y, Dong Q. Effects of wet torrefaction on the physicochemical properties and pyrolysis product properties of rice husk. Energy Convers Manag 2017;141:403–9. https://doi.org/10.1016/j.enconman.2016.10.002.
[140] Tarves PC, Serapiglia MJ, Mullen CA, Boateng AA, Volk TA. Effects of hot water extraction pretreatment on pyrolysis of shrub willow. Biomass Bioenergy 2017;107:299–304. https://doi.org/10.1016/j.biombioe.2017.10.024.
[141] Stephanidis S, Nitsos C, Kalogiannis K, Iliopoulou EF, Lappas AA, Triantafyllidis KS. Catalytic upgrading of lignocellulosic biomass pyrolysis vapours: effect of hydrothermal pre-treatment of biomass. Catal Today 2011;167:37–45. https://doi.org/10.1016/j.cattod.2010.12.049.
[142] Le Roux É, Chaouch M, Diouf PN, Stevanovic T. Impact of a pressurized hot water treatment on the quality of bio-oil produced from aspen. Biomass Bioenergy 2015;81:202–9. https://doi.org/10.1016/j.biombioe.2015.07.005.
[143] Zheng A, Zhao Z, Chang S, Huang Z, Zhao K, Wei G, et al. Comparison of the effect of wet and dry torrefaction on chemical structure and pyrolysis behavior of corncobs. Bioresour Technol 2015;176:15–22. https://doi.org/10.1016/j.biortech.2014.10.157.
[144] Zeng K, He X, Yang H, Wang X, Chen H. The effect of combined pretreatments on the pyrolysis of corn stalk. Bioresour Technol 2019;281:309–17. https://doi.org/10.1016/j.biortech.2019.02.107.
[145] Su Y, Liu L, Dong Q, Xie Y, Wang P, Zhang S, et al. Investigation of molten salt in wet torrefaction and its effects on fast pyrolysis behaviors. Energy Sources, Part A Recovery, Util Environ Eff 2019:1–9. https://doi.org/10.1080/15567036.2019.1587104.
[146] Hu J, Jiang B, Wang J, Qiao Y, Zuo T, Sun Y, et al. Physicochemical characteristics and pyrolysis performance of corn stalk torrefied in aqueous ammonia by microwave heating. Bioresour Technol 2019;274:83–8. https://doi.org/10.1016/j.biortech.2018.11.076.
[147] Granados DA, Basu P, Nhuchhen DR, Chejne F. Investigation into torrefaction kinetics of biomass and combustion behaviors of raw, torrefied and char samples. Biofuels 2019:1–11. https://doi.org/10.1080/17597269.2018.1558837.
[148] Bach Q-V, Tran K-Q, Ø Skreiberg, Trinh TT. Effects of wet torrefaction on pyrolysis of woody biomass fuels. Energy 2015;88:443–56. https://doi.org/10.1016/j.energy.2015.05.062.
[149] Biswas AK, Umeki K, Yang W, Blasiak W. Change of pyrolysis characteristics and structure of woody biomass due to steam explosion pretreatment. Fuel Process Technol 2011;92:1849–54. https://doi.org/10.1016/j.fuproc.2011.04.038.
[150] Inagaki T, Siesler HW, Mitsui K, Tsuchikawa S. Difference of the crystal structure of cellulose in wood after hydrothermal and aging degradation: a NIR spectroscopy and XRD study. Biomacromolecules 2010;11:2300–5. https://doi.org/10.1021/bm100403y.
[151] Li M-F, Shen Y, Sun J-K, Bian J, Chen C-Z, Sun R-C. Wet torrefaction of bamboo in hydrochloric acid solution by microwave heating. ACS Sustainable Chem Eng 2015;3:2022–9. https://doi.org/10.1021/acssuschemeng.5b00296.
[152] Lynam JG, Coronella CJ, Yan W, Reza MT, Vasquez VR. Acetic acid and lithium chloride effects on hydrothermal carbonization of lignocellulosic biomass. Bioresour Technol 2011;102:6192–9. https://doi.org/10.1016/j.biortech.2011.02.035.
[153] Xu X, Tu R, Sun Y, Wu Y, Jiang E, Zhen J. The influence of combined pretreatment with surfactant/ultrasonic and hydrothermal carbonization on fuel properties, pyrolysis and combustion behavior of corn stalk. Bioresour Technol 2019;271:427–38. https://doi.org/10.1016/j.biortech.2018.09.066.
[154] Kumar P, Barrett DM, Delwiche MJ, Stroeve P. Methods for pretreatment of lignocellulosic biomass for efficient hydrolysis and biofuel production. Ind Eng Chem Res 2009;48:3713–29. https://doi.org/10.1021/ie801542g.
[155] Balan V, Bals B, Chundawat SPS, Marshall D, Dale BE. Lignocellulosic biomass pretreatment using AFEX. In: Mielenz JR, editor. Biofuels, vol. 581. Totowa, NJ: Humana Press; 2009. p. 61–77. https://doi.org/10.1007/978-1-60761-214-8_5.
[156] Chundawat SPS, Donohoe BS, da Costa Sousa L, Elder T, Agarwal UP, Lu F, et al. Multi-scale visualization and characterization of lignocellulosic plant cell wall deconstruction during thermochemical pretreatment. Energy Environ Sci 2011;4:973. https://doi.org/10.1039/c0ee00574f.
[157] Balan V, Bals B, Chundawat SPS, Marshall D, Dale BE. Lignocellulosic biomass pretreatment using AFEX. In: Mielenz JR, editor. Biofuels, vol. 581. Totowa, NJ: Humana Press; 2009. p. 61–77. https://doi.org/10.1007/978-1-60761-214-8_5.
[158] Jacquet N, Maniet G, Vanderghem C, Delvigne F, Richel A. Application of steam explosion as pretreatment on lignocellulosic material: a review. Ind Eng Chem Res 2015;54:2593–8. https://doi.org/10.1021/ie503151g.
[159] Deepa B, Abraham E, Cherian BM, Bismarck A, Blaker JJ, Pothan LA, et al. Structure, morphology and thermal characteristics of banana nano fibers obtained by steam explosion. Bioresour Technol 2011;102. https://doi.org/10.1016/j.biortech.2010.09.030. 1988–97.
[160] Shi W, Li S, Jia J, Zhao Y. Highly efficient conversion of cellulose to bio-oil in hot-compressed water with ultrasonic pretreatment. Ind Eng Chem Res 2013;52:586–93. https://doi.org/10.1021/ie3024966.
[161] Tarves PC, Serapiglia MJ, Mullen CA, Boateng AA, Volk TA. Effects of hot water extraction pretreatment on pyrolysis of shrub willow. Biomass Bioenergy 2017;107:299–304. https://doi.org/10.1016/j.biombioe.2017.10.024.
[162] Le Roux É, Diouf PN, Stevanovic T. Analytical pyrolysis of hot water pretreated forest biomass. J Anal Appl Pyrol 2015;111:121–31. https://doi.org/10.1016/j.jaap.2014.11.023.
[163] Eisenbies MH, Volk TA, Amidon TE, Shi S. Influence of blending and hot water extraction on the quality of wood pellets. Fuel 2019;241:1058–67. https://doi.org/10.1016/j.fuel.2018.12.120.
[164] Sindhu R, Binod P, Pandey A. Biological pretreatment of lignocellulosic biomass – an overview. Bioresour Technol 2016;199:76–82. https://doi.org/10.1016/j.biortech.2015.08.030.
[165] Vasco-Correa J, Ge X, Li Y. Biological pretreatment of lignocellulosic biomass. Biomass fractionation technologies for a lignocellulosic feedstock based biorefinery. Elsevier; 2016. p. 561–85. https://doi.org/10.1016/B978-0-12-802323-5.00024-4.
[166] Yu Y, Zeng Y, Zuo J, Ma F, Yang X, Zhang X, et al. Improving the conversion of biomass in catalytic fast pyrolysis via white-rot fungal pretreatment. Bioresour Technol 2013;134:198–203. https://doi.org/10.1016/j.biortech.2013.01.167.
[167] Longe LF, Couvreur J, Leriche Grandchamp M, Garnier G, Allais F, Saito K. Importance of mediators for lignin degradation by fungal laccase. ACS Sustainable Chem Eng 2018;6:10097–107. https://doi.org/10.1021/acssuschemeng.8b01426.
[168] Yang X, Ma F, Yu H, Zhang X, Chen S. Effects of biopretreatment of corn stover with white-rot fungus on low-temperature pyrolysis products. Bioresour Technol 2011;102:3498–503. https://doi.org/10.1016/j.biortech.2010.11.021.
[169] You T, Li X, Wang R, Zhang X, Xu F. Effects of synergistic fungal pretreatment on structure and thermal properties of lignin from corncob. Bioresour Technol 2019;272:123–9. https://doi.org/10.1016/j.biortech.2018.09.145.
[170] Yan K, Liu F, Chen Q, Ke M, Huang X, Hu W, et al. Pyrolysis characteristics and kinetics of lignin derived from enzymatic hydrolysis residue of bamboo pretreated with white-rot fungus. Biotechnol Biofuels 2016;9. https://doi.org/10.1186/s13068-016-0489-y.
[171] Agbor VB, Cicek N, Sparling R, Berlin A, Levin DB. Biomass pretreatment: fundamentals toward application. Biotechnol Adv 2011;29:675–85. https://doi.org/10.1016/j.biotechadv.2011.05.005.
[172] Adhikari S, Srinivasan V, Fasina O. Catalytic pyrolysis of raw and thermally treated lignin using different acidic zeolites. Energy & Fuels 2014;28:4532–8. https://doi.org/10.1021/ef500902x.
[173] Ly HV, Choi JH, Woo HC, Kim S-S, Kim J. Upgrading bio-oil by catalytic fast pyrolysis of acid-washed Saccharina japonica alga in a fluidized-bed reactor. Renew Energy 2019;133:11–22. https://doi.org/10.1016/j.renene.2018.09.103.
[174] Hoff TC, Gardner DW, Thilakaratne R, Wang K, Hansen TW, Brown RC, et al. Tailoring ZSM-5 zeolites for the fast pyrolysis of biomass to aromatic hydrocarbons. ChemSusChem 2016;9:1473–82. https://doi.org/10.1002/cssc.201600186.
[175] Li X, Dong W, Zhang J, Shao S, Cai Y. Preparation of bio-oil derived from catalytic upgrading of biomass vacuum pyrolysis vapor over metal-loaded HZSM-5 zeolites. J Energy Inst 2019. https://doi.org/10.1016/j.joei.2019.06.005. S1743967119303599.
[176] Veses A, Puértolas B, López JM, Callén MS, Solsona B, García T. Promoting deoxygenation of bio-oil by metal-loaded hierarchical ZSM-5 zeolites. ACS Sustainable Chem Eng 2016;4:1653–60. https://doi.org/10.1021/acssuschemeng.5b01606.
[177] Lee S, Lee M-G, Park J. Catalytic upgrading pyrolysis of pine sawdust for bio-oil with metal oxides. J Mater Cycles Waste Manag 2018;20:1553–61. https://doi.org/10.1007/s10163-018-0716-7.

[178] Lin X, Zhang Z, Zhang Z, Sun J, Wang Q, Pittman CU. Catalytic fast pyrolysis of a wood-plastic composite with metal oxides as catalysts. Waste Manag 2018;79:38–47. https://doi.org/10.1016/j.wasman.2018.07.021.

[179] Kumar R, Strezov V, Lovell E, Kan T, Weldekidan H, He J, et al. Enhanced bio-oil deoxygenation activity by Cu/zeolite and Ni/zeolite catalysts in combined in-situ and ex-situ biomass pyrolysis. J Anal Appl Pyrol 2019. https://doi.org/10.1016/j.jaap.2019.03.008.

[180] Wang K, Johnston PA, Brown RC. Comparison of in-situ and ex-situ catalytic pyrolysis in a micro-reactor system. Bioresour Technol 2014;173:124–31. https://doi.org/10.1016/j.biortech.2014.09.097.

[181] Huang Y, Wei L, Crandall Z, Julson J, Gu Z. Combining Mo–Cu/HZSM-5 with a two-stage catalytic pyrolysis system for pine sawdust thermal conversion. Fuel 2015;150:656–63. https://doi.org/10.1016/j.fuel.2015.02.071.

[182] Hu C, Xiao R, Zhang H. Ex-situ catalytic fast pyrolysis of biomass over HZSM-5 in a two-stage fluidized-bed/fixed-bed combination reactor. Bioresour Technol 2017;243:1133–40. https://doi.org/10.1016/j.biortech.2017.07.011.

[183] Adjaye JD, Bakhshi NN. Production of hydrocarbons by catalytic upgrading of a fast pyrolysis bio-oil. Part I: conversion over various catalysts. Fuel Process Technol 1995;45:161–83. https://doi.org/10.1016/0378-3820(95)00034-5.

[184] Leung A, Boocock DGB, Konar SK. Pathway for the catalytic conversion of carboxylic acids to hydrocarbons over activated alumina. Energy Fuels 1995;9:913–20. https://doi.org/10.1021/ef00053a026.

[185] Shi Y, Xing E, Wu K, Wang J, Yang M, Wu Y. Recent progress on upgrading of bio-oil to hydrocarbons over metal/zeolite bifunctional catalysts. Catalysis Science & Technology 2017;7:2385–415. https://doi.org/10.1039/C7CY00574A.

[186] Rahimi N, Karimzadeh R. Catalytic cracking of hydrocarbons over modified ZSM-5 zeolites to produce light olefins: a review. Appl Catal Gen 2011;398:1–17. https://doi.org/10.1016/j.apcata.2011.03.009.

[187] Hernando H, Hernández-Giménez AM, Ochoa-Hernández C, Bruijnincx PCA, Houben K, Baldus M, et al. Engineering the acidity and accessibility of the zeolite ZSM-5 for efficient bio-oil upgrading in catalytic pyrolysis of lignocellulose. Green Chem 2018. https://doi.org/10.1039/C8GC01722K.

[188] Puértolas B, Veses A, Callén MS, Mitchell S, García T, Pérez-Ramírez J. Porosity-Acidity interplay in hierarchical ZSM-5 zeolites for pyrolysis oil valorization to aromatics. ChemSusChem 2015;8:3283–93. https://doi.org/10.1002/cssc.201500685.

[189] Gou J, Wang Z, Li C, Qi X, Vattipalli V, Cheng Y-T, et al. The effects of ZSM-5 mesoporosity and morphology on the catalytic fast pyrolysis of furan. Green Chem 2017;19:3549–57. https://doi.org/10.1039/C7GC01395G.

[190] Baloch HA, Nizamuddin S, Siddiqui MTH, Riaz S, Jatoi AS, Dumbre DK, et al. Recent advances in production and upgrading of bio-oil from biomass: a critical overview. J. Environ. Chem. Eng. 2018;6:5101–18. https://doi.org/10.1016/j.jece.2018.07.050.

[191] Lian X, Xue Y, Zhao Z, Xu G, Han S, Yu H. Progress on upgrading methods of bio-oil: a review: upgrading progress of bio-oil. Int J Energy Res 2017;41:1798–816. https://doi.org/10.1002/er.3726.

[192] Srinivasan V, Adhikari S, Chattanathan SA, Park S. Catalytic pyrolysis of torrefied biomass for hydrocarbons production. Energy & Fuels 2012;26:7347–53. https://doi.org/10.1021/ef301469t.

[193] Neupane S, Adhikari S, Wang Z, Ragauskas AJ, Pu Y. Effect of torrefaction on biomass structure and hydrocarbon production from fast pyrolysis. Green Chem 2015;17:2406–17. https://doi.org/10.1039/C4GC02383H.

[194] Chen Z, Wang M, Jiang E, Wang D, Zhang K, Ren Y, et al. Pyrolysis of torrefied biomass. Trends Biotechnol 2018;36:1287–98. https://doi.org/10.1016/j.tibtech.2018.07.005.

[195] Zhang S, Zhang H, Liu X, Zhu S, Hu L, Zhang Q. Upgrading of bio-oil from catalytic pyrolysis of pretreated rice husk over Fe-modified ZSM-5 zeolite catalyst. Fuel Process Technol 2018;175:17–25. https://doi.org/10.1016/j.fuproc.2018.03.002.

[196] Custodis VBF, Hemberger P, Ma Z, van Bokhoven JA. Mechanism of fast pyrolysis of lignin: studying model compounds. J Phys Chem B 2014;118:8524–31. https://doi.org/10.1021/jp5036579.

[197] Bu Q, Lei H, Qian M, Yadavalli G. A thermal behavior and kinetics study of the catalytic pyrolysis of lignin. RSC Adv 2016;6:100700–7. https://doi.org/10.1039/C6RA22967K.

[198] Arteaga-Pérez LE, Jiménez R, Grob N, Gómez O, Romero R, Ronsse F. Catalytic upgrading of biomass-derived vapors on carbon aerogel-supported Ni: effect of temperature, metal cluster size and catalyst-to-biomass ratio. Fuel Process Technol 2018;178:251–61. https://doi.org/10.1016/j.fuproc.2018.05.036.

[199] Bach Q-V, Tran K-Q, Skreiberg Ø, Trinh TT. Effects of wet torrefaction on pyrolysis of woody biomass fuels. Energy 2015;88:443–56. https://doi.org/10.1016/j.energy.2015.05.062.

[200] Stephanidis S, Nitsos C, Kalogiannis K, Iliopoulou EF, Lappas AA, Triantafyllidis KS. Catalytic upgrading of lignocellulosic biomass pyrolysis vapours: effect of hydrothermal pre-treatment of biomass. Catal Today 2011;167:37–45. https://doi.org/10.1016/j.cattod.2010.12.049.

[201] Arteaga-Pérez LE, Gómez Cápiro O, Romero R, Delgado A, Olivera P, Ronsse F, et al. In situ catalytic fast pyrolysis of crude and torrefied Eucalyptus globulus using carbon aerogel-supported catalysts. Energy 2017;128:701–12. https://doi.org/10.1016/j.energy.2017.04.024.

[202] Mahadevan R, Adhikari S, Shakya R, Wang K, Dayton DC, Li M, et al. Effect of torrefaction temperature on lignin macromolecule and product distribution from HZSM-5 catalytic pyrolysis. J Anal Appl Pyrol 2016;122:95–105. https://doi.org/10.1016/j.jaap.2016.10.011.

[203] Chen D, Li Y, Deng M, Wang J, Chen M, Yan B, et al. Effect of torrefaction pretreatment and catalytic pyrolysis on the pyrolysis poly-generation of pine wood. Bioresour Technol 2016;214:615–22. https://doi.org/10.1016/j.biortech.2016.04.058.

[204] Persson H, Yang W. Catalytic pyrolysis of demineralized lignocellulosic biomass. Fuel 2019;252:200–9. https://doi.org/10.1016/j.fuel.2019.04.087.

[205] Baral NR, Shah A. Comparative techno-economic analysis of steam explosion, dilute sulfuric acid, ammonia fiber explosion and biological pretreatments of corn stover. Bioresour Technol 2017;232:331–43. https://doi.org/10.1016/j.biortech.2017.02.068.

[206] Brown TR, Zhang Y, Hu G, Brown RC. Techno-economic analysis of biobased chemicals production via integrated catalytic processing. Biofuels, Bioprod Bioref 2012;6:73–87. https://doi.org/10.1002/bbb.344.

[207] Shemfe M, Gu S, Fidalgo B. Techno-economic analysis of biofuel production via bio-oil zeolite upgrading: an evaluation of two catalyst regeneration systems. Biomass Bioenergy 2017;98:182–93. https://doi.org/10.1016/j.biombioe.2017.01.020.

[208] Rogers JG, Brammer JG. Estimation of the production cost of fast pyrolysis bio-oil. Biomass Bioenergy 2012;36:208–17. https://doi.org/10.1016/j.biombioe.2011.10.028.

[209] Chai L, Saffron CM, Yang Y, Zhang Z, Munro RW, Kriegel RM. Integration of decentralized torrefaction with centralized catalytic pyrolysis to produce green aromatics from coffee grounds. Bioresour Technol 2016;201:287–92. https://doi.org/10.1016/j.biortech.2015.11.065.

[210] Oasmaa A, Kyt M, Sipil K. Pyrolysis oil combustion tests in an industrial boiler. In: Bridgwater AV, editor. Progress in thermochemical biomass conversion. Oxford, UK: Blackwell Science Ltd; 2001. p. 1468–81. https://doi.org/10.1002/9780470694954.ch121.

[211] Cataluña R, Kuamoto PM, Petzhold CL, Caramão EB, Machado ME, da Silva R. Using bio-oil produced by biomass pyrolysis as diesel fuel. Energy & Fuels 2013;27:6831–8. https://doi.org/10.1021/ef401644v.

MACQUARIE University

MACQUARIE UNIVERSITY
AUTHORSHIP CONTRIBUTION STATEMENT

In accordance with the *Macquarie University Code for the Responsible Conduct of Research* and the *Authorship Standard*, researchers have a responsibility to their colleagues and the wider community to treat others fairly and with respect, to give credit where appropriate to those who have contributed to research.

Note for HDR students: *Where research papers are being included in a thesis, this template must be used to document the contribution of authors to each of the proposed or published research papers. The contribution of the candidate must be sufficient to justify inclusion of the paper in the thesis.*

1. DETAILS OF PUBLICATION & CORRESPONDING AUTHOR

Title of Publication (can be a holding title)		**Publication Status** Choose an item.
Thermochemcial production of bio-oil: A review of downstream processing technologies for bio-oil upgrading, production of hydrogen and high value-added products		☐ In Progress or Unpublished work for thesis submission ☐ Submitted for Publication ☐ Accepted for Publication ☑ Published
Name of **corresponding author**	Department/Faculty	**Publication details:** indicate the name of the journal/ conference/ publisher/other outlet
Ravinder Kumar	Earth and Environmental Sciences/ Science & Engineering	Renewable & Sustainable Energy Reviews

2. STUDENTS DECLARATION (if applicable)

Name of HDR thesis author (If the same as corresponding author - write "as above")	Department/Faculty	Thesis title
As above	Earth and Environmental Sciences/ Science & Engineering	Catalytic Upgrading of Bio-oil Produced from Fast Pyrolysis of Pinewood Sawdust

Description of HDR thesis author's contribution to planning, execution, and preparation of the work if there are multiple authors

(for example, how much as a percent did you contribute to the conception of the project, the design of methodology or experimental protocol, data collection, analysis, drafting the manuscript, revising it critically for important intellectual content, etc.)

In this article, I helped in designing the project, data collection and writing 85% of the manuscript.

I declare that the above is an accurate description of my contribution to this publication, and the contributions of other authors are as described below.	**Student signature** **Date**	02/26/2021

MACQUARIE University

3. Description of all other author contributions

Use an Asterisk * to denote if the author is also a current student or HDR candidate.

The HDR candidate or corresponding author must, for each paper, list all authors and provide details of their role in the publication. Where possible, also provide a percentage estimate of the contribution made by each author.

Name and affiliation of author	**Intellectual contribution(s)** (for example to the: conception of the project, design of methodology/experimental protocol, data collection, analysis, drafting the manuscript, revising it critically for important intellectual content etc.)
Vladimir Strezov Macquarie University	Conception, supervision, critical revision
	Provide summary for any additional Authors in this cell.

4. Author Declarations

I agree to be named as one of the authors of this work, and confirm:

i. *that I have met the authorship criteria set out in the* Authorship Standard, *accompanying the* Macquarie University Research Code,

ii. *that there are no other authors according to these criteria,*

iii. *that the description in Section 3 or 4 of my contribution(s) to this publication is accurate*

iv. *that I have agreed to the planned authorship order following the* Authorship Standard

Name of author	**Authorised *** By Signature or refer to other written record of approval (eg. pdf of a signed agreement or an email record)	**Date**
Vladimir Strezov		24/02/2021
	Provide other written record of approval for additional authors (eg. pdf of a signed agreement or an email record)	

5. Data storage

The original data for this project are stored in the following location, in accordance with the *Research Data Management Standard* accompanying the *Macquarie University Research Code*.

If the data have been or will be deposited in an online repository, provide the details here with any corresponding DOI.

Data description/format	**Storage Location or DOI**	**Name of custodian** if other than the corresponding author

A copy of this form must be retained by the corresponding author and must accompany the thesis submitted for examination.

Chapter 4

Thermochemical production of bio-oil: A review of downstream processing technologies for bio-oil upgrading, production of hydrogen and high value-added products

Kumar, R., & Strezov, V. (2021). Thermochemical production of bio-oil: a review of downstream processing technologies for bio-oil upgrading, production of hydrogen and high value-added products. Renewable and Sustainable Energy Reviews, 135, 1-31. [110152]. https://doi.org/10.1016/j.rser.2020.110152

Renewable and Sustainable Energy Reviews 135 (2021) 110152

Contents lists available at ScienceDirect

Renewable and Sustainable Energy Reviews

journal homepage: http://www.elsevier.com/locate/rser

Thermochemical production of bio-oil: A review of downstream processing technologies for bio-oil upgrading, production of hydrogen and high value-added products

R. Kumar *, V. Strezov

Department of Earth and Environmental Sciences, Faculty of Science & Engineering, Macquarie University, Sydney, NSW, 2109, Australia

ARTICLE INFO

Keywords:
Bio-oil upgrading
Hydrotreatment
Solvent addition
Emulsification
Microfiltration
Electrocatalytic hydrogenation
Steam reforming

ABSTRACT

Bio-oil produced from biomass pyrolysis and hydrothermal liquefaction is considered as the most sustainable alternative for depleting fossil fuels. However, the poor bio-oil properties, such as high viscosity, presence of solid particles, low calorific value and high instability are restricting its use as a drop-in fuel. The bio-oil properties can be significantly improved using different methods, such as catalytic upgrading, biomass pre-treatment and downstream bio-oil upgrading. This article focusses on the widely used methods for downstream bio-oil upgrading, such as hydrotreatment, solvent addition, emulsification, microfiltration and electrocatalytic hydrogenation. The bio-oil upgrading using non-polar solvents or preparing emulsions using surfactants have shown a significant increase in the calorific values and a considerable decrease in viscosity of the bio-oil. On the other hand, filtration of the bio-oil using membranes can remove the char particles and alkali and alkali earth metals from the bio-oil, consequently, leading to higher stability of the bio-oil. Electrocatalytic hydrogenation of the bio-oil has shown promising results to increase the content of hydrocarbons and increased pH by removing the carbonyl group-containing compounds from the bio-oil. The bio-oil can also be upgraded to other clean fuels, such as H_2 using steam reforming approach, has been critically reviewed. Basic principles of the processes and effects of different parameters on bio-oil upgrading are thoroughly discussed. In addition, techno-economic analysis, policy analysis, challenges and future recommendations related to downstream processes are provided in the article. Overall, this review article provides critical information about downstream bio-oil upgrading and production of other high value-added fuels.

1. Introduction

The world economy continues to grow at a Gross Domestic Product (GDP) rate of 3.25% and has been estimated to grow at a faster rate in Asia, particularly in India and China [1]. Significant energy sources are also required to meet the desired economic development. The total energy demand is expected to increase worldwide by 28% by 2040 [1]. Among all the energy sectors, transport sector, which mainly relies on liquid fuels, consumes the largest part of the energy and is predicted to reach nearly 3.3 Billion toe worldwide by 2040 [1]. There are predictions of the significant increase in electric vehicles (cars and buses) or solar-assisted vehicles that may decrease the demand of liquid fuel, however high-power transport vehicles, such as aeroplanes, long-haul trucks and ships, will still require high energy-density fuels. Therefore, potential alternatives to liquid fuels are required to meet the energy demand since the conventional liquid fuels (petrol and diesel) are depleting. The most desirable alternatives could be renewable and sustainable fuels or fuels that can be produced from renewable feedstocks and their combustion produces less greenhouse gas (GHG) emissions. In this regard, biomass has been considered the most suitable renewable energy source for production of various second-generation liquid fuels. This is mainly because biomass is a dominant source of carbon and contains less nitrogenous and sulphur contents. There are promising technologies that can convert biomass into high energy-density fuels [2–6]. In addition, it has been also reported that the combustion of fuels produced from biomass emits lower amount of NO_x and SO_x compared to conventional liquid fuels, like bio-oil [7,8] or bio-based jet fuel [9], which consequently could help to reduce GHG emissions.

Pyrolysis and hydrothermal liquefaction (HTL) are the most widely used approaches to convert the dry and wet lignocellulose biomass or organic wastes into liquid or other fuels and value-added chemicals

Nomenclature

AEM	Anion Exchange Membrane
Al	aluminium
C	Carbon
Ca	calcium
CO_2	carbon dioxide
CEM	Cation Exchange Membrane
cP	Centipoise
cSt	Centistokes
DMF	N N-dimethylformamide
DMSO	dimethyl sulfoxide,
ER	Energy recovery
ECR	energy conversion rate
CHR	carbon and hydrogen recovery
Fe	iron
GDP	Gross Domestic Product
GHG	greenhouse gas
Gt	gigaton
h	hydrogen
h	hour
HCl	Hydrochloric Acid
HER	Hydrogen Evolution Reaction
HTL	hydrothermal liquefaction
HHV	higher heating values
HLB	Hydrophilic-Lipophilic Balance
HVF	Hot Vapour Filtration
l	litre
kg	kilogram
KJ	Kilo Joule
m	metre
M	Molar
Mg	magnesium
MJ	Mega Joule
mg	milligram
Mg	magnesium
MPa	Mega Pascal
MFC	microbial fuel cell
N	nitrogen
Na	sodium
Ni	nickel
NO_x	nitrogen oxides
NaCl	sodium chloride
NaOH	sodium hydroxide
O	oxygen
O/W	Oil in Water
P	phosphorus
PEG	polyethylene glycol
PEG-DPHS	Polyethylene Glycol-Dipolyhydroxy Stearate
ppm	parts per million
s	second
Si	silicon
SO_x	sulphur oxides
SR	steam reforming
S/C	steam/carbon
T	temperature
W	watt
W/O	Water in Oil
μm	micro meter
°C	degree Celsius

[12–17]. Pyrolysis is a thermochemical process that degrades the various interlinkages between the biomass components as an effect of heating in an inert atmosphere where the main biomass components, such as cellulose, hemicellulose and lignin, are further degraded into different organic compounds [18,19]. Fig. 1 shows the major component of lignocellulose biomass. The biomass pyrolysis usually results in three types of products, bio-oil, bio-char and pyrolytic gases. The yield of the products mainly depends on the composition of biomass and the pyrolysis temperature. Generally, at the temperature of 500–600 °C, the biomass with a higher proportion of cellulose results in a higher bio-oil yield, while the pyrolysis of biomass with a higher amount of hemicellulose and lignin may result in higher gas and char yield, respectively [20–22]. Other pyrolytic parameters, such as heating rate, flow rate of carrier gas or residence time, holding time, and particle size of the feedstock, also influence the product yield or the composition of bio-oil [23]. On the other hand, HTL involves decomposition of biomass (wet or dry biomass) in the presence of a solvent (water, methanol, ethanol, acetone etc.) at the temperature of 250–550 °C and pressure of 5–25 MPa [24,25]. The process of biomass HTL firstly comprises the depolymerization of biomass into their individual components, followed by their decomposition via various reactions, such as dehydration, cleavage, decarboxylation and deamination. In the last step, the reactive molecules are recombined or repolymerized to form high-molecular-weight compounds. Similar to pyrolysis, the HTL process also generates three types of fuels, mainly bio-oil, bio-char, gases and also a water phase that contains a high content of carbon, and their yields depend on the type of feedstock and operating parameters of the process. For example, de Caprariis et al. [26] suggested that an increased bio-oil yield could be obtained with the biomass containing higher content of lignin, while the minimum bio-oil yield was obtained with the biomass containing a higher content of cellulose. Generally, the temperature range of 250–330 °C is suitable to obtain a higher bio-oil yield. The solvents with higher density and ability to promote the solvolysis and hydration reactions are highly advantageous in the HTL process [27,47,48]. Other parameters, such as pressure, heating rate and residence time also play a critical role to obtain quality bio-oil.

The bio-oil produced using either pyrolysis or HTL has been considered a clean and environmentally friendly energy fuel as its combustion generates lower GHG emissions compared to the conventional fossil fuels [28,29]. For example, a study demonstrated the comparison of bio-oil combustion with heavy fuel oil in an industrial boiler and the results showed that the NO_x emissions for bio-oil were 88 mg/MJ, while the combustion of heavy fuel oil produced NO_x emissions of 193 mg/MJ [30]. However, the bio-oil properties, such as high acidity, low stability, low higher heating values (HHV), presence of solid char particles make it an unsuitable drop-in fuel [19,31,32]. Therefore, bio-oil upgrading is essential to produce bio-oil as a transport fuel or for its direct use in the boilers and turbines for heat and power generation. There are different strategies to improve the properties of bio-oil, mainly based on the biomass pre-treatment, such as dry torrefaction [33,34], wet torrefaction [35,36], acid and alkali treatment [37–39], steam explosion etc. [40] and downstream treatment of the bio-oil such as emulsification [41,42], solvent addition [43,44], filtration etc. [45,46]. In terms of bio-oil upgrading, the biomass pre-treatment methods are usually advantageous to increase the conversion of oxygenated compounds into hydrocarbons, increase the bio-oil yield and HHV [47,48], while the downstream treatment methods generally help to increase the bio-oil stability and HHV, and decrease the viscosity and the amount of solid char particles. In addition, the bio-oil can also be upgraded using electrochemical hydrogenation, which generally converts the carbonyl-containing compounds into hydrocarbons or other value-added compounds [49,50]. Alternatively, the application of different catalysts during pyrolysis and HTL is a significant approach to improve the kinetics of the process and enhance the bio-oil properties,

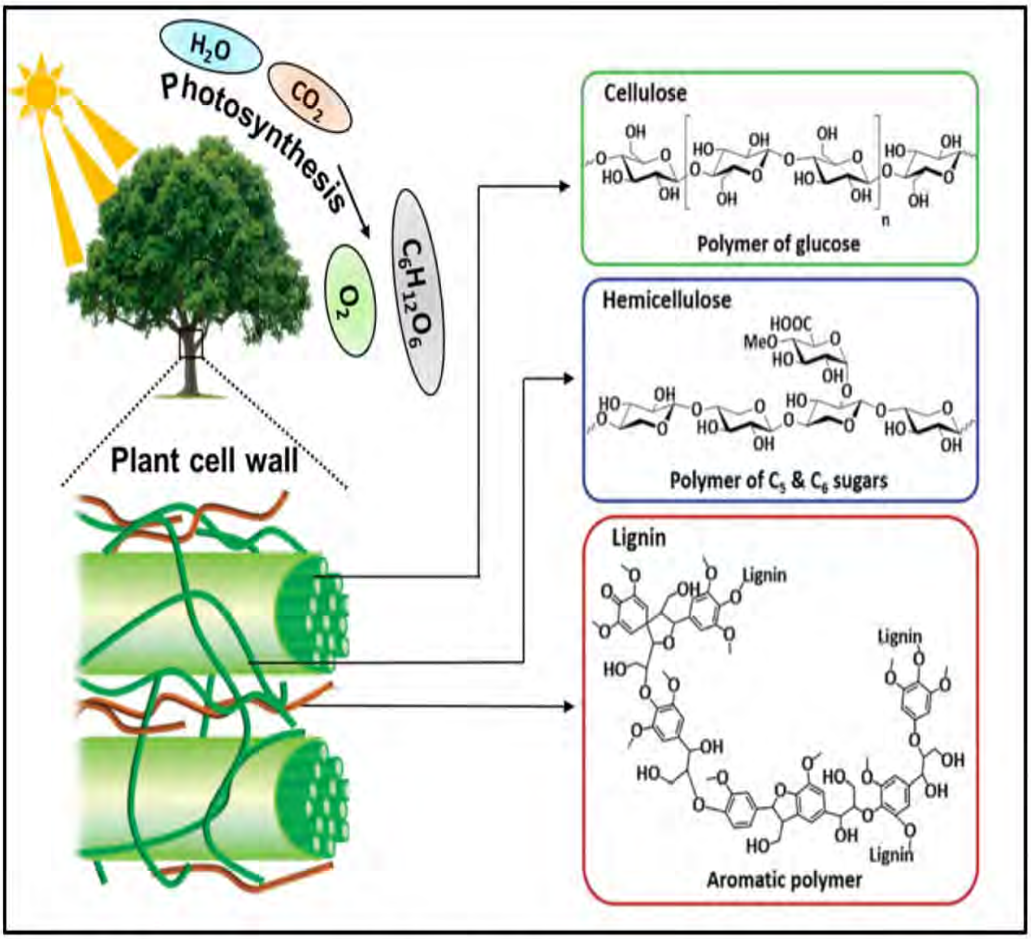

Fig. 1. Structure of lignocellulosic biomass with cellulose, hemicellulose, and lignin represented. Reproduced with permission from Refs. [10,11].

and has been widely used for bio-oil upgrading in pyrolysis as well as in HTL [24,51,52]. Hydrotreatment is considered highly efficient for bio-oil upgrading as it removes oxygen in the form of H_2O while in cracking oxygen is removed in the form of CO_2 and CO which decreases the total carbon yield [53,54]. Hydrotreatment of bio-oil obtained from pyrolysis and HTL process has been reported in several studies with various types of catalysts utilized for hydrotreatment of bio-oil to either convert it into a more valuable fuel with improved physicochemical properties or other value-added products. For instance, Biller et al. [55] studied the application of sulphided $NiMo/Al_2O_3$ and $CoMo/Al_2O_3$ for hydrotreatment of bio-oil obtained from HTL of *Chlorella*. The results reported considerable increase in the conversion of oxygenated compounds into hydrocarbons with application of sulphided catalysts, as a high number of hydrocarbons was observed in the upgraded bio-oil [55].

The bio-oil obtained from thermochemical techniques could also be a suitable feedstock for steam reforming (SR) for production of H_2 or a mixture of CO and H_2, called syngas [56–61]. H_2 produced from SR of bio-oil can be further used as a clean fuel, while syngas can be further subjected to Fischer-Tropsch process for production of hydrocarbons. SR is a process involving conversion of bio-oil containing oxygenated compounds or hydrocarbons into hydrogen in the presence of water at a temperature range of 350–1000 °C [62,63]. The technique also requires highly active catalyst to enhance the conversion efficiency and hydrogen yield. Several studies have reported the application of various types for catalysts with promising results for hydrogen production [60,62].

Bio-oil is foreseen as a potential drop-in fuel; hence, the bio-oil upgrading is highly important to make it competitive to the conventional energy fuels. The methods used for bio-oil upgrading, such as catalytic cracking, hydrodeoxygenation [10,13,64], biomass pre-treatments such as torrefaction and wet-torrefaction [35,35,65] have been comprehensively reviewed in previous publications. For example, Zacher et al. [66] critically reviewed hydrotreatment process for bio-oil upgrading and discussed various parameters, techno-economic analysis and challenges associated with the technique. Recently, Nishu et al. [67] published a review article focused on catalytic pyrolysis with ZSM-based catalysts for bio-oil upgrading. On the other hand, Bach and Skreiberg [65] published a review article on the effect of dry and wet torrefaction on bio-oil upgrading and other biofuel production. It was noticed that less attention has been paid to review the methods applied for downstream bio-oil upgrading and no review article has been published recently. In recent years, a number of research articles and reports have been published on various downstream techniques for bio-oil upgrading and production of other value-added fuels. Therefore, considering the significance of these methods for biofuel production this article aims to provide the recent advances in the downstream upgrading of bio-oil produced either using the pyrolysis process or HTL. The article begins with providing critical insights for the potential of biomass as a renewable resource and the conversion efficiency of pyrolysis and liquefaction for biofuel production. Later, it discusses the widely used methods for downstream bio-oil upgrading, such as solvent addition, emulsification, filtration, electrochemical hydrogenation and hydrotreatment. Basic principles of the processes and effects of different parameters on bio-oil upgrading are thoroughly discussed, while key challenges and possible solutions are also provided. Bio-oil can be successfully converted to clean fuel like H_2 using steam reforming technique (SR), which is critically discussed in the article. In addition, techno-economic analysis, policy analysis, challenges and future recommendations related to downstream processes are provided in later sections of the article. Overall, this review article provides

critical information about downstream bio-oil upgrading and production of other high value-added fuels.

2. Biomass as a renewable feedstock for bio-oil production

Biomass is a non-fossil, complex organic-inorganic solid product, mainly derived from plants and could also be obtained from animals, bacteria, fungi etc. A recent study has estimated the amount of biomass among all the taxa (plants, bacteria, fungi, animals, viruses, archaea, protists) on Earth [68,97]. The study showed that approximately 550 Gt C is present on Earth with 80%, or ~450 Gt C, is covered by terrestrial plants, while the rest is dominant by bacteria and others [68]. Therefore, it could be suggested that out of the total biomass on earth, 80% of biomass could be estimated as the potential feedstock in different thermochemical technologies for biofuel production. Biomass is considered as a renewable energy source since it does not contribute to the greenhouse effect because of CO_2 neutral conversion. The biomass plants store the energy in the primary products (monosaccharides) as a result of photosynthesis process, which involves the uptake of water, CO_2 and solar energy by the plant pigments and are converted into organic chemicals (monosaccharides like glucose) and oxygen, as shown in eq. (1).

$$6H_2O + 6CO_2 + radiant\ energy \rightarrow C_6H_{12}O_6(glucose) + 6O_2 \quad (1)$$

These primary products produced after photosynthesis act as precursors for synthesis of all types of organic components of biomass and are further converted into the secondary products, such as polysaccharides, proteins, lipids and several other organic compounds. The biomass synthesis in the plants greatly depends on the photosynthesis efficiency, which varies for different biomass species. Generally, the higher the photosynthesis efficiency, the greater is the biomass synthesis. It has been reported that the plants that fix CO_2 via C_3 pathway show higher photosynthesis efficiency at warm temperatures, while the plants fixing CO_2 via C_4 pathway exhibit higher rates of photosynthesis at cool temperatures [69]. Therefore, from higher biomass production point of view, C_3 or C_4 plants can be cultured according to the preferred climate conditions in different parts of the world to enhance production of biomass in shorter span of time, which can be further utilized in various technologies for biofuel production.

The organic-inorganic composition and energy content of the biomass are pivotal parameters for their utilization in conversion processes for the production of bio-oil or other biofuels. For example, the biomass that exhibits higher content of moisture could not be suitable for pyrolysis process, while it could be a suitable feedstock for HTL as the excess water could be used as a reactant medium, or in anaerobic or fermentation processes for methane or bioethanol production. Similarly, the ash content is highly undesirable in the biomass as its higher content lowers the organic matter in the biomass and consequently decreases the HHV of the biomass. The ash content also contains certain metal oxides, such as calcium and potassium, which might affect the conversion processes due to their catalytic behavior, and their further presence in the bio-oil makes it highly unstable as these metal oxides may start the polymerization reactions. It is evident and well known that different biomass exhibits varying composition, chemical structures and carbon contents. Generally, biomass with higher carbon content in reduced form shows higher heating value, while the higher degree of oxygenation reduces the heating value of the biomass. For example, the monosaccharides contain carbon contents of nearly 40% and their estimated HHV is 15.6 MJ/kg, while terpenes and lipids exhibit approximately 88% and 77% of carbon content and hence show higher HHV of 45.2 MJ/kg and 39.8 MJ/kg, respectively [70]. Table 1 shows the carbon content and HHV of specific biomass components.

An extensive research has been carried on both pyrolysis and HTL technologies for bio-oil production for optimization of process parameters and selection of biomass feedstock to obtain higher yield and quality of bio-oil. These parameters have been discussed in detail in several articles published already [20,21,91,92], therefore, are not reviewed in this article. However, the key differences between the pyrolysis and HTL in terms of bio-oil quality and energy conversion rate (ECR) are briefly discussed. ECR of the pyrolysis (or HTL) for a biomass feedstock at any temperature can be obtained using equations (2) and (3).

Table 1
Typical carbon content and heating value of selected biomass components. Reproduced with permission from Ref. [70].

Component	Carbon (wt%) on dry basis	HHV (MJ/kg)
Monosaccharides	40	15.6
Disaccharides	42	16.7
Polysaccharides	44	17.5
Crude proteins	53	24.0
Lignin	63	25.1
Lipids	76–77	39.8
Terpenes	88	45.2
Crude carbohydrates	41–44	16.7–17.7
Crude fibers	47–50	18.8–19.8
Crude triglycerides	74–78	36.5–40.0

$$\eta = \frac{Q_{recovered} - Q_{pyrolysis}}{Q_{biomass}} \times 100\% \quad (2)$$

where

$$Q_{recovered} = HHV_{gas} \times mass_{gas} + HHV_{liquid} \times mass_{liquid} + HHV_{char} \times mass_{char} \quad (3)$$

The comparative studies of pyrolysis and HTL suggest that HTL produces better bio-oil quality compared to pyrolysis [62,84,85]. For instance, Jena and Das [71] compared the quality of bio-oil produced from pyrolysis and HTL. They used *Spirulina platensis* as the feedstock and carried out the pyrolysis process at temperatures of 350 and 550 °C, with a heating rate of 3.5 °C/min and 7 °C/min, respectively, while the HTL process was carried out in a 1.8-L Parr reactor at 350 °C with the water pressure of 20.6 MPa and a heating rate of 3.3 °C/min, and the residence time of 60 min. The properties of the bio-oil resulted from both processes are shown in Table 2, which suggests that the bio-oil from HTL showed better thermal stability and HHV as compared to the pyrolytic oils [71]. However, the higher content of inorganic species was found in the bio-oil collected from HTL process, which could be mainly because of the leaching of inorganic species from the char into the bio-oil, as the liquid and solid products are usually kept in the reactor until the reactor is cooled down and the bio-oil is separated from the solid char [93,94]. In terms of ECR, HTL also proved more efficient than pyrolysis process. The study showed that HTL could convert approximately 67.9% of energy present in biomass into the bio-oil, while the ECR during pyrolysis was only 33.9% and 46.7% for the bio-oils obtained at the temperature of 350 and 500 °C, respectively [71]. The lower ECR in pyrolysis could be attributed to more energy inputs required for the pyrolysis process, mainly for drying the biomass feedstock before pyrolysis. The conversion efficiency of the pyrolysis process could be further enhanced if the energy inputs are provided by the energy products generated during the pyrolysis or using the solar thermal energy. In a recent study, Weldekidan et al. [95] showed that the pyrolysis process could be highly efficient if heat required to carry out the pyrolysis process is supplied by combustion of the evolved pyrolytic gas products. In this scenario, the ECR (for all pyrolytic products) calculated for the pyrolysis of rice husk biomass (at 500 °C and heating rate of 10 °C/min) was 89% and if the solar thermal energy is used for the pyrolysis process, the ECR of 94% could also be achieved [95]. Overall, it can be suggested that pyrolysis could be an efficient and equivalent approach for bio-oil production when compared to HTL.

Pyrolysis is a commercial process used for bio-oil production at a pilot scale. For example, KiOR and Envergent use Circulating Fluid Bed configuration, while Dynamotive applies Bubbling Fluidized Bed for

Table 2
Physical properties, ultimate analysis, inorganic elements of algal bio-oil samples, and energy and mass balance in HTL and pyrolysis processes, reproduced with permission from Ref. [71]. Copyright © 2011, American Chemical Society.

Bio-oil properties	HTL[a] (350 °C)	Pyr[b] (350 °C)	Pyr[b] (550 °C)
color	black	reddish brown	reddish brown
odor	smoky	acrid smoky	acrid smoky
pH	9.60	9.35	9.52
density, kg/L	0.97	1.20	1.05
viscosity, cP			
at 60 °C	51.20	34.30	23.10
at 40 °C	189.90	100.67	79.20
C, %	73.73	67.52	74.66
H, %	8.90	9.82	10.57
N, %	6.30	10.71	7.13
S, %	0.90	0.45	0.81
O, %	10.17	11.34	6.81
H/C ratio	1.44	1.73	1.68
O/C ratio	0.10	0.13	0.06
HHV, MJ/kg	34.20	29.30	33.62
Inorganics in Ash, mg/kg			
Na	14.6	14.6	14.0
Mg	69.3	11.3	2.3
Al	60.1	58.8	10.7
Si	115	54.8	15.5
P	249	63.2	39.6
Ca	116	35.4	7.6
Fe	848	135	180
Ni	72.1	6.4	24.1
Energy and Mass Balance			
ER[c], %	67.9	33.9	46.7
ECR[d], net energy ratio	0.70	2.11	1.56
CHR[e], %	71.7	39.3	51.3

[a] HTL: hydrothermal liquefaction.
[b] Pyr: pyrolysis.
[c] ER: Energy recovery.
[d] ECR: net energy ratio.
[e] CHR: carbon and hydrogen recovery.

biomass pyrolysis [96]. BTG-Bioliquids is using Rotating Cone Reactor fast pyrolysis technology for bio-oil production at a commercial level, and claims to obtain 70% of bio-oil yield. However, the bio-oil produced at the commercial level is still of low quality in terms of calorific value and H/C ratios, hence, the companies have to use an upgrading approach to improve the bio-oil properties. On the other hand, HTL has not been used at a commercial level yet mainly because of the high capital cost for the system. Other key challenges of HTL are associated with reactor designs, high cost for solvent, catalyst and purification of the bio-oil. A continuous reactor system is required to scale up the HTL process for bio-oil production as the batch reactors possess certain limitations regarding process parameters and mixture of bio-oil and biochar in the reactor which further requires a purification step to separate [97]. However, continuous reactors have some challenges when operates under high pressures and temperature conditions. For example, they require preparation of biomass slurries and pumping into the reactor, which is a challenging task to perform under high pressures. The requirement for pumping instrumentation and operation is also an economic challenge as it increases the total operating cost. The development of highly effective, cheaper and simple purification techniques, application of advanced, cost-effective and versatile catalysts, and minimizing the use of solvents are major breakthroughs required for successful application of HTL at a commercial level.

Table 3 and Table 4 summarize few studies on production of bio-oil using general pyrolysis and HTL (without any upgrading approach), respectively. It can be estimated that the bio-oil produced using either pyrolysis or HTL cannot be directly used as a drop-in fuel and thus it is highly important to improve its properties and increase the energy content to make it a competitive fuel to the currently available conventional fuels. In this regard, several methods have been demonstrated for bio-oil upgrading, which can be applied during pyrolysis or HTL process that mainly contain catalytic approaches, such as catalytic cracking, hydrodeoxygenation and esterification, or pre-pyrolysis or pre-HTL approaches which mainly involve biomass pre-treatment methods, such as torrefaction, acid and alkali treatments, or steam explosion. Alternatively, the bio-oil properties can be improved during post-pyrolysis or HTL process, such as with solvent addition, emulsification, filtration, electrochemical hydrogenation and hydrotreatment, which are comprehensively discussed in the further sections of the article.

3. Methods for downstream bio-oil upgrading

In this section, major downstream approaches for bio-oil upgrading have been comprehensively reviewed. Basic principles of the processes, effect of key parameters on bio-oil properties, challenges and feasibility of the processes have been thoroughly discussed.

Table 3
Properties of bio-oils obtained from biomass pyrolysis without using any upgrading technique.

Biomass	Pyrolysis temp. (°C)	Pyrolysis reactor	**Bio-oil yield (wt %)**	Bio-oil properties						Reference
				HHV (MJ/kg)	Water content (wt %)	pH	Viscosity	TAN	Density (g/ml)	
Pine wood	500	/	/	19.5	/	/	175 cP	/	/	[42]
Saccharina japonica	300	Fluidized-bed	31.27	28.63	1.76	5.9	–	/	/	[72]
Pine wood	450	Auger reactor	/	22.49	16.9	3.08	55.2 cSt	69.5	1.18	[73]
Pine wood	450	Auger reactor	54.00	16.1	20.83	2.65	6.49 cSt	90.06	1.17	[74]
Sweetgum	450	Auger reactor	52.00	2.65	38.3	2.65	8.26 cSt	119.2	1.16	[75]
Switchgrass	450	Auger reactor	33.00	2.98	61.7	2.98	1.51 cSt	88.4	1.08	[75]
Corn stover	450	Auger reactor	35.00	2.66	54.7	2.66	1.60 cSt	85.8	1.08	[75]
Saccharina japonica	470	Fixed-bed	/	35.0	34.7	/	/	43	1.13	[76]
Eucalyptus bark	550	FFFP unit	52.79	12.77	29.89	2.38	/	/	1.14	[77]
Eucalyptus bark	500	FFFP unit	55.54	12.23	32.86	2.87	/	/	1.14	[77]
Eucalyptus bark	450	FFFP unit	64.99	13.89	27.98	2.76	/	/	1.15	[77]
Eucalyptus bark	400	FFFP unit	58.25	12.45	26.07	2.78	/	/	1.13	[77]
Walnut shell	550	Spouted bed	/	/	18.87	4.38	7.98 cSt	/	0.94	[78]
Walnut shell	550	Spouted bed	/	/	23.29	4.28	3.29 cSt	/	0.95	[32]
Prairie cord grass	400	Spouted bed	/	15.2	/	2.59	2.5 cP	/	1.25	[32]
Switchgrass	400	Spouted bed	/	14.9	/	2.77	2.1 cP	/	1.25	[32]
Napier grass	600	Fixed-bed	30.06	20.97	26.01	2.95	2.71 cP	/	1.05	[79]
Pine wood	500	/	/	14.46	29.78	/	18.49 cSt	40.7	/	[80]

TAN-total acid number (mg of KOH/g), FFFP unit-free-fall fast pyrolysis unit.

Table 4
Properties of bio-oils obtained from HTL process without using any upgrading technique.

Feedstock	HTL Process				Bio-oil fuel properties								Reference
	T (°C)	Pressure (MPa)	Reaction time (min)	Solvent	HHV (MJ/kg)	Water content (wt %)	pH	Viscosity	TAN	Density (g/ml)	H/C	O/C	
Spirulina platensis	350	20.6	60	water	34.21	/	9.60	51.20 cP	/	0.97	1.44	0.10	[71]
Aspen wood	400	32	/	/	37.4	1.4	/	2.10×10^5 cP	/	1.07	1.25	0.10	[81]
Blackcurrant Pomace	300	1	60	Ethyl acetate	33.4	/	3.2	/	134	/	/	/	[82]
Blackcurrant Pomace	300	1	60	hexane	38.4	/	3.2	/	159	/	/	/	[82]
Blackcurrant Pomace	300	1	60	acetone	35.0	/	3.2	/	134	/	/	/	[82]
Blackcurrant Pomace	300	1	60	Isopropyl alcohol	34.6	/	3.2	/	137				[82]
Barley straw	500	35	15	water	17.19	/	/	/	/	/	0.95	0.56	[83]
Swine manure	340	6.8	15	water	36.05	2.37	/	843 cP	/	/	1.61	0.13	[84]
Chlorella pyrenoidosa	300	/	20	water	19.01	/	/	/	/	/	1.49	0.53	[85]
Barley straw	300	9	15	water	24.87	/	/	/	/	/	1.23	0.36	[86]
Nannochloropsis sp.	320	3.4	240	/	40.1	/	/	/	256.5	/	1.63	0.06	[87]
Nannochloropsis sp.	320		30	water	36.44	1.25	/	68.83 cSt	23.26	/	1.64	0.06	[88]
Sewage sludge	350	9.4–10.1	20	ethanol	36.14	/	/	818.3 cP	/	0.91	1.56	0.11	[89]
Rice straw	350	9.4–10.1	20	ethanol	33.90	/	/	1224 cP	/	1.03	1.38	0.17	[89]
Spirulina sp.	350	9.4–10.1	20	ethanol	34.33	/	/	962 cP	/	0.97	1.49	0.12	[89]
Litsea cubeba seed	290	/	60	water	40.8	8	/	/	100	/	1.9	0.10	[90]

Table 5
Solvents used to improve physicochemical properties of bio-oil.

Bio-oil properties				Solvents with bio-oil	Upgraded Bio-oil properties				Reference
Viscosity (mm^2/s)	Water content (wt%)	pH	HHV (MJ/kg)		Viscosity (mm^2/s)	Water content (wt%)	pH	HHV (MJ/kg)	
1244.60	9.36	4.84	19.31	50% Ethyl acetate	6.16	8.12	4.43	26.48	[44]
1244.60	9.36	4.84	19.31	50% Acetone	6.50	7.31	5.48	29.03	[44]
1244.60	9.36	4.84	19.31	50% n-octanol	35.74	9.09	4.92	25.76	[44]
1244.60	9.36	4.84	19.31	50% PEG 400[a]	127.54	8.96	3.30	33.22	[44]
1244.60	9.36	4.84	19.31	50% Ethyl acetate + ultrasonication-150 W, 12 min	18.52	6.96	3.88	29.24	[44]
1244.60	9.36	4.84	19.31	50% Acetone + ultrasonication-150 W, 12 min	22.51	7.33	4.18	29.93	[44]
1244.60	9.36	4.84	19.31	50% n-octanol + ultrasonication-150 W, 12 min	34.13	9.04	4.80	35.21	[44]
1244.60	9.36	4.84	19.31	50% PEG 400[a] + ultrasonication-150 W, 12 min	127.29	8.93	5.42	34.77	[44]
560.77	16.64	3.36	22.55	10% Methanol	78.82	17.35	3.66	22.38	[103]
560.77	16.64	3.36	22.55	10% Acetone	76.04	17.04	3.49	23.06	[103]
560.77	16.64	3.36	22.55	10% Ethyl acetate	93.86	17.35	3.48	22.60	[103]
178.2	23.5	/	18.9	4.3% Glycerol, 1.9% methanol	130.1	/	/	18.90	[31]
178.2	23.5	/	18.9	22.8%, Glycerol, 13.4%methanol	40.3	/	/	19.08	[31]
178.2	23.5	/	18.9	10.8%, Glycerol, 51.1% methanol	22.5	/	/	19.48	[31]
12.14	21.77	4.14	/	2.42% n-butanol, 2.32% DMSO[b], 3.25% ethyl acetate	8.26	19.39	4.43	/	[78]
12.14	21.77	4.14	/	1.96% n-butanol, 5.03% DMSO[b], 1% ethyl acetate	9.34	19.50	4.40	/	[78]
/	32.86	2.87	12.23	2.5% Ethanol	/	32.61	2.50	12.23	[77]
/	32.86	2.87	12.23	5% Ethanol	/	32.76	2.53	13.65	[77]
/	32.86	2.87	12.23	10% Ethanol	/	31.25	2.55	15.62	[77]
/	32.86	2.87	12.23	2.5% Methanol	/	32.31	2.47	12.46	[77]
/	32.86	2.87	12.23	5% Methanol	/	31.21	2.54	13.30	[77]
/	32.86	2.87	12.23	10% Methanol		27.48	2.57	14.63	[77]
6.43	28.03	4.04	/	8% Methanol	4.54	24.12	4.38	/	[32]
6.43	28.03	4.04	/	8% Acetone	4.95	24.30	4.36	/	[32]
6.43	28.03	4.04	/	8% DMF	4.67	23.97	4.42	/	[32]
6.43	28.03	4.04	/	1% Methanol, 1.94% acetone, 5.06% DMF	4.36	24.03	4.49	/	[32]

T = temperature.
[c] *N,N*-dimethylformamide (DMF).
[a] Polyethylene glycol (PEG).
[b] Dimethyl sulfoxide (DMSO).

3.1. Solvent addition

The application of polar solvents has shown to improve certain properties of the bio-oil. The main objective of using solvents is to increase the stability and decrease the viscosity of the bio-oil. The increase in viscosity during the storage is generally linked with the formation of water, which subsequently results in the separation of a lignin-rich sludge at the bottom. The bio-oil along with water contains other oxygenated compounds and degraded lignin. Upon aging, the quantity of water-insoluble fraction increases, which further leads to the increase in average molecular mass and viscosity of the bio-oil. The formation of water and water-insoluble fraction is usually due to the occurrence of condensation and polymerization reactions. The presence of impurities in the bio-oil, like char particles or heavy metals absorbed from the biomass during pyrolysis or HTL process, can catalyse the condensation and polymerization reactions. The addition of a solvent generally affects the viscosity of the bio-oil mainly by diluting the bio-oil without affecting the chemical reaction rate. In addition, the chemical reactions between the solvent and the bio-oil components also help to prevent the polymerization reactions. The primary chemical reactions that occur between the alcohol solvent (such as ethanol and methanol) and the bio-oil components are esterification and acetalization. Table 5 shows some examples of solvents used to improve physicochemical properties bio-oil. Several solvents, such as ethanol, isopropanol, methanol, acetone and N, N-dimethylformamide (DMF), have been successfully demonstrated for the bio-oil upgrading. For example, Oasmaa et al. [98] investigated the effect of alcohol on the improvement of bio-oil properties. The results demonstrated that adding 5% of ethanol or isopropanol increased the solubility of hydrophobic components of the bio-oil and the amount of water content decreased approximately 7 wt % in the top phase (that constitutes nearly 25% of the total liquid product) of the bio-oil, while no significant change in the water content was observed in the bottom phase. Moreover, the addition of solvent decreased the viscosity and density, whereas the heating value of the bio-oil increased proportionally with the concentration of the solvent, reaching maximum of 17.5 MJ/kg with 10% of isopropanol [98]. A recent study demonstrated the use of different proportions of methanol from 3 wt% to 15 wt% to improve the storage stability of bio-oil from pine wood pyrolysis [99]. The increasing concentration of methanol demonstrated decrease in viscosity, which could be attributed to the change in the bio-oil microstructure, physical dilution and prevention of chain reactions due to the interactions between methanol and bio-oil constituents [99,100]. In addition, the concentration above 6 wt% of methanol showed to increase the pH with the storage time, which could be ascribed to the fact that the neutral dilution effect of methanol or methanol could also inhibit the activity of H^+ in the bio-oil [99,101]. In a similar study, Liu et al. [102] investigated the influence of varying concentrations of acetone (3 wt%-15 wt%) on physicochemical properties of bio-oil obtained from the pyrolysis of pinewood at 500 °C in a continuously fed bubbling fluidized bed reactor. The results indicated that acetone had a significant effect on improving the overall bio-oil properties. The increasing concentration of acetone increased the pH of bio-oil proportionally, while the formation of water content decreased with increase in the concentration, obtaining approximately 12% decrease with 15 wt% acetone. On the other hand, a maximum of 84.6% decrease was observed in the viscosity with the addition of 15 wt% of acetone in the bio-oil [102].

The previous studies discussed above utilized an individual solvent separately to analyze its effect on bio-oil upgrading, however, a compound additive comprising two or more solvents in varying proportions has been also tested to improve the bio-oil quality that showed better results for bio-oil upgrading compared to its single solvent counterparts. For example, a compound additive with 1 wt% methanol, 5.06 wt% DMF, and 1.94 wt % acetone proved the best combination to produce the most significant quality bio-oil as compared to the either of the single solvents and increased the overall storage properties of the bio-oil [32]. The addition of compound additive was believed to prevent the polymerization of low-molecular compounds during the aging. In a similar demonstration, Zhu et al. [78] examined the effect of a compound additive (2.42 wt% n-butanol, 2.32 wt% dimethyl sulfoxide and 3.25 wt% ethyl acetate) on bio-oil properties during its storage at 80 °C for up to 48 h. It was reported that the compound additive showed noteworthy bio-oil stability as compared to the single solvent. For instance, the water content in the bio-oil with ethyl acetate was 8.18%, which decreased to 1.60% with the compound additive used in the study [78]. Moreover, Zhang et al. [103] also investigated the application of a mixed additive, containing methanol, acetone, and ethyl acetate in certain percentages for bio-oil upgrading and the results were satisfactory, showing substantial improvement in the viscosity and water content in the bio-oil. In comparison to single solvent, mixed additives proved more advantageous for bio-oil upgrading, which can be attributed to the chemical activity of the solvents in the compound additive that react with a greater number of constituents of the bio-oil and also prevent the polymerization reactions, consequently, leading to a stable bio-oil.

The bio-oil upgrading with solvents can be further improved with physical treatments, such as ultrasonication, that could result in frequent particle movements and hence could allow the solvents molecules to interact better with the constituents of bio-oil. Noticeably, Xu et al. [44] successfully demonstrated the application of ultrasonication for bio-oil upgrading. They used *n*-octanol as the solvent mixed with the bio-oil in a ratio of 1:1 and the ultrasonic power of 150 W was applied for different exposure times from 2 to 20 min. The results revealed that increasing the exposure time of ultrasonication enhanced the bio-oil properties. For example, the bio-oil without ultrasonication showed lower pH of 4.92 and HHV of 25.76 MJ/kg, while the ultrasonication with an exposure time of 20 min increased the pH to 5.11 and HHV to 38.32 MJ/kg [44]. The increase in pH was attributed to the increase in alcoholysis of organic compounds of bio-oil upon ultrasonication. It was also suggested that ultrasonication promotes mechanical and cavitation effects at higher temperatures which triggers the decomposition of large chain compounds into smaller compounds that can be evaporated as gas, consequently, leading to decrease in moisture content of the bio-oil. A recent study also investigated the effect of ultrasonication power and exposure time on bio-oil properties, such as HHV, viscosity and moisture content using methanol and octanol blends [104]. Authors reported that bio-oil blends with solvents without ultrasonication treatment showed the HHV of 26 MJ/kg, viscosity of 316 mPa s, and moisture content of 17%, while ultrasonication of the blends at power of 55 W/L for 11 min increased the HHV to 34.2 MJ/kg and reduced the viscosity and moisture content to 260 mPa s and 14.4%, respectively [104]. The enhanced properties of the blends were attributed to breaking of larger compounds and formation of free radicals upon ultrasonication, which reacted with other group of compounds in the bio-oil and formed stable compounds [104]. Ultrasonication was also believed to promote ring opening and hemiacetalation reactions by breaking the double bonds in ketones, alcohols and polyaromatic hydrocarbons, leading to the reduction in the content of ketones and alcohols and increase in the content of alkanes and alkynes in the bio-oil [105].

The application of solvents is quite simple and significant approach to enhance the bio-oil properties, such as viscosity and calorific value. The solvents also react with the constituents of the bio-oil, such as organic compounds, minerals and alkali metals, and prevent the polymerization reactions, thereby leading to a stable bio-oil. However, less information is available about the reaction mechanism between the solvent and bio-oil constituents due to the complexity and bio-oil composition. Therefore, more research should be conducted to understand the chemical reactions between the solvent and constituents of bio-oil.

3.2. Emulsification

Similar to the solvent addition, emulsification can also be used to

improve the bio-oil properties and increase the total energy content of the resultant bio-oil. Where the polar solvents are miscible in the bio-oil, emulsification involves two immiscible liquids in which the tiny particles of one liquid are suspended in the larger particles of the second liquid. The successful emulsion of the two liquids may result in different sizes of droplets, such as 1–10 μm, while the emulsion that results in the droplets of the size 1–100 nm is termed as microemulsions [41]. Emulsion and microemulsions are formed almost in a similar way but there are some key factors that differentiate them with each other. It has been stated that microemulsions are thermodynamically more stable than emulsions and hence possess less probability of phase separation at a broad range of temperature. On the other hand, emulsions are comparatively less stable and require more energy to form [106]. Emulsification is a simple and effective approach for bio-oil upgrading as the resultant mixture can be directly used for heat or power generation [41]. Generally, the bio-oil is emulsified with other petroleum fuels, such as diesel or biodiesel. Since the bio-oil and diesel are less miscible is nature, their emulsification could be carried out in the presence of a surfactant (such as Atlox 4914, Tween 80 and Span 80) and sometimes co-surfactants (for example, methanol, ethanol and n-butanol) can also be used to improve the emulsion stability [107]. Generally, the surfactant molecules are made up of two parts, a polar hydrophilic 'head' and a nonpolar lipophilic 'tail'. During the emulsion of a polar liquid, such as bio-oil, and a nonpolar liquid like diesel, the hydrophilic part of the surfactant adsorbs on to the droplet's surface and the lipophilic part points outward into the nonpolar liquid. The surfactant molecules form a thin layer around the droplets and protect it to coalesce when they interact with each other in the emulsion. This type of emulsion is known as water in oil (W/O) emulsion. Alternatively, when the droplets of a nonpolar liquid are dispersed in an aqueous liquid they are termed as oil in water (O/W) emulsion, as shown in Fig. 2A. In addition to this, other physical methods such as ultrasonication, stirring and the selection of favourable parameters can be employed to obtain the stable emulsions, which ultimately affect the physicochemical properties of the resultant bio-oil. Usually, the bio-oil upgrading through emulsification with diesel reduces the viscosity and enhances the calorific value and cetane number as the liquid fuel [106]. Table 6 compares the fuel properties of bio-oils and emulsions prepared using bio-oil and emulsifiers.

To obtain a stable emulsion, the volumetric ratios of bio-oil/diesel and the concentration of the emulsifier/surfactant are the important parameters, while other factors like temperature, stirring intensity, and mixing time are also critical to obtain a stable emulsion which subsequently would affect the bio-oil upgrading. In other words, a stable emulsion would result in a high-quality bio-oil having a longer stability duration, while the unstable emulsion would lead to a poor-quality bio-oil. Jiang and Ellis [108] investigated the emulsification of bio-oil with biodiesel optimization using octanol as the surfactant and studied the effect of various parameters on the stability of emulsion and their effect on the bio-oil properties. The study concluded that the mixing ratio of bio-oil/biodiesel of 40%/60% produced the most stable emulsion, while 4% of octanol (surfactant) was optimum to obtain a stable emulsion. They found that at the lower concentrations of octanol, the mixture was unstable due to the agglomeration of the oil droplets, whereas the emulsion disrupted due to rapid coalescence at the higher concentrations of octanol [41,108,109]. Emulsification of the bio-oil with biodiesel decreased the viscosity to 4.66 mPa s compared to 67.39 mPa s of the sole bio-oil, while the HHV of the mixture significantly increased from 15.28 MJ/kg to 35.76 MJ/kg [108]. In a recent study, the bio-oil was emulsified with diesel using Span 80 and Tween 60 as surfactants, the resultant mixture showed HHV value of 44.32 MJ/kg that was close to the commercial diesel fuel (45.65 MJ/kg) [110]. Another important factor that plays a key role to obtain a stable emulsion and thereby a high-quality bio-oil is hydrophilic-lipophilic balance (HLB) number of the surfactant. HLB is a measure of the degree to which a surfactant is hydrophilic or lipophilic in nature. HLB generally varies between 0 and 18. Fig. 2B shows the scale of HLB values, indicating that a surfactant having an HLB range of 4–8 would result in W/O emulsions while a surfactant with an HLB range of 9–12 would lead to O/W emulsions. Bio-oil emulsification with diesel or biodiesel using surfactants of varying HLB values has been investigated to improve the bio-oil stability and other properties. For instance, Martin et al. [111] demonstrated the effect of surfactant polyethylene glycol-dipolyhydroxystearate (PEG-DPHS) of varying HLB values on the stability of bio-oil emulsion with diesel fuel. The results revealed that the surfactant with HLB of 4.75 produced the most stable emulsion with uniform size (~0.48 μm) of droplets when the ratio of diesel/bio-oil/surfactant of 32:8:1 was used in the experiments. It was further reported that the droplets were quite stable until seven days as no coalescence was observed. Such an emulsion showed greatly improved fuel properties, exhibiting the HHV value of 41.2 MJ/kg, which was approximately 75% higher than the raw bio-oil. A significant decrease in the viscosity and water content was also observed which were 5.94 cP and 1.74 wt%, respectively [111]. In a

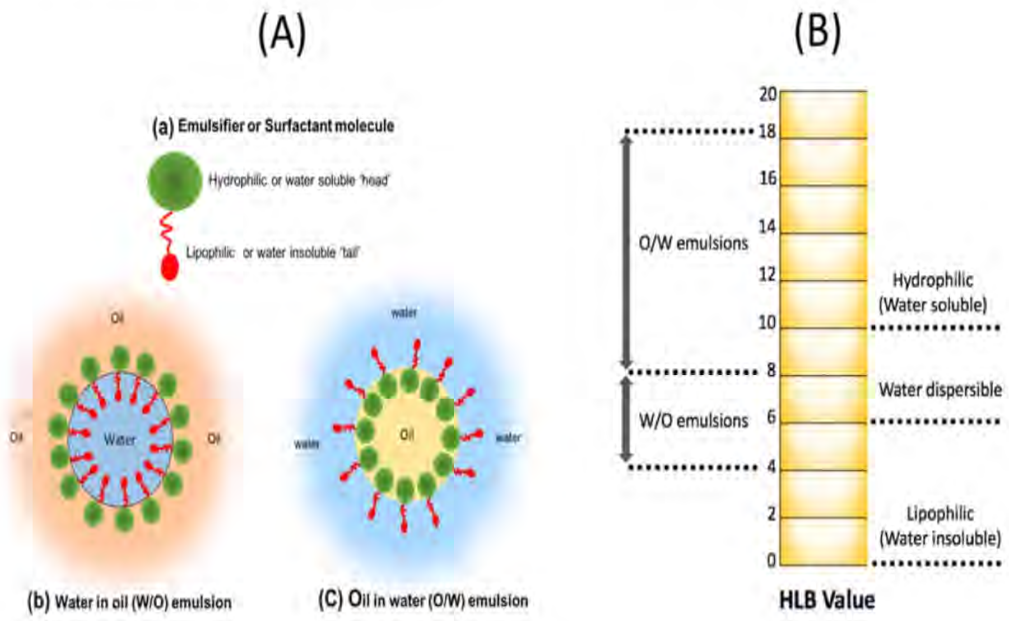

Fig. 2. (A) Type of emulsions and (B) HLB values for different emulsions and mixture behaviors.

Table 6
Comparative analysis of bio-oil fuel properties and emulsions fuel properties.

Bio-oil fuel properties					Emulsification			Emulsions fuel properties					Reference
C wt %	H wt %	O wt %	N wt %	HHV (MJ/kg)	Mixture	Emulsifier	HLB	C wt %	H wt %	O wt %	N wt %	HHV (MJ/kg)	
42.60	8.47	48.85	0.08	19.50	BO + 10% CG	/	/	42.11	8.54	49.27	0.08	19.40	[42]
42.60	8.47	48.85	0.08	19.50	BO + 20% CG	/	/	41.62	8.61	49.70	0.07	19.30	[42]
42.60	8.47	48.85	0.08	19.50	BO + 10% CG	0.5% Span 80	/	42.21	8.55	49.17	0.08	19.40	[42]
47.02	7.63	44.81	0.54	21.38	BO[a] + 90% D	5% (Span 80 and Tween 60)	7.3	82.47	13.56	0	3.97	44.32	[110]
47.02	7.63	44.81	0.54	21.38	BO[a] + 86% D	6.6% (Span 80 and Tween 60)	7.3	83.26	13.66	0.06	3.97	43.68	[110]
61.35	6.34	32.07	0.24	23.50	BO + 80% D	/	/	80.93	12.26	6.77	0.05	41.20	[114]
61.35	6.34	32.07	0.24	23.50	BO + 80% Et	/	/	53.98	11.77	34.20	0.05	28.60	[114]
75.65	5.20	18.97	0.17	28.90	BO + 80% D	/	/	84.11	12.06	3.79	0.03	42.30	[114]
42.64	7.55	49.59	0.22	18.90	BO + 4.35% G + 1.95% Mt	/	/	42.39	7.69	49.72	0.20	18.90	[31]
42.64	7.55	49.59	0.22	18.90	BO + 10.8% G + 5% Mt	/	/	42.0	7.92	49.90	0.18	18.95	[31]
42.64	7.55	49.59	0.22	18.90	BO + 22.8% G + 13.4% Mt	/	/	41.15	8.47	50.24	0.14	19.08	[31]
42.64	7.55	49.59	0.22	18.90	BO + 30.1% G + 23.1% Mt	/	/	40.40	9.03	50.47	0.10	19.24	[31]
42.64	7.55	49.59	0.22	18.90	BO + 42.7% G + 32.6% Mt	/	/	39.47	9.65	50.83	0.05	19.40	[31]
42.64	7.55	49.59	0.22	18.90	BO + 51.1% G + 38.1% Mt	/	/	38.89	10.02	51.07	0.02	19.48	[31]
39.96	7.74	52.19	0.11	15.27	BO + 60% D	4% octanol	/	77.54	11.75	9.71	1.00	41.43	[108]
/	/	/	/	13.8	BO + 90% D	10% Tween 80	/	/	/	/	/	41.38	[115]
/	/	/	/	13.8	BO + 90% D	10% Brij 58	/	/	/	/	/	41.18	[115]

BO-bio-oil; CG-crude glycerol; G-Glycerol; D-diesel; Et-ethanol; Mt-methanol; HLB-hydrophilic-lipophilic balance; [a]BO-ether extracted bio-oil was used in the study.

separate study, Farooq et al. [110] investigated emulsification of bio-oil with diesel using the surfactant of varying HBL values. Firstly, they treated the raw bio-oil with ether and used the ether extracted bio-oil for emulsification with diesel. Two surfactants, Tween 60 (HLB of 14.6) and Span 80 (4.3) were mixed to obtain the final surfactant with HLB range of 4.3–8.8. An emulsion of bio-oil/surfactant/diesel was prepared with a ratio of 5/5/90 wt% and the results showed that the surfactant with HLB of 7.3 was optimal to obtain the stable emulsion. The resultant emulsion showed a very high HHV value of 44.32 MJ/kg, which was nearly 107% higher than the raw bio-oil [110]. Based on the results from previous two studies, it can be suggested that to obtain a stable emulsion, the optimal HLB value may differ to the type of surfactant and might vary depending on the composition of the bio-oil. For example, if the bio-oil contains higher proportion of aromatic hydrocarbons it would be miscible with diesel and may require a surfactant with lower HLB value to produce a stable emulsion. On the hand, the bio-oil with no hydrocarbons and rich in oxygenated compounds may demand a surfactant with a higher HLB value to make a stable emulsion.

The emulsification of bio-oil with other than diesel or biodiesel fuel has been also investigated for bio-oil upgrading. For example, Zhang et al. [112] demonstrated the emulsification of bio-oil with crude glycerol using Span 80 as the surfactant. They studied the effect of various parameters to produce the stable emulsion with crude glycerol and found that the concentration of surfactant of 1% and temperature of below 45 °C was favourable to produce stable bio-oil/glycerol emulsions. However, they also reported the presence of some impurities in the crude glycerol, such as water, salt and alkali metals, that significantly decreased the stability of emulsions [112]. The bio-oil emulsification can also be achieved without using any surfactant, which could make the process simpler and more cost-effective. It has been demonstrated that ultrasound emulsification with mechanical agitation is effective to break the droplets to produce stable emulsions and therefore, could prove highly advantageous over conventional emulsification and can also prevent the use of surfactants [42,113]. For instance, Zhang et al. [42] in their further study demonstrated the emulsification of bio-oil with crude glycerol using ultrasound and mechanical agitation. To prepare a stable emulsion with bio-oil, the amount of glycerol was controlled so that it contains 1% of soap content to prevent the re-coalescence of droplets, while the ultrasound at 40% amplitude for 4 min and mechanical agitation for 2 min was applied to obtain a stable emulsion. The ultrasound treatment could help in the effective breakdown of droplets while the mechanical agitation could prevent the re-coalescence of droplets. The results showed that the applied combined approach resulted in the emulsion that could be stable for maximum of 15 h and improved the fuel properties compared to the raw bio-oil. For example, the produced emulsion showed a viscosity of 119.2 mPa s, which was approximately 32% lower than the sole bio-oil [42].

Similar to solvent addition, emulsification could be a remarkable approach to improve the bio-oil properties but it requires other physical techniques, such as stirring, ultrasonication to produce a stable emulsion and the use of additional surfactant that increases the cost of overall bio-oil upgrading.

3.3. Filtration to remove solid char residue

The crude bio-oil contains some solid char particles (1–10 μm) that encompass metal ions as well, which are usually present in the biomass and are retained in the char particles during the pyrolysis process. The metal ions may act as a catalyst and promote the polymerization and condensation reactions during bio-oil storage, adversely affecting the chemical composition of the bio-oil and making it highly unstable to use as a drop-in fuel [116]. The char particles can also agglomerate and transform into larger particles, which can easily be deposited in engine valves and may block them, adversely affecting the ignition process in engines. The char particles can also cause corrosion problems to the engines. Therefore, it is highly imperative to remove the char particles and metal ions to improve the bio-oil properties. In this regard, some successful attempts have been demonstrated using filtration techniques to remove the char particles from the bio-oil [45,46,117–122]. The filtration process can be divided mainly into two types, liquid phase filtration and hot vapour filtration (HVF). Both modes of bio-oil filtration have shown positive results for removal of char particles as well as improved bio-oil stability [66]. Fig. 3a shows schematic diagram of fast pyrolysis unit with HVF.

Liquid phase filtration is considered as post pyrolysis treatment or a complete downstream bio-oil processing approach. It can be used to separate solid particles of 1–10 μm size [45,119]. Evidently, Javaid et al. [45] demonstrated the application of tubular ceramic membranes with pore size of 0.5–0.8 μm for microfiltration of bio-oil at a temperature range of 38–45 °C and *trans*-membrane pressures of 1–3 bars. The authors reported the significant reduction in the char particles and overall ash content in the bio-oil, as confirmed by the microscopic analysis. However, insignificant changes were observed in the chemical composition of the bio-oil after the filtration process [45]. The most concerned problem of using membranes for bio-oil filtration is fouling of the membranes in long run filtration, which can occur due to pore constriction, partial or complete blockage of pores and formation of a cake layer on its surface. Therefore, the regular washing of membranes with solvents, like methanol or acetic acid, is important to hamper the fouling.

On the other hand, HVF has proven more advantageous to remove char particles as well as to improve the bio-oil properties. It has been shown that char particles <10 μm can be removed using HVF. Unlike liquid filtration that is a post-treatment method, HVF upgrades the bio-oil in mid pyrolysis process, prior to the condensation. HVF can be further classified into two types based on the introduction of the filter that is *ex-situ* HVF and *in-situ* HVF. In *ex-situ* HVF, the filter can be placed downstream the pyrolysis process but before the vapour condensation. Alternatively in *in-situ* HVF, the filter is introduced in a continuous fluid bed pyrolysis system [66]. It has been observed that *ex-situ* HVF results in significant decrease in bio-oil yield while *in-situ* HVF could be advantageous to obtain higher bio-oil yields and lower cake formation on the filter [121]. Generally, an HVF unit is comprised of porous and permeable filter elements like filter candle, filter media and membrane. Filters are usually made up of ceramic and metal elements applicable for high temperature. Filter candles are cylindrical in shape and made up of ceramic monolith or other materials with 1–3 m in length, depending on the type of materials, and a diameter of 60–150 mm [124]. Filter media is made up of high or low-density ceramic like silicon carbide alumina or cordierite or metal filter media which is made up of sintered metal or metal alloy. HVF units are coupled with pyrolysis system for bio-oil filtration. During filtration, the pyrolytic vapours are passed through the filters where the treated pyrolytic vapours leave the filter through an open end, while the untreated vapours enter the filter candles. Dust particles are also formed during the process which aggregate on the surface of the candle and form cake layer (shown in Fig. 3b). The char particles or alkali and alkali earth metals are filtered in the HVF mainly by two mechanisms, surface filtration and depth filtration. In surface filtration, generally the particles larger than pore size of filters are filtered through a sieving mechanism where they attach on the surface of the filter. The cake on the filter is removed using jet pulsing techniques [124]. In depth filtration, particles are filtered on filter media where the particles are trapped through diffusion mechanism. The integration of HVF with pyrolysis unit is challenging since the pyrolytic vapours form a sticky cake layer inside the filters which requires additional efforts to remove. Therefore, efficient techniques are required to remove the cake more easily and prevent blocking of the filters.

Ex-situ HVF has been widely used for bio-oil upgrading. For example, Baldwin et al. [117] demonstrated the application of *ex-situ* HVF to remove the char particles from bio-oil produced from oak wood by employing the pyrolysis reactor, which was operated in the entrained-flow mode. The hot vapour filter comprised of either porous sintered stainless-steel metal powder or sintered ceramic powder was placed slipstream from the pyrolysis process development unit so that the filtered and unfiltered bio-oils could be separately collected for the comparison, while the bio-oil condensation and collection system was interfaced to the slipstream filter unit. The results demonstrated that the bio-oil obtained after the HVF using either of the filtration systems showed significantly less amount of the alkali metals compared to the unfiltered bio-oil. For example, the bio-oil obtained from the filtration system using porous sintered stainless-steel metal powder showed concentrations of sodium and potassium at 7 and 14 ppm, which were 49 and 50 ppm in the unfiltered bio-oil, respectively. Similarly, the concentrations of sodium and potassium in the bio-oil obtained from the sintered ceramic powder filtration system were less than 5 ppm. Consequently, the significant effect on aging of the bio-oil and reduction in viscosity was noticed in the filtered bio-oil. However, stainless-steel filter was not found appropriate as a high concentration of iron was detected in the bio-oil filtered using a stainless-steel filter that was probably due to leaching from the filter, which indicates the importance of filter material for the effective bio-oil upgrading. Another important observation in the study was the major decrease of 10–30% in the bio-oil yield, which was attributed to the catalytic activity of alkali metals and char present on the filter that probably reduced the activation energy of secondary cracking reactions for the pyrolytic vapours and increased the production of hydrogen and methane [117].

The temperature of the filter unit plays an important role in the removal of alkali metals, physical properties of the bio-oil and the yields of pyrolytic products (bio-oil, bio-char, gases). Mei et al. [120] demonstrated the effect of temperature of HVF on the removal of alkali metals and analyzed its effect on the bio-oil properties. They utilized ceramic hot vapour filter for upgrading of the bio-oil produced under fast pyrolysis of pine wood in a fluidized-bed reactor and varying HVF temperature from 350 to 500 °C. The results showed higher bio-oil yield

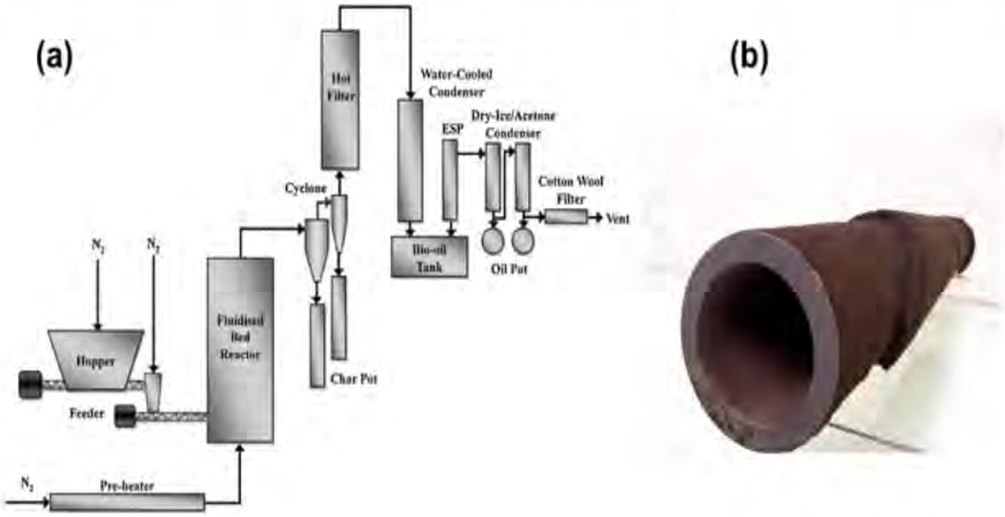

Fig. 3. (a) Schematic diagram of fast pyrolysis unit with hot vapour filter [123] (b) Filter candle with a cake layer [46].

obtained under HVF temperature of 400 °C when compared to 350 or 500 °C, while the concentrations of alkali metals and solid contents were also lower in the bio-oil obtained at this temperature. Consequently, the filtered bio-oil showed the HHV value of 23.29 MJ/kg, which was slightly lower than the bio-oil produced at 500 °C (25.88 MJ/kg), however, the viscosity of 26.9 mm^2/s was the lowest compared to either 350 or 500 °C, which were 28.6 and 37.6 mm^2/s, respectively [120]. Similarly, Chen et al. [119] investigated the effect of HVF to filter the char and solid particles in rice husk bio-oil and showed a noticeable decrease in the contents of char and alkali metals compared to unfiltered bio-oil. This study also reported a decrease of ~2.2% in the bio-oil with HVF process. Another study demonstrated the effect of filter temperature on yields of pyrolytic products with results shown in Fig. 4, which suggests an increase in the bio-oil yield from 400 to 475 °C, while decrease in the bio-oil yield was noticed as the temperatures increased to 550 °C [123]. Significant increase in char and gas yields was observed with HVF compared to non HVF fast pyrolysis [123]. The decrease in bio-oil yield is mainly attributed to the promotion of secondary cracking reactions catalysed by char and metal particles present in the cake layer. A study revealed that during the filtration process major cracking reactions occur in the homogeneous gas phase, while some other reactions like dehydration and decarboxylation take place heterogeneously by char particles or metals present in the cake layer [46]. The physical characteristics of the cake, concentration of metals and porosity may have significant effect on bio-oil composition, which should be studied in the future. Hence, it can be suggested that *ex-situ* HVF could prove significant for the removal of char and metal particles but the bio-oil yield could decrease due to the catalytic activity of char and metal particles attached to the filter that promote the secondary cracking reactions [66,117,120]. However, these challenges encountered in *ex-situ* HVF can be overcome and the filter fouling can be diminished if the filter is used *in-situ* in a continuous fluidized bed pyrolysis system. Hoekstra et al. [121] successfully tested *in-situ* filtration of the char particles using wire mesh filters with a 5 μm pore size. The results revealed less filter fouling and efficient process stability achieved during the continuous run of 2 h, while a significant decrease in solid contents and alkali metals was noticed in the filtered bio-oil. Besides, the liquid yield of approximately 61–62% was achieved which was comparably higher than that of pyrolysis without HVF process [121].

This technique is highly advantageous to remove the solid char particles that, if present in the bio-oil, could initiate the polymerization and condensation reactions, making the bio-oil highly unstable, hence, filtration can increase the bio-oil stability and also decreases the viscosity. However, HVF may reduce bio-oil yield significantly. The presence of char and alkali metals promotes secondary cracking reactions of pyrolytic vapours and extra residence time in the filter might also boost the cracking reactions, thereby reducing the bio-oil yields and increasing gas and char yields. Cake formation on the filter also leads to pressure deviations in filter media, which can make the operation process of filtration quite challenging. Therefore, it is very important to maintain the cake removal or regeneration to prevent pressure deviations and make filtration process stable for bio-oil upgrading. In addition, the use of filtration may increase the cost of bio-oil upgrading as the membranes used in the process are highly expensive. Besides, they need regular washing with solvents which can further make the process costly. Therefore, cost-effective and more efficient membranes should be developed for bio-oil upgrading to make the process economical and more significant. Very little or nothing has been studied to estimate the cost of filtration for bio-oil upgrading. Hence, a techno-economic study is further proposed to determine the capital and operational costs of the process and estimate the cost of the upgraded bio-oil. Filtration process removes contaminants and improves certain bio-oil properties like viscosity but high oxygen and water content and low HHV make the bio-oil a poor drop-in fuel. Therefore, filtration technique should be further integrated with other bio-oil upgrading technique such as hydrotreatment to improve the calorific value.

3.4. Electrochemical or electrocatalytic upgrading of bio-oil

Electrochemical upgrading or widely known as electrocatalytic hydrogenation is a well-known process to convert the oxygenated or carbonyl containing compounds into value-added organic compounds or hydrocarbons [125–127]. However, only recently, electrocatalytic upgrading of bio-oil has been reported, which is believed to be a noteworthy alternative for conventional hydrogenation process that occurs at high temperatures and hydrogen pressures of up to 2000 MPa. Electrocatalytic hydrogenation is generally carried out in an electrolytic membrane fuel cell. The fuel cell utilizes the protons for bio-oil hydrogenation that result from the oxidation of water, therefore, eliminates the use of high-pressure hydrogen and high temperature for bio-oil upgrading, which decreases the cost of bio-oil upgrading or other chemicals. Fig. 5 shows an electrochemical cell used for bio-oil upgrading, made up of two compartments i.e. the anode and the cathode, separated by a polymer membrane that could be either cation exchange membrane (CEM) or anion exchange membrane (AEM). At the anode, the oxidation of H_2O takes place, releasing O_2 and H^+, while at the cathode, the oxygenated compounds (in this case, bio-oil containing oxygenated compounds) are hydrogenated by the addition of H^+ transferred through the membrane from the anode, evolving hydrogen during the process. At the cathode, a catalyst can be used to reduce the

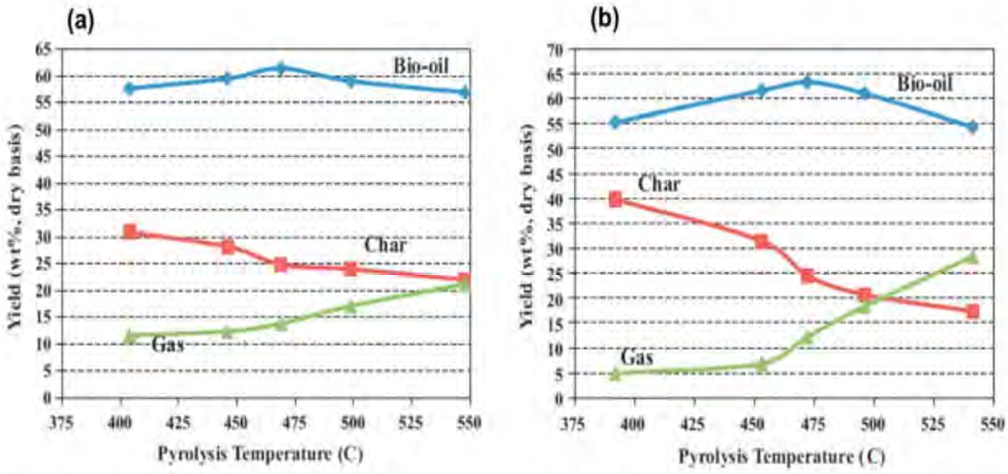

Fig. 4. Effect of temperature on product yields from fast pyrolysis of cassava rhizome (a) without hot vapour filter and (b) with hot vapour filter. Reproduced with permission from Ref. [123].

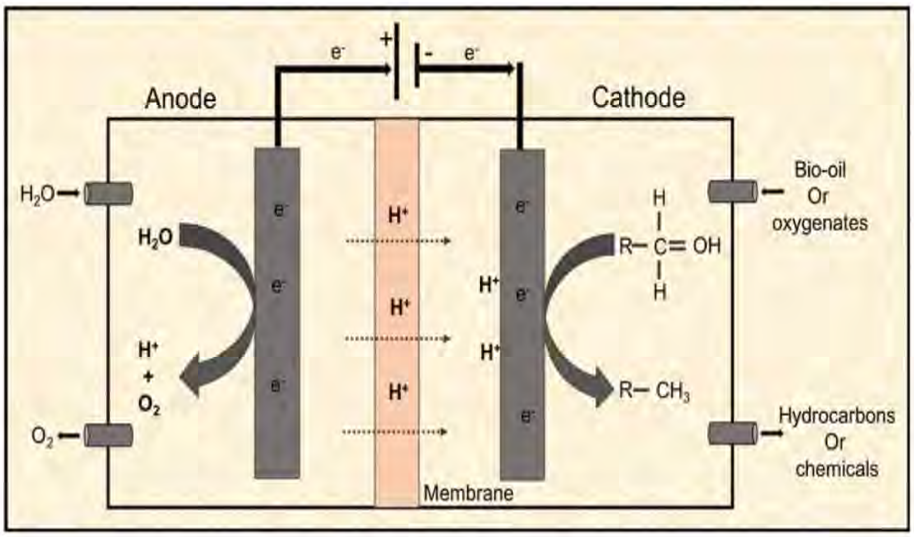

Fig. 5. Electrochemical cell for bio-oil upgrading.

overpotential of hydrogen evolution reaction (HER) and increase the conversion efficiency of the compound to the desired product. Similarly, the anode can also be modified with catalysts to improve the efficiency.

A number of studies have reported the electrocatalytic hydrogenation of bio-oil model compounds to stable or value-added compounds, however, only a few studies have demonstrated the application of electrochemical cells for real bio-oil upgrading. For example, Zhao et al. [125] demonstrated the electrocatalytic hydrogenation of furfural to furfuryl alcohol. Furfural is one of the main compounds formed during pyrolysis of hemicellulose, which can be hydrogenated to a high-value compounds i.e. furfuryl alcohol, which is widely used in chemical and polymer industries. Conventionally, furfuryl alcohol is prepared by vapour phase catalytic hydrogenation of furfural under high temperatures and high hydrogen pressures. Alternatively, electrocatalytic hydrogenation can be operated at mild temperatures and can eliminate the external supply of hydrogen, which otherwise uses the *in-situ* produced H_2 during the electrocatalytic hydrogenation. The study by Zhao et al. [173] used H-type electrochemical cell for hydrogenation of furfural with different metal and metal-activated carbon fibre catalysts at the cathode. The results showed that sole platinum cathode showed better selectivity of approximately 99% for furfuryl alcohol as compared to copper, lead and nickel cathodes. However, the conversion or hydrogenation efficiency was found lower (8%) for the platinum cathode due to low active surface area. Subsequently, the platinum cathode was modified with high surface area activated carbon fibre catalysts, which enhanced the conversion efficiency to 82% [125]. Similarly, electrocatalytic hydrogenation of some other bio-oil model compounds has been demonstrated. For instance, phenol, guaiacol and syringol are the dominant compounds in the bio-oil composition which are usually formed during the pyrolysis of lignin content of the feedstock. Evidently, Li et al. [128] investigated the electrocatalytic hydrogenation of guaiacol in ruthenium/activated carbon cathode based two-chamber H-type electrochemical cell, Nafion-117 membrane and catholyte containing HCl, NaCl and NaOH. The major product of guaiacol hydrogenation was found to be cyclohexanol, while phenol was found to be the intermediate product. The study also suggested that during the electrochemical hydrogenation of guaiacol, demethoxygenation was the dominant deoxygenation reaction while in conventional catalytic upgrading of guaiacol, demethylation is one the major deoxygenation pathways, indicating that the former process retains more carbon in the liquid products than the latter and hence can prove more advantageous for enhanced bio-oil upgrading.

After the successful demonstration of electrocatalytic hydrogenation of bio-oil model compounds, this approach has been applied for real bio-oil upgrading in few studies that showed considerable positive results for bio-oil deoxygenation. For example, Elangovan et al. [126] demonstrated bio-oil deoxygenation using an oxygen ion conducting ceramic membrane-based electrochemical cells, operated at 550 °C, while a condenser was attached to the cell to condense the vapours and was kept at 10 °C. The results reported that approximately 24.5% oxygen reduction was observed in the bio-oil after electrochemical hydrogenation and approximately 16% increase in carbon content was achieved, which could be attributed to the conversion of oxygenated compounds into hydrocarbons. However, it was difficult to estimate the correct deoxygenation pathways due to the presence of numerous compounds in the bio-oil composition. In a recent study, bio-oil produced from the pine wood pyrolysis was upgraded in a dual membrane electrochemical cell, an AEM attached to the cathode and a CEM attached to the anode [127]. This demonstration showed improvements in few properties of the bio-oil, such as the pH increased from 2.6 to 4.5 and the total acid number decreased from 193 to 149 (mg of KOH/g, dry). This decrease in total acid number was attributed to the removal of carbonyl group-containing compounds, such as carboxylic acids and aldehydes, suggesting the successful hydrogenation of carbonyl moieties during the process [127].

Electrocatalytic upgrading could prove effective to convert the oxygenated compounds into hydrocarbons. However, the technique has not been used extensively for real bio-oil upgrading due to some major challenges. For example, the technique utilizes costly membranes and hydrogen, which makes the process highly expensive compared to the other techniques. Moreover, it requires supply of electricity to initiate the reactions. This electricity could also be provided from other renewable technology such as microbial fuel cells (MFCs) that can produce sufficient power for electrocatalytic hydrogenation. MFCs are also the electrochemical cells that use microorganisms to convert the chemical energy present in organic compounds into electricity [129, 130]. Overall, it needs more development and research to make this technique more efficient and advanced to use for real bio-oil upgrading at a pilot-scale. Table 7 provides the main advantages and challenges of all methods for downstream bio-oil upgrading discussed in the previous sections. Besides making the bio-oil to a gasoline like product, it can also be upgraded to produce other clean fuels, has been discussed in the following section.

3.5. Hydrotreatment of bio-oil

Hydrotreatment of bio-oil is the treatment with hydrogen in the presence of an active catalyst made up of metal or metal/support at

Table 7
Advantages and challenges of methods used for bio-oil upgrading.

No.	Method	Advantages	Challenges
1	Solvent addition	- a very simple approach for bio-oil upgrading - decreases viscosity of bio-oil - enhances stability of bio-oil - increases heating value	- may increase water content - may decrease pH of bio-oil - increases overall cost for bio-oil upgrading - requires more research to understand the chemical reactions between the solvent and compounds of bio-oil
2	Emulsification	- a simple and effective approach for bio-oil upgrading - reduces bio-oil viscosity - enhances the calorific value and cetane number - increases bio-oil stability	- the reaction mechanisms could be complex to understand - requires other physical technique to produce a stable emulsion - process parameters such as temperature and stirring are critical to obtain a stable emulsion - requires an additional surfactant that increases the cost
3	Filtration	- an efficient approach to remove char particles and alkali metals - filtered bio-oil exhibits lower viscosity and higher stability due to the removal of solid particles that can initiate the polymerization and condensation reactions. - reduction in ageing reaction rate during storage - removal of contaminants protects downstream equipment from corrosion and catalysts from poisoning	- membranes are highly expensive - membranes requires regular washing with solvents that can increase the cost - some filter units require higher temperature - cake formation causes pressure drops in the filter - increases water content - reduces HHV of bio-oil - decreases bio-oil yield and increases char and gas yields by promoting secondary cracking reactions of vapours
4 5.	Electrocatalytic Upgrading Hydrotreatment	- increases the content of hydrocarbons in the bio-oil - increases pH of bio-oil - decreases acid number mainly due to the removal of carbonyl group-containing compounds - can be used to convert bio-oil into high value-added compounds - increases the content of hydrocarbons in the bio-oil - other valuable products like phenols are also enhanced - increases calorific value of bio-oil - cost of upgraded bio-oil would be in range of $0.74–1.80/L	- an energy intensive process - supply of hydrogen makes the process expensive - the use of membranes could be uneconomical - needs more investigation to understand the chemical reactions during electrocatalytic bio-oil upgrading - use of hydrogen makes the process highly expensive - transportation and storage of hydrogen add the cost - needs extra precautionary steps - catalyst deactivation is a major challenge - sulphur leaching from sulphided catalyst contaminates bio-oil that requires additional purification step

temperatures between 200 and 500 °C and pressure in the range of 3–30 MPa [53,54]. It involves the removal of oxygen from oxygenated compounds of bio-oil through hydrodeoxygenation (HDO) reaction to produce hydrocarbons and water as the by-product. The main reactions involved in bio-oil upgrading under hydrotreatment are i) hydrogenation of C – C and C – O bonds, ii) breaking of C – C bond by retro-aldol condensation and decarbonylation, iii) dehydration of C – OH groups and iv) hydrogenolysis of C – O – C bonds. Hydrotreatment is considered highly efficient for bio-oil upgrading compared to cracking since it removes oxygen in the form of H_2O while in cracking oxygen is removed in the form of CO_2 and CO which decreases the total carbon yield [19,53,131]. More information on the reaction mechanisms involved in the conversion of oxygenated compounds to hydrocarbons can be found elsewhere [132–134]. Numerous studies have been conducted to examine the hydrotreatment of bio-oils and has proven most valuable approach among above discussed downstream technologies for bio-oil upgrading.

Hydrotreatment of bio-oils can be carried out in different reactors, such as batch, continuous and down flow reactors [135,136], are shown in Fig. 6. Generally, the hydrotreatment is carried out in two steps. Firstly, the bio-oil is stabilized at lower temperature of between 100 and 300 °C in the presence of catalyst to convert the carboxyl and carbonyl functional groups to alcohol. Secondly, the stabilized bio-oil is treated at higher temperature around 350–400 °C where it undergoes HDO and cracking reactions in the presence of active catalysts [138,139]. The reactors can be operated at different optimized operating parameters such as temperature, pressure, relative flow rate and type of catalyst to obtain efficient bio-oil upgrading and less coke formation on the catalyst to prevent its early deactivation. For instance, temperature is one of the most important parameters to obtain the higher conversion of oxygenated compounds into hydrocarbons and hence decrease the oxygen content and increase the carbon and hydrogen content in the bio-oils. A number of studies suggest that in stabilization step of hydrotreatment, a temperature range of 100–300 °C, pressures between 29 and 290 bar and reaction time interval of 0.5–4 h are ideal to obtain the bio-oil yield in the range of 17–92 wt% and oxygen content of 1–16 wt% in the bio-oils [140,141]. However, for second step of hydrotreatment, higher temperatures of more than 300 °C are required to crack the larger molecules in the bio-oil but may vary depending on the type of catalyst used for the hydrotreatment. For example, Auersvald et al. [53] investigated the effect of temperature on bio-oil hydrotreatment in a continuous flow reactor in the presence of commercial sulphide $NiMo/Al_2O_3$ catalyst. Authors applied a range of temperatures of 240–360 °C and pressure of 2–8 MPa, while the hydrogen flow rate of 90 lh^{-1} was used in the experiments. Fig. 7 shows the results for the effect of temperature on physicochemical properties of bio-oils. It can be clearly observed from the figure that undesirable properties of the bio-oils, such as acid number and content, significantly decreased with increase in temperature from 240 to 360 °C, while the desirable properties, such as heating value and degree of deoxygenation, considerably increased with increase in the reaction temperature. Therefore, it can be estimated that the higher temperatures enhanced the deoxygenation reactions like dehydration, decarboxylation, decarbonylation which were accompanied with hydrogenation reactions, leading to increase in H/C atomic ratio of bio-oils and decreasing O/C atomic ratio. The study also revealed that increase in hydrogen pressure from 2 to 8 MPa enhanced hydrogenation reactions, confirmed with the increase in H/C atomic ratio of bio-oils [53]. The selection of a temperature range is also essential to minimize the coke formation onto the catalyst surface during hydrotreatment of bio-oils. It is evident that temperature has a great influence on activation energies of the reactions that take place during hydrotreatment of bio-oils and it may promote the aromatization and polymerization reactions that usually favour coke formation and ultimately can lead to blockage of the reactor. Gholizadeh et al. [140] provided insightful information on the effect of temperature (370–470 °C) on coke formation and bio-oil properties during hydrotreatment of

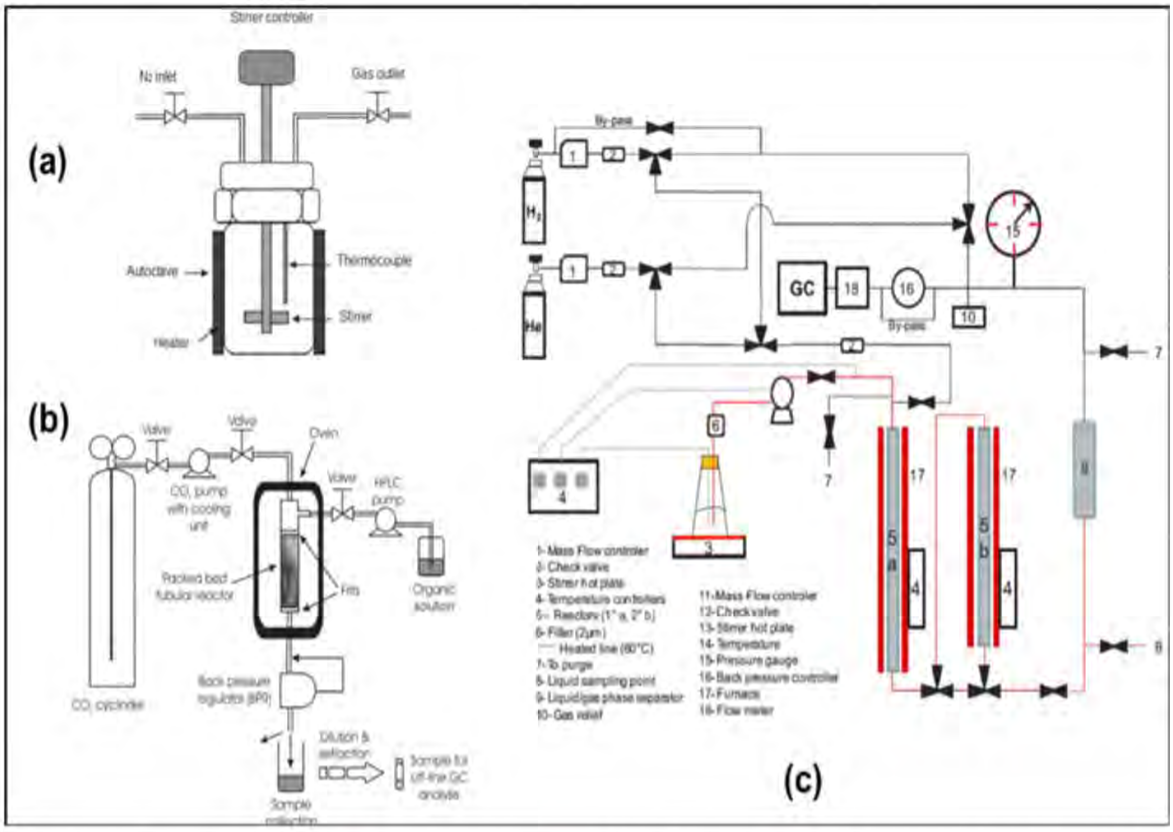

Fig. 6. Schematic diagrams of batch reactor [135], continuous reactor [136] and down flow reactor [137] for hydrotreatment of bio-oils. Reproduced with permission from respective references.

mallee wood pyrolysis oil in a continuous flow reactor using pre-sulphided $NiMo/Al_2O_3$ catalyst. The results showed that increasing the temperature augmented the coke formation considerably. The study reported the formation of small and large aromatic ring structures that probably occupied the active sites of catalyst and deactivated the catalyst. The study also revealed that the increase in temperature from 375 to 400 °C achieved the lowest oxygen content and highest carbon content in the bio-oils irrespective of varying bio-oil feed, however, further increase in temperature up to 450 °C marginally decreased the carbon content and increased the oxygen content in the bio-oils. The increase in oxygen content at higher temperatures can be attributed to reduced activity of the catalyst due to coke deposition [140]. The amount of coke formation on catalyst surface can be reduced by heating the hydrogen at the inlet point of the reactor. Evidently, a study demonstrated the application of active hydrogen at the inlet point of bio-oil to heat and activate the catalyst [142]. The results showed decreased coke deposition and lesser reactor blockage during hydrotreatment of bio-oil. This is probably because the active hydrogen enhanced cracking activity and reduced polymerization of polycyclic aromatics of the bio-oils.

Similarly, other operating parameters such as hydrogen pressure, relative flow rate and catalyst to bio-oil feed ratio are also highly important to obtain the bio-oil with high carbon and less oxygen content, and improved calorific values. It has been noticed that increasing the hydrogen pressure enhances hydrogenation and hydrodeoxygenation reactions, subsequently, increases deoxygenation activity and improves the conversion of oxygenated compounds to gasoline like products and less heavy products, while the lower hydrogen pressure may favour condensation reactions and increases heavy products in the bio-oil. Fig. 7 shows the results for the effect of hydrogen pressure on physicochemical properties of bio-oil, investigated by Auersvald et al. [53]. It can be observed from the figure that the higher hydrogen pressure of 8 MPa showed the maximum deoxygenation activity of nearly 85% compared to the lower hydrogen pressure of 2 MPa. The study reported that high hydrogen pressure of 8 MPa enhanced the hydrogenation of oxygenated compounds and produced approximately 8% of heavy products, while a higher yield of nearly 12% of heavy products was obtained with 2 MPa, owing to the promotion of condensation reactions at the lower hydrogen pressure. In addition, the values for undesirable physicochemical properties such as density, acid number, viscosity and water content decreased constantly with increase in hydrogen pressure [53]. On the other hand, the catalyst to bio-oil ratio in case of batch reactor or liquid hourly space velocity (LHSV) in continuous bed reactor plays a significant role in the distribution of organic compounds in the bio-oil and coke formation on the catalyst, which ultimately affects the bio-oil quality and catalyst deactivation. LHSV is the rate at which bio-oil is fed into the hydrotreatment reactor and can be measured as h^{-1}. A number of studies reported the application of catalyst to bio-oil ratio of 1:20 and reaction time of 1–4 h in batch reactors and LHSV of 0.05–2 h^{-1} in continuous bed reactors. For instance, Gholizadeh et al. [141] investigated the influence of LHSV on product distribution during hydrotreatment of bio-oil in a continuous bed reactor. They applied LHSV of 1, 2 and 3 h^{-1} with different amount of bio-oil (100–900 mL) at constant temperature of 375 °C and hydrogen pressure of 7 MPa. The yields of organics from the hydrotreatment of bio-oil as a function of the volume of bio-oil fed into the reactor and LHSV are shown in Fig. 8, which suggests that increasing the LHSV from 1 to 3 h^{-1} increased the yield of organics and reaches plateau values when more than 500 mL of bio-oil was fed into the reactor. The study also revealed that a low LHSV of 1 h^{-1} produced less coke yield compared to the LHSV of 3 h^{-1}. This is probably because increasing LHSV offered less residence time, providing less time for hydrotreatment reactions. Moreover, the number of accessible active sites of hydrogen decreases as the concentration of heavy liquid increases in the reactor with increase in LHSV. Consequently, in the absence of active hydrogen, hydrogenation and hydrocracking reactions are less favoured while polymerization reactions could be enhanced which ultimately could

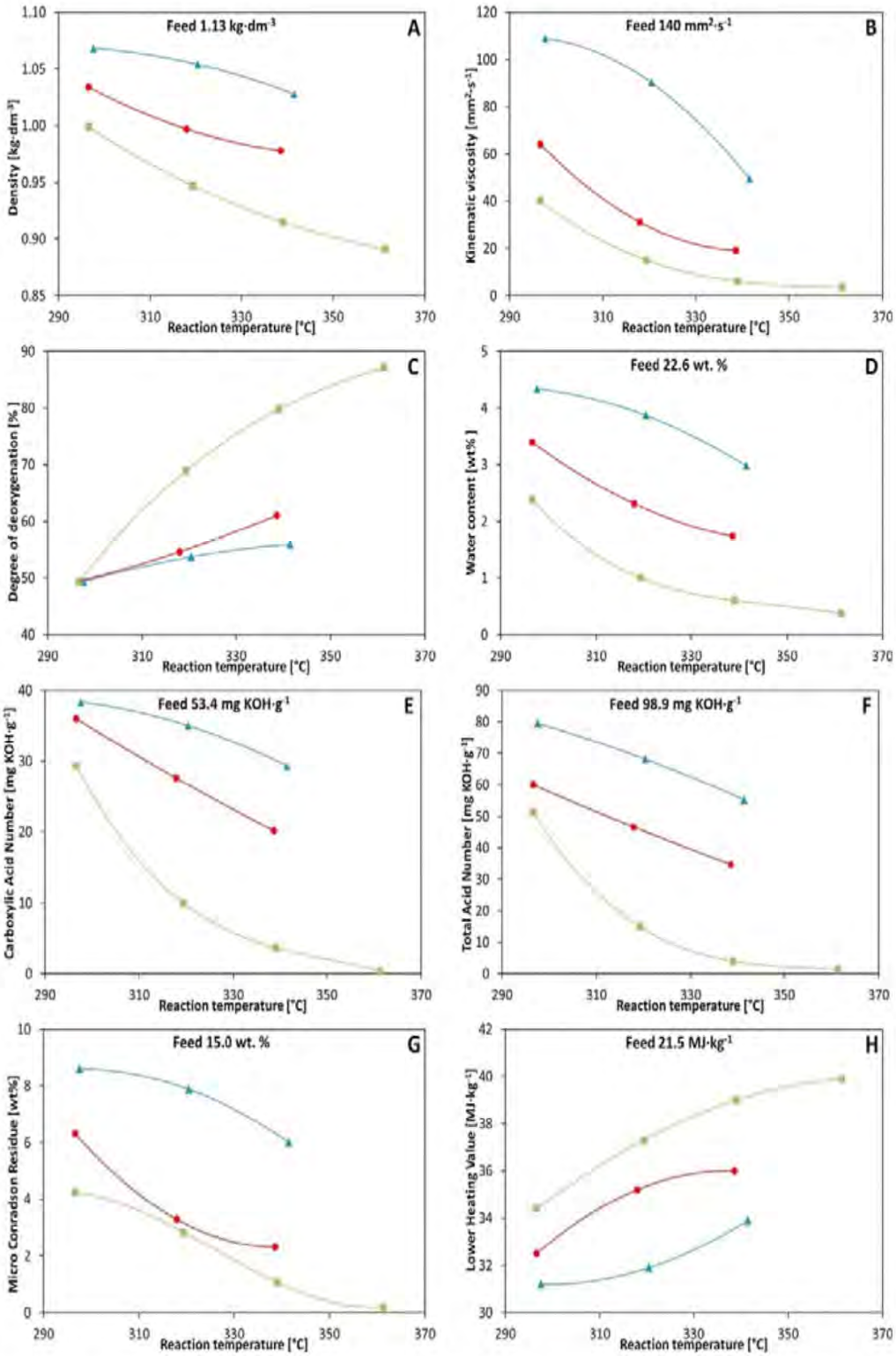

Fig. 7. Effect of temperature and pressure on physico-chemical properties of organic phase of products: density (A), kinematic viscosity (B), degree of deoxygenation (DOD) (C), water content (D), carboxylic acid number (CAN) (E), total acid number (TAN) (F), micro Conradson carbonization residue (MCR) (G), lower heating value (H); blue triangle – 2 MPa, red circle – 4 MPa, green square – 8 MPa. Reproduced with permission from Refs. [53]. (For interpretation of the references to color in this figure legend, the reader is referred to the Web version of this article.)

result in the formation of heavy products and carbonaceous species.

Hydrotreatment of bio-oil obtained from pyrolysis and HTL process has been reported in several studies and various types of catalysts have been utilized for hydrotreatment of bio-oil to either convert it into a more valuable fuel with improved physico-chemical properties or other value-added products [138,155,156]. The major catalyst types used for HDO include the commercialized metal sulphides (MoS_2, Ni–MoS_2, and Co–MoS_2), efficient noble metals (Ru, Rh, Pd, Pt, Re) and most commonly used transition metal-based catalysts (Cu, Fe, Mo, Co and Ni) [137,157,158]. Noble metal-based catalysts are considered markedly favourable for bio-oil upgrading through HDO pathway [158]. However, their high cost and high hydrogenation activity leads to excessive hydrogen consumption, which increases the overall cost of the process [135,137]. These catalysts are highly prone to poisoning of sulphur

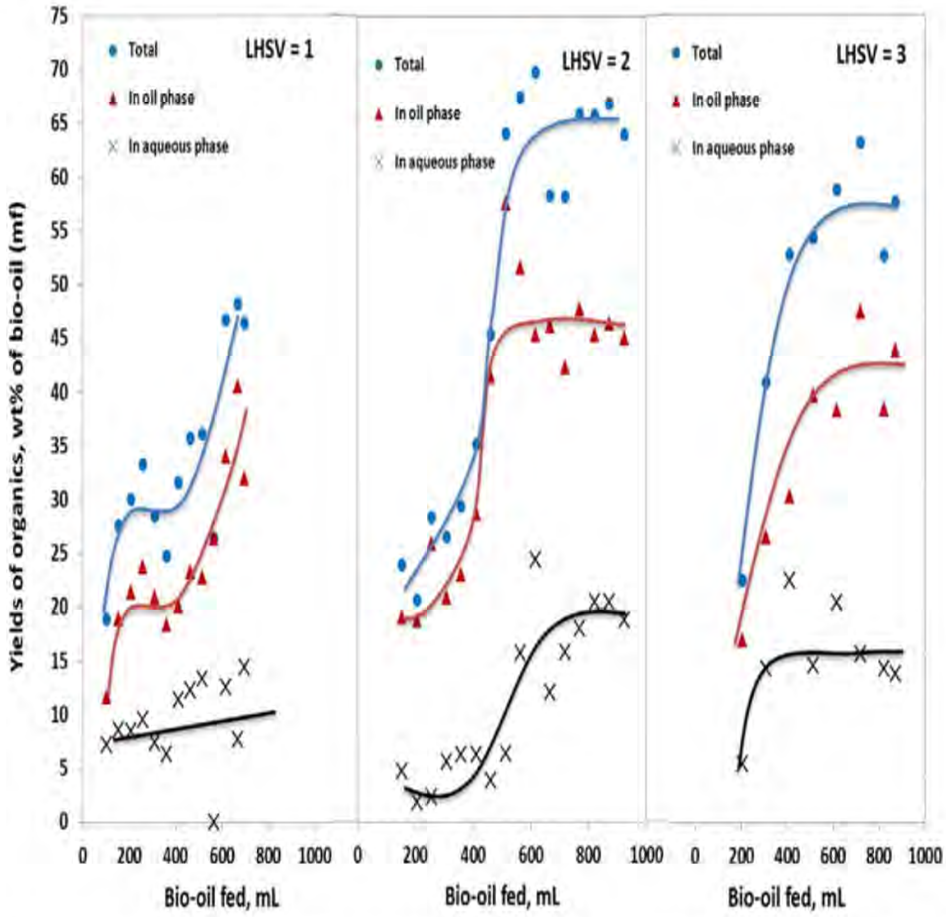

Fig. 8. The yields of organics from the hydrotreatment of bio-oil as a function of the volume of bio-oil fed into the reactor and LHSV (h^{-1}). Reproduced with permission from Refs. [141].

content present in the bio-oils. On the other hand, transition metals are comparatively cheaper and possess competitive activity for bio-oil upgrading and therefore have been extensively studied for hydrotreatment of bio-oil as well as bio-oil model compounds. Table 8 presents the summary of catalysts used for hydrotreatment of bio-oil and the properties of upgraded bio-oils.

Metal sulphide catalysts like $NiMoS/Al_2O_3$ and $CoMoS/Al_2O_3$ are commercialized catalysts used in petroleum refining and have been successfully utilized for hydrotreatment of bio-oils [146,159,160]. In these catalysts, Mo and S act as active parts of the catalyst. The retention of sulphur content is highly important to keep the catalyst active during the hydrotreatment of bio-oils. Since the bio-oil contains very low amount of sulphur, sulphur containing compounds like dimethyl sulphide, H_2S are required to add with the feed to overcome the loss of sulphur and avoid the catalyst deactivation [159]. The presence of sulphur vacancies in the catalysts, mainly at the catalyst edges are thought to work as active sites in metal sulphide catalysts that catalyse the hydrodeoxygenation reactions [134], while the catalysts support like Al_2O_3 also contains acidic sites that catalyse various deoxygenation reactions like dehydration, decarboxylation, decarbonylation and convert acids, aldehydes, ketones into hydrocarbons [161]. The addition of transition metals Ni and Cu can be used as promoters for Mo and are also believed to enhance the number of sulphur vacancies [146,160]. These promoters can donate their valence electrons to Mo, subsequently can make $Mo - S$ weaker, resulting into more active sulphur vacancies. During hydrodeoxygenation on metal sulphide catalysts, the oxygen atom of the functional groups of the reactant is attached to sulphur vacancies and promote the breaking of $C - O$ bond [162]. In addition, activated hydrogen from $S - H$ groups is believed to saturate the oxygen atom released from the breaking of $C - O$[162]. A number of studies have reported the successful application of metal sulphide catalysts for hydrotreatment of bio-oils. For instance, Grilc et al. [163] investigated the influence of metal sulphide catalysts like $NiMo/Al_2O_3$ and MoS_2 for hydrotreatment of bio-oils produced from HTL of spruce and fir sawdust at a temperature of 300 °C and hydrogen pressure of 8 MPa, and compared their activity with other catalysts like Pd/Al_2O_3, Pd/C, and $Ni/Al_2O_3–SiO_2$. The authors examined the comparative effect of different catalysts studied on various reactions (such as hydrodeoxygenation, decarbonylation, decarboxylation and catalytic cracking) and yield of upgraded bio-oils. The results suggested that sulphide NiMo catalysts produced higher yield of upgraded bio-oil compared to oxide and reduced form of NiMo catalysts but lower than Pd/Al_2O_3 and Pd/C. In addition, sulphide NiMo catalysts showed high hydrodeoxygenation, decarboxylation and catalytic cracking activity. Reduced form of NiMo catalyst also showed high hydrodeoxygenation activity but could not favour decarbonylation, decarboxylation and cracking much efficiently compared to sulphide NiMo catalyst. On the other hand, Pd/Al_2O_3, Pd/C, and $Ni/Al_2O_3–SiO_2$ exhibited lower activity for all the reactions compared to either reduced or sulphide NiMo catalysts [163]. Biller et al. [55] studied the application of sulphided $NiMo/Al_2O_3$ and $CoMo/Al_2O_3$ for hydrotreatment of bio-oil obtained from HTL of *Chlorella*. The hydrotreatment of bio-oil using both the catalysts was investigated in a batch reactor at two temperatures of 350 and 405 °C, 13.8 MPa hydrogen pressure and catalyst to bio-oil ratio of 0.2 [55]. The results reported that the application of sulphided catalysts considerably increased the conversion of oxygenated compounds into hydrocarbons, as a high number of hydrocarbons was observed in the upgraded bio-oil [55]. Although the application of metal sulphide catalysts is highly advantageous for hydrotreatment technique to obtain the bio-oil with enhanced physicochemical properties and energy density, it

Table 8
Catalysts applied for hydrotreatment of bio-oils and properties of upgraded bio-oils.

Catalyst	Hydrotreatment operating parameters						Upgraded bio-oil properties (wt%)					Reference
	Reactor type	Bio-oil source	Temp (°C)	Pressure (MPa)	Time (h) or LHSV (h^{-1})	C/B	Bio-oil yield	C	H	O	H_2O	
$NiCu/TiO_2$	Batch	Pine wood	350	20.0	1 h	1:10	45.5	73.0	9.1	15.1	3.6	[143]
$NiCu/Al_2O_3$	Batch	Wheat straw	340	8.0	4 h	1:20	17.9	74.9	9.7	14.3	/	[144]
$NiMo/SiO_2$–Al_2O_3	Batch	Pine wood	350	14.0	4 h	1:20	42.4	77.2	9.6	13.2	2.9	[145]
$NiMoCe/\delta$-Al_2O_3	Batch	Cassava rhizome	300	1.0	1 h	1:6.7	/	67.8	7.1	22.2	/	[146]
$NiCu/CeO_2$–ZrO_2	Batch	Pine wood	350	20.0	1 h	1:10	40.6	78.3	8.5	13.2	8.1	[143]
$NiCu/ZrO_2$	Batch	Pine wood	350	20.0	1 h	1:10	38.9	72.1	8.7	16.1	4.1	[143]
NiCu/CRH	Batch	Pine wood	350	20.0	1 h	1:10	44.9	76.2	8.1	17.7	3.9	[143]
NiCu/Sibunite	Batch	Pine wood	350	20.0	1 h	1:10	35.9	87.6	6.8	5.4	12.5	[143]
$NiCu/\delta$-Al_2O_3	Batch	Pine wood	350	20.0	1 h	1:10	42.2	74.5	8.4	17.1	4.1	[143]
Ni/Cr_2O_3	Batch	Beech wood	225	8.0	2 h	1:20	42.86	58.3	8.0	33.7	10.5	[147]
$Ni–Cr/Cr_2O_3$	Batch	Beech wood	225	8.0	2 h	1:20	37.48	60.1	8.2	31.7	10.1	[147]
Ru/C	Batch	Beech wood	225	8.0	2 h	1:20	46.41	59.9	8.1	31.8	10.6	[147]
$NiCu/Al_2O_3$	Batch	Wheat straw	250	8.0	4 h	1:20	/	71.4	9.3	18.2	11.8	[144]
Ru/C	Batch	Pine wood	350	14.0	4 h	1:20	41.5	81.4	9.5	9.0	4.4	[145]
Ni/SiO_2–Al_2O_3	Batch	Pine wood	350	140	4 h	1:20	52.7	75.8	9.0	15.0	5.2	[145]
$NiCu/SiO_2$–Al_2O_3	Batch	Pine wood	350	14.0	4 h	1:20	49.5	76.0	9.1	14.8	4.6	[145]
$NiPd/SiO_2$	Batch	Pine wood	350	14.0	4 h	1:20	52.5	75.1	9.2	15.5	4.7	[145]
$NiPdCu/SiO_2$	Batch	Pine wood	350	14.0	4 h	1:20	53.1	75.8	9.2	14.9	5.6	[145]
$NiMoCu/SiO_2$–Al_2O_3	Batch	Pine wood	350	14.0	4 h	1:20	43.2	77.1	9.4	13.3	2.9	[145]
$NiMo/\delta$-Al_2O_3	Batch	Cassava rhizome	300	1.0	1 h	1:6.7	/	59.2	6.8	31.3	/	[146]
$NiMoCu//\delta$-Al_2O_3	Batch	Cassava rhizome	300	1.0	1 h	1:6.7	/	67.7	7.1	22.3	/	[146]
Ni/C	Batch	/	275	10.0	4 h	1:20	47.6	50.83	9.19	39.24	/	[148]
Ru/C	Packed bed	Pine wood	300	10.0	0.4 h^{-1}	/	49.0	75.0	12.2	10.2	0.44	[149]
Ru/C	Batch	Pine wood	350	20.0	4 h	1:31.5	17.5	79.1	9.3	11.6	/	[150]
Pt/C	Batch	Switchgrass	320	14.5	4 h	1:18	46.6	75.4	8.48	15.04	2.1	[151]
Ru/C	Batch	Corn stover	300	12.5	4 h	/	54.4	78.6	9.69	8.8	2.1	[139]
Pd/C	Batch	Corn stover	300	12.5	4 h	/	52.6	77.8	9.30	10.6	1.8	[139]
Ru/C	Batch	Hardwood	300	5.0	3 h	1:20	63.5	71.0	8.5	20.5	/	[152]
Ni/AC	Batch	Hardwood	300	5.0	3 h	1:20	60.0	72.8	8.3	18.8	/	[152]
NiP/AC	Batch	Hardwood	300	5.0	3 h	1:20	59.1	80.0	8.4	18.1	/	[152]
NiRu/AC	Batch	Hardwood	300	5.0	3 h	1:20	55.4	73.4	9.0	17.6	/	[152]
NiRuP/AC	Batch	Hardwood	300	5.0	3 h	1:20	58.7	73.0	8.5	18.3	/	[152]
Co/AC	Batch	Hardwood	300	5.0	3 h	1:20	58.4	72.6	8.2	19.2	/	[152]
CoP/AC	Batch	Hardwood	300	5.0	3 h	1:20	37.2	73.0	7.7	19.2	/	[152]
CoRu/AC	Batch	Hardwood	300	5.0	3 h	1:20	61.2	71.8	8.4	19.7	/	[152]
CoRuP/AC	Batch	Hardwood	300	5.0	3 h	1:20	63.5	73.2	8.4	18.4	/	[152]
Ni/SiO_2–Al_2O_3	Batch	PJ chips	350	7.0	1 h	1:5	55.7	69.2	10.4	20.1	/	[153]
Ni/SiO_2–Al_2O_3	Batch	PJ chips	400	7.0	1 h	1:5	49.4	75.1	12.5	12.2	/	[153]
Ni/SiO_2–Al_2O_3	Batch	PJ chips	450	7.0	1 h	1:5	44.8	83.4	16.4	0.0	/	[153]
Ni/Al_2O_3	Batch	Wheat straw	340	8.0	1.6 h	1:20	76.2	73.5	9.5	15.9	4.7	[154]
$NiCu/Al_2O_3$	Batch	Wheat straw	340	8.0	1.6 h	1:20	78.0	69.8	9.8	19.4	6.8	[154]
Ni/SiO_2	Batch	Wheat straw	340	8.0	1.6 h	1:20	76.0	70.0	9.2	19.7	6.8	[154]
Ni/ZrO_2	Batch	Wheat straw	340	8.0	1.6 h	1:20	76.5	69.9	9.1	20.0	7.4	[154]
NiW/AC	Batch	Wheat straw	340	8.0	1.6 h	1:20	76.0	70.4	9.4	19.3	6.9	[154]
Ni/TiO_2	Batch	Wheat straw	340	8.0	1.6 h	1:20	76.8	73.0	9.1	16.8	4.9	[154]
Ru/C	Batch	Wheat straw	340	8.0	1.6 h	1:20	78.0	71.6	10.5	16.9	5.4	[154]

Note: PJ-Pinyon juniper, C/B-catalyst to bio-oil ratio.

may also lead to coke formation and subsequently, undesirable blockage of the reactor. The use of additives like methanol has shown to reduce the coke formation. Methanol may also react with carboxylic or esters groups of the bio-oil and help to reduce its corrosivity [159]. The other drawback of using sulphided catalysts is the leaching of catalyst bound sulphur into the upgraded bio-oil. Therefore, additional upgrading approach may require to remove the impurities, which ultimately can increase the overall cost of the bio-oil upgrading.

The other type of catalysts widely used for hydrotreatment of bio-oils are noble metals-based catalysts, such as Rh/C, Rh/ZrO_2, Ru/C, Pt/SiO_2 and Pd/C, Pd/Al_2O_3 [139,150,158]. These catalysts show a high reactivity for H_2 activation and thus can effectively saturate the oxygen atom of the functional groups of the oxygenated compounds in the bio-oil, making them highly favourable candidates for hydrotreatment of bio-oils [138]. The other advantage of noble metal-based catalysts is that they are less prone to deactivation by water or sulphur contents present in the bio-oil [133]. Consequently, a number of studies deployed noble metals on different catalytic supports for hydrotreatment of bio-oil and showed considerable improvement in the bio-oil properties and increase in H/C ratio, indicating the successful conversion of oxygenated compounds into hydrocarbons. For example, Wildschut et al. [150] demonstrated the hydrotreatment of fast pyrolysis oil at 250 and 350 °C and hydrogen pressures of 10 and 20 MPa using Ru and Pt on different supports like Ru/C, Pt/C, Pd/C, Ru/Al_2O_3, and Ru/TiO_2. The results revealed that Ru/C achieved the highest yield of upgraded bio-oil and deoxygenation activity which were 60 wt% and 90 wt%, respectively, while Ru/TiO_2 showed the least deoxygenation activity that can be attributed to low surface area of TiO_2 [150]. Authors further suggested that other physicochemical properties of bio-oils like viscosity, water content and density were significantly reduced and notable increase in HHV of bio-oils was observed. Evidently, the HHV of upgraded bio-oil obtained using Ru/C was 43 MJ/kg, which was approximately two

times higher than the feed bio-oil of 20 MJ/kg [150]. A recent study reported the application of Ru/α-Al_2O_3 and Ru/γ-Al_2O_3 on hydrotreatment of rice husk pyrolysis oil at 240 °C and hydrogen pressure of 4 MPa, reaction time of 24 h. The results showed that Ru/α-Al_2O_3 achieved superior activity for hydrotreatment compared to Ru/γ-Al_2O_3. Markedly, Ru/α-Al_2O_3 showed a higher bio-oil yield of nearly 80 wt%, while Ru/γ-Al_2O_3 could achieve a maximum bio-oil yield of 58.4 wt%. Ru/α-Al_2O_3 showed less coke formation than Ru/γ-Al_2O_3 which was ascribed to the higher acidic character of the latter catalyst [150]. In addition, Ru/α-Al_2O_3 produced 23.15% yield of hydrocarbons comprised of alkyl-substituted cyclohexane and alkyl-substituted benzene. The use of noble metals based catalysts showed promising results of bio-oil upgrading through hydrotreatment approach, however, noble metals are considered rare earth metals and not present abundantly. Moreover, noble metal-based catalysts are highly expensive that restricts their industrial-scale application for bio-oil upgrading. Therefore, comparatively cheaper catalysts can make the hydrotreatment approach more economical for bio-oil upgrading.

Transition metals based catalysts are considered highly cost-effective and substantially efficient for hydrotreatment of bio-oils. Considering their low cost and lower hydrogen consumption, transition metals like Ni, Cu, Co, and Fe have been extensively used with and without different supports as potential catalysts for hydrotreatment of bio-oils [133,146,157]. The presence of valence electrons in their d-orbitals allows them to interact with reactants, however, electron density in the d-orbitals plays a key role in the determination of vacant coordination sites [133]. The mechanism of hydrodeoxygenation reactions over transition metals based catalysts can be understood more clearly using model compounds of the bio-oil components [164–166]. Consequently, many attempts have been made to understand the reaction mechanisms using model compounds, such as guaiacol, anisole, phenol and p-cresol [166–168].

Several studies have reported hydrotreatment of bio-oils using different monometallic and bimetallic catalysts. For instance, Yin et al. [145] investigated the effect of different transition metals based catalysts such as Ni/SiO_2–ZrO_2, NiCu/SiO_2–ZrO_2, NiMo/SiO_2 and NiMo-Cu/SiO_2 for hydrotreatment of pine wood bio-oil at 350 and 400 °C and hydrogen pressure of 14 MPa for 4 h. The results suggested that upgraded bio-oil showed higher H/C ratio with NiMo/SiO_2 and NiMo-Cu/SiO_2 catalysts compared to Ni/SiO_2–ZrO_2, NiCu/SiO_2–ZrO_2. A noticeable point was that Mo based catalysts yielded more CH_4 due to enhanced methanation reactions, which could be an undesirable product in order to retain more carbon in the bio-oil [145]. Similar to transition metals, the application of metal oxides [133,146], metal phosphides [148,152,165], carbides [137,151] and nitrides [132,133] have also shown promising results for hydrotreatment of bio-oils.

Hydrotreatment of bio-oils has proven an advantageous approach, nevertheless, the use of external hydrogen, arduous transport and exorbitant storage makes the overall process highly expensive. Therefore, it is important to adopt cost-effective measurements to develop the technique more affordable at industrial-scale. In order to reduce the cost of external hydrogen supply, liquid hydrogen donors, such as formic acid, ethanol and methanol can be used which can be successfully converted into hydrogen through catalytic aqueous phase reforming process. Subsequently, the produced hydrogen can be utilized in hydrodeoxygenation of bio-oils [169–171]. This approach is called *in-situ* hydrodeoxygenation where hydrogen is not supplied from outside rather provided from reforming reactions of hydrogen donating chemicals. In a recent study, Mohammed et al. [170] demonstrated the application of methanol in *in-situ* hydrodeoxygenation of Napier pyrolytic oil in the presence of Pd/C and Pt/C catalysts. The process was carried out at 350 °C, 2 wt% catalyst, 20 wt% methanol and 1 h reaction time. The results showed that the oxygenated compounds in the bio-oil were successfully converted into hydrocarbons. As a result, the upgraded bio-oil showed enhanced physicochemical properties compared to feed bio-oil. For example, feed bio-oil showed H/C ratio of 1.44, while H/C ratios of bio-oil obtained with Pd/C and Pt/C were 1.68 and 1.66, respectively. In addition, HHV was increased from 29.18 MJ/kg of feed bio-oil to 39.32 with Pd/C and 38.07 with Pt/C [170]. Alternative to the application of liquid hydrogen donors, hydrogen can also be generated from water using suitable catalysts. For instance, zinc hydrolysis can lead to generation of H_2 ($Zn + H_2O = ZnO + H_2$), which can be further utilized for hydrotreatment of bio-oil [172]. Bio-oils also contain approximately 15–30 wt% of water content which can be converted to hydrogen and the *in-situ* produced hydrogen can be used for bio-oil upgrading making the whole process highly independent from external source of hydrogen. However, the amount of water present in the bio-oil might not be enough to act as solvent for all reactants to form a supercritical reaction system, hence, demanding the addition of water. A study attempted *in-situ* hydrodeoxygenation of bio-oil using the water content of bio-oil to produce hydrogen but the authors also added water and methanol since the bio-oil contained 14.5 wt% water only, which might not be adequate to generate required amount of hydrogen for the treatment [135]. In a typical experiment, authors utilized 6 g zinc powder, 5 g Pd/C catalyst, 50 g bio-oil, 50 mL deionized water and 63 mL methanol as solvents and loaded them in a 500 mL autoclave reactor. The experiments were carried out at 200–300 °C and 5 h reaction time. The results suggested significant production of hydrocarbons in the upgraded bio-oils, producing 12.47 wt% at 200 °C and 19.36 wt% at 300 °C, while 250 °C produced the maximum hydrocarbons of 24.09 wt %. The oxygenated compounds like phenols, acids, aldehydes, ketones were reduced considerably, although esters were substantially increased. This was possibly because during hydrotreatment process ketones and aldehydes were hydrogenated into alcohols that further underwent esterification reactions to yield esters [156,173]. Therefore, *in-situ* hydrodeoxygenation could be an advantageous approach economically as it reduces the cost of external hydrogen supply but it also produces a low-quality bio-oil, hence, a comparative techno-economic study considering the quality of bio-oils should be conducted to understand the impact of both types of hydrodeoxygenations.

4. Commercial applications of bio-oils

The main goal of bio-oil upgrading is to make it a competitive fuel to replace heavy fuel oil or light fuel oil for heat generation or using it as a transport fuel. The early bio-oil combustion tests for heating applications at the industrial scale have indicated the bio-oil as a suitable fuel to replace heavy fuel oil. To date, few commercial-scale applications of bio-oil have been reported for combustion in boilers, turbines and diesel engines. However, some specific modifications are required in the combustion equipment for bio-oil as compared to the conventional fuels. In boilers, a variety of fuels can be used for heat generation where bio-oil has also proved to be a suitable fuel for boilers for heat generation with acceptable emissions. For example, the combustion properties of bio-oils were tested in a test boiler on 4 MW output level in Finland [30]. The study demonstrated the combustion of different bio-oils in the boiler, modified with a special type of front head to avoid heat loss and an extra cylinder inside the furnace to obtain higher temperature and faster volatilization. The bio-oil samples were added with 10% methanol to increase the homogeneity and to enhance the combustibility and ignition. The combustion results suggested that the bio-oils were of high grade and the NO_x emissions were competitive to heavy fuel oil and extremely lower to the standard emission value (120 mg/MJ for 50–150 MW boiler) in Finland. Noticeably, the NO_x emissions were reported to be 88 mg/MJ for bio-oil, while the combustion of heavy fuel oil produced NO_x emissions of 88 mg/MJ [30]. Alternatively, combustion of bio-oil has been also tested in a gas turbine for heat generation. Earlier [174], carried out bio-oil combustion in small gas turbine type T216 with capacity to generate 75 kW electric power. The combustion chamber of the gas turbine was modified with inline fuel nozzles i.e. an ignition nozzle and second the main nozzle. The gas turbine was started using diesel oil, firstly, diesel oil was used to operate the ignition nozzle

and the bio-oil was supplied to the main nozzle using an external fuel pump. This gas turbine with dual fuel operation generated power of 580 kWth, which was lower to sole diesel fuel operation (791 kWth). However, the former mode resulted in lower NOx emissions as compared to the latter [174]. Recently, a study also reported the bio-oil combustion in a micro gas turbine [28]. The tests were performed using pure bio-oil and bio-oil/ethanol ratios of 20/80 and 50/50% (volume fractions), and the results were compared with the combustion of sole diesel fuel and ethanol. The results reported that pure bio-oil and the blend fuels with a higher fraction of bio-oil showed higher emissions of CO and NO_x than sole diesel fuel and ethanol. These increased emissions of CO and NO_x were attributed to the formation of larger droplets by the viscous bio-oil and fuel-bound nitrogen, respectively. However, the blend fuels showed better electrical efficiency compared to the diesel fuel, which was ascribed to the higher production of water vapour during the combustion process [28]. In addition to boilers and turbines, combustion of bio-oil has been successfully demonstrated in diesel engines for power generation. Generally, the diesel engines show higher efficiency for power generation as compared to boilers and turbines. Laesecke et al. [8] demonstrated the combustion of bio-oil in a diesel engine using 0.45 L Ricardo single cylinder direct injection diesel engine. The bio-oil showed approximately similar thermal efficiency to the diesel fuel, however, combustion air preheating of bio-oil (55 °C) was required for ignition. The longer ignition delay time with the bio-oil could be related to the chemical composition of the bio-oil. Recently, another demonstration showed the combustion behavior of bio-oil and its blends with biodiesel in a single cylinder research engine [29]. The testing results indicated that pure bio-oil and the blend fuels with the higher concentration of bio-oil showed longer ignition delays as compared to the diesel fuel, due to the reduction in cetane number and lower heating values.

The above discussion suggests that the bio-oil has a great potential to serve as a potential fuel in turbines, boilers and diesel engines for heat and power generation. However, some modifications are still required either in the combustion units or mixing the bio-oil with the solvents like ethanol, methanol or diesel fuel to avoid the ignition time delays. On the other hand, application of bio-oil as a transport fuel needs more investigation. Currently, the lower heating values, chemical instability and other poor physical properties restrict its use in internal combustion engines. The bio-oil upgrading to a suitable transport fuel needs complete removal of oxygenated compounds and presence of naphthenes, paraffins and aromatic hydrocarbons and the other physical properties should also be improved to make it a realistic drop-in fuel. Besides, the production of bio-oil at a large scale similar to the cost of conventional fuels is one of the key challenges to overcome to make the bio-oil economical and affordable to the consumers.

5. Bio-oil upgrading to hydrogen/syngas via steam reforming

The bio-oil generated from biomass pyrolysis or HTL process could also be a suitable feedstock for steam reforming (SR) technique for the production of H_2 gas and synthesis gas (also termed as syngas is a mixture of CO and H_2)·H_2 produced from SR of bio-oil can be further used as a clean fuel as its combustion produces water and no harmful gases are generated or it can also be used in hydrodeoxygenation of bio-oil for the synthesis of gasoline-like products, while syngas can be further subjected to Fischer-Tropsch process for the production of hydrocarbons. SR is a process that involves the conversion of bio-oil containing oxygenated compounds or hydrocarbons into hydrogen in the presence of water at a temperature range of 350–1000 °C [62,63]. SR of an oxygenated compound of bio-oil can be represented as following in eq. (4).

$$C_n H_m O_k + (n-k)H_2O \rightarrow nCO + \left(n + \frac{m}{2} - k\right)H_2 \quad (4)$$

The presence of the higher amount of steam in the process can lead to water-gas shift reaction (WGSR) that involves the conversion of CO into CO_2 and H_2 gas, as shown in eq. (5), while at low temperatures, H_2 produced in the process can combine with CO to generate methane, as given in eq. (6).

$$CO + H_2O \leftrightarrow CO_2 + H_2 \quad (5)$$

$$CO + 3H_2 \leftrightarrow CH_4 + H_2O \quad (6)$$

It is also interesting to note that for a complete SR reaction, 1 mol of CO is lost for each mole of H_2 produced (eq. (5)), and in methanation reaction (eq. (6)), 3 mol of hydrogen are lost for each mole of CH_4. From thermodynamics point of view, the reforming reaction (eq. (4)) is an endothermic reaction and occurs at high temperature and low pressures, while WGSR and methanation shown in eqs. (5) and (6), respectively are exothermic reactions and take place at lower temperatures [175]. Therefore, the endothermic reforming reaction is usually performed in the high-temperature reactor, and the resultant products are transferred to another reactor of lower temperature to carry out the exothermic conversion reactions.

SR of bio-oil can be carried out in different types of reactors, such as combined two stage pyrolysis-reforming reactor, separate fixed bed reactor and fluidized bed reactor, tubular quartz micro-reactor, membrane reactor, spouted bed reactor, and nozzle-fed reactor [56]. Some reactors are shown in Figs. 9–11. Several studies have employed fixed bed reactor for SR of bio-oil [56,175,176]. However, it is believed that fixed-bed reactor is convenient to reform only lighter model compounds of bio-oil such as acetic acid and ethanol, while the reforming of larger model compounds or crude bio-oil leaves large amount of residue in the reactor and subsequent heating may lead to thermal degradation and formation of coke. Therefore, to reduce the coke formation during SR of bio-oil or larger bio-oil model compounds, fluidized bed reactor has been widely used and it is thought that the reforming process can be operated more efficiently than fixed bed reactor [56,59,60]. Where in fixed bed reactor a layer of coke can be easily formed, in fluidized bed reactor the circulated catalyst particles are in direct contact with bio-oil components and thus less coke formation and more hydrogen yield can be obtained. Evidently, a study compared the activity of SR of bio-oil for hydrogen production in a fixed and fluidized bed reactor using Ni based catalyst and also observed the coke formation in both reactors at similar reaction conditions [177]. The results revealed that carbon deposition was severe in fixed bed reactor compared to fluidized bed which suggests quicker catalyst deactivation in the former. Since the fluidized bed showed lesser coke formation, it produced a higher yield of hydrogen, approximately 76%, which was 7% greater than the fixed bed [177]. However, coke deposition is still one of the limitations in fluidized beds. Other limitations associated with catalyst deactivation in fluidized beds are sintering and attrition. These processes result in the loss of active components of catalysts. More information on the mechanism of attrition of catalyst in fluidized bed can be found elsewhere [178]. Fluidized bed reactors could be made up of two beds, in which one bed is used for SR process and the other is used to regenerate the catalyst by gasification or oxidation. Alternatively, combined fixed and fluidized bed reactor can also be used for SR of bio-oil which allows to carry out the whole process at two different temperatures [56,179]. In this combined unit, fluidized bed is used to evaporate the bio-oil at lower temperatures of 430–500 °C, while steam reforming is carried out in the fixed bed at higher temperature of >700 °C in the presence of an active catalyst [179].

Another alternative to reduce the coke deposition on catalyst is the application of two stage catalytic reforming process, as shown in Fig. 11 [180,181]. In the first stage, a less active catalyst is used at temperature of 400–600 °C, while the second stage is operated with more active catalyst at temperature >700 °C. It is believed that in two stage reactor systems, coke generating precursors are reduced in the first stage, converting macromolecules of bio-oil into smaller compounds that lowers coke deposition in the second stage, consequently, it produces enhanced yield of syngas or H_2 and stabilizes the activity of a catalyst in long term

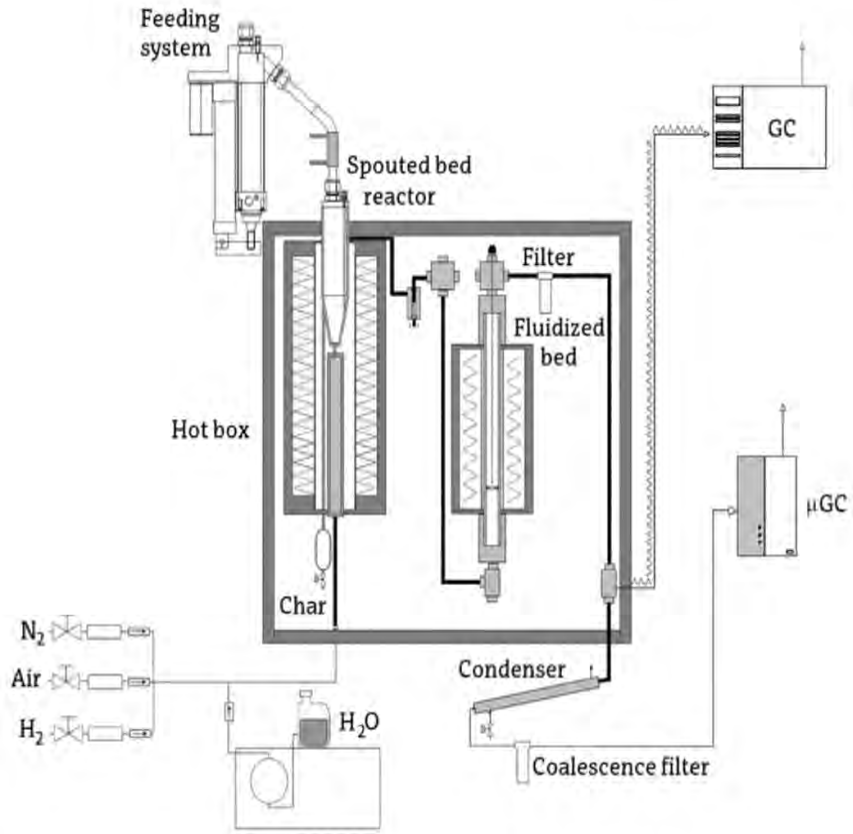

Fig. 9. Scheme of the bench scale plant for continuous biomass pyrolysis-reforming. Reproduced with permission from Ref. [182].

reaction. For example, Ren et al. [181] demonstrated the application of two stage SR of bio-oil, using quartz sand in first-stage fluidized bed reactor and Ni/dolomite for second stage fixed bed reactor and compared the reforming results with single stage fixed bed SR at 800 °C. The results showed that two stage SR produced a higher H_2 yield of 85.3% in 1 h of reaction time, while single stage could produce 80% of H_2 yield. After 3 h of reaction time, H_2 yield decreased nearly 10% in single stage fixed reactor but only 5.6% reduction in H_2 yield was noticed in two stage system, owing to reduced coke formation in the system [181]. Another study by Liu et al. [180] performed two stage catalytic SR of bio-oil using Fe/biochar in the first stage (or pre-reforming) at 350–600 °C and Ni–Ca/γ-Al_2O3 in second stage at 700 °C. The study suggested that Fe/biochar in the pre-reforming stage converted coke precursors like polycyclic aromatics, naphthalenes and benzene into furans, phenols and other non-aromatic compounds, which were successfully converted to H_2 and syngas in the second stage by Ni catalyst. The decrease in coke precursor compounds inhibits polymerization of volatiles and hence the coke formation on the catalyst in the second stage [181]. As a result, enhanced yield of H_2 was achieved, indicating two stage catalytic reforming process an advantageous and efficient approach to reduce the coke formation and obtain a higher yield of H_2.

SR of bio-oil can be performed in different reactors on the type or composition of bio-oil under varying operating parameters, such as temperature, steam/carbon (S/C) ratio and weight hourly space velocity (WHSV) or space time which greatly influence the conversion rate of bio-oil, yield of H_2, and coke formation on the catalyst [62,175,183]. Generally, the smaller compounds like acetic acid require a low temperature of nearly 450 °C for its full conversion, while the larger compounds or polyaromatic compounds require a higher temperature of >750 °C for its complete conversion in the process. Therefore, SR of bio-oil is usually carried out between 400 and 1000 °C in a fixed or fluidized bed reactor. Valle et al. [184] investigated the effect of temperature range of 550–700 °C on H_2 yield, bio-oil conversion and coke formation during SR of pine wood bio-oil in a continuous two-step system using Ni/La_2O_3-αAl_2O_3 as the catalyst. It was found that H_2 yield and bio-oil conversion increased with increase in temperature, showing the H_2 yield of nearly 30% at 550 °C which increased to above 70% at 700 °C with a space time of >0.10 $g_{catalyst}$ h/$g_{bio\text{-}oil}$ and S/C ratio of 1.5. However, increase in the temperature showed increased the coke deposition on the Ni catalyst. For example, 14.8 wt% coke was observed at 600 °C where 700 °C produced 21.4 wt% of coke with 0.04 $g_{catalyst}$ h/$g_{bio\text{-}oil}$ of space time, S/C ratio of 1.5 and 5 h of reaction time [184]. It was further noticed that 550–650 °C range produced filamentous type of coke which does not block the active sites of the catalyst and therefore has less impact on the catalyst deactivation [184]. Similarly, Remiro et al. [185] examined the effect of temperature range of 500–800 °C on SR of aqueous fraction of bio-oil. The results revealed that a complete bio-oil conversion was achieved at 700 °C and the highest H_2 yield of 95% was obtained with 5 h of reaction time [185].

Another key parameter for SR is S/C ratio to achieve a higher yield of H_2 [183,186]. Generally, water is added to the bio-oil to obtain the desirable S/C ratio. Studies have shown that higher S/C ratio (>3) is advantageous to change the thermodynamic equilibrium of reforming and WGSR towards H_2 production, consequently leading to the higher yield of H_2. For instance, a study showed approximately 93% H_2 yield with S/C ratio of 6, while S/C ratio of 1.5 could achieve a maximum H_2 yield of nearly 78% [183]. Moreover, the higher amount of steam can also help to gasify some amount of carbonaceous species, thus, minimizing the risk of catalyst deactivation. However, the higher amount of steam can reduce the energy efficiency of SR process since it requires higher amount of energy to evaporate water at the required temperature [187]. Therefore, a suitable S/C ratio is pivotal to achieve the maximum H_2 yield. In addition to S/C ratio, the selection of space time or WHSV is highly important to obtain optimum yield of H_2 and bio-oil conversion in reforming reaction. Higher the space time or WHSV means longer the time catalyst can react with bio-oil components and therefore could be favourable to produce high H_2 yield. Valle et al. [184] applied different

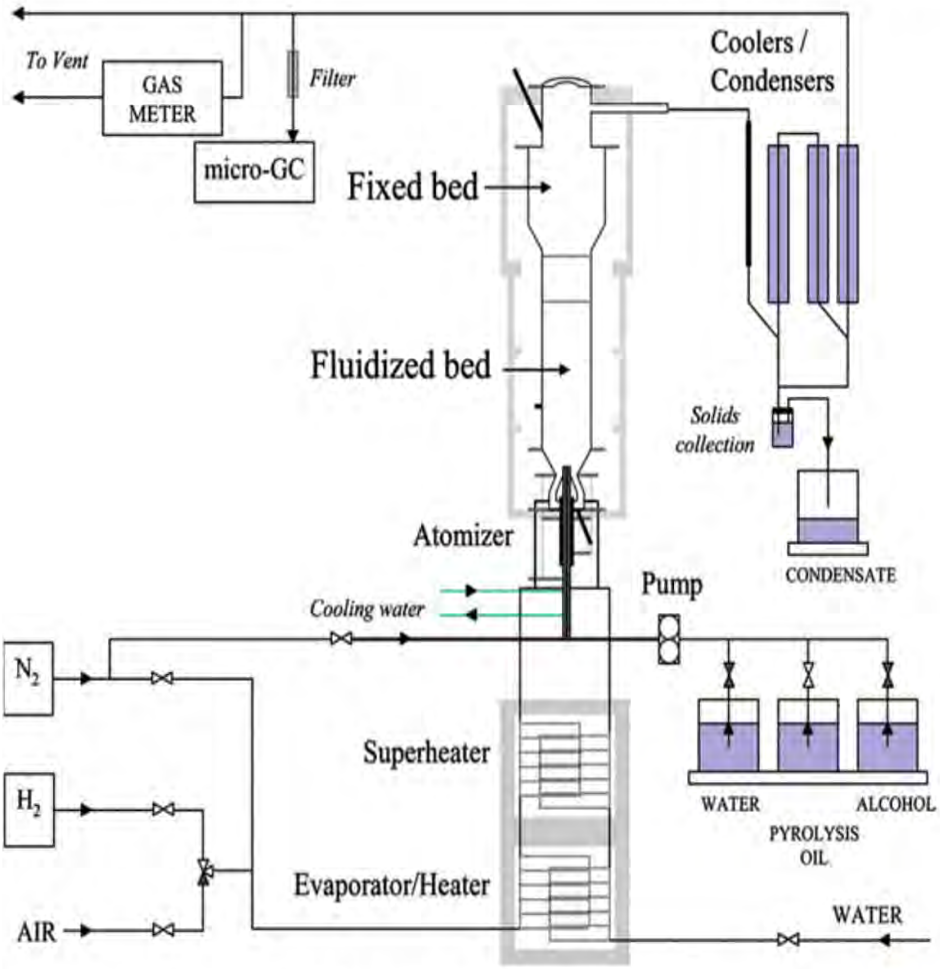

Fig. 10. Schematic overview of the fluidized-bed setup for bio-oil reforming. Reproduced with permission from Ref. [179].

space time (0.04, 0.10, 0.19 and 0.38 $g_{catalyst}$ h/$g_{bio\text{-}oil}$) for SR of bio-oil and examined its effect on hydrogen production. The results of the study are shown in Fig. 12, which suggested that a space time of 0.19 $g_{catalyst}$ h/$g_{bio\text{-}oil}$ was favourable to convert the all bio-oil into H2, obtaining the maximum H_2 yield of nearly 93% with a S/C ratio of 6 and temperature of 700 °C. In addition, these operating condition were also ideal to form undesirable by-products, such as CH_4 and C_2–C_4 hydrocarbons as negligible amount of CH_4 and nearly no C_2–C_4 hydrocarbons were found with a space time of 0.19 $g_{catalyst}$ h/$g_{bio\text{-}oil}$ [184]. On the other hand, increase in space time from 0.04 to 0.38 $g_{catalyst}$ h/$g_{bio\text{-}oil}$ showed a constant decrease in coke formation, 0.04 $g_{catalyst}$ h/$g_{bio\text{-}oil}$ producing the largest amount of coke of 17.3 wt% which reduced significantly to 6.7 wt% with 0.38 $g_{catalyst}$ h/$g_{bio\text{-}oil}$ [184].

A highly active and stable catalyst is usually required to enhance the rate of SR reaction and increase the yield of H_2 [188]. A desirable catalyst should be able to promote WGSR and favour the breaking of C–C, C–H, and O═H bonds, and less prone to deactivation due to coke formation [189]. In this regard, noble metals like Pt and Rh or non-noble metals such as Ni, Co, Ce and Fe dispersed on different supports like Al_2O_3, ZrO_2, CeO_3–Al_2O_3, HZSM-5 and carbon nanotubes (CNT) have been widely explored in various modes of SR of bio-oil [62,182,188]. For instance, a study compared the activity of the noble metals Pt and Rh supported on Al_2O_3 and $CeZrO_2$ for SR for beech wood bio-oil [190]. The results of the study are shown in Fig. 13. It can be predicted from the results that Al_2O_3 based catalysts were less active for hydrogen production compared to $CeZrO_2$ catalysts. This is probably because $CeZrO_2$ exhibits redox properties and may carry out additional set of reactions compared to Al_2O_3 based catalysts. It was further noticed that Rh/$CeZrO_2$ and Pt/$CeZrO_2$ catalysts showed almost similar yields of H_2 but Pt/$CeZrO_2$ catalyst was found to maintain the reforming activity for a long-term reaction, producing more than 50% of H_2 over 9 h, which can be attributed to better WGSR activity of Pt [190]. On the other hand, among non-noble metals, Ni-based catalysts have shown promising activity for WGSR and bond breaking and hence different Ni-based monometallic and bimetallic catalysts have been widely used for SR of bio-oil for enhanced H_2 production. For example, Santamaria et al. [182] demonstrated the application of Ni/ZrO_2 for SR of the bio-oil (produced from pyrolysis of pine wood at 500 °C) in a fluidized bed reactor at 600 °C and achieved a maximum H_2 yield of 92.4%. In a separate study, Bizkarra et al. [58] carried out SR of bio-oil in a continuous fixed bed reactor using different Ni-based monometallic and bimetallic catalysts. The SR reactions were operated using S/C ratio of 5 and at atmospheric pressure. The results showed that monometallic catalyst, Ni/Al_2O_3 showed a maximum H_2 yield of 90%, which continuously decreased and reached to 35% after 3 h of operating time, attributing to the faster deactivation of the catalyst due to coke formation. However, Ni/CeO_3–Al_2O_3 showed more resistance to the coke formation and maintained high activity for H_2 production for a longer period, which was attributed to the higher oxygen mobility by the ceria particles as compared to the sole Al_2O_3 [58]. Noticeably, compared to the monometallic catalysts, the bimetallic catalyst, Rh–Ni/CeO_3–Al_2O_3 showed better activity and stability for H_2 for a longer period of time. The catalyst showed a H_2 yield of nearly 60% from starting to the end of the reaction, which was ascribed to the significant activity of the catalyst for oxidation of carbon instead of favoring carbon deposition, consequently, resulting in the higher resistance to catalyst deactivation and better catalytic activity towards H_2 production [58]. Several other catalysts using different metals and supports have been utilized for SR of

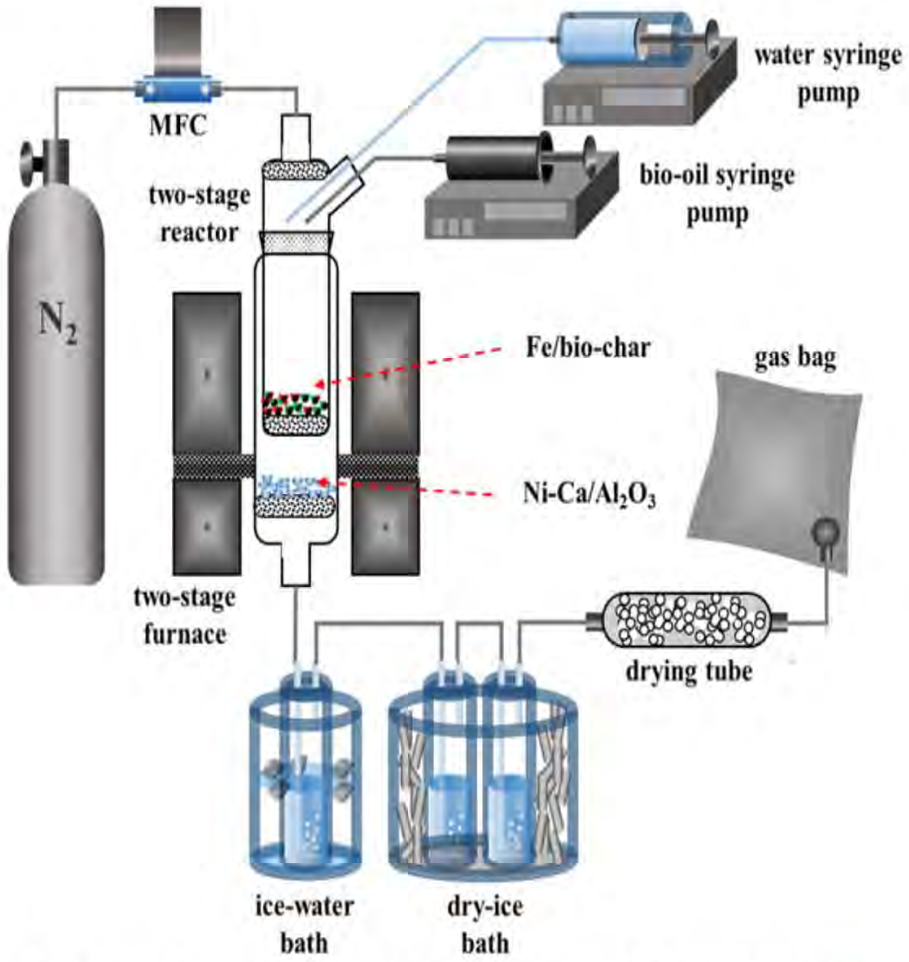

Fig. 11. Schematic diagram of two-stage catalytic reforming system. Reproduced with permission from Ref. [180].

bio-oil, some examples are given in Table 9.

The kinetics of SR process for bio-oil has been less explored so far. Although several studies have been conducted to understand the SR reactions using model compounds like butanol and ethanol [191–193]. For instance, Vaidya and Rodrigues [193] examined the kinetics of ethanol reforming for hydrogen production in the presence of Ru/Al_2O_3 catalyst at 600 and 700 °C. The authors concluded that SR of ethanol over Ru/Al_2O_3 catalyst involves three reactions in which the first reaction is irreversible and the latter two are reversible:

1. $C_2H_5OH + H_2O \rightarrow CO_2 + CH_4 + 2H_2$ (7)

2. $CH_4 + H_2O \leftrightarrow CO + 3H_2$ (8)

4. $CO + H_2O \leftrightarrow CO_2 + H_2$ (9)

The study suggests that the increase in temperature enhances ethanol conversion and above 700 °C, intermediate products like CH_4, C_2H_4, C_2H_6 and CH_2CHO are also formed that are steam reformed to produce CO_2 and H_2 [193]. A total of 6 mol of H_2 and 2 mol of CO_2 could be produced. It was further noticed that ethanol reforming follows first order kinetics and requires an activation energy of 96 kJ mol^{-1} [193]. However, the kinetics of ethanol reforming to hydrogen production under similar conditions over different catalysts can be varied and different values of activation energies can be obtained [192,194]. Similarly, the kinetics of other oxygenated compounds like acetic acid has been widely studied on different types of catalysts.

Overall, SR of bio-oil is a promising approach to generate clean fuel like H_2 and the studies have shown that significant conversion rates of bio-oil to H_2 or a higher H_2 yield of more than 90% can be obtained using catalytic SR. The main concern of catalytic SR is the catalyst deactivation. As the reaction is carried out usually at higher temperatures, the metals such as Ni in the catalyst can be sintered, which consequently affect the catalytic activity during the SR reaction. The formation of carbonaceous species during the reaction could occupy or block the active sites on the catalyst surface, initiating the prompt deactivation of the catalyst and leading to decreased catalytic activity. In addition, Ni is believed to be less active for WGSR and more active for methanation, which may result into lower H_2 yields. Therefore, the performance of Ni based catalysts can be further improved by its modification with the addition of Cu and Co metals that are highly active WGSR and less active for methanation. The addition of metal oxides, such as CeO_2 and MgO can also increase adsorption and activation of water, thereby increasing WGSR. Metal oxides can also enhance the oxygen storage capacity which can help to gasify carbonaceous species and minimize the catalyst deactivation. Therefore, the development of versatile catalysts with multiple functions that are highly efficient and less prone to deactivation is necessary for the successful conversion of different compounds in SR process.

6. Trends and future perspectives

6.1. Techno-economic analysis

Thermochemical technologies, like fast pyrolysis and HTL, are used for bio-oil production and subsequently, upgrading techniques are applied to enhance the bio-oil properties to make a competitive fuel for real applications. In addition to the quality of bio-oil, it is also important to examine the cost involved in different steps of these processes and estimate the price of upgraded bio-oil. Additionally, a comparative

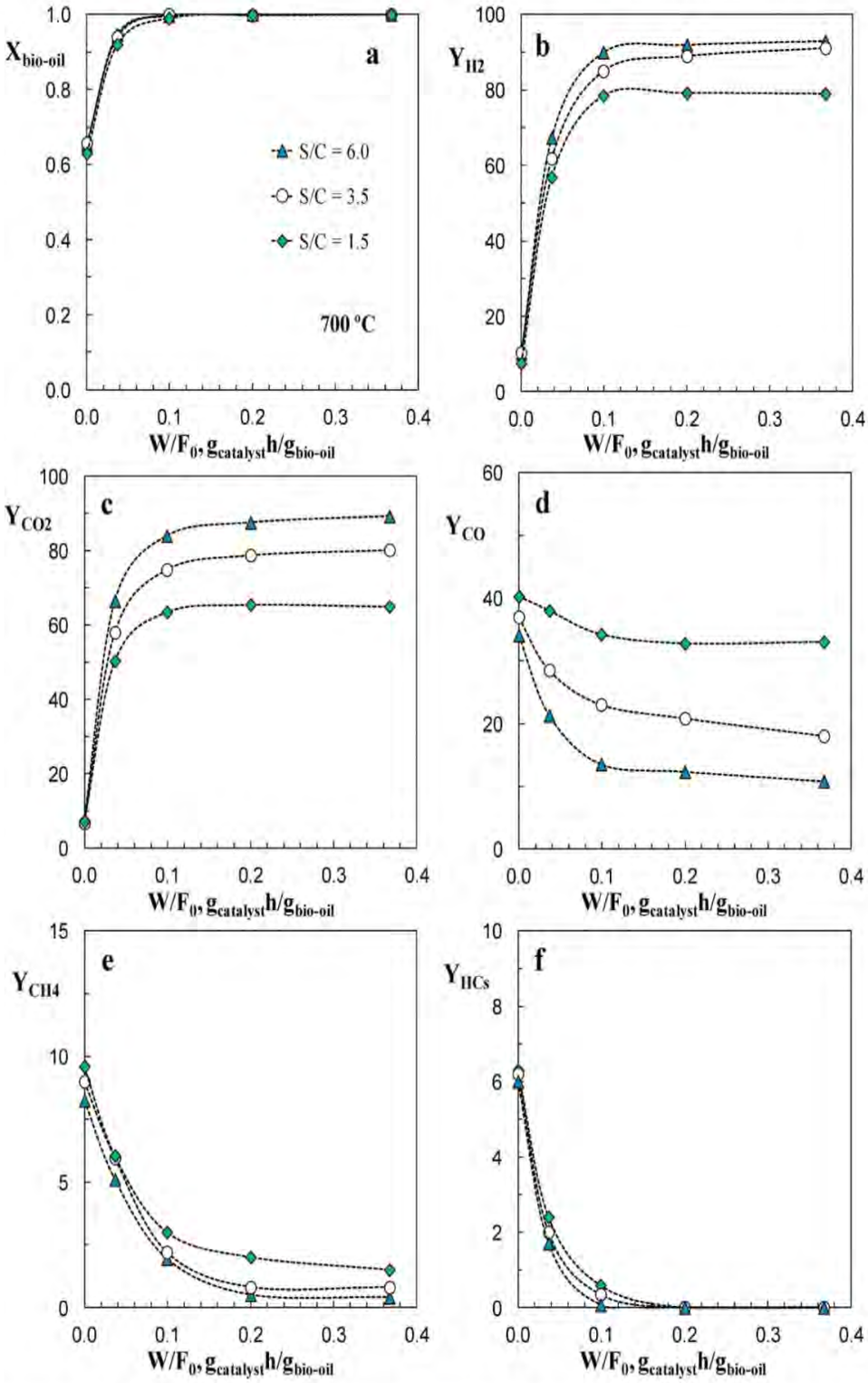

Fig. 12. Effect of space-time on the values at zero time on (a) bio-oil conversion and yields of (b) H_2 (c), CO_2 (d), CO (e), CH_4 (f), and C_2–C_4 hydrocarbons at 700 °C and for different values of S/C ratio. Reproduced with permission from Ref. [184].

techno-economic analysis between different approaches can help to adopt the appropriate technique that suggests highest energy conversion efficiency and maximum bio-oil production with minimum investment. In this regard, several techno-economic studies have been conducted for bio-oil production from fast pyrolysis, HTL and combined upgrading techniques [199–201]. The major cost involved in pyrolysis bio-oil production is from buying, transporting and drying of feedstocks, and electrical consumption during pyrolysis process. The total cost for electrical consumption can be reduced if the bio-oil produced from the pyrolysis process is used in a diesel engine for power generation. In this case, approximately 18% of bio-oil would be consumed. The cost of bio-oil production could be further reduced to 18% by selling the bio-char that is also produced during the pyrolysis process [202]. The estimated cost for bio-oil production from fast pyrolysis of energy crops like willow and miscanthus is $12-$26/GJ [202]. A comparative techno-economic study between pyrolysis and HTL using a similar feedstock can provide better insights for economical bio-oil production. To confirm this, a recent study conducted a comparative

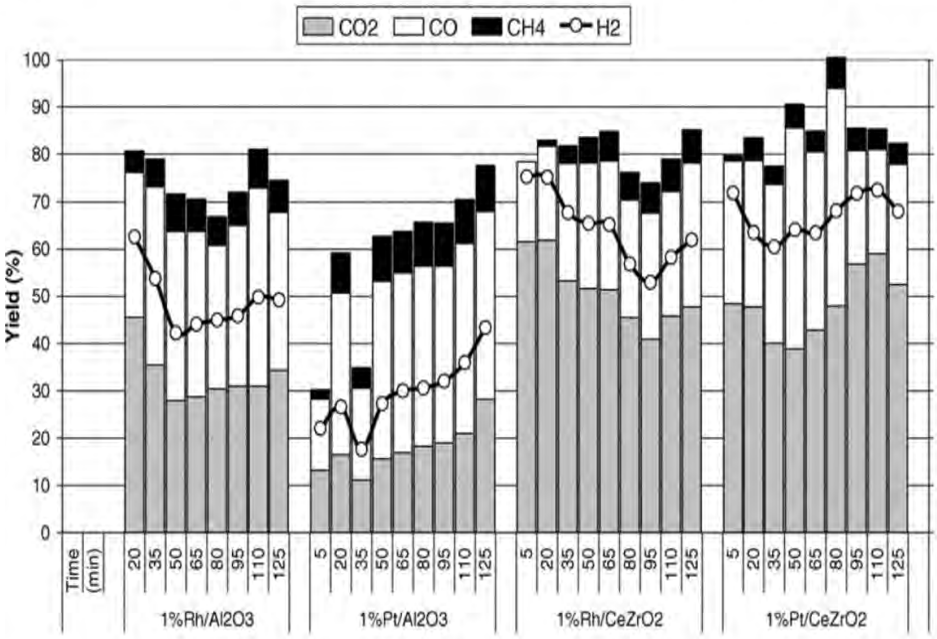

Fig. 13. Activity of various catalysts for steam reforming of bio-oil as a function of time on stream. Experimental conditions: 200 catalyst +1000 mg cordierite; T = 860 °C ± 30 °C; liquid flow rate: bio-oil = 14.0 μL min^{-1}, H_2O = 96.8 μL min^{-1}; S/C = 10.8; GeHSV = 3090 h^{-1}. Reproduced with permission from Ref. [190].

Table 9
Catalytic steam reforming of bio-oil for hydrogen production.

Bio-oil source	Catalyst	SR operating parameters					Maximum H_2 yield	Reference
		Reactor	Temperature (°C)	Pressure	S/C molar ratio	Space time/WHSV[a]		
Pine wood sawdust	Ni/ZrO_2	Fluidized bed	600	/	7.7	20 g_{cat} min/$g_{bio-oil}$	92.4 wt%	[182]
Pine wood sawdust	Ni/Al_2O_3	Fixed bed	800	1 atm	5	1.45 g_{cat} h/$g_{bio-oil}$	~90 wt%	[58]
Pine wood sawdust	Ni/CeO_2–Al_2O_3	Fixed bed	800	1 atm	5	1.45 g_{cat} h/$g_{bio-oil}$	~88 wt%	[58]
Pine wood sawdust	Ni/La_2O_3–Al_2O_3	Fixed bed	800	1 atm	5	1.45 g_{cat} h/$g_{bio-oil}$	~73 wt%	[58]
Pine wood sawdust	Pd–Ni/CeO_2–Al_2O_3	Fixed bed	800	1 atm	5	1.45 g_{cat} h/$g_{bio-oil}$	~70 wt%	[58]
Pine wood sawdust	Pt–Ni/CeO_2–Al_2O_3	Fixed bed	800	1 atm	5	1.45 g_{cat} h/$g_{bio-oil}$	~72 wt%	[58]
Pine wood sawdust	Rh–Ni/CeO_2–Al_2O_3	Fixed bed	800	1 atm	5	1.45 g_{cat} h/$g_{bio-oil}$	~61 wt%	[58]
Pine wood sawdust	Ni/La_2O_3-αAl_2O_3	Fluidized bed	700	/	6	0.38 g_{cat} h/$g_{bio-oil}$	93% wt%	[183]
Coconut shell	Ni/Al_2O_3	Fixed bed	750	/	/	/	58.21 wt%	[57]
Cotton stalk	Ni/Al_2O_3	Fixed bed	750	/	/	/	57.95 wt%	[57]
Palm kernel shell	Ni/Al_2O_3	Fixed bed	750	/	/	/	57.36 wt%	[57]
Rice Husk	Ni/Al_2O_3	Fixed bed	750	/	/	/	57.63 wt%	[57]
Sugarcane	Ni/Al_2O_3	Fixed bed	750	/	/	/	59.23 wt%	[57]
Wheat straw	Ni/Al_2O_3	Fixed bed	750	/	/	/	54.06 wt%	[57]
Pine wood sawdust	Rh/CeO_2– ZrO_2	Fluidized bed	700	/	6	0.15 g_{cat} h/$g_{bio-oil}$	0.95[c]	[63]
Pine wood sawdust	Ni/Al_2O_3	Fluidized bed	600	/	7.7	20 g_{cat} min/$g_{bio-oil}$	~90 wt%	[195]
Pine wood sawdust	Ni/MgO	Fluidized bed	600	/	7.7	20 g_{cat} min/$g_{bio-oil}$	~88 wt%	[195]
Pine wood sawdust	Ni/SiO_2	Fluidized bed	600	/	7.7	20 g_{cat} min/$g_{bio-oil}$	~12 wt%	[195]
Pine wood sawdust	Ni/TiO_2	Fluidized bed	600	/	7.7	20 g_{cat} min/$g_{bio-oil}$	~65 wt%	[195]
Commercial bio-oil	Ni–MgO/Al_2O_3	Fixed bed	850	/	1[b]	30 h^{-1}	61 wt%	[176]
Pine wood	Ni/Al	Fixed bed	600	1 atm	5.58	1.67 g_{cat} min/$g_{bio-oil}$	0.064 g/g_{org}	[187]
Pine wood	Ni/Al	Fixed bed	700	1 atm	5.58	1.67 g_{cat} min/$g_{bio-oil}$	0.097 g/g_{org}	[187]
Pine wood	Ni/Al	Fixed bed	800	1 atm	5.58	1.67 g_{cat} min/$g_{bio-oil}$	0.087 g/g_{org}	[187]
Pine wood sawdust	Ni–Co/Al–Mg	Fixed bed	650	1 atm	7.6	4 g_{cat} min/$g_{bio-oil}$	0.17 g/g_{org}	[196]
Pine wood sawdust	Ni–Co/Al–Mg	Fluidized bed	650	1 atm	7.6	4 g_{cat} min/$g_{bio-oil}$	0.07 g/g_{org}	[196]
Maize stalk	Ni–Ce/Al_2O_3	Fixed bed	900	/	6	12 h^{-1}	71.4 wt%	[59]
Pine wood sawdust	NiO/MgO	Fluidized bed	800	/	10	1.0 h^{-1}	77.6%	[197]

[a] WHSV-weight hourly space velocity.
[b] Bio-oil/water ratio.
[c] H_2 yield was calculated as: Y_{H2}=F_{H2}/F^{o}_{H2}, where F_{H2} is the H_2 molar flow rate in the product stream and F^{o}_{H2} is the stoichiometric molar flow rate.

techno-economic analysis for biofuel production through HTL and pyrolysis using sugarcane bagasse as the feedstock [198]. The estimated costs involved in different steps of pyrolysis and HTL of sugarcane bagasse have been outlined in Table 10 [198]. The study suggested that pyrolysis technique is more profitable for biofuel production compared to HTL. The results showed that liquefaction of biomass requires more energy inputs, mainly to pump liquefaction slurry at a high flow rate and liquefaction pressure. Besides, the use of ethanol also increases the operating cost in liquefaction process which is not required in pyrolysis. The total operating costs were estimated at $14.57 million/year for liquefaction and $6.16 million/year for pyrolysis process using the similar amount of the feedstock. On the other hand, the revenue obtained from unit price for HTL was higher compared to the pyrolysis, which could be attributed to the generation of different annual volumes of the products. Since the operating costs are higher than the revenue, unit margin (US$/L) is more suitable to compare the profits or losses of

Table 10
Economic results of modelling of liquefaction and pyrolysis. Reproduced with permission from Ref. [198].

Quantity	Liquefaction	Pyrolysis
Plant capacity, tonnes/year feed as received	84,000	84,000
Capital cost estimates, million US$		
Total Installed Cost	17.87	23.20
Location-adjusted Direct Cost	44.46	38.42
Total Indirect Costs	16.20	4.95
Working Capital	12.13	8.67
Total Capital Cost	72.79	52.05
Operating Costs, million US$/year		
Feedstock Cost	2.04	2.04
Electricity	0.30	<0.01
Heating	1.01	–
Ethanol or Amine Make-up	3.37	–
Catalyst replacements	0.12	0.31
Hydrogen	1.77	1.17
Steam Supply	2.07	–
Trade Waste Handling	0.06	<0.01
Water	1.46	0.60
Labour	1.17	1.17
Maintenance (2% FCI)	1.21	0.87
Total Operating Costs	14.57	6.16
Total Products, million litre/year	25.78	11.58
Revenue, million US$/year	8.44	3.79
Base Economic Indicators		
Annual Cash Flow, Million US$	−6.13	−2.37
Net present value, Million US$	−113.7	−65.7

the process, which can be calculated with the following formula:

$$Unit\ margin\left(\frac{US\$}{L}\right)=\frac{Annual\ revenue-Annual\ opearational\ costs}{Annual\ production\ volume}$$

The authors further suggested that the lower negative value of the unit margin indicates cost-effectiveness or profitability of the process. In this regard, the unit margin for pyrolysis was estimated to be $-0.21/L, while it was $-0.24/L for liquefaction [198]. Therefore, it can be suggested that pyrolysis technique is more favourable or economical for bio-oil production compared to liquefaction process. Various techno-economic studies of biomass fast pyrolysis estimated the cost of produced bio-oil to be in the range of $0.11-$0.65/Litre [200,203].

Integration of bio-oil production from either pyrolysis or liquefaction process with any upgrading approach such as solvent addition or hydrotreatment further increases the cost of bio-oil. Techno-economic analysis of an integrated process has been widely studied for hydrotreatment but has been rarely reported for other approaches like emulsification, solvent addition and electrochemical treatment. For example, Wright et al. [203] estimated the cost of bio-oil produced from fast pyrolysis of corn stover and upgraded with hydrotreatment, assuming two scenarios, one of which includes hydrogen production from a fraction of the bio-oil produced during the pyrolysis process and the other relies on purchasing hydrogen. Initial economic results showed that purchasing hydrogen for bio-oil upgrading would be more economical compared to producing the hydrogen as hydrogen production requires higher capital investment which would be approximately $287 millions compared to merchant hydrogen of $200 millions. The study further suggested that the upgraded bio-oil would cost nearly $1.73 and $0.90 per litre for hydrogen production and merchant hydrogen scenarios, respectively [203]. Sensitivity results indicated that process variables such as biomass cost and electricity supply in both scenarios had great influence on the final cost of the bio-oil, while the low fuel conversion yield could also be achieved due to reduced performance of the pyrolysis reactor, losses occurred during bio-oil collection and storage, and poor bio-oil upgrading yields [203]. On the other hand, Zhu et al. [204] conducted techno-economic analysis of bio-oil production through HTL and its further upgrading via hydrotreatment. Two scenarios were applied to evaluate the bio-oil production cost. The first scenario was based on using the parameters currently available and the second was based on advanced technologies in a commercial system. The annual production rates for upgraded bio-oil for the first and second scenario were $42.9 millions and $69.9 millions GGE (gallon gasoline-equivalent), respectively. The second scenario assumes the utilization of advanced technology that could reduce the organic loss and enhance the bio-oil yield compared to the first scenario, showing approximately 40.5% bio-oil yield which was estimated to be 29.4% for the first scenario. The minimum fuel selling price for the upgraded bio-oil was estimated to be $0.74/Litre for the second and $1.29/Litre for the first scenario [204]. The major factors affecting the bio-oil production cost were found to be feedstock cost, product yield and cost of upgrading equipment [204]. Furthermore, it has been inferred that the production of upgraded bio-oil which is equivalent to gasoline or diesel like liquid fuel could be economically attractive if the bio-oil is available at the cost of $0.11/Litre and should be sold at the cost of more than $0.31/Litre [96]. However, previous studies suggest that the cost of upgraded bio-oil production is still higher than the desired cost to make it a commercial liquid fuel. Therefore, more efforts are required to reduce the operating cost of the processes to obtain the bio-oil at cheaper prices.

The economic feasibility of hydrogen production through SR of bio-oil has been also investigated [201,205,206]. Sarkar and Kumar [205] carried out fast pyrolysis of forest (whole-tree biomass and forest residue) and agricultural biomass (wheat and barley straw) for bio-oil production at a plant capacity of 2000 dry tonnes/day and its further SR for hydrogen production at a plant which has a capacity of processing 1198 tonnes bio-oil/day. The results showed that hydrogen production from forest biomass is economically more feasible compared to agricultural biomass, suggesting the cost of hydrogen production around $2.40/kg of H_2 from whole-tree biomass, $3.00/kg of H_2 for forest residue and $4.55/kg of H_2 for agricultural biomass. Costs for feedstock transport and capital cost for bio-oil production were major contributions for production of H_2 cost, contributing almost 34% of the total cost. In a separate study, Zhang et al. [201] estimated the cost of hydrogen production via SR of bio-oil and suggested that a total capital investment of $333 millions would be required at a 2000 t/day capacity plant, which could produce hydrogen around 160 t/day, indicating the cost of H_2 in a range of $2.33 and $4.33/kg of H_2.

6.2. Policy analysis

Renewable Energy Directive of European commission has set the target to have 32% renewable fuels in the energy mix by 2030 which was nearly 17.5% in 2017. Pyrolysis and HTL technologies have shown promising potential to produce a low-cost liquid fuel that is bio-oil, which is foreseen to compete with conventional fossil fuels in the near future. However, poor physicochemical properties of the bio-oil mainly due to the high oxygen content is great challenge to make it a drop-in fuel. Although several approaches can be employed to improve poor physicochemical properties and convert oxygen containing compounds into high energy density hydrocarbons, the bio-oil is still not regarded as a drop-in fuel. This is mainly associated with production cost of bio-oil regardless of the production technology and the integration with bio-oil upgrading technique that influences the commercialization of bio-oil. Different techno-economic studies estimate high cost for feedstock sourcing, capital and operating expenses, lower process yields that ultimately contribute to the high cost of produced bio-oil. Moreover, the degree of sensitivity for these parameters could vary for different bio-oil upgrading approaches. Therefore, there is a high need of dedicated policies to reduce the capital and operating costs to promote the development and commercialization of bio-oil. To reduce the cost of feedstock transportation, the establishment of facilities for bio-oil production near to the feedstock source could be a feasible option. A sustainable management of land use is required for growing desirable crops that result in higher yield of bio-oil that could be advantageous for economical bio-oil production at a large-scale. On the other hand, the

capital investment for bio-oil upgrading can be minimized by integrating the bio-oil production unit with the existing oil refining industry. In this way, the already built infrastructure can be used for bio-oil upgrading facilities and can minimize the capital cost. It has been estimated that oil refineries around the world would be used less for gasoline production and more for diesel and jet fuels, projecting the change in petroleum feed from fluid catalytic cracking units to hydrocracking units [96]. Therefore, oil refineries can be employed for hydrotreatment of bio-oils. Overall, effective policies are essentially required to reduce the capital cost for bio-oil production and commercialization of bio-oil to achieve the desirable target of renewable fuel generation.

6.3. Challenges and future recommendations

The downstream approaches employed for bio-oil upgrading have shown promising results to improve certain physicochemical properties of the bio-oil. There are also certain challenges associated with the techniques which can be seen as possible research opportunities in the near future. For example, solvent addition and emulsification approaches are highly advantageous to increase the stability and calorific value of bio-oil. However, solvent addition can also increase water content of the bio-oil and decreases the pH, while to obtain a stable emulsion, additional physical techniques like ultrasonication and stirring are required. The necessity of surfactant in emulsification further increases the cost for bio-oil upgrading. Very less is known about the reaction mechanisms between solvents and bio-oil components. Therefore, more research studies can be conducted using bio-oil model compounds to understand the reaction chemistry during solvent addition and emulsification techniques. On the other hand, filtration removes the solid char particles from the bio-oil which otherwise could be detrimental for bio-oil stability as they can promote polymerization and condensation reactions. However, the use of filtration may increase the cost of bio-oil upgrading as the membranes used in the process are highly expensive. In addition, membranes need regular washing with solvents which can further make the process costly. Therefore, cost effective and more efficient membranes should be developed for bio-oil upgrading to make the process economical.

Electrocatalytic hydrogenation approach is still in its infancy stage for real bio-oil upgrading although it has been widely used for processing of model compounds. The major challenges associated with the technique is utilization of high-priced membranes and hydrogen. Thus, development of cost-effective and high-performance ion exchange membrane is essentially required to make the technique economical. To decrease the hydrogen cost, electrochemical cells can be integrated with other systems such as steam reforming that can utilize bio-oil for hydrogen production, although converting it into a reality would require extensive research work since it requires significant capital investment and operational costs. Other main challenge in electrochemical hydrogenation is supply of electricity to initiate the reactions. To minimize the cost of electricity and make the technique more sustainable it can be integrated with other renewable technologies, such as microbial fuel cells that can produce required electricity that can be supplied to electrocatalytic hydrogenation of bio-oil. Furthermore, techno-economic analysis should be carried out to examine the extent of deoxygenation of bio-oil in electrochemical cells to optimize operating cost, use of external hydrogen, and greenhouse gas emissions.

Hydrotreatment of bio-oil is considered the most promising approach to obtain hydrocarbon rich bio-oil, has shown almost 100% of conversion of oxygenated compounds to hydrocarbons and other high value-added products. Nevertheless, the technique faces critical challenges which should be addressed to make the process feasible at the commercial scale. The major challenge is associated with the cost of external hydrogen, its storage and transportation. To reduce the cost of external hydrogen supply, some liquid hydrogen donors such as ethanol can be used for *in-situ* hydrogen production and the produced hydrogen can be utilized in hydrodeoxygenation of bio-oil. However, feasibility of the process to produce affordable bio-oil has not been examined so far. Therefore, a techno-economic study should be conducted to determine the operating cost and degree of bio-oil upgrading. Other challenges in hydrotreatment process are associated with the application of catalysts. For example, metal sulphide catalysts are highly prone to coke formation which may lead to unfavorable blockage of the reactor. The other disadvantage of using sulphided catalysts is the leaching of catalyst bound sulphur into the upgraded bio-oil which demands additional upgrading approach to remove the impurities, which ultimately can increase the overall cost of the bio-oil upgrading. Noble metal-based catalysts are highly expensive that restricts their industrial-scale application for bio-oil upgrading. On the other hand, transition metal-based catalysts are also sensitive to coke deposition at high temperature and pressure conditions, which leads to their early deactivation. The acidic nature of catalyst supports like Al_2O_3, zeolite is also unfavorable as the water content present in the bio-oils adsorbs onto active sites, resulting in the catalyst deactivation [138]. The formation of aromatic hydrocarbons is suitable up to certain concentrations, for instance, 40% in gasoline as aromatics act as precursors for coke formation and thus their high concentrations are prone to coking reactions and ultimately reactor plugging. Hydrogenation of aromatic rings is quite challenging because it requires highly active catalysts and stringent reaction conditions like high temperatures and hydrogen pressures of up to 8 MPa [158]. To produce more stable bio-oil and less coke deposition, two stage hydrotreatment can be carried out. In the first stage, lower temperatures up to 250 °C can be applied in the presence of a less active catalyst that converts large molecular compounds (which are thought to contribute for coke formation) into smaller compounds, the resultant bio-oil with intermediate compounds is considered stabilized. In the second stage, higher temperatures >350 °C can be applied in the presence of a more active catalyst to successfully convert the oxygenated compounds into high energy density hydrocarbons.

SR of bio-oil is a promising approach to generate H_2 or syngas. The main concern of catalytic SR is the catalyst deactivation. The metals such as Ni in the catalyst can be sintered at higher temperatures, which consequently affect the catalytic activity during the SR reaction. In addition, coke formation blocks the active sites on the catalyst surface, initiating the prompt deactivation of the catalyst and leading to reduced catalytic activity. Therefore, the development of advanced catalysts that are highly efficient and less prone to deactivation is necessary for the SR process. The catalysts can be promoted with metal oxides like CeO_2 and MgO that increase adsorption and activation of water, which helps to enhance WGSR. Oxygen storage capacity of metal oxides can also help to gasify carbonaceous species and minimize the catalyst deactivation.

7. Conclusions

This review article comprehensively reviewed predominantly applied downstream processing techniques such as solvent addition, emulsification, filtration, hydrotreatment, electrochemical hydrogenation for bio-oil upgrading, and steam reforming of bio-oil for hydrogen production. Significant improvement in bio-oil properties can be achieved using these techniques. It has been shown that in the downstream bio-oil upgrading, certain bio-oil properties, such as viscosity, pH, HHV and bio-oil stability can be considerably improved with polar solvents, like ethanol and methanol, and by preparing emulsions with diesel using surfactants, like Span 80 and Tween 60. However, the addition of solvents may increase the water content and decrease pH of the bio-oils. In addition, less is known about the reaction mechanisms between solvents and bio-oil components. Therefore, more research studies can be conducted to understand the mechanisms, which can help to make the process more feasible for enhanced bio-oil upgrading. Microfiltration and hot vapour filtration methods are highly beneficial to separate char particles and inorganic species present in the bio-oil but at the expense of a decrease in bio-oil yield due to enhanced secondary cracking reactions promoted by char particles and metals. Since filtration removes

contaminants from the bio-oil it protects downstream equipment from corrosion and catalysts from poisoning. Formation of cake layer on filter is another challenge with hot vapour filtration associated with fast pyrolysis. Therefore, it is very important to maintain the cake removal or regeneration to make filtration process stable for bio-oil upgrading.

Hydrotreatment has proven an advantageous approach to obtain the bio-oil rich in hydrocarbons and high energy density, nevertheless, the use of external hydrogen, transport and storage makes the overall process highly expensive. The cost of upgraded bio-oil obtained from hydrotreatment has been estimated between $0.74 and $1.80/L, which is still higher than the desired cost to make it a commercial liquid fuel. Therefore, more efforts are required to reduce the operating cost of the processes to obtain the bio-oil at cheaper prices. Recently, electrocatalytic hydrogenation has emerged as a novel approach for bio-oil upgrading and is effective to remove carbonyl-containing compounds in the bio-oil. It also improves the bio-oil-properties, such as increasing the pH and decreasing the acid values. However, the technique requires external supply of electricity and utilizes costly membranes and hydrogen, which makes the process highly expensive compared to the other techniques. Extensive research is required to make this technique more efficient and advanced to use for real bio-oil upgrading at a pilot-scale.

Alternatively, the bio-oil could also be subjected to steam reforming to generate H_2 and syngas, where H_2 can be directly used a clean fuel, while syngas can be further subjected to Fischer-Tropsch process for production of hydrocarbons. The main concern of catalytic steam reforming is the catalyst deactivation. As the reaction is carried out usually at higher temperatures, the metals such as Ni in the catalyst can be sintered, which consequently affect the catalytic activity during the SR reaction. The addition of metals like Cu, Co and metal oxides, such as CeO_2 and MgO increase adsorption and activation of water, thereby increases water gas shift reaction and hydrogen production. Coke formation is a major challenge for steam reforming of bio-oil. Thus, the development of versatile catalysts with multiple functions that are highly efficient and less prone to deactivation is necessary for the successful conversion of different compounds in SR process.

To sum up, the bio-oil is still not regarded as a drop-in fuel. This is mainly associated with production cost of bio-oil regardless of the production technology and the integration with bio-oil upgrading technique. Therefore, there is a high need of dedicated policies to reduce the capital and operating costs to promote the development and commercialization of bio-oil.

Declaration of competing interest

The authors declare that they have no known competing financial interests or personal relationships that could have appeared to influence the work reported in this paper.

Acknowledgments

This work did not receive any specific grant from funding agencies in the public, commercial, or not-for-profit sectors. Some figures included in the article have been reproduced from the given references and copyrights have been taken from the respective publishers.

References

[1] Capuano DL. International Energy Outlook 2000;2018(IEO2018):21.
[2] He J, Strezov V, Kan T, Weldekidan H, Asumadu-Sarkodie S, Kumar R. Effect of temperature on heavy metal(loid) deportment during pyrolysis of Avicennia marina biomass obtained from phytoremediation. Bioresour Technol 2019. https://doi.org/10.1016/j.biortech.2019.01.101.
[3] Hognon C, Delrue F, Texier J, Grateau M, Thiery S, Miller H, et al. Comparison of pyrolysis and hydrothermal liquefaction of Chlamydomonas reinhardtii. Growth studies on the recovered hydrothermal aqueous phase. Biomass Bioenergy 2015; 73:23–31. https://doi.org/10.1016/j.biombioe.2014.11.025.
[4] Kumar R, Strezov V, Lovell E, Kan T, Weldekidan H, He J, et al. Enhanced bio-oil deoxygenation activity by Cu/zeolite and Ni/zeolite catalysts in combined in-situ and ex-situ biomass pyrolysis. J Anal Appl Pyrol 2019. https://doi.org/10.1016/j.jaap.2019.03.008.
[5] Kumar R, Kumar P. Future microbial applications for bioenergy production: a perspective. Front Microbiol 2017;8. https://doi.org/10.3389/fmicb.2017.00450.
[6] Zhou YJ, Kerkhoven EJ, Nielsen J. Barriers and opportunities in bio-based production of hydrocarbons. Nature Energy 2018;3:925–35. https://doi.org/10.1038/s41560-018-0197-x.
[7] Khodier A, Kilgallon P, Legrave N, Simms N, Oakey J, Bridgwater T. Pilot-scale combustion of fast-pyrolysis bio-oil: ash deposition and gaseous emissions. Environ Prog Sustain Energy 2009;28:397–403. https://doi.org/10.1002/ep.10379.
[8] Shihadeh A, Hochgreb S. Diesel engine combustion of biomass pyrolysis oils. Energy Fuels 2000;14:260–74. https://doi.org/10.1021/ef990044x.
[9] Moore RH, Thornhill KL, Weinzierl B, Sauer D, D'Ascoli E, Kim J, et al. Biofuel blending reduces particle emissions from aircraft engines at cruise conditions. Nature 2017;543:411–5. https://doi.org/10.1038/nature21420.
[10] Alonso DM, Wettstein SG, Dumesic JA. Bimetallic catalysts for upgrading of biomass to fuels and chemicals. Chem Soc Rev 2012;41:8075. https://doi.org/10.1039/c2cs35188a.
[11] Sudarsanam P, Peeters E, Makshina EV, Parvulescu VI, Sels BF. Advances in porous and nanoscale catalysts for viable biomass conversion. Chem Soc Rev 2019;48:2366–421. https://doi.org/10.1039/C8CS00452H.
[12] Araújo A, Queiroz G, Maia D, Gondim A, Souza L, Fernandes V, et al. Fast pyrolysis of sunflower oil in the presence of microporous and mesoporous materials for production of bio-oil. Catalysts 2018;8:261. https://doi.org/10.3390/catal8070261.
[13] Baloch HA, Nizamuddin S, Siddiqui MTH, Riaz S, Jatoi AS, Dumbre DK, et al. Recent advances in production and upgrading of bio-oil from biomass: a critical overview. Journal of Environmental Chemical Engineering 2018;6:5101–18. https://doi.org/10.1016/j.jece.2018.07.050.
[14] Li R, Xie Y, Yang T, Li B, Wang W, Kai X. Effects of Chemical–Biological pretreatment of corn stalks on the bio-oils produced by hydrothermal liquefaction. Energy Convers Manag 2015;93:23–30. https://doi.org/10.1016/j.enconman.2014.12.089.
[15] Lian X, Xue Y, Zhao Z, Xu G, Han S, Yu H. Progress on upgrading methods of bio-oil: a review: upgrading progress of bio-oil. Int J Energy Res 2017;41:1798–816. https://doi.org/10.1002/er.3726.
[16] Weldekidan H, Strezov V, Kan T, Kumar R, He J, Town G. Solar assisted catalytic pyrolysis of chicken-litter waste with in-situ and ex-situ loading of CaO and char. Fuel 2019;246:408–16. https://doi.org/10.1016/j.fuel.2019.02.135.
[17] Weldekidan H, Strezov V, Town G. Review of solar energy for biofuel extraction. Renew Sustain Energy Rev 2018;88:184–92. https://doi.org/10.1016/j.rser.2018.02.027.
[18] Dhyani V, Bhaskar T. A comprehensive review on the pyrolysis of lignocellulosic biomass. Renew Energy 2018;129:695–716. https://doi.org/10.1016/j.renene.2017.04.035.
[19] Mohan D, Pittman CU, Steele PH. Pyrolysis of wood/biomass for bio-oil: a critical review. Energy Fuels 2006;20:848–89. https://doi.org/10.1021/ef0502397.
[20] Fan L, Zhang Y, Liu S, Zhou N, Chen P, Cheng Y, et al. Bio-oil from fast pyrolysis of lignin: effects of process and upgrading parameters. Bioresour Technol 2017; 241:1118–26. https://doi.org/10.1016/j.biortech.2017.05.129.
[21] Guedes RE, Luna AS, Torres AR. Operating parameters for bio-oil production in biomass pyrolysis: a review. J Anal Appl Pyrol 2018;129:134–49. https://doi.org/10.1016/j.jaap.2017.11.019.
[22] Zhao S, Liu M, Zhao L, Zhu L. Influence of interactions among three biomass components on the pyrolysis behavior. Ind Eng Chem Res 2018;57:5241–9. https://doi.org/10.1021/acs.iecr.8b00593.
[23] Sharma A, Pareek V, Zhang D. Biomass pyrolysis—a review of modelling, process parameters and catalytic studies. Renew Sustain Energy Rev 2015;50:1081–96. https://doi.org/10.1016/j.rser.2015.04.193.
[24] Gollakota ARK, Kishore N, Gu S. A review on hydrothermal liquefaction of biomass. Renew Sustain Energy Rev 2018;81:1378–92. https://doi.org/10.1016/j.rser.2017.05.178.
[25] Toor SS, Rosendahl L, Rudolf A. Hydrothermal liquefaction of biomass: a review of subcritical water technologies. Energy 2011;36:2328–42. https://doi.org/10.1016/j.energy.2011.03.013.
[26] de Caprariis B, De Filippis P, Petrullo A, Scarsella M. Hydrothermal liquefaction of biomass: influence of temperature and biomass composition on the bio-oil production. Fuel 2017;208:618–25. https://doi.org/10.1016/j.fuel.2017.07.054.
[27] Akhtar J, Amin NAS. A review on process conditions for optimum bio-oil yield in hydrothermal liquefaction of biomass. Renew Sustain Energy Rev 2011;15: 1615–24. https://doi.org/10.1016/j.rser.2010.11.054.
[28] Buffi M, Cappelletti A, Rizzo AM, Martelli F, Chiaramonti D. Combustion of fast pyrolysis bio-oil and blends in a micro gas turbine. Biomass Bioenergy 2018;115: 174–85. https://doi.org/10.1016/j.biombioe.2018.04.020.
[29] Laesecke J, Ellis N, Kirchen P. Production, analysis and combustion characterization of biomass fast pyrolysis oil – biodiesel blends for use in diesel engines. Fuel 2017;199:346–57. https://doi.org/10.1016/j.fuel.2017.01.093.
[30] Oasmaa A, Kyt M, Sipil K. Pyrolysis oil combustion tests in an industrial boiler. In: Bridgwater AV, editor. Progress in thermochemical biomass conversion. Oxford, UK: Blackwell Science Ltd; 2001. p. 1468–81. https://doi.org/10.1002/9780470694954.ch121.

[31] Zhang M, Wu H. Phase behavior and fuel properties of bio-oil/glycerol/methanol blends. Energy Fuels 2014;28:4650–6. https://doi.org/10.1021/ef501176z.
[32] Zhu L, Li K, Zhang Y, Zhu X. Upgrading the storage properties of bio-oil by adding a compound additive. Energy Fuels 2017;31:6221–7. https://doi.org/10.1021/acs.energyfuels.7b00864.
[33] Bert V, Allemon J, Sajet P, Dieu S, Papin A, Collet S, et al. Torrefaction and pyrolysis of metal-enriched poplars from phytotechnologies: effect of temperature and biomass chlorine content on metal distribution in end-products and valorization options. Biomass Bioenergy 2017;96:1–11. https://doi.org/10.1016/j.biombioe.2016.11.003.
[34] Chen W-H, Wang C-W, Kumar G, Rousset P, Hsieh T-H. Effect of torrefaction pretreatment on the pyrolysis of rubber wood sawdust analyzed by Py-GC/MS. Bioresour Technol 2018;259:469–73. https://doi.org/10.1016/j.biortech.2018.03.033.
[35] He C, Tang C, Li C, Yuan J, Tran K-Q, Bach Q-V, et al. Wet torrefaction of biomass for high quality solid fuel production: a review. Renew Sustain Energy Rev 2018;91:259–71. https://doi.org/10.1016/j.rser.2018.03.097.
[36] Zhang D, Wang F, Zhang A, Yi W, Li Z, Shen X. Effect of pretreatment on chemical characteristic and thermal degradation behavior of corn stalk digestate: comparison of dry and wet torrefaction. Bioresour Technol 2019;275:239–46. https://doi.org/10.1016/j.biortech.2018.12.044.
[37] Cao B, Wang S, Hu Y, Abomohra AE-F, Qian L, He Z, et al. Effect of washing with diluted acids on Enteromorpha clathrata pyrolysis products: towards enhanced bio-oil from seaweeds. Renew Energy 2019;138:29–38. https://doi.org/10.1016/j.renene.2019.01.084.
[38] Chen H, Cheng H, Zhou F, Chen K, Qiao K, Lu X, et al. Catalytic fast pyrolysis of rice straw to aromatic compounds over hierarchical HZSM-5 produced by alkali treatment and metal-modification. J Anal Appl Pyrol 2018;131:76–84. https://doi.org/10.1016/j.jaap.2018.02.009.
[39] Liu G, Mba Wright M, Zhao Q, Brown RC. Hydrocarbon and ammonia production from catalytic pyrolysis of sewage sludge with acid pretreatment. ACS Sustainable Chem Eng 2016;4:1819–26. https://doi.org/10.1021/acssuschemeng.6b00016.
[40] Wang H, Srinivasan R, Yu F, Steele P, Li Q, Mitchell B. Effect of acid, alkali, and steam explosion pretreatments on characteristics of bio-oil produced from pinewood. Energy Fuels 2011;25:3758–64. https://doi.org/10.1021/ef2004909.
[41] Leng L, Li H, Yuan X, Zhou W, Huang H. Bio-oil upgrading by emulsification/microemulsification: a review. Energy 2018;161:214–32. https://doi.org/10.1016/j.energy.2018.07.117.
[42] Zhang M, Yewe-Siang Lee Shee We M, Wu H. Direct emulsification of crude glycerol and bio-oil without addition of surfactant via ultrasound and mechanical agitation. Fuel 2018;227:183–9. https://doi.org/10.1016/j.fuel.2018.04.099.
[43] Li H, Xia S, Ma P. Upgrading fast pyrolysis oil: solvent–anti-solvent extraction and blending with diesel. Energy Convers Manag 2016;110:378–85. https://doi.org/10.1016/j.enconman.2015.11.043.
[44] Xu X, Li Z, Sun Y, Jiang E, Huang L. High-quality fuel from the upgrading of heavy bio-oil by the combination of ultrasonic treatment and mutual solvent. Energy Fuels 2018;32:3477–87. https://doi.org/10.1021/acs.energyfuels.7b03483.
[45] Javaid A, Ryan T, Berg G, Pan X, Vispute T, Bhatia SR, et al. Removal of char particles from fast pyrolysis bio-oil by microfiltration. J Membr Sci 2010;363:120–7. https://doi.org/10.1016/j.memsci.2010.07.021.
[46] Ruiz M, Martin E, Blin J, Van de Steene L, Broust F. Understanding the secondary reactions of flash pyrolysis vapors inside a hot gas filtration unit. Energy Fuels 2017;31:13785–95. https://doi.org/10.1021/acs.energyfuels.7b02923.
[47] Kumar R, Strezov V, Kan T, Weldekidan H, He J, Jahan S. Investigating the effect of mono- and bimetallic/zeolite catalysts on hydrocarbon production during bio-oil upgrading from *ex situ* pyrolysis of biomass. Energy Fuels 2019. https://doi.org/10.1021/acs.energyfuels.9b02724. acs.energyfuels.9b02724.
[48] Kumar R, Strezov V, Weldekidan H, He J, Singh S, Kan T, et al. Lignocellulose biomass pyrolysis for bio-oil production: a review of biomass pre-treatment methods for production of drop-in fuels. Renew Sustain Energy Rev 2020;123:109763. https://doi.org/10.1016/j.rser.2020.109763.
[49] Carroll KJ, Burger T, Langenegger L, Chavez S, Hunt ST, Román-Leshkov Y, et al. Electrocatalytic hydrogenation of oxygenates using earth-abundant transition-metal nanoparticles under mild conditions. ChemSusChem 2016;9. https://doi.org/10.1002/cssc.201600290. 1904–10.
[50] Elangovan S, Larsen D, Bay I, Mitchell E, Hartvigsen J, Millett B, et al. Electrochemical upgrading of bio-oil. ECS Transactions 2017;78:3149–58. https://doi.org/10.1149/07801.3149ecst.
[51] Ding K, Zhong Z, Wang J, Zhang B, Fan L, Liu S, et al. Improving hydrocarbon yield from catalytic fast co-pyrolysis of hemicellulose and plastic in the dual-catalyst bed of CaO and HZSM-5. Bioresour Technol 2018;261:86–92. https://doi.org/10.1016/j.biortech.2018.03.138.
[52] Iisa K, French RJ, Orton KA, Yung MM, Johnson DK, ten Dam J, et al. In situ and ex situ catalytic pyrolysis of pine in a bench-scale fluidized bed reactor system. Energy Fuels 2016;30:2144–57. https://doi.org/10.1021/acs.energyfuels.5b02165.
[53] Auersvald M, Shumeiko B, Vrtiška D, Straka P, Staš M, Šimáček P, et al. Hydrotreatment of straw bio-oil from ablative fast pyrolysis to produce suitable refinery intermediates. Fuel 2019;238:98–110. https://doi.org/10.1016/j.fuel.2018.10.090.
[54] Zhang X, Wang T, Ma L, Zhang Q, Jiang T. Hydrotreatment of bio-oil over Ni-based catalyst. Bioresour Technol 2013;127:306–11. https://doi.org/10.1016/j.biortech.2012.07.119.
[55] Biller P, Sharma BK, Kunwar B, Ross AB. Hydroprocessing of bio-crude from continuous hydrothermal liquefaction of microalgae. Fuel 2015;159:197–205. https://doi.org/10.1016/j.fuel.2015.06.077.
[56] Adeniyi AG, Otoikhian KS, Ighalo JO. Steam reforming of biomass pyrolysis oil: a review. Int J Chem React Eng 2019;17. https://doi.org/10.1515/ijcre-2018-0328.
[57] Akubo K, Nahil MA, Williams PT. Pyrolysis-catalytic steam reforming of agricultural biomass wastes and biomass components for production of hydrogen/syngas. J Energy Inst 2018. https://doi.org/10.1016/j.joei.2018.10.013. S1743967118308742.
[58] Bizkarra K, Bermudez JM, Arcelus-Arrillaga P, Barrio VL, Cambra JF, Millan M. Nickel based monometallic and bimetallic catalysts for synthetic and real bio-oil steam reforming. Int J Hydrogen Energy 2018;43:11706–18. https://doi.org/10.1016/j.ijhydene.2018.03.049.
[59] Fu P, Yi W, Li Z, Bai X, Zhang A, Li Y, et al. Investigation on hydrogen production by catalytic steam reforming of maize stalk fast pyrolysis bio-oil. Int J Hydrogen Energy 2014;39:13962–71. https://doi.org/10.1016/j.ijhydene.2014.06.165.
[60] Santamaria L, Arregi A, Alvarez J, Artetxe M, Amutio M, Lopez G, et al. Performance of a Ni/ZrO2 catalyst in the steam reforming of the volatiles derived from biomass pyrolysis. J Anal Appl Pyrol 2018;136:222–31. https://doi.org/10.1016/j.jaap.2018.09.025.
[61] Singh S, Kumar R, Setiabudi HD, Nanda S, Vo D-VN. Advanced synthesis strategies of mesoporous SBA-15 supported catalysts for catalytic reforming applications: a state-of-the-art review. Appl Catal Gen 2018;559:57–74. https://doi.org/10.1016/j.apcata.2018.04.015.
[62] Choi I-H, Hwang K-R, Lee K-Y, Lee I-G. Catalytic steam reforming of biomass-derived acetic acid over modified Ni/γ-Al2O3 for sustainable hydrogen production. Int J Hydrogen Energy 2019;44:180–90. https://doi.org/10.1016/j.ijhydene.2018.04.192.
[63] Remiro A, Ochoa A, Arandia A, Castaño P, Bilbao J, Gayubo AG. On the dynamics and reversibility of the deactivation of a Rh/CeO2ZrO2 catalyst in raw bio-oil steam reforming. Int J Hydrogen Energy 2019;44:2620–32. https://doi.org/10.1016/j.ijhydene.2018.12.073.
[64] Dabros TMH, Stummann MZ, Høj M, Jensen PA, Grunwaldt J-D, Gabrielsen J, et al. Transportation fuels from biomass fast pyrolysis, catalytic hydrodeoxygenation, and catalytic fast hydropyrolysis. Prog Energy Combust Sci 2018;68:268–309. https://doi.org/10.1016/j.pecs.2018.05.002.
[65] Bach Q-V, Ø Skreiberg. Upgrading biomass fuels via wet torrefaction: a review and comparison with dry torrefaction. Renew Sustain Energy Rev 2016;54:665–77. https://doi.org/10.1016/j.rser.2015.10.014.
[66] Zacher AH, Olarte MV, Santosa DM, Elliott DC, Jones SB. A review and perspective of recent bio-oil hydrotreating research. Green Chem 2014;16:491–515. https://doi.org/10.1039/C3GC41382A.
[67] Nishu Liu R, Rahman MdM, Sarker M, Chai M, Li C, et al. A review on the catalytic pyrolysis of biomass for the bio-oil production with ZSM-5: focus on structure. Fuel Process Technol 2020;199:106301. https://doi.org/10.1016/j.fuproc.2019.106301.
[68] Bar-On YM, Phillips R, Milo R. The biomass distribution on Earth. Proc Natl Acad Sci Unit States Am 2018;115:6506–11. https://doi.org/10.1073/pnas.1711842115.
[69] Pearcy RW, Ehleringer J. Comparative ecophysiology of C3 and C4 plants. Plant Cell Environ 1984;7:1–13. https://doi.org/10.1111/j.1365-3040.1984.tb01194.x.
[70] Klass DL. Biomass for renewable energy, fuels, and chemicals. San Diego: Academic Press; 1998.
[71] Jena U, Das KC. Comparative evaluation of thermochemical liquefaction and pyrolysis for bio-oil production from microalgae. Energy Fuels 2011;25:5472–82. https://doi.org/10.1021/ef201373m.
[72] Choi JH, Kim S-S, Ly HV, Kim J, Woo HC. Effects of water-washing Saccharina japonica on fast pyrolysis in a bubbling fluidized-bed reactor. Biomass Bioenergy 2017;98:112–23. https://doi.org/10.1016/j.biombioe.2017.01.006.
[73] Hassan EM, Steele PH, Ingram L. Characterization of fast pyrolysis bio-oils produced from pretreated pine wood. Appl Biochem Biotechnol 2009;154:3–13. https://doi.org/10.1007/s12010-008-8445-3.
[74] Wang H, Srinivasan R, Yu F, Steele P, Li Q, Mitchell B. Effect of acid, alkali, and steam explosion pretreatments on characteristics of bio-oil produced from pinewood. Energy Fuels 2011;25:3758–64. https://doi.org/10.1021/ef2004909.
[75] Wang H, Srinivasan R, Yu F, Steele P, Li Q, Mitchell B, et al. Effect of acid, steam explosion, and size reduction pretreatments on bio-oil production from sweetgum, switchgrass, and corn stover. Appl Biochem Biotechnol 2012;167:285–97. https://doi.org/10.1007/s12010-012-9678-8.
[76] Choi J, Choi J-W, Suh DJ, Ha J-M, Hwang JW, Jung HW, et al. Production of brown algae pyrolysis oils for liquid biofuels depending on the chemical pretreatment methods. Energy Convers Manag 2014;86:371–8. https://doi.org/10.1016/j.enconman.2014.04.094.
[77] Pidtasang B, Udomsap P, Sukkasi S, Chollacoop N, Pattiya A. Influence of alcohol addition on properties of bio-oil produced from fast pyrolysis of eucalyptus bark in a free-fall reactor. J Ind Eng Chem 2013;19:1851–7. https://doi.org/10.1016/j.jiec.2013.02.031.
[78] Zhu L, Li K, Ding H, Zhu X. Studying on properties of bio-oil by adding blended additive during aging. Fuel 2018;211:704–11. https://doi.org/10.1016/j.fuel.2017.09.106.
[79] Mohammed IY, Abakr YA, Kazi FK, Yusuf S. Effects of pretreatments of napier grass with deionized water, sulfuric acid and sodium hydroxide on pyrolysis oil characteristics. Waste and Biomass Valorization 2017;8:755–73. https://doi.org/10.1007/s12649-016-9594-1.

[80] Ye J, Jiang J, Xu J. Effect of alcohols on simultaneous bio-oil upgrading and separation of high value-added chemicals. Waste and Biomass Valorization 2018; 9:1779–85. https://doi.org/10.1007/s12649-017-9934-9.
[81] Yu J, Biller P, Mamahkel A, Klemmer M, Becker J, Glasius M, et al. Catalytic hydrotreatment of bio-crude produced from the hydrothermal liquefaction of aspen wood: a catalyst screening and parameter optimization study. Sustainable Energy Fuels 2017;1:832–41. https://doi.org/10.1039/C7SE00090A.
[82] Anouti S, Haarlemmer G, Déniel M, Roubaud A. Analysis of physicochemical properties of bio-oil from hydrothermal liquefaction of blackcurrant pomace. Energy Fuels 2016;30:398–406. https://doi.org/10.1021/acs.energyfuels.5b02264.
[83] Zhu Z, Rosendahl L, Toor SS, Yu D, Chen G. Hydrothermal liquefaction of barley straw to bio-crude oil: effects of reaction temperature and aqueous phase recirculation. Appl Energy 2015;137:183–92. https://doi.org/10.1016/j.apenergy.2014.10.005.
[84] Xiu S, Shahbazi A, Shirley V, Cheng D. Hydrothermal pyrolysis of swine manure to bio-oil: effects of operating parameters on products yield and characterization of bio-oil. J Anal Appl Pyrol 2010;88:73–9. https://doi.org/10.1016/j.jaap.2010.02.011.
[85] Xu Y, Zheng X, Yu H, Hu X. Hydrothermal liquefaction of Chlorella pyrenoidosa for bio-oil production over Ce/HZSM-5. Bioresour Technol 2014;156:1–5. https://doi.org/10.1016/j.biortech.2014.01.010.
[86] Zhu Z, Toor SS, Rosendahl L, Yu D, Chen G. Influence of alkali catalyst on product yield and properties via hydrothermal liquefaction of barley straw. Energy 2015; 80:284–92. https://doi.org/10.1016/j.energy.2014.11.071.
[87] Duan P, Savage PE. Upgrading of crude algal bio-oil in supercritical water. Bioresour Technol 2011;102:1899–906. https://doi.org/10.1016/j.biortech.2010.08.013.
[88] Shakya R, Adhikari S, Mahadevan R, Hassan EB, Dempster TA. Catalytic upgrading of bio-oil produced from hydrothermal liquefaction of Nannochloropsis sp. Bioresour Technol 2018;252:28–36. https://doi.org/10.1016/j.biortech.2017.12.067.
[89] Huang H, Yuan X, Zhu H, Li H, Liu Y, Wang X, et al. Comparative studies of thermochemical liquefaction characteristics of microalgae, lignocellulosic biomass and sewage sludge. Energy 2013;56:52–60. https://doi.org/10.1016/j.energy.2013.04.065.
[90] Wang F, Chang Z, Duan P, Yan W, Xu Y, Zhang L, et al. Hydrothermal liquefaction of Litsea cubeba seed to produce bio-oils. Bioresour Technol 2013;149:509–15. https://doi.org/10.1016/j.biortech.2013.09.108.
[91] Chan YH, Yusup S, Quitain AT, Tan RR, Sasaki M, Lam HL, et al. Effect of process parameters on hydrothermal liquefaction of oil palm biomass for bio-oil production and its life cycle assessment. Energy Convers Manag 2015;104:180–8. https://doi.org/10.1016/j.enconman.2015.03.075.
[92] Kan T, Strezov V, Evans TJ. Lignocellulosic biomass pyrolysis: a review of product properties and effects of pyrolysis parameters. Renew Sustain Energy Rev 2016; 57:1126–40. https://doi.org/10.1016/j.rser.2015.12.185.
[93] Doassans-Carrère N, Ferrasse J-H, Boutin O, Mauviel G, Lédé J. Comparative study of biomass fast pyrolysis and direct liquefaction for bio-oils production: products yield and characterizations. Energy Fuels 2014;28:5103–11. https://doi.org/10.1021/ef500641c.
[94] Vardon DR, Sharma BK, Blazina GV, Rajagopalan K, Strathmann TJ. Thermochemical conversion of raw and defatted algal biomass via hydrothermal liquefaction and slow pyrolysis. Bioresour Technol 2012;109:178–87. https://doi.org/10.1016/j.biortech.2012.01.008.
[95] Weldekidan H, Strezov V, He J, Kumar R, Sarkodie SA, Doyi I, et al. Energy conversion efficiency of pyrolysis of chicken litter and rice husk biomass. Energy Fuels 2019. https://doi.org/10.1021/acs.energyfuels.9b01264. acs.energyfuels.9b01264.
[96] Karatzos S, McMillan JD, Saddler JN. The potential and challenges of drop-in biofuels: a report by IEA Bioenergy Task 2014;39.
[97] Beims RF, Hu Y, Shui H, Xu C, Charles). Hydrothermal liquefaction of biomass to fuels and value-added chemicals: products applications and challenges to develop large-scale operations. Biomass Bioenergy 2020;135:105510. https://doi.org/10.1016/j.biombioe.2020.105510.
[98] Oasmaa A, Kuoppala E, Selin J-F, Gust S, Solantausta Y. Fast pyrolysis of forestry residue and pine. 4. Improvement of the product quality by solvent addition. Energy Fuels 2004;18:1578–83. https://doi.org/10.1021/ef040038n.
[99] Mei Y, Chai M, Shen C, Liu B, Liu R. Effect of methanol addition on properties and aging reaction mechanism of bio-oil during storage. Fuel 2019;244:499–507. https://doi.org/10.1016/j.fuel.2019.02.012.
[100] Chen D, Zhou J, Zhang Q, Zhu X. Evaluation methods and research progresses in bio-oil storage stability. Renew Sustain Energy Rev 2014;40:69–79. https://doi.org/10.1016/j.rser.2014.07.159.
[101] Kim T-S, Kim J-Y, Kim K-H, Lee S, Choi D, Choi I-G, et al. The effect of storage duration on bio-oil properties. J Anal Appl Pyrol 2012;95:118–25. https://doi.org/10.1016/j.jaap.2012.01.015.
[102] Liu R, Fei W, Shen C. Influence of acetone addition on the physicochemical properties of bio-oils. J Energy Inst 2014;87:127–33. https://doi.org/10.1016/j.joei.2013.08.001.
[103] Zhang L, Liu R, Yin R, Mei Y, Cai J. Optimization of a mixed additive and its effect on physicochemical properties of bio-oil. Chem Eng Technol 2014;37:1181–90. https://doi.org/10.1002/ceat.201300786.
[104] Qin L, Shao Y, Hou Z, Jia Y, Jiang E. Ultrasonic-assisted upgrading of the heavy bio-oil obtained from pyrolysis of pine nut shells with methanol and octanol solvents. Energy Fuels 2019;33:8640–8. https://doi.org/10.1021/acs.energyfuels.9b01248.
[105] Mohapatra H, Kleiman M, Esser-Kahn AP. Mechanically controlled radical polymerization initiated by ultrasound. Nat Chem 2017;9:135–9. https://doi.org/10.1038/nchem.2633.
[106] Jiang X, Ellis N. Upgrading bio-oil through emulsification with biodiesel: thermal stability. Energy Fuels 2010;24:2699–706. https://doi.org/10.1021/ef901517k.
[107] de Luna MDG, Cruz LAD, Chen W-H, Lin B-J, Hsieh T-H. Improving the stability of diesel emulsions with high pyrolysis bio-oil content by alcohol co-surfactants and high shear mixing strategies. Energy 2017;141:1416–28. https://doi.org/10.1016/j.energy.2017.11.055.
[108] Jiang X, Ellis N. Upgrading bio-oil through emulsification with biodiesel: mixture production. Energy Fuels 2010;24:1358–64. https://doi.org/10.1021/ef9010669.
[109] Guo Z, Wang S, Wang X. Stability mechanism investigation of emulsion fuels from biomass pyrolysis oil and diesel. Energy 2014;66:250–5. https://doi.org/10.1016/j.energy.2014.01.010.
[110] Farooq A, Shafaghat H, Jae J, Jung S-C, Park Y-K. Enhanced stability of bio-oil and diesel fuel emulsion using Span 80 and Tween 60 emulsifiers. J Environ Manag 2019;231:694–700. https://doi.org/10.1016/j.jenvman.2018.10.098.
[111] Martin JA, Mullen CA, Boateng AA. Maximizing the stability of pyrolysis oil/diesel fuel emulsions. Energy Fuels 2014;28:5918–29. https://doi.org/10.1021/ef5015583.
[112] Zhang M, Wu H. Stability of emulsion fuels prepared from fast pyrolysis bio-oil and glycerol. Fuel 2017;206:230–8. https://doi.org/10.1016/j.fuel.2017.06.010.
[113] Abismaïl B, Canselier JP, Wilhelm AM, Delmas H, Gourdon C. Emulsification by ultrasound: drop size distribution and stability. Ultrason Sonochem 1999;6: 75–83. https://doi.org/10.1016/S1350-4177(98)00027-3.
[114] Martin JA, Mullen CA, Boateng AA. Maximizing the stability of pyrolysis oil/diesel fuel emulsions. Energy Fuels 2014;28:5918–29. https://doi.org/10.1021/ef5015583.
[115] Chong YY, Thangalazhy-Gopakumar S, Ng HK, Ganesan PB, Gan S, Lee LY, et al. Emulsification of bio-oil and diesel. Chemical Engineering Transactions 2017;56: 1801–6. https://doi.org/10.3303/CET1756301.
[116] Yang Z, Kumar A, Huhnke RL. Review of recent developments to improve storage and transportation stability of bio-oil. Renew Sustain Energy Rev 2015;50: 859–70. https://doi.org/10.1016/j.rser.2015.05.025.
[117] Baldwin RM, Feik CJ. Bio-oil stabilization and upgrading by hot gas filtration. Energy Fuels 2013;27:3224–38. https://doi.org/10.1021/ef400177t.
[118] Case PA, Wheeler MC, DeSisto WJ. Effect of residence time and hot gas filtration on the physical and chemical properties of pyrolysis oil. Energy Fuels 2014;28: 3964–9. https://doi.org/10.1021/ef500850y.
[119] Chen T, Wu C, Liu R, Fei W, Liu S. Effect of hot vapor filtration on the characterization of bio-oil from rice husks with fast pyrolysis in a fluidized-bed reactor. Bioresour Technol 2011;102:6178–85. https://doi.org/10.1016/j.biortech.2011.02.023.
[120] Mei Y, Liu R, Wu W, Zhang L. Effect of hot vapor filter temperature on mass yield, energy balance, and properties of products of the fast pyrolysis of pine sawdust. Energy Fuels 2016;30:10458–69. https://doi.org/10.1021/acs.energyfuels.6b01877.
[121] Hoekstra E, Hogendoorn KJA, Wang X, Westerhof RJM, Kersten SRA, van Swaaij WPM, et al. Fast pyrolysis of biomass in a fluidized bed reactor: in situ filtering of the vapors. Ind Eng Chem Res 2009;48:4744–56. https://doi.org/10.1021/ie8017274.
[122] Elliott DC, Wang H, French R, Deutch S, Iisa K. Hydrocarbon liquid production from biomass via hot-vapor-filtered fast pyrolysis and catalytic hydroprocessing of the bio-oil. Energy Fuels 2014;28:5909–17. https://doi.org/10.1021/ef501536j.
[123] Pattiya A, Suttibak S. Production of bio-oil via fast pyrolysis of agricultural residues from cassava plantations in a fluidised-bed reactor with a hot vapour filtration unit. J Anal Appl Pyrol 2012;95:227–35. https://doi.org/10.1016/j.jaap.2012.02.010.
[124] Heidenreich S. Hot gas filtration – a review. Fuel 2013;104:83–94. https://doi.org/10.1016/j.fuel.2012.07.059.
[125] zhao B, Chen M, Guo Q, Fu Y. Electrocatalytic hydrogenation of furfural to furfuryl alcohol using platinum supported on activated carbon fibers. Electrochim Acta 2014;135:139–46. https://doi.org/10.1016/j.electacta.2014.04.164.
[126] Elangovan S, Larsen D, Bay I, Mitchell E, Hartvigsen J, Millett B, et al. Electrochemical upgrading of bio-oil. ECS Transactions 2017;78:3149–58. https://doi.org/10.1149/07801.3149ecst.
[127] Lister TE, Diaz LA, Lilga MA, Padmaperuma AB, Lin Y, Palakkal VM, et al. Low-temperature electrochemical upgrading of bio-oils using polymer electrolyte membranes. Energy Fuels 2018;32:5944–50. https://doi.org/10.1021/acs.energyfuels.8b00134.
[128] Li Z, Garedew M, Lam CH, Jackson JE, Miller DJ, Saffron CM. Mild electrocatalytic hydrogenation and hydrodeoxygenation of bio-oil derived phenolic compounds using ruthenium supported on activated carbon cloth. Green Chem 2012;14:2540. https://doi.org/10.1039/c2gc35552c.
[129] Kumar R, Singh L, Zularisam AW, Hai FI. Microbial fuel cell is emerging as a versatile technology: a review on its possible applications, challenges and strategies to improve the performances: microbial fuel cell is emerging as a versatile technology. Int J Energy Res 2018;42:369–94. https://doi.org/10.1002/er.3780.
[130] Kumar R, Singh L, Zularisam AW. Exoelectrogens: recent advances in molecular drivers involved in extracellular electron transfer and strategies used to improve it for microbial fuel cell applications. Renew Sustain Energy Rev 2016;56: 1322–36. https://doi.org/10.1016/j.rser.2015.12.029.

[131] Chen B, Shi Z, Jiang S, Tian H. Catalytic cracking mechanisms of tar model compounds. J Cent South Univ 2016;23:3100–7. https://doi.org/10.1007/s11771-016-3375-7.
[132] Si Z, Zhang X, Wang C, Ma L, Dong R. An overview on catalytic hydrodeoxygenation of pyrolysis oil and its model compounds. Catalysts 2017;7:169. https://doi.org/10.3390/catal7060169.
[133] Kim S, Kwon EE, Kim YT, Jung S, Kim HJ, Huber GW, et al. Recent advances in hydrodeoxygenation of biomass-derived oxygenates over heterogeneous catalysts. Green Chem 2019. https://doi.org/10.1039/C9GC01210A. 10.1039. C9GC01210A.
[134] Ruddy DA, Schaidle JA, Ferrell III JR, Wang J, Moens L, Hensley JE. Recent advances in heterogeneous catalysts for bio-oil upgrading via "ex situ catalytic fast pyrolysis": catalyst development through the study of model compounds. Green Chem 2014;16:454–90. https://doi.org/10.1039/C3GC41354C.
[135] Cheng S, Wei L, Alsowij MR, Corbin F, Julson J, Boakye E, et al. In situ hydrodeoxygenation upgrading of pine sawdust bio-oil to hydrocarbon biofuel using Pd/C catalyst. J Energy Inst 2018;91:163–71. https://doi.org/10.1016/j.joei.2017.01.004.
[136] Lau PL, Allen RWK, Styring P. Continuous-flow Heck synthesis of 4-methoxybiphenyl and methyl 4-methoxycinnamate in supercritical carbon dioxide expanded solvent solutions. Beilstein J Org Chem 2013;9:2886–97. https://doi.org/10.3762/bjoc.9.325.
[137] Sanna A, Vispute TP, Huber GW. Hydrodeoxygenation of the aqueous fraction of bio-oil with Ru/C and Pt/C catalysts. Appl Catal B Environ 2015;165:446–56. https://doi.org/10.1016/j.apcatb.2014.10.013.
[138] Han Y, Gholizadeh M, Tran C-C, Kaliaguine S, Li C-Z, Olarte M, et al. Hydrotreatment of pyrolysis bio-oil: a review. Fuel Process Technol 2019;195:106140. https://doi.org/10.1016/j.fuproc.2019.106140.
[139] Capunitan JA, Capareda SC. Hydrotreatment of corn stover bio-oil using noble metal catalysts. Fuel Process Technol 2014;125:190–9. https://doi.org/10.1016/j.fuproc.2014.03.029.
[140] Gholizadeh M, Gunawan R, Hu X, de Miguel Mercader F, Westerhof R, Chaitwat W, et al. Effects of temperature on the hydrotreatment behaviour of pyrolysis bio-oil and coke formation in a continuous hydrotreatment reactor. Fuel Process Technol 2016;148:175–83. https://doi.org/10.1016/j.fuproc.2016.03.002.
[141] Gholizadeh M, Gunawan R, Hu X, Hasan MM, Kersten S, Westerhof R, et al. Different reaction behaviours of the light and heavy components of bio-oil during the hydrotreatment in a continuous pack-bed reactor. Fuel Process Technol 2016;146:76–84. https://doi.org/10.1016/j.fuproc.2016.01.026.
[142] Gholizadeh M, Gunawan R, Hu X, Kadarwati S, Westerhof R, Chaiwat W, et al. Importance of hydrogen and bio-oil inlet temperature during the hydrotreatment of bio-oil. Fuel Process Technol 2016;150:132–40. https://doi.org/10.1016/j.fuproc.2016.05.014.
[143] Ardiyanti AR, Khromova SA, Venderbosch RH, Yakovlev VA, Melián-Cabrera IV, Heeres HJ. Catalytic hydrotreatment of fast pyrolysis oil using bimetallic Ni–Cu catalysts on various supports. Appl Catal Gen 2012;449:121–30. https://doi.org/10.1016/j.apcata.2012.09.016.
[144] Boscagli C, Yang C, Welle A, Wang W, Behrens S, Raffelt K, et al. Effect of pyrolysis oil components on the activity and selectivity of nickel-based catalysts during hydrotreatment. Appl Catal Gen 2017;544:161–72. https://doi.org/10.1016/j.apcata.2017.07.025.
[145] Yin W, Venderbosch RH, He S, Bykova MV, Khromova SA, Yakovlev VA, et al. Mono-, bi-, and tri-metallic Ni-based catalysts for the catalytic hydrotreatment of pyrolysis liquids. Biomass Conv Bioref 2017;7:361–76. https://doi.org/10.1007/s13399-017-0267-5.
[146] Sangnikul P, Phanpa C, Xiao R, Zhang H, Reubroycharoen P, Kuchonthara P, et al. Role of copper- or cerium-promoters on NiMo/γ-Al2O3 catalysts in hydrodeoxygenation of guaiacol and bio-oil. Appl Catal Gen 2019;574:151–60. https://doi.org/10.1016/j.apcata.2019.02.004.
[147] Carriel Schmitt C, Zimina A, Fam Y, Raffelt K, Grunwaldt J-D, Dahmen N. Evaluation of high-loaded Ni-based catalysts for upgrading fast pyrolysis bio-oil. Catalysts 2019;9:784. https://doi.org/10.3390/catal9090784.
[148] Schmitt CC, Raffelt K, Zimina A, Krause B, Otto T, Rapp M, et al. Hydrotreatment of fast pyrolysis bio-oil fractions over nickel-based catalyst. Top Catal 2018;61:1769–82. https://doi.org/10.1007/s11244-018-1009-z.
[149] Kim G, Seo J, Choi J-W, Jae J, Ha J-M, Suh DJ, et al. Two-step continuous upgrading of sawdust pyrolysis oil to deoxygenated hydrocarbons using hydrotreating and hydrodeoxygenating catalysts. Catal Today 2018;303:130–5. https://doi.org/10.1016/j.cattod.2017.09.027.
[150] Wildschut J, Mahfud FH, Venderbosch RH, Heeres HJ. Hydrotreatment of fast pyrolysis oil using heterogeneous noble-metal catalysts. Ind Eng Chem Res 2009;48:10324–34. https://doi.org/10.1021/ie9006003.
[151] Elkasabi Y, Mullen CA, Pighinelli ALMT, Boateng AA. Hydrodeoxygenation of fast-pyrolysis bio-oils from various feedstocks using carbon-supported catalysts. Fuel Process Technol 2014;123:11–8. https://doi.org/10.1016/j.fuproc.2014.01.039.
[152] Guo C, Rao KTV, Yuan Z, He SQ, Rohani S, Xu CC. Hydrodeoxygenation of fast pyrolysis oil with novel activated carbon-supported NiP and CoP catalysts. Chem Eng Sci 2018;178:248–59. https://doi.org/10.1016/j.ces.2017.12.048.
[153] Jahromi H, Agblevor FA. Upgrading of pinyon-juniper catalytic pyrolysis oil via hydrodeoxygenation. Energy 2017;141:2186–95. https://doi.org/10.1016/j.energy.2017.11.149.
[154] Boscagli C, Raffelt K, Grunwaldt J-D. Reactivity of platform molecules in pyrolysis oil and in water during hydrotreatment over nickel and ruthenium catalysts. Biomass Bioenergy 2017;106:63–73. https://doi.org/10.1016/j.biombioe.2017.08.013.
[155] Ardiyanti AR, Bykova MV, Khromova SA, Yin W, Venderbosch RH, Yakovlev VA, et al. Ni-based catalysts for the hydrotreatment of fast pyrolysis oil. Energy Fuels 2016;30:1544–54. https://doi.org/10.1021/acs.energyfuels.5b02223.
[156] Reyhanitash E, Tymchyshyn M, Yuan Z, Albion K, van Rossum GC, Xu C. Hydrotreatment of fast pyrolysis oil: effects of esterification pre-treatment of the oil using alcohol at a small loading. Fuel 2016;179:45–51. https://doi.org/10.1016/j.fuel.2016.03.074.
[157] Jahromi H, Agblevor FA. Hydrodeoxygenation of aqueous-phase catalytic pyrolysis oil to liquid hydrocarbons using multifunctional nickel catalyst. Ind Eng Chem Res 2018;57:13257–68. https://doi.org/10.1021/acs.iecr.8b02807.
[158] Mu W, Ben H, Du X, Zhang X, Hu F, Liu W, et al. Noble metal catalyzed aqueous phase hydrogenation and hydrodeoxygenation of lignin-derived pyrolysis oil and related model compounds. Bioresour Technol 2014;173:6–10. https://doi.org/10.1016/j.biortech.2014.09.067.
[159] Horáček J, Kubička D. Bio-oil hydrotreating over conventional CoMo & NiMo catalysts: the role of reaction conditions and additives. Fuel 2017;198:49–57. https://doi.org/10.1016/j.fuel.2016.10.003.
[160] Kadarwati S, Hu X, Gunawan R, Westerhof R, Gholizadeh M, Hasan MDM, et al. Coke formation during the hydrotreatment of bio-oil using NiMo and CoMo catalysts. Fuel Process Technol 2017;155:261–8. https://doi.org/10.1016/j.fuproc.2016.08.021.
[161] Eschenbacher A, Saraeian A, Jensen PA, Shanks BH, Li C, Duus JØ, et al. Deoxygenation of wheat straw fast pyrolysis vapors over Na-Al2O3 catalyst for production of bio-oil with low acidity. Chem Eng J 2020;394:124878. https://doi.org/10.1016/j.cej.2020.124878.
[162] Romero Y, Richard F, Brunet S. Hydrodeoxygenation of 2-ethylphenol as a model compound of bio-crude over sulfided Mo-based catalysts: promoting effect and reaction mechanism. Appl Catal B Environ 2010;98:213–23. https://doi.org/10.1016/j.apcatb.2010.05.031.
[163] Grilc M, Likozar B, Levec J. Hydrodeoxygenation and hydrocracking of solvolysed lignocellulosic biomass by oxide, reduced and sulphide form of NiMo, Ni, Mo and Pd catalysts. Appl Catal B Environ 2014;150–151:275–87. https://doi.org/10.1016/j.apcatb.2013.12.030.
[164] Jin W, Pastor-Pérez L, Villora-Picó JJ, Sepúlveda-Escribano A, Gu S, Reina TR. Investigating new routes for biomass upgrading: "H_2 -free" hydrodeoxygenation using Ni-based catalysts. ACS Sustainable Chem Eng 2019;7:16041–9. https://doi.org/10.1021/acssuschemeng.9b02712.
[165] Li K, Wang R, Chen J. Hydrodeoxygenation of anisole over silica-supported Ni_2P, MoP, and NiMoP catalysts. Energy Fuels 2011;25:854–63. https://doi.org/10.1021/ef101258j.
[166] Tu C, Chen J, Li W, Wang H, Deng K, Vinokurov VA, et al. Hydrodeoxygenation of bio-derived anisole to cyclohexane over bi-functional IM-5 zeolite supported Ni catalysts. Sustainable Energy Fuels 2019;3:3462–72. https://doi.org/10.1039/C9SE00554D.
[167] Dongil AB, Ghampson IT, García R, Fierro JLG, Escalona N. Hydrodeoxygenation of guaiacol over Ni/carbon catalysts: effect of the support and Ni loading. RSC Adv 2016;6:2611–23. https://doi.org/10.1039/C5RA22540J.
[168] Zhang J, Fidalgo B, Kolios A, Shen D, Gu S. Mechanism of deoxygenation in anisole decomposition over single-metal loaded HZSM-5: experimental study. Chem Eng J 2018;336:211–22. https://doi.org/10.1016/j.cej.2017.11.128.
[169] Wang Z, Zeng Y, Lin W, Song W. In-situ hydrodeoxygenation of phenol by supported Ni catalyst – explanation for catalyst performance. Int J Hydrogen Energy 2017;42:21040–7. https://doi.org/10.1016/j.ijhydene.2017.07.053.
[170] Mohammed IY, Abakr YA, Mokaya R. Catalytic upgrading of pyrolytic oil via in-situ hydrodeoxygenation. Waste Biomass Valor 2020;11:2935–47. https://doi.org/10.1007/s12649-019-00613-0.
[171] Wang L, Ye P, Yuan F, Li S, Ye Z. Liquid phase in-situ hydrodeoxygenation of bio-derived phenol over Raney Ni and Nafion/SiO2. Int J Hydrogen Energy 2015;40:14790–7. https://doi.org/10.1016/j.ijhydene.2015.09.014.
[172] Lv M, Zhou J, Yang W, Cen K. Thermogravimetric analysis of the hydrolysis of zinc particles. Int J Hydrogen Energy 2010;35:2617–21. https://doi.org/10.1016/j.ijhydene.2009.04.017.
[173] Hilten R, Weber J, Kastner JR. Continuous upgrading of fast pyrolysis oil by simultaneous esterification and hydrogenation. Energy Fuels 2016;30:8357–68. https://doi.org/10.1021/acs.energyfuels.6b01906.
[174] Strenziok R, Hansen U, Knstner H. Combustion of bio-oil in a gas turbine. In: Bridgwater AV, editor. Progress in thermochemical biomass conversion. Oxford, UK: Blackwell Science Ltd; 2001. p. 1452–8. https://doi.org/10.1002/9780470694954.ch119.
[175] Trane R, Dahl S, Skjøth-Rasmussen MS, Jensen AD. Catalytic steam reforming of bio-oil. Int J Hydrogen Energy 2012;37:6447–72. https://doi.org/10.1016/j.ijhydene.2012.01.023.
[176] Seyedeyn-Azad F, Abedi J, Sampouri S. Catalytic steam reforming of aqueous phase of bio-oil over Ni-based alumina-supported catalysts. Ind Eng Chem Res 2014;53:17937–44. https://doi.org/10.1021/ie5034705.
[177] Lan P, Xu Q, Zhou M, Lan L, Zhang S, Yan Y. Catalytic steam reforming of fast pyrolysis bio-oil in fixed bed and fluidized bed reactors. Chem Eng Technol 2010;33:2021–8. https://doi.org/10.1002/ceat.201000169.
[178] Werther J, Reppenhagen J. Catalyst attrition in fluidized-bed systems. AIChE J 1999;45:2001–10. https://doi.org/10.1002/aic.690450916.
[179] van Rossum G, Kersten SRA, van Swaaij WPM. Staged catalytic gasification/steam reforming of pyrolysis oil. Ind Eng Chem Res 2009;48:5857–66. https://doi.org/10.1021/ie900194j.

[180] Liu Q, Xiong Z, Syed-Hassan SSA, Deng Z, Zhao X, Su S, et al. Effect of the pre-reforming by Fe/bio-char catalyst on a two-stage catalytic steam reforming of bio-oil. Fuel 2019;239:282–9. https://doi.org/10.1016/j.fuel.2018.11.029.
[181] Ren Z-Z, Lan P, Ma H-R, Wang T, Shi X-H, Zhang S-P, et al. Hydrogen production via catalytic steam reforming of bio-oil model compound in a two-stage reaction system. Energy Sources, Part A Recovery, Util Environ Eff 2014;36:1921–30. https://doi.org/10.1080/15567036.2011.582615.
[182] Santamaria L, Lopez G, Arregi A, Amutio M, Artetxe M, Bilbao J, et al. Influence of the support on Ni catalysts performance in the in-line steam reforming of biomass fast pyrolysis derived volatiles. Appl Catal B Environ 2018;229:105–13. https://doi.org/10.1016/j.apcatb.2018.02.003.
[183] Valle B, Aramburu B, Benito PL, Bilbao J, Gayubo AG. Biomass to hydrogen-rich gas via steam reforming of raw bio-oil over Ni/La2O3-αAl2O3 catalyst: effect of space-time and steam-to-carbon ratio. Fuel 2018;216:445–55. https://doi.org/10.1016/j.fuel.2017.11.151.
[184] Valle B, Aramburu B, Olazar M, Bilbao J, Gayubo AG. Steam reforming of raw bio-oil over Ni/La2O3-αAl2O3: influence of temperature on product yields and catalyst deactivation. Fuel 2018;216:463–74. https://doi.org/10.1016/j.fuel.2017.11.149.
[185] Remiro A, Valle B, Aguayo AT, Bilbao J, Gayubo AG. Operating conditions for attenuating Ni/La2O3–αAl2O3 catalyst deactivation in the steam reforming of bio-oil aqueous fraction. Fuel Process Technol 2013;115:222–32. https://doi.org/10.1016/j.fuproc.2013.06.003.
[186] Arregi A, Lopez G, Amutio M, Artetxe M, Barbarias I, Bilbao J, et al. Role of operating conditions in the catalyst deactivation in the in-line steam reforming of volatiles from biomass fast pyrolysis. Fuel 2018;216:233–44. https://doi.org/10.1016/j.fuel.2017.12.002.
[187] Bimbela F, Oliva M, Ruiz J, García L, Arauzo J. Hydrogen production via catalytic steam reforming of the aqueous fraction of bio-oil using nickel-based coprecipitated catalysts. Int J Hydrogen Energy 2013;38:14476–87. https://doi.org/10.1016/j.ijhydene.2013.09.038.
[188] Xing R, Dagle VL, Flake M, Kovarik L, Albrecht KO, Deshmane C, et al. Steam reforming of fast pyrolysis-derived aqueous phase oxygenates over Co, Ni, and Rh metals supported on MgAl2O4. Catal Today 2016;269:166–74. https://doi.org/10.1016/j.cattod.2015.11.046.
[189] Chen J, Sun J, Wang Y. Catalysts for steam reforming of bio-oil: a review. Ind Eng Chem Res 2017;56:4627–37. https://doi.org/10.1021/acs.iecr.7b00600.
[190] Rioche C, Kulkarni S, Meunier FC, Breen JP, Burch R. Steam reforming of model compounds and fast pyrolysis bio-oil on supported noble metal catalysts. Appl Catal B Environ 2005;61:130–9. https://doi.org/10.1016/j.apcatb.2005.04.015.
[191] Yadav AK, Vaidya PD. Reaction kinetics of steam reforming of *n* -butanol over a Ni/hydrotalcite catalyst. Chem Eng Technol 2018;41:890–6. https://doi.org/10.1002/ceat.201600738.
[192] Llera I, Mas V, Bergamini ML, Laborde M, Amadeo N. Bio-ethanol steam reforming on Ni based catalyst. Kinetic study. Chem Eng Sci 2012;71:356–66. https://doi.org/10.1016/j.ces.2011.12.018.
[193] Vaidya PD, Rodrigues AE. Kinetics of steam reforming of ethanol over a Ru/Al $_2$ O $_3$ catalyst. Ind Eng Chem Res 2006;45:6614–8. https://doi.org/10.1021/ie051342m.
[194] Arregi A, Lopez G, Amutio M, Barbarias I, Santamaria L, Bilbao J, et al. Kinetic study of the catalytic reforming of biomass pyrolysis volatiles over a commercial Ni/Al2O3 catalyst. Int J Hydrogen Energy 2018;43:12023–33. https://doi.org/10.1016/j.ijhydene.2018.05.032.
[195] Santamaria L, Lopez G, Arregi A, Amutio M, Artetxe M, Bilbao J, et al. Stability of different Ni supported catalysts in the in-line steam reforming of biomass fast pyrolysis volatiles. Appl Catal B Environ 2019;242:109–20. https://doi.org/10.1016/j.apcatb.2018.09.081.
[196] Remón J, Broust F, Valette J, Chhiti Y, Alava I, Fernandez-Akarregi AR, et al. Production of a hydrogen-rich gas from fast pyrolysis bio-oils: comparison between homogeneous and catalytic steam reforming routes. Int J Hydrogen Energy 2014;39:171–82. https://doi.org/10.1016/j.ijhydene.2013.10.025.
[197] Zhang S, Li X, Li Q, Xu Q, Yan Y. Hydrogen production from the aqueous phase derived from fast pyrolysis of biomass. J Anal Appl Pyrol 2011;92:158–63. https://doi.org/10.1016/j.jaap.2011.05.007.
[198] Ramirez JA, Rainey TJ. Comparative techno-economic analysis of biofuel production through gasification, thermal liquefaction and pyrolysis of sugarcane bagasse. J Clean Prod 2019;229:513–27. https://doi.org/10.1016/j.jclepro.2019.05.017.
[199] Magdeldin M, Kohl T, Järvinen M. Techno-economic assessment of the by-products contribution from non-catalytic hydrothermal liquefaction of lignocellulose residues. Energy 2017;137:679–95. https://doi.org/10.1016/j.energy.2017.06.166.
[200] Patel M, Zhang X, Kumar A. Techno-economic and life cycle assessment on lignocellulosic biomass thermochemical conversion technologies: a review. Renew Sustain Energy Rev 2016;53:1486–99. https://doi.org/10.1016/j.rser.2015.09.070.
[201] Zhang Y, Brown TR, Hu G, Brown RC. Comparative techno-economic analysis of biohydrogen production via bio-oil gasification and bio-oil reforming. Biomass Bioenergy 2013;51:99–108. https://doi.org/10.1016/j.biombioe.2013.01.013.
[202] Rogers JG, Brammer JG. Estimation of the production cost of fast pyrolysis bio-oil. Biomass Bioenergy 2012;36:208–17. https://doi.org/10.1016/j.biombioe.2011.10.028.
[203] Wright MM, Daugaard DE, Satrio JA, Brown RC. Techno-economic analysis of biomass fast pyrolysis to transportation fuels. Fuel 2010;89:S2–10. https://doi.org/10.1016/j.fuel.2010.07.029.
[204] Zhu Y, Biddy MJ, Jones SB, Elliott DC, Schmidt AJ. Techno-economic analysis of liquid fuel production from woody biomass via hydrothermal liquefaction (HTL) and upgrading. Appl Energy 2014;129:384–94. https://doi.org/10.1016/j.apenergy.2014.03.053.
[205] Sarkar S, Kumar A. Large-scale biohydrogen production from bio-oil. Bioresour Technol 2010;101:7350–61. https://doi.org/10.1016/j.biortech.2010.04.038.
[206] Wright MM, Román-Leshkov Y, Green WH. Investigating the techno-economic trade-offs of hydrogen source using a response surface model of drop-in biofuel production via bio-oil upgrading: modeling and Analysis: techno-economic tradeoffs of hydrogen source in bio-oil upgrading. Biofuels, Bioprod Bioref 2012;6:503–20. https://doi.org/10.1002/bbb.1340.

MACQUARIE University

MACQUARIE UNIVERSITY
AUTHORSHIP CONTRIBUTION STATEMENT

In accordance with the *Macquarie University Code for the Responsible Conduct of Research* and the *Authorship Standard*, researchers have a responsibility to their colleagues and the wider community to treat others fairly and with respect, to give credit where appropriate to those who have contributed to research.

Note for HDR students: *Where research papers are being included in a thesis, this template must be used to document the contribution of authors to each of the proposed or published research papers. The contribution of the candidate must be sufficient to justify inclusion of the paper in the thesis.*

1. DETAILS OF PUBLICATION & CORRESPONDING AUTHOR

Title of Publication (can be a holding title)		**Publication Status** Choose an item
Enhanced bio-oil deoxygenation activity by Cu/zeolite and Ni/zeolite catalysts in combined in-situ and ex-situ biomass pyrolysis		☐ In Progress or Unpublished work for thesis submission ☐ Submitted for Publication ☐ Accepted for Publication ☒ Published
Name of **corresponding author**	Department/Faculty	**Publication details:** indicate the name of the journal/ conference/ publisher/other outlet
Ravinder Kumar	Earth and Environmental Sciences/ Science & Engineering	Journal of Analytical and Applied Pyrolysis

2. STUDENTS DECLARATION (if applicable)

Name of HDR thesis author (If the same as corresponding author - write "as above")	Department/Faculty	Thesis title
as above	Earth and Environmental Sciences/ Science & Engineering	Catalytic Upgrading of Bio-oil Produced from Fast Pyrolysis of Pinewood Sawdust

Description of HDR thesis author's contribution to planning, execution, and preparation of the work if there are multiple authors

(for example, how much as a percent did you contribute to the conception of the project, the design of methodology or experimental protocol, data collection, analysis, drafting the manuscript, revising it critically for important intellectual content, etc.)

In this article, I contributed in designing the project, carried out 70% of the experimental work, analyzed the data and wrote 80% of the manuscript.

I declare that the above is an accurate description of my contribution to this publication, and the contributions of other authors are as described below.	**Student signature** **Date**	 02/22/2021

MACQUARIE University

3. Description of all other author contributions

Use an Asterisk * to denote if the author is also a current student or HDR candidate.

The HDR candidate or corresponding author must, for each paper, list all authors and provide details of their role in the publication. Where possible, also provide a percentage estimate of the contribution made by each author.

Name and affiliation of author	**Intellectual contribution(s)** (for example to the: conception of the project, design of methodology/experimental protocol, data collection, analysis, drafting the manuscript, revising it critically for important intellectual content etc.)
Vladimir Strezov Macquarie University	conception, supervision, critical revision
Emma Lovell UNSW	experimental, data analysis, critical revision
Tao Kan Macquarie University	experimental, supervision, critical revision
Haftom Weldekidan Macquarie University	experimental, data analysis, critical revision
Jing He Macquarie University	experimental, data analysis, critical revision
*Behnam Dastjerdi Macquarie University	data analysis, critical revision
Jason Scott UNSW	experimental, data analysis, critical revision
Sayka Jahan	critical revision
	Provide summary for any additional Authors in this cell.

4. Author Declarations

I agree to be named as one of the authors of this work, and confirm:

i. *that I have met the authorship criteria set out in the* Authorship Standard, *accompanying the* Macquarie University Research Code,

ii. *that there are no other authors according to these criteria,*

iii. *that the description in Section 3 or 4 of my contribution(s) to this publication is accurate*

iv. *that I have agreed to the planned authorship order following the* Authorship Standard

Name of author	Authorised * By Signature or refer to other written record of approval (eg. pdf of a signed agreement or an email record)	Date
Vladimir Strezov		24/02/2021
Emma Lovell		26/02/2021
Tao Kan		22/02/2021
Haftom Weldekidan		22/02/202
Jing He		22/02/2021
Behnam Dastjerdi		02/22/2021
Jason Scott		26/02/2021
Sayka Jahan		25/02/2021
	Provide other written record of approval for additional authors (eg. pdf of a signed agreement or an email record)	

5. Data storage

The original data for this project are stored in the following location, in accordance with the *Research Data Management Standard* accompanying the *Macquarie University Research Code*.

If the data have been or will be deposited in an online repository, provide the details here with any corresponding DOI.

Data description/format	Storage Location or DOI	Name of custodian if other than the corresponding author

A copy of this form must be retained by the corresponding author and must accompany the thesis submitted for examination.

Chapter 5

Enhanced bio-oil deoxygenation activity by Cu/zeolite and Ni/zeolite catalysts in combined *in-situ* and *ex-situ* biomass pyrolysis

Ravinder Kumar[a], Vladimir Strezov[a], Emma Lovell[b], Tao Kan[a], Haftom Weldekidan[a], Jing He[a], Sayka Jahan[a], Behnam Dastjerdi[a], Jason Scott[b]

[a]Department of Environmental Sciences, Faculty of Science & Engineering, Macquarie University, Sydney, NSW 2109, Australia

[b]Particles and Catalysis Research Group, School of Chemical Engineering, The University of New South Wales, Sydney, NSW 2052, Australia

Previous chapters reviewed different approaches including catalytic, biomass pre-treatment and downstream processing technologies, which indicate that catalytic approach is comparatively advantageous for bio-oil upgrading. Catalytic biomass pyrolysis in a fixed bed reactor can be of three types that is sole *in-situ*; *ex-situ*; and combined *in-situ* and *ex-situ.* This chapter aims to compare three modes of pyrolysis for bio-oil deoxygenation and select the best pyrolysis mode for further experiments. Pinewood sawdust was taken as the feedstock and pyrolysis was carried out at 700 °C. Cu/zeolite and Ni/zeolite were prepared using wet-impregnation method and employed as catalysts in three modes of the pyrolysis.

Kumar, R., Strezov, V., Lovell, E., Kan, T., Weldekidan, H., He, J., Jahan, S., Dastjerdi, B., & Scott, J. (2019). Enhanced bio-oil deoxygenation activity by Cu/zeolite and Ni/zeolite catalysts in combined in-situ and ex-situ biomass pyrolysis. Journal of Analytical and Applied Pyrolysis, 140, 148-160. https://doi.org/10.1016/j.jaap.2019.03.008

Journal of Analytical and Applied Pyrolysis 140 (2019) 148–160

Contents lists available at ScienceDirect

Journal of Analytical and Applied Pyrolysis

journal homepage: www.elsevier.com/locate/jaap

Enhanced bio-oil deoxygenation activity by Cu/zeolite and Ni/zeolite catalysts in combined *in-situ* and *ex-situ* biomass pyrolysis

Ravinder Kumar[a,*], Vladimir Strezov[a], Emma Lovell[b], Tao Kan[a], Haftom Weldekidan[a], Jing He[a], Sayka Jahan[a], Behnam Dastjerdi[a], Jason Scott[b]

[a] Department of Environmental Sciences, Faculty of Science & Engineering, Macquarie University, Sydney, NSW 2109, Australia
[b] Particles and Catalysis Research Group, School of Chemical Engineering, The University of New South Wales, Sydney, NSW 2052, Australia

ARTICLE INFO

Keywords:
Bio-oil upgrading
Combined pyrolysis
Cu/zeolite
Ni/zeolite

ABSTRACT

The presence of oxygenated compounds in pyrolytic oil makes it highly acidic and unsuitable energy source for real-world applications. *In-situ* and *ex-situ* catalytic pyrolysis have been considered the most significant approaches to convert these oxygenated compounds into hydrocarbons or less oxygenated compounds, thereby increasing the carbon and hydrogen content in the bio-oil and improving its overall quality. A remarkable conversion of oxygenated compounds could also be achieved using a combined *in-situ* and *ex-situ* catalytic pyrolysis approach. Therefore, this study aimed to prepare Cu10%/zeolite and Ni10%/zeolite catalysts using a wet-impregnation method and investigate their potential for bio-oil upgrading in a combined *in-situ* and *ex-situ* catalytic pyrolysis mode and the results were compared with sole *in-situ* and *ex-situ* catalytic pyrolysis. In combined pyrolysis, Cu/zeolite was used *in-situ* and Ni/zeolite in *ex-situ* mode with four different catalyst to biomass (C/B) ratios (2, 3, 4 and 5). Interestingly, the results demonstrated that the combined pyrolysis with a C/B ratio of 5 achieved the highest deoxygenation activity (~98%) and total hydrocarbon production (~72%) as compared to sole *in-situ* (C/B ratio of 5) or *ex-situ* catalytic pyrolysis (C/B ratio of 3). It was further noticed that both the catalysts in sole *in-situ* pyrolysis promoted the formation of acids (~28% by Cu/zeolite with C/B ratio of 5) in the bio-oil, but a negligible proportion of acids (~1%) was obtained in sole *ex-situ* and combined pyrolysis mode. The major hydrocarbons detected in all the bio-oil samples were ethylidenecyclobutane, retene, fluorene, phenanthrene, and pyrene. The enhanced deoxygenation activity and hydrocarbon production by the catalysts can be attributed to the abundant acidic sites present inside the pores or on the surface of the catalysts that carried out major deoxygenation reactions, such as dehydration, decarboxylation, decarbonylation, aldol condensation, and aromatization. Overall, this study suggested that a combined *in-situ* and *ex-situ* catalytic pyrolysis approach could be advantageous for bio-oil upgrading as compared to sole *in-situ* or *ex-situ* catalytic pyrolysis mode.

1. Introduction

Pyrolysis has been considered a promising technique for many decades to produce economical and renewable energy fuels and chemicals from different lignocellulose biomasses [1–4]. The major application of pyrolysis that has been extensively studied to the date is bio-oil production, which is foreseen as one of the second-generation energy carriers. However, the bio-oil produced from pyrolysis is generally an aqueous and a highly oxygenated mixture of phenols, acids and a fraction of hydrocarbons [5–7]. Moreover, its high acidity, low stability, corrosive nature, high viscosity, and low vapour pressure are other major limitations that restrict its direct application as a drop-in energy fuel. It is believed that bio-oil could be a suitable energy source for the production of high-grade transportation fuels. Therefore, bio-oil upgrading is highly essential to make it a feasible transportation fuel in the nearest future.

There are two major catalytic routes to deoxygenate the bio-oil, the first is catalytic hydroprocessing such as hydrocracking, hydrodeoxygenation and secondly, catalytic cracking of oxygenated compounds [8–11]. The catalytic hydroprocessing approach could be advantageous over cracking to produce a high-quality bio-oil with a low oxygen and high H/C ratio but it requires a considerable amount of hydrogen that makes the process economically expensive. Therefore, catalytic cracking might prove comparatively cost-effective and could

be preferred over catalytic hydroprocessing for bio-oil upgrading. In catalytic cracking, the pyrolysis can be operated in two configurations based on the addition of a catalyst. The first mode called *in-situ* pyrolysis involves the addition of a catalyst mixed with the biomass, whereas in the second configuration that is *ex-situ* pyrolysis, the catalyst is separately placed downstream to the biomass and the produced pyrolytic vapours are passed through the catalyst bed [3,12,13]. The catalyst either in *in-situ* or *ex-situ* mode converts the oxygenated compounds into various hydrocarbons, less oxygenated compounds and different pyrolytic gases through various reactions, such as dehydration, decarboxylation, decarbonylation, aldol condensation, and aromatization [14–17]. A number of different catalysts used in both modes of pyrolysis have achieved successful results to deoxygenate the bio-oil [18–21]. *In-situ* catalytic pyrolysis has proven to reduce the content of oxygenated compounds and increase the proportion of hydrocarbons in the bio-oil. For example, different catalysts were applied for *in-situ* catalytic upgrading of bio-oil in a fixed bed pyrolysis reactor [16]. The results demonstrated that the catalysts with higher surface area, such as ZSM-5 and zirconia/titania resulted in higher organic liquid yields with less oxygenated compounds and maximum hydrocarbons [20]. In a separate study, Zhang et al. [21] applied HZSM-5 with varying Si/Al ratios (20–300) in *in-situ* pyrolysis of biomass at 450 °C. The results reported that *in-situ* catalytic pyrolysis produced a higher number of hydrocarbons and light phenols in the bio-oil samples [21]. It has been also noticed that *in-situ* pyrolysis could result in higher liquid yield as compared to *ex-situ* pyrolysis. Evidently, Gamliel et al. [18] investigated the effect of ZSM-5 on bio-oil deoxygenation in *in-situ* pyrolysis mode and compared the results with *ex-situ* pyrolysis. The authors found that *in-situ* pyrolysis mode produced the higher liquid carbons and the lower gas carbon yields as compared to the *ex-situ* pyrolysis [18]. Besides, it was noticed that ZSM-5 favoured the production of naphthalenes during *in-situ* pyrolysis, while in *ex-situ* pyrolysis, ZSM-5 promoted the formation of monocyclic-aromatic hydrocarbons (*e.g.*, benzene, toluene) in the bio-oil samples. Another advantage of *in-situ* pyrolysis is higher biomass conversion rate to liquid products or liquid aromatics. This is because during *in-situ* mode the catalyst could react with a higher amount of pyrolytic vapours as the catalyst is in direct contact with the vapours released from the pyrolyzing biomass, while during *ex-situ* pyrolysis mode the pyrolytic vapours get diluted with the carrier gas first before reacting with the catalyst bed [22]. It has been also argued that vapour residence time in the catalyst pores is higher for *in-situ* pyrolysis mode as compared to *ex-situ* mode, which could be a key factor to enhance the conversion of oxygenated compounds to hydrocarbons [14]. Therefore, it can be suggested that *in-situ* pyrolysis provides better opportunity for efficient biomass conversion to obtain more liquid products, while higher residence time allows pyrolytic vapours to react effectively with acids sites in the catalyst, resulting in higher production of hydrocarbons. However, the previous studies also suggested that *in-situ* pyrolysis results in the higher coke formation on the catalyst surface as the catalyst is in direct contact with the biomass, leading to the faster catalyst deactivation, in contrast, *ex-situ* pyrolysis results in less coke formation [18]. It has been also argued that the pyrolytic vapours generated during *in-situ* mode could not contact significant amount of the catalyst, thereby demanding a higher catalyst to biomass (C/B) ratio to achieve better deoxygenation activity [14]. In addition to this, the catalyst regeneration in *in-situ* pyrolysis is comparatively challenging as the catalyst is properly mixed with the biomass, whereas in *ex-situ* pyrolysis, the catalyst can be easily retrieved from the reactor and can be used in the successive demonstrations.

Due to significant advantages of *ex-situ* catalytic pyrolysis, it has been preferred over *in-situ* pyrolysis for bio-oil upgrading and has also shown competitive deoxygenation activity as compared to *in-situ* pyrolysis mode [22,23]. Noticeably, Iisa et al. (2016) proved that an *in-situ* configuration generated a higher amount of oxygenated and acid compounds as compared to *ex-situ* configuration, attributing to the faster deactivation of the catalyst. The results also reported the higher production of naphthalenes and aromatic hydrocarbons in the bio-oil from *ex-situ* pyrolysis as compared to the *in-situ* mode [23]. In a separate study, Veses et al. [24] compared the performance of different metal cations/ZSM-5 catalysts for bio-oil upgrading during *ex-situ* pyrolysis of biomass at 450 °C. The study demonstrated that Ni/ZSM-5 and Cu/ZSM-5 generated higher number of hydrocarbons as compared to Mg/ZSM-5 and H-ZSM-5 catalysts. Evidently, the results reported that Ni/ZSM-5 and Cu/ZSM-5 produced the bio-oil with hydrocarbons of approximately 35% and 31%, respectively, while Mg/ZSM-5 and H-ZSM-5 catalysts could produce 29% hydrocarbons in the bio-oil samples [24]. In an alternative study, Yung et al. [25] applied Ni/ZSM-5 catalyst with different loadings of Ni (1.2%, 3.1%, 6.2%) for bio-oil upgrading in *ex-situ* pyrolysis of pine wood biomass. The results showed that the catalyst enhanced the conversion of oxygenated compounds into aromatic hydrocarbons, and the number of aromatics increased with increase in Ni loading, catalyst with 6.2% Ni produced higher aromatics as compared to the catalyst with 1.2% Ni. There are several other examples that demonstrated the application of different types of mono or bi-metallic catalysts for deoxygenation of bio-oil in *ex-situ* pyrolysis [1,6,26].

The results from previous studies suggested that the substantial deoxygenation of bio-oil could be achieved using *in-situ* and *ex-situ* catalytic pyrolysis. On one hand, *in-situ* pyrolysis could be advantageous to convert oxygenated compounds into hydrocarbons and produce higher liquid yield and on the other hand, *ex-situ* pyrolysis could be effective to achieve a higher hydrocarbon production and less coke formation onto the catalyst. Hence, a combination of *in-situ* and *ex-situ* pyrolysis could be highly significant to obtain an efficient bio-oil deoxygenation. Such an approach for combined *in-situ* and *ex-situ* catalytic pyrolysis has been less explored so far. The literature also indicates that Ni/zeolite and Cu/zeolite catalysts have shown promising results for bio-oil upgrading and the application of Cu/zeolite and Ni/zeolite catalysts for combined *in-situ* and *ex-situ* pyrolysis has not reported to the date. Therefore, this study aimed to prepare Cu/zeolite and Ni/zeolite catalysts and demonstrate their potential for bio-oil deoxygenation in combined *in-situ* and *ex-situ* pyrolysis. These two different catalysts with different catalytic activity could produce more diverse type of hydrocarbons in the bio-oil, which is essential for a quality bio-oil. The catalysts are hypothesized to produce hydrocarbons and other phenolic and acid compounds during *in-situ* pyrolysis which can be further converted to different aliphatic or aromatic hydrocarbons in *ex-situ* pyrolysis by various reactions such as dehydration, cracking, decarboxylation, and decarbonylation. The combined catalytic pyrolysis process could be advantageous to obtain a higher deoxygenation of bio-oil as compared to either *in-situ* or *ex-situ* catalytic pyrolysis.

2. Experimental

2.1. Pine wood biomass

Radiata pine sawdust used in this study was the same sample utilized in the previous study [27]. It contains very low content of ash (0.3%) and a higher proportion of volatile matter (87.5%), while 50.1% of carbon, 6.07% of hydrogen and 43.2% of oxygen is reported in the biomass, and the content of nitrogen and sulphur is very less at 0.21% and 0.08%, respectively [18].

2.2. Synthesis and characterization of catalysts

The zeolite (Silica-25% alumina with 0.35% Na_2O) used in this study was provided in the form of pellets (3 mm) from Saint-Gobain (Paris). The pellets were crushed and sieved with a 40 mesh sieve to obtain the particle size of 0.42 mm. Further, the zeolite was calcined at 550 °C for 2.5 h prior to use in the catalyst preparation. Previous studies

suggest that 10% metal loading in a catalyst is suitable to obtain sufficient number of stronger acid sites and hence for higher bio-oil deoxygenation, while the higher metal percentages reduce the number of stronger acidic sites and result in lower bio-oil deoxygenation [26]. Therefore, Cu10%/zeolite and Ni10%/zeolite catalysts were prepared by a wet-impregnation method. To prepare 15 mg of Cu/zeolite or Ni/zeolite, 5.70 g of $Cu(NO_3)_2.3H_2O$ or 7.43 g of $Ni(NO_3)_2.6H_2O$ was dissolved in 50 ml Milli Q water. Then the required amount of zeolite was slowly added in the metal solution and the ultrasonic vibration at 40 kHz for 2 h was employed for better dispersion of the active metals on the zeolite. The mixture was stirred for 22 h on a magnetic stirrer. The resultant solution was heated on a hot plate at 80 °C to evaporate water and subsequently dried in a vacuum oven at 110 °C overnight. The material was further calcined at 550 °C for 5.5 h. The calcined material was achieved as the final catalyst. The concentration of metals in the catalysts was estimated by X-ray fluorescence (XRF), Olympus Delta Pro spectrometers using Ta tube (50 kV). XRF analysis was repeated three times and an average value has been taken to obtain the final result, which showed that 10.38% of Cu and 12.01% of Ni was present in Cu/zeolite and Ni/zeolite catalysts, respectively.

The prepared catalysts were characterized by XRD on PANalytical X'Pert Pro MPD X-ray diffractometer by employing CuK_α radiations ($\lambda = 1.54056$ Å) and Ni-filter by measuring the X-ray intensity over a diffraction 2θ angle from 5 to 90. The crystallite size of the metal was calculated using the following Scherrer equation:

$$d_{\text{crystallite}}\text{size}(nm) = \frac{0.94\lambda}{B \times \cos\theta} \quad (1)$$

where B is full-width at half-maximum (FWHM) of the most intense peak in the spectrum.

The morphology of the catalyst was examined using TEM (Philips CM10, Netherlands) with an operating voltage of 100 kV and Olympus SIS Megaview G2 digital camera.

N_2 adsorption-desorption isotherms and Brunauer-Emmett-Teller (BET) specific surface areas (SSA) were obtained on a Micromeritics Tristar 3030 instrument at −196 °C. Prior to analysis, the samples were degassed at 150 °C for 3 h under vacuum.

Ammonia temperature programmed desorption (NH_3-TPD) and hydrogen temperature programmed reduction (H_2-TPR) were carried out to analyse the acidity and the presence of reducible metal species in the catalysts, respectively. Both the measurements were conducted on a Micromeritics Autochem 2920 with a thermal conductivity detector (TCD). In the H_2-TPR analysis, approximately 100 mg of sample was loaded into a quartz U-tube atop a plug of quartz wool. The sample was successively pre-treated by heating to 150 °C (at 10 °C/min) and holding for 0.5 h under 20 mL/min Ar (Coregas Ar; > 99.999%), cooled to room temperature and then heated to 850 °C at 5 °C/min under 20 mL/min 10% H_2 in Ar (Coregas, 10.05% H_2 in Ar). Alternatively, in an NH_3-TPD study, ~100 mg of sample was also loaded into the quartz U-tube on a plug of quartz wool. Prior to analysis, the samples were pre-reduced by heating from room temperature to 550 °C at 5 °C/min under 20 mL/min 10% H_2 in Ar with a 1 h hold, subsequently cooled to 50 °C under He (20 mL/min, Coregas He; > 99.999%). Then NH_3 in He (Coregas, 5.13% NH_3 in He) was passed over the sample at 20 mL/min for 2 h at 50 °C. Any physiosorbed NH_3 was purged from the system by holding at 50 °C for 2 h under 20 mL/min prior to heating (in He) at 5 °C/min to 800 °C with a 1 h hold at 800 °C.

2.3. Pyrolysis operation

An infrared image gold furnace (SINKU-RIKO) was used for pyrolysis experiments. All the experiments were carried out at 700 °C with a heating rate of 100 °C/min. The temperature 700 °C was selected because the previous studies demonstrated higher production of hydrocarbons between 650 and 720 °C [7,28]. The biomass and catalysts were loaded in an inner silica fixed bed reactor tube and a surrounding graphite rod was applied to maintain the uniform heat across the reactor tube. Approximately 100 mg of feedstock was utilized in all the experiments, was placed upstream of the catalyst. For *in-situ* pyrolysis, the catalyst was properly mixed with the feedstock. The required amounts of biomass and catalyst were added in a glass vial and manually shaken for 2–3 min to obtain the mixture. In the *ex-situ* mode, the catalyst was placed downstream of the feedstock and in combined pyrolysis mode, Cu/zeolite was used *in-situ* and Ni/zeolite was used *ex-situ*. The quantities of feedstock and catalysts used in all pyrolysis modes are given in Table 1. In all pyrolysis experiments, helium was used as the carrier gas at a flow rate of 50 mL/min.

Table 1
Quantity of feedstock and catalyst used in *in-situ*, *ex-situ* and combined pyrolysis modes.

Catalyst abbreviation	Catalyst type	Quantity of catalyst (mg)	Quantity of feedstock (mg)	C/B
In-situ pyrolysis				
Z-1	Zeolite	100	100	1
Z-3	Zeolite	300	100	3
Z-5	Zeolite	500	100	5
CuZ-1	Cu/zeolite	100	100	1
CuZ-3	Cu/zeolite	300	100	3
CuZ-5	Cu/zeolite	500	100	5
NiZ-1	Ni/zeolite	100	100	1
NiZ-3	Ni/zeolite	300	100	3
NiZ-5	Ni/zeolite	500	100	5
Ex-situ pyrolysis				
Z-1	Zeolite	100	100	1
Z-2	Zeolite	200	100	2
Z-3	Zeolite	300	100	3
CuZ-1	Cu/zeolite	100	100	1
CuZ-2	Cu/zeolite	200	100	2
CuZ-3	Cu/zeolite	300	100	3
NiZ-1	Ni/zeolite	100	100	1
NiZ-2	Ni/zeolite	200	100	2
NiZ-3	Ni/zeolite	300	100	3
Combined Pyrolysis				
CP-2	*In-situ*-Cu/zeolite	100	100	2
	Ex-situ-Ni/zeolite	100		
CP-3	*In-situ*-Cu/zeolite	100	100	3
	Ex-situ-Ni/zeolite	200		
CP-4	*In-situ*-Cu/zeolite	200	100	4
	Ex-situ-Ni/zeolite	200		
CP-5	*In-situ*-Cu/zeolite	300	100	5
	Ex-situ-Ni/zeolite	200		

The bio-oil was collected at room temperature by condensing the pyrolytic organic vapours on quartz wool filled at the tube end. Successively, the bio-oil was then dissolved in dichloromethane (DCM) solvent and filtered through glass wool and sodium sulfate three times each. The solution was analyzed by GC–MS consisting of Agilent 7890B gas chromatograph with an HP-5MS column (60 m × 0.25 μm) coupled with a 5977A mass spectrometer. The oven temperature of the GC stayed initially at 40 °C for 2 min then increased to 310 °C at 2 °C/min. The quadruple mass spectrometer temperature was kept at 150 °C while temperatures of the transfer line and mass spectrometer detector were set to 310 °C. MassHunter software was applied to analyse the compounds with match factor for the database set to over 80. Approximately 200 compounds were detected by MS library in all the bio-oil samples. But 40 compounds with the largest peak areas in each spectrum were selected for the analysis and were further classified in eight major groups, namely aliphatic hydrocarbons, aromatic

hydrocarbons, phenols, acids, nitrogenous compounds (amines, amides and nitriles), furans, aldehydes, ketones and the remaining compounds were designated as others that mainly contained haloalkanes, and thio and silicon-containing compounds.

2.4. Analysis of coke formation

A thermogravimetric analyzer (apparatus model TGA/DSC 1 STARe system, Mettler Toledo, Ltd.) was used for temperature programmed oxidation (TPO) to examine the carbon deposition on the spent catalysts after the *ex-situ* pyrolysis process and the results were compared with fresh catalysts. In the TPO analysis, approximately 20 mg of the catalyst was loaded in the furnace and heated from room temperature to a final temperature of 900 °C at a heating rate of 10 °C/min, using compressed air and nitrogen gas at a flow rate of 100 ml/min and 20 ml/min, respectively. The carbon deposition was estimated by taking the percentage of the difference between initial mass and residual mass of the sample.

The catalysts were also tested to evaluate the stability tests in *ex-situ* pyrolysis mode at 700 °C with a heating rate of 100 °C/min. The catalysts were used for three consecutive runs without any regeneration process. All the tests were performed with a catalyst to biomass ratio of 3. The results are shown in Fig. S2 in the supplementary information.

3. Results & discussion

3.1. Catalyst properties

The physiochemical properties of the prepared catalysts were analyzed by various techniques such as XRD, BET, H_2-TPR, and NH_3-TPD. Fig. 1 represents the XRD diffraction of fresh and spent catalysts (recovered after *ex-situ* pyrolysis reaction). The results revealed that the metals in fresh Cu/zeolite and Ni/zeolite catalysts were in oxide forms that is CuO and NiO, respectively, which were reduced to their metallic form (Cu and Ni) during the pyrolysis reaction. Evidently, fresh Cu/zeolite showed diffraction peaks at 2θ of 35.1°, 39.3°, 48.7°, 53.44°, 58.3°, 61.4°, and 75.2° which can be indexed to (002), (200), (202), (020), (−113), (−311), and (−222) planes of crystalline CuO, respectively and the average crystallite size of CuO was estimated 30.5 nm. Similarly, fresh Ni-zeolite showed the diffraction peaks at 2θ of 37.1°, 43.4°, 62.5°, and 75.5° which were indexed to (111), (200), (220), and (311) planes of crystalline NiO. The crystallite size of NiO in this catalyst was estimated at 7.7 nm. These results were consistent with the standard values of CuO and NiO, well matched with International Centre for Diffraction Data (ICDD) reference codes 00-045-0937 and 01-089-7390. In contrast, the spent catalysts also showed intense diffraction peaks at respective 2θ angles, which can be attributed to the highly crystalline form of Ni and Cu in the catalysts. These findings are in agreement with the previous studies which showed that catalytic pyrolysis reaction can lead to the *in-situ* reduction of metal oxides into their metal forms [25].

Fig. 2 shows TEM images of the catalysts, which indicate that in comparison to sole zeolite, significant morphological changes can be observed for Cu/zeolite and Ni/zeolite catalysts. Therefore, it can be assumed that metal nanoparticles were present on the zeolite support. The metal content in the catalysts was nearly 10%, hence it can be expected that the metal nanoparticles were appropriately dispersed throughout the zeolite support. The lower crystallite size of NiO compared to CuO might indicate its better dispersion on the zeolite, which may result in the improved catalytic activity.

Table 2 compares the specific surface area and porous properties of the catalysts, while Fig. 3 depicts N_2-adsorption-desorption curves and pore distribution in the catalysts. The results demonstrated that sole zeolite exhibited a specific surface area of 412 m^2/g and the catalysts exhibited the characteristic IUPAC type IV isotherm, indicating the mesoporous structure of the catalysts. The addition of CuO or NiO

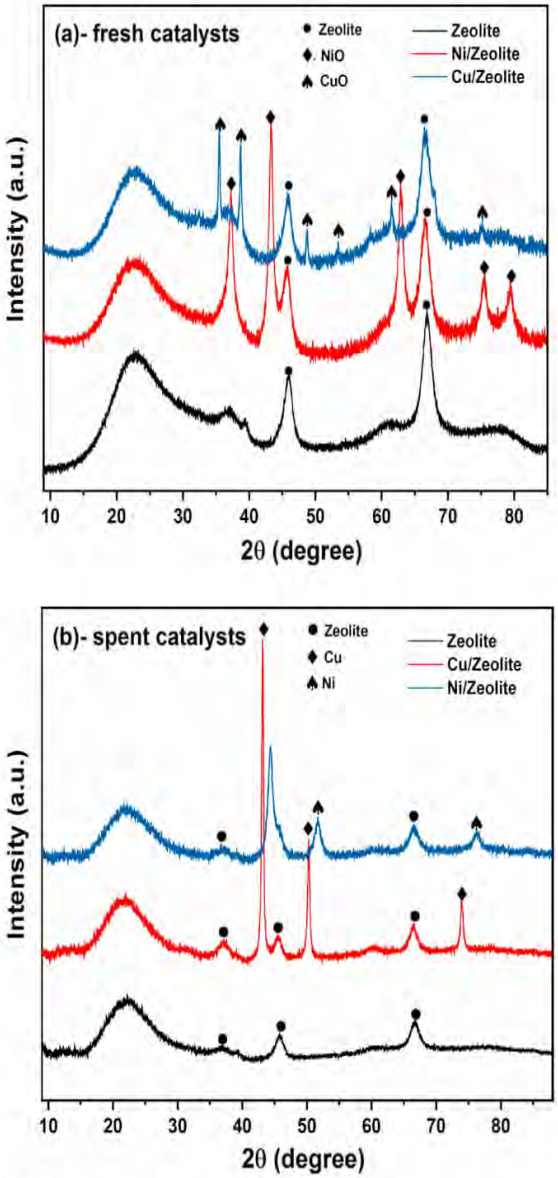

Fig. 1. XRD pattern of (a) fresh zeolite, Cu/zeolite and Ni/zeolite and (b) spent zeolite, Cu/zeolite and Ni/zeolite catalysts.

remarkably decreased the surface area. Noticeably, Ni/zeolite showed a specific surface area of 295 m^2/g, which was 39.6% lower than the sole zeolite and nearly equal percent higher than Cu/zeolite. This decrease in the surface area of the catalysts can be attributed to the incorporation of metal ions onto the surface of zeolite or inside the pores of the zeolite structure. Besides, the total pore volume was found lower in Cu/zeolite and Ni/zeolite as compared to the sole zeolite (0.69 cm^3/g), exhibiting the pore volume of 0.51 and 0.55 cm^3/g, respectively. The reduction of pore volume upon metal loading also indicates the pore blockage, which can be further attributed to the successful loading of the metals on zeolite surface or potential to be within the pores of the zeolite (particularly NiO with a crystal size < 8 nm). These results are in line with previous studies that also showed a decrease in the surface area after the addition of a metal in the catalyst support [29,30]. Besides, the results demonstrated that addition of metals slightly increased the pore diameter in the catalysts compared to sole zeolite (6.51 nm), Cu/zeolite and Ni/zeolite showing an average pore diameter of 7.76 nm and 6.76 nm, respectively. However, in all the catalysts, the pore diameter was found in a range of 2–17 nm. Previous studies suggested that the catalyst with higher pore diameter (*e.g.*, in a range of 30–50 nm) results in more polycyclic aromatic hydrocarbons, which are considered

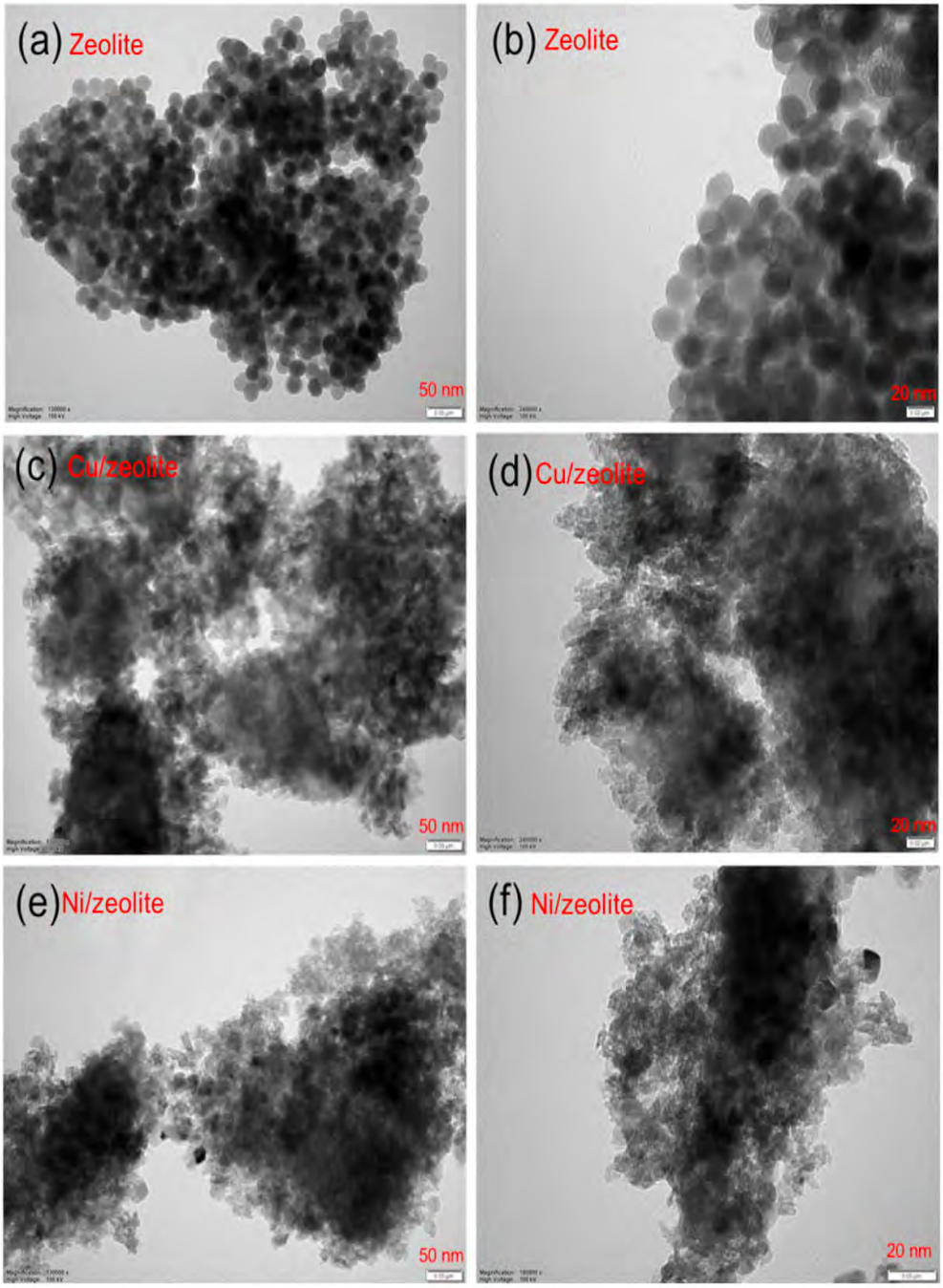

Fig. 2. TEM images of (a, b) zeolite, (c, d) Cu/zeolite, and (e, f) Ni/zeolite.

hazardous to the environment and highly undesirable for a quality bio-oil. For example, Adam et al. [31] demonstrated that MCM-41 based catalysts with increase in pore diameter resulted in the higher production of polycyclic aromatic hydrocarbons.

The acidic characteristics of all the catalysts were analyzed by NH_3-TPD technique. The acidic character in zeolite based catalysts mainly arise due to the presence of Brönsted acidic proton, which consists of a hydrogen atom bonded to the oxygen that connects the tetrahedrally coordinated cation, can be represented as $[M]^{n+}$—H—O [32]. Table 3 and Fig. 1 indicate that total acidity increases with metal loading. Evidently, sole zeolite exhibited a total acidity of 65 μmol/g, while Cu/zeolite and Ni/zeolite showed total acidity of 73 and 94 μmol/g. The extent of the increase is dependent on the metal loaded, with Ni facilitating a greater increase in total acidity. These results support the findings of Iliopoulou et al. [26] who showed that addition of Ni on ZSM-5 support increased the total acidity of the catalyst, ZSM-5

Table 2
BET results of catalysts.

Catalyst	Specific surface area (m^2/g)	Average pore size (nm)	Pore volume (cm^3/g)	Crystallite size of metal oxide (nm)
Zeolite	412	6.51	0.696	–
Cu/zeolite	212	7.76	0.513	30.5
Ni/zeolite	295	6.76	0.552	7.7

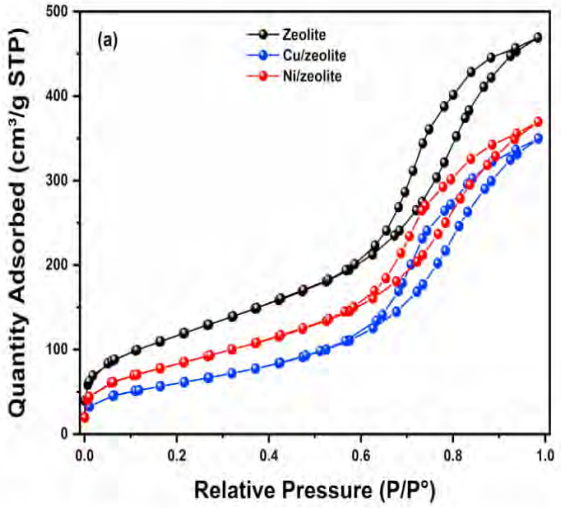

Fig. 3. (a) N_2 adsorption-desorption curves and (b) pore distribution in Cu/zeolite and Ni/zeolite catalysts.

Table 3
Acidity results of catalysts.

Sample	Relative acidity (μmol/g)			Peak Temperature (°C)			Total Acidity (μmol/g)
	a	b	c	a	b	c	
Zeolite	27	–	38	130	–	755	65
Cu/zeolite	–	42	31	–	250	685	73
Ni/zeolite	39	29	26	150	390	790	94

showing the total acidity of 54.6 μmol/g and Ni 5%/ZSM-5 of 76.5 μmol/g, but the addition of 10% Ni decreased the total acidity to 62.8 μmol/g, which was mainly due to the significant decrease in Lewis acidity (from 54.6 to 43.6 μmol/g) while Brönsted acidity was slightly decreased from 21.9 to 19.2 μmol/g [26]. Besides, it can be seen that addition of Cu and Ni created a new peak (b) in the spectra, which can be attributed to the presence of new acidic sites on the zeolite support. Whilst the total acidity increases, it is clear that the distribution and strength of the acidic sites varies significantly. The loading of metal resulted in a reduction in the quantity of strong acidic sites (which can be regarded as Brönsted acid sites), evidenced by the reduction in the higher temperature peak (labelled peak c). Simultaneously, the weak and moderate acidic sites (peaks a and b, which can be ascribed to Lewis acid sites) increased on metal loading. Previous studies showed that the metal loading increases the total acidity of the catalyst, but

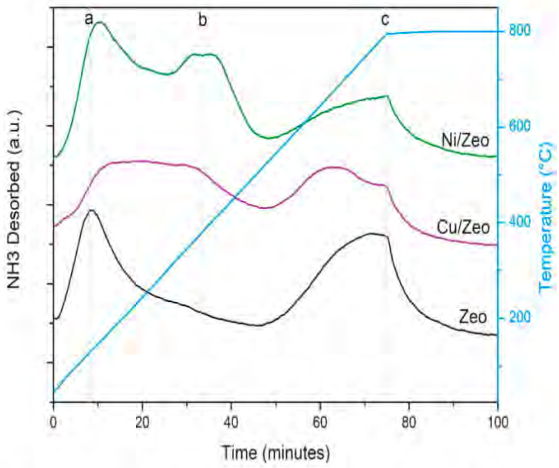

Fig. 4. NH_3-TPD results for zeolite, Cu/zeolite and Ni/zeolite catalysts.

decreases the number of Brönsted acid sites and increases the number of Lewis acid sites [6,26]. Therefore, the increase in total acidity can be mainly attributed to the increase in Lewis acid sites [15,33]. Moreover, the decrease in Brönsted acid sites also suggests that part of the acidic protons in zeolite were ion-exchanged by Cu or Ni ions during the wet-impregnation procedure. Based on the results from previous studies, it can be assumed that the addition of Cu and Ni decreased the number of Brönsted acid sites and increased the number of Lewis acid sites in the catalysts (Fig. 4).

H_2-TPR is a useful technique to analyse the presence of reducible metal species in the catalysts. In a typical H_2-TPR spectrum, a peak indicates the presence of a reducible species, whereas the temperature signifies the interaction of the metal species with zeolite support [34]. For example, a peak at a lower temperature (*e.g.*, 150 °C) suggests weaker or no interaction between the metal particles and the support, in contrast, a peak at the higher temperature (*e.g.*, 550 °C) indicates the stronger interaction between the metal particles and the support that might result from the better dispersion of the metal particles on the zeolite support or successful exchange of metal cations with H^+ in the zeolite structure [4]. Fig. 5 shows H_2-TPR results of Cu/zeolite and Ni/zeolite catalysts. It can be observed from the data that Cu/zeolite showed an intense peak at around 245 °C and a moderate peak at 283 °C, which can be attributed to the reduction of CuO particles in the catalyst. The occurrence of these peaks at the lower temperatures demonstrates a weaker or no interaction with zeolite support and CuO particles are believed to present on the zeolite surface rather inside the

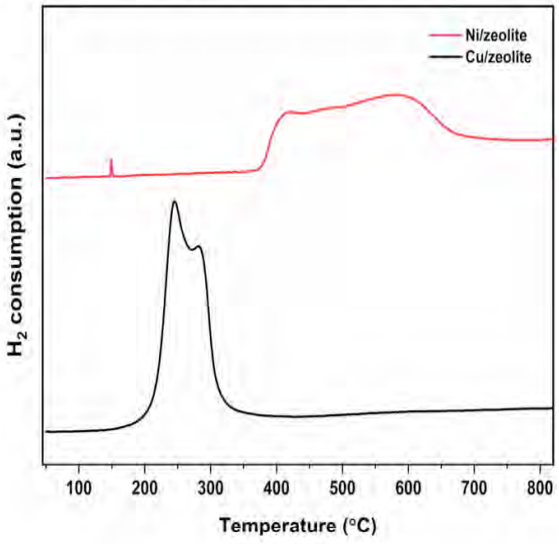

Fig. 5. H_2-TPR results for Cu/zeolite and Ni/zeolite.

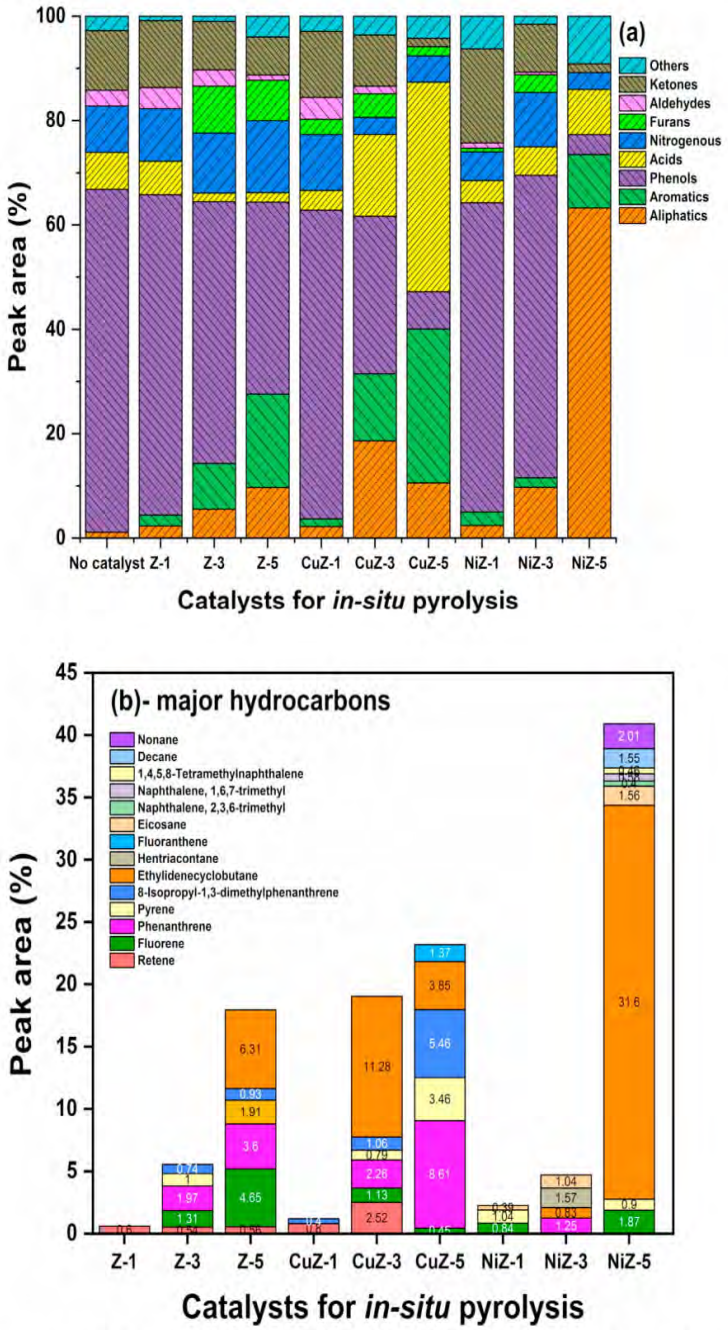

Fig. 6. (a) Bio-oil composition and (b) hydrocarbons obtained from *in-situ* pyrolysis of pine wood at 700 °C with a heating rate of 100 °C/min.

pores as no peaks at the higher temperature were detected in the spectra. Ni/zeolite exhibited two major peaks in the spectra, one at 419 °C and another at 589 °C, corresponding the reduction of NiO particles in the catalyst. In comparison to Cu/zeolite, the peaks were detected at the higher temperatures for Ni/zeolite, which suggested the stronger interaction of NiO particles with the zeolite support. These stronger interactions can be attributed to the smaller crystallite size of NiO particles (as revealed by XRD results) that resulted in its better dispersion on the surface and inside the zeolite support.

3.2. Bio-oil deoxygenation in in-situ pyrolysis

Fig. 6a presents the composition of bio-oil obtained from catalytic and non-catalytic *in-situ* pyrolysis of pine wood. It can be seen from the data that non-catalytic pyrolysis resulted in the bio-oil highly rich in oxygenated compounds, mainly producing approximately 47.5% phenols, 8.28% of ketones and 5.1% acids. This higher proportion of phenols was expected to result in primarily from the pyrolysis of lignin component of the biomass while the production of acids and ketones could be chiefly attributed to the thermal degradation of cellulose, hemicellulose and some portion of lignin [35,36]. Further analysis with the addition of a catalyst showed a significant decrease in the formation of these oxygenated compounds. It was observed that sole zeolite also demonstrated a substantial deoxygenation activity, Z-3 and Z-5 decreased the phenol percentage to 31.8% and 23.9%, respectively. Besides, the proportion of ketones and acids was also found lower in the bio-oil samples with a higher concentration of zeolite catalyst when compared with non-catalytic pyrolysis. It was further noticed that sole zeolite catalyst promoted the formation of furans in the bio-oil such as benzofurans, which can be attributed to the ability of zeolite catalyst to catalyse Diels-Alder condensation reaction, the main route to form furans [37].

The addition of Cu and Ni on the zeolite catalyst showed considerable deoxygenation for phenols, ketones and aldehydes. The

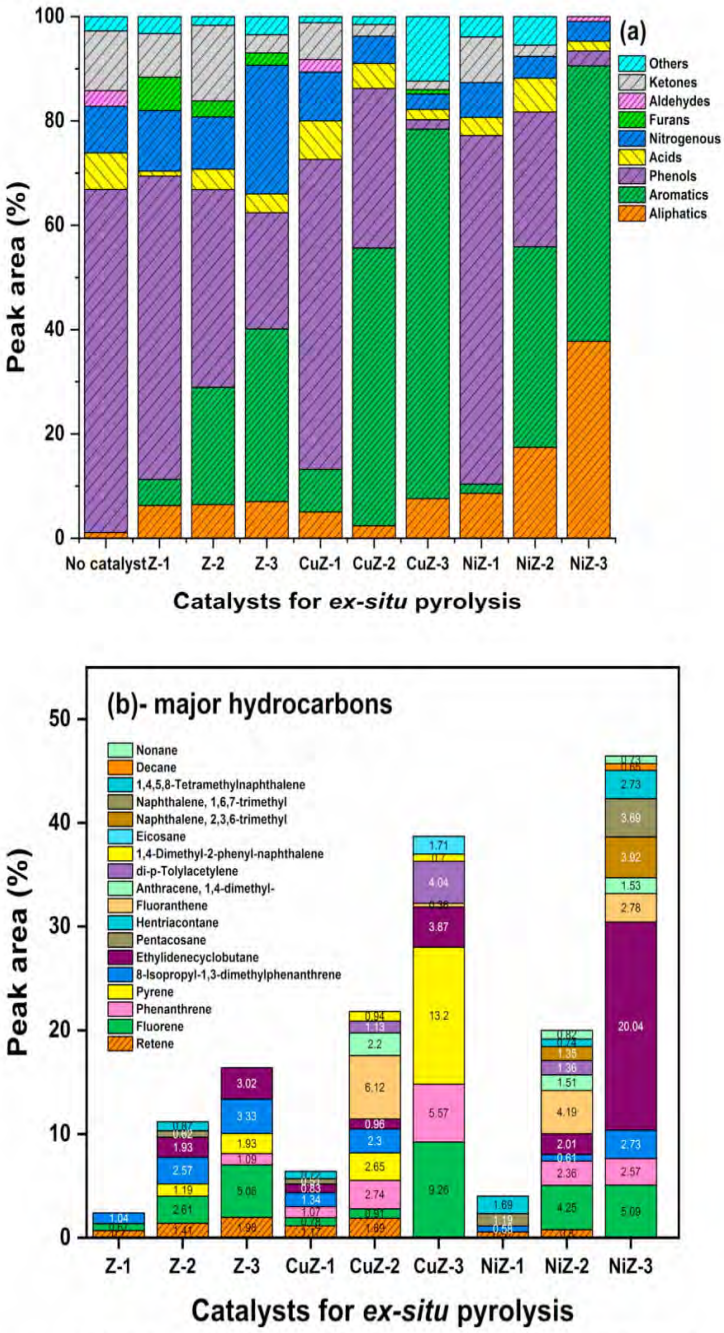

Fig. 7. (a) Bio-oil composition and (b) hydrocarbons obtained from *ex-situ* pyrolysis of pine wood at 700 °C with a heating rate of 100 °C/min.

catalyst with a highest C/B ratio of 5 produced the least proportion of oxygenated compounds and maximum proportion of hydrocarbons in the bio-oil samples. This is because the higher amount of catalyst presented maximum number of active sites to react with pyrolytic vapours, which resulted in enhanced bio-oil deoxygenation and hydrocarbon production as compared to the catalyst with lower C/B ratios. Noticeably, CuZ-5 produced 5.05% of phenols, 1.16% of ketones and NiZ-5 generated 2.24% of phenols, 1.02% of ketones, while no aldehydes were detected in either of the bio-oil samples. Therefore, it could be suggested that the catalysts favoured the deoxygenation pathways, such as dehydration, decarboxylation and decarboxylation to remove these oxygenated compounds [16]. Cu/zeolite and Ni/zeolite catalysts were also assumed to catalyse Diels-Alder condensation reaction as some furans were also detected in the bio-oil. It was noticed that Cu/zeolite catalysts promoted the formation of acids significantly, whereas Ni/zeolite catalysts also increased the concentration of acids slightly in the bio-oil samples and its concentration increased with increase in C/B ratio. For example, CuZ-1 produced 3.11% acids in the bio-oil that increased to 28.58% with CuZ-5. Similarly, NiZ-1 catalysed pyrolysis resulted in 3.14% of acids in the bio-oil that slightly increased to 5.16% with NiZ-5. These results were found contrary to the previous reports, which could be possible due to two reasons. Firstly, the observed results can be attributed to the variations in the porous and acidic properties of zeolite catalysts. It is evident that the acid sites present at the mesopore walls and at the external surface of zeolites participate in the deoxygenation reactions [38]. Therefore, less accessibility of acid sites present at the mesopore walls during *in-situ* process might also results in deviated results. The second potential reason for this could be that the acidic sites at the external surface of zeolites promoted the probable reactions, such as dehydration, C–C bond cleavage, direct C–O cleavage etc. that lead to the depolymerization of cellulose and hemicellulose, which are believed to be the main source for the formation of acids [36,39]. Besides, the better deoxygenation activity of Ni/zeolite compared to Cu/zeolite can be attributed to its higher surface area,

porosity and enhanced number of total acid sites, as suggested by BET and NH_3-TPD results.

Fig. 6b presents the distribution of hydrocarbons produced in the bio-oil samples during *in-situ* pyrolysis of pine wood. The findings suggested that a variety of aromatic and aliphatic hydrocarbons were obtained from the *in-situ* mode of catalytic pyrolysis. Overall, all the catalysts produced a significant amount of hydrocarbons but the production of aliphatic or aromatic hydrocarbons was found selective to the type of catalyst. For example, sole zeolite and Cu/zeolite catalysts produced a higher proportion of aromatic hydrocarbons as compared to aliphatic hydrocarbons, whereas Ni/zeolite catalysts comparatively favoured the production of aliphatic hydrocarbons. For example, Z-5 and CuZ-5 produced 11.66% and 20.97% of aromatic hydrocarbons, respectively, and NiZ-5 yielded 37.5% of aliphatic hydrocarbons and 6.12% of aromatic hydrocarbons in the bio-oil. This is because zeolite and Cu/zeolite catalysts carried out aromatization reactions more efficiently than Ni/zeolite catalysts during *in-situ* pyrolysis mode. The major aliphatic hydrocarbons observed in the bio-oil samples were ethylidenecyclobutane, eicosane, decane, and nonane. It was noticed that a higher content of ethylidenecyclobutane was observed in the bio-oil samples with the higher C/B ratios. For instance, Z-5 and NiZ-5 produced 6.31% and 31.6% of ethylidenecyclobutane in the bio-oils, respectively. The production of ethylidenecyclobutane could be possible mainly by two catalytic pathways favoured by the catalysts. The first could be attributed to the hydrogenation activity of metal cations, which could be exchanged with protons in the zeolite structure. These metal cations can use the hydronium ions for dehydration and the in-situ produced hydrogen gas for hydrogenation reaction to convert the oxygenated compounds into cycloalkanes such as ethylidenecyclobutane [40]. The second route to convert the oxygenated compounds into cycloalkanes could be dehydration and direct cracking reactions [41]. Other aliphatic hydrocarbons such as decane and nonane were observed in the bio-oils with the highest amount of Ni/zeolite catalysts, NiZ-5 producing 1.55% of decane and 2.01% of nonane in the bio-oil. In contrast, the dominant aromatic hydrocarbons were pyrene, retene, fluorene, and phenanthrene in the bio-oil samples catalysed with sole zeolite and Cu/zeolite catalysts, while naphthalenes were also detected in the bio-oils with Ni/zeolite catalysts. The production of higher proportion of hydrocarbons by Ni/zeolite catalysts as compared to Cu/zeolite can be ascribed to its physiochemical properties, such as higher BET surface area compared to Cu/zeolite. Besides, Ni/zeolite also showed higher number of acidic sites (Table 3) that probably acted as the active sites to carry out deoxygenation reactions and aromatization reactions to form aromatic hydrocarbons.

3.3. Bio-oil deoxygenation in ex-situ pyrolysis

Fig. 7a shows the composition of bio-oil obtained from *ex-situ* catalytic pyrolysis of pine wood. These results confirmed that the catalysts behaved differently in *ex-situ* pyrolysis as compared to *in-situ* pyrolysis and the former showed the better conversion of oxygenated compounds than the latter. During *ex-situ* pyrolysis, a C/B ratio of 3 for all the catalysts proved most significant to obtain the maximum bio-oil deoxygenation. This is probably because the higher amount of catalyst presented the highest number of active sites to react with pyrolytic vapours, which resulted in enhanced bio-oil deoxygenation and hydrocarbon production compared to the catalyst with lower C/B ratios. Moreover, a lower C/B ratio (*e.g.*, 3) in *ex-situ* pyrolysis was sufficient and highly significant to deoxygenate the bio-oil in comparison to a higher C/B ratio of 5 used in *in-situ* pyrolysis mode. This finding supports previous research that suggested that a higher amount of the catalyst is required in *in-situ* mode, as the pyrolytic vapours generated during *in-situ* mode could not contact a considerable amount of the catalyst [23]. As shown in Fig. 7a, all the catalysts showed a remarkable reduction in the proportion of all types of oxygenated compounds, and this decrease was observed directly proportional to the increase in the C/B ratio. The addition of Cu or Ni further enhanced the efficiency of the catalysts to deoxygenate the bio-oil. Noticeably, CuZ-3 produced only 1.06% of phenols and 0.97% of ketones. The most noteworthy finding was that Cu/zeolite catalysts favoured the production of acids during the *in-situ* mode of pyrolysis but in *ex-situ* pyrolysis mode, the proportion of acids was greatly reduced. For example, CuZ-3 resulted in 1.16% of acids in the bio-oil as compared to 5.11% achieved with non-catalytic pyrolysis, whereas CuZ-5 in *in-situ* mode produced approximately 28.5% of acids. Similarly, Ni/zeolite catalysts also showed a remarkable tendency to deoxygenate acids in *ex-situ* mode, which were also found to increase the proportion of acids in *in-situ* mode. Vese et al. [15] demonstrated that the extent of bio-oil deoxygenation increases with the amount of Lewis acid sites, which are created by cation incorporation at the external surface and mesopore walls. The study showed that the catalysts such as Cu/ZSM-5 and Mg/ZSM-5 achieved higher deoxygenation rate with increase in Lewis acid sites [12]. The results of current study further indicate that the catalysts were able to catalyze the deoxygenation reactions more efficiently in *ex-situ* mode as compared to *in-situ* mode. In contrary to *in-situ* mode, an insignificant proportion of aldehydes and no ketones were observed in the bio-oil samples with a higher C/B ratio in *ex-situ* mode of pyrolysis, which means the catalysts favoured decarboxylation, decarbonylation and aldol condensation as the main deoxygenation reactions in *ex-situ* mode. In comparison to *in-situ* pyrolysis, the catalysts were assumed not to catalyse Diels-Alder condensation reaction as no furans were detected in the bio-oil samples.

Fig. 7b shows the distribution of main hydrocarbons generated from *ex-situ* pyrolysis of pine wood. The results demonstrated that in *ex-situ* pyrolysis mode, the catalysts produced an almost similar type of hydrocarbons to *in-situ* mode, but a few aromatic hydrocarbons such as pentacosane, anthracene, 1,4-dimethyl, di-p-Tolylacetylene and 1,4-Dimethyl-2-phenyl-naphthalene were also detected in the bio-oil samples from *ex-situ* pyrolysis. The findings also suggested that *ex-situ* pyrolysis resulted in a higher proportion of total hydrocarbons as compared to *in-situ* pyrolysis mode, which indicated that pyrolytic vapours could access extensive catalytic surface in the former mode than the latter, thereby increasing the efficiency of the catalysts for the conversion of oxygenated compounds to hydrocarbons. It can be seen in Fig. 7b that the highest C/B ratio of 3 resulted in the maximum percentage of the hydrocarbons. Similar to *in-situ* pyrolysis, sole zeolite and Cu/zeolite catalysts favoured the production of aromatic hydrocarbons over aliphatic hydrocarbons. However, Ni/zeolite catalysts not only generated a significant amount of aromatic hydrocarbons but also produced a higher number of aliphatic hydrocarbons as compared to the sole zeolite and Cu/zeolite catalysts. Noticeably, NiZ-3 obtained 30.54% of aromatic hydrocarbons and 21.85% of aliphatic hydrocarbons in the bio-oil. This efficient production of hydrocarbons can be attributed to the excellent catalytic activity by Ni cations and physiochemical properties such as higher surface area and enhanced number of acidic sites. The dominant aliphatic hydrocarbon obtained in almost all the bio-samples was ethylidenecyclobutane, NiZ-3 producing its maximum proportion of approximately 20% of the total bio-oil composition. The possible pathway for ethylidenecyclobutane generation could be the similar as discussed in the previous section, mainly *via* hydrogenation activity by metal cations, direct cracking and dehydration reactions [41]. Alternatively, the major aromatic hydrocarbons observed in the bio-oil samples were fluorene, retene, phenanthrene, pyrene, fluoranthene, and naphthalenes. Noticeably, Z-3, CuZ-3, and NiZ-3 produced fluorene of 5.06%, 9.26%, and 5.09%, respectively. A higher percentage of pyrene (5.57%) and phenanthrene (13.2%) was observed in the bio-oil with CuZ-3. The production of aromatic hydrocarbons can be attributed to the aromatization activity carried out by the acidic sites present in the catalysts and other deoxygenations pathways such as dehydration, decarboxylation and decarbonylation that were efficiently catalysed by the catalysts.

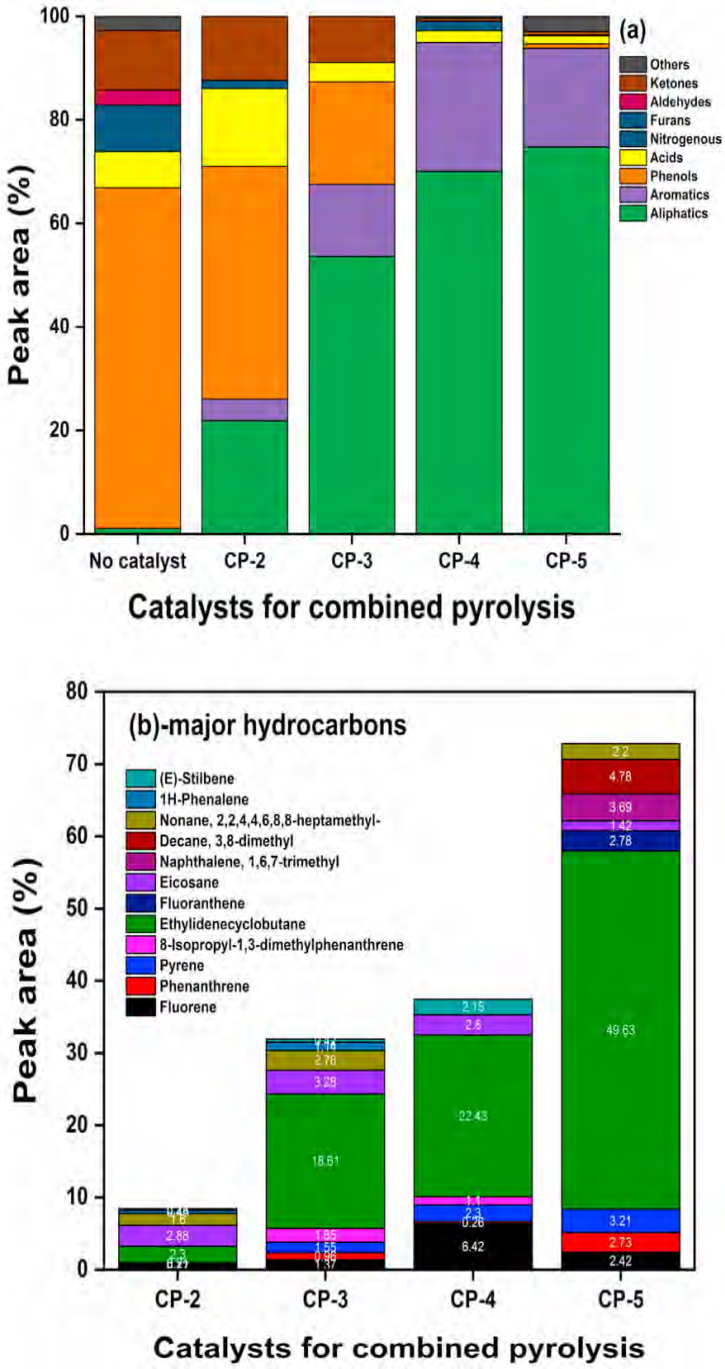

Fig. 8. (a) Bio-oil composition and (b) hydrocarbons obtained from combined pyrolysis of pine wood 700 °C with a heating rate of 100 °C/min.

3.4. Bio-oil deoxygenation in combined in-situ and ex-situ pyrolysis

The sole *in-situ* and *ex-situ* pyrolysis results indicate that Cu/zeolite and Ni/zeolite catalysts favoured the production of both aromatic and aliphatic hydrocarbons. However, Cu/zeolite in *ex-situ* favoured the production of aromatics, while Ni/zeolite in *in-situ* favoured the production of aliphatics. Therefore, to obtain a better quality of bio-oil with aromatic and aliphatic hydrocarbons, in combined pyrolysis, Cu/zeolite was used in *in-situ* mode and Ni/zeolite in *ex-situ* mode. Fig. 8a compares the results of the bio-oil composition obtained with combined *in-situ* and *ex-situ* pyrolysis with different C/B ratios. The results demonstrated that the combined pyrolysis process proved a better approach than the sole *in-situ* or *ex-situ* pyrolysis, and the increasing C/B ratio showed enhanced conversion of the oxygenated compounds. For example, CP-5 converted almost 98% of the oxygenated compounds to hydrocarbons or non-oxygenated compounds, producing only 0.63% of phenols, 0.55% of ketones, while no aldehydes or furans were detected in the bio-oil samples. Similarly, CP-4 also obtained a bio-oil composition with almost negligible oxygenated compounds and rich in hydrocarbons. In the combined pyrolysis approach, it can be assumed that the oxygenated compounds that could not react with the catalyst during *in-situ* process were successfully converted into hydrocarbons or other compounds [42]. Moreover, it can also be suggested that *in-situ* catalysis promoted the formation of acids as indicated by the results of sole *in-situ* pyrolysis (Section 3.2), and because acids contain carbonyl groups, these acid compounds were further converted to various hydrocarbons during *ex-situ* catalysis mainly *via* aldol condensation, decarbonylation and decarboxylation reactions [43]. This enhanced deoxygenation during combined pyrolysis must also be attributed to improved textural and increased acidic properties of the Cu/zeolite and

Ni/zeolite catalysts that helped to convert the oxygenated compounds into hydrocarbons.

Fig. 8b shows the distribution of major hydrocarbons obtained from combined *in-situ* and *ex-situ* pyrolysis. The findings suggested that the combined pyrolysis produced a similar type of hydrocarbons to the sole *in-situ* or *ex-situ* pyrolysis and their proportion increased with rise in C/B ratio. Evidently, CP-5 produced 58.22% of aliphatic compounds and 14.85% of aromatic compounds, whereas CP-1 generated 7.53% of aliphatic hydrocarbons and 1.44% of aromatic hydrocarbons. The results obtained for bio-oil deoxygenation and hydrocarbon production in this study were competitive to previously published studies that utilized combined pyrolysis approach or two-stage *ex-situ* catalytic pyrolysis. For example, the previous study by Lee et al. [44] utilized the combined pyrolysis approach for lignin pyrolysis using natural zeolite in *in-situ* and HZSM-5 in *ex-situ* mode. The study reported 8.69% production of BTEX (benzene, toluene, ethylbenzene, xylenes) and approximately 5% other mono aromatics with a combined pyrolysis approach, while the single stage *ex-situ* pyrolysis with HZSM-5 could produce 5.65% of BTEX [44]. In a separate study, Wang et al. [45] demonstrated the application of red mud and HZSM-5 in a two-stage catalytic pyrolysis of lignin at 550 °C, which reported the formation of 41.27% of monocyclic aromatic hydrocarbons and 22.65% polycyclic aromatic hydrocarbons in the bio-oil [45]. The most dominant hydrocarbon produced in the bio-oil samples from combined pyrolysis was ethylidenecyclobutane, contributing major proportion of the total bio-oil composition, which suggested the main deoxygenation pathways favoured by the catalysts were dehydration and hydrogenation activity [40,41]. The other aliphatic hydrocarbons such as eicosane, decane, and nonane detected in the bio-oil samples were present in comparatively lower proportions. Alternatively, retene, fluorene, phenanthrene, pyrene, and naphthalene were amongst the major aromatic hydrocarbons in the bio-oil samples. Noticeably, the higher proportion of fluorene (6.42%) and naphthalene (3.69%) was achieved in CP-4 and CP-5, respectively. The production of aromatic hydrocarbons can be attributed to the excellent aromatization activity carried out by the acidic sites present in Cu/zeolite and Ni/zeolite catalysts [32]. The oxygenated compounds were also assumed to convert into various hydrocarbons *via* other deoxygenations reactions such as dehydration, decarboxylation, decarbonylation and aldol condensation [32,34,36]. Overall, this study suggested that the combined pyrolysis process in a batch mode could be considered an advantageous approach to achieve the remarkable conversion of the oxygenated compounds into hydrocarbons and consequently, improving the quality of bio-oil. This process could be more economical to achieve efficient bio-oil upgrading in continuous type of pyrolysis reactor which could allow to retrieve the catalyst from the mixture with char and after the effective regeneration process by treating with oxygen it could be used for successive experiments for bio-oil upgrading.

3.5. Analysis of coke deposition on the catalysts

TPO is a useful technique to estimate the deposition of carbonaceous species on the catalysts during the pyrolysis process. The coke formation over the catalysts usually occurs due to the formation of mono or polycyclic aromatic hydrocarbons [6]. It has been also reported that the higher acidity of catalysts can also lead to coke formation, which could ultimately lead to catalyst deactivation [14]. Fig. 9 shows TPO results for fresh and spent catalysts. The results revealed that the total carbon deposition on sole zeolite was estimated to be 10.79 wt%, which was slightly higher than Cu/zeolite (10.35 wt%), whereas Ni/zeolite catalyst achieved the coke deposition of 11.94 wt%. The coke deposition over all the catalysts can be attributed to the accumulation of various types of hydrocarbons on their surface, resulting from the catalytic conversion of oxygenated compounds [17]. As shown in Fig. 9b, all the fresh catalysts did not show any peak in the spectra, indicating the absence of any carbonaceous species or coke formation on the catalysts. However, the sharp and intense peaks can be observed

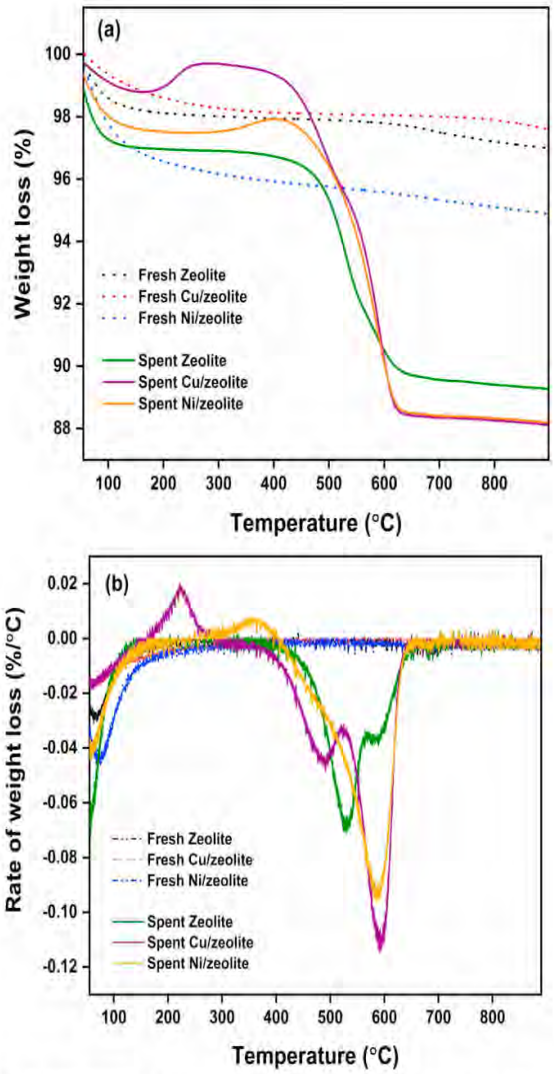

Fig. 9. TPO analysis of fresh and spent catalysts, at a heating rate of 10 °C/min in compressed air with a flow rate of 100 ml/min.

for all the spent catalysts, which demonstrated an effective deposition of carbonaceous species during the pyrolysis reaction. For spent Cu/zeolite and Ni/zeolite, positive peaks were observed at around 220 °C and 390 °C, respectively. This slight weight gain can be attributed to the oxidation of metal particles of Cu and Ni (which are believed to be present in the catalysts after the pyrolysis process) into their oxide forms of CuO or NiO [46,47], while no positive peaks for weight gain were observed for fresh catalysts as the metal particles were already in their oxide forms, as suggested by the XRD results. A similar weight gain was observed in the thermogravimetric analysis by Wolf et al. [46], which was attributed to the oxidation of Pd particles into its oxide forms, such as PdO and PdO_2. It was further noticed that all the spent catalysts showed a peak at a higher temperature of approximately 595 °C, which can be attributed to the presence of almost similar kind of carbon species that may be deposited deep inside the pores of the catalysts or having strong interactions with metal/metal oxide particles or zeolite structure [6]. In addition to this, spent zeolite and Cu/zeolite also showed intense peaks at 530 and 490 °C, respectively, which can be ascribed to the presence of carbon species with comparatively weaker interaction with metal/metal oxide particles/zeolite structure or the carbon species may also be present on the surface of zeolite structure. Overall, this study suggested that the catalysts proved effective to deoxygenate the bio-oil but can also be deactivated by the deposition of carbonaceous species on their surface.

4. Conclusion

The present study successfully demonstrated that Cu/zeolite and Ni/zeolite achieved approximately 98% removal of oxygenated compounds in combined *in-situ* and *ex-situ* pyrolysis (CP-5), which was higher than either sole *in-situ* or *ex-situ* approach. The study also showed that CP-5 achieved the maximum proportion of total hydrocarbons (73%) in the bio-oil, which was higher than NiZ-3 (52%) and CuZ-3 (46%) produced in the bio-oil from *ex-situ* or NiZ-5 (43%) and CuZ-5 (28%) produced in *in-situ* pyrolysis mode. After comparing the bio-oil quality with petroleum crude oil (naphthenes-49%, paraffins-30%, aromatic hydrocarbons-15%), it can be suggested that the combined pyrolysis approach (CP-5) obtained a competitive proportion of aromatic hydrocarbons (~15%) and naphthenes (~48%) but could not produce sufficient paraffins in the bio-oil. The major aliphatic hydrocarbon detected in all the bio-oil samples was ethylidenecyclobutane, while retene, fluorene, phenanthrene, and pyrene were the primary aromatic hydrocarbons in all the bio-oil samples. The enhanced deoxygenation activity and hydrocarbon production by the catalysts can be attributed to the presence of abundant acidic sites insides the pores or on the surface of the catalysts that carried out major deoxygenation reactions, such as dehydration, decarboxylation, decarbonylation, aldol condensation, and aromatization. Overall, this study demonstrated that the combined pyrolysis process could be highly advantageous to achieve the significant conversion of the oxygenated compounds into hydrocarbons and consequently, improving the quality of bio-oil.

Appendix A. Supplementary data

Supplementary material related to this article can be found, in the online version, at doi:https://doi.org/10.1016/j.jaap.2019.03.008.

References

[1] C. Mukarakate, M.J. Watson, J. ten Dam, X. Baucherel, S. Budhi, M.M. Yung, H. Ben, K. Iisa, R.M. Baldwin, M.R. Nimlos, Upgrading biomass pyrolysis vapors over β-zeolites: role of silica-to-alumina ratio, Green Chem. 16 (2014) 4891–4905, https://doi.org/10.1039/C4GC01425A.

[2] H. Weldekidan, V. Strezov, G. Town, Review of solar energy for biofuel extraction, Renew. Sustain. Energy Rev. 88 (2018) 184–192, https://doi.org/10.1016/j.rser.2018.02.027.

[3] P. Ghorbannezhad, M.D. Firouzabadi, A. Ghasemian, P.J. de Wild, H.J. Heeres, Sugarcane bagasse ex-situ catalytic fast pyrolysis for the production of Benzene, Toluene and Xylenes (BTX), J. Anal. Appl. Pyrolysis 131 (2018) 1–8, https://doi.org/10.1016/j.jaap.2018.02.019.

[4] Y. Zheng, F. Wang, X. Yang, Y. Huang, C. Liu, Z. Zheng, J. Gu, Study on aromatics production via the catalytic pyrolysis vapor upgrading of biomass using metal-loaded modified H-ZSM-5, J. Anal. Appl. Pyrolysis 126 (2017) 169–179, https://doi.org/10.1016/j.jaap.2017.06.011.

[5] C. Li, J. Ma, Z. Xiao, S.B. Hector, R. Liu, S. Zuo, X. Xie, A. Zhang, H. Wu, Q. Liu, Catalytic cracking of Swida wilsoniana oil for hydrocarbon biofuel over Cu-modified ZSM-5 zeolite, Fuel. 218 (2018) 59–66, https://doi.org/10.1016/j.fuel.2018.01.026.

[6] W.B. Widayatno, G. Guan, J. Rizkiana, J. Yang, X. Hao, A. Tsutsumi, A. Abudula, Upgrading of bio-oil from biomass pyrolysis over Cu-modified β-zeolite catalyst with high selectivity and stability, Appl. Catal. B Environ. 186 (2016) 166–172, https://doi.org/10.1016/j.apcatb.2016.01.006.

[7] H. Weldekidan, V. Strezov, T. Kan, G. Town, Waste to energy conversion of chicken litter through a solar-driven pyrolysis process, Energy Fuels 32 (2018) 4341–4349, https://doi.org/10.1021/acs.energyfuels.7b02977.

[8] T. Kan, V. Strezov, T.J. Evans, Lignocellulosic biomass pyrolysis: a review of product properties and effects of pyrolysis parameters, Renew. Sustain. Energy Rev. 57 (2016) 1126–1140, https://doi.org/10.1016/j.rser.2015.12.185.

[9] D. Mohan, C.U. Pittman, P.H. Steele, Pyrolysis of wood/biomass for bio-oil: a critical review, Energy Fuels 20 (2006) 848–889, https://doi.org/10.1021/ef0502397.

[10] R. Kumar, V. Strezov, E. Lovell, T. Kan, H. Weldekidan, J. He, B. Dastjerdi, J. Scott, Bio-oil upgrading with catalytic pyrolysis of biomass using Copper/zeolite-Nickel/zeolite and Copper-Nickel/zeolite catalysts, Bioresour. Technol. 279 (2019) 404–409, https://doi.org/10.1016/j.biortech.2019.01.067.

[11] J. He, V. Strezov, T. Kan, H. Weldekidan, S. Asumadu-Sarkodie, R. Kumar, Effect of temperature on heavy metal(loid) deportment during pyrolysis of Avicennia marina biomass obtained from phytoremediation, Bioresour. Technol. 278 (2019) 214–222, https://doi.org/10.1016/j.biortech.2019.01.101.

[12] X. Huo, J. Xiao, M. Song, L. Zhu, Comparison between in-situ and ex-situ catalytic pyrolysis of sawdust for gas production, J. Anal. Appl. Pyrolysis 135 (2018) 189–198, https://doi.org/10.1016/j.jaap.2018.09.003.

[13] X. Chen, H. Yang, Y. Chen, W. Chen, T. Lei, W. Zhang, H. Chen, Catalytic fast pyrolysis of biomass to produce furfural using heterogeneous catalysts, J. Anal. Appl. Pyrolysis 127 (2017) 292–298, https://doi.org/10.1016/j.jaap.2017.07.022.

[14] A. Galadima, O. Muraza, In situ fast pyrolysis of biomass with zeolite catalysts for bioaromatics/gasoline production: a review, Energy Convers. Manage. 105 (2015) 338–354, https://doi.org/10.1016/j.enconman.2015.07.078.

[15] A. Veses, B. Puértolas, J.M. López, M.S. Callén, B. Solsona, T. García, Promoting deoxygenation of bio-oil by metal-loaded hierarchical ZSM-5 zeolites, ACS Sustain. Chem. Eng. 4 (2016) 1653–1660, https://doi.org/10.1021/acssuschemeng.5b01606.

[16] J. Zhang, B. Fidalgo, A. Kolios, D. Shen, S. Gu, Mechanism of deoxygenation in anisole decomposition over single-metal loaded HZSM-5: experimental study, Chem. Eng. J. 336 (2018) 211–222, https://doi.org/10.1016/j.cej.2017.11.128.

[17] C. Zhao, J.A. Lercher, Upgrading pyrolysis oil over Ni/HZSM-5 by cascade reactions, Angew. Chem. 124 (2012) 6037–6042, https://doi.org/10.1002/ange.201108306.

[18] D.P. Gamliel, S. Du, G.M. Bollas, J.A. Valla, Investigation of in situ and ex situ catalytic pyrolysis of miscanthus × giganteus using a PyGC–MS microsystem and comparison with a bench-scale spouted-bed reactor, Bioresour. Technol. 191 (2015) 187–196, https://doi.org/10.1016/j.biortech.2015.04.129.

[19] C. Hu, R. Xiao, H. Zhang, Ex-situ catalytic fast pyrolysis of biomass over HZSM-5 in a two-stage fluidized-bed/fixed-bed combination reactor, Bioresour. Technol. 243 (2017) 1133–1140, https://doi.org/10.1016/j.biortech.2017.07.011.

[20] S.D. Stefanidis, K.G. Kalogiannis, E.F. Iliopoulou, A.A. Lappas, P.A. Pilavachi, In-situ upgrading of biomass pyrolysis vapors: catalyst screening on a fixed bed reactor, Bioresour. Technol. 102 (2011) 8261–8267, https://doi.org/10.1016/j.biortech.2011.06.032.

[21] Y. Zhang, P. Chen, H. Lou, In situ catalytic conversion of biomass fast pyrolysis vapors on HZSM-5, J. Energy Chem. 25 (2016) 427–433, https://doi.org/10.1016/j.jechem.2016.03.014.

[22] K. Wang, P.A. Johnston, R.C. Brown, Comparison of in-situ and ex-situ catalytic pyrolysis in a micro-reactor system, Bioresour. Technol. 173 (2014) 124–131, https://doi.org/10.1016/j.biortech.2014.09.097.

[23] K. Iisa, R.J. French, K.A. Orton, M.M. Yung, D.K. Johnson, J. ten Dam, M.J. Watson, M.R. Nimlos, In situ and ex situ catalytic pyrolysis of pine in a bench-scale fluidized bed reactor system, Energy Fuels 30 (2016) 2144–2157, https://doi.org/10.1021/acs.energyfuels.5b02165.

[24] A. Veses, B. Puértolas, M.S. Callén, T. García, Catalytic upgrading of biomass derived pyrolysis vapors over metal-loaded ZSM-5 zeolites: effect of different metal cations on the bio-oil final properties, Microporous Mesoporous Mater. 209 (2015) 189–196, https://doi.org/10.1016/j.micromeso.2015.01.012.

[25] M.M. Yung, A.K. Starace, C. Mukarakate, A.M. Crow, M.A. Leshnov, K.A. Magrini, Biomass catalytic pyrolysis on Ni/ZSM-5: effects of nickel pretreatment and loading, Energy Fuels 30 (2016) 5259–5268, https://doi.org/10.1021/acs.energyfuels.6b00239.

[26] E.F. Iliopoulou, S.D. Stefanidis, K.G. Kalogiannis, A. Delimitis, A.A. Lappas, K.S. Triantafyllidis, Catalytic upgrading of biomass pyrolysis vapors using transition metal-modified ZSM-5 zeolite, Appl. Catal. B Environ. 127 (2012) 281–290, https://doi.org/10.1016/j.apcatb.2012.08.030.

[27] V. Strezov, B. Moghtaderi, J.A. Lucas, Thermal Study of Decomposition of Selected Biomass Samples, (2003), p. 8.

[28] M. Garcia-Perez, X.S. Wang, J. Shen, M.J. Rhodes, F. Tian, W.-J. Lee, H. Wu, C.-Z. Li, Fast pyrolysis of oil mallee woody biomass: effect of temperature on the yield and quality of pyrolysis products, Ind. Eng. Chem. Res. 47 (2008) 1846–1854, https://doi.org/10.1021/ie071497p.

[29] P. Li, D. Li, H. Yang, X. Wang, H. Chen, Effects of Fe-, Zr-, and Co-modified zeolites and pretreatments on catalytic upgrading of biomass fast pyrolysis vapors, Energy Fuels 30 (2016) 3004–3013, https://doi.org/10.1021/acs.energyfuels.5b02894.

[30] A.J. Maia, B. Louis, Y.L. Lam, M.M. Pereira, Ni-ZSM-5 catalysts: detailed characterization of metal sites for proper catalyst design, J. Catal. 269 (2010) 103–109, https://doi.org/10.1016/j.jcat.2009.10.021.

[31] J. Adam, E. Antonakou, A. Lappas, M. Stöcker, M.H. Nilsen, A. Bouzga, J.E. Hustad, G. Øye, In situ catalytic upgrading of biomass derived fast pyrolysis vapours in a fixed bed reactor using mesoporous materials, Microporous Mesoporous Mater. 96 (2006) 93–101, https://doi.org/10.1016/j.micromeso.2006.06.021.

[32] H. Hernando, A.M. Hernández-Giménez, C. Ochoa-Hernández, P.C.A. Bruijnincx, K. Houben, M. Baldus, P. Pizarro, J.M. Coronado, J. Fermoso, J. Čejka, B.M. Weckhuysen, D.P. Serrano, Engineering the acidity and accessibility of the zeolite ZSM-5 for efficient bio-oil upgrading in catalytic pyrolysis of lignocellulose, Green Chem. (2018), https://doi.org/10.1039/C8GC01722K.

[33] X.-Y. Ren, J.-P. Cao, X.-Y. Zhao, Z. Yang, T.-L. Liu, X. Fan, Y.-P. Zhao, X.-Y. Wei, Catalytic upgrading of pyrolysis vapors from lignite over mono/bimetal-loaded mesoporous HZSM-5, Fuel 218 (2018) 33–40, https://doi.org/10.1016/j.fuel.2018.01.017.

[34] G. Dai, S. Wang, S. Huang, Q. Zou, Enhancement of aromatics production from catalytic pyrolysis of biomass over HZSM-5 modified by chemical liquid deposition, J. Anal. Appl. Pyrolysis (2018), https://doi.org/10.1016/j.jaap.2018.07.010.

[35] V.B.F. Custodis, P. Hemberger, Z. Ma, J.A. van Bokhoven, Mechanism of fast pyrolysis of lignin: studying model compounds, J. Phys. Chem. B 118 (2014) 8524–8531, https://doi.org/10.1021/jp5036579.

[36] H. Yang, R. Yan, H. Chen, D.H. Lee, C. Zheng, Characteristics of hemicellulose, cellulose and lignin pyrolysis, Fuel 86 (2007) 1781–1788, https://doi.org/10.1016/j.fuel.2006.12.013.

[37] Y.-T. Cheng, G.W. Huber, Chemistry of furan conversion into aromatics and olefins over HZSM-5: a model biomass conversion reaction, ACS Catal. 1 (2011) 611–628,

https://doi.org/10.1021/cs200103j.
[38] B. Puértolas, A. Veses, M.S. Callén, S. Mitchell, T. García, J. Pérez-Ramírez, Porosity-acidity interplay in hierarchical ZSM-5 zeolites for pyrolysis oil valorization to aromatics, ChemSusChem 8 (2015) 3283–3293, https://doi.org/10.1002/cssc.201500685.
[39] P.R. Patwardhan, R.C. Brown, B.H. Shanks, Product distribution from the fast pyrolysis of hemicellulose, ChemSusChem 4 (2011) 636–643, https://doi.org/10.1002/cssc.201000425.
[40] C. Zhao, Y. Kou, A.A. Lemonidou, X. Li, J.A. Lercher, Highly selective catalytic conversion of phenolic bio-oil to alkanes, Angew. Chem. 121 (2009) 4047–4050, https://doi.org/10.1002/ange.200900404.
[41] B. Op de Beeck, M. Dusselier, J. Geboers, J. Holsbeek, E. Morré, S. Oswald, L. Giebeler, B.F. Sels, Direct catalytic conversion of cellulose to liquid straight-chain alkanes, Energy Environ. Sci. 8 (2015) 230–240, https://doi.org/10.1039/C4EE01523A.
[42] A.G. Gayubo, A.T. Aguayo, A. Atutxa, R. Aguado, J. Bilbao, Transformation of oxygenate components of biomass pyrolysis oil on a HZSM-5 zeolite. I. Alcohols and Phenols, Ind. Eng. Chem. Res. 43 (2004) 2610–2618, https://doi.org/10.1021/ie030791o.
[43] A.G. Gayubo, A.T. Aguayo, A. Atutxa, R. Aguado, M. Olazar, J. Bilbao, Transformation of oxygenate components of biomass pyrolysis oil on a HZSM-5 zeolite. II. Aldehydes, ketones, and acids, Ind. Eng. Chem. Res. 43 (2004) 2619–2626, https://doi.org/10.1021/ie030792g.
[44] H.W. Lee, Y.-M. Kim, J. Jae, B.H. Sung, S.-C. Jung, S.C. Kim, J.-K. Jeon, Y.-K. Park, Catalytic pyrolysis of lignin using a two-stage fixed bed reactor comprised of in-situ natural zeolite and ex-situ HZSM-5, J. Anal. Appl. Pyrolysis 122 (2016) 282–288, https://doi.org/10.1016/j.jaap.2016.09.015.
[45] S. Wang, Z. Li, X. Bai, W. Yi, P. Fu, Catalytic pyrolysis of lignin in a cascade dual-catalyst system of modified red mud and HZSM-5 for aromatic hydrocarbon production, Bioresour. Technol. 278 (2019) 66–72, https://doi.org/10.1016/j.biortech.2019.01.037.
[46] M.M. Wolf, H. Zhu, W.H. Green, G.S. Jackson, Kinetic model for polycrystalline Pd/PdOx in oxidation/reduction cycles, Appl. Catal. A Gen. 244 (2003) 323–340, https://doi.org/10.1016/S0926-860X(02)00604-X.
[47] A.W. Coats, J.P. Redfern, Thermogravimetric analysis. A review, Analyst 88 (1963) 906, https://doi.org/10.1039/an9638800906.

MACQUARIE University

MACQUARIE UNIVERSITY
AUTHORSHIP CONTRIBUTION STATEMENT

In accordance with the *Macquarie University Code for the Responsible Conduct of Research* and the *Authorship Standard*, researchers have a responsibility to their colleagues and the wider community to treat others fairly and with respect, to give credit where appropriate to those who have contributed to research.

Note for HDR students: *Where research papers are being included in a thesis, this template must be used to document the contribution of authors to each of the proposed or published research papers. The contribution of the candidate must be sufficient to justify inclusion of the paper in the thesis.*

1. DETAILS OF PUBLICATION & CORRESPONDING AUTHOR

Title of Publication (can be a holding title)		**Publication Status** Choose an item.
Investigating the effect of mono/bi-metallic-zeolite catalysts on the selectivity of hydrocarbons during bio-oil upgrading from ex-situ pyrolysis of biomass		☐ In Progress or Unpublished work for thesis submission ☐ Submitted for Publication ☐ Accepted for Publication ■ Published
Name of **corresponding author**	Department/Faculty	**Publication details:** indicate the name of the journal/ conference/ publisher/other outlet
Vladimir Strezov, Tao Kan	Earth and Environmental Sciences/ Science & Engineering	Energy & Fuels

2. STUDENTS DECLARATION (if applicable)

Name of HDR thesis author (If the same as corresponding author - write "as above")	Department/Faculty	Thesis title
Ravinder Kumar	Earth and Environmental Sciences /Science & Engineering	Catalytic Upgrading of Bio-oil Produced from Fast Pyrolysis of Pinewood Sawdust

Description of HDR thesis author's contribution to planning, execution, and preparation of the work if there are multiple authors

(for example, how much as a percent did you contribute to the conception of the project, the design of methodology or experimental protocol, data collection, analysis, drafting the manuscript, revising it critically for important intellectual content, etc.)

In this article, I contributed in designing the project, carried out 70% of the experimental work, analyzed the data and wrote 80% of the manuscript.

I declare that the above is an accurate description of my contribution to this publication, and the contributions of other authors are as described below.	**Student signature** **Date**	02/22/2021

MACQUARIE University

3. Description of all other author contributions

Use an Asterisk * to denote if the author is also a current student or HDR candidate.

The HDR candidate or corresponding author must, for each paper, list all authors and provide details of their role in the publication. Where possible, also provide a percentage estimate of the contribution made by each author.

Name and affiliation of author	**Intellectual contribution(s)** (for example to the: conception of the project, design of methodology/experimental protocol, data collection, analysis, drafting the manuscript, revising it critically for important intellectual content etc.)
Vladimir Strezov Macquarie University	conception, supervision, critical revision
Tao Kan Macquarie University	conception, supervision, experimental, critical revision
Haftom Weldekidan Macquarie University	experimental, critical revision
Jing He Macquarie University	experimental, critical revision
Sayka Jahan Macquarie University	experimental, critical revision
	Provide summary for any additional Authors in this cell.

4. Author Declarations

I agree to be named as one of the authors of this work, and confirm:

i. *that I have met the authorship criteria set out in the* Authorship Standard, *accompanying the* Macquarie University Research Code,

ii. *that there are no other authors according to these criteria,*

iii. *that the description in Section 3 or 4 of my contribution(s) to this publication is accurate*

iv. *that I have agreed to the planned authorship order following the* Authorship Standard

Name of author	**Authorised *** By Signature or refer to other written record of aporoval (eg. pdf of a signed agreement or an email record)	**Date**
Vladimir Strezov		24/02/2021
Tao Kan		22/02/2021
Haftom Weldekidan		22/02/202
Jing He		22/02/2021
Sayka Jahan		25/02/2021
	Provide other written record of approval for additional authors (eg. pdf of a signed agreement or an email record)	

5. Data storage

The original data for this project are stored in the following location, in accordance with the *Research Data Management Standard* accompanying the *Macquarie University Research Code*.

If the data have been or will be deposited in an online repository, provide the details here with any corresponding DOI.

Data description/format	**Storage Location or DOI**	**Name of custodian** if other than the corresponding author

A copy of this form must be retained by the corresponding author and must accompany the thesis submitted for examination.

Chapter 6

Investigating the effect of mono and bimetallic/zeolite catalysts on hydrocarbon production during bio-oil upgrading from *ex-situ* pyrolysis of biomass

Ravinder Kumar, Vladimir Strezov, Tao Kan, Haftom Weldekidan, Jing He, Sayka Jahan

Department of Earth and Environmental Sciences, Faculty of Science & Engineering, Macquarie University, Sydney, NSW 2109, Australia

The previous chapter suggests that *ex-situ* pyrolysis is economically better than other pyrolysis modes and also showed outstanding bio-oil deoxygenation. Therefore, further experiments were conducted in *ex-situ* pyrolysis mode. This chapter aims to compare the bio-oil deoxygenation between monometallic and bimetallic catalysts. To achieve this, monometallic catalysts (Cu/zeolite and Ni/zeolite) and a bimetallic (CuNi/zeolite) were prepared using dry-impregnation method and employed in one-stage *ex-situ* pyrolysis mode. Preparation of catalysts and characterization results of catalysts are provided in supporting information.

Reprinted (adapted) with permission from Kumar, R., Strezov, V., Kan, T., Weldekidan, H., He, J., & Jahan, S. (2020). Investigating the effect of mono and bimetallic/zeolite catalysts on hydrocarbon production during bio-oil upgrading from ex-situ pyrolysis of biomass. Energy and Fuels, 34(1), 389-400. https://doi.org/10.1021/acs.energyfuels.9b02724.

energy&fuels

Article

Cite This: Energy Fuels 2020, 34, 389−400

pubs.acs.org/EF

Investigating the Effect of Mono- and Bimetallic/Zeolite Catalysts on Hydrocarbon Production during Bio-oil Upgrading from *Ex Situ* Pyrolysis of Biomass

Ravinder Kumar, Vladimir Strezov,* Tao Kan,* Haftom Weldekidan, Jing He, and Sayka Jahan

Department of Earth and Environmental Sciences, Faculty of Science & Engineering, Macquarie University, Sydney, New South Wales 2109, Australia

Supporting Information

ABSTRACT: Catalytic fast pyrolysis of biomass offers an opportunity for upgrading of pyrolysis bio-oils using mono- and bimetallic-supported catalysts, which have been demonstrated to improve the bio-oil qualities. However, the influence of mono- and bimetallic catalysts on different pyrolytic products is less explored. Therefore, this study aimed to examine the effect of mono- and bimetallic catalysts on different pyrolytic products with more emphasis on bio-oil upgrading from *ex situ* pyrolysis of pine wood biomass. Cu/zeolite and Ni/zeolite were used as the monometallic catalysts, while CuNi/zeolite was used as the bimetallic catalyst in the study. The catalysts were used in *ex situ* pyrolysis with three different catalyst/biomass ratios: 1, 2, and 3. The results revealed that mono- and bimetallic catalysts with the highest catalyst/biomass ratio of 3 obtained the minimum percentage of oxygen-containing compounds in the bio-oils compared to the sole zeolite. For instance, Cu/zeolite and Ni/zeolite with a catalyst/biomass ratio of 3 (CuZ-2 and NiZ-3) produced the total proportion of hydrocarbons of 50.8 and 41.8%, respectively, while the bimetallic catalyst produced the total hydrocarbons of 54.5% in the bio-oil. It was further revealed that Cu/zeolite favored production of aliphatic hydrocarbons, such as ethylidenecyclobutane and cyclohexene, with CuZ-3 producing 49.6% aliphatic hydrocarbons and 1.25% aromatic hydrocarbons, while Ni/zeolite produced both aromatic and aliphatic hydrocarbons, with NiZ-3 producing 26.8% aromatic hydrocarbons and 15.1% aliphatic hydrocarbons in the bio-oils. The main aromatic hydrocarbons found in the bio-oil were benzene, naphthalene, and phenanthrene. CuNi/zeolite showed better deoxygenation efficiency than monometallic catalysts and produced a comparatively higher percentage of aromatic hydrocarbons at 14.3% and aliphatic hydrocarbons at 39.9%. The main deoxygenation pathway during monometallic catalytic pyrolysis was found to be dehydration and decarboxylation because a higher CO_2 yield was observed during the reaction. The CuNi/zeolite converted the oxygenated compounds into hydrocarbons via dehydration, decarboxylation, and decarbonylation because higher yields of both CO_2 and CO were observed. Overall, CuNi/zeolite catalytic pyrolysis of biomass resulted in improved bio-oil quality when compared to the monometallic counterparts.

1. INTRODUCTION

In the last 3 decades, fast pyrolysis (FP) has gained increasing interest for the production of sustainable biofuels from lignocellulosic biomass or biomass waste materials.[1−4] FP is generally termed as the fast heating of biomass in an inert atmosphere to depolymerize biomass into various multiphase renewable biofuels, mainly liquids (bio-oil or pyrolytic oil), gases (hydrocarbons, H_2, CO_2, and CO), and biochar in a solid phase.[5,6] FP is an efficient and promising way to mitigate the overdependence upon fossil fuels, simultaneously leading to the development of a sustainable economy. However, biofuels generated through FP cannot be directly used for any application. For example, bio-oil produced from FP generally contains highly oxygenated compounds, such as alcohols, phenols, acids, and ketones. Furthermore, its low pH, high instability, and low calorific value are among the major limitations that restrict the use of bio-oil at a commercial scale. It is therefore imperative to improve the overall bio-oil properties to develop into a potential transportation fuel.

Catalytic fast pyrolysis (CFP) is considered an efficient approach to convert oxygen-rich bio-oil compounds into aromatic or aliphatic hydrocarbons, thereby enhancing the bio-oil quality.[7−9] On the basis of the application of a catalyst, there are two types of pyrolysis processes, that is, either *in situ*, where a catalyst is combined with biomass, or *ex situ*, where a catalyst is placed separately at a certain distance from the biomass and the produced vapors are passed through the catalyst bed.[10,11] In practice, *ex situ* pyrolysis is economically advantageous over *in situ* because the catalyst can be easily recovered in the former process and can be further reused in the pyrolysis. A plethora of catalysts have been successfully investigated for bio-oil upgrading, which have shown a considerable decrease in the oxygenated compounds and an increase in the content of aromatic or aliphatic hydrocarbons and calorific values.[12−16] Zeolite-based catalysts (e.g., Ni/ZSM-5, Fe/HZSM-5, etc.) have shown the best deoxygenation activity for bio-oil upgrading and are the most widely used heterogeneous catalysts in petrochemical refineries. This is mainly because of their acidity and micro-/mesoporosity, which allows for the diffusion of the reactant molecules into the zeolite structure and access to its internal active sites.[10,17,18] Zeolites contain SiO_4 and a negatively charged $[AlO_4]^-$

Received: August 15, 2019
Revised: November 25, 2019
Published: November 27, 2019

DOI: 10.1021/acs.energyfuels.9b02724
Energy Fuels 2020, 34, 389−400

tetrahedra, which is compensated by a cation to ensure electroneutrality. Because of the bond between these counter cations and the ionic nature of the zeolite framework, the cation can be easily exchanged by a proton or other type of cations without changing the crystalline structure of the material. The presence of a proton, as bridging hydroxyl groups between the tetrahedral framework of Si and Al atoms, results in the acidic character of zeolites. This acidic character of zeolites is considered useful for bio-oil deoxygenation.[19] However, a high number of acid sites may favor the formation of aromatic hydrocarbons but can also simultaneously enhance the production of coke or carbonaceous species, which may lead to the rapid deactivation of the catalyst.[20] Therefore, it is highly important to balance the number as well as type of acid sites in a catalyst to achieve higher deoxygenation and minimize charring. Moreover, sole zeolite catalysts deoxygenate the bio-oil mainly via the dehydration reaction at lower temperatures, which decreases the availability of hydrogen atoms because H_2O is removed in the main deoxygenation pathway.[21] Therefore, the addition of a transition metal at an optimized proportion can be useful to improve the deoxygenation activity of zeolite-based catalysts. The metal ions can be dispersed on the catalyst surface or can be introduced as the compensation cations in the zeolite structure. Additionally, it has been suggested that the metals on the zeolite catalyst promote decarboxylation and decarbonylation reactions, thereby maintaining more hydrogen atoms, which can be used for hydrocarbon production.[22−24]

Several studies have been applied for a number of metal/zeolite catalysts for bio-oil upgrading, showing a significant increase in aromatic and aliphatic hydrocarbons.[15,25−27] For example, Zheng et al.[25] prepared six catalysts using different metals (Cu, Mg, Zn, Ga, Ni, and Co) using H-ZSM-5 as the support and applied for *ex situ* upgrading of the pine wood bio-oil. All metal-loaded/H-ZSM-5 catalysts selectively increased the concentration of mono- and polycyclic aromatic hydrocarbons.[25] Zn/ZSM-5 catalysts produced the highest concentration of monocyclic aromatic hydrocarbons compared to the other comparative catalysts, producing xylenes and toluene with the contents of 35.32 and 36.52 wt %, respectively. In contrast, Ni/ZSM-5 yielded the highest (31.36%) content of polycyclic aromatic hydrocarbons in the liquid product. This substantial deoxygenation and selective aromatization was attributed to the increased Lewis and Brönsted acid sites in the metal/ZSM-5 catalysts and enhanced hydrogen transfer reactions during pyrolysis.[19,28] A recent study demonstrated the application of different Cu loadings (0−30 wt %) on ZSM-5 for the bio-oil upgrading from *ex situ* pyrolysis of *Swida wilsoniana*.[29] The results revealed that the addition of Cu increased the total acidic sites without affecting the crystalline structure of the original ZSM-5. The optimum concentration of Cu loading was found at 10%, achieving the highest hydrocarbon production of nearly 89%.[22] In addition to monometallic catalysts, many studies have also investigated the potential of bimetallic catalysts to convert the oxygenated compounds to aromatic or aliphatic hydrocarbons. For instance, Ren et al.[26] demonstrated the upgrading of pine wood bio-oil using Ni/Co-ZSM-5 and Mo/Co-ZSM-5. It was shown that Ni/Co-ZSM-5 generated more benzene derivative compounds (47.2 wt %) compared to a monometallic catalyst (Co-ZSM-5), while Mo/Co-ZSM-5 favored the generation of naphthalene derivative compounds, producing 37 wt %, while Co-ZSM-5 produced 32 wt %.[26] *Ex situ* catalytic pyrolysis using highly active mono- or bimetallic catalysts could prove highly efficient and economical for bio-oil upgrading or viable hydrocarbon production at industrial scale. In comparison to *in situ* pyrolysis, the primary advantage of *ex situ* pyrolysis is in the higher yield of aromatic hydrocarbons and lower carbon deposition on catalysts.[30] *Ex situ* pyrolysis also requires less amount of catalysts compared to *in situ* pyrolysis because lower catalyst/biomass ratios could achieve efficient bio-oil deoxygenation and hydrocarbon production.[23,31]

The previous studies suggest that different hydrocarbons are selectively generated by a particular catalyst during the pyrolysis reactions. Moreover, most of the studies are focused on the application of mono- or bimetallic catalysts to increase the production of aromatic hydrocarbons in bio-oil using model compounds. The effect of mono- and bimetallic catalysts on different product yields and selectivity of hydrocarbons from pyrolysis of real biomass have not been sufficiently explored. The literature also suggests that Ni/zeolite and Cu/zeolite catalysts contribute to improved bio-oil upgrading. The synergetic effect of Ni and Cu metals could carry out an enhanced number of deoxygenation reactions, which could prove significant for bio-oil upgrading. Therefore, as a result of the efficient catalytic activity, this study prepared mono- and bimetallic catalysts using Cu and Ni with zeolite as the support and investigated their effect on different product yields and selectivity of hydrocarbons using pine wood pyrolysis while determining the optimum catalyst/biomass ratio for efficient deoxygenation of bio-oils. Cu/zeolite and Ni/zeolite as the monometallic catalysts and CuNi/zeolite as the bimetallic catalyst were prepared with a zeolite support using incipient wetness impregnation. Three catalyst/biomass ratios of 1, 2, and 3 were used in *ex situ* pyrolysis mode to demonstrate the effect on hydrocarbon selectivity and the overall bio-oil upgrading. The possible pathways for bio-oil deoxygenation are also discussed.

2. MATERIALS AND METHODS

2.1. Biomass Analysis. Radiata pine sawdust was selected as the biomass sample for the pyrolysis experiments. The biomass was obtained from Sydney, Australia. The biomass was dried at 60 °C for 24 h in a vacuum oven, then refined, and sieved with a 40-mesh sieve, resulting in biomass with a particle diameter of 0.18 mm, which was used as feedstock in this study. The biomass was further dried in a vacuum oven at 100 °C for 1 h prior to pyrolysis.

The proximate and ultimate analyses of the selected pine wood sample, conducted in a standard procedure described elsewhere,[32] are shown in Table 1. The proximate analysis showed that biomass

Table 1. Analysis of Pine Wood Biomass

proximate analysis			ultimate analysis				
ash (%)	volatile matter (%)	fixed carbon (%)	C (%)	H (%)	N (%)	O (%)	total S (%)
0.3	87.5	12.2	50.1	6.07	0.21	43.2	0.08

contains the volatile matter of 87.5% and 0.3% ash content. The ultimate analysis confirmed the presence of 50.1% carbon and 6.07% hydrogen in the biomass, while the content of nitrogen was very low (0.21%), suggesting the pine wood biomass as a suitable feedstock for biofuel production.[32]

Thermogravimetric (TG) analysis of biomass was performed to evaluate the mass loss with respect to the temperature with a TG analyzer (apparatus model TGA/DSC 1 STARe system, Mettler Toledo, Ltd.). Approximately 15 mg of the biomass sample was

loaded in the furnace and heated from room temperature to a final temperature of 900 °C at a heating rate of 50 °C/min, using high-purity nitrogen at a flow rate of 20 mL/min as the carrier gas. Furthermore, the rate of mass loss %/°C (DTG curve) was calculated by differentiating the TG data.

2.2. Catalysts. The zeolite and preparation of the Cu/zeolite, Ni/zeolite, and CuNi/zeolite catalysts used in this study were described previously.[33] Zeolite contained silica−25% alumina with 0.35% Na_2O. In monometallic catalysts (Cu/zeolite and Ni/zeolite), the concentration of Cu and Ni was 10%, while in the bimetallic catalyst (CuNi/zeolite), the concentration of Cu and Ni was 5% each. This ratio was selected because 10% metal loading in a catalyst has been shown to produce a sufficient number of stronger acid sites to carry out the deoxygenation reactions, which then start to reduce if the metal percentage is increased.[34]

2.3. Pyrolysis Experiments. The *ex situ* pyrolysis experiments were conducted in an infrared image gold furnace (SINKU-RIKO) with a cylindrical inner silica reactor tube. The amount of feedstock (pine wood) was nearly 100 mg for all of the pyrolysis experiments, while the amount of catalyst was varied to obtain three catalyst/biomass ratios of 1, 2, and 3. The feedstock was placed in a silica reactor tube; a catalyst bed was placed downstream of the feedstock; and the remaining tube was filled with quartz wool. The tube containing the feedstock and the catalyst was purged with He gas for 20−30 min to remove oxygen. An abbreviation has been used for the catalysts according to the catalyst/biomass ratio. Cu/zeolite catalysts are named as CuZ-1, CuZ-2, and CuZ-3, and Ni/zeolite catalysts are named as NiZ-1, NiZ-2, and NiZ-3, while CuNi/zeolite catalysts are termed as CuNiZ-1, CuNiZ-2, and CuNiZ-2. First, the pyrolysis process was carried out at four temperatures (500, 600, 700, and 800 °C) at 100 °C/min to determine the favorable temperature to achieve the highest bio-oil yield. Preliminary results suggested that the highest bio-oil yields are produced at 500 °C; therefore, the further experiments were conducted at this temperature using He at 50 mL/min. During the pyrolysis process, the gases were analyzed online using a M200 micro gas chromatograph (GC), while the pyrolytic vapors were condensed on quartz wool. The bio-oil attached to the wool was dissolved in a certain amount of dichloromethane (DCM) solvent, which was filtered 3 times through glass wool and sodium sulfate each to remove the solid impurities. The solution was further condensed with Ar gas and heated at 60 °C for 30 min. The samples were subjected for gas chromatography−mass spectroscopy (GC−MS) to examine the bio-oil composition. GC−MS used in the study contains an Agilent 7890A gas chromatograph with a HP-5MS column (60 m × 0.25 μm) coupled with a 5977A mass spectrometer. The product yields, bio-oil, gas, and char yields, were calculated as mentioned in the previous studies.[35,35]

3. RESULTS AND DISCUSSION

3.1. Thermogravimetric Analysis (TGA) of Biomass. TGA and differential weight loss thermogram (DTG) are shown in Figure 1 presenting the weight loss and weight loss rate for pine wood biomass at a heating rate of 50 °C/min. These data are used to estimate the loss of biomass mass during the pyrolysis reactions. Pine wood is mainly composed of three components that are cellulose, hemicellulose, and lignin. Besides, it also contains very small amounts of water and various substances extractable with water or organic solvents, such as benzene and alcohol. Cellulose is the primary structural component present in the cell wall of plants, a polysaccharide made up of approximately 100−15 000 linked D-glucose units in a linear chain, contributing to ca. 32% wood mass.[36] The thermal decomposition of cellulose usually starts around 200 °C until 380 °C. On the other hand, hemicellulose is a branched polysaccharide, with each branch made up of ~500−3000 glucose units, constituting 20−35% dry matter of wood. Hemicellulose is comparatively less thermally stable compared

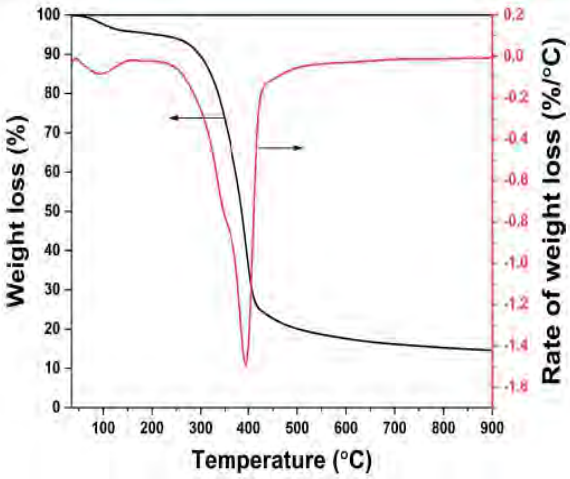

Figure 1. TG and DTG curves of pine wood biomass at a heating rate of 10 °C/min.

to cellulose, and its decomposition starts at ~180 °C and finishes at around 350 °C.[37] Moreover, a large proportion of lignin is a heterogeneous three-dimensional polymer of phenylpropane, containing phenolic hydroxyl groups in the *para* position and methoxy groups in the *meta* position to the side chain. Lignin constitutes 24−28% of the total wood, and it thermally degrades between 180 and 800 °C.

From the data in Figure 1, it can be analyzed that there was an initial mass loss between the starting temperature of 35 and 150 °C, which can be attributed to the loss of water and other volatile substances present in the biomass. The actual decomposition of biomass slowly started at 180 °C and increased sharply after 250−350 °C. The DTG curve also showed two peak areas, first starting from 250 to 350 °C and second between 350 and 500 °C. The first peak area indicated approximately 32 wt % weight loss, which can be ascribed to the depolymerization of all three components of the biomass, cellulose, hemicellulose, and lignin, while hemicellulose was completely decomposed by 350 °C.[38] A steep weight loss of ca. 40 wt % was noticed between 350 and 410 °C, which marked the complete decomposition of cellulose and depolymerization of lignin polymers into monomer units.[37] At 500 °C, a further 10 wt % weight loss was observed, ascribed to lignin decomposition that continued at higher temperatures and resulted in approximately 18 wt % char residue after the final temperature.

3.2. Effect of Mono- and Bimetallic Catalysts on Product Yields. Table 2 shows the yield distribution of the pyrolytic products produced after pyrolysis. Initially, the pyrolysis of pine wood was performed at four temperatures (500, 600, 700, and 800 °C) to identify the most suitable temperature to achieve the maximum bio-oil yield. The preliminary observations showed that 500 °C was favorable to achieve a maximum bio-oil yield of 62.7 wt % compared to the higher temperatures studied, with the minimum yield of 17.9 wt % was produced at 700 °C. The results are also consistent with the earlier studies that obtained a higher bio-oil yield at 500 °C.[20,39] It is evident that mainly decomposition of cellulose and hemicellulose is responsible for bio-oil production, which decompose at temperatures up to 500 °C, while at higher temperatures, the major part of biomass is converted into gases, resulting in a comparatively lower bio-oil yield and higher yield of pyrolytic gases.[8,40] The yield of

Table 2. Product Yields Obtained Using No Catalyst and Mono-/Bimetallic Catalysts during Pyrolysis of Pine Wood

catalyst[a]	gas yield (wt %)	char yield (wt %)	bio-oil yield (wt %)
C-500	15.3	22	62.7
C-600	34.9	18	47.1
C-700	50.1	32	17.9
C-800	38.3	27	34.7
Z-1	14.6	23	62.4
Z-2	15.5	27	57.5
Z-3	21.6	22	56.4
CuZ-1	26.2	23	50.8
CuZ-2	22	21	57
CuZ-3	25.4	22	52.6
NiZ-1	20.1	29	50.9
NiZ-2	31.9	27	41.1
NiZ-3	29.3	22	48.7
CuNiZ-1	28.8	17	54.2
CuNiZ-2	30.8	21	48.2
CuNiZ-3	30.7	22	47.3

[a]C represents control or no catalyst, while Z is used to present zeolite.

pyrolytic gases was minimum at 500 °C (15.3 wt %), which increased to the maximum of 50.1 wt % at 700 °C. On the other hand, the char yield was found to be less at lower temperatures. A char yield of 32 wt % was obtained at 700 °C, reducing to 27 wt % at 800 °C.

The introduction of mono- and bimetallic/zeolite catalysts at different catalyst/biomass ratios showed a significant change in the gas and bio-oil yields. A higher bio-oil yield was obtained at lower catalyst/biomass ratios and vice versa. For instance, sole zeolite with a catalyst/biomass ratio of 1 (Z-1) produced a bio-oil yield of 62.4 wt %, which decreased to 56.4 wt % with a catalyst/biomass ratio of 3. The decrease in the bio-oil yield could be attributed to the generation of pyrolytic gases, which generally resulted with an increase in the number of deoxygenation reactions favored by the higher catalyst/biomass ratios. For Cu/zeolite and Ni/zeolite catalysts, a small deviation was observed in the results for product yields, CuZ-2 showed higher bio-oil yields compared to CuZ-1, and NiZ-2 showed a lower bio-oil yield compared to NiZ-3, which could be compensated with a higher char yield for the NiZ-2 catalyst. For bimetallic catalysts, the bio-oil yield decreased proportionally to the increase in the catalyst/biomass ratio, with CuNiZ-1 producing the maximum bio-oil yield of 54.24 wt %, which decreased to 47.32 wt % with CuNiZ-3.

3.3. Effect of Non-catalytic Pyrolysis on the Bio-oil Composition. Peak area % is typically reported to estimate the proportion of compounds as a result of the difficulty for quantifying a very large range of complex compounds found in the pyrolysis oils.[2,26,35] More than 180 compounds in the bio-oils were detected in this study, with 60 compounds showing the highest peak areas, as shown in Figure S1 of the Supporting Information, which were selected for further analysis and classified on the basis of the functional groups. Figure 2a illustrates the bio-oil composition obtained at varying temperatures (500, 600, 700, and 800 °C) from *ex situ* pyrolysis at a heating rate of 100 °C/min. The results demonstrated that the bio-oil samples obtained at all temperatures were highly rich in oxygenated compounds. The major compounds in the bio-oils were phenols (phenol, 2-methoxy, phenol, and 2-methyl), ranging from 40 to 47.6%. The proportion of phenols slightly decreased with the temperature until 700 °C and then further

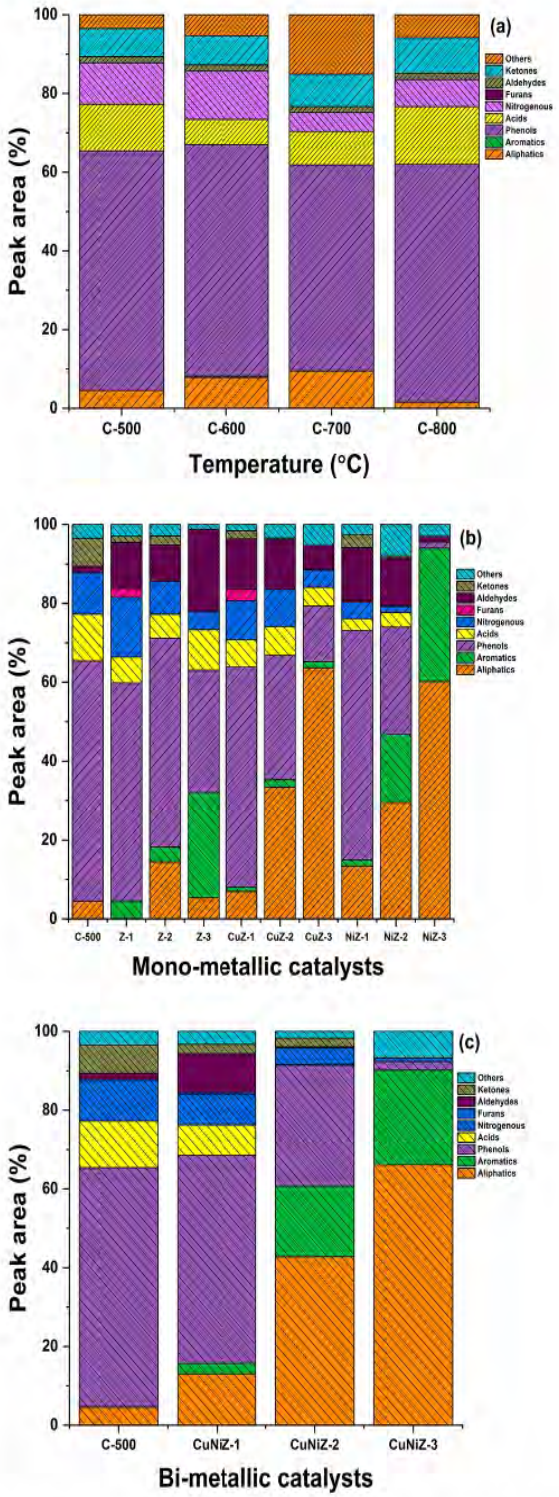

Figure 2. Bio-oil composition obtained (a) without catalysts at different temperatures and (b) with mono- and (c) bimetallic catalysts at 500 °C with a heating rate of 100 °C/min.

increased at 800 °C. The phenols are formed by the pyrolysis of the lignin fraction of the pine wood biomass.[39,41] The thermal decomposition of lignin is primarily initiated by the free radical reactions to produce monomeric phenolic compounds, which further undergo recombination and rearrangement reactions to form tri- or tetramers of phenolic compounds.[42] The other dominant compounds in the obtained bio-oils were acids (hexadecenoic, dodecanoic, and

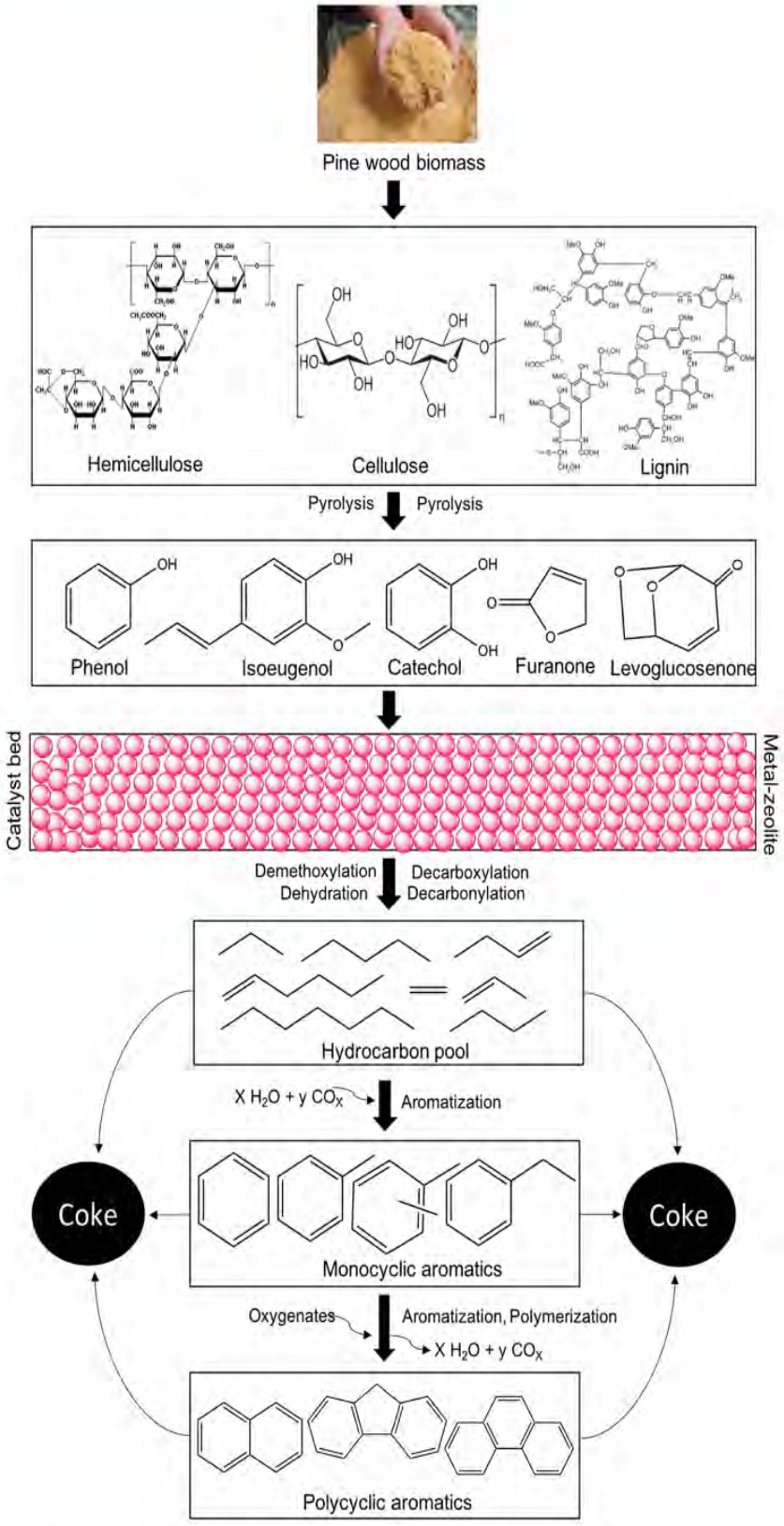

Figure 3. Possible reaction mechanism for deoxygenation reactions during the catalytic pyrolysis of pine wood.

octadecenoic acids). The highest percentage of acid was obtained at 800 °C, which was 10.82%, while the minimum proportion of acid (4.91%) was found in the bio-oil extracted at 600 °C. The other major categories of oxygenated compounds were ketones [2-cyclopenten-1-one and 2(5*H*)-furanone] and aldehydes. The data showed that ketones were present in a range of 5.57−6.64%; on the other hand, the aldehydes were almost similar (~1.2%) in the bio-oils extracted at all temperatures. The compounds containing carbonyl groups, such as aldehydes and carboxylic acids, are

generally produced from thermal degradation of the major portion of cellulose and hemicellulose of the lignocellulose biomass, and pyrolysis of some part of lignin also results in the formation of these types of compounds. The decomposition of cellulose and hemicellulose can be divided into two steps. During cellulose pyrolysis, a glucosyl cation is generated after the cleavage of a glycosidic bond between pyranose rings stabilized by the generation of a 1,6-anhydride molecule.[43] Further breakdown of the glycosidic bond linked between the anhydride molecule and end of the polymer chain leads to production of levoglucasan. Levoglucasan is the primary intermediate product during cellulose pyrolysis, which decomposes into different compounds by various pathways, such as direct breaking of the C−C and C−O bonds and dehydration.[44] Alternatively, in hemicellulose (such as xylan) pyrolysis, a xylosyl cation is created after breakage of a glycosidic bond between pyranose rings, but a stable anhydride cannot be formed as a result of the absence of the sixth carbon and substituted oxygen at the fourth position.[45,46] Therefore, the xylosyl cation could undergo further breaking of the glycosidic bond to produce 5-hydroxy-2*H*-pyran-4(3*H*)-one via dehydration, or xylose could also be formed after the breaking of the glycosidic bond as a result of the inclusion of OH^- and H^+.[22] Many nitrogenous compounds were detected in the bio-oil samples at varying temperatures, with imidazole, oxazolidine, and piperidine representing the largest fractions. For example, 8.21% nitrogen-containing compounds were present in the bio-oil obtained at 500 °C, while only 3.64% nitrogen-containing compounds were detected at 700 °C. In addition to many oxygenated compounds, few aliphatic hydrocarbons and haloalkanes were also obtained with non-catalytic pyrolysis of pine wood. The bio-oil produced at 500 °C contained 3.53% aliphatic hydrocarbons, while 800 °C could generate 1.18% in the bio-oil.

Overall, this analysis suggests that pyrolysis without catalysts resulted in highly oxygenated bio-oils and much lower amounts of non-oxygenated hydrocarbons. Because a higher bio-oil yield was achieved at 500 °C, this temperature was selected to upgrade the bio-oil using mono- and bimetallic catalysts.

3.4. Effect of Monometallic Catalysts on Bio-oil Deoxygenation. Figure 2b shows the composition of bio-oils produced using sole zeolite and monometallic catalysts (CuZ and NiZ) at three catalyst/biomass ratios (1, 2, and 3). The results revealed that the use of a catalyst demonstrated a significant conversion of oxygen-containing compounds into aromatic and aliphatic hydrocarbons. Even the sole zeolite showed a competitive deoxygenation activity and simultaneous production of aromatic hydrocarbons. For instance, Z-3 decreased the proportion of phenols from 37.6 to 16.91% when compared to the non-catalytic pyrolysis. The other oxygenated compounds, such as acids and ketones, were also reduced using sole zeolite but surprisingly favored the production of aldehydes, with percentages increasing with an increase in the catalyst amount. A substantial reduction in the proportion of nitrogenous compounds was noticed in the bio-oil samples. Zeolite at a lower concentration, such as Z-2, promoted the formation of aliphatic hydrocarbons, producing 9.62% aliphatic hydrocarbons and 2.5% aromatic hydrocarbons, while Z-3 favored the generation of aromatic hydrocarbons, producing 14.42% aromatic hydrocarbons and 2.91% aliphatic hydrocarbons. The deoxygenation activity of zeolite catalysts can be assigned to the higher surface area and presence of strong Brönsted acid sites inside the pores. The addition of a metal (Cu or Ni) on a zeolite support further enhanced the removal of oxygenated compounds and hydrocarbon production in the bio-oil. Additionally, increasing the catalyst amount (higher catalyst/biomass ratio) achieved a higher deoxygenation efficiency as well as a greater production of hydrocarbons. The Cu/zeolite catalysts enhanced the formation of aliphatic hydrocarbons, with CuZ-3 producing a maximum proportion of 49.58% aliphatic hydrocarbons, which was ∼2 and ∼9 times higher than CuZ-2 and CuZ-1, respectively. CuZ-3 also showed a higher production of aliphatic hydrocarbons than Z-3 but produced a comparatively less number of aromatic hydrocarbons. However, CuZ-3 showed an enhanced deoxygenation activity for phenols, acids, and ketones, decreasing their proportion to 10.96, 3.7, and 0% in the bio-oil samples, respectively. The deoxygenation of acids, ketones, and aldehydes is generally carried out via three pathways, such as dehydration, decarbonylation, and decarboxylation, producing water, CO, and CO_2 as byproducts. The dehydration of these compounds may occur through aldol condensation reactions.[47] The decarbonylation occurs via cracking of ketone or carboxylic group to generate hydrocarbon gases and CO.[48] The hydrocarbon volatiles can further form aliphatic and aromatic hydrocarbons through aromatization. On the other hand, the decarboxylation reaction is produced by cracking of the carboxylic group and removing oxygen from the carboxylic acids as CO_2.[17] The possible deoxygenation pathways followed by the catalysts are shown in Figure 3.

Similar to sole zeolites, the Cu/zeolite catalyst also favored the formation of aldehydes, such as 3-benzofurancarboxaldehyde, in the bio-oils, while some furans [benzofuran, 3-(4-methoxyphenyl)-2,6-dimethyl, and 3,7-benzofurandiol, 2,3-dihydro-2,2-dimethyl] were also detected with CuZ-1 and CuZ-3. It is well-known that furan is a good source for the Diels−Alder condensation reaction, promoting the formation of benzofurans. Therefore, it can be suggested that Cu/zeolite catalysts favored the Diels−Alder condensation reaction and promoted the formation of benzofurans.[49] In addition to this, benzofurans can further undergo the decarbonylation reaction to form benzene and CO.

In comparison to the Cu/zeolite and sole zeolite catalysts, Ni/zeolite catalysts showed the best deoxygenation activity for the bio-oil samples and mixed formation of aliphatic and aromatic hydrocarbons, where Cu/zeolite catalysts only favored the formation of aliphatic hydrocarbons. This is because Ni/zeolite catalysts exhibited comparatively higher surface area, smaller deposit size, and increased Brönsted acidic sites. Additionally, Ni/zeolite catalysts also enhanced the aromatization and hydrogenation reactions, where Cu/zeolite could not catalyze these reactions efficiently, hence resulting in less aromatic hydrocarbons. Ni/zeolite catalysts decreased the proportion of oxygen-rich compounds, such as acids, phenols, ketones, and aldehydes, as well as nitrogenous compounds. The following trend was observed in the reduction of the oxygen-rich compounds and increased production of aliphatic or aromatic hydrocarbons: NiZ-3 > NiZ-2 > NiZ-1. NiZ-3 produced bio-oil with only 0.7% phenols with no acids, ketones, and nitrogenous compounds in the bio-oil. Alternatively, NiZ-3 generated the proportions of ∼15% aromatic hydrocarbons and 26.78% aliphatic hydrocarbons, which were several and ∼2.5 times higher than NiZ-1, respectively. Ni/zeolite catalysts enhanced the deoxygenation pathways, such as decarbonylation, decarboxylation, dehydration, and Diels−

Table 3. Hydrocarbon Products (Peak Area %) Obtained Using Mono- and Bimetallic Catalysts during Pyrolysis of Pine Wood at 500 °C

		catalyst type												
hydrocarbon	chemical formula	no catalyst	Z-1	Z-2	Z-3	CuZ-1	CuZ-2	CuZ-3	NiZ-1	NiZ-2	NiZ-3	CuNiZ-1	CuNiZ-2	CuNiZ-3
ethylidenecyclobutane	C_6H_{10}	0.28		3.39	2.91		15.62	43.2	5.75	7.87	18.27	5.07	23.6	34.45
cyclohexene	C_6H_{10}	0.1	0.11			0.15						0.35		4.96
pentacosane	$C_{25}H_{52}$	0.52				0.99								
heptacosane	$C_{27}H_{56}$	1.91		1.05		1.37								
hentriacontane	$C_{31}H_{64}$	0.43		1.36		1.44			1.17			1.13		
stigmasta-3,5-diene	$C_{29}H_{48}$	0.27		0.8										
phenanthrene	$C_{14}H_{10}$		2.88	1.63	2.77	0.64	0.51		0.49	2.23			0.52	
retene	$C_{18}H_{18}$		0.52	0.87		0.18						2.24		
cyclohexadiene	C_6H_8											0.2		
hexacosane	$C_{26}H_{54}$				0.63		2.09		1.15	2.5				
naphthalene	$C_{10}H_8$				7.13					4.7	9.42			2.86
indene	C_9H_8				0.64						0.95		0.24	1.31
trimethylazulene	$C_{13}H_{14}$				0.39									
fluorene	$C_{13}H_{10}$				1.75		0.85	0.78		0.36	2.42		2.18	2.74
anthracene	$C_{14}H_{10}$				0.61								0.21	
octadiene	C_8H_{14}					0.9				0.47				
cycloheptatriene	C_7H_8						0.38							
ethylene	C_2H_2						0.28							
nonane	C_9H_{20}						1.04	2.21						
hexadecane	$C_{16}H_{34}$						1.53							
heneicosane	$C_{21}H_{44}$						2.09							
benzene	C_6H_6							0.45	0.67	1.92			5.31	1.33
pentalene	C_8H_6									1.8				
indacene	$C_{12}H_8$									0.42				
tetracosane	$C_{24}H_{50}$									2.56				
heneicosane	$C_{21}H_{44}$									1.61				
chamazulene	$C_{14}H_{16}$										0.36			
cyclopentane	C_5H_{10}											2.62		
pyrene	$C_{16}H_{10}$												0.54	
propene	C_3H_{10}													0.52
(*E*)-stilbene	$C_{14}H_{12}$												0.3	3.2

Alder condensation reactions to convert benzofurans into aromatic hydrocarbons.[24,49]

Table 3 shows the types of hydrocarbons obtained in the bio-oil samples using monometallic catalysts, while the main hydrocarbons are depicted in Figure 4. The data demonstrate that neat zeolite and the metal/zeolite catalysts produced varying proportions of aromatic and aliphatic hydrocarbons. It was further noticed that almost all catalysts consistently favored the production of ethylidenecyclobutane as the primary aliphatic hydrocarbon in the bio-oils. The proportion of ethylidenecyclobutane was found to be higher with an increase in the catalyst amount, suggesting the conversion of oxygenated compounds mainly into ethylidenecyclobutane. For instance, CuZ-2 produced a proportion of 15.62% ethylidenecyclobutane in the bio-oil, which increased to 43.2% in the bio-oil obtained with CuZ-3. Similarly, NiZ-1 produced only 5.75% ethylidenecyclobutane, while 18.27% of the hydrocarbons were detected in the bio-oil with NiZ-3. The generation of ethylidenecyclobutane over monometallic catalysts may be followed by two routes. First, the conversion of all oxygenated compounds occurs via direct dehydration and cracking reactions.[48] The second route can include hydrogenation activity by Cu and Ni metals, which can use the hydronium ions for the dehydration reaction and hydrogen gas (produced *in situ* during pyrolysis) for the hydrogenation reaction to transform the oxygen-containing compounds into cycloalkanes, such as cyclobutane, in this study.[50] The other major aliphatic hydrocarbons were cyclohexene, hentriacontane, and hexacosane. Cyclohexene was detected in the bio-oil samples from the pyrolysis catalyzed by Z-1 and CuZ-1 but in a very small proportion. The maximum proportions of hentriacontane and hexacosane were achieved with CuZ-1 and NiZ-2, which were 1.44 and 2.5%, respectively. On the other hand, the dominant aromatic hydrocarbons were benzene derivative compounds, naphthalene derivative compounds, phenanthrene, retene, and fluorene. The sole zeolite catalyst, Z-3, produced a higher percentage of naphthalene derivative compounds that were 7.13%, while Cu/zeolite-catalyzed *ex situ* pyrolysis did not favor the production of naphthalenes in the bio-oil, suggesting the inability of the Cu metal to carry out the aromatization reactions. However, Ni/zeolite catalysts enhanced production of naphthalenes with NiZ-3, producing a maximum proportion of these aromatic compounds in the bio-oil that collectively contributed to 9.42% of the total bio-oil composition. The other highly important and most desirable aromatic hydrocarbons were benzene derivative hydrocarbons. The higher percentage of aromatic hydrocarbons over Ni/zeolite catalysts can be credited to the improved rate of deoxygenation reactions that enhanced the conversion of oxygen-rich compounds into carbon- and hydrogen-rich compounds. The results also revealed that sole zeolites could not produce any benzene

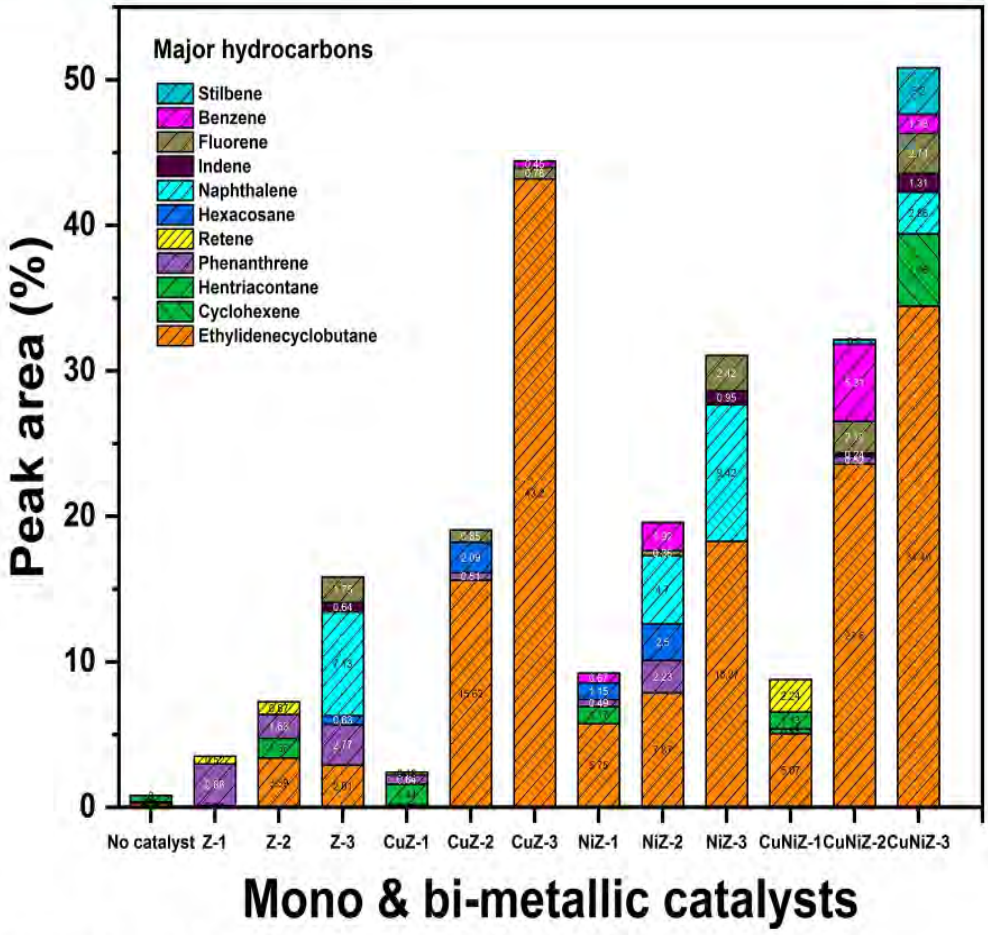

Figure 4. Distribution of major hydrocarbons obtained in the bio-oil samples using mono- and bimetallic catalysts.

hydrocarbons, while CuZ-3- and NiZ-2-catalyzed pyrolysis could form a small percentage of benzene compounds in the bio-oil at 0.45 and 1.92%, respectively. Meanwhile, phenanthrene and fluorene were detected in approximately all bio-oil samples. The sole zeolite catalyst, Z-3, showed a maximum proportion of phenanthrene (2.77%), while 1.75% fluorene was present in the bio-oil. Cu/zeolite catalysts showed a slightly lower proportion of the aromatic hydrocarbons; however, NiZ-2 produced 2.23% phenanthrene, while NiZ-3 enhanced the formation of fluorene (2.42%) in the bio-oil.

3.5. Reaction Mechanism of Bio-oil Upgrading. The results of non-catalytic pyrolysis showed that bio-oil was highly rich with different oxygenated compounds, while the catalytic pyrolysis with mono- and bimetallic catalysts showed considerable conversion of these compounds into various aliphatic and aromatic hydrocarbons. In this regard, various types of reactions could be involved, mainly deoxygenation reactions, cracking reactions including C−C bond cleavage, hydrogen transfer and isomerization, aromatization of olefins into aromatics, aldol condensation, and ketonization reactions.[23,51,52] All of these reactions are typically catalyzed by the Brönsted sites present inside the pore of the mono- or bimetallic catalysts, while some could also be carried out by Lewis acid sites present on the external surface of the catalyst. In this study, the major oxygenated compounds found in non-catalytic pyrolysis were phenols that are usually formed from thermal degradation of the lignin component of pine wood. The catalytic conversion of phenolic compounds into aromatic hydrocarbons has been suggested to take place via various reactions. It has been observed that Brönsted sites enhance demethoxylation, dehydroxylation, and methyl substitution reactions to produce monocyclic aromatic hydrocarbons, including benzene and toluene.[53] The monocyclic aromatic hydrocarbons could undergo polymerization reactions to produce polycyclic aromatic hydrocarbons, such as naphthalene. The phenolic compounds, for instance, *m*-cresol, could also undergo direct deoxygenation reactions, including dehydration, to form aromatic hydrocarbons.[53,54] The conversion of carboxylic acids can take place primarily via decarbonylation and decarboxylation reactions to produce CO_2 and H^-. In the next step, the carboxylic acids could undergo cracking reactions to form light-chain hydrocarbons, which can further undergo a chain elongation step to form olefins and an aromatization reaction to form aromatics.[55,56] Some furans were also observed in the bio-oil produced from non-catalytic pyrolysis, which could be converted into aliphatic and aromatic hydrocarbons in the presence of catalysts via Diels−Alder condensation, dehydration, decarbonylation, and aromatization reactions, which could be carried out by Brönsted as well as Lewis acid sites of the catalysts.[57]

3.6. Effect of the Bimetallic Catalyst on Bio-oil Deoxygenation. Generally, the bimetallic catalysts may prove advantageous over monometallic catalysts for a variety of reasons. For example, inclusion of a second metal may improve the stability of a catalytically active metal by inhibiting the sintering process or reducing the coke formation, and second, the synergistic effect of both metals may increase the catalytic activity and modify selectivity of the products, as in

Table 4. Pyrolytic Gas Yields without Catalyst and with Mono-/Bimetallic Catalysts during Pyrolysis of Pine Wood

catalyst[a]	CH_4 (wt %)	CO_2 (wt %)	C_2H_4 (wt %)	C_2H_6 (wt %)	H_2 (wt %)	CO (wt %)
C-500	1.67	5.30	0.14	0.18	3.84	4.16
Z-1	1.61	9.10	0.20	0.25	0.07	3.37
Z-2	1.29	10.53	0.20	0.22	0.04	3.27
Z-3	2.41	13.89	0.32	0.36	0.07	4.52
CuZ-1	1.90	19.36	0.28	0.23	0.79	3.68
CuZ-2	2.06	15.60	0.28	0.29	0.14	3.65
CuZ-3	0.88	18.78	0.14	0.14	0.03	5.41
NiZ-1	1.11	14.68	0.11	0.14	0.10	4.01
NiZ-2	2.49	20.90	0.32	0.35	3.05	4.82
NiZ-3	0.86	15.41	0.59	0.65	3.65	8.11
CuNiZ-1	0.72	15.42	0.13	0.05	0.80	11.64
CuNiZ-2	1.85	15.36	0.23	0.30	1.12	11.98
CuNiZ-3	1.80	17.55	0.22	0.28	0.41	10.42

[a]C represents control or no catalyst, while Z is used to present zeolite.

this case, the hydrocarbons.[26,58] Figure 2c shows the composition of bio-oils obtained using bimetallic catalysts at three catalyst/biomass ratios (1, 2, and 3). It can be observed that CuNi/zeolite showed better deoxygenation activity than Cu/zeolite and competitive deoxygenation activity compared to Ni/zeolite but obtained a higher proportion of the total hydrocarbons than both Cu/zeolite and Ni/zeolite. Similar to the monometallic catalysts, the bimetallic catalyst demonstrated an increased reduction in oxygenated compounds with the rise in the catalyst/biomass ratio. Evidently, CuNiZ-3 showed the best deoxygenation activity when compared to CuNiZ-2, CuNiZ-1, and CuZ-3. For instance, bio-oil obtained with CuNiZ-3 contained only 1.33% phenols, whereas no acids or ketones were noticed in the bio-oil. In contrast, CuNiZ-2 produced bio-oil with 16.9% phenols, 0.06% acids, and 1.21% ketones, while the bio-oil obtained with CuZ-3 was comparatively richer with phenols, acids, and aldehydes, contributing 10.9, 3.7, and 4.76%, respectively. However, CuNiZ-3 showed a competitive decrease in oxygenated compounds compared to NiZ-3 because no acids, ketones, and nitrogenous compounds were detected in both bio-oil samples, while the proportion of phenols was also much lower. This enhanced catalytic activity of CuNi/zeolite can be attributed to its improved physical properties and synergetic effect of Cu and Ni in the catalyst. Noticeably, CuNi/zeolite showed the higher acidity compared to either Ni/zeolite or Cu/zeolite and a competitive surface area, which consequently signifies the higher number of active sites for deoxygenation reactions. The removal of oxygen by the bimetallic catalysts is also carried out by the deoxygenation pathways, similar to the monometallic catalysts. For example, aldol condensation, decarboxylation, decarbonylation, dehydration, and Diels–Alder reactions participate in the conversion of highly oxygenated compounds to different types of hydrocarbons.[41,49,50,59] In addition, the micro GC results demonstrated that the bimetallic catalysts produced approximately equal amounts of CO_2 and CO, while monometallic catalysts generated more CO_2 than CO, which suggested that the main deoxygenation pathway for the latter was decarboxylation, while the former deoxygenated the bio-oil via both decarboxylation and decarbonylation reactions. In comparison to the monometallic catalysts, the bimetallic catalyst exhibited balanced production of the hydrocarbons, which are considered more desirable in a bio-oil composition for a possible transportation fuel. CuNiZ showed an increased production of the hydrocarbons (aliphatic and aromatic) with an increase in the catalyst amount, following the trend where CuNiZ-3 > CuNiZ-2 > CuNiZ-1. CuNiZ-3 produced 39.9% aliphatic hydrocarbons and 14.5% aromatic hydrocarbons, which were 69.2 and 46.6% higher than CuNiZ-2, respectively. Moreover, CuNiZ-3 produced several times more aromatic hydrocarbons than CuZ-3 and almost a similar amount to NiZ-3, but CuNiZ-3 showed ca. 49% higher proportion of aliphatic hydrocarbons compared to NiZ-3.

Table 3 shows the proportion of hydrocarbons obtained in the bio-oils using the CuNi/zeolite catalyst, and the main hydrocarbons are also depicted in Figure 4. An initial observation indicates that CuNiZ catalysts produced the type of hydrocarbons similar to the monometallic catalysts but also formed a number of additional hydrocarbons. For example, cyclopentane, propene, stilbene, and pyrene were present in the bio-oil produced with CuNi/zeolite, which were not found in the bio-oil samples with any monometallic catalyst. Therefore, the synergistic catalytic effect of both metals changed the selectivity of the products and resulted in a variety of aliphatic and aromatic hydrocarbons. CuNi/zeolite-catalyzed pyrolysis of pine wood resulted in bio-oil enriched with major aliphatic hydrocarbons, such as ethylidenecyclobutane and cyclohexene, and aromatic hydrocarbons, such as benzene, naphthalene, fluorene, and stilbene. The results demonstrate that CuNiZ-3 produced the highest proportion of ethylidenecyclobutane (34.45%) and cyclohexene (4.96%) compared to CuNiZ-2, CuNiZ-1, and other monometallic catalysts, such as CuZ-3 and NiZ-3. In contrast, CuNiZ-2 generated 23.6% ethylidenecyclobutane in the bio-oil, which was 4.6 times higher than CuNiZ-1, 3 times more than NiZ-2, and 1.5 times greater than CuZ-2. Noticeably, CuNiZ-1 favored the formation of cyclopentane (2.62%) and cyclohexadiene (0.2%), which were not detected in any other bio-oil sample. The bimetallic catalyst also produced competitive mono- and polycyclic aromatic hydrocarbons. It was observed that varying the amount of the catalyst used in pyrolysis favored the formation of different hydrocarbons in the bio-oil samples. CuNiZ-1 could only produce retene (2.24%) in the bio-oil, while CuNiZ-2 produced different aromatic hydrocarbons, such as benzene (5.31%), fluorene (2.18%), phenanthrene (0.52%), stilbene (0.3%), and indene (0.24%). A further increase in the CuNiZ-3 catalyst amount also produced almost similar hydrocarbons to CuNiZ-2 but with an increased proportion. CuNiZ-3 showed a higher percentage of

fluorene (2.74%), indene (1.31%), and stilbene (3.2%). CuNiZ-3 generated lower percentages of benzene (1.33%) than CuNiZ-2 but instead favored the generation of naphthalene, contributing 2.86% of the total bio-oil composition.

3.7. Effect of Mono- and Bimetallic Catalysts on Pyrolytic Gases. Table 4 summarizes the generation of different pyrolytic gases obtained at 500 °C using different concentrations of mono- and bimetallic catalysts. The main gases obtained during the pyrolysis of pine wood were CO_2, CO, CH_4, H_2, C_2H_4, and C_2H_6. However, the amounts of CO_2 and CO were comparatively higher than other gases. The quantities of CO_2 and CO at 500 °C were 5.30 and 4.16 wt %, respectively. Pine wood biomass is known to contain a variety of compounds with functional groups, such as ROR′, ROH, RR′CO, RCHO, and RCO_2H. The release of CO_2 can be accredited to the cracking of the carboxyl functional group (RCO_2H), and the evolution of CO can be attributed to the cracking of either carboxyl (RCO_2H) or carbonyl (RR′CO) functional groups. The generation of H_2 can be attributed to the cracking and deformation of C=C and C−H bonds during the pyrolysis reaction. Moreover, CH_4 is mainly formed as a result of the release of $O-CH_3$ groups during the reaction.

In further pyrolysis experiments with mono- and bimetallic catalysts, the main volatiles were also CO_2 and CO, which indicated that the main deoxygenation pathways during the catalytic pyrolysis were decarboxylation and decarbonylation. However, it was observed that monometallic catalysts promoted the decarboxylation reaction over decarbonylation because higher yields of CO_2 were obtained during the pyrolysis. For example, CuZ-1 obtained a yield of 19.36 wt % for CO_2, while only 3.68 wt % CO was obtained for the same reaction. Similarly, NiZ-3 also showed a higher CO_2 yield in comparison to CO, which were 15.41 and 8.11 wt %, respectively. During catalytic biomass pyrolysis, the catalyst/biomass ratio also had a significant effect on the release of pyrolytic gases. It was observed that zeolite and Ni/zeolite catalysts achieved higher gas yields with increasing catalyst/biomass ratios. For example, Z-1 generated a CO_2 yield of 9.1 wt % and CO yield of 3.37 wt %, while Z-3 increased the yield of CO_2 and CO to 13.89 and 4.52 wt %, respectively. Similarly, NiZ-1 showed the production of 14.18 wt % CO_2 and 4.01 wt % CO, which increased to 20.9 and 4.82 wt %, respectively, with NiZ-2; however, NiZ-3 showed a decrease in the CO_2 yield and a significant increase in CO, while a noticeable yield of H_2 was also achieved. On the other hand, bimetallic catalysts showed higher yields of CO_2 and CO, indicating that both decarboxylation and decarbonylation reactions were favored by the bimetallic catalysts. For example, CuNiZ-1 achieved a CO_2 yield of 15.42 wt % and a CO yield of 11.64 wt %. The yields of CO_2 and CO obtained with CuNiZ-2 were 15.36 and 11.98 wt %, respectively, and the yields of CO_2 and CO obtained with CuNiZ-3 were 17.55 and 10.42 wt %, respectively. Meanwhile, a small amount of CH_4 (~1.8%) was observed in the gas composition catalyzed by CuNiZ-2 and CuNiZ-3, suggesting demethoxylation as the third preferred deoxygenation pathway by bimetallic catalysts during pyrolysis.

3.8. Estimation of the Bio-oil Quality. The primary aim of CFP is not only to convert all of the oxygen-rich compounds into aromatic hydrocarbons but also to generate the bio-oil enriched with different types of hydrocarbons, at least similar to the composition of petroleum crude oil. On average, crude oil generally contains naphthenes that include cycloalkanes (49%), paraffins which contain acyclic saturated hydrocarbons (30%), aromatics (15%), and others (6%). Therefore, the bio-oil composition was classified into these aforementioned categories to compare the quality of the bio-oil samples produced in this work to petroleum crude oil, as shown in Table 5. The data suggest that there were some catalytic

Table 5. Comparison of Bio-oil Composition to Petroleum Crude Oil

bio-oil type[a]	naphthene (%)	aromatic (%)	paraffin (%)	others (%)
crude oil	49.00	15.00	30.00	6.00
Z-1	0.11	3.40	0	2.30
Z-2	3.39	2.50	2.41	1.93
Z-3	2.91	14.42	0.63	0.64
CuZ-1	0.15	0.84	3.99	1.26
CuZ-2	16.00	1.37	4.94	2.41
CuZ-3	43.20	1.25	6.82	4.10
NiZ-1	5.75	1.17	1.82	1.97
NiZ-2	7.87	9.75	8.47	4.56
NiZ-3	18.27	15.06	0	1.36
CuNiZ-1	8.24	2.24	1.13	2.75
CuNiZ-2	23.60	9.91	0	0.95
CuNiZ-3	39.41	14.53	0.53	4.10

[a]Z represents zeolite.

pyrolysis reactions that produced a competitive amount of naphthenes and aromatics in the bio-oils, while the percentage of paraffins was comparatively lower than that in the crude oil. For example, in monometallic catalysts, CuZ-3-catalyzed pyrolysis resulted in 43.20% naphthenes, while NiZ-3 could produce 18.27% naphthenes in the bio-oils. Alternatively, Z-3- and NiZ-3-catalyzed pyrolysis generated 14.42 and 15.06% aromatic hydrocarbons, respectively, which were close to the quantity present in the crude oil (15%). On the other hand, in comparison to monometallic catalysts, bimetallic catalysts produced a better quality of bio-oil and showed relatively higher percentages of naphthenes and aromatics. Noticeably, CuNiZ-3 formed 39.41% naphthenes and 14.53% aromatics in the bio-oil. However, the desired percentage of paraffins was not achieved in this study. Therefore, it is highly imperative to produce a bio-oil composition that is approximately close to that of the crude petroleum oil, which is not only rich in aromatic hydrocarbons but also contains the required amount of naphthenes and paraffins.

4. CONCLUSION

The study successfully demonstrated the excellent bio-oil deoxygenation activity by mono- and bimetallic catalysts during *ex situ* pyrolysis of biomass. The biomass/catalyst ratio of 3 was found to achieve the highest percentage of hydrocarbon production. For example, NiZ-3 produced 41.84% of total hydrocarbons, and only 5.65% oxygenated compounds were found in the bio-oil. All catalysts favored the production of ethylidenecyclobutane, and its proportion was increased in the bio-oil with an increase in the catalyst amount. Cu/zeolite catalysts promoted the production of only aliphatic hydrocarbons, while Ni/zeolite also promoted the formation of aromatic hydrocarbons. However, CuNi/zeolite showed better deoxygenation efficiency than Cu/zeolite or Ni/zeolite and also produced comparatively a variety of aromatic hydrocarbons (14.53%) and aliphatic hydrocarbons (39.94%), attributing to its higher acidity that created a higher number

of active sites for deoxygenation reactions. The main deoxygenation pathway for monometallic catalysts was decarboxylation, while the bimetallic catalyst favored the decarboxylation and decarbonylation reactions as the main deoxygenation pathways. In comparison the quality of produced bio-oils with petroleum crude oil, it can be suggested that CuNi/zeolite produced a better quality of bio-oil when compared to either Cu/zeolite or Ni/zeolite.

■ ASSOCIATED CONTENT

Supporting Information

The Supporting Information is available free of charge at https://pubs.acs.org/doi/10.1021/acs.energyfuels.9b02724.

GC–MS chromatograms in the bio-oil samples obtained from non-catalytic and catalytic biomass pyrolysis (Figure S1) (PDF)

■ AUTHOR INFORMATION

Corresponding Authors

*E-mail: vladimir.strezov@mq.edu.au.

*E-mail: tao.kan@mq.edu.au.

ORCID

Vladimir Strezov: 0000-0002-9129-9284

Tao Kan: 0000-0002-8468-4475

Haftom Weldekidan: 0000-0002-4682-6583

Notes

The authors declare no competing financial interest.

■ ACKNOWLEDGMENTS

The authors are thankful to the Microscopy Unit, Faculty of Science and Engineering, Macquarie University, for helping with transmission electron microscopy analysis.

■ REFERENCES

(1) Kan, T.; Strezov, V.; Evans, T. J. Lignocellulosic Biomass Pyrolysis: A Review of Product Properties and Effects of Pyrolysis Parameters. *Renewable Sustainable Energy Rev.* **2016**, *57*, 1126–1140.

(2) Weldekidan, H.; Strezov, V.; Kan, T.; Town, G. Waste to Energy Conversion of Chicken Litter through a Solar-Driven Pyrolysis Process. *Energy Fuels* **2018**, *32* (4), 4341–4349.

(3) Czernik, S.; Bridgwater, A. V. Overview of Applications of Biomass Fast Pyrolysis Oil. *Energy Fuels* **2004**, *18* (2), 590–598.

(4) Eschenbacher, A.; Jensen, P. A.; Henriksen, U. B.; Ahrenfeldt, J.; Li, C.; Duus, J. Ø.; Mentzel, U. V.; Jensen, A. D. Impact of ZSM-5 Deactivation on Bio-Oil Quality during Upgrading of Straw Derived Pyrolysis Vapors. *Energy Fuels* **2019**, *33* (1), 397–412.

(5) Mohan, D.; Pittman, C. U.; Steele, P. H. Pyrolysis of Wood/Biomass for Bio-Oil: A Critical Review. *Energy Fuels* **2006**, *20* (3), 848–889.

(6) Hilten, R.; Weber, J.; Kastner, J. R. Continuous Upgrading of Fast Pyrolysis Oil by Simultaneous Esterification and Hydrogenation. *Energy Fuels* **2016**, *30* (10), 8357–8368.

(7) Ardiyanti, A. R.; Khromova, S. A.; Venderbosch, R. H.; Yakovlev, V. A.; Melián-Cabrera, I. V.; Heeres, H. J. Catalytic Hydrotreatment of Fast Pyrolysis Oil Using Bimetallic Ni–Cu Catalysts on Various Supports. *Appl. Catal., A* **2012**, *449*, 121–130.

(8) Liu, C.; Wang, H.; Karim, A. M.; Sun, J.; Wang, Y. Catalytic Fast Pyrolysis of Lignocellulosic Biomass. *Chem. Soc. Rev.* **2014**, *43* (22), 7594–7623.

(9) Jahromi, H.; Agblevor, F. A. Upgrading of Pinyon-Juniper Catalytic Pyrolysis Oil via Hydrodeoxygenation. *Energy* **2017**, *141*, 2186–2195.

(10) Hu, C.; Xiao, R.; Zhang, H. Ex-Situ Catalytic Fast Pyrolysis of Biomass over HZSM-5 in a Two-Stage Fluidized-Bed/Fixed-Bed Combination Reactor. *Bioresour. Technol.* **2017**, *243*, 1133–1140.

(11) Kan, T.; Strezov, V.; Evans, T. Catalytic Pyrolysis of Coffee Grounds Using NiCu-Impregnated Catalysts. *Energy Fuels* **2014**, *28* (1), 228–235.

(12) Mukarakate, C.; Watson, M. J.; Ten Dam, J.; Baucherel, X.; Budhi, S.; Yung, M. M.; Ben, H.; Iisa, K.; Baldwin, R. M.; Nimlos, M. R. Upgrading Biomass Pyrolysis Vapors over β-Zeolites: Role of Silica-to-Alumina Ratio. *Green Chem.* **2014**, *16* (12), 4891–4905.

(13) Taarning, E.; Osmundsen, C. M.; Yang, X.; Voss, B.; Andersen, S. I.; Christensen, C. H. Zeolite-Catalyzed Biomass Conversion to Fuels and Chemicals. *Energy Environ. Sci.* **2011**, *4* (3), 793–804.

(14) Yung, M. M.; Starace, A. K.; Mukarakate, C.; Crow, A. M.; Leshnov, M. A.; Magrini, K. A. Biomass Catalytic Pyrolysis on Ni/ZSM-5: Effects of Nickel Pretreatment and Loading. *Energy Fuels* **2016**, *30* (7), 5259–5268.

(15) Zhao, C.; Lercher, J. A. Upgrading Pyrolysis Oil over Ni/HZSM-5 by Cascade Reactions. *Angew. Chem.* **2012**, *124* (24), 6037–6042.

(16) Kumar, R.; Strezov, V.; Kan, T.; Weldekidan, H.; He, J. Investigating the Effect of Cu/Zeolite on Deoxygenation of Bio-Oil from Pyrolysis of Pine Wood. *Energy Procedia* **2019**, *160*, 186–193.

(17) Gayubo, A. G.; Aguayo, A. T.; Atutxa, A.; Aguado, R.; Olazar, M.; Bilbao, J. Transformation of Oxygenate Components of Biomass Pyrolysis Oil on a HZSM-5 Zeolite. II. Aldehydes, Ketones, and Acids. *Ind. Eng. Chem. Res.* **2004**, *43* (11), 2619–2626.

(18) Veses, A.; Puértolas, B.; Callén, M. S.; García, T. Catalytic Upgrading of Biomass Derived Pyrolysis Vapors over Metal-Loaded ZSM-5 Zeolites: Effect of Different Metal Cations on the Bio-Oil Final Properties. *Microporous Mesoporous Mater.* **2015**, *209*, 189–196.

(19) Hernando, H.; Hernández-Giménez, A. M.; Ochoa-Hernández, C.; Bruijnincx, P. C. A.; Houben, K.; Baldus, M.; Pizarro, P.; Coronado, J. M.; Fermoso, J.; Čejka, J.; Weckhuysen, B. M.; Serrano, D. P. Engineering the Acidity and Accessibility of the Zeolite ZSM-5 for Efficient Bio-Oil Upgrading in Catalytic Pyrolysis of Lignocellulose. *Green Chem.* **2018**, *20*, 3499–3511.

(20) Yildiz, G.; Lathouwers, T.; Toraman, H. E.; van Geem, K. M.; Marin, G. B.; Ronsse, F.; van Duren, R.; Kersten, S. R. A.; Prins, W. Catalytic Fast Pyrolysis of Pine Wood: Effect of Successive Catalyst Regeneration. *Energy Fuels* **2014**, *28* (7), 4560–4572.

(21) Hertzog, J.; Carré, V.; Jia, L.; Mackay, C. L.; Pinard, L.; Dufour, A.; Mašek, O.; Aubriet, F. Catalytic Fast Pyrolysis of Biomass over Microporous and Hierarchical Zeolites: Characterization of Heavy Products. *ACS Sustainable Chem. Eng.* **2018**, *6* (4), 4717–4728.

(22) Liu, W.-J.; Li, W.-W.; Jiang, H.; Yu, H.-Q. Fates of Chemical Elements in Biomass during Its Pyrolysis. *Chem. Rev.* **2017**, *117* (9), 6367–6398.

(23) Ruddy, D. A.; Schaidle, J. A.; Ferrell, J. R., III; Wang, J.; Moens, L.; Hensley, J. E. Recent Advances in Heterogeneous Catalysts for Bio-Oil Upgrading via "Ex Situ Catalytic Fast Pyrolysis": Catalyst Development through the Study of Model Compounds. *Green Chem.* **2014**, *16* (2), 454–490.

(24) Valle, B.; Gayubo, A. G.; Aguayo, A. T.; Olazar, M.; Bilbao, J. Selective Production of Aromatics by Crude Bio-Oil Valorization with a Nickel-Modified HZSM-5 Zeolite Catalyst. *Energy Fuels* **2010**, *24* (3), 2060–2070.

(25) Zheng, Y.; Wang, F.; Yang, X.; Huang, Y.; Liu, C.; Zheng, Z.; Gu, J. Study on Aromatics Production via the Catalytic Pyrolysis Vapor Upgrading of Biomass Using Metal-Loaded Modified H-ZSM-5. *J. Anal. Appl. Pyrolysis* **2017**, *126*, 169–179.

(26) Ren, X.-Y.; Cao, J.-P.; Zhao, X.-Y.; Yang, Z.; Liu, T.-L.; Fan, X.; Zhao, Y.-P.; Wei, X.-Y. Catalytic Upgrading of Pyrolysis Vapors from Lignite over Mono/Bimetal-Loaded Mesoporous HZSM-5. *Fuel* **2018**, *218*, 33–40.

(27) Du, Z.; Ma, X.; Li, Y.; Chen, P.; Liu, Y.; Lin, X.; Lei, H.; Ruan, R. Production of Aromatic Hydrocarbons by Catalytic Pyrolysis of Microalgae with Zeolites: Catalyst Screening in a Pyroprobe. *Bioresour. Technol.* **2013**, *139*, 397–401.

(28) Mihalcik, D. J.; Mullen, C. A.; Boateng, A. A. Screening Acidic Zeolites for Catalytic Fast Pyrolysis of Biomass and Its Components. *J. Anal. Appl. Pyrolysis* **2011**, *92* (1), 224−232.
(29) Li, C.; Ma, J.; Xiao, Z.; Hector, S. B.; Liu, R.; Zuo, S.; Xie, X.; Zhang, A.; Wu, H.; Liu, Q. Catalytic Cracking of Swida Wilsoniana Oil for Hydrocarbon Biofuel over Cu-Modified ZSM-5 Zeolite. *Fuel* **2018**, *218*, 59−66.
(30) Huo, X.; Xiao, J.; Song, M.; Zhu, L. Comparison between In-Situ and Ex-Situ Catalytic Pyrolysis of Sawdust for Gas Production. *J. Anal. Appl. Pyrolysis* **2018**, *135*, 189−198.
(31) Hu, C.; Xiao, R.; Zhang, H. Ex-Situ Catalytic Fast Pyrolysis of Biomass over HZSM-5 in a Two-Stage Fluidized-Bed/Fixed-Bed Combination Reactor. *Bioresour. Technol.* **2017**, *243*, 1133−1140.
(32) Strezov, V.; Moghtaderi, B.; Lucas, J. A. Thermal Study of Decomposition of Selected Biomass Samples. *J. Therm. Anal. Calorim.* **2003**, *72*, 1041−1048.
(33) Kumar, R.; Strezov, V.; Lovell, E.; Kan, T.; Weldekidan, H.; He, J.; Dastjerdi, B.; Scott, J. Bio-Oil Upgrading with Catalytic Pyrolysis of Biomass Using Copper/Zeolite-Nickel/Zeolite and Copper-Nickel/Zeolite Catalysts. *Bioresour. Technol.* **2019**, *279*, 404−409.
(34) Iliopoulou, E. F.; Stefanidis, S. D.; Kalogiannis, K. G.; Delimitis, A.; Lappas, A. A.; Triantafyllidis, K. S. Catalytic Upgrading of Biomass Pyrolysis Vapors Using Transition Metal-Modified ZSM-5 Zeolite. *Appl. Catal., B* **2012**, *127*, 281−290.
(35) Weldekidan, H.; Strezov, V.; Town, G.; Kan, T. Production and Analysis of Fuels and Chemicals Obtained from Rice Husk Pyrolysis with Concentrated Solar Radiation. *Fuel* **2018**, *233*, 396−403.
(36) Anderson, A. B. The Composition and Structure of Wood. *J. Chem. Educ.* **1958**, *35* (10), 487.
(37) Sanchez-Silva, L.; López-González, D.; Villaseñor, J.; Sánchez, P.; Valverde, J. L. Thermogravimetric−Mass Spectrometric Analysis of Lignocellulosic and Marine Biomass Pyrolysis. *Bioresour. Technol.* **2012**, *109*, 163−172.
(38) Williams, P. T.; Besler, S. Thermogravimetric Analysis of the Components of Biomass. In *Advances in Thermochemical Biomass Conversion*; Bridgwater, A. V., Ed.; Springer: Dordrecht, Netherlands, 1993; pp 771−783, DOI: 10.1007/978-94-011-1336-6_60.
(39) Westerhof, R. J. M.; Brilman, D. W. F.; Garcia-Perez, M.; Wang, Z.; Oudenhoven, S. R. G.; Kersten, S. R. A. Stepwise Fast Pyrolysis of Pine Wood. *Energy Fuels* **2012**, *26* (12), 7263−7273.
(40) Garcia-Perez, M.; Wang, X. S.; Shen, J.; Rhodes, M. J.; Tian, F.; Lee, W.-J.; Wu, H.; Li, C.-Z. Fast Pyrolysis of Oil Mallee Woody Biomass: Effect of Temperature on the Yield and Quality of Pyrolysis Products. *Ind. Eng. Chem. Res.* **2008**, *47* (6), 1846−1854.
(41) Custodis, V. B. F.; Hemberger, P.; Ma, Z.; van Bokhoven, J. A. Mechanism of Fast Pyrolysis of Lignin: Studying Model Compounds. *J. Phys. Chem. B* **2014**, *118* (29), 8524−8531.
(42) Patwardhan, P. R.; Brown, R. C.; Shanks, B. H. Understanding the Fast Pyrolysis of Lignin. *ChemSusChem* **2011**, *4* (11), 1629−1636.
(43) Yang, H.; Yan, R.; Chen, H.; Lee, D. H.; Zheng, C. Characteristics of Hemicellulose, Cellulose and Lignin Pyrolysis. *Fuel* **2007**, *86* (12−13), 1781−1788.
(44) Piskorz, J.; Radlein, D.; Scott, D. S. On the Mechanism of the Rapid Pyrolysis of Cellulose. *J. Anal. Appl. Pyrolysis* **1986**, *9* (2), 121−137.
(45) Patwardhan, P. R.; Brown, R. C.; Shanks, B. H. Product Distribution from the Fast Pyrolysis of Hemicellulose. *ChemSusChem* **2011**, *4* (5), 636−643.
(46) Zhang, J.; Choi, Y. S.; Yoo, C. G.; Kim, T. H.; Brown, R. C.; Shanks, B. H. Cellulose−Hemicellulose and Cellulose−Lignin Interactions during Fast Pyrolysis. *ACS Sustainable Chem. Eng.* **2015**, *3* (2), 293−301.
(47) Adjaye, J. D.; Bakhshi, N. N. Catalytic Conversion of a Biomass-Derived Oil to Fuels and Chemicals I: Model Compound Studies and Reaction Pathways. *Biomass Bioenergy* **1995**, *8* (3), 131−149.
(48) Op de Beeck, B.; Dusselier, M.; Geboers, J.; Holsbeek, J.; Morré, E.; Oswald, S.; Giebeler, L.; Sels, B. F. Direct Catalytic Conversion of Cellulose to Liquid Straight-Chain Alkanes. *Energy Environ. Sci.* **2015**, *8* (1), 230−240.
(49) Cheng, Y.-T.; Huber, G. W. Chemistry of Furan Conversion into Aromatics and Olefins over HZSM-5: A Model Biomass Conversion Reaction. *ACS Catal.* **2011**, *1* (6), 611−628.
(50) Zhao, C.; Kou, Y.; Lemonidou, A. A.; Li, X.; Lercher, J. A. Highly Selective Catalytic Conversion of Phenolic Bio-Oil to Alkanes. *Angew. Chem.* **2009**, *121* (22), 4047−4050.
(51) Hemberger, P.; Custodis, V. B. F.; Bodi, A.; Gerber, T.; van Bokhoven, J. A. Understanding the Mechanism of Catalytic Fast Pyrolysis by Unveiling Reactive Intermediates in Heterogeneous Catalysis. *Nat. Commun.* **2017**, *8*, 15946.
(52) Asadieraghi, M.; Ashri Wan Daud, W. M.; Abbas, H. F. Heterogeneous Catalysts for Advanced Bio-Fuel Production through Catalytic Biomass Pyrolysis Vapor Upgrading: A Review. *RSC Adv.* **2015**, *5* (28), 22234−22255.
(53) To, A. T.; Resasco, D. E. Role of a Phenolic Pool in the Conversion of M-Cresol to Aromatics over HY and HZSM-5 Zeolites. *Appl. Catal., A* **2014**, *487*, 62−71.
(54) Jiang, X.; Zhou, J.; Zhao, J.; Shen, D. Catalytic Conversion of Guaiacol as a Model Compound for Aromatic Hydrocarbon Production. *Biomass Bioenergy* **2018**, *111*, 343−351.
(55) Leung, A.; Boocock, D. G. B.; Konar, S. K. Pathway for the Catalytic Conversion of Carboxylic Acids to Hydrocarbons over Activated Alumina. *Energy Fuels* **1995**, *9* (5), 913−920.
(56) Psarras, A. C.; Michailof, C. M.; Iliopoulou, E. F.; Kalogiannis, K. G.; Lappas, A. A.; Heracleous, E.; Triantafyllidis, K. S. Acetic Acid Conversion Reactions on Basic and Acidic Catalysts under Biomass Fast Pyrolysis Conditions. *Molecular Catalysis* **2019**, *465*, 33−42.
(57) Zhao, Y.; Pan, T.; Zuo, Y.; Guo, Q.-X.; Fu, Y. Production of Aromatic Hydrocarbons through Catalytic Pyrolysis of 5-Hydroxymethylfurfural from Biomass. *Bioresour. Technol.* **2013**, *147*, 37−42.
(58) Alonso, D. M.; Wettstein, S. G.; Dumesic, J. A. Bimetallic Catalysts for Upgrading of Biomass to Fuels and Chemicals. *Chem. Soc. Rev.* **2012**, *41* (24), 8075.
(59) Gunawardena, D. A.; Fernando, S. D. Screening of Transition Metal/Oxide-Impregnated ZSM-5 Catalysts for Deoxygenation of Biomass Oxygenates via Direct Methane Intervention. *Biofuels* **2018**, *9* (1), 113−120.

Supporting information

Investigating the effect of mono and bimetallic/zeolite catalysts on hydrocarbon production during bio-oil upgrading from *ex-situ* pyrolysis of biomass

Ravinder Kumar, Vladimir Strezov, Tao Kan, Haftom Weldekidan, Jing He, Sayka Jahan

Department of Earth and Environmental Sciences, Faculty of Science & Engineering, Macquarie University, Sydney, NSW 2109, Australia

1. Experimental

1.1. Synthesis and characterization of catalysts

The zeolite (Saint-Gobain, Paris) used in this study had a composition of Silica-25% alumina with 0.35% Na_2O, was provided in the form of pellets (3 mm). The pellets were crushed and sieved with a 40-mesh sieve to obtain the particle size of 0.42 mm. The zeolite was calcined at 550 °C for 2.5 h before using in the catalyst preparation. Cu10%/zeolite and Ni10%/zeolite as the mono-metallic catalysts and Cu5%-Ni5%/zeolite as a bimetallic catalyst were prepared by an incipient wetness impregnation method. To prepare 15g of mono-metallic catalyst, 5.70g of $Cu(NO_3)_2.3H_2O$ or 7.43g of $Ni(NO_3)_2.6H_2O$ was dissolved in 30 ml Milli Q water, followed by the addition of the required amount of zeolite in the metal solution. The ultrasonic vibration at 40 kHz for 2 h was applied for better dispersion of the active metals on the zeolite. The resultant slurry was held at room temperature for 22 h and subsequently dried in a vacuum oven at 110 °C overnight. Successively, the material was calcined at 550 °C for 5.5 h. The material obtained after the calcination process was used as the final catalyst. A similar method was used to prepare the bi-metallic catalyst utilizing the required amount of the metal precursors. Moreover, the concentration of metals in the catalysts was estimated by X-ray fluorescence (XRF), Olympus Delta Pro spectrometers using Ta tube (50 kV). The XRF results showed that the concentrations of Cu and Ni were 9.9% and 11.29% in mono-metallic catalysts, respectively, whereas 6.02% of Cu and 4.74% of Ni was present in the bi-metallic catalyst, demonstrating the formation of the catalysts with estimated concentrations of the metals.

The mono-metallic and bi-metallic catalysts were characterized by XRD on PANalytical X'Pert Pro MPD X-ray diffractometer by employing CuKα radiations (λ = 1.54056 Å) and Ni-

filter by measuring the X-ray intensity over a diffraction 2θ angle from 5 to 90. The crystallite size of the metal was measured using the following Scherrer equation:

$$d_{\text{crystallite size}}(nm) = \frac{0.94\lambda}{B \times \cos\theta} \quad (1)$$

where B is full-width at half-maximum (FWHM) of the most intense peak in the spectrum.
The morphology of all the catalysts was examined using TEM (Philips CM10, Netherlands) with an operating voltage of 100 kV and Olympus SIS Megaview G2 digital camera.

N_2 adsorption-desorption isotherms and Brunauer-Emmett-Teller (BET) specific surface areas (SSA) were analyzed on a Micromeritics Tristar 3030 instrument at -196 °C. The samples were degassed at 150 °C for 3 h under vacuum prior to analysis.

Ammonia temperature programmed desorption (NH_3-TPD) and hydrogen temperature programmed reduction (H_2-TPR) were carried out to analyze the acidity and the presence of reducible metal species in the catalysts, respectively. Both the measurements were conducted on a Micromeritics Autochem 2920 with a thermal conductivity detector (TCD). In the H_2-TPR analysis, around 100 mg of sample was loaded into a quartz U-tube atop a plug of quartz wool. The sample was successively pre-treated by heating to 150 °C (at 10 °C/min) and holding for 0.5 h under 20 mL/min Ar (Coregas Ar; >99.999 %), cooled to room temperature and then heated to 850 °C at 5 °C/min under 20mL/min 10% H_2 in Ar (Coregas, 10.05 % H_2 in Ar). Alternatively, in an NH_3-TPD study, ~100 mg of sample was also loaded into the quartz U-tube on a plug of quartz wool. Prior to analysis, the samples were pre-reduced by heating from room temperature to 550 °C at 5 °C/min under 20mL/min 10% H_2 in Ar with a 1 h hold, subsequently cooled to 50 °C under He (20 mL/min, Coregas He; > 99.999 %). Then NH_3 in He (Coregas, 5.13% NH_3 in He) was passed over the sample at 20 mL/min for 2 h at 50 °C. Any physiosorbed NH_3 was purged from the system by holding at 50 °C for 2 h under 20 mL/min prior to heating (in He) at 5 °C/min to 800 °C with a 1 h hold at 800 °C.

2. Results and discussion

2. 1. Characterization of catalysts

XRD technique was carried out to examine the crystallinity and the presence of metals in fresh mono and bi-metallic catalysts, while the spent catalysts were also subjected to XRD to confirm the status of metal species in the catalysts, the results are shown in Fig. S1. In Fig. S1a, it can be noticed that zeolite was not present in a highly pure crystalline form but few sharp peaks in the pattern can be attributed to a crystalline form of zeolite. For example, the peaks at 2θ of 39.7°, 46.1°, 66.7°, and 85.06° can be ascribed to crystalline zeolite, which is consistent with the standard values of zeolite, International Centre for Diffraction data (ICDD) reference code 98-009-3736. Further, it was observed that the metals were present in their oxide forms (CuO and

NiO) in both mono and bi-metallic catalysts. Noticeably, Cu/zeolite exhibited diffraction peaks at 2θ of 35.1°, 39.3°, 48.7°, 53.44°, 58.3°, 61.4°, and 75.2° which can be indexed to (002), (200), (202), (020), (-113), (-311), and (-222) planes of CuO, respectively. These results were in a close line with the standard values of CuO, ICDD reference code 00-045-0937. The crystallite size of CuO was estimated to be 29.81 nm in the catalyst. Alternatively, Ni/zeolite showed the diffraction peaks at the respective 2θ angles which were in the agreement with the standard values of NiO, ICDD reference code-01-089-7390. The determined crystallite size of NiO was 7.62 nm in this catalyst. Similarly, the bi-metallic catalyst, CuNi/zeolite showed main diffraction peaks at 2θ of 37.1°, 39.3°, 43.4°, 62.5°, 75.5° which can be attributed to NiO and CuO present in the catalyst. The XRD patterns of the spent catalysts are given in Fig. S1b, which revealed that the metal oxides present in the catalysts were successfully converted into their metal forms during the pyrolysis reaction. These results support the findings of other research that also showed the transformation of metal oxides into their metal forms [1,2].

The morphology of all the catalysts was examined using TEM. Fig. S2 shows TEM micrographs of mono and bi-metallic catalysts. It can be observed from the figure that there were substantial morphological changes in mono and bi-metallic catalysts when compared to sole zeolite, which indicated that successful introduction of the metal oxides onto zeolite support. TEM results were also supported by XRD analysis that confirmed the presence of CuO and NiO in the catalysts. XRD study also suggested that in Ni/zeolite, the crystallite size of NiO was smaller as compared to CuO in Cu/zeolite, which might result into better dispersion of the former on the zeolite, and consequently improve its stability and catalytic activity.

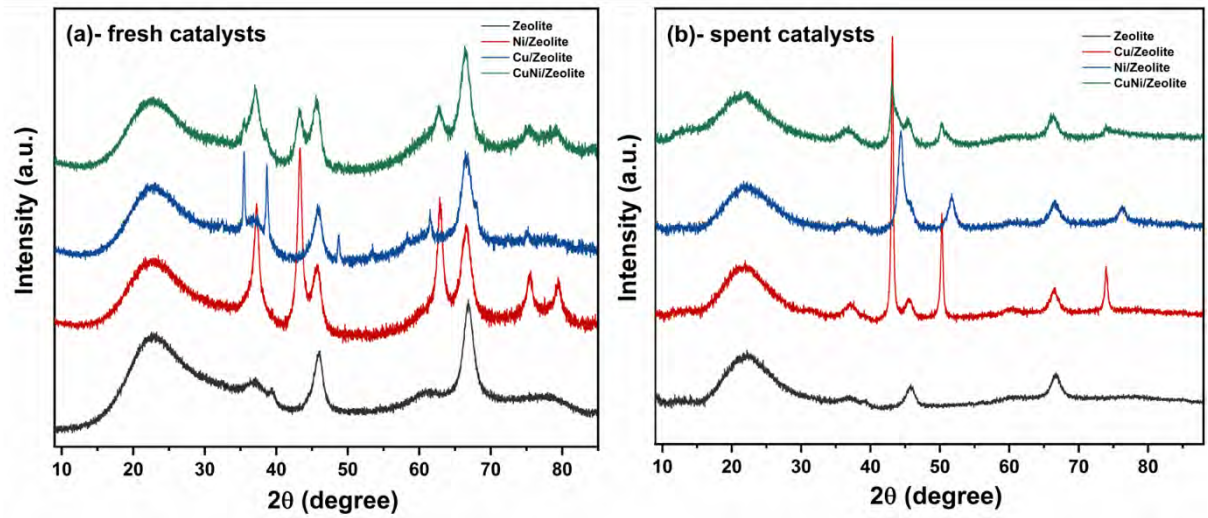

Figure S1. XRD pattern of catalysts, (a) fresh catalyst, (b) spent catalysts.

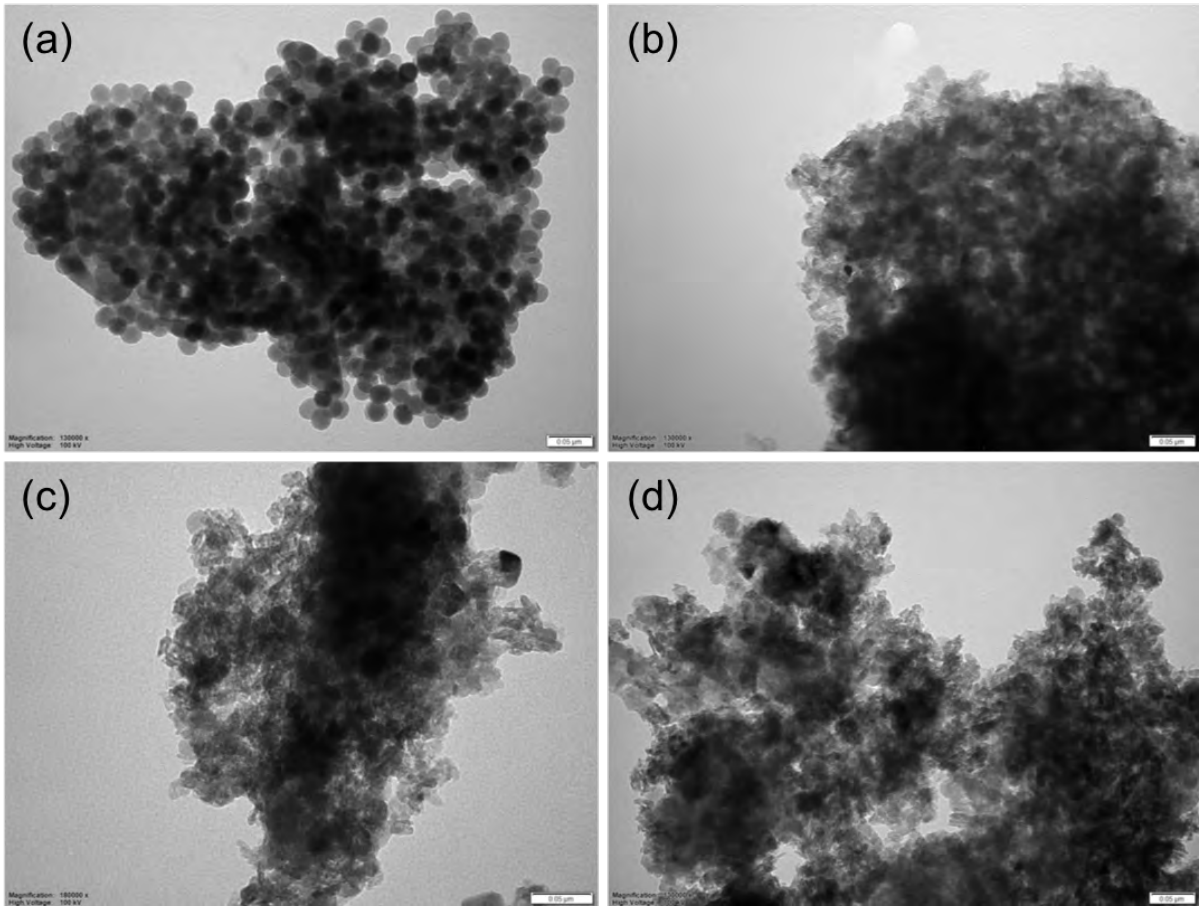

Figure S2. TEM images of (a) zeolite, (b) Cu/zeolite, (c) Ni/zeolite, and (d) CuNi/zeolite.

The BET results for mono and bi-metallic catalysts are given in Table S1. One can see in the table, sole zeolite demonstrated the highest BET surface area of 412 m^2/g among all the catalysts. Further, it was noticed that the incorporation of metals on to the zeolite drastically reduced the surface area, indicating the successful accumulation of metal oxide particles on to zeolite surface or inside the pores. Expectedly, Cu/zeolite showed a BET surface area of 195 m^2/g and Ni/zeolite achieved the surface area of 307 m^2/g. The higher surface area of Ni/zeolite can be credited to the smaller crystallite size of NiO particles that resulted in its better dispersion on the zeolite surface, whereas the crystallite size of CuO particles was observed higher in Cu/zeolite, which might have blocked the pores on the zeolite surface, resulting in the lower surface area. Moreover, the bi-metallic catalyst obtained the surface area of 253 m^2/g, which can be attributed to the mutual distribution of NiO and CuO on to the zeolite surface. These results support the reports of other studies that also exhibited the substantial reduction in the surface area after the addition of a metal in the zeolite catalyst [3,4]. For example, [4] revealed that the sole ZSM-5 catalyst showed a BET surface area of 392 m^2/g, while the addition of 6% Ni decreased the surface area to 316 m^2/g.

Table S1. BET results of mono and bi-metallic catalysts.

Catalyst	Specific surface area (m^2/g)	Average pore size (nm)	Pore volume (cm^3/g)
Zeolite	412	6.51	0.696
Cu/zeolite	195	8.08	0.485
Ni/zeolite	307	6.77	0.554
CuNi/zeolite	253	7.22	0.511

The acidic characteristic of mono and bi-metallic catalysts was measured by NH_3-TPD. The acidic character in zeolite arise due to the presence of Brønsted acidic protons in its framework. A Brønsted acidic proton contains a hydrogen atom bonded to the oxygen that connects the tetrahedrally coordinated cation, which can be represented as $[M]^{n+}$—H—O [5]. These acidic sites in the catalyst play a pivotal role its catalytic activity and aromatization of hydrocarbons [6]. Figure S3a showing NH_3-TPD results revealed a broad peak at approximately 133 °C for the sole zeolite, which can be credited to the weak Brønsted acid sites in the catalyst. No peak was detected at the higher temperature, indicating the absence of strong Brønsted acid sites in the sole zeolite catalyst. However, Cu/zeolite showed a decrease in weak Brønsted acid sites as a lower intensity peak was observed at ~140 °C but exhibited a broad peak at approximately 659 °C, which can be attributed to the strong and new Brønsted acid sites created by Cu cations or other Cu cluster species in the catalyst [7]. Alternatively, Ni/zeolite exhibited a large and broad peak at 150 °C, corresponding to the presence of weak Brønsted acid sites in the catalyst. It was noticed that this peak shifted to a higher temperature when compared to the sole zeolite (133 °C), suggesting that the addition of Ni improved the acidity of the catalyst. Moreover, Ni/zeolite showed two peaks at 360 °C and 410 °C, which marked the formation of two new types of Brønsted acid sites by Ni cations in the catalyst [4]. The bi-metallic catalyst, CuNi/zeolite demonstrated a desorption signal at approximately 155 °C, attributing to the occurrence of weak acidic sites. Further, a low intensity and broad peak can be observed at 592 °C, which can be attributed to the formation of new acidic sites by Cu and Ni cations in the catalyst [2]. Overall, it can be suggested that the mono and bi-metallic catalysts showed a combination of weak and strong acidic sites than the sole zeolite, which would affect their catalytic activity and consequently, the selectivity of hydrocarbons in the bio-oil.

Figure S3b shows H_2-TPR results for mono and bi-metallic catalysts, which confirmed the presence of reducible metal species in the catalysts. One can notice two intense peaks at 236 and 278 °C for Cu/zeolite catalyst. The first peak at 236 °C could be attributed to the reduction of CuO particles having less or weak interaction with zeolite support, whereas the second peak at a higher temperature can be credited to the reduction of CuO particles with the stronger interaction with zeolite support. These results support the findings of Widayatno et al. [7] that also reported almost

similar data for the reduction of Cu/zeolite catalyst. Alternatively, Ni/zeolite exhibited a broad peak that can be divided into two zones, one starting from the temperature of 353 to 450 °C and the second starting from 450 to 654 °C. A study by Maia et al. [4] demonstrated the reduction patterns of Ni/zeolite catalyst and proposed three reduction zones: (a) 430−470 °C, (b) 520−560 °C, and (c) 630−720 °C. The first reduction zone can be attributed the bulk NiO and the latter two could be due to the smaller NiO particles. Besides, it was also concluded that Ni^{2+} requires a higher temperature to reduce if it is exchanged with H^{+} on the zeolite structure [4]. Therefore, in this case, it can be suggested that bulk NiO and smaller NiO particles with strong zeolite interaction were present in the catalyst. In addition, the NiO particles could also be present within zeolite pores, which are usually difficult to reduce as indicated by the reduction peak at the higher temperatures. The bi-metallic catalyst showed an intense peak at 255 °C and two other small and broad peaks at 325 and 390 °C, which suggested that CuO and NiO particles had weak or no interaction with zeolite support and these metal oxide particles were mostly present on the zeolite surface as no peaks were detected at the higher temperatures. Overall, it can be suggested that Ni/zeolite showed the better dispersion of NiO particles as compared to Cu/zeolite catalyst, while the addition of Cu affected the dispersion of Ni particles in the bi-metallic catalyst, resulting in the comparatively weaker interaction with zeolite support. These findings are also supported by XRD and BET results which confirmed the smaller crystallite size of NiO particles and a higher surface area of the catalyst, respectively.

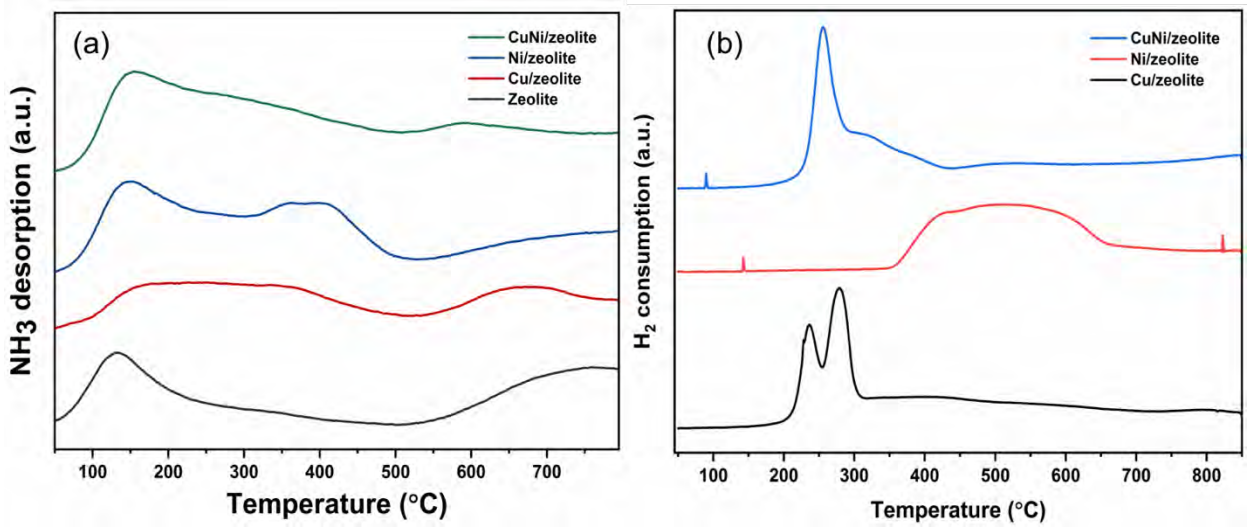

Figure S3. (a) NH_3-TPD curves for mono and bi-metallic catalysts (b) H_2-TPR curves for mono and bi-metallic catalysts.

References

[1] Li C, Ma J, Xiao Z, Hector SB, Liu R, Zuo S, et al. Catalytic cracking of Swida wilsoniana oil for hydrocarbon biofuel over Cu-modified ZSM-5 zeolite. Fuel 2018;218:59–66. https://doi.org/10.1016/j.fuel.2018.01.026.

[2] Ren X-Y, Cao J-P, Zhao X-Y, Yang Z, Liu T-L, Fan X, et al. Catalytic upgrading of pyrolysis vapors from lignite over mono/bimetal-loaded mesoporous HZSM-5. Fuel 2018;218:33–40. https://doi.org/10.1016/j.fuel.2018.01.017.

[3] Hernando H, Hernández-Giménez AM, Ochoa-Hernández C, Bruijnincx PCA, Houben K, Baldus M, et al. Engineering the acidity and accessibility of the zeolite ZSM-5 for efficient bio-oil upgrading in catalytic pyrolysis of lignocellulose. Green Chemistry 2018. https://doi.org/10.1039/C8GC01722K.

[4] Maia AJ, Louis B, Lam YL, Pereira MM. Ni-ZSM-5 catalysts: Detailed characterization of metal sites for proper catalyst design. Journal of Catalysis 2010;269:103–9. https://doi.org/10.1016/j.jcat.2009.10.021.

[5] Niwa M, Katada N. Measurements of acidic property of zeolites by temperature programmed desorption of ammonia n.d.:12.

[6] Du Z, Ma X, Li Y, Chen P, Liu Y, Lin X, et al. Production of aromatic hydrocarbons by catalytic pyrolysis of microalgae with zeolites: Catalyst screening in a pyroprobe. Bioresource Technology 2013;139:397–401. https://doi.org/10.1016/j.biortech.2013.04.053.

[7] Widayatno WB, Guan G, Rizkiana J, Yang J, Hao X, Tsutsumi A, et al. Upgrading of bio-oil from biomass pyrolysis over Cu-modified β-zeolite catalyst with high selectivity and stability. Applied Catalysis B: Environmental 2016;186:166–72. https://doi.org/10.1016/j.apcatb.2016.01.006.

MACQUARIE University

MACQUARIE UNIVERSITY
AUTHORSHIP CONTRIBUTION STATEMENT

In accordance with the *Macquarie University Code for the Responsible Conduct of Research* and the *Authorship Standard*, researchers have a responsibility to their colleagues and the wider community to treat others fairly and with respect, to give credit where appropriate to those who have contributed to research.

Note for HDR students: *Where research papers are being included in a thesis, this template must be used to document the contribution of authors to each of the proposed or published research papers. The contribution of the candidate must be sufficient to justify inclusion of the paper in the thesis.*

1. DETAILS OF PUBLICATION & CORRESPONDING AUTHOR

Title of Publication (can be a holding title)		**Publication Status** Choose an item
Bio-oil upgrading with catalytic pyrolysis of biomass using Copper/zeolite-Nickel/zeolite and Copper-Nickel/zeolite catalysts		☐ In Progress or Unpublished work for thesis submission ☐ Submitted for Publication ☐ Accepted for Publication ■ Published
Name of **corresponding author**	Department/Faculty	**Publication details:** indicate the name of the journal/ conference/ publisher/other outlet
Ravinder Kumar	Earth and Environmental Sciences/ Science & Engineering	Bioresource Technology

2. STUDENTS DECLARATION (if applicable)

Name of HDR thesis author (If the same as corresponding author - write "as above")	Department/Faculty	Thesis title
as above	Earth and Environmental Sciences/ Science & Engineering	Catalytic Upgrading of Bio-oil Produced from Fast Pyrolysis of Pinewood Sawdust

Description of HDR thesis author's contribution to planning, execution, and preparation of the work if there are multiple authors

(for example, how much as a percent did you contribute to the conception of the project, the design of methodology or experimental protocol, data collection, analysis, drafting the manuscript, revising it critically for important intellectual content, etc.)

In this article, I contributed in designing the project, carried out 70% of the experimental work, analyzed the data and wrote 80% of the manuscript.

I declare that the above is an accurate description of my contribution to this publication, and the contributions of other authors are as described below.	**Student signature** **Date**	 02/22/2021

MACQUARIE University

3. Description of all other author contributions

Use an Asterisk * to denote if the author is also a current student or HDR candidate.

The HDR candidate or corresponding author must, for each paper, list all authors and provide details of their role in the publication. Where possible, also provide a percentage estimate of the contribution made by each author.

Name and affiliation of author	Intellectual contribution(s) (for example to the: conception of the project, design of methodology/experimental protocol, data collection, analysis, drafting the manuscript, revising it critically for important intellectual content etc.)
Vladimir Strezov Macquarie University	conception, supervision, critical revision
Emma Lovell UNSW	experimental, data analysis, critical revision
Tao Kan Macquarie University	experimental, data analysis, supervision, critical revision
Haftom Weldekidan Macquarie University	experimental, data analysis, critical revision
Jing He Macquarie University	experimental, data analysis, critical revision
*Behnam Dastjerdi Macquarie University	data analysis, critical revision
Jason Scott UNSW	experimental, data analysis, critical revision
	Provide summary for any additional Authors in this cell.

4. Author Declarations

I agree to be named as one of the authors of this work, and confirm:

i. *that I have met the authorship criteria set out in the* Authorship Standard, *accompanying the* Macquarie University Research Code,

ii. *that there are no other authors according to these criteria,*

iii. *that the description in Section 3 or 4 of my contribution(s) to this publication is accurate*

iv. *that I have agreed to the planned authorship order following the* Authorship Standard

Name of author	**Authorised *** By Signature or refer to other written record of approval (eg. pdf of a signed agreement or an email record)	**Date**
Vladimir Strezov		24/02/2021
Emma Lovell		26/02/2021
Tao Kan		22/02/2021
Haftom Weldekidan		22/02/202
Jing He		22/02/2021
Behnam Dastjerdi		02/22/2021
Jason Scott		26/02/2021
	Provide other written record of approval for additional authors (eg. pdf of a signed agreement or an email record)	

5. Data storage

The original data for this project are stored in the following location, in accordance with the *Research Data Management Standard* accompanying the *Macquarie University Research Code*.

If the data have been or will be deposited in an online repository, provide the details here with any corresponding DOI.

Data description/format	**Storage Location or DOI**	**Name of custodian** if other than the corresponding author

A copy of this form must be retained by the corresponding author and must accompany the thesis submitted for examination.

Chapter 7

Bio-oil upgrading with catalytic pyrolysis of biomass using Copper/zeolite-Nickel/zeolite and Copper-Nickel/zeolite catalysts

Ravinder Kumar[a,], Vladimir Strezov[a], Emma Lovell[b], Tao Kan[a], Haftom Weldekidan[a], Jing He[a], Behnam Dastjerdi[a], Jason Scott[b]

[a]Department of Environmental Sciences, Faculty of Science & Engineering, Macquarie University, Sydney, NSW 2109, Australia
[b]Particles and Catalysis Research Group, School of Chemical Engineering, The University of New South Wales, Sydney, NSW 2052, Australia

The previous chapter compares the bio-oil deoxygenation activity of monometallic catalysts (Cu/zeolite and Ni/zeolite) and a bimetallic (CuNi/zeolite) in one-stage *ex-situ* pyrolysis mode and showed that synergistic effect of Ni and Cu as a bimetallic catalyst achieved better bio-oil deoxygenation. This chapter aims to compare the bio-oil deoxygenation between combined monometallic catalysts in two-stage *ex-situ* mode and a bimetallic catalyst in one-stage *ex-situ* pyrolysis mode. Similar catalysts employed in the previous chapter were utilized in this chapter and the details are given in the supporting information of the previous chapter.

Kumar, R., Strezov, V., Lovell, E., Kan, T., Weldekidan, H., He, J., Dastjerdi, B., & Scott, J. (2019). Bio-oil upgrading with catalytic pyrolysis of biomass using Copper/ zeolite-Nickel/zeolite and Copper-Nickel/zeolite catalysts. Bioresource Technology, 279, 404-409. https://doi.org/10.1016/j.biortech.2019.01.067

Bioresource Technology 279 (2019) 404–409

Contents lists available at ScienceDirect

Bioresource Technology

journal homepage: www.elsevier.com/locate/biortech

Short Communication

Bio-oil upgrading with catalytic pyrolysis of biomass using Copper/zeolite-Nickel/zeolite and Copper-Nickel/zeolite catalysts

Ravinder Kumar[a,*], Vladimir Strezov[a], Emma Lovell[b], Tao Kan[a], Haftom Weldekidan[a], Jing He[a], Behnam Dastjerdi[a], Jason Scott[b]

[a] Department of Environmental Sciences, Faculty of Science & Engineering, Macquarie University, Sydney, NSW 2109, Australia
[b] Particles and Catalysis Research Group, School of Chemical Engineering, The University of New South Wales, Sydney, NSW 2052, Australia

GRAPHICAL ABSTRACT

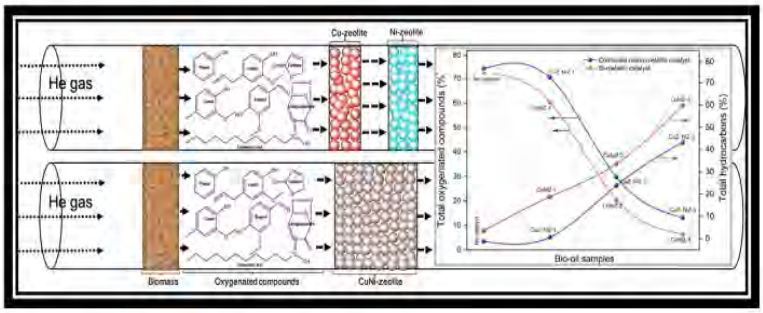

ARTICLE INFO

Keywords:
Catalytic fast pyrolysis
Bio-oil upgrading
Combined mono-metallic
Bi-metallic
Hydrocarbons

ABSTRACT

The bio-oil obtained from a general pyrolysis process contains a higher concentration of oxygenated compounds and the resultant physical and chemical properties make it an unsuitable drop-in fuel. The oxygenated compounds in the bio-oil can be converted into hydrocarbons or less oxygenated compounds with the application of catalysts. This study demonstrated the bio-oil upgrading with the application of catalysts, comparing the catalytic effect of combined mono-metallic catalysts (Cu/zeolite and Ni/zeolite) and sole bi-metallic catalyst (CuNi/zeolite) on the composition of bio-oil and pyrolytic gases. The results demonstrated that in comparison to the combined mono-metallic catalysts, the sole bi-metallic catalyst showed better deoxygenation for all the oxygenated compounds and favoured the production of aliphatic hydrocarbons, whereas the combination of mono-metallic catalysts generated higher proportion of aromatic hydrocarbons in the bio-oil. In both cases, the catalysts equally favoured decarboxylation and decarbonylation reactions, as CO_2/CO of approximately 1 was obtained during the pyrolysis process.

1. Introduction

Bio-oil or pyrolytic oil generated from the fast pyrolysis of biomass is foreseen as the future source of renewable energy and many other useful chemicals (Kan et al., 2016; Li et al., 2018; Wang et al., 2018; Weldekidan et al., 2018). However, the bio-oil without any upgrading or downstream processing cannot be used as a drop-in fuel. This is because the general pyrolysis of biomass produces the bio-oil that is highly rich in oxygenated compounds, such as phenols, alcohols, carboxylic acids, ketones and aldehydes, while the content of non-

* Corresponding author.
E-mail address: ravinder.kumar@hdr.mq.edu.au (R. Kumar).

https://doi.org/10.1016/j.biortech.2019.01.067
Received 3 December 2018; Received in revised form 16 January 2019; Accepted 17 January 2019
Available online 18 January 2019
0960-8524/

oxygenated hydrocarbons is usually very low (Westerhof et al., 2012). The dominant presence of the oxygenated compounds makes the bio-oil highly acidic in nature (pH of 2–3) and some other unfavourable physical or chemical properties, such as low calorific value, poor volatility and instability, restrict its direct application as a fuel (Gayubo et al., 2004). Therefore, it is highly essential to advance the overall quality of bio-oil and make it a competitive fuel that is deficient of oxygenated compounds and rich in aliphatic and aromatic hydrocarbons.

Catalytic fast pyrolysis (CFP) is considered a significant approach to convert the oxygenated compounds into a variety of hydrocarbons and improving the bio-oil quality. The introduction of a catalyst generally decreases the temperature of the pyrolysis process and removes the oxygen via various reactions, such as dehydration (removing oxygen as H_2O), decarboxylation (removing oxygen as CO_2) and decarbonylation (removing oxygen as CO) (Hernando et al., 2018; Hertzog et al., 2018). A plethora of studies has successfully demonstrated the application of different types of catalysts to upgrade the pyrolytic oil (Li et al., 2018; Thangalazhy-Gopakumar et al., 2012; Zhang et al., 2017). However, zeolites, such as ZSM-5 or H-ZSM-5 based catalysts have shown enhanced conversion of oxygenated compounds into hydrocarbons as compared to other catalysts (Dai et al., 2018; Hernando et al., 2018; Ren et al., 2018; Zheng et al., 2017), which is generally attributed to their acidic and porous characteristics (Hertzog et al., 2018; Mihalcik et al., 2011). The catalytic activity and stability of zeolite catalysts can be further improved with the introduction of a metal or two metals, preparing mono-metallic or bi-metallic catalysts, respectively. In this regard, several mono and bi-metallic catalysts have been utilized to upgrade the bio-oil with results suggesting that adding a metal to zeolite support enhances the deoxygenation activity by favouring the specific deoxygenation reactions, such as decarboxylation and decarbonylation, and decreases the coke formation onto the catalyst (Gunawardena and Fernando, 2018; Iliopoulou et al., 2012; Ren et al., 2018; Zheng et al., 2017). For example, Li et al. (2016) prepared different zeolite-based mono-metallic catalysts (Fe/HZSM-5, Zr/HZSM-5 and Co/HZSM-5) and investigated their catalytic activity using *ex-situ* pyrolysis of pine wood sawdust. The results demonstrated that metal-substituted catalysts resulted in a significant increase in the yield of aromatic hydrocarbons. It was reported that Zr/HZSM-5 catalyst enhanced the formation of benzene derivative compounds, which was attributed to the promoted intermolecular hydrogen-transfer reaction with consequent consumption of olefins to form benzene and its derivatives while Fe/HZSM-5 promoted the production of naphthalene derivatives in the bio-oil samples (Li et al., 2016). In an alternative study, different metal loaded ZSM-5 catalysts were tested for bio-oil upgrading (Veses et al., 2016). The study indicated that Cu/ZSM-5 catalyst deoxygenated bio-oil via decarbonylation of acids and ketones at Cu cations incorporated at ion exchange positions, while Ni/ZSM-5 catalyst removed oxygen from the oxygenated compounds through decarbonylation and decarboxylation reactions at the Lewis acid sites on the catalyst (Veses et al., 2016). Similar to mono-metallic catalysts, bi-metallic catalysts have also shown remarkable tendency to enhance the bio-oil deoxygenation. In a bi-metallic catalyst, the synergetic activity of two metals generally increases the overall catalytic efficiency of the catalyst and also creates new type of catalytic sites, which ultimately could affect the selectivity of hydrocarbons in the bio-oil. For instance, MoZn/HZSM-5 was applied for *ex-situ* pyrolysis of torrefied switchgrass at 700 °C (Yang et al., 2017). This bi-metallic catalyst showed better catalytic activity and produced a higher number of aromatic hydrocarbons as compared to mono-metallic catalysts. A maximum aromatic hydrocarbons yield of 39.31% was obtained in the study (Yang et al., 2017).

It is evident from the earlier studies that the bi-metallic catalysts could be more effective for bio-oil deoxygenation as compared to mono-metallic catalysts. However, the difference in the catalytic effect between combined mono-metallic catalysts and a bi-metallic catalyst of the same metals for bio-oil deoxygenation is still not sufficiently understood. The aim of this study was to provide a comparative investigation of the difference between the combined mono-metallic and bi-metallic catalysts for upgrading of the bio-oils produced during pyrolysis of biomass. The study was carried out using Cu/zeolite and Ni/zeolite as mono-metallic catalysts and CuNi/zeolite as the bi-metallic catalyst. Three different combinations of mono-metallic catalysts with total catalyst to biomass ratios of 1, 2 and 3 and the bi-metallic catalyst with the similar catalyst to biomass ratios were applied in a fixed bed tube reactor at 500 °C in an *ex-situ* pyrolysis mode. The bio-oil samples extracted from the pyrolysis process were subjected to gas chromatography-mass spectrometry to analyse their compounds, while the pyrolytic gases were examined online using a micro-gas chromatography.

2. Materials and methods

2.1. Analysis of biomass

Pine wood biomass used in this study was collected from Sydney, Australia. The methods for feedstock preparation and the results of its proximate and ultimate analysis are discussed in the Supplementary information.

2.2. Catalyst preparation and characterization

The mono-metallic (Cu10%/zeolite and Ni10%/zeolite) and bi-metallic catalysts (Cu 5%-Ni5%/zeolite) were prepared by an incipient wetness impregnation method, and characterized by different physio-chemical techniques, such as X-ray diffraction (XRD), Brunauer–Emmett–Teller (BET), transmission electron microscopy (TEM), hydrogen-temperature programmed reduction (H_2-TPR) and ammonia-temperature programmed desorption (NH_3-TPD). The preparation method of catalysts, methods and results of characterization techniques are comprehensively discussed in the Supplementary information.

2.3. Pyrolysis operation

An infrared image gold furnace (SINKU-RIKO) was used for *ex-situ* pyrolysis of pine wood at 500 °C with a heating rate of 100 °C/min. The quantity of biomass used was approximately 100 mg throughout the experiments, which was loaded in an inner silica reactor tube. For combined mono-metallic catalysts, a catalyst bed of each catalyst with equal amount (~2 cm distant from each other) was placed downstream to the biomass in the reactor tube, resulting in three catalyst to biomass ratios of 1, 2 and 3. For example, 50 mg of Cu/zeolite and 50 mg of Ni/zeolite were used to obtain the final catalyst to biomass ratio of 1. The combinations of mono-metallic catalysts with three catalyst to biomass ratios of 1, 2 and 3 were named as CuZ:NiZ-1, CuZ:NiZ-2 and CuZ:NiZ-3, respectively. Similarly, three catalyst to biomass ratios of 1, 2 and 3 were also used for the bi-metallic catalyst, designating them as CuNiZ-1, CuNiZ-2 and CuNiZ-3, respectively. The previous studies have shown that the lower amount of catalyst is unable to react with generated pyrolytic vapours in the process, resulting in inefficient conversion of oxygenated compounds into hydrocarbons, while increasing the catalyst content enhances the production of aromatic hydrocarbons (Yang et al., 2017; Balasundram et al., 2017). Therefore, three different catalyst to biomass ratios were applied in this study. Helium was used as the carrier gas at a flow rate of 50 mL/min in all pyrolysis experiments. The bio-oil was collected at room temperature by condensing the pyrolytic organic vapours on quartz wool filled at the end of reactor tube. Subsequently, the bio-oil was then dissolved in dichloromethane (DCM) solvent and filtered through glass wool and sodium sulfate three times each. The solution was analyzed by GC–MS consisting of Agilent 7890A gas chromatograph with an HP-5MS column (60 m × 0.25 μm) coupled with a 5977A mass spectrometer. MassHunter software was applied to

analyse the compounds with match factor for the database set to over 80 and approximately 60 compounds with the largest peak areas in each spectrum were selected for the analysis and further classified in eight major groups, namely aliphatic hydrocarbons, aromatic hydrocarbons, phenols, acids, nitrogenous compounds (amines, amides and nitriles), furans, aldehydes, ketones and the remaining compounds were designated as others that mainly contained haloalkanes, and thio and silicon-containing compounds. Chromatograms obtained from GC-MS results of bio-oils during catalytic pyrolysis of pine wood are given in Fig. S5.

Pyrolysis gases produced during the pyrolysis reaction were examined online with M200 micro-gas chromatograph (GC). The micro-GC used in this study comprises of two channels: Channel A, a polymer paraplot U column maintained at 40 °C to analyse CO_2, CH_4, C_2H_4 and C_2H_6, and Channel B, column molecular sieve of 5A kept at 60 °C, to examine H_2 and CO products. Chromatograms were recorded every 100 s using a thermal conductivity detector.

The product yields (wt%) from the pyrolysis process were calculated as mentioned in Weldekidan et al. (2018). Firstly, the weight of residue biomass (char) was measured and the percentage of char/initial biomass was taken as char yield, while to estimate the gas yield, volume of each pyrolysis gas was quantified from standard mixture of gases with known concentrations, then the weight percentage of each gas was calculated using the ideal gas equation. The sum of all individual gases was used as the total gas yield. The bio-oil yield was calculated from the mass difference between the total sample weight and the sum of the produced char and pyrolytic gases.

3. Results and discussion

3.1. Effect of catalytic pyrolysis on product yields

Table 1 represents the distribution of bio-oil yield, pyrolytic gas yield and char yield obtained from *ex-situ* pyrolysis of pine wood at 500 °C. The results showed significant changes in bio-oil and pyrolytic gas yields with and without the introduction of any catalyst, while a subtle change was noticed in the char yield, with 20–24 wt% of char yield obtained in all pyrolysis reactions. Noticeably, the non-catalytic pyrolysis showed a bio-oil yield of 71.7 wt%, while the combined mono-metallic catalysts produced bio-oil yields in a decreasing order with respect to increasing catalyst to biomass ratio. These results are consistent with previous studies that also obtained a similar trend of pyrolytic products at 500 °C (Balasundram et al., 2017; Kan et al., 2014). In this work, the bi-metallic catalyst with the lowest catalyst to biomass ratio (CuNiZ-1) produced the highest bio-oil yield of 70 wt% and CuNiZ-3 generated the minimum bio-oil yield (61 wt%). The decrease in liquid products can be attributed to the efficient catalytic activity of the catalysts that promoted the deoxygenation reactions (e.g., decarboxylation, decarbonylation etc.) and increased the content of the pyrolytic gases. Evidently, the gas yield increased with rising in the catalyst to biomass ratio. However, it was noticed that in case of the combined mono-metallic catalysts, there was a slight increase in gas yield, CuZ:NiZ-1 and CuZ:NiZ-3 generating a gas yield of 7.96 wt% and 9.96%, respectively. On the other hand, a remarkable rise was observed in the gas yield from pyrolysis catalysed by the sole bi-metallic catalyst as a maximum gas yield of 15.9% was achieved by CuNiZ-3, which was nearly 76% higher than CuNiZ-1. The possible reason for this could be that the synergetic effect of Cu and Ni metals enhanced the cracking and other deoxygenation reactions such as decarboxylation and decarbonylation, which are consistent with GC results that showed highest evolution of CO_2 and CO gases, respectively (Yang et al., 2017).

Table 1
Distribution of product yields using combined mono-metallic and sole bi-metallic catalysts during pyrolysis of pine wood at 500 °C.

Catalyst	Gas yield (wt%)	Char yield (wt%)	Bio-oil yield (wt%)
No catalyst	6.31	22	71.6
CuZ:NiZ-1	7.96	20	72.0
CuZ:NiZ-2	8.51	24	67.4
CuZ:NiZ-3	9.96	24	66.0
CuNiZ-1	8.98	21	70.0
CuNiZ-2	9.49	21	69.5
CuNiZ-3	15.8	23	61.1

3.2. Bio-oil deoxygenation and hydrocarbon production

Fig. 1 shows the distribution of various types of compounds detected in the bio-oil samples after *ex-situ* pyrolysis of pine wood with and without the introduction of catalysts. The results demonstrated that non-catalytic pyrolysis produced highly oxygenated bio-oil, approximately 75% oxygenated compounds including phenols, phenols, acids and ketones were found in the bio-oil. However, the addition of either combined mono-metallic or sole bi-metallic catalysts significantly deoxygenated the bio-oil and increased the proportion of hydrocarbons. Fig. 2 compares the deoxygenation activity between the combined mono-metallic catalysts and sole bi-metallic catalyst. As shown in the figure, the deoxygenation activity increased with rising in the catalyst to biomass ratio. Noticeably, CuZ:NiZ-1 and CuNiZ-1 showed negligible deoxygenation activity while the hydrocarbon production was also much lower with CuZ:NiZ-1, suggesting the quantity of the catalyst was not sufficient to react with pyrolytic vapours. Alternatively, CuZ:NiZ-3 remarkably reduced the percentage of oxygenated compounds as compared to non-catalytic pyrolysis, as only 6.42% of phenols, 1.81% of acids and 0.4% of ketones were found in the bio-oil. This substantial decrease in oxygenated compounds can be attributed to the excellent catalytic activity of the catalysts that converted oxygenated compounds into hydrocarbons and gases *via* various reactions, such as cracking, dehydration, decarboxylation, decarbonylation and oligomerization. In the combined mono-metallic catalysts, some compounds are assumed to deoxygenate firstly by Cu/zeolite and the remaining were further deoxygenated by Ni/zeolite catalyst. In comparison to the combined mono-metallic catalysts, sole bi-metallic catalyst showed better deoxygenation activity for all the oxygenated compounds. For instance, only 0.11% phenols and 0.33% of acids were found, while no ketones or aldehydes were detected in the bio-oil from pyrolysis of the pine wood sample with CuNiZ-3. The catalysts in this study showed higher deoxygenation activity for phenols as compared to Mo/Co-HZSM-5 and Ni/Co-HZSM-5 as demonstrated by Ren et al. (2018) that reported 16.7% and 24.1% phenols in bio-oils. The deoxygenation of phenols could be carried out primarily through dehydration to produce an alkene or naphthene, cracking or ring opening of naphthene to generate straight chain alcohols, which may further undergo cracking to produce olefins (Zheng et al., 2017). The olefins can further undergo aromatization reactions to generate aromatic hydrocarbons. The carboxylic acids, ketones and aldehydes contain carbonyl groups in their compounds. These compounds are mainly converted to non-oxygenated compounds or hydrocarbons through decarboxylation and decarbonylation, or can undergo dehydration reaction through Aldol condensation, which involves the reaction of a protonated carbonyl group and an intermediate enol, resulting in water as a by-product (Adjaye and Bakhshi, 1995; Op de Beeck et al., 2015). Overall, it can be suggested that the synergetic catalytic activity of the two metals in the sole bi-metallic catalyst promoted more efficiently than the combined mono-metallic catalysts the deoxygenation reactions, specially decarboxylation and decarbonylation, as no ketones or aldehydes were present in the bio-oil and carboxylic acids were also very lower.

Table 2 shows the distribution of all hydrocarbons obtained using combined mono-metallic catalysts and sole bi-metallic catalyst, while Fig. 3 depicts the major hydrocarbons present in the bio-oil samples. The results demonstrated that all the catalysts enhanced the proportion of aliphatic and aromatic hydrocarbons, which increased with

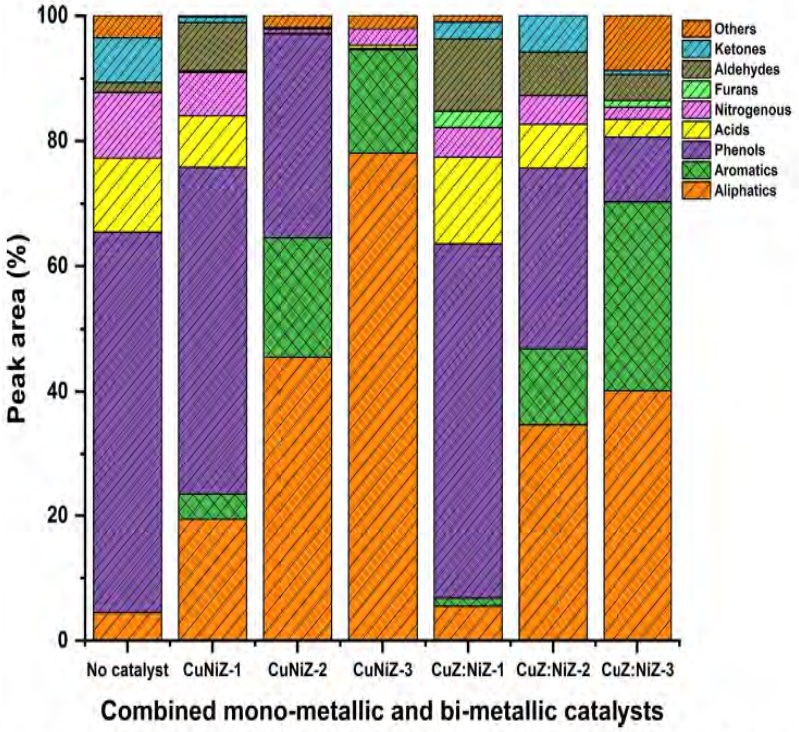

Fig. 1. Bio-oil composition obtained using combined mono-metallic catalysts and bi-metallic catalyst during *ex-situ* pyrolysis of pine wood at 500 °C with a heating rate of 100 °C/min.

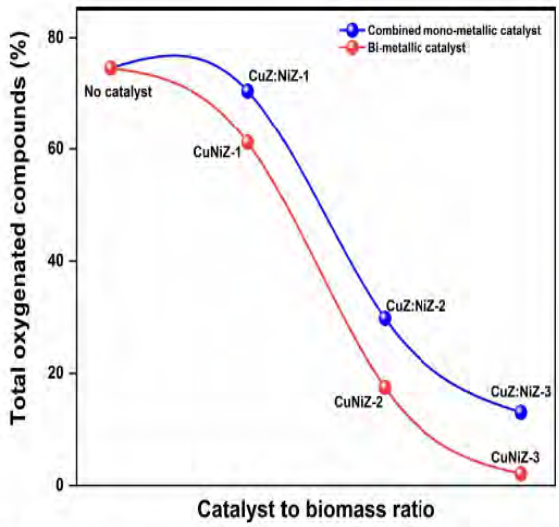

Fig. 2. A comparison of deoxygenation activity between combined mono-metallic catalysts and sole bi-metallic catalyst.

increasing the catalyst to biomass ratio. For example, in case of the combined mono-metallic catalysts, CuZ:NiZ-2 produced 19.5% of aliphatic hydrocarbons and 6.8% of aromatic hydrocarbons, while CuZ:NiZ-3 increased the percentage of aliphatic and aromatic hydrocarbons to 25.1% and 18.9%, respectively. The results obtained in this study are competitive to the previous studies that utilized advanced catalysts for bio-oil upgrading. For example, Yang et al. (2017) applied MoZn/HZSM-5 for bio-oil upgrading using torrefied switchgrass and achieved a maximum proportion of 18.17% in the bio-oil. For the sole bi-metallic catalyst, CuNiZ-1 produced 15.6% of aliphatic and 3.17% of aromatic hydrocarbons, increasing to 49.3% and 10.4%, respectively with CuNiZ-3. It was noticed that the combined mono-metallic catalysts favoured the production of aromatic hydrocarbons when compared to the sole bi-metallic catalyst, whereas a higher percentage of aliphatic hydrocarbons was formed by the latter as compared to the former. The higher percentage of aromatic hydrocarbons by combined mono-metallic catalysts could be because Cu/zeolite favoured mainly dehydration, decarboxylation and decarbonylation reactions, while in addition to these reactions Ni/zeolite also carried out aromatization reactions more efficiently and enhanced the production of aromatic hydrocarbons. The enhanced aromatization reactions can also be attributed to the higher acidity of Ni/zeolite and a better dispersion of NiO particles or Ni cations on the surface or into the pores of the zeolite support, as indicated by NH_3-TPD and H_2-TPR results (Supplementary information).

The main aliphatic hydrocarbon detected in almost all the bio-oil samples was ethylidenecyclobutane and its proportion was found to increase at higher catalyst to biomass ratios, which indicates that the zeolite supported catalysts converted the major content of oxygenated compounds into ethylidenecyclobutane. The production of ethylidenecyclobutane over mono or bi-metallic catalysts can be attributed to their efficient catalytic activity for direct dehydration and cracking reactions (Op de Beeck et al., 2015). It was further noticed that the lower catalyst to biomass ratio favoured the formation of cyclohexene and cyclopentane, while the higher amount of catalyst produced decane and dodecane. On the other hand, a variety of aromatic hydrocarbons, such as benzene, naphthalene, phenanthrene and fluorene, were predominantly detected in the bio-oil samples with the higher catalyst to biomass ratios. Evidently, the combined mono-metallic catalyst, CuZ:NiZ-2 produced 2.69% benzene but in contrast, CuNiZ-2 resulted in a higher proportion of benzene in the bio-oil at 5.2%. Besides, CuZ:NiZ-3 and its counterpart CuNiZ-3 produced 4.06% and 2.09% of naphthalene in the bio-oil, respectively. It has been reported that the acidic sites at the mesopore surface of zeolite play a central role in aromatization reactions and cracking of the oxygenated compounds in pyrolytic vapours (Veses et al., 2016). In this study, all the catalysts also showed a higher number of weak and strong acid sites created by the incorporation of metal cation at specific exchange sites, as indicated by NH_3-TPD results (Supplementary information). Overall, this study indicates that a sole bi-metallic catalyst could be advantageous to obtain a higher content of aliphatic hydrocarbons, whereas a combination of two mono-metallic catalysts could be useful to achieve a higher amount of aromatic hydrocarbons in the bio-oil.

Table 2
Distribution of all hydrocarbons obtained using combined mono-metallic catalysts and sole bimetallic catalyst during pyrolysis of pine wood at 500 °C.

Hydrocarbon	Formula	Catalyst type						
		No catalyst	CuZ:NiZ-1	CuZ:NiZ-2	CuZ:NiZ-3	CuNiZ-1	CuNiZ-2	CuNiZ-3
Cyclohexene	C_6H_{10}	0.1	0.79					
Cyclopentane	C_5H_{10}		3.44			0.34		
Retene	$C_{18}H_{18}$	0.52	0.48					
Phenanthrene	$C_{14}H_{10}$	1.93	0.47	0.14	3.1	0.24	0.5	
Ethylidenecyclobutane	C_6H_{10}	0.28		19.46	23.06	11.77	23.6	49.34
Benzene	C_6H_6			2.69	1.57		5.2	
Indene	C_9H_8			0.19			0.24	2.51
Fluorene	$C_{13}H_{10}$			0.22	0.8	2.2	2.3	3.54
s-Indacene	$C_{12}H_8$			0.16	0.75			
1,1′-biphenyl, 2,4,6-trimethyl	$C_{15}H_{16}$			0.43	1.66			
Stilbene	$C_{14}H_{12}$			0.2			0.2	2.1
Fluoranthene	$C_{16}H_{10}$			1.2				
Anthracene	$C_{14}H_{10}$			0.7	2.38		0.75	
Decane	$C_{10}H_{22}$				1.49		0.85	
Naphthalene	$C_{10}H_8$				4.06			2.09
Tolylacetylene	C_9H_8				1.07		0.24	
Dodecane	$C_{12}H_{26}$				0.51			
Nonane	C_9H_{20}						0.85	
Pyrene	$C_{16}H_{10}$						0.55	
Heptacosane	$C_{27}H_{56}$	1.91						

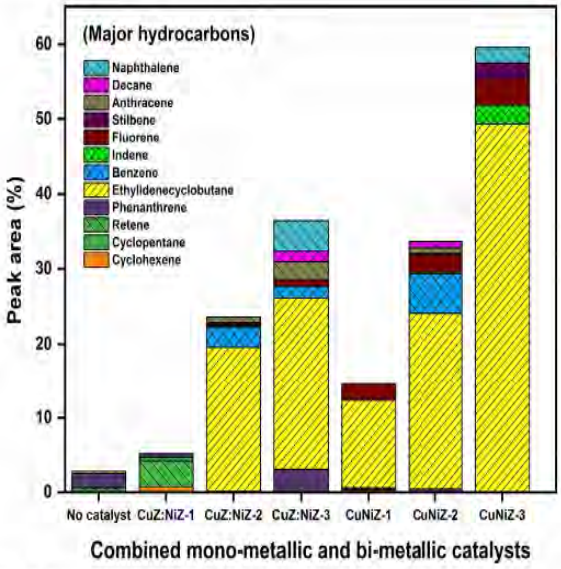

Fig. 3. Distribution of major hydrocarbons detected in the bio-oil samples from catalytic *ex-situ* pyrolysis by combined mono-metallic catalysts and bi-metallic catalyst.

When the quality of bio-oil samples obtained in this study was compared with petroleum crude oil (naphthenes-49%, paraffins-30%, aromatic hydrocarbons-15%), it could be suggested that the sole bi-metallic catalyst, CuNiZ-3 produced 49.34% of naphthenes, which is competitive but less diverse to the proportion present in petroleum crude oil. In contrast, the combined mono-metallic catalysts could not obtain the desired amount of naphthenes or paraffins, although CuZ:NiZ-3 produced suitable proportion of different aromatic hydrocarbons (18.8%) in the bio-oil. This study suggests that the application of sole bi-metallic catalyst in the biomass pyrolysis process would significantly reduce the requirement for hydrothermal upgrading of the bio-oils to produce drop-in fuels.

3.3. Pyrolytic gases

The emission of various gases during the pyrolysis reaction provides a pivotal information about the main catalytic reactions favoured by the catalysts for efficient deoxygenation of bio-oils. Table 3 shows the

Table 3
Yield distribution of pyrolytic gases obtained using combined Cu/zeolite-Ni/zeolite and CuNi/zeolite catalysts during pyrolysis of pine wood.

Catalyst	CH_4 (wt%)	CO_2 (wt%)	C_2H_4 (wt%)	C_2H_6 (wt%)	H_2 (wt%)	CO (wt%)	CO_2:CO (wt%)
No catalyst	0.53	1.68	0.06	0.08	2.28	1.66	1.01
CuZ:NiZ-1	0.5	2.78	1.77	0.15	0.17	2.59	1.07
CuZ:NiZ-2	0.75	2.77	1.76	0.13	0.14	2.95	0.93
CuZ:NiZ-3	0.57	3.82	2.43	0.11	0.15	2.88	1.32
CuNiZ-1	0.655	3.35	2.13	0.08	0.1	2.67	1.25
CuNiZ-2	0.76	3.17	2.02	0.12	0.29	3.13	1.01
CuNiZ-3	0.92	5.06	3.22	0.15	0.94	5.58	0.90

results for each pyrolytic gas yield obtained from the pyrolysis reactions. The main gases obtained in this study were CO_2, CO, CH_4, C_2H_4, C_2H_6 and H_2. It was observed that the introduction of catalysts produced a higher amount of gases as compared to non-catalytic pyrolysis. The results further suggest that both combined mono-metallic catalysts and the sole bi-metallic catalyst produced a comparatively higher amount of CO_2, CO, C_2H_4 in each reaction and their concentrations increased with increase in the catalyst to biomass ratio. Pine wood biomass contains many compounds with different functional groups, such as ROH, ROR′, RCHO, RR′CO, and RCO_2H (Wang et al., 2015). Therefore, the formation of CO_2 can be attributed to the cracking of carboxyl functional group (RCO_2H), while the release of CO can be related to the cracking of either carbonyl (RR′CO) or carboxyl (RCO_2H) functional groups (Zhang et al., 2013). CO_2 can also be formed through water–gas shift reaction using *in-situ* produced CO and water vapours. Moreover, it was noticed that all the catalysts produced almost equal amount of CO_2 and CO during the pyrolysis reaction as CO_2 to CO ratio was found nearly 1, suggesting decarbonylation and decarboxylation were equally favoured by the combined mono-metallic catalysts and sole bi-metallic catalyst. Besides, the bi-metallic catalyst produced a higher concentration of CO_2 and CO than the combined mono-metallic catalysts, CuNiZ-3 producing 5.06 wt% of CO_2 and 5.58 wt% of CO, while CuZ:NiZ-3 could produce 3.82 wt% of CO_2 and 2.88 wt% of CO. The other dominant gas observed during catalytic pyrolysis was C_2H_4 and its concentration was also found directly proportional to the catalyst to biomass ratio. The generation of C_2H_4 can be attributed to the cracking of alkyl groups in oxygenated compounds, such as acids, ketones and aldehydes. and it can also be produced by cracking of alkyl

groups attached to alcohol or phenol molecules (Adjaye and Bakhshi, 1995). Markedly, the sole bi-metallic catalyst produced a slightly higher amount of C_2H_4 as compared to the combined mono-metallic catalysts, suggesting the former showed better cracking activity than the latter.

4. Conclusion

The present study demonstrated that in comparison to combined mono-metallic catalysts, sole bi-metallic catalyst proved better deoxygenation activity as only 0.11% of phenols and 0.33% of acids were obtained in the bio-oil samples, while ketones and aldehydes were completely converted to liquid and gaseous products. Besides, it was observed that sole bi-metallic catalyst preferred the production of aliphatic hydrocarbons, CuNiZ-3 generating 49.34% of aliphatic hydrocarbons, whereas the combination of mono-metallic catalysts favoured the production of aromatic hydrocarbons, CuZ:NiZ-3 producing 18.87% of aromatics in the bio-oil. The major deoxygenation reactions promoted by the catalysts were found to be cracking, aromatization, dehydration, decarboxylation and decarbonylation.

Appendix A. Supplementary data

Supplementary data to this article can be found online at https://doi.org/10.1016/j.biortech.2019.01.067.

References

Adjaye, J.D., Bakhshi, N.N., 1995. Catalytic conversion of a biomass-derived oil to fuels and chemicals I: model compound studies and reaction pathways. Biomass Bioenergy 8, 131–149.

Balasundram, V., Ibrahim, N., Kasmani, R.M., Isha, R., Hamid, M.K.Abd., Hasbullah, H., 2017. Catalytic pyrolysis of sugarcane bagasse using molybdenum modified HZSM-5 zeolite. Energy Procedia 142, 793–800.

Dai, G., Wang, S., Huang, S., Zou, Q., 2018. Enhancement of aromatics production from catalytic pyrolysis of biomass over HZSM-5 modified by chemical liquid deposition. J. Anal. Appl. Pyrol.

Gayubo, A.G., Aguayo, A.T., Atutxa, A., Aguado, R., Olazar, M., Bilbao, J., 2004. Transformation of oxygenate components of biomass pyrolysis oil on a HZSM-5 zeolite. II. Aldehydes, ketones, and acids. Ind. Eng. Chem. Res. 43, 2619–2626.

Gunawardena, D.A., Fernando, S.D., 2018. Screening of transition metal/oxide-impregnated ZSM-5 catalysts for deoxygenation of biomass oxygenates via direct methane intervention. Biofuels 9, 113–120.

Hernando, H., Hernández-Giménez, A.M., Ochoa-Hernández, C., Bruijnincx, P.C.A., Houben, K., Baldus, M., Pizarro, P., Coronado, J.M., Fermoso, J., Čejka, J., Weckhuysen, B.M., Serrano, D.P., 2018. Engineering the acidity and accessibility of the zeolite ZSM-5 for efficient bio-oil upgrading in catalytic pyrolysis of lignocellulose. Green Chem. 20, 3499.

Hertzog, J., Carré, V., Jia, L., Mackay, C.L., Pinard, L., Dufour, A., Mašek, O., Aubriet, F., 2018. Catalytic fast pyrolysis of biomass over microporous and hierarchical zeolites: characterization of heavy products. ACS Sustain. Chem. Eng. 6, 4717–4728.

Iliopoulou, E.F., Stefanidis, S.D., Kalogiannis, K.G., Delimitis, A., Lappas, A.A., Triantafyllidis, K.S., 2012. Catalytic upgrading of biomass pyrolysis vapors using transition metal-modified ZSM-5 zeolite. Appl. Catal. B 127, 281–290.

Kan, T., Strezov, V., Evans, T., 2014. Catalytic pyrolysis of coffee grounds using NiCu-impregnated catalysts. Energy Fuels 28, 228–235.

Kan, T., Strezov, V., Evans, T.J., 2016. Lignocellulosic biomass pyrolysis: a review of product properties and effects of pyrolysis parameters. Renewable Sustainable Energy Rev. 57, 1126–1140.

Li, P., Li, D., Yang, H., Wang, X., Chen, H., 2016. Effects of Fe-, Zr-, and Co-modified zeolites and pretreatments on catalytic upgrading of biomass fast pyrolysis vapors. Energy Fuels 30, 3004–3013.

Li, X., Zhang, X., Shao, S., Dong, L., Zhang, J., Hu, C., Cai, Y., 2018. Catalytic upgrading of pyrolysis vapor from rape straw in a vacuum pyrolysis system over La/HZSM-5 with hierarchical structure. Bioresour. Technol. 259, 191–197.

Mihalcik, D.J., Mullen, C.A., Boateng, A.A., 2011. Screening acidic zeolites for catalytic fast pyrolysis of biomass and its components. J. Anal. Appl. Pyrol. 92, 224–232.

Op de Beeck, B., Dusselier, M., Geboers, J., Holsbeek, J., Morré, E., Oswald, S., Giebeler, L., Sels, B.F., 2015. Direct catalytic conversion of cellulose to liquid straight-chain alkanes. Energy Environ. Sci. 8, 230–240.

Ren, X.-Y., Cao, J.-P., Zhao, X.-Y., Yang, Z., Liu, T.-L., Fan, X., Zhao, Y.-P., Wei, X.-Y., 2018. Catalytic upgrading of pyrolysis vapors from lignite over mono/bimetal-loaded mesoporous HZSM-5. Fuel 218, 33–40.

Thangalazhy-Gopakumar, S., Adhikari, S., Chattanathan, S.A., Gupta, R.B., 2012. Catalytic pyrolysis of green algae for hydrocarbon production using H+ZSM-5 catalyst. Bioresour. Technol. 118, 150–157.

Veses, A., Puértolas, B., López, J.M., Callén, M.S., Solsona, B., García, T., 2016. Promoting deoxygenation of bio-oil by metal-loaded hierarchical ZSM-5 zeolites. ACS Sustainable Chem. Eng. 4, 1653–1660.

Wang, W., Li, X., Ye, D., Cai, L., Shi, S.Q., 2018. Catalytic pyrolysis of larch sawdust for phenol-rich bio-oil using different catalysts. Renewable Energy 121, 146–152.

Wang, S., Ru, B., Lin, H., Sun, W., Luo, Z., 2015. Pyrolysis behaviors of four lignin polymers isolated from the same pine wood. Bioresour. Technol. 182, 120–127.

Weldekidan, H., Strezov, V., Kan, T., Town, G., 2018. Waste to energy conversion of chicken litter through a solar-driven pyrolysis process. Energy Fuels 32, 4341–4349.

Westerhof, R.J.M., Brilman, D.W.F., Garcia-Perez, M., Wang, Z., Oudenhoven, S.R.G., Kersten, S.R.A., 2012. Stepwise fast pyrolysis of pine wood. Energy Fuels 26, 7263–7273.

Yang, Z., Kumar, A., Apblett, A.W., Moneeb, A.M., 2017. Co-Pyrolysis of torrefied biomass and methane over molybdenum modified bimetallic HZSM-5 catalyst for hydrocarbons production. Green Chem. 19, 757–768.

Zhang, H., Xiao, R., Jin, B., Xiao, G., Chen, R., 2013. Biomass catalytic pyrolysis to produce olefins and aromatics with a physically mixed catalyst. Bioresour. Technol. 140, 256–262.

Zhang, H., Shao, S., Luo, M., Xiao, R., 2017. The comparison of chemical liquid deposition and acid dealumination modified ZSM-5 for catalytic pyrolysis of pinewood using pyrolysis-gas chromatography/mass spectrometry. Bioresour. Technol. 244, 726–732.

Zheng, Y., Wang, F., Yang, X., Huang, Y., Liu, C., Zheng, Z., Gu, J., 2017. Study on aromatics production via the catalytic pyrolysis vapor upgrading of biomass using metal-loaded modified H-ZSM-5. J. Anal. Appl. Pyrol. 126, 169–179.

MACQUARIE University

MACQUARIE UNIVERSITY
AUTHORSHIP CONTRIBUTION STATEMENT

In accordance with the *Macquarie University Code for the Responsible Conduct of Research* and the *Authorship Standard*, researchers have a responsibility to their colleagues and the wider community to treat others fairly and with respect, to give credit where appropriate to those who have contributed to research.

Note for HDR students: *Where research papers are being included in a thesis, this template must be used to document the contribution of authors to each of the proposed or published research papers. The contribution of the candidate must be sufficient to justify inclusion of the paper in the thesis.*

1. DETAILS OF PUBLICATION & CORRESPONDING AUTHOR

Title of Publication (can be a holding title)		**Publication Status** Choose an item.
Synergistic effect of transition metals on ZSM-5-supported catalysts for ex-situ bio-oil upgrading		■ In Progress or Unpublished work for thesis submission ☐ Submitted for Publication ☐ Accepted for Publication ☐ Published
Name of **corresponding author**	Department/Faculty	**Publication details:** indicate the name of the journal/ conference/ publisher/other outlet
	Earth and Environmental Sciences/ Science & Engineering	

2. STUDENTS DECLARATION (if applicable)

Name of HDR thesis author (If the same as corresponding author - write "as above")	Department/Faculty	Thesis title
Ravinder Kumar	Earth and Environmental Sciences/ Science & Engineering	Catalytic Upgrading of Bio-oil Produced from Fast Pyrolysis of Pinewood Sawdust

Description of HDR thesis author's contribution to planning, execution, and preparation of the work if there are multiple authors

(for example, how much as a percent did you contribute to the conception of the project, the design of methodology or experimental protocol, data collection, analysis, drafting the manuscript, revising it critically for important intellectual content, etc.)

In this article, I contributed in designing the project, carried out 90% of the experimnetal work, analyzed the data and wrote 80% of the manuscript.

I declare that the above is an accurate description of my contribution to this publication, and the contributions of other authors are as described below.	**Student signature** **Date**	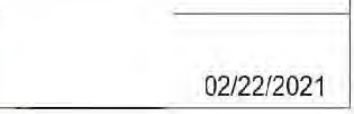 02/22/2021

MACQUARIE University

3. Description of all other author contributions

Use an Asterisk * to denote if the author is also a current student or HDR candidate.

The HDR candidate or corresponding author must, for each paper, list all authors and provide details of their role in the publication. Where possible, also provide a percentage estimate of the contribution made by each author.

Name and affiliation of author	Intellectual contribution(s) (for example to the: conception of the project, design of methodology/experimental protocol, data collection, analysis, drafting the manuscript, revising it critically for important intellectual content etc.)
Vladimir Strezov Macquarie University	conception, supervision, critical revision
Jing He Macquarie University	experimental, critical revision
Yutong Zhao Macquarie University	experimental, critical revision
*Behnam Dastjerdi Macquarie University	data analysis, critical revision
Tao Kan Macquarie University	conception, supervision, experimental, critical revision
Haimei Xu Macquarie University	experimental, critical revision
Yijiao Jiang Macquarie University	experimental, critical revision
	Provide summary for any additional Authors in this cell.

4. Author Declarations

I agree to be named as one of the authors of this work, and confirm:

i. *that I have met the authorship criteria set out in the* Authorship Standard, *accompanying the* Macquarie University Research Code,

ii. *that there are no other authors according to these criteria,*

iii. *that the description in Section 3 or 4 of my contribution(s) to this publication is accurate*

iv. *that I have agreed to the planned authorship order following the* Authorship Standard

Name of author	Authorised * By Signature or refer to other written record of approval (eg. pdf of a signed agreement or an email record)	Date
Vladimir Strezov		24/02/2021
Jing He		22/02/2021
Yutong Zhao		22/02/2021
Haimei Xu		24/02/2021
Tao Kan		22/02/2021
Behnam Dastjerdi		02/22/2021
Yijiao Jiang		24/02/2021
	Provide other written record of approval for additional authors (eg. pdf of a signed agreement or an email record)	

5. Data storage

The original data for this project are stored in the following location, in accordance with the *Research Data Management Standard* accompanying the *Macquarie University Research Code*.

If the data have been or will be deposited in an online repository, provide the details here with any corresponding DOI.

Data description/format	Storage Location or DOI	Name of custodian if other than the corresponding author

A copy of this form must be retained by the corresponding author and must accompany the thesis submitted for examination.

Chapter 8

Synergistic effect of transition metals on ZSM-5-supported catalysts for *ex-situ* bio-oil upgrading

Ravinder Kumar[a*], Vladimir Strezov[a], Jing He[a], Yutong Zhao[b], Haimei Xu[b], Tao Kan[a], Behnam Dastjerdi[a], Yijiao Jiang[b]

[a]Department of Earth and Environmental Sciences, Faculty of Science & Engineering, Macquarie University, Sydney, NSW 2109, Australia
[b]School of Engineering, Macquarie University, North Ryde, NSW 2109, Australia

Abstract

The study investigates the synergistic effect of transition metals (Ni, Cu, Fe and Mo) supported ZSM-5 bimetallic catalysts on bio-oil deoxygenation and hydrocarbon production during *ex-situ* pyrolysis of pinewood sawdust. The pyrolysis process was carried out in a fixed-bed reactor at 500 ºC with three catalyst to biomass (C/B) ratios (1, 2 and 3), and the pyrolytic products were characterized with physicochemical techniques. The results showed that all bimetallic catalysts achieved significant bio-oil yield that decreased with an increase in C/B ratio. The gas yield was found to rise with the increase in C/B, while an insignificant effect was noticed in the char yield. Further, it was found that the synergistic effect of Ni and Cu on ZSM-5 showed maximum removal of oxygen in bio-oil, where nearly 31.90 wt% was observed in the bio-oil and achieved high bio-oil quality with a higher heating value (HHV) of 24.28 MJ/kg. The synergistic effect of Ni with Fe was also effective for bio-oil deoxygenation, producing bio-oil with 23.06 MJ/kg of HHV. The synergistic effect of different metals had a noticeable effect on the selectivity of hydrocarbons, probably due to the preference of selective deoxygenation pathways. The results revealed that NiCu/ZSM-5 produced biphenyl derived aromatics, anthracene and alkanes, such as tridecane, heneicosane and tetracosane. However, Ni with Mo favored the production of alkanes like nonane, decane and dodecane, while only few aromatics, mainly naphthalene, were found in the bio-oils. The combination of Fe with either Ni or Cu favored the catalytic routes to form benzene derived aromatics and cyclic aliphatics. The synergistic effect of Fe with Mo promoted the formation of indene aromatics, benzene and cyclic hydrocarbons, like cycloheptatriene. The results of gas composition indicate that the synergistic effect of Ni-Cu and Ni-Mo favored decarboxylation reactions. In contrast, Ni with Fe preferred decarbonylation reactions predominantly for bio-oil upgrading. The synergistic effect of Fe and Cu equally promoted the decarboxylation and decarbonylation reactions. Overall, it can be suggested that bimetallic catalysts with different metals could be highly effective for bio-oil deoxygenation, and their synergistic effect can help to obtain quality bio-oils enriched with varying hydrocarbons.

1. Introduction

The increasing environmental concerns of climate change and depleting fossil fuels have necessitated the generation of eco-friendly, renewable drop-in fuels and sustainable chemicals to create a green world with less greenhouse gas emissions. In this regard, fast pyrolysis of lignocellulose biomass and organic wastes is considered one of the viable approaches to produce green energy fuels and commodity chemical feedstocks [1,2]. The primary product of biomass pyrolysis is bio-oil or pyrolysis oil that exhibits approximately 40-70 wt% of the pyrolytic products [3]. There are several pyrolysis plants operating around the world that generate bio-oil at a commercial scale [4,5]. Although bio-oil contains several high value-added chemicals or source

compounds that can be converted to energy fuels, it cannot be used as a drop-in fuel, because bio-oil predominantly contains oxygen-containing compounds of low calorific values that make it highly acidic and unstable. Bio-oil can be processed either to extract high value-added chemicals, which can be further used for commercial applications, or it can be upgraded into a high calorific energy fuel for heat or power generation. However, the isolation of sustainable chemicals from bio-oil and downstream bio-oil upgrading would require other techniques in addition to pyrolysis, which would make the overall process expensive. Considering the significance of bio-oil applications, it is imperative to employ cost-effective and efficient techniques for bio-oil upgrading and convert it into a drop-in fuel. Particularly, catalytic bio-oil upgrading, which can be used during the pyrolysis process, is considered an effective and economical approach to convert the oxygen-rich compounds into high energy density hydrocarbons, such as benzene, toluene, xylenes, naphthalenes, cycloalkanes, alkenes and alkanes [6–8]. The approach that employs catalysts for bio-oil upgrading during pyrolysis is termed catalytic biomass pyrolysis (CBP) [9].

CBP can consist mainly of two types based on the addition of a catalyst during the pyrolysis process: *in-situ* and *ex-situ* CBP [10–12]. In *in-situ* CBP, a catalyst is mixed with biomass. In *ex-situ* CBP, the catalyst(s) is placed downstream of the biomass, and the generated pyrolytic vapors are passed through the catalytic bed. *Ex-situ* CBP is generally preferred over *in-situ* CBP for bio-oil upgrading due to less coke formation, a requirement of low catalyst amount, easier regeneration and higher deoxygenation catalytic activities [12–15]. Thus, considering the advantages, the *ex-situ* CBP has been commonly adopted for bio-oil upgrading. The catalysts that favor the cleavage of $C-O$ bond and formation of the $C-C$ bond are commonly preferred in CBP, which can remove oxygen and promote hydrocarbon formation [16]. A number of nanomaterials with acidic to basic properties, such as microporous and mesoporous zeolites, mordenites, aluminosilicates, or metal oxides, such as TiO_2, Al_2O_3, and basic catalysts like CaO and MgO have been applied in *ex-situ* CBP for bio-oil upgrading [17–21]. The results of several studies suggest that zeolites, especially, Zeolite Socony Mobil-5 (ZSM-5)-based catalysts show remarkable cracking activity and produce maximum proportion of hydrocarbons, owing to their desirable characteristics, such as high surface area, suitable Brønsted acid sites, regular pore structure and shape selectivity [22–24]. Zeolites are generally modified or loaded with mono, bi or tri metals to enhance the overall catalytic activity of the catalyst and to promote deoxygenation reactions, including dehydration, decarboxylation, decarbonylation and aromatization, consequently, achieving bio-oil with higher content of hydrocarbons and improved physicochemical properties [12,25,26]. It is evident from the literature that bimetallic catalysts with compatible metals and appropriate composition are catalytically more active compared to monometallic catalysts and thus show better activity for bio-oil upgrading [27–29]. The catalytic activity of bimetallic catalysts can be enhanced because the two metals can create special geometric and electronic effects, and their synergistic, bifunctional

and oxophilic effects may promote deoxygenation reactions [28,30]. Moreover, incorporation of the second metal may alter the surface structure of other metal and their interaction can create additional synergistically catalytic active sites, which might prove advantageous to carry out selective deoxygenation reactions which otherwise might not be favorable on monometallic catalysts [28]. For example, Huang et al. [31] demonstrated the application of zeolite-based mono and bimetallic catalysts (Mo/HZSM-5, Cu/HZSM-5 and MoCu/HZSM-5) for bio-oil upgrading using pyrolysis of pine sawdust. The authors suggested that MoCu bimetals on HZSM-5 surface were able to convert gaseous methane into liquid aromatic hydrocarbons through aromatization reaction and also improved the cracking activity to generate more light phenols [31]. The catalytic activity of MoCu/HZSM-5 produced the maximum yield of C_6-C_{12} hydrocarbons compared to monometallic catalysts [31]. There are several other studies that provided inclusive evidences to prove the superiority of bimetallic catalysts to convert oxygenated compounds into hydrocarbons or other sustainable chemicals [30,32,33]. For instance, Wu et al. [28] studied the synergistic catalytic effect of $CuCo/Al_2O_3$ catalyst for hydrogenation of ethyl levulinate to 1,4-pentanediol. The results reported that the addition of Co species in the bimetallic catalyst improved the dispersion of Cu, while the strong electronic interaction at the interface of the Cu and neighboring CoO_x species altered the chemical states of Cu species to create Cu^0/Cu^+ distributions and synergic catalytic sites containing Cu and electron deficient CoO_x species [28]. The overall modifications in metallic distributions and the generation of synergic catalytic sites provided outstanding catalytic activity for the bimetallic catalyst compared to monometallic counterparts as reflected by the reduction in the activation energy of the rate-determining step and greater selectivity for 1,4-pentanediol [28]. Evidently, the activation energy for Cu/Al_2O_3 was 100.2 kJ mol^{-1}, which significantly decreased to 65.1 kJ mol^{-1} for $CuCo/Al_2O_3$, while the selectivity for the bimetallic catalyst was reported 93% compared to 52% for Cu/Al_2O_3 [28]. Another study demonstrating hydrodeoxygenation selectivity of anisole using Ru and Fe on TiO_2-supported catalysts was carried out by Phan et al. [32], which revealed that Ru/TiO_2 catalyst converted anisole to methoxycyclohexane, mainly favoring hydrogenation reaction pathway, while the addition of Fe changed the main reaction pathway from hydrogenation to direct deoxygenation. This change in the reaction mechanism can be attributed to synergistic effects of Ru and Fe species on TiO_2 surfaces [32]. Overall, the literature suggests that the combination of two active metals can bring some significant changes in overall metal distribution on the catalyst and their synergistic effects can increase the catalytic activity and favor selective deoxygenation reactions to obtain the enhanced yield of the desired products.

The catalytic activities of several bimetallic catalysts have been demonstrated for bio-oil upgrading using model compounds in either catalytic cracking or hydrodeoxygenation processes, which have provided valuable information for understanding the favorable deoxygenation

reactions on the bimetal surfaces. However, less information is available on the application of bimetallic catalysts for bio-oil upgrading using lignocellulose biomass as the feedstock as well as their effect on energy conversion efficiency in pyrolytic products. C the importance of real bio-oil upgrading and its applications as a future energy fuel it is essential to examine the performance of bimetallic catalysts for real bio-oil upgrading, their effects on pyrolysis products, energy distribution as well as coke formation during biomass pyrolysis. Therefore, this study aimed to investigate the effect of active transition metals supported on ZSM-5 as bimetallic catalysts on production of hydrocarbons and sustainable chemicals. Bimetallic catalysts with combination of four metals (Ni, Cu, Fe, and Mo) supported on ZSM-5 were prepared and employed in *ex-situ* pyrolysis mode to study their synergistic effects for bio-oil deoxygenation and selectivity of hydrocarbons. Bio-oil was characterized using quantitative and qualitative analysis methods. The study is important to enhance the understanding of bimetallic catalysts for bio-oil deoxygenation and energy conversion efficiency in pyrolytic products.

2. Experimental Section

2.1. Biomass

Pinewood sawdust applied in previous studies [12,34] was used in this study as feedstock in *ex-situ* pyrolysis for bio-oil production.

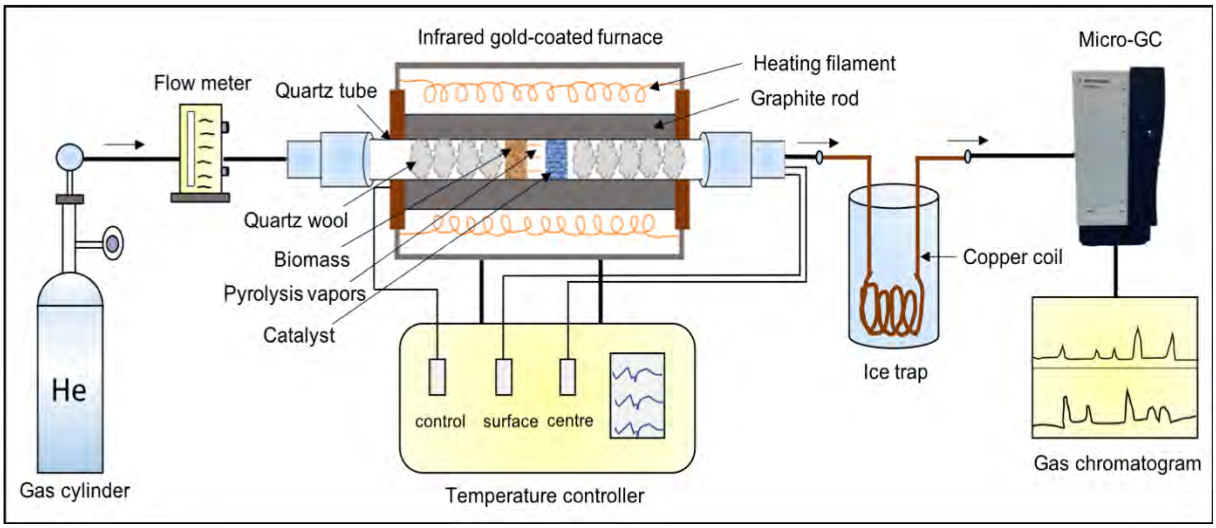

Figure 1. A schematic diagram of horizontal fixed-bed pyrolysis set-up.

2.2. Pyrolysis operation

Pine wood pyrolysis with all bimetallic catalysts was carried out in an infrared gold-coated furnace containing a quartz tube horizontal fixed-bed reactor. A schematic diagram of the pyrolysis set-up is shown in Figure 1. Approximately 100 mg of the feedstock was loaded in the quartz tube reactor, and the catalyst of 100, 200 and 300 mg was loaded downstream of the biomass to obtain

a catalyst to biomass ratio of 1, 2 and 3, respectively. The remaining space in the quartz tube was filled with quartz wool. All the pyrolysis experiments were performed at 500 ºC (retention time of 2 min for the final temperature) with a heating rate of 100 ºC/min and He as a carrier gas at a flow rate of 50 ml/min. Prior to each pyrolysis experiment He gas was purged in the reactor for 30 min to ensure oxygen free conditions. Pyrolysis experiments were repeated twice with each catalyst to confirm data reliability.

The pyrolytic bio-oil product and pyrolytic gases were analyzed with gas chromatography-mass spectroscopy (GC-MS, Agilent) and micro-gas chromatography (micro-GC, Agilent 490), respectively. As shown in Figure 1 micro-GC was attached to the gas outlet of the quartz reactor. Gases were analyzed online during the pyrolysis. The micro-GC was calibrated with a standard gas mixture of CO (3%), CO_2 (3.05%), H_2 (1.16%), CH_4 (1%), C_2H_4 (0.98%), and C_2H_6 (0.99%). Agilent 490 micro-GC contains two channels. Channel A (PoraPLOT U) identifies CO_2, CH_4, C_2H_4, and C_2H_6 while channel B (molecular sieve 5A) detects H_2 and CO. Channel A and channel B were maintained at 40 ºC and 60 ºC, respectively and pressure of 20 psi. Chromatograms were obtained after each 150 sec with a sampling span of 15 sec. All gases were quantified from standard gas mixture and each weight was estimated from the ideal gas equation.

Bio-oil condensed on the quartz wool at the end of the quartz reactor was collected and extracted by dissolving in dichloromethane (DCM), filtered through glass wool and sodium sulfate three times each to remove all solid impurities and dehydrate the bio-oil samples. The bio-oil samples were condensed with argon gas, heated for 30 min at 60 ºC and subjected to GC-MS analysis. Agilent 7890B GC/5977A MS system with a HP-5MS capillary column (60 m × 0.25 µm) linked to a 5977A mass spectrometry system was used to analyze the bio-oil composition. MassHunter software was used to identify the compounds, where the compounds with a matching score of 80 or above were selected and grouped in different families based on their main functional groups.

Biochar was retrieved from the quartz reactor after pyrolysis experiment and weighed. Product yield (wt%) of the biochar and other pyrolytic products were calculated using the following equation:

$$Product\ yield\ i\ (wt\%) = 100.[(mass\ i\ (g))/biomass(g)] \quad (1)$$

where *i* is gas, char, bio-oil.

2.3. Energy yield of pyrolytic products

To calculate the energy content of pyrolytic products, biomass pyrolysis with all bimetallic catalysts at 500 ºC was carried out with a C/B ratio of 2 and heating rate of 100 ºC /min. C/B ratio of 2 was selected to obtain adequate amount of bio-oil for elemental analysis. The C, H, N and S contents of the bio-oil and char were quantified using Vario MICRO cube elemental analysers

(Elementar Analysensysteme GmbH, Germany). The values of CHNS for bio-oil and char samples were calculated from a standard sample of known composition. The higher heating values (HHV) of bio-oil and char samples were determined using equation 2:

$$HHV\ i\ (MJ/kg) = 0.3491\mathrm{C} + 1.1783\mathrm{H} + 0.1005\mathrm{S} - 0.1034\mathrm{O} - 0.0151\mathrm{N} - 0.0211\mathrm{A} \quad (2)$$

where C, H, O, N, S and A represents carbon, hydrogen, oxygen, sulphur and ash contents of *i* wt%.

Oxygen distribution in bio-oil was determined according to equation 3:

$$O_{bio-oil}\ (wt\%) = 100 \times [(O_{bio-oil}(wt\%)/(O_{biomass}(wt\%)] \quad (3)$$

HHV of pyrolytic gases was calculated from equation 4:

$$HHV_i = [(n_i \times\ HHV_i)/Sum\ of\ gases\ (wt\%)] \quad (4)$$

where n_i is wt% of a gas and HHV_i is HHV value of gas at standard conditions [35].

The energy yield of any pyrolytic product (*i*) was calculated using equation 5 [36]:

$$Energy\ yield\ i\ (\%) = 100 \times [\frac{HHV_i \times\ mass\ yield_i}{HHV_{biomass}}] \quad (5)$$

2.4. Catalyst preparation and characterization

ZSM-5 (Si/Al=30, CBV 3024E) was obtained from Zeolyst International, USA in powder form and pelletized using hydraulic pressure machine. The pellets were crushed using a mortar and pestle and sieved with a 40-mesh sieve to obtain the particle size of 0.42 mm of ZSM-5. ZSM-5 was calcined at 550 °C for 2.5 hours to convert into its protonic form of HZSM-5. HZSM-5 was used as the catalyst and support for bimetallic catalysts. The concentration of each metal was projected 5wt% in all bimetallic catalysts, NiCu/ZSM-5, NiMo/ZSM-5, NiFe/ZSM-5, CuMo/ZSM-5, CuFe/ZSM-5, and FeMo/ZSM-5. Bimetallic catalysts were prepared using incipient wetness impregnation method. $Cu(NO_3)_2.3H_2O$, $Ni(NO_3)_2.6H_2O$, $Fe(NO_3)_3.9H_2O$ and $(NH_4)_6Mo_7O_{24}.4H_2O$ were used as metal precursors for Cu, Ni, Fe and Mo, respectively. To prepare 10 g of the catalyst, the required amounts of metal precursors were dissolved in 15 ml Milli Q water and stirred for 10 min on a magnetic stirrer, followed by slow addition of HZSM-5 particles. To improve the dispersion of metals on zeolite, the obtained slurry was placed in ultrasonic vibrator at 40 kHz for 2 h, and after removing from ultrasonication kept for 22 h at room temperature. The mixture was dried in a vacuum oven at 110 °C overnight. Dried samples were calcined at 550 °C for 5.5 h in air muffle furnace. Calcined samples were sieved with 40-mesh sieve to remove fine particles and obtain particle sizes of 0.42 mm. The final product was used for further characterization and pyrolysis experiments. X-ray fluorescence (XRF), Olympus Delta Pro spectrometers using Ta tube (50 kV) was used to estimate probable concentrations of metals in catalysts. The results suggest 5.19% Ni and 5.74% Cu in NiCu/ZSM-5, 5.27% Ni and 4.78% Mo in NiMo/ZSM-5, 5.06% Ni and 5.21% Fe in NiFe/ZSM-5, 5.95% Cu and 4.63% in CuMo/ZSM-

5, 5.55% Cu and 5.13% Fe in CuFe/ZSM-5, and 5.28% Fe and 4.71% Mo in FeMo/ZSM-5. Abbreviations mentioned in Table 1 have been used for the catalysts.

X-ray diffraction (XRD) of fresh and spent bimetallic catalysts was carried out using a PANalytical X'Pert Pro MPD X-ray diffractometer with CuKα radiations (λ=1.54056 Å) and X-ray generator tube operating at 45 kV, 40 mA. Samples were scanned by measuring the X-ray intensity over a range of 2θ between 5 and 90 at a scanning rate of 50 sec per step, using Ni-filter, 1-16 divergent slit and 13 mm mask.

Textural properties of all catalysts were characterized by nitrogen adsorption-desorption isotherms at -196 °C on a Micromeritics TriStar II volumetric adsorption analyzer (Micromeritics Instrument Corporation, GA, USA). Before the analysis, the samples were dried and degassed at 300 °C for 12 h under vacuum. Brunauer–Emmett–Teller (BET) method was applied to determine specific surface areas by applying the relative pressure range between 0 and 1. The total pore volume was evaluated from the amount of gas adsorbed at $P/P^o = 0.95$.

Table 1. Quantity of feedstock and catalyst used in *ex-situ* pyrolysis of pinewood at 500 °C at a heating rate of 100 °C/min.

Catalyst abbreviation	**Catalyst type**	**Quantity of catalyst (mg)**	**Quantity of feedstock (mg)**	**C/B**
Z-1	ZSM-5	100	100	1
Z-2	ZSM-5	200	100	2
Z-3	ZSM-5	300	100	3
NCZ-1	NiCu/ZSM-5	100	100	1
NCZ-2	NiCu/ZSM-5	200	100	2
NCZ-3	NiCu/ZSM-5	300	100	3
NMZ-1	NiMo/ZSM-5	100	100	1
NMZ-2	NiMo/ZSM-5	200	100	2
NMZ-3	NiMoZSM-5	300	100	3
NFZ-1	NiFe/ZSM-5	100	100	1
NFZ-2	NiFe/ZSM-5	200	100	2
NFZ-3	NiFe/ZSM-5	300	100	3
CMZ-1	CuMo/ZSM-5	100	100	1
CMZ-2	CuMo/ZSM-5	200	100	2
CMZ-3	CuMo/ZSM-5	300	100	3
CFZ-1	CuFe/ZSM-5	100	100	1
CFZ-2	CuFe/ZSM-5	200	100	2
CFZ-3	CuFe/ZSM-5	300	100	3
FMZ-1	FeMo/ZSM-5	100	100	1
FMZ-2	FeMo/ZSM-5	200	100	2
FMZ-3	FeMo/ZSM-5	300	100	3

Acidic properties of the catalysts were characterized using NH_3 temperature programmed desorption (NH_3-TPD) on ChemBET Pulsar (USA) with a thermal conductivity detector. Approximately 0.1 g of sample was used for the analysis. The sample was loaded into a quartz U-tube plugged with quartz wool. Firstly, the sample was dried in inert conditions heating from room

temperature to 350 °C at 5 °C/min under 15 ml/min He with a 2 h hold. The system was cooled to 50 °C and then NH_3 (5% NH_3 in He) was passed over the sample at 20 ml/min for 45 min at 50 °C. Data for NH_3-desorption was recorded by removing physiosorbed NH_3 from the system by heating the sample from 50 to 650 °C at a heating rate of 5 °C/min under 15 ml/min He.

High resolution transmission electron microscopy (HRTEM) of catalysts was conducted on Jeol Jem-2100F operated at 200 kV. X-ray photoelectron spectroscopy (XPS) of catalysts was carried out on Thermo ESCALAB 250Xi surface analysis system.

Carbon deposition on spent bimetallic catalysts was examined using a thermogravimetric analyzer (TGA/DSC 1 Stare system, Mettler Toledo, Ltd.) Approximately 25 mg of the spent catalyst in a crucible was placed in the furnace. The sample was heated from 25 to 700 °C at 10 °C/min in compressed air (100 ml/min) and nitrogen (20 ml/min).

To examine the presence of different functional groups in the bio-oils, Fourier transform infrared spectroscopy (FTIR) was carried in the wavelength range of 400 and 4000 cm^{-1} using a Nicolet 6700 FTIR spectrometer (Thermo Fisher Scientific, Inc.). Bio-oil samples obtained from catalytic pyrolysis with C/B ratio of 3 were examined for FTIR analysis. An attenuated total reflectance (ATR) accessory with a diamond crystal was used with a total scan of 32 and spectral resolution of 4 cm^{-1}.

3. Results & discussion

3.1. Pyrolysis products

Figure 2a shows the yields (wt%) of pyrolytic products obtained with bimetallic catalysts. The primary pyrolytic product with the highest yield was bio-oil in both cases of non-catalytic and catalytic pyrolysis. Non-catalytic pyrolysis produced the maximum bio-oil yield of 69.53 wt%. The application of catalysts significantly decreased the bio-oil yield and a decreasing trend in bio-oil yield was observed with all bimetallic catalysts when the C/B ratio was increased from 1 to 3. For example, NCZ-1 achieved a bio-oil yield of 58.97 wt% while NCZ-3 obtained the bio-oil yield of 46.99 wt%. The decrease in bio-oil yield with catalysts can be attributed to their efficient catalytic activity and carrying out various deoxygenation reactions to upgrade the pyrolytic vapors [36]. The increase in C/B ratio provided greater amount of catalyst to react with pyrolytic vapors that presented higher number of active sites and thus enhanced the number of deoxygenation reactions. In addition to increase in gas yield, enhanced formation of water due to dehydration reactions promoted by catalysts and coke deposition on catalyst surface also led to decrease in bio-oil yield [37]. On the other hand, the gas yield increased with the C/B ratio. For instance, FMZ-1 produced a gas yield of 15.7 wt% that increased to 33.92 wt% with FMZ-3. Similar increasing trend of the gas yield with C/B was observed with all the catalysts. The results are consistent with previous studies that showed similar trends for pyrolytic products in the presence of

catalysts[36,38]. On the other hand, C/B had insignificant effect on the char yield, 15-18 wt% of char yield was obtained from all catalysts with varying C/B ratio. Char formation can be ascribed primarily to the carbonization of lignin and slightly from hemicellulose components of the biomass [39].

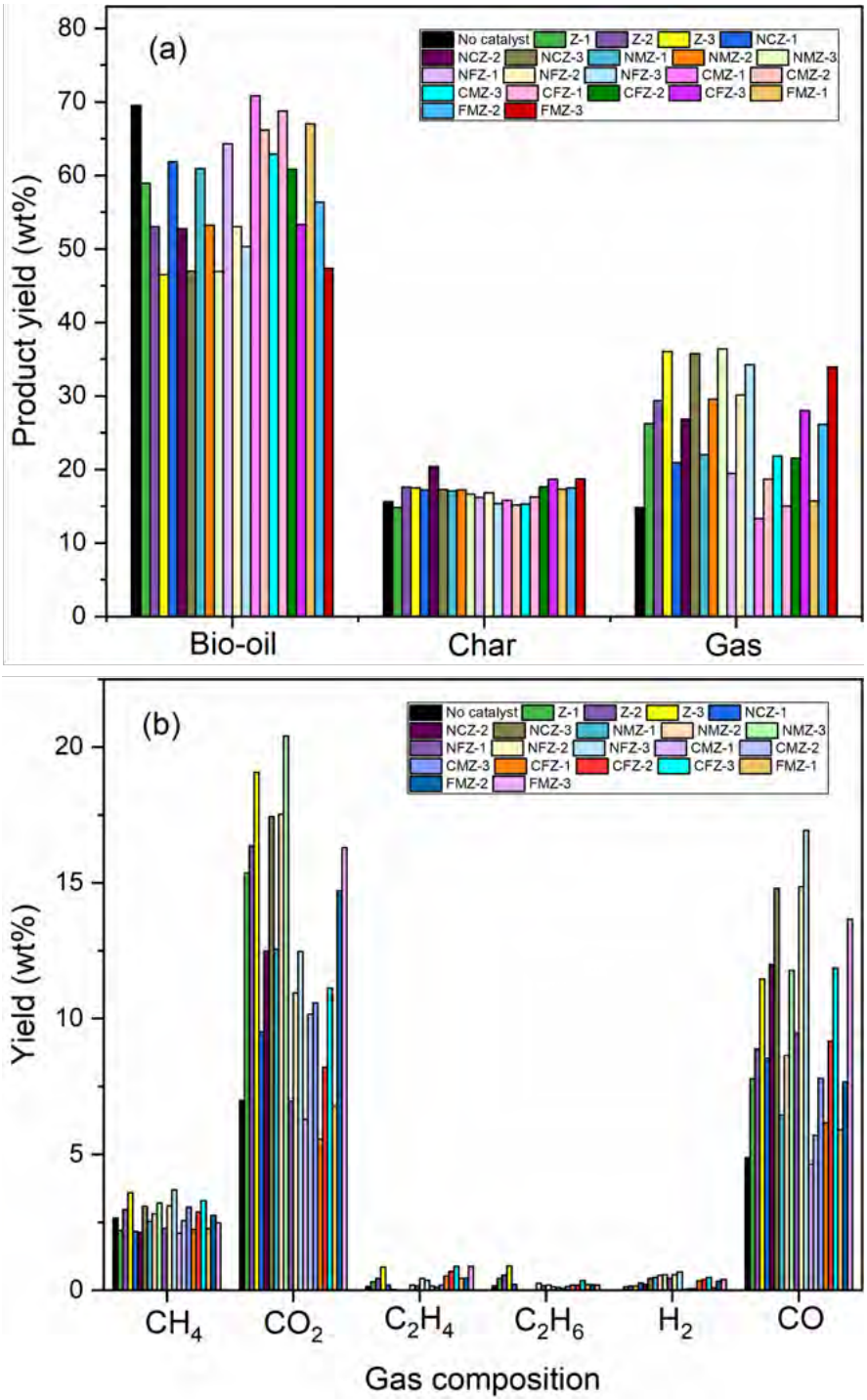

Figure 2. (a) Distribution of pyrolytic product yield (wt%) and (b) gas composition obtained with bimetallic catalysts from biomass pyrolysis at 500 °C with heating rate of 100 °C/min and C/B ratios of 1, 2 and 3.

Figure 2b shows the yield (wt%) of gas composition obtained during the catalytic pyrolysis. Primary gases detected in this study during the pyrolysis were CO, CO_2, H_2, CH_4, C_2H_4 and C_2H_6. The release of gases could also reflect the type of reactions carried out by the catalysts

during bio-oil upgrading. For example, the release of CO can be attributed to decarbonylation reactions which can be formed by cracking of RR'CO or RCO_2H groups [6]. Similarly, evolution of CO_2 can be credited to decarboxylation reactions and from cracking of RCO_2H groups [40]. The production of CH_4 is mainly ascribed to demethylation of methoxy groups from the lignin structure [41]. H_2 can be produced due to the cracking of $C-H$ and $C=C$ bonds in the organic compounds. H_2 can also be generated via water gas shift reaction (WGSR) favored by the catalysts by reacting CO and H_2O produced during pyrolysis [41]. On the other hand, gaseous olefins are formed by cracking of alkyl aromatics or decarbonylation of light oxygenated compounds. The results indicated that with increase in C/B ratio, the amount of gases, mainly CO and CO_2 significantly increased with all catalysts, while some catalysts also produced small proportion of H_2. Noticeably, the synergistic effect of Ni-Cu and Ni-Mo favoured decarboxylation reactions for bio-oil upgrading and produced higher amount of CO_2 of 17.44 wt% and 20.4 wt%. Ni with Fe promoted decarbonylation reactions as higher amount of CO (16.93 wt%) was obtained compared to CO_2 (12.48 wt%). However, the synergistic effect of Fe and Cu promoted decarboxylation and decarbonylation reactions equally since nearly similar quantities of CO (11.86 wt%) and CO_2 (11.13 wt%) were achieved. The variation in yields of gases indicates the preference of deoxygenation pathways, and the results showed that the synergistic effect of metals selects unique pathways to convert the oxygenated compounds into hydrocarbons.

Table 2. Elemental composition and HHV values of bio-oils obtained in *ex-situ* pyrolysis with bimetallic catalysts from biomass pyrolysis at 500 °C with a heating rate of 100 °C /min and C/B of 2.

Catalyst	**C (wt%)**	**H (wt%)**	**N (wt%)**	**O (wt%)**	**HHV (MJ/kg)**
No catalyst	44.79	5.59	0.00	49.62	17.09
ZSM-5	54.49	3.11	0.00	42.40	18.30
NiCu/ZSM-5	63.51	4.59	0.00	31.90	24.28
NiMo/ZSM-5	54.35	3.51	0.00	42.14	18.75
NiFe/ZSM-5	60.10	4.84	0.00	35.06	23.06
CuMo/ZSM-5	42.17	3.87	0.00	53.96	13.70
CuFe/ZSM-5	52.39	4.11	0.06	43.44	18.64
FeMo/ZSM-5	53.81	3.45	0.00	42.74	18.43

Note: O (wt%) was calculated by the difference.

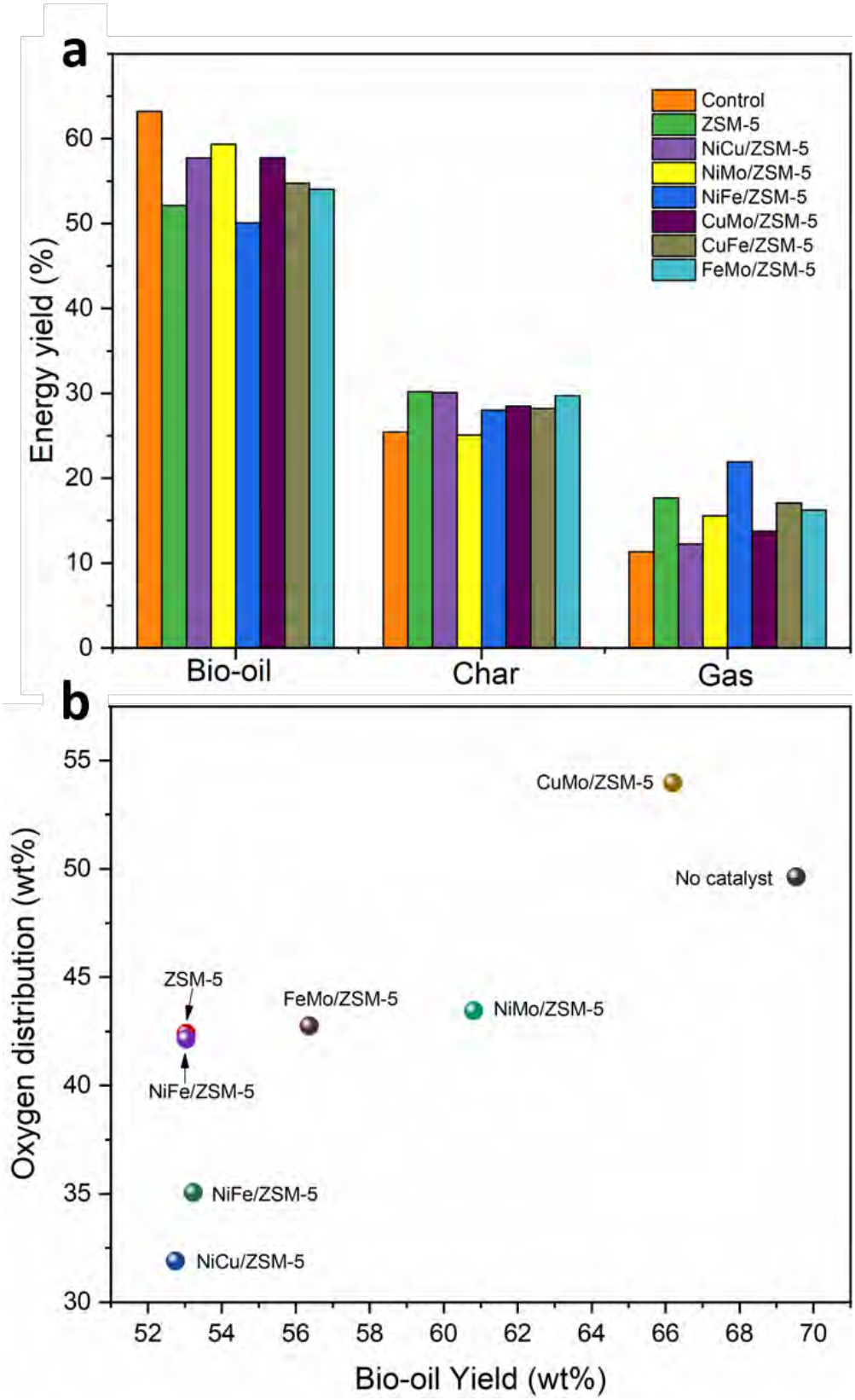

Figure 3. Comparative analysis of catalyst performance for (a) energy yield (%) in pyrolytic products and (b) oxygen distribution (wt%) in bio-oil samples obtained from biomass pyrolysis at 500 °C with a heating rate of 100 °C /min and C/B of 2.

Table 3. Elemental composition and HHV values of bio-chars obtained in *ex-situ* pyrolysis with bimetallic catalysts from biomass pyrolysis at 500 °C with a heating rate of 100 °C/min and C/B of 2.

Catalyst	C (wt%)	H (wt%)	N (wt%)	O (wt%)	Ash (wt%)	HHV (MJ/kg)
No catalyst	83.41	2.47	0.03	14.09	5.92	30.58
ZSM-5	85.64	2.75	0.03	11.58	4.09	31.98
NiCu/ZSM-5	87.40	2.74	0.03	9.83	5.83	32.72
NiMo/ZSM-5	81.88	2.62	0.02	15.48	3.30	30.14
NiFe/ZSM-5	87.74	2.78	0.00	9.48	1.59	33.01
CuMo/ZSM-5	81.23	2.38	0.01	16.38	4.33	29.51
CuFe/ZSM-5	87.99	2.75	0.00	9.26	2.02	33.08
FeMo/ZSM-5	87.06	2.79	0.04	10.11	5.49	32.64

Note: O (wt%) was calculated by the difference

3.3. Energy yield and bio-oil deoxygenation

A realistic approach is important to estimate the oxygen distribution and chemical energy available in the bio-oil to compare the efficiency of bimetallic catalysts for bio-oil upgrading. Therefore, elemental composition and HHV of the bio-oils were determined [36]. Table 2 shows the elemental composition and HHV values of the bio-oil samples obtained from noncatalytic and catalytic pyrolysis, while Figure 3b compares the oxygen concentration of bio-oils with respect to the bio-yield. It is evident from the results that pyrolysis without catalyst resulted in bio-oil with low carbon and high oxygen content, and consequently had low HHV of 17.09 MJ/kg. On the other hand, catalytic pyrolysis significantly enhanced the carbon content in the bio-oils and reduced the oxygen proportion. Among all bimetallic catalysts, NiCu/ZSM-5 showed the highest carbon (63.51 wt%) and lowest oxygen concentration (31.90 wt%) and thus the maximum HHV of 24.28 MJ/kg. The increased HHV of the bio-oil can be attributed to the excellent synergistic catalytic activity of Ni and Cu on ZSM-5 that carried out various deoxygenation reactions, such as dehydration, decarboxylation, decarbonylation, and polymerization, and condensation reactions to convert oxygenated compounds into energy-rich aromatic and aliphatic hydrocarbons. The bio-oils obtained with other catalysts also showed noticeable improvement in HHV, owing to increased concentration of carbon due to their efficient synergistic catalytic activities to reduce the proportion of oxygenated compounds and increase the concentration of valuable hydrocarbons. The biochars showed retention of higher content of carbon and almost similar HHV were obtained for all samples (Table 3). It should be noted that HHV of bio-oils can be further improved with higher C/B ratios but at the expense of decreased bio-oil yield.

Figure 3a shows the energy yield of pyrolytic products. Compared to the results of product yield (wt%), a different trend was obtained for the energy yield (%) of pyrolytic products. It was observed that most of the chemical energy was present in bio-oils and may contain up to 60% of the energy present in the raw biomass. For product yield (wt%), higher amount of gas than char

was obtained, but in terms of energy yield (%), char contributes to higher energy yield and gases retain the lowest amount of energy than char and bio-oil. For example, NiCu/ZSM-5 showed energy yield of 57.7% for bio-oil, 30.1% for biochar and 12.2% for gases. A similar trend can be seen for other samples. A probable way to enhance the energy yield for bio-oil could be to reduce the char formation during pyrolysis, which can be obtained by applying biomass-pretreatment methods to reduce the lignin content in the feedstock and retain the cellulose component largely for the pyrolysis that generally contributes most to the bio-oil yield [42].

3.4. Bio-oil composition

The bio-oil composition generally contains more than 200 compounds, and it is not possible to identify them all. GC-MS is usually considered as a semi-quantitative approach for bio-oil analysis since it cannot detect all the compounds of bio-oil. It is evident that GC-MS is unable to detect the oligomers produced from the pyrolysis of three biopolymers of lignin component. Moreover, in this study, peak area % was considered to estimate the bio-oil composition which provides qualitative analysis of the organic compounds. The organic compounds detected were further grouped in different families based on their main functional groups. Table 4 presents the bio-oil composition obtained from pyrolysis with all bimetallic catalysts. The results showed that pyrolysis without any catalyst produced bio-oil enriched with oxygenated compounds dominantly phenols, ketones, esters and alcohols, and nitrogen containing compounds. These oxygenated compounds are generated from thermal degradation of cellulose, hemicellulose and lignin components of pinewood. Thermal degradation of cellulose could result into different anhydrosugars, such as levoglucosan (LGA) and levoglucosenone (LGO), and furans, such as hydroxymethyl furfural (HMF) and pyrans like dianhydroglucopyranose (DAGP), acids and aldehydes [43]. Hemicellulose also contributes to light oxygenates and furans [40]. Lignin contains monolignols (*p*-coumaryl, coniferyl, and sinapyl alcohols) which act as intermediate compounds in formation of various phenolic compounds like eugenol, 2-methyl-4-vinylphenol, creosol [44–46]. Negligible proportion of hydrocarbons was obtained with noncatalytic pyrolysis. However, the application of sole ZSM-5 and supported bimetallic catalysts showed excellent conversion of oxygenated compounds into high energy density aromatic hydrocarbons. Furthermore, the formation of hydrocarbons was significantly improved with increase in C/B ratio, while the undesirable oxygenated compounds like acids, ketones, phenols and esters were drastically reduced. The primary aromatics obtained in bio-oils using ZSM-5 were naphthalene, naphthalene derived and phenanthrene derived aromatics. The acidic sites (Brønsted as well as Lewis acid sites) present in the zeolite are well known to catalyze various deoxygenation reactions to convert the generated oxygenated compounds into hydrocarbons. For instance, naphthalenes were chief hydrocarbons in the bio-oils, which are assumed to generate from

hydroxymethyl furfural and furans possibly via Diels-Alder condensation, decarboxylation, decarbonylation, oligomerization and aromatization reactions [47]. The phenolic compounds have also been reported to undergo direct deoxygenation and dehydration reactions to form aromatics [48]. Brønsted acid sites in ZSM-5 promote the demethoxylation, dehydroxylation and methyl substitution reactions to produce monocyclic aromatics, like benzene and toluene, which further undergo secondary polymerization reactions to form polycyclic aromatics, like naphthalene, methylnaphthalene and phenanthrene [49].

On bimetallic catalysts, in addition to naphthalene derived aromatics, the synergistic effect of metals produced a variety of additional aromatic and aliphatic hydrocarbons. For instance, the synergistic effect of Ni and Cu produced biphenyl derived aromatics, anthracene and alkanes, such as tridecane, heneicosane and tetracosane. However, Ni with Mo nanoparticles favored the production of alkanes, like nonane, decane and dodecane, while only few aromatics, mainly naphthalene, were found in the bio-oils. The combination of Fe with either Ni or Cu also showed substantial production of hydrocarbons and favored the catalytic routes to form benzene derived aromatics and cycloalkanes. The synergistic effect of Fe and Mo produced a variety of additional hydrocarbons. Evidently, FeMo/ZSM-5 contributed to the formation of indene aromatics, benzene, acenaphthene and cyclic hydrocarbons, like cycloheptatriene. The combination of Cu and Mo did not lead to the deoxygenation reactions as they favored formation of oxygenation compounds, like phenols, ketones, esters and alcohols. This unfavorable catalytic activity of CuMo/ZSM-5 can also be attributed partially to its physicochemical properties of low acidic sites and surface area.

Table 4. Bio-oil composition obtained from pyrolysis with bimetallic catalysts.

Catalyst	Bio-oil composition (peak area %)											
	Aromatic	**Aliphatic**	**Phenol**	**Ketone**	**Ester**	**Aldehyde**	**Alcohol**	**Acid**	**Furan**	**Nitro**	**Sugars**	**Others**
Control	1.35	1.39	31.37	13.79	5.79	2.69	4.06	0.90	1.23	7.44	1.89	3.35
Z-1	30.26	1.35	28.36	3.07	0.41	0.00	2.77	0.00	0.00	1.96	0.00	1.26
Z-2	59.73	4.76	3.95	0.00	2.13	0.00	1.64	0.00	0.52	0.00	0.00	0.00
Z-3	65.09	1.25	0.00	0.00	1.04	0.00	0.00	0.00	0.50	0.00	0.00	0.00
NCZ-1	14.19	6.76	42.80	7.37	0.60	0.00	3.85	2.15	1.42	5.03	0.00	0.18
NCZ-2	45.35	0.00	18.96	0.43	1.43	0.00	2.02	0.00	0.41	0.00	0.00	2.20
NCZ-3	75.52	1.90	8.47	0.30	2.28	0.00	3.78	1.61	0.75	0.00	0.00	0.30
NMZ-1	4.64	0.36	46.89	5.76	0.28	0.72	6.72	0.00	0.00	2.82	0.00	0.97
NMZ-2	6.46	1.09	45.59	1.59	1.31	0.00	10.72	3.05	4.10	0.00	0.00	2.07
NMZ-3	8.06	14.38	13.08	3.59	23.27	0.44	0.00	1.75	0.00	2.90	0.00	5.42
NFZ-1	15.20	0.91	43.52	7.58	0.83	0.47	3.34	0.00	0.31	1.35	0.58	0.00
NFZ-2	57.93	0.49	12.21	1.06	0.69	1.51	1.74	0.97	0.74	2.54	0.00	0.00
NFZ-3	68.19	0.46	1.41	1.13	1.60	1.74	1.41	0.91	3.58	0.00	0.00	0.00
CMZ-1	3.73	1.51	30.19	17.49	5.60	3.24	0.60	1.19	0.00	2.79	0.95	2.24
CMZ-2	4.02	2.22	48.47	14.91	4.29	1.27	1.45	0.43	0.27	0.84	1.72	1.97
CMZ-3	5.34	1.18	41.00	12.72	2.29	2.47	10.79	2.46	0.27	1.49	1.80	0.54
CFZ-1	37.79	1.23	26.00	4.05	0.57	0.00	0.88	0.00	2.06	3.13	0.00	0.31
CFZ-2	50.40	0.41	15.52	2.81	0.00	0.00	0.00	1.52	1.64	1.76	0.00	1.41
CFZ-3	85.25	0.00	1.34	0.22	0.16	0.82	0.95	0.58	1.47	0.00	0.00	0.00
FMZ-1	18.14	0.40	43.32	6.75	0.00	0.00	1.35	0.00	0.78	0.83	0.00	0.00
FMZ-2	23.17	0.00	17.10	3.62	1.05	0.00	4.83	7.20	1.10	1.10	0.00	0.00
FMZ-3	54.27	0.88	7.32	1.68	1.32	0.43	1.80	0.38	2.55	0.00	0.00	2.67

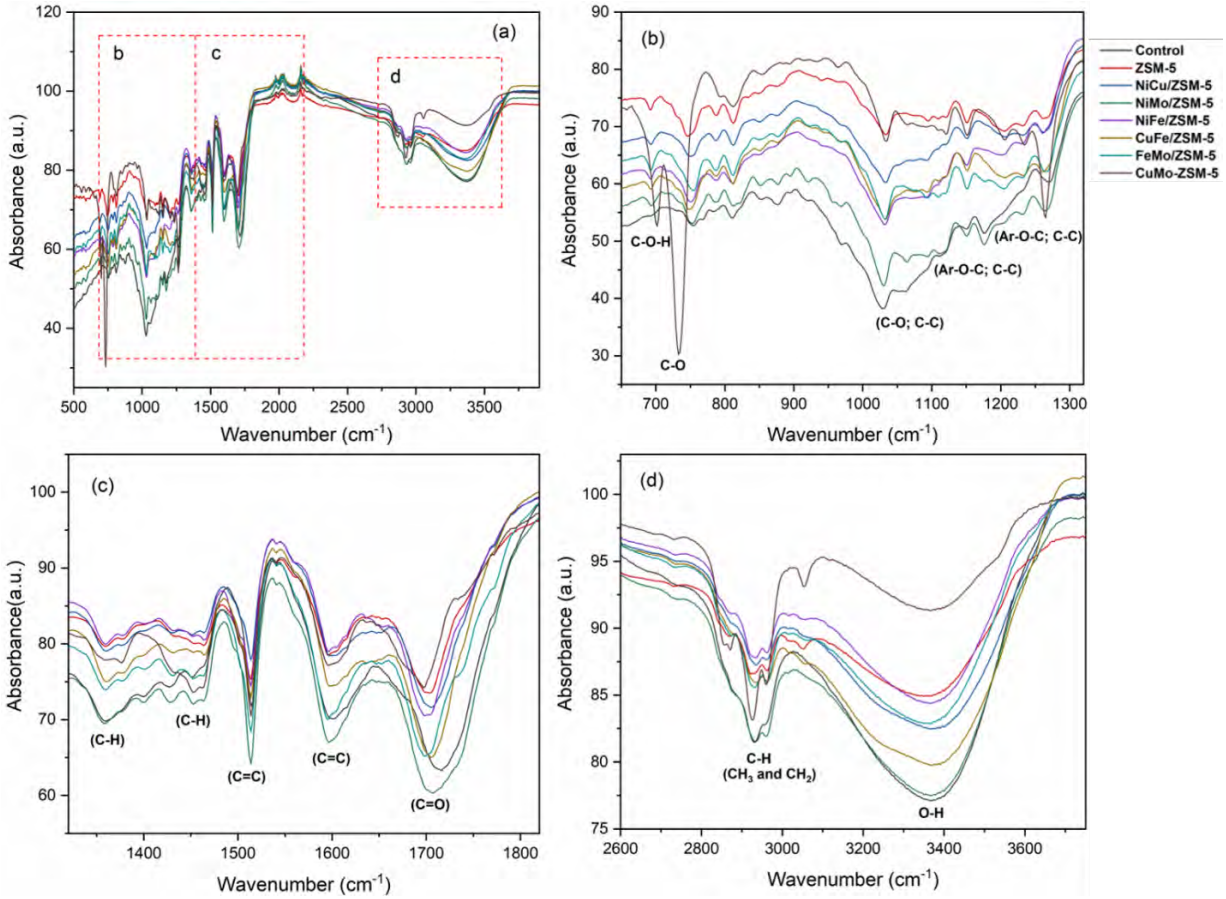

Figure 4. FTIR scans of bio-oil samples obtained from catalytic pyrolysis.

3.5. FTIR of bio-oils

Figure 4a shows FTIR scans of the bio-oil samples while b, c, and d are enlarged regions shown in part a. The absorbance peaks shown in the scans suggest the type of functional groups and family of compounds present in the bio-oil samples. It can be observed from the figures that all bio-oil samples showed strong IR absorbance at different regions. Noticeably, the peaks between 2600 and 3100 cm^{-1} can be attributed to $C-H$ stretch present in the saturated and unsaturated aliphatic and aromatic compounds, while $C-H$ stretch present between 1350 and 1500 cm^{-1} are often associated with alcohols, aldehydes and ketones [50,51]. The peaks between 1000 and 1310 cm^{-1} are designated to $C-O$ and $C-C$ bonds which might be present in the family compounds of alkanes, alcohols, phenols and ethers [52]. The $C=O$ stretch at around 1705 cm^{-1} suggesting presence of aldehydes, acids and ketones, can be seen for all bio-oil samples but its intensity was reduced for bimetallic catalysts compared to the noncatalytic pyrolysis which indicates the reduction in the oxygenated compounds in the bio-oils. In addition, strong absorbance peaks were observed at 1514 and 1598 cm^{-1} ascribed to $C=C$ functional groups of aromatic hydrocarbons. A significant increase in the vibrations can be observed for bimetallic catalysts, suggesting the presence of more aromatic hydrocarbons in

the bio-oil samples. $O-H$ stretch at 3370 cm^{-1} suggests presence of water, alcohols and phenols in the bio-oil. Low intensity of $O-H$ stretch for the bio-oils obtained from catalytic pyrolysis indicates low concentrations of phenols and alcohols compared to noncatalytic pyrolysis.

3.6. Catalyst characterization

Figure 5a shows X-ray diffraction of fresh ZSM-5 and ZSM-5 supported bimetallic catalysts. It can be observed from the figure that ZSM-5 and the impregnated metal nanoparticles were crystalline in nature as sharp and less intense peaks can be clearly identified. The impregnated metal nanoparticles were found in their oxide forms, such as NiO, CuO, MoO_3 and Fe_2O_4 on the zeolite support. In all catalysts, diffraction peaks at 2θ degree of 9.03, 9.83, 26.67, 27.65, 28.26 correspond to 101, 111, 051, 313, 323 index planes of crystalline ZSM-5, respectively and belong to the crystal system: orthorhombic; space group: Pnma. The results match well with standard data given in JCPDS (Joint Committee on Powder Diffraction Standards) no. 891421. In bimetallic catalysts containing Ni, the diffraction peaks at 2θ degree of 43.23, 50.54 and 74.27 are designated to 111, 200 and 220 index planes of NiO, respectively, corresponding to cubic crystal system and space group of Fm-3m. These results are well in line with standard NiO crystallographic results (reference code-01-073-1523). The catalysts comprising Cu (such as NiCu/ZSM-5, CuMo/ZSM-5, CuFe/ZSM-5) show diffraction peaks at 2θ degree of 62.17 and 69.51 that are indexed to 020 and 202 planes of CuO, belonging to monoclinic crystal system and C2/c space group. In Fe containing catalysts, diffraction peak observed at 2θ degree of 41.43 corresponds to 311 planes of crystalline Fe_3O_4, which belongs to the cubic crystal system and Fd-3m space group (reference code-01-089-0950). In addition, Mo impregnated catalysts showed sharp diffraction peaks at 2θ degree of 29.82, 31.59, 45.56 and 57.82 which suggest presence of 040, 021, 060 and 002 planes of the crystalline MoO_3 in the catalysts, respectively. The results were in line with standard data of MoO_3 (reference code-00-005-0508) which suggests that MoO_3 belongs to the orthorhombic crystal system and Pbnm space group.

Figure 5b shows X-ray diffraction patterns of spent ZSM-5 and supported bimetallic catalysts. The impregnated metals present in the fresh catalysts in their oxide forms, such as NiO, CuO, MoO_3 and Fe_3O_4, were detected reduced to Ni, Cu, MoO_2 and FeO after the pyrolysis process. It is well known that metal oxide species can be reduced to their metallic forms after reacting with hydrogen and other gases produced during the pyrolysis and other catalytic reactions such as hydrogenation and water-gas shift reaction (WGSR) carried out on

the surface of the catalysts. Diffraction peaks at 2θ degree of 30.22, 43.06, 63.10 are aligned to 110, 020, 211 planes of MoO_2 (reference code-01-078-1072). Diffraction peaks at 50.62 and 59.75 correspond to 111 and 200 planes of Cu metal (reference code-00-004-0836). In addition, the peaks at 2θ degree of 51.34 and 53.08 can be indexed to the Ni (200) and FeO (110) planes, respectively.

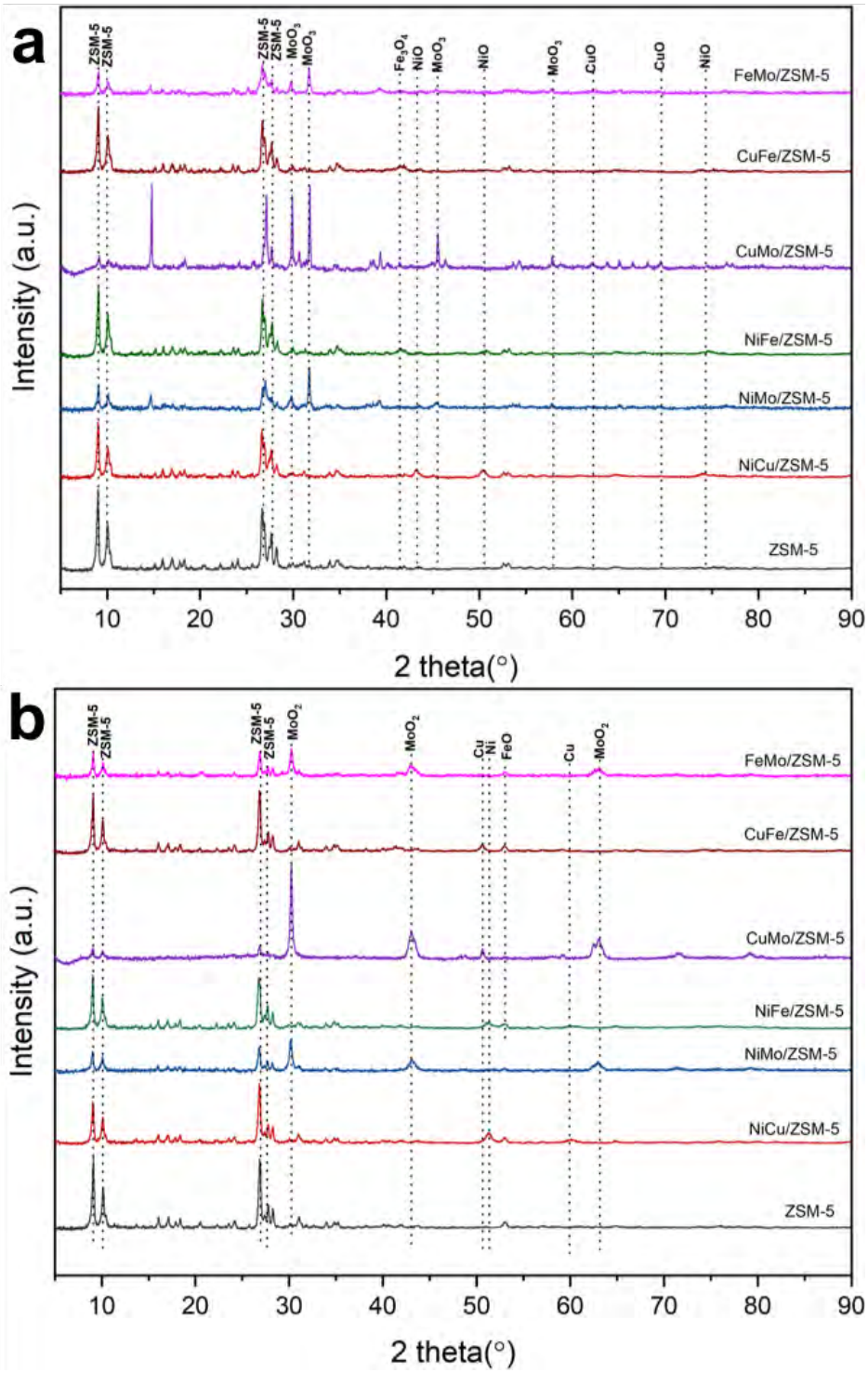

Figure 5. X-ray diffraction patterns of (a) fresh and (b) spent ZSM-5 and supported bimetallic catalysts.

Table 5. Textural properties of fresh and spent bimetallic catalysts.

No.	Catalyst	BET surface area (m^2/g)	External Surface area (m^2/g)	Micropore volume (cm^3/g)	Average Pore size (nm)
	Fresh catalysts				
1	ZSM-5	403.23	135.64	0.25	1.12
2	NiCu/ZSM-5	278.35	85.66	0.17	1.05
3	NiMo/ZSM-5	162.05	42.21	0.10	1.06
4	NiFe/ZSM-5	257.92	75.96	0.17	1.05
5	CuMo/ZSM-5	166.18	86.33	0.12	1.34
6	CuFe/ZSM-5	272.39	88.20	0.17	1.09
7	FeMo/ZSM-5	154.43	51.96	0.10	1.23
			Spent catalysts		
1	ZSM-5	280.35	47.35	0.17	1.02
2	NiCu/ ZSM-5	158.62	36.74	0.09	1.27
3	NiMo/ZSM-5	121.37	29.32	0.07	1.02
4	NiFe/ZSM-5	215.77	56.18	0.13	1.05
5	CuMo/ZSM-5	112.47	14.78	0.03	1.30
6	CuFe/ZSM-5	184.13	46.62	0.11	1.05
7	FeMo/ZSM-5	119.69	34.80	0.07	1.20

Nitrogen sorption isothermal curves of fresh and spent bimetallic catalysts are shown in supplementary Figure S1 and S2 while textural properties of the catalysts are given in Table 5. All catalysts either fresh or spent showed type I isotherm curve, which suggests the microporous nature of the prepared materials. Evidently, the average pore size in all catalysts was around 1 nm. ZSM-5 support showed the highest surface area and pore volume of 403.23 m^2/g and 0.25 cm^3/g, respectively. The addition of metals on ZSM-5 significantly reduced the surface area as well as the micropore volume. For instance, NiCu/ZSM-5 showed surface area of 278.35 m^2/g and micropore volume of 0.17 cm^3/g. Other catalysts showed lower surface area and pore volume compared to ZSM-5 and NiCu/ZSM-5. The reduction in surface area and micropore volume can be attributed to the addition of metal nanoparticles on the zeolite surface that blocked the pores on ZSM-5 and consequently, resulted in lesser adsorption of N_2 gas molecules on the catalyst surface. Moreover, the microporous properties of ZSM-5 restricted the distribution of metal nanoparticles probably on its surface and could not access the internal pores of ZSM-5. Another noticeable point observed in the results was that the bimetallic catalysts containing Mo metal showed lower surface area compared to other catalysts. This can be explained with the observed agglomeration of Mo nanoparticles in the Mo-incorporated catalysts, which blocked the pores on the zeolite surface that were inaccessible for N_2 adsorption. Agglomeration of Mo nanoparticles was evident from HRTEM images, and XRD results also showed comparatively sharp intensity peaks for Mo compared to other metal (Ni, Cu and Fe) impregnated catalysts, suggesting the presence of crystalline Mo nanoparticles.

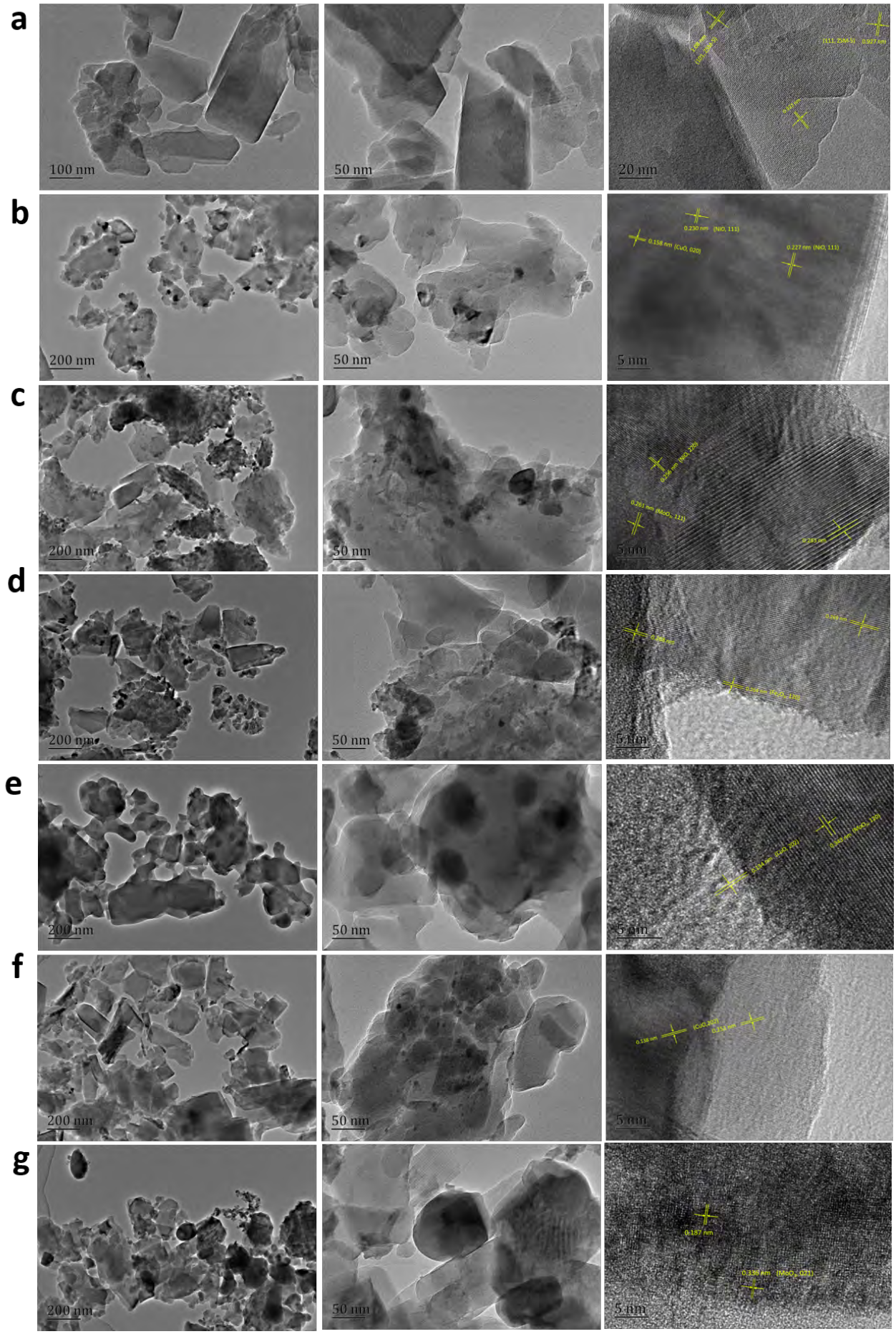

Figure 6. HRTEM images of (a) ZSM-5, (b) NiCu/ZSM-5, (c) NiMo/ZSM-5, (d) NiFe/ZSM-5, (e) CuMo/ZSM-5, (f) CuFe/ZSM-5, and (g) FeMo/ZSM-5.

BET results of spent catalysts showed noticeable decrease in both surface area and pore volume. During the pyrolysis, catalysts carry out several deoxygenation reactions and convert different oxygenated compounds into monocyclic and polycyclic aromatic compounds. Generally, the polycyclic aromatic compounds or the hydrocarbons with larger structure than the pore diameter could not escape the pores of the catalyst and block the pores as well the active sites. Accumulation of polycyclic aromatics leads to coke formation and collectively leads to the decrease in surface area and pore volume, which subsequently may lead to catalyst deactivation.

The dispersion of metal nanoparticles on ZSM-5 was examined using HRTEM. Figure 6 shows HRTEM images of bimetallic catalysts. Compared to the pristine zeolite, presence of smaller to larger metal nanoparticles can be clearly observed for bimetallic catalysts. The metal nanoparticles are assumed to be predominantly present on the zeolite surface. In addition, in case of NiMo/ZSM-5 and CuMo/ZSM-5 catalysts, agglomeration of metal nanoparticles can be seen, indicating the impregnation method might be inefficient for these catalysts.

ZSM-5 is well known for its high acidity that plays a crucial role in its catalytic activity. ZSM-5 exhibits both Lewis and Brønsted types of acidic sites and are responsible to carry out the deoxygenation reactions to convert oxygenated compounds into hydrocarbons [38,53,54]. Acidic properties of the prepared catalysts were examined using NH_3-TPD. The results are shown in Figure 7, indicating that all catalysts showed noticeable desorption peaks at lower and higher temperatures, indicating presence of weak and strong acidic sites. Sole ZSM-5 showed total acidity of 103.46 μmol/g. For bimetallic catalysts NiCu/ZSM-5 and NiFe/ZSM-5, total acidity increased significantly to 136.43 and 123.51 μmol/g, respectively and slightly increased for NiMo/ZSM-5 showing acidity of 105.6 μmol/g. It has been demonstrated previously that the addition of metals on zeolite decreases strong Brønsted sites and produces new types of Lewis acidic sites [38,55]. Therefore, increase in total acidity for Ni incorporated bimetallic catalysts can be attributed mainly to the increase in Lewis acidic sites. However, peaks around 525 °C for NiCu/ZSM-5 and small peaks between 350 and 470 °C also indicate the presence of strong Lewis or Brønsted sites. This can be attributed to better dispersion of Ni and other metal nanoparticles on zeolite surface allowing adsorption of more NH_3 molecules on the catalyst surface. On the other hand, CuFe/ZSM-5 and CuMo/ZSM-5 showed lower acidity of 96.48 and 67.70 μmol/g, respectively, while no peak was observed at higher temperatures, indicating the presence of only weak Lewis acidic sites in the catalysts. Low acidity by CuFe/ZSM-5 and CuMo/ZSM-5 can also be attributed to agglomeration of metal nanoparticles on ZSM-5 surface that blocked the pores, leading to adsorption of smaller number of NH_3 molecules. In addition, FeMo/ZSM-5 achieved total acidity of 86.30 μmol/g, small peaks between 170 and 430 °C indicate the existence of some strong acidic sites as well. The catalysts with higher acidic sites are expected to catalyze higher number of

deoxygenation reactions and produce more hydrocarbons in bio-oil samples, however, may also be prone to faster catalyst deactivation.

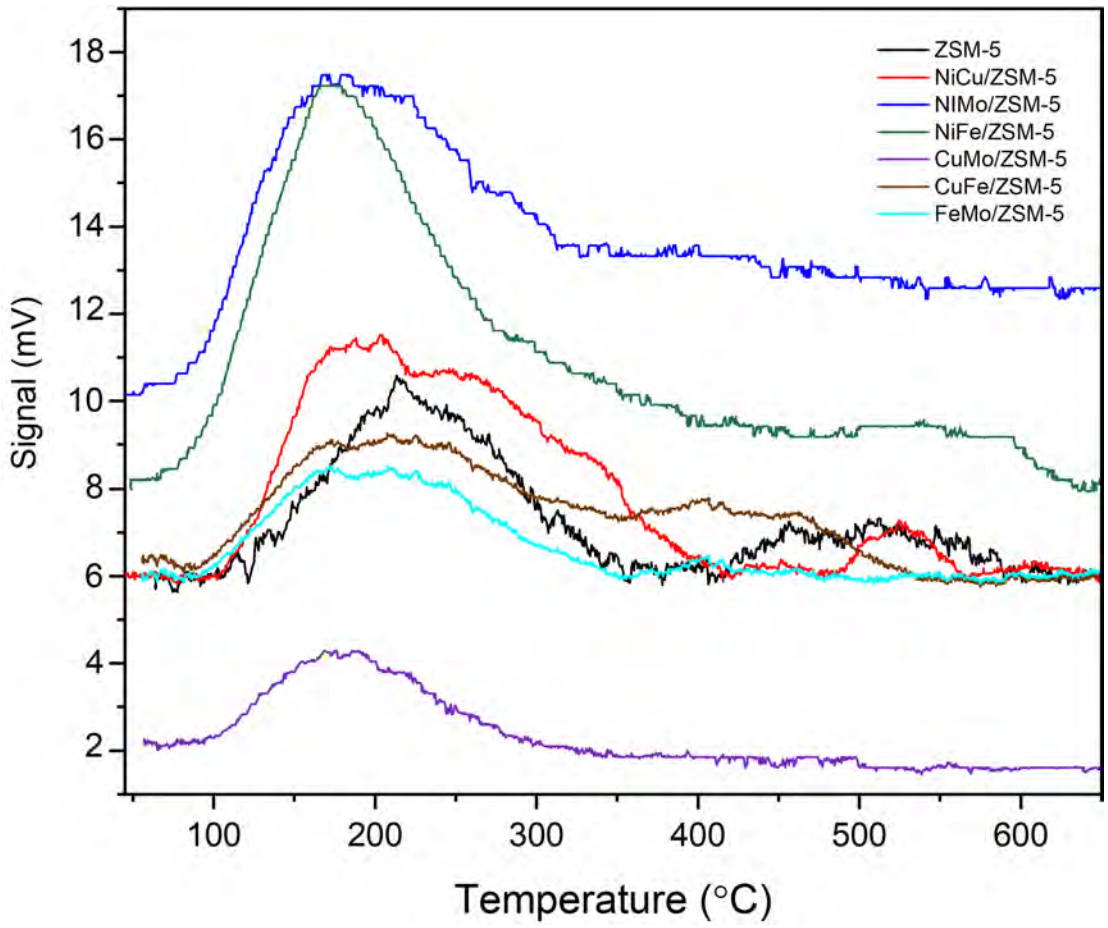

Figure 7. TPD analysis of bimetallic catalysts.

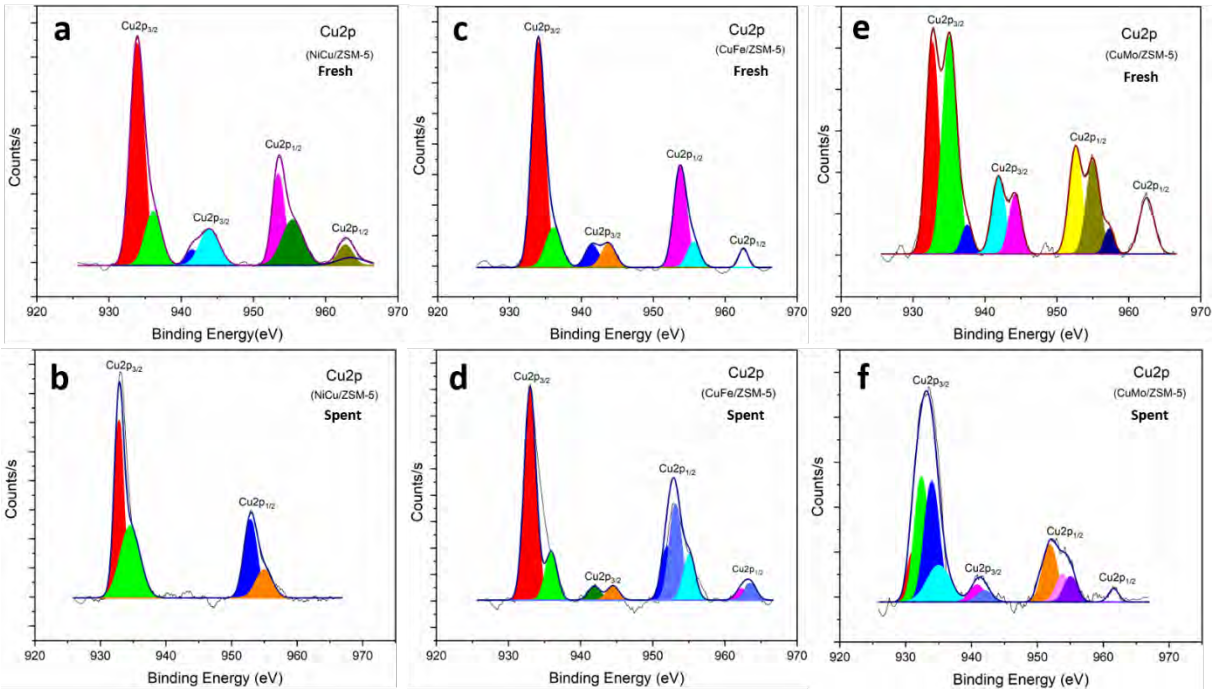

Figure 8. Cu2p photoelectron spectra of fresh catalysts (a) NiCu/ZSM-5, (c) CuFe/ZSM-5 and (e) CuMo/ZSM-5 and spent catalysts (b) NiCu/ZSM-5, (d) CuFe/ZSM-5 and (f) CuMo/ZSM-5.

Elemental composition of the catalysts was analyzed using XPS. Results are shown in Figures 8-11. Figure 8 shows Cu2p photoelectron spectra of Cu containing fresh (a, c and e) and spent catalysts (b, d and f). Significant changes can be clearly observed in Cu2p spectra of fresh and spent catalysts. In fresh catalysts, highly intense main peaks at binding energy of 934 eV and 953.04 eV can be attributed to $Cu2p_{3/2}$ and $Cu2p_{1/2}$ of CuO in the catalysts. The presence of shake-up satellites indicates the presence of Cu^{2+} state of the metal. On the other hand, for spent NiCu/ZSM-5, shake-up satellites were completely disappeared, suggesting the reduction of CuO into metallic form of Cu [56]. In addition, for CuFe/ZSM-5 and CuMo/ZSM-5, the intensity of shake-up satellites significantly decreased and the main peaks were observed at lower values of binding energy, revealing high reduction in CuO species and transformation of Cu^{2+} into Cu^{0} form [56].

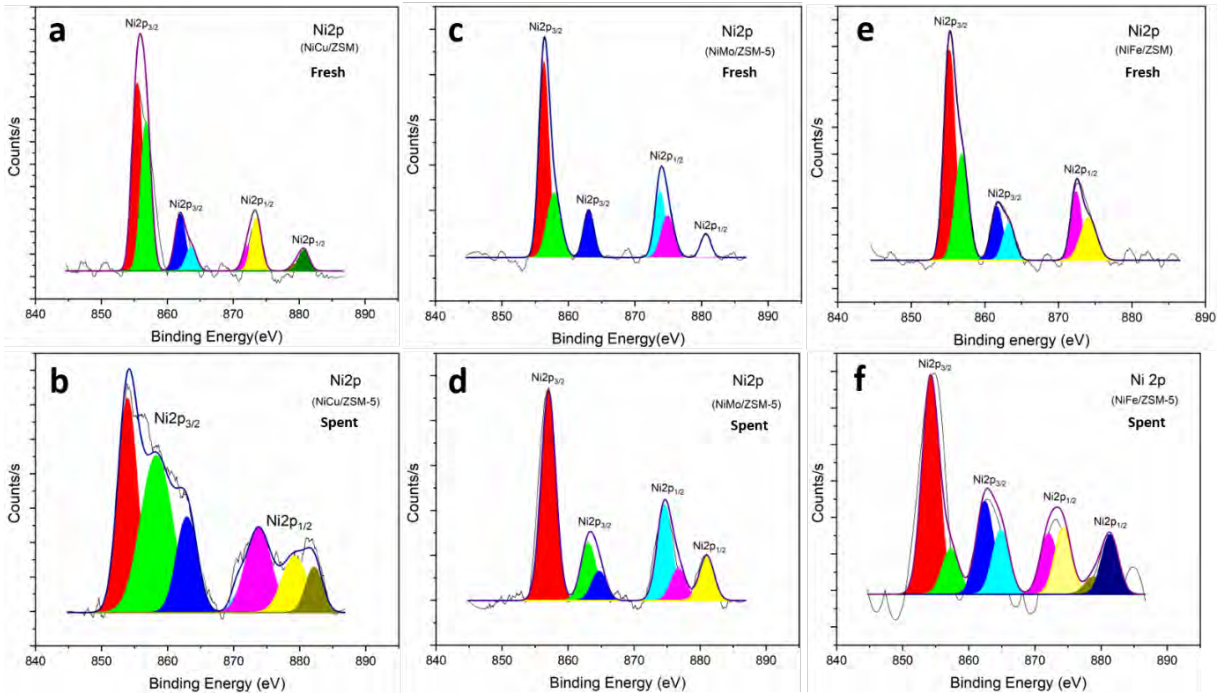

Figure 9. Ni2p photoelectron spectra of fresh catalysts (a) NiCu/ZSM-5, (c) NiMo/ZSM-5 and (e) NiFe/ZSM-5 and spent catalysts (b) NiCu/ZSM-5, (d) NiMo/ZSM-5 and (f) NiFe/ZSM-5.

Figure 9 shows Ni2p photoelectron spectra of Ni containing fresh (a, c and e) and spent catalysts (b, d and f). In all catalysts, Ni2p spectra can be divided into two main peaks present at 855.1 and 872.55 eV, and along with two shake-up satellites (except fresh NiFe/ZSM-5, where only one shake-up satellite is present) at 863.9 and 880.75 eV, which can be ascribed to $Ni2p_{3/2}$ and $Ni2p_{1/2}$ of NiO present in the catalysts [57]. Intense satellites at 855.1 eV can be assigned to Ni^{3+} state of NiO. In contrast, in spent catalyst, intense peaks at 854.14 are attributed to the presence of Ni^{2+}, indicating the reduction of NiO to Ni during the pyrolysis process [58].

Figure 10 shows Mo3d photoelectron spectra of Mo containing fresh (a, c and e) and spent catalysts (b, d and f). It can be observed from the figures that all fresh catalysts showed

approximately similar spectra of Mo3d. Noticeably, two main peaks at 232.99 and 239.09 can be attributed to $Mo3d_{5/2}$ and $Mo3d_{3/2}$ of MoO_3, indicating the presence of Mo^{4+} and Mo^{6+} species in the catalysts. On the other hand, in spent catalysts, an additional peak at a lower binding energy of 229.7 eV can be clearly observed, which can be assigned to Mo^{4+} of MoO_2. These results are consistent with previous studies [59].

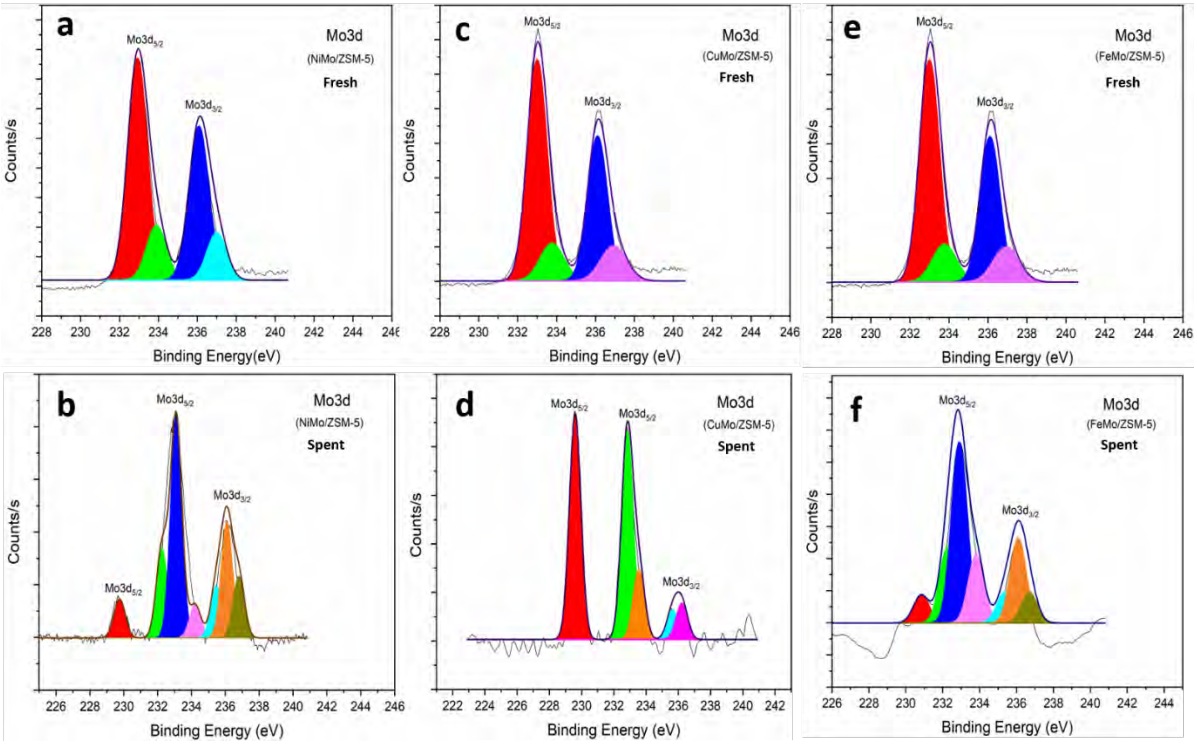

Figure 10. Mo3d photoelectron spectra of fresh catalysts (a) NiMo/ZSM-5, (c) CuMo/ZSM-5 and (e) FeMo/ZSM-5 and spent catalysts (b) NiMo/ZSM-5, (d) CuMo/ZSM-5 and (f) FeMo/ZSM-5.

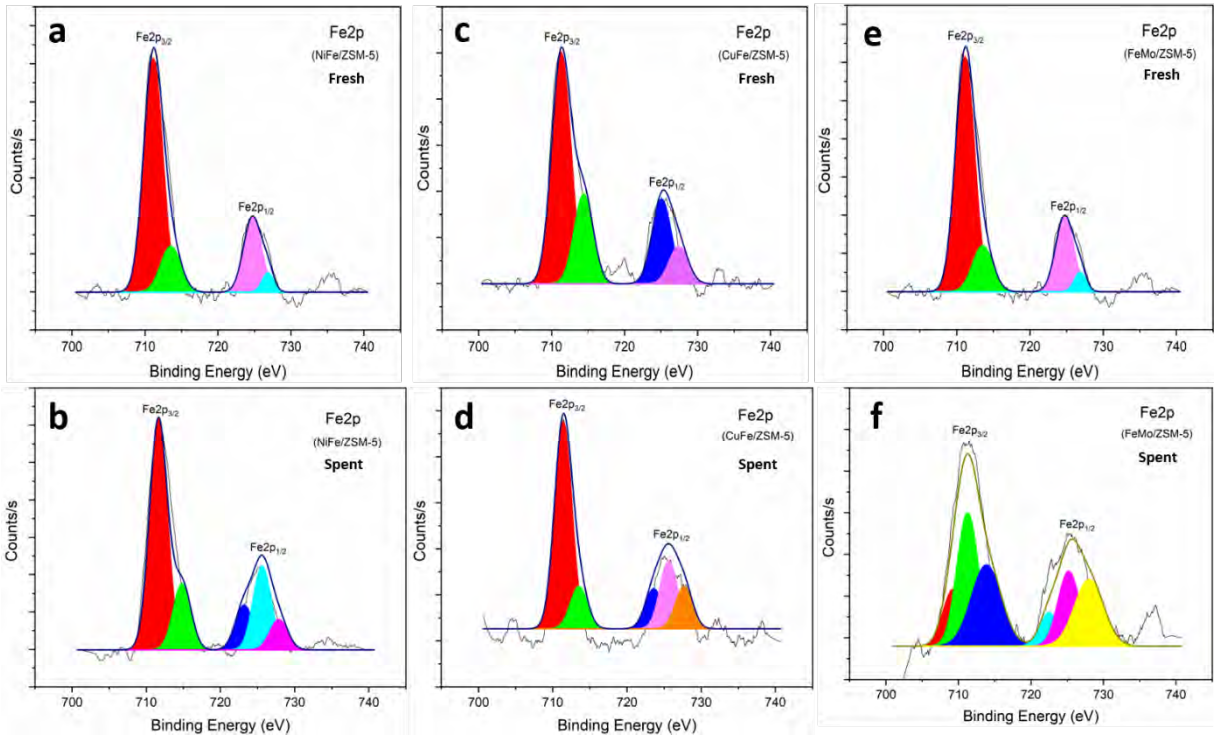

Figure 11. Fe2p photoelectron spectra of fresh catalysts (a) NiFe/ZSM-5, (c) CuFe/ZSM-5 and (e) FeMo/ZSM-5 and spent catalysts (b) NiFe/ZSM-5, (d) CuFe/ZSM-5 and (f) FeMo/ZSM-5.

Figure 11 shows Fe2p photoelectron spectra of Fe containing fresh (a, c and e) and spent catalysts (b, d and f). All fresh catalysts showed two main peaks at 711.25 and 724.8 eV, which are assigned to $Fe2p_{3/2}$ and $Fe2p_{1/2}$ of Fe_3O_4 present in the catalysts. In addition, Fe metal was present in Fe^{2+} and Fe^{3+} states. In contrast, in spent catalysts, additional peaks at 723.3 and 725.7 eV can be attributed to FeO and Fe_2O_3, respectively, indicating the reduction of Fe^{3+} to Fe^{2+} during the pyrolysis process. These results are also consistent with XRD results that showed the presence of Fe_3O_4 in fresh catalysts and FeO in spent catalysts.

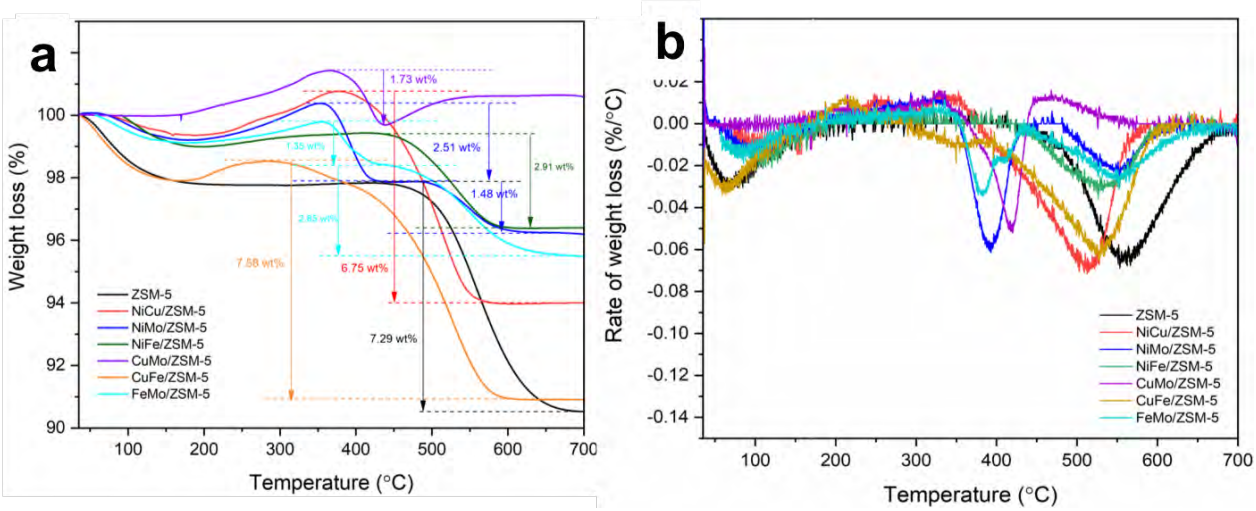

Figure 8. TPO analysis of spent bimetallic catalysts.

3.7. Coke deposition

Figure 8 shows TPO results of spent bimetallic catalysts, while TPO results of fresh catalysts are provided in supplementary Figure S3. It was concluded form the results that fresh catalysts did not show any coke deposition and the insignificant weight decrease can be attributed to the removal of moisture and impurities, while significant coke deposition was observed for spent catalysts. On one hand, the higher acidic characteristics of the catalysts could be advantageous to enhance their catalytic activity and convert the oxygenated compounds into more valuable aromatic hydrocarbons, but on the other hand, the formation of excessive hydrocarbons (mainly polycyclic aromatic) may also lead to coke formation and thus to catalyst deactivation. The results suggested that higher coke deposition was achieved for the bimetallic catalysts that showed efficient cracking activity for hydrocarbon formation. For example, spent ZSM-5, NiCu/ZSM-5 and CuFe/ZSM-5 showed coke deposition of 7.29, 6.75 and 7.58 wt%, respectively. Two sharp peaks at different temperatures (lower and higher) can be observed for NiMo/ZSM-5 and FeMo/ZSM-5 catalysts, suggesting the presence of two types of carbon species on the catalyst. The lower temperature peaks (around 382 and 392 °C) can be attributed to the carbon with weaker interactions with catalyst (zeolite or metal (oxide)) or their deposition on the outer part of pores, while peaks at higher temperature (around 550 °C) can be ascribed to the carbon species with

stronger interactions with catalyst or their deposition deep inside the pores. The initial mass increase at around 200 °C in the spent catalysts can be credited to the oxidation of metal particles inside the catalysts, as reported in the previous studies [34,60].

4. Conclusion

This work demonstrated the synergistic effect of ZSM-5 supported bimetallic catalysts on conversion of low-energy oxygen-containing compounds into energy-rich hydrocarbons. Among all the studied catalysts, it can be concluded the synergistic effect of Ni and Cu on ZSM-5 was found advantageous, owing to their better physicochemical properties, such as higher surface area and a large number of acidic sites, and the combined catalytic activity of Ni^{3+}/Cu^{2+}/ZSM-5 that paved the way to convert the oxygenated compounds into hydrocarbons. Evidently, NiCu/ZSM-5 produced bio-oil with the least amount of oxygen (31.90 wt%) and maximum carbon content (63.51wt%), resulting in HHV of 24.28 MJ/kg. The synergistic effect of other metal combinations was also found useful for bio-oil deoxygenation and producing bio-oils with improved calorific values. For instance, NiFe/ZSM-5 and CuFe/ZSM-5 produced bio-oils with HHVs of 23.06 and 18.64 MJ/kg, respectively. The bio-oil compositions indicate the formation of varying types of hydrocarbons, which can be ascribed to the synergistic effect of the bi-metals.

References

[1] Kumar R, Strezov V. Thermochemical production of bio-oil: A review of downstream processing technologies for bio-oil upgrading, production of hydrogen and high value-added products. Renewable and Sustainable Energy Reviews 2021;135:110152. https://doi.org/10.1016/j.rser.2020.110152.

[2] Yu IKM, Chen H, Abeln F, Auta H, Fan J, Budarin VL, et al. Chemicals from lignocellulosic biomass: A critical comparison between biochemical, microwave and thermochemical conversion methods. Critical Reviews in Environmental Science and Technology 2020:1–54. https://doi.org/10.1080/10643389.2020.1753632.

[3] Ansari KB, Arora JS, Chew JW, Dauenhauer PJ, Mushrif SH. Fast Pyrolysis of Cellulose, Hemicellulose, and Lignin: Effect of Operating Temperature on Bio-oil Yield and Composition and Insights into the Intrinsic Pyrolysis Chemistry. Ind Eng Chem Res 2019:acs.iecr.9b00920. https://doi.org/10.1021/acs.iecr.9b00920.

[4] Cai W, Liu R, He Y, Chai M, Cai J. Bio-oil production from fast pyrolysis of rice husk in a commercial-scale plant with a downdraft circulating fluidized bed reactor. Fuel Processing Technology 2018;171:308–17. https://doi.org/10.1016/j.fuproc.2017.12.001.

[5] Cai W, Liu R. Performance of a commercial-scale biomass fast pyrolysis plant for bio-oil production. Fuel 2016;182:677–86. https://doi.org/10.1016/j.fuel.2016.06.030.

[6] Asadieraghi M, Ashri Wan Daud WM, Abbas HF. Heterogeneous catalysts for advanced bio-fuel production through catalytic biomass pyrolysis vapor upgrading: a review. RSC Adv 2015;5:22234–55. https://doi.org/10.1039/C5RA00762C.

[7] Lappas AA, Kalogiannis KG, Iliopoulou EF, Triantafyllidis KS, Stefanidis SD. Catalytic pyrolysis of biomass for transportation fuels: Catalytic pyrolysis of biomass for transportation fuels. WENE 2012;1:285–97. https://doi.org/10.1002/wene.16.

[8] Kan T, Strezov V, Evans T, He J, Kumar R, Lu Q. Catalytic pyrolysis of lignocellulosic biomass: A review of variations in process factors and system structure. Renewable and Sustainable Energy Reviews 2020;134:110305. https://doi.org/10.1016/j.rser.2020.110305.
[9] Samolada MC, Papafotica A, Vasalos IA. Catalyst Evaluation for Catalytic Biomass Pyrolysis. Energy & Fuels 2000;14:1161–7. https://doi.org/10.1021/ef000026b.
[10] Weldekidan H, Strezov V, Kan T, Kumar R, He J, Town G. Solar assisted catalytic pyrolysis of chicken-litter waste with in-situ and ex-situ loading of CaO and char. Fuel 2019;246:408–16. https://doi.org/10.1016/j.fuel.2019.02.135.
[11] Lee HW, Kim Y-M, Jae J, Sung BH, Jung S-C, Kim SC, et al. Catalytic pyrolysis of lignin using a two-stage fixed bed reactor comprised of in-situ natural zeolite and ex-situ HZSM-5. Journal of Analytical and Applied Pyrolysis 2016;122:282–8. https://doi.org/10.1016/j.jaap.2016.09.015.
[12] Kumar R, Strezov V, Kan T, Weldekidan H, He J, Jahan S. Investigating the Effect of Mono- and Bimetallic/Zeolite Catalysts on Hydrocarbon Production during Bio-oil Upgrading from *Ex Situ* Pyrolysis of Biomass. Energy Fuels 2019:acs.energyfuels.9b02724. https://doi.org/10.1021/acs.energyfuels.9b02724.
[13] Huo X, Xiao J, Song M, Zhu L. Comparison between in-situ and ex-situ catalytic pyrolysis of sawdust for gas production. Journal of Analytical and Applied Pyrolysis 2018;135:189–98. https://doi.org/10.1016/j.jaap.2018.09.003.
[14] Wang K, Johnston PA, Brown RC. Comparison of in-situ and ex-situ catalytic pyrolysis in a micro-reactor system. Bioresource Technology 2014;173:124–31. https://doi.org/10.1016/j.biortech.2014.09.097.
[15] Heracleous E, Pachatouridou E, Hernández-Giménez AM, Hernando H, Fakin T, Paioni AL, et al. Characterization of deactivated and regenerated zeolite ZSM-5-based catalyst extrudates used in catalytic pyrolysis of biomass. Journal of Catalysis 2019;380:108–22. https://doi.org/10.1016/j.jcat.2019.10.019.
[16] Ruddy DA, Schaidle JA, Ferrell III JR, Wang J, Moens L, Hensley JE. Recent advances in heterogeneous catalysts for bio-oil upgrading via “ex situ catalytic fast pyrolysis”: catalyst development through the study of model compounds. Green Chem 2014;16:454–90. https://doi.org/10.1039/C3GC41354C.
[17] Chen H, Shi X, Zhou F, Ma H, Qiao K, Lu X, et al. Catalytic fast pyrolysis of cellulose to aromatics over hierarchical nanocrystalline ZSM-5 zeolites prepared using sucrose as a template. Catalysis Communications 2018;110:102–5. https://doi.org/10.1016/j.catcom.2018.03.016.
[18] Chaihad N, Karnjanakom S, Kurnia I, Yoshida A, Abudula A, Reubroycharoen P, et al. Catalytic upgrading of bio-oils over high alumina zeolites. Renewable Energy 2019;136:1304–10. https://doi.org/10.1016/j.renene.2018.09.102.
[19] Lin X, Zhang Z, Zhang Z, Sun J, Wang Q, Pittman CU. Catalytic fast pyrolysis of a wood-plastic composite with metal oxides as catalysts. Waste Management 2018;79:38–47. https://doi.org/10.1016/j.wasman.2018.07.021.
[20] Eschenbacher A, Saraeian A, Jensen PA, Shanks BH, Li C, Duus JØ, et al. Deoxygenation of wheat straw fast pyrolysis vapors over Na-Al2O3 catalyst for production of bio-oil with low acidity. Chemical Engineering Journal 2020;394:124878. https://doi.org/10.1016/j.cej.2020.124878.
[21] Araújo A, Queiroz G, Maia D, Gondim A, Souza L, Fernandes V, et al. Fast Pyrolysis of Sunflower Oil in the Presence of Microporous and Mesoporous Materials for Production of Bio-Oil. Catalysts 2018;8:261. https://doi.org/10.3390/catal8070261.
[22] Feliczak-Guzik A. Hierarchical zeolites: Synthesis and catalytic properties. Microporous and Mesoporous Materials 2018;259:33–45. https://doi.org/10.1016/j.micromeso.2017.09.030.
[23] Ennaert T, Schutyser W, Dijkmans J, Dusselier M, Sels BF. Conversion of Biomass to Chemicals. Zeolites and Zeolite-Like Materials, Elsevier; 2016, p. 371–431. https://doi.org/10.1016/B978-0-444-63506-8.00010-0.

[24] Hoff TC, Gardner DW, Thilakaratne R, Wang K, Hansen TW, Brown RC, et al. Tailoring ZSM-5 Zeolites for the Fast Pyrolysis of Biomass to Aromatic Hydrocarbons. ChemSusChem 2016;9:1473–82. https://doi.org/10.1002/cssc.201600186.
[25] Balasundram V, Ibrahim N, Kasmani RMd, Isha R, Hamid MohdKAbd, Hasbullah H. Catalytic upgrading of biomass-derived pyrolysis vapour over metal-modified HZSM-5 into BTX: a comprehensive review. Biomass Conv Bioref 2020. https://doi.org/10.1007/s13399-020-00909-5.
[26] Cai Q, Yu T, Meng X, Zhang S. Selective generation of aromatic hydrocarbons from hydrotreating-cracking of bio-oil light fraction with MOx modified HZSM-5 (M = Ga, Mo and Zn). Fuel Processing Technology 2020;204:106424. https://doi.org/10.1016/j.fuproc.2020.106424.
[27] Alonso DM, Wettstein SG, Dumesic JA. Bimetallic catalysts for upgrading of biomass to fuels and chemicals. Chemical Society Reviews 2012;41:8075. https://doi.org/10.1039/c2cs35188a.
[28] Wu J, Gao G, Sun P, Long X, Li F. Synergetic Catalysis of Bimetallic CuCo Nanocomposites for Selective Hydrogenation of Bioderived Esters. ACS Catal 2017;7:7890–901. https://doi.org/10.1021/acscatal.7b02837.
[29] Zhang J, Fidalgo B, Wagland S, Shen D, Zhang X, Gu S. Deoxygenation in anisole decomposition over bimetallic catalysts supported on HZSM-5. Fuel 2019;238:257–66. https://doi.org/10.1016/j.fuel.2018.10.129.
[30] Han Q, Rehman MU, Wang J, Rykov A, Gutiérrez OY, Zhao Y, et al. The synergistic effect between Ni sites and Ni-Fe alloy sites on hydrodeoxygenation of lignin-derived phenols. Applied Catalysis B: Environmental 2019;253:348–58. https://doi.org/10.1016/j.apcatb.2019.04.065.
[31] Huang Y, Wei L, Crandall Z, Julson J, Gu Z. Combining Mo–Cu/HZSM-5 with a two-stage catalytic pyrolysis system for pine sawdust thermal conversion. Fuel 2015;150:656–63. https://doi.org/10.1016/j.fuel.2015.02.071.
[32] Phan TN, Ko CH. Synergistic effects of Ru and Fe on titania-supported catalyst for enhanced anisole hydrodeoxygenation selectivity. Catalysis Today 2018;303:219–26. https://doi.org/10.1016/j.cattod.2017.08.025.
[33] Zhou J, An W, Wang Z, Jia X. Hydrodeoxygenation of phenol over Ni-based bimetallic single-atom surface alloys: mechanism, kinetics and descriptor. Catal Sci Technol 2019;9:4314–26. https://doi.org/10.1039/C9CY01082C.
[34] Kumar R, Strezov V, Lovell E, Kan T, Weldekidan H, He J, et al. Enhanced bio-oil deoxygenation activity by Cu/zeolite and Ni/zeolite catalysts in combined in-situ and ex-situ biomass pyrolysis. Journal of Analytical and Applied Pyrolysis 2019. https://doi.org/10.1016/j.jaap.2019.03.008.
[35] Weldekidan H, Strezov V, He J, Kumar R, Sarkodie SA, Doyi I, et al. Energy conversion efficiency of pyrolysis of chicken litter and rice husk biomass. Energy & Fuels 2019:acs.energyfuels.9b01264. https://doi.org/10.1021/acs.energyfuels.9b01264.
[36] Hernando H, Jiménez-Sánchez S, Fermoso J, Pizarro P, Coronado JM, Serrano DP. Assessing biomass catalytic pyrolysis in terms of deoxygenation pathways and energy yields for the efficient production of advanced biofuels. Catal Sci Technol 2016;6:2829–43. https://doi.org/10.1039/C6CY00522E.
[37] Aysu T. Catalytic pyrolysis of Eremurus spectabilis for bio-oil production in a fixed-bed reactor: Effects of pyrolysis parameters on product yields and character. Fuel Processing Technology 2015;129:24–38. https://doi.org/10.1016/j.fuproc.2014.08.014.
[38] Hernando H, Hernández-Giménez AM, Ochoa-Hernández C, Bruijnincx PCA, Houben K, Baldus M, et al. Engineering the acidity and accessibility of the zeolite ZSM-5 for efficient bio-oil upgrading in catalytic pyrolysis of lignocellulose. Green Chemistry 2018. https://doi.org/10.1039/C8GC01722K.
[39] Aysu T, Küçük MM. Biomass pyrolysis in a fixed-bed reactor: Effects of pyrolysis parameters on product yields and characterization of products. Energy 2014;64:1002–25. https://doi.org/10.1016/j.energy.2013.11.053.

[40] Kan T, Strezov V, Evans TJ. Lignocellulosic biomass pyrolysis: A review of product properties and effects of pyrolysis parameters. Renewable and Sustainable Energy Reviews 2016;57:1126–40. https://doi.org/10.1016/j.rser.2015.12.185.
[41] Mohan D, Pittman, CU, Steele PH. Pyrolysis of Wood/Biomass for Bio-oil: A Critical Review. Energy & Fuels 2006;20:848–89. https://doi.org/10.1021/ef0502397.
[42] Kumar R, Strezov V, Weldekidan H, He J, Singh S, Kan T, et al. Lignocellulose biomass pyrolysis for bio-oil production: A review of biomass pre-treatment methods for production of drop-in fuels. Renewable and Sustainable Energy Reviews 2020;123:109763. https://doi.org/10.1016/j.rser.2020.109763.
[43] Ansari KB, Arora JS, Chew JW, Dauenhauer PJ, Mushrif SH. Fast Pyrolysis of Cellulose, Hemicellulose, and Lignin: Effect of Operating Temperature on Bio-oil Yield and Composition and Insights into the Intrinsic Pyrolysis Chemistry. Ind Eng Chem Res 2019:acs.iecr.9b00920. https://doi.org/10.1021/acs.iecr.9b00920.
[44] Zhao C, Jiang E, Chen A. Volatile production from pyrolysis of cellulose, hemicellulose and lignin. Journal of the Energy Institute 2017;90:902–13. https://doi.org/10.1016/j.joei.2016.08.004.
[45] Kurnia I, Karnjanakom S, Bayu A, Yoshida A, Rizkiana J, Prakoso T, et al. In-situ catalytic upgrading of bio-oil derived from fast pyrolysis of lignin over high aluminum zeolites. Fuel Processing Technology 2017;167:730–7. https://doi.org/10.1016/j.fuproc.2017.08.026.
[46] Patwardhan PR, Brown RC, Shanks BH. Understanding the Fast Pyrolysis of Lignin. ChemSusChem 2011;4:1629–36. https://doi.org/10.1002/cssc.201100133.
[47] Gou J, Wang Z, Li C, Qi X, Vattipalli V, Cheng Y-T, et al. The effects of ZSM-5 mesoporosity and morphology on the catalytic fast pyrolysis of furan. Green Chem 2017;19:3549–57. https://doi.org/10.1039/C7GC01395G.
[48] Zheng Y, Chen D, Zhu X. Aromatic hydrocarbon production by the online catalytic cracking of lignin fast pyrolysis vapors using Mo2N/γ-Al2O3. Journal of Analytical and Applied Pyrolysis 2013;104:514–20. https://doi.org/10.1016/j.jaap.2013.05.018.
[49] Jiang X, Zhou J, Zhao J, Shen D. Catalytic conversion of guaiacol as a model compound for aromatic hydrocarbon production. Biomass and Bioenergy 2018;111:343–51. https://doi.org/10.1016/j.biombioe.2017.06.026.
[50] Li B, Lv W, Zhang Q, Wang T, Ma L. Pyrolysis and catalytic pyrolysis of industrial lignins by TG-FTIR: Kinetics and products. Journal of Analytical and Applied Pyrolysis 2014;108:295–300. https://doi.org/10.1016/j.jaap.2014.04.002.
[51] Wang D, Xiao R, Zhang H, He G. Comparison of catalytic pyrolysis of biomass with MCM-41 and CaO catalysts by using TGA–FTIR analysis. Journal of Analytical and Applied Pyrolysis 2010;89:171–7. https://doi.org/10.1016/j.jaap.2010.07.008.
[52] He J, Strezov V, Kumar R, Weldekidan H, Jahan S, Dastjerdi BH, et al. Pyrolysis of heavy metal contaminated Avicennia marina biomass from phytoremediation: Characterisation of biomass and pyrolysis products. Journal of Cleaner Production 2019;234:1235–45. https://doi.org/10.1016/j.jclepro.2019.06.285.
[53] Busca G. Acidity and basicity of zeolites: A fundamental approach. Microporous and Mesoporous Materials 2017;254:3–16. https://doi.org/10.1016/j.micromeso.2017.04.007.
[54] Puértolas B, Veses A, Callén MS, Mitchell S, García T, Pérez-Ramírez J. Porosity-Acidity Interplay in Hierarchical ZSM-5 Zeolites for Pyrolysis Oil Valorization to Aromatics. ChemSusChem 2015;8:3283–93. https://doi.org/10.1002/cssc.201500685.
[55] Dai G, Wang S, Zou Q, Huang S. Improvement of aromatics production from catalytic pyrolysis of cellulose over metal-modified hierarchical HZSM-5. Fuel Processing Technology 2018;179:319–23. https://doi.org/10.1016/j.fuproc.2018.07.023.
[56] Surface Oxidation and Reduction of CuO and Cu2O Studied Using XPS and XAES n.d.:10.
[57] Liu D, Li D, Yang D. Size-dependent magnetic properties of branchlike nickel oxide nanocrystals. AIP Advances 2017;7:015028. https://doi.org/10.1063/1.4974307.
[58] Grosvenor AP, Biesinger MC, Smart RStC, McIntyre NS. New interpretations of XPS spectra of nickel metal and oxides. Surface Science 2006;600:1771–9. https://doi.org/10.1016/j.susc.2006.01.041.

[59] Baltrusaitis J, Mendoza-Sanchez B, Fernandez V, Veenstra R, Dukstiene N, Roberts A, et al. Generalized molybdenum oxide surface chemical state XPS determination via informed amorphous sample model. Applied Surface Science 2015;326:151–61. https://doi.org/10.1016/j.apsusc.2014.11.077.
[60] Wolf MM, Zhu H, Green WH, Jackson GS. Kinetic model for polycrystalline Pd/PdOx in oxidation/reduction cycles. Applied Catalysis A: General 2003;244:323–40. https://doi.org/10.1016/S0926-860X(02)00604-X.

Supporting Information

Synergistic effect of transition metals on ZSM-5-supported catalysts for *ex-situ* bio-oil upgrading

Ravinder Kumar[a*], Vladimir Strezov[a], Jing He[a], Yutong Zhao[b], Haimei Xu[b], Tao Kan[a], Behnam Dastjerdi[a], Yijiao Jiang[b]

[a]Department of Earth and Environmental Sciences, Faculty of Science & Engineering, Macquarie University, Sydney, NSW 2109, Australia
[b]School of Engineering, Macquarie University, North Ryde, NSW 2109, Australia

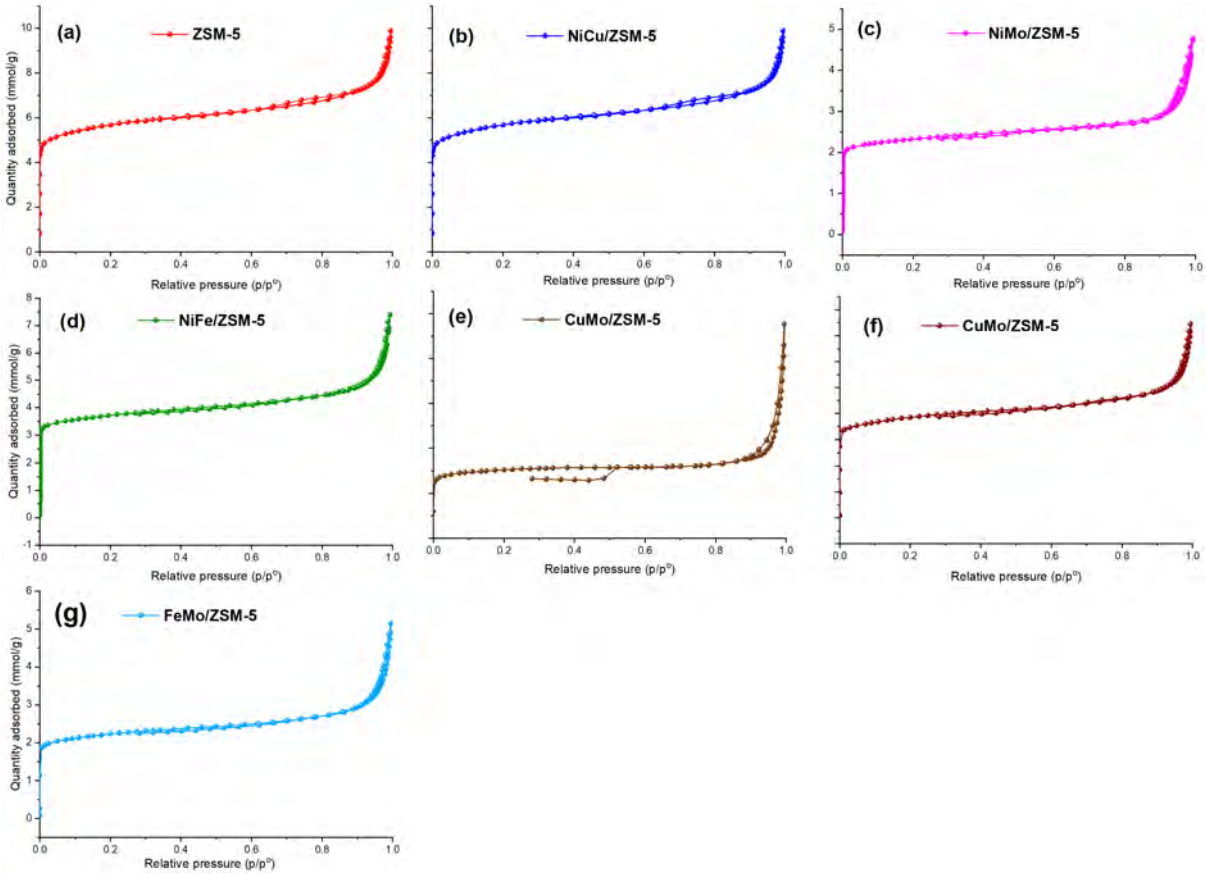

Figure S1. Nitrogen adsorption-desorption isotherm curves of fresh ZSM-5 and bimetallic catalysts.

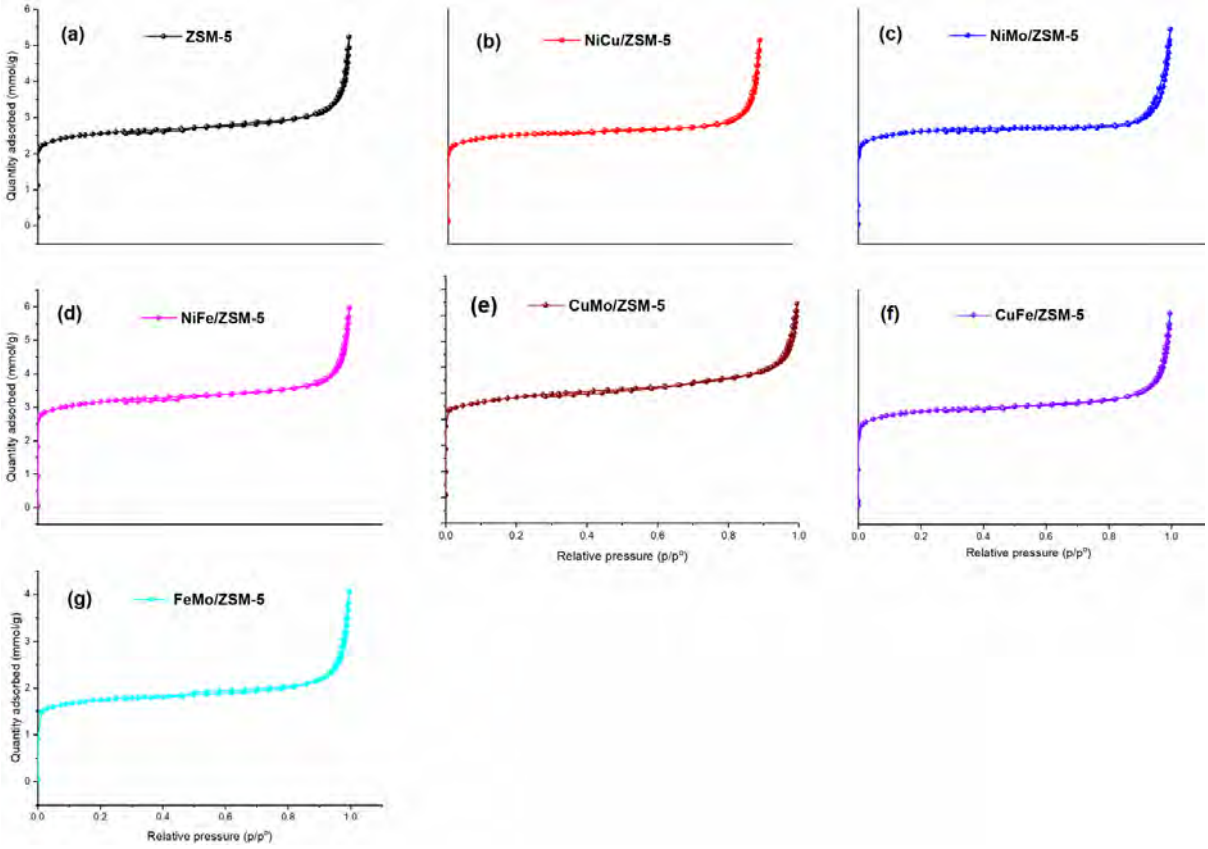

Figure S2. Nitrogen adsorption-desorption isotherm curves of spent ZSM-5 and bimetallic catalysts.

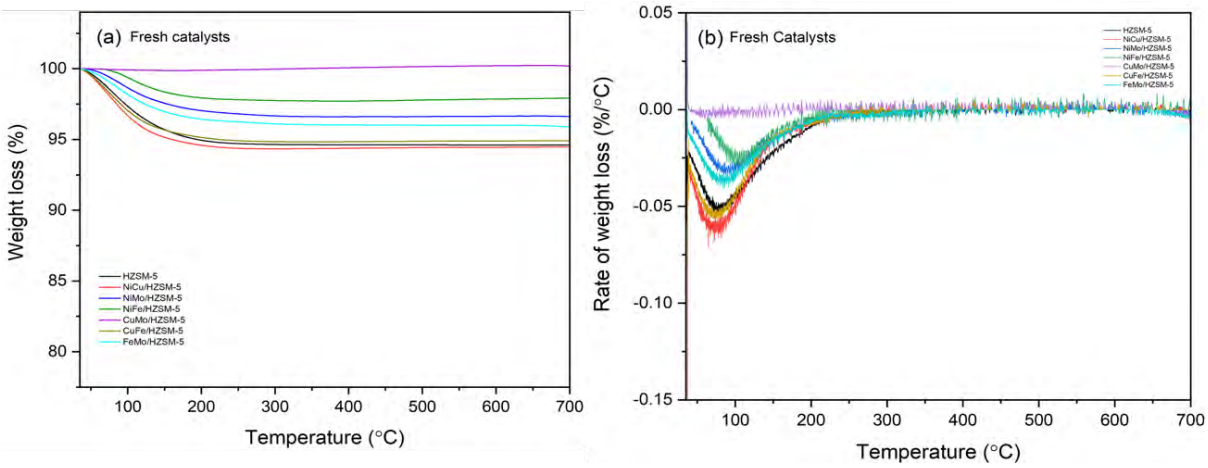

Figure S3. TPO analysis of fresh ZSM-5 and bimetallic catalysts.

MACQUARIE University

MACQUARIE UNIVERSITY
AUTHORSHIP CONTRIBUTION STATEMENT

In accordance with the *Macquarie University Code for the Responsible Conduct of Research* and the *Authorship Standard*, researchers have a responsibility to their colleagues and the wider community to treat others fairly and with respect, to give credit where appropriate to those who have contributed to research.

Note for HDR students: *Where research papers are being included in a thesis, this template must be used to document the contribution of authors to each of the proposed or published research papers. The contribution of the candidate must be sufficient to justify inclusion of the paper in the thesis.*

1. DETAILS OF PUBLICATION & CORRESPONDING AUTHOR

Title of Publication (can be a holding title)		**Publication Status** Choose an item.
Effect of catalyst supports with and without Nickel on bio-oil upgrading and energy distribution in pyrolytic products during one and two-stage ex-situ biomass pyrolysis		■ In Progress or Unpublished work for thesis submission ☐ Submitted for Publication ☐ Accepted for Publication ☐ Published
Name of **corresponding author**	Department/Faculty	**Publication details:** indicate the name of the journal/ conference/ publisher/other outlet
	Earth and Environmental Sciences /Science & Engineering	

2. STUDENTS DECLARATION (if applicable)

Name of HDR thesis author (If the same as corresponding author - write "as above")	Department/Faculty	Thesis title
Ravinder Kumar	Earth and Environmental Sciences /Science & Engineering	Catalytic Upgrading of Bio-oil Produced from Fast Pyrolysis of Pinewood Sawdust

Description of HDR thesis author's contribution to planning, execution, and preparation of the work if there are multiple authors

(for example, how much as a percent did you contribute to the conception of the project, the design of methodology or experimental protocol, data collection, analysis, drafting the manuscript, revising it critically for important intellectual content, etc.)

In this article, I contributed in designing the project, carried out 90% of the experimnetal work, analyzed the data and wrote 80% of the manuscript.

I declare that the above is an accurate description of my contribution to this publication, and the contributions of other authors are as described below.	**Student signature** **Date**	02/22/2021

MACQUARIE University

3. Description of all other author contributions

Use an Asterisk * to denote if the author is also a current student or HDR candidate.

The HDR candidate or corresponding author must, for each paper, list all authors and provide details of their role in the publication. Where possible, also provide a percentage estimate of the contribution made by each author.

Name and affiliation of author	Intellectual contribution(s) (for example to the: conception of the project, design of methodology/experimental protocol, data collection, analysis, drafting the manuscript, revising it critically for important intellectual content etc.)
Vladimir Strezov Macquarie University	conception, supervision, critical revision
Jing He Macquarie University	experimental, data analysis, critical revision
Yutong Zhao Macquarie University	experimental, critical revision
Behnam Dastjerdi Macquarie University	data analysis, critical revision
Tao Kan Macquarie University	experimental, supervision, critical revision
Haimei Xu Macquarie University	experimental, critical revision
Yijiao Jiang Macquarie University	experimental, critical revision
	Provide summary for any additional Authors in this cell.

4. Author Declarations

I agree to be named as one of the authors of this work, and confirm:

i. *that I have met the authorship criteria set out in the* Authorship Standard, *accompanying the* Macquarie University Research Code,

ii. *that there are no other authors according to these criteria,*

iii. *that the description in Section 3 or 4 of my contribution(s) to this publication is accurate*

iv. *that I have agreed to the planned authorship order following the* Authorship Standard

Name of author	Authorised * By Signature or refer to other written record of approval (eg. pdf of a signed agreement or an email record)	Date
Vladimir Strezov		24/02/2021
Jing He		22/02/2021
Yutong Zhao		22/02/2021
Haimei Xu		24/02/2021
Tao Kan		22/02/2021
Behnam Dastjerdi		02/22/2021
Yijiao Jiang		24/02/2021
	Provide other written record of approval for additional authors (eg. pdf of a signed agreement or an email record)	

5. Data storage

The original data for this project are stored in the following location, in accordance with the *Research Data Management Standard* accompanying the *Macquarie University Research Code*.

If the data have been or will be deposited in an online repository, provide the details here with any corresponding DOI.

Data description/format	Storage Location or DOI	Name of custodian if other than the corresponding author

A copy of this form must be retained by the corresponding author and must accompany the thesis submitted for examination.

Chapter 9

Effect of catalyst supports with and without nickel on bio-oil upgrading and energy distribution in pyrolytic products during one and two-stage *ex-situ* biomass pyrolysis

Ravinder Kumar[a*], Vladimir Strezov[a], Jing He[a], Yutong Zhao[b], Behnam Dastjerdi[a], Tao Kan[a] Haimei Xu[b], Yijiao Jiang[b]

[a]Department of Earth and Environmental Sciences, Faculty of Science & Engineering, Macquarie University, Sydney, NSW 2109, Australia
[b]School of Engineering, Macquarie University, North Ryde, NSW 2109, Australia

Abstract

The present study examines the effect of different catalytic supports (ZSM-5, Al_2O_3, Al_2O_3/CaO/MgO, and CaO) with and without nickel impregnation for bio-oil deoxygenation in one-stage *ex-situ* pyrolysis, and compares the results for bio-oil deoxygenation in a two-stage mode using various combinations of the catalysts. The stability of Ni-modified catalysts was tested for bio-oil deoxygenation. All pyrolysis experiments were carried out at 500 ºC. In one-stage *ex-situ* pyrolysis, three catalyst to biomass (C/B) ratios (1, 2 and 3) were applied, while two-stage pyrolysis was demonstrated with C/B of 2. The results revealed that microporous and mesoporous acidic catalysts in one-stage pyrolysis achieved substantial bio-oil deoxygenation. For example, Ni/ZSM-5 produced bio-oil with 29.54 wt% oxygen content and 60.21 wt% carbon content, with a higher heating value (HHV) of 23.6 MJ/kg. Ni/Al_2O_3 obtained bio-oil with an HHV of 20.6 MJ/kg. In contrast, basic catalysts were inefficient to produce desired concentrations of hydrocarbons in one-stage pyrolysis. For instance, Ni/CaO could produce bio-oil with HHV of 16.41 MJ/kg. However, the combination of basic catalysts with either micro or mesoporous acidic catalysts was useful for significant bio-oil upgrading in two-stage pyrolysis. Noticeably, Ni/CaO and ZSM-5 produced a superior quality bio-oil, with HHV of 24.40 MJ/kg. Two-stage pyrolysis produced a variety of hydrocarbons, attributing to the diverse physicochemical properties and active sites of the two catalysts, which favoured additional deoxygenation reactions, resulting in enhanced bio-oil deoxygenation. The stability tests of Ni-modified catalysts revealed that Ni/ZSM-5 was least affected by coke deposition, while Ni/CaO achieved the highest coke deposition. Consequently, Ni/ZSM-5 produced better quality of bio-oil even after four successive pyrolysis experiments.

1. Introduction

Pyrolytic oil or bio-oil is considered a biofuel, an intermediate bioenergy carrier that can be upgraded to sustainable chemicals and high value-added products [1,2]. The large-scale production of bio-oil may contribute to renewable energy generation, reduce our dependence on fossil fuels, and substantially decrease carbon dioxide emissions. In addition, bio-oil production can also help create employment in the areas of feedstock harvesting, transportation and facility management [3]. Therefore, considering the ecological and economic significance of bio-oil, it is essential to produce high-quality bio-oil with improved physicochemical properties for its direct applications. Catalytic biomass pyrolysis (CBP) is a well-known and promising technique for bio-oil upgrading, generating renewable hydrocarbons and high value-added products [4–6]. CBP can be successfully applied to enhance bio-oil carbon content, which increases the calorific value of the bio-oil and improves other physicochemical properties.

Different modes of CBP have been employed for bio-oil upgrading. *Ex-situ* CBP has been widely accepted for enhanced bio-oil upgrading and operational advantages, such as low coke deposition, low catalyst requirement and easier recovery of the catalyst [7,8]. *Ex-situ* CBP could be either one-stage or two-stage based on the number of catalytic beds used in the process [9,10]. In one-stage mode, an individual catalyst bed is employed. In contrast, in the two-stage, a cascade system involving two catalytic beds of similar or varying physicochemical and catalytic properties is utilized where the pyrolytic vapours are passed through the first catalyst bed. The reacted vapours are then passed through the second catalyst bed. Several catalysts have been used for bio-oil upgrading in both modes of *ex-situ* CBP. A large number of studies indicate that zeolites, chiefly ZSM-5-based catalysts, are most efficient in converting the oxygenated compounds into aromatics [1,8,11]. The excellent deoxygenation activity of ZSM-5 is mainly attributed to its high Brønsted acid sites, uniform pore diameters (5.2-5.9 Å), shape selectivity, and high thermal stability [12]. Although the Brønsted acid sites are present on external surfaces as well as internal pores of zeolites, the majority of chemical reactions are believed to carry out by the acid sites present inside the pores [13,14]. Therefore, pore sizes play a pivotal role in the diffusion and mass transfer of molecules and thus in the conversion of oxygenated compounds into aromatics [15]. The major catalytic reactions carried out by zeolites in CBP are reported to be cracking, dehydration, decarboxylation, decarbonylation, aromatization and oligomerization reactions [16,17]. The higher acidity of zeolites promotes cracking and aromatization reactions, which results in enhanced formation of polycyclic aromatics and, ultimately, leading to rapid catalyst deactivation [18]. Consequently, it adversely affects the conversion of oxygenated compounds into aromatics and decreases the bio-oil yield. Therefore, catalysts with optimal acidity are preferred for efficient hydrocarbon production.

Al_2O_3-based catalysts are mesoporous and mild acidic solid catalysts with high Lewis and low Brønsted acid sites, considerable surface area (>200 m^2/g) considered suitable alternatives for zeolites for bio-oil upgrading [19,20]. These catalysts with larger pore sizes show better mass transfer kinetics and significant cracking activity, and effectively catalyse deoxygenation reactions, like dehydration, decarboxylation and decarbonylation [21]. Consequently, Al_2O_3-based catalysts have been used in *ex-situ* CBP for hydrocarbon production. For example, Che et al. [22] demonstrated the upgrading of pinewood pyrolysis vapours into aromatics using Al_2O_3 catalysts. The results reported that Lewis acid sites of Al_2O_3 promoted cleavage of $C-O$ bonds and showed significant deoxygenation activity [22]. Especially, the proportion of heavy molecular weight compounds derived from lignin pyrolysis were noticeably reduced and monocyclic aromatics like toluene were significantly increased [22]. Another study also confirmed the outstanding deoxygenation activity of Al_2O_3 catalyst, showing higher production of C_5-C_{11} hydrocarbons, like 1-heptene, 1,3,5-cycloheptatriene and 1-octene, from *ex-situ* CBP of Jatropha wastes [23].

Solid basic catalysts, such as CaO and MgO, as sole catalysts or impregnated with other catalyst supports like zeolites and Al_2O_3 have also been investigated for bio-oil upgrading in *ex-situ* CBP of biomass [24–26]. On one hand, oxides like CaO can be used to lower the strong acid sites of zeolites to obtain the overall optimal acidity of the catalyst. On the other hand, the catalytic activity of oxides can also help to improve the yield of aromatics. CaO is known to decrease the concentration of oxygenated compounds through dehydration reactions and directly fixing the active quasi-CO_2 intermediates [26,27]. For instance, Lin et al. [26] investigated the potential of CaO for bio-oil upgrading and showed that CaO catalyzed dehydration reactions of cellulose and hemicellulose. As a result, the proportions of furfuryl and furfuryl alcohol was also increased [26]. In addition, CaO at higher concentrations may promote phenol formation via demethoxylation reactions of lignin components. Similarly, MgO catalysts are reported to deoxygenate the bio-oil via decarboxylation, ketonization and aldol condensation reactions [28,29].

Although one-stage *ex-situ* pyrolysis has been extensively studied for bio-oil upgrading, two-stage *ex-situ* pyrolysis has not been explored so far. Therefore, this study aims to demonstrate the effect of different types of catalysts for bio-oil upgrading in two-stage *ex-situ* pyrolysis. To achieve this, diverse types of catalytic supports, like ZSM-5, Al_2O_3, Al_2O_3/CaO/MgO and CaO, were impregnated with nickel metal and explored their activity for bio-oil deoxygenation, hydrocarbon production and energy distribution in pyrolytic products. Nickel-modified catalysts were tested for their stability and the effect of deactivation on their physicochemical properties and, consequently, on yields of pyrolytic products and bio-oil deoxygenation were thoroughly studied.

2. Materials & methods

2.1. Biomass

Pinewood sawdust applied in previous studies [8,30] was used as feedstock in *ex-situ* pyrolysis for bio-oil production.

2.2. Pyrolysis operation

Pinewood pyrolysis with and without catalysts was carried out in an infrared gold-coated furnace containing a quartz tube horizontal fixed-bed reactor. A schematic diagram of pyrolysis set-up is shown in Figure 1. For one-stage *ex-situ* pyrolysis, approximately 100 mg of the feedstock was loaded in the quartz tube reactor and 100, 200 and 300 mg catalyst was loaded downstream of the biomass to obtain a catalyst to biomass ratio (C/B) of 1, 2 and 3, respectively. For all experiments in the two-stage *ex-situ* pyrolysis, C/B ratio of 2 was utilized using 100 mg of the catalyst each in bed 1 and 2, while using 100 mg of the feedstock. The catalysts used for bed 1 and 2 are given in Table 1. The remaining space in the quartz tube was filled with quartz wool. All the

pyrolysis experiments were performed at 500 ºC (retention time of 2 min for the final temperature) with a heating rate of 100 ºC/min and He as a carrier gas at a flow rate of 50 ml/min. Prior to each pyrolysis experiment He gas was purged in the reactor for 30 min to ensure oxygen free conditions. Pyrolysis experiments were repeated twice with each catalyst to confirm data reliability.

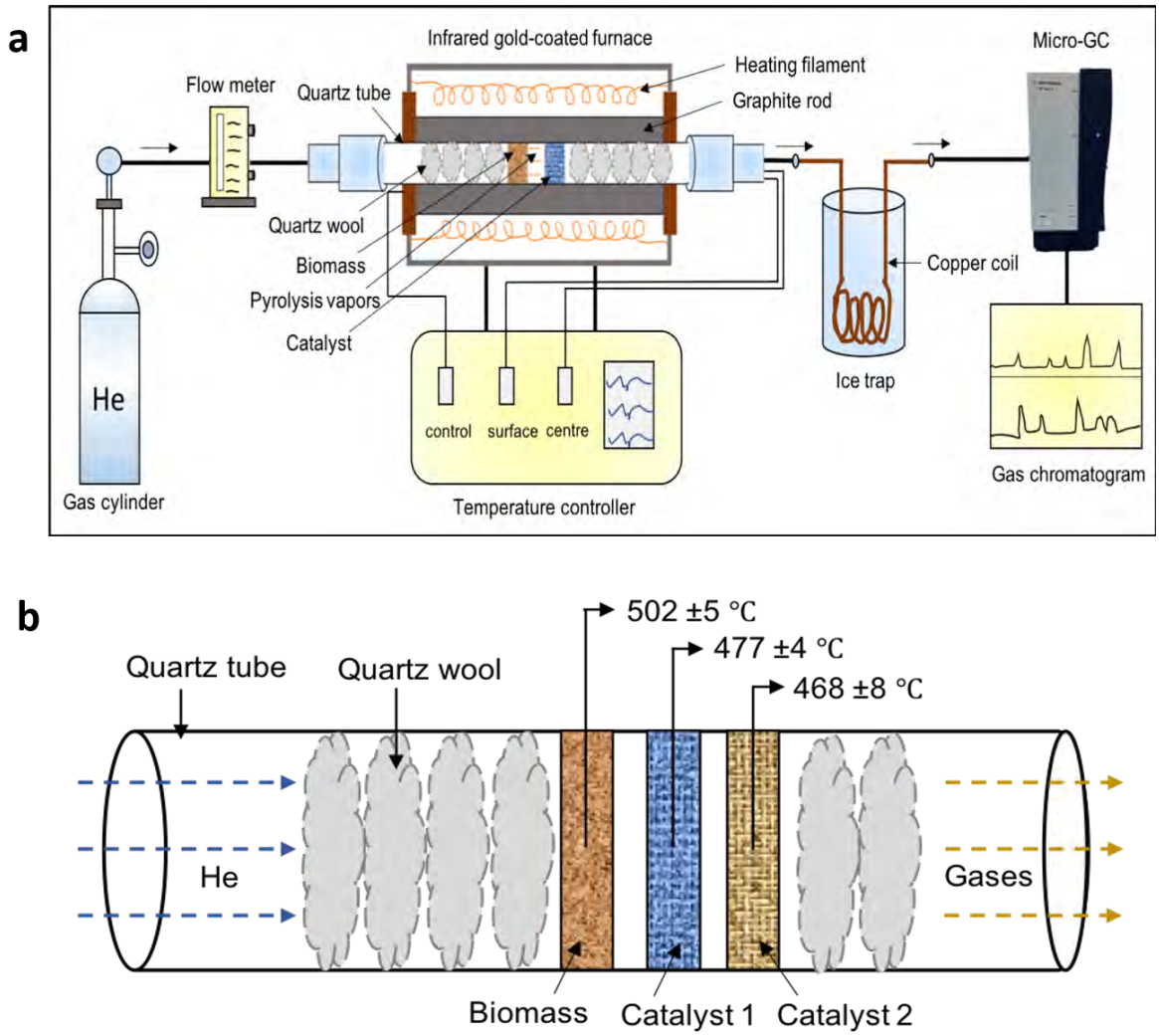

Figure 1. (a) A schematic diagram of horizontal fixed-bed pyrolysis set-up (b) quartz tube reactor showing central temperatures for biomass and catalyst beds.

The pyrolytic bio-oil and gas products were analyzed with gas chromatography-mass spectroscopy (GC-MS, Agilent) and micro-gas chromatography (micro-GC, Agilent 490), respectively. As shown in Figure 1 micro-GC was attached to the gas outlet of the quartz reactor. Gases were analyzed online during the pyrolysis. The micro-GC was calibrated with a standard gas mixture of CO (3%), CO_2 (3.05%), and H_2, (1.16%) CH_4, (1%) C_2H_4 (0.98%) and C_2H_6 (0.99%). Agilent 490 micro-GC contains two channels. Channel A (PoraPLOT U) identifies CO_2, CH_4, C_2H_4, and C_2H_6 while channel B (molecular sieve 5A) detects H_2 and CO. Channel A and channel B were maintained at 40 ºC and 60 ºC, respectively and pressure of 20 psi. Chromatograms were obtained after each 150 sec with a sampling span of 15 sec. All gases were quantified from standard gas mixture and weight of each was estimated from ideal gas equation.

Bio-oil condensed on quartz wool at the end of the quartz reactor was collected and extracted by dissolving in dichloromethane (DCM), filtered three times each through glass wool and sodium sulfate to remove all solid impurities and dehydrate the bio-oil samples. Bio-oil samples were condensed with argon gas and heated for 30 min at 60 ºC and subjected for GC-MS analysis. An Agilent 7890B GC/5977A MS system with a HP-5MS capillary column (60 m × 0.25 µm) linked to a 5977A mass spectrometry system was used to analyze the bio-oil composition. MassHunter software was used to identify the compounds, compounds with a matching score of 80 or above were selected and grouped in different families based on their main functional groups.

To examine the presence of different functional groups in the bio-oils, Fourier Transform Infrared spectroscopy (FTIR) was carried in the wavelength range of 400 and 4000 cm^{-1} using Nicolet 6700 FTIR spectrometer (Thermo Fisher Scientific, Inc.). Bio-oil samples obtained from catalytic pyrolysis (with C/B ratio of 3 for one-stage and C/B ratio of 2 for two-stage pyrolysis) were examined for FTIR analysis. An attenuated total reflectance (ATR) accessory with a diamond crystal was used with a total scan of 32 and spectral resolution of 4 cm^{-1}.

Bio-char was retrieved from the quartz reactor after pyrolysis and weighed. Product yield (wt%) of bio-char and other pyrolytic products was calculated using the following equation:

$$Product\ yield\ i\ (wt\%) = 100.[(mass\ i\ (g))/biomass(g)] \quad (1)$$

where *i* is gas, bio-char, bio-oil.

2.3. Energy yield of pyrolytic products

To calculate the energy content of pyrolytic products, one stage and two-stage *ex-situ* pyrolysis experiments were carried out at 500 ºC with a C/B ratio of 2 and heating rate of 100 ºC/min. C/B ratio of 2 was selected to obtain adequate amount of bio-oil for elemental analysis since higher C/B ratios produce lower bio-oil yield. The C, H, N and S contents of bio-oil and bio-char were quantified using Vario MICRO cube elemental analysers (Elementar Analysensysteme GmbH, Germany). The values of CHNS for bio-oil and bio-char samples were calculated from a standard sample of known composition. Further the higher heating values (HHV) of bio-oil and bio-char samples were determined using equation 2:

$$HHV\ i\ (MJ/kg) = 0.3491\mathrm{C} + 1.1783\mathrm{H} + 0.1005\mathrm{S} - 0.1034\mathrm{O} - 0.0151\mathrm{N} - 0.0211\mathrm{A} \quad (2)$$

where C, H, O, N, S and A represents carbon, hydrogen, oxygen, sulphur and ash contents of *i* wt%.

Oxygen distribution in bio-oil was determined according to equation 3:

$$O_{bio-oil}\ (wt\%) = 100 \times [(O_{bio-oil}(wt\%)/(O_{biomass}(wt\%)] \quad (3)$$

HHV of pyrolytic gases was calculated from equation 4:

$$HHV_i = [(n_i \times\ HHV_i)/Sum\ of\ gases\ (wt\%)] \quad (4)$$

where n_i is wt% of a gas and HHV_i is HHV value of gas at standard conditions [31].

The energy yield of any pyrolytic product (i) was calculated using equation 5 [32]:

$$Energy\ yield\ i\ (\%) = 100 \times [\frac{HHV_i \times mass\ yield_i}{HHV_{biomass}}] \quad (5)$$

2.4. Catalyst preparation and characterization

ZSM-5 (Si/Al=30, CBV 3024E) was obtained from Zeolyst International, USA in powder form, which was pelletized using hydraulic pressure machine. The pellets were crushed using a mortar and pestle and sieved with a 40-mesh sieve to obtain the particle size of 0.42 mm of ZSM-5. ZSM-5 was calcined at 550 °C for 2.5 hours to convert into its protonic form of HZSM-5. Al_2O_3 and Al_2O_3/CaO/MgO (4.5% CaO and 0.5% MgO) were provided by Saint-Gobain (Paris) in pellets. The pellets were crushed using mortar and pestle and sieved with a 40-mesh sieve to obtain particle size of 0.42 mm. Al_2O_3 and Al_2O_3/CaO/MgO were calcined at 550 °C for 2.5 hours to remove any type of impurities. Calcium carbonate was purchased from Sigma-Aldrich and was calcined at 750 °C for 3 h to convert into CaO [27]. Ni (10 wt%) loaded catalysts were prepared using incipient wetness impregnation method. $Ni(NO_3)_2.6H_2O$ was used as the metal precursor. To prepare 10 g of the catalyst, the required amount of $Ni(NO_3)_2.6H_2O$ was dissolved in 15 ml Milli Q water and stirred for 10 min on a magnetic stirrer, followed by slow addition of the support. To improve the dispersion of metals on zeolite, the obtained slurry was placed in ultrasonic vibrator at 40 kHz for 2 h, and after removing from ultrasonication kept it for 22 h at room temperature. The mixture was dried in a vacuum oven at 110 °C overnight. Dried samples were calcined at 550 °C for 5.5 h in air muffle furnace. Calcined samples were sieved with 40-mesh sieve to remove fine particles and obtain particle sizes of 0.42 mm. The final product was used for further characterization and pyrolysis experiments. X-ray fluorescence (XRF), Olympus Delta Pro spectrometers using Ta tube (50 kV) was used to estimate probable concentrations of Ni in catalysts. The results suggested the all catalysts contained 10.3-10.5 wt% of Ni.

X-ray diffraction (XRD) of fresh and spent catalysts was carried out using PANalytical X'Pert Pro MPD X-ray diffractometer with CuKα radiations (λ=1.54056 Å) and X-ray generator tube operating at 45 kV and 40 mA. The samples were scanned by measuring the X-ray intensity over a range of 2θ between 5 and 90 at a scanning rate of 50 sec per step, using Ni-filter, 1-16 divergent slit and 13 mm mask.

Textural properties of all catalysts were characterized by nitrogen adsorption-desorption isotherms at -196 °C on a Micromeritics TriStar II volumetric adsorption analyzer (Micromeritics Instrument Corporation, GA, USA). Before the analysis, the samples were dried and degassed at 300 °C for 12 h under vacuum. Brunauer–Emmett–Teller (BET) method was applied to determine

specific surface areas by applying the relative pressure range between 0 and 1. The total pore volume was evaluated from the amount of gas adsorbed at $P/P^o = 0.95$.

Table 1. Quantity of feedstock and catalyst used in two-stage *ex-situ* pyrolysis of pine wood at 500 °C at heating rate of 100 °C/min.

Sample	**Catalyst**		**Feedstock** (mg)
	Catalyst 1 (100 mg)	Catalyst 2 (100 mg)	
Control			100
Rxn1	Ni/ZSM-5	Al_2O_3	100
Rxn2	Ni/ZSM-5	AlCaOMgO	100
Rxn3	Ni/ZSM-5	CaO	100
Rxn4	Ni/Al_2O_3	ZSM-5	100
Rxn5	Ni/Al_2O_3	AlCaOMgO	100
Rxn6	Ni/Al_2O_3	CaO	100
Rxn7	Ni/AlCaOMgO	ZSM-5	100
Rxn8	Ni/AlCaOMgO	Al_2O_3	100
Rxn9	Ni/AlCaOMgO	CaO	100
Rxn10	Ni/CaO	ZSM-5	100
Rxn11	Ni/CaO	Al_2O_3	100
Rxn12	Ni/CaO	AlCaOMgO	100
Rxn13	Al_2O_3	Ni/ZSM-5	100
Rxn14	Al_2O_3	Ni/AlCaOMgO	100
Rxn15	Al_2O_3	Ni/CaO	100
Rxn16	ZSM-5	Ni/Al_2O_3	100
Rxn17	ZSM-5	Ni/AlCaOMgO	100
Rxn18	ZSM-5	Ni/CaO	100
Rxn19	AlCaOMgO	Ni/ZSM-5	100
Rxn20	AlCaOMgO	Ni/Al_2O_3	100
Rxn21	AlCaOMgO	Ni/CaO	100
Rxn22	CaO	Ni/ZSM	100
Rxn23	CaO	Ni/Al_2O_3	100
Rxn24	CaO	AlCaOMgO	100

Acidic properties of the catalysts were characterized using NH_3 temperature programmed desorption (NH_3-TPD) on ChemBET Pulsar (USA) with a thermal conductivity detector. Approximately 0.1 g of sample was used for the analysis. The sample was loaded into a quartz U-tube plugged with quartz wool. Firstly, the sample was dried in inert conditions heating from room temperature to 350 °C at 5 °C/min under 15 ml/min He with a 2 h hold. The system was cooled to 50 °C and then NH_3 (5% NH_3 in He) was passed over the sample at 20 ml/min for 45 min at 50 °C. Data for NH_3-desorption was recorded by removing physiosorbed NH_3 from the system by heating the sample from 50 to 650 °C at a heating rate of 5 °C/min under 15 ml/min He.

High resolution transmission electron microscopy (HRTEM) of the catalysts was conducted on Jeol Jem-2100F operated at 200 kV. X-ray photoelectron spectroscopy (XPS) of the catalysts was carried out on Thermo ESCALAB 250Xi surface analysis system.

Carbon deposition on the spent catalysts was examined using thermogravimetric analyzer (TGA/DSC 1 Stare system, Mettler Toledo, Ltd.) Approximately 25 mg of the spent catalyst in a

crucible was placed in the TGA furnace. The sample was heated from 25 to 900 °C at 10 °C/min in compressed air (100 ml/min) and nitrogen (20 ml/min).

The stability of Ni-loaded catalysts was examined in one-stage *ex-situ* pyrolysis with C/B of 3 for 4 consecutive runs without regenerating the catalysts. Pyrolytic products were examined with similar methods and the catalysts were characterized under similar conditions.

3. Results & discussion

3.1. Catalyst characterization

The prepared catalysts were examined for the presence of crystalline structures using XRD technique. The results of XRD analysis are shown in Figure 2. It can be analyzed from the figure that ZSM-5 and CaO with and without Ni showed sharp peaks at designated 2θ angles, suggesting the crystalline nature of the catalysts. For instance, high intensity diffraction peaks were observed at 2θ degree of 9.03, 9.83, 26.67, 27.65, 28.26, which can be attributed to 101, 111, 051, 313, 323 index planes of crystalline ZSM-5, respectively. The results were in line with standard data provided in JCPDS (Joint Committee on Powder Diffraction Standards) no. 891421 and suggest the material has orthorhombic crystal system and Pnma space group. For CaO-based catalysts, sharp diffraction peaks at 2θ of 33.32 and 39.76 can be ascribed to 111 and 200 index planes of crystalline CaO_4. The results resemble with standard data of CaO_4 (reference code-00-021-055). On the other hand, Al_2O_3 and Al_2O_3/CaO/MgO with and without Ni showed very low intensity broad peaks, indicating the amorphous properties of the catalysts. In addition, the results showed that Ni was in its oxide (NiO) form in all Ni-modified catalysts. Evidently, diffraction peaks at 2θ degree of 43.23, 50.54 and 74.27 were clearly found for Ni/ZSM-5 and Ni/CaO observed which can be designated to 111, 200 and 220 index planes of NiO, respectively, corresponding to cubic crystal system and space group of Fm-3m. For Ni/Al_2O_3 and Ni/Al_2O_3/CaO/MgO, low intensity broad diffraction peak at 43.23 can be clearly seen. This peak can be attributed to 111 index planes, confirming the presence of amorphous NiO in catalysts. The results match well with the standard NiO crystallographic results (reference code-01-073-1523).

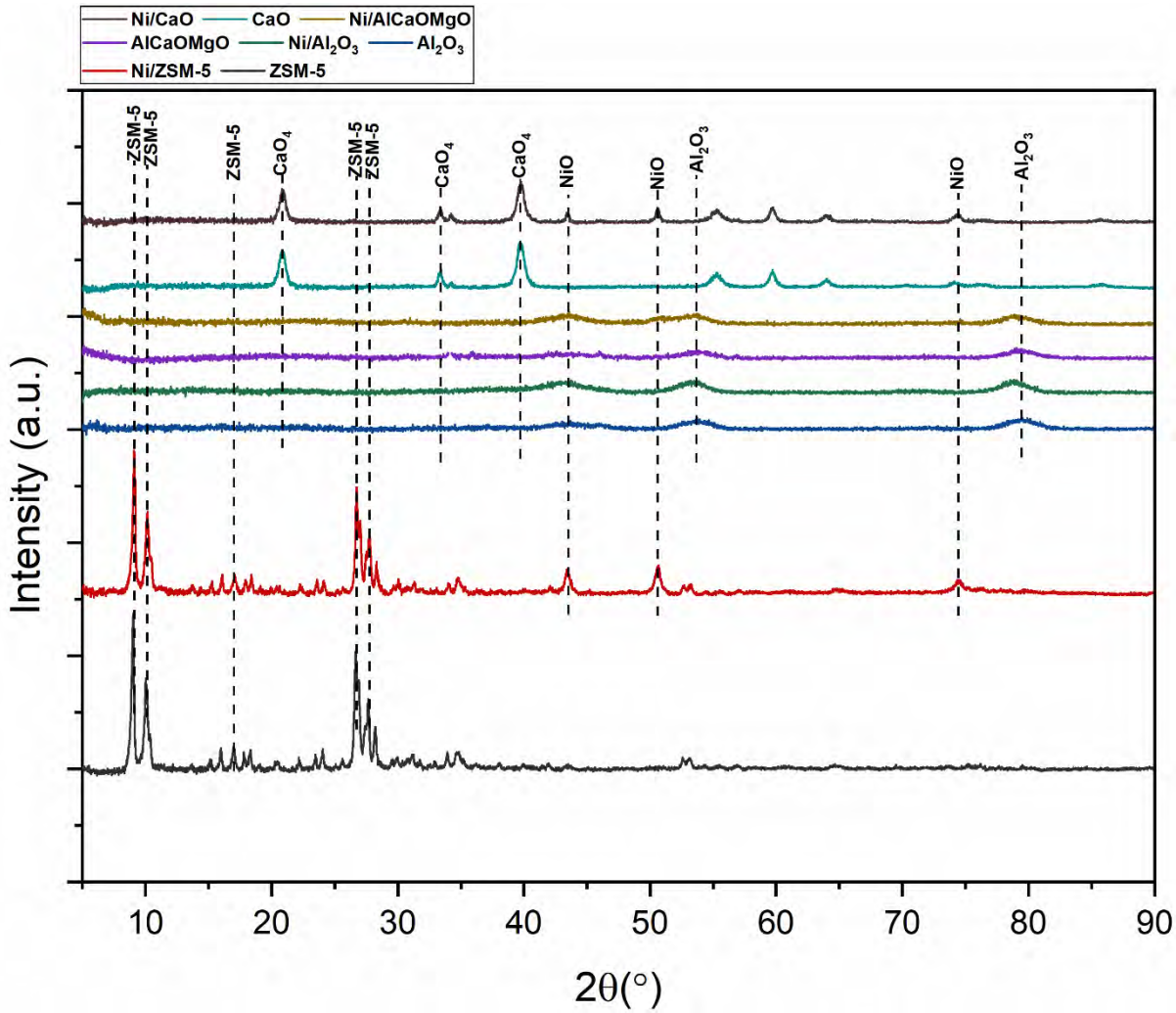

Figure 2. XRD pattern of catalysts with and without nickel.

Figure 3 shows HRTEM images of all catalysts. Ni nanoparticles can be clearly observed in the images compared to the sole supports. Thus, it can be assumed that Ni nanoparticles were successfully dispersed on the surface of the catalytic supports. For microporous supports, like ZSM-5 and CaO that exhibit very small pore size (<2 nm), Ni nanoparticles are assumed to present primarily on the surface, while for mesoporous supports with large pore diameters (>15 nm), several Ni nanoparticles are assumed to exist inside the pores.

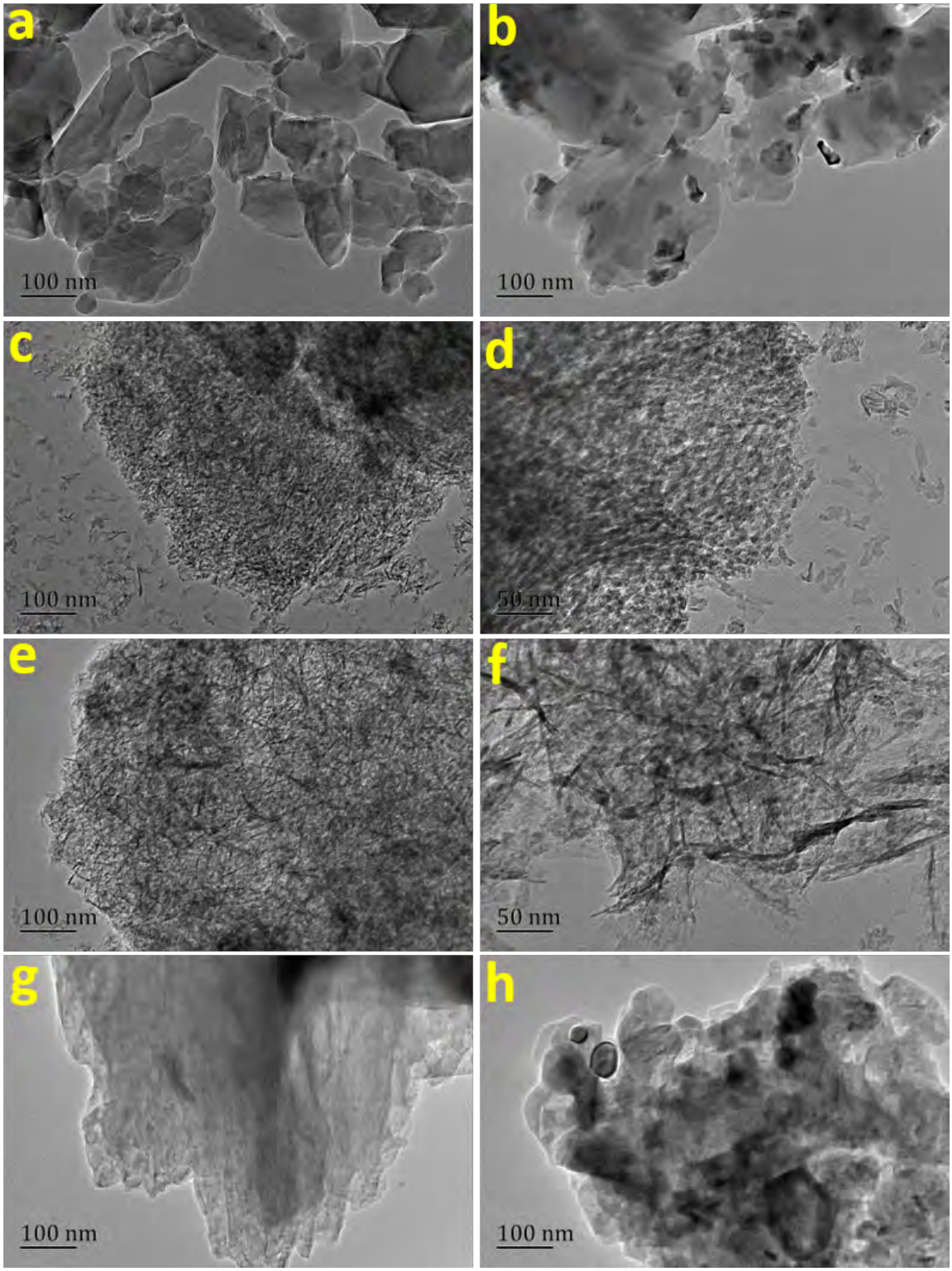

Figure 3. HRTEM images (a) ZSM-5, (b) Ni/ZSM-5, (c) Al_2O_3 (d) Ni/Al_2O_3, (e) Al_2O_3/CaO/MgO, (f) Ni/ Al_2O_3/CaO/MgO, (g) CaO, and (h) Ni/CaO.

Table 2. Textural properties of catalysts.

No.	Catalyst	BET surface area (m^2/g)	External Surface area (m^2/g)	Micropore volume (cm^3/g)	Average Pore size (nm)
1	ZSM-5	403.23	135.64	0.249	1.12
2	Al_2O_3	218.39	210.43	0.576	15.89
3	Al_2O_3/CaO/MgO	222.20	208.99	0.502	15.90
4	CaO	4.50	3.50	0.007	2.54
5	Ni/ZSM-5	280.35	93.80	0.174	1.16
6	Ni/Al_2O_3	199.39	192.80	0.476	15.89
7	Ni/Al_2O_3/CaO/MgO	208.75	200.13	0.471	15.90
8	Ni/CaO	4.59	2.53	0.007	2.35

Textural properties of the catalysts were examined using nitrogen sorption isotherm. Results are presented in supplementary Figure S1 and Table 2. It was observed from the figures that ZSM-5 and CaO with and without Ni showed type I isotherm, which suggests the microporous nature of the catalysts, while Al_2O_3 and Al_2O_3/CaO/MgO with and without Ni showed type IV isotherm, indicating the presence of mesopores in the catalysts. Evidently, the average pore size in ZSM-5 and CaO based catalysts was around 1 and 2 nm, while the average pore size in Al_2O_3 and Al_2O_3/CaO/MgO based catalysts was 15.9 nm. On the other hand, sole catalytic supports showed higher surface areas and micropore volume compared to Ni-modified catalysts. For instance, ZSM-5 showed higher surface area of 403.23 m^2/g and micropore volume of 0.24 cm^3/g, which significantly decreased to 280.35 m^2/g and 0.17 cm^3/g. This decrease in surface area and pore volume can be attributed to successful dispersion of Ni nanoparticles on the catalyst surface, and occupied majority of the pores on ZSM-5 [4]. In addition, on ZSM-5, Ni nanoparticles are assumed to disperse predominantly on its surface rather than entering the pores due the microporous nature of ZSM-5. As a result, Ni nanoparticles might block the pores and reduce the adsorption of N_2 molecules on its surface, thus decreasing the surface area and pore volume [33]. In contrast, a slight decrease in the surface area and micropore volume was noticed on mesoporous supports (Al_2O_3 and Al_2O_3/CaO/MgO) after addition of Ni. For example, Al_2O_3 showed the surface area of 218.39 m^2/g and micropore volume of 0.57 cm^3/g, while Ni/ Al_2O_3 achieved the surface area of 199.39 m^2/g and micropore volume of 0.47 cm^3/g. Thus, it can be assumed that majority of Ni nanoparticles (mainly smaller than the pore diameter) successfully entered the pores and merely a fraction of Ni nanoparticles (larger particle than pore diameter) were present on the surface.

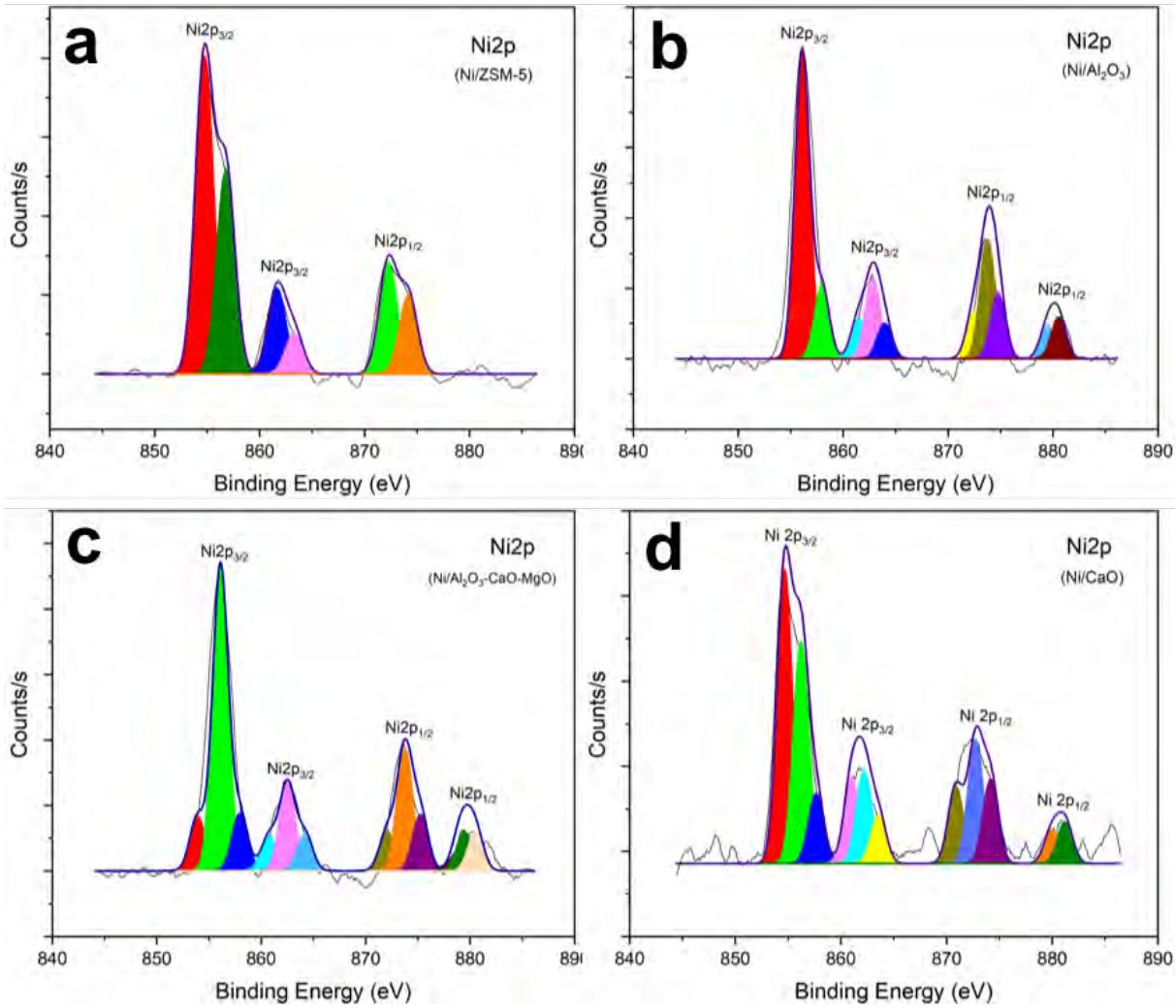

Figure 4. Photoelectron spectra of Ni2p in fresh (a) Ni/ZSM-5 (b) Ni/Al_2O_3 (c) Ni/AlCaOMgO and (d) Ni/CaO.

Figure 4 shows Ni2p spectra of fresh Ni-modified catalysts. In all catalysts, Ni2p spectra can be divided into two main peaks. One peak present around 853.9 and 856 eV, and the second main peak present around 872.3 and 873.85 eV, can be ascribed to $Ni2p_{3/2}$ and $Ni2p_{1/2}$ of NiO present in the catalysts [34]. These two main peaks are assigned to Ni^{2+} present in NiO. A slight variation in the binding energies of the main peaks in all catalysts can be attributed to varying strengths of Ni metal with catalytic supports [35].

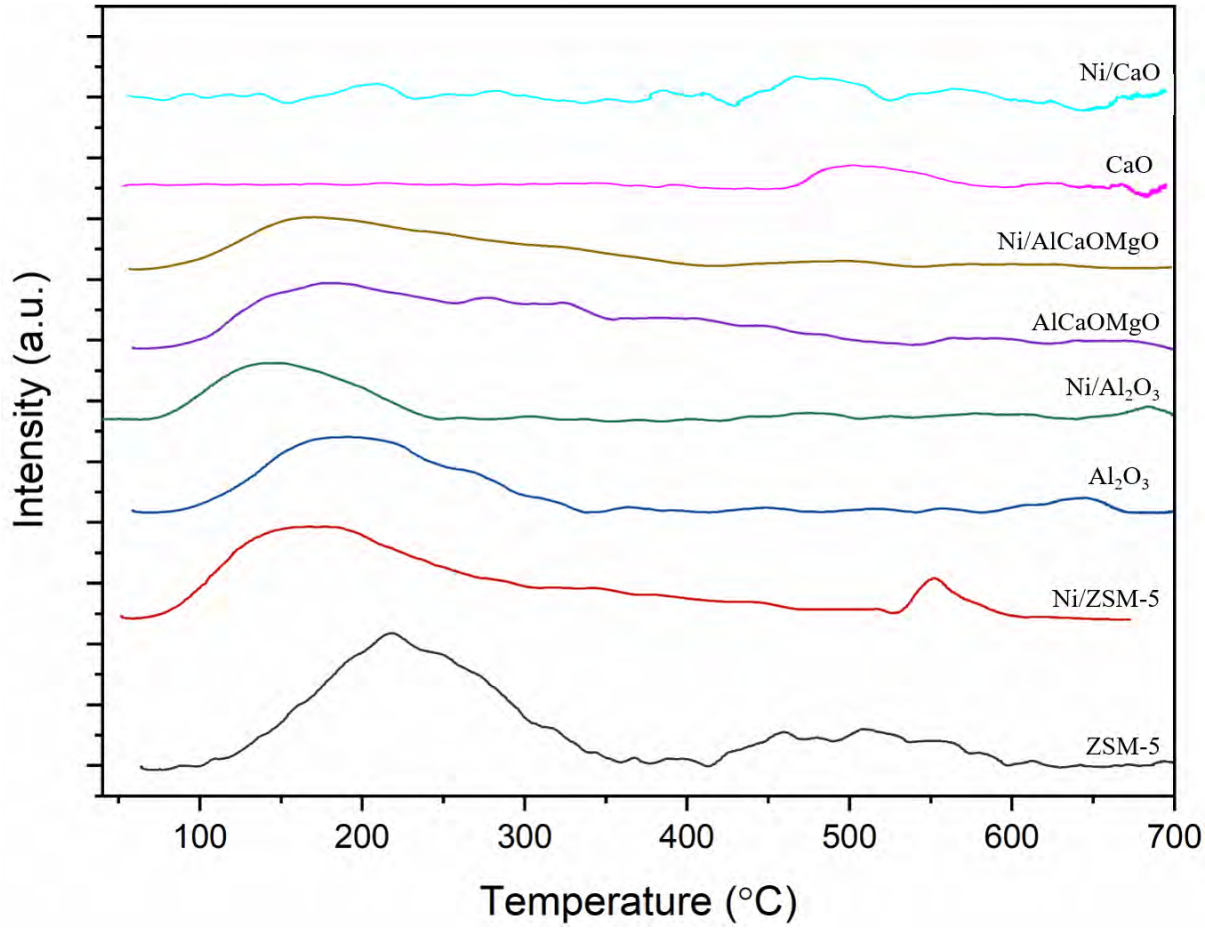

Figure 5. TPD analysis of all the catalysts.

Acidic sites associated to either Lewis or Brønsted acid sites are considered active sites to carry out the necessary deoxygenation reactions to transform oxygen rich compounds into carbon rich hydrocarbons [14,36]. The acidic sites might be present on the catalyst surface as well as inside the pores. TPD analysis was conducted to estimate the amount of acidic sites in pristine and Ni-impregnated catalysts. The results are shown in Figure 5. As expected, ZSM-5 showed the highest acidity of 103.46 µmol/g. A broad peak at 220 °C indicates the presence of weak Lewis acidic sites, while small broad peaks between 415 and 595 °C suggest the occurrence of strong Brønsted acid sites in the catalyst. The addition of Ni slightly decreased the total acidity to 97.81 µmol/g, however, a sharp peak at 552 °C confirms the availability of strong acidic sites, which would be advantageous to improve its catalytic activity. Mesoporous Al_2O_3-based catalysts also showed noticeable desorption peaks below 200 °C, indicating the presence of mainly weak Lewis acid sites. Sole Al_2O_3 and Ni/Al_2O_3 achieved the total acidity of 93.50 and 84.63 µmol/g, respectively. The decrease in acidity upon Ni impregnation can be attributed to the blockage of active sites by Ni nanoparticles, resulting in the adsorption of a smaller number of NH_3 molecules. Similarly, Ni/AlCaOMgO achieved low acidity (65.44 µmol/g) compared to sole AlCaOMgO (72.16 µmol/g). For AlCaOMgO, desorption peaks at 277 and 325 °C indicate the presence of weak to medium acidic sites in the catalyst. Kumar et al. [37] demonstrated that when an acidic support is mixed with a basic chemical, it neutralizes the strong acidity and new weak and medium

acidic sites are created due to the charge redistribution in the structure of mixed metal oxide. In contrast, CaO-based catalysts showed negligible amount of NH_3 adsorption and thus, contain insignificant acidic sites. In Ni/CaO, the addition of Ni created trivial Lewis acidic sites, indicated by the emergence of small broad peaks. Generally, the average electronegativity of the metal ions contributes to the acidity of the catalyst. Hence it could be suggested that impregnation of Ni nanoparticles improved the average electronegativity of the metal ions in Ni/CaO [37].

3.2. Product yields in one and two-stage pyrolysis

Tables 3 and 4 show the distribution of pyrolytic products obtained from one and two-stage pyrolysis with all catalysts. In one-stage pyrolysis, the results demonstrated that the primary pyrolytic product was bio-oil that accounted for approximately 50-78 wt%, while gases and bio-char were secondary and tertiary products at higher C/B of 3 and 2, respectively, and vice-versa at C/B ratio of 1. Comparatively, for acidic catalysts, the increase in C/B ratio from 1 to 3 decreased the bio-oil yield considerably and increased the gas yield. For instance, a bio-oil yield of 63.29 wt% and a gas yield of 18.43 wt% was obtained with 1 C/B of Ni/ZSM-5, while C/B of 3 decreased the bio-oil yield to 49.80 wt% and increased the gas yield to 32.55 wt%. This can be attributed to the excellent activity of the catalysts where the increased amount of the catalyst provided enhanced number of active sites that carried out the deoxygenation reactions, and finally, contributed to the increased gas yield. In contrast, the basic catalysts CaO and Ni/CaO produced much lower gas yields than the other catalysts. The substantial decrease in gas yield for CaO based catalysts can be attributed to their excellent activity to act as CO_2 sorbent and fix CO_2 containing compounds to form active quasi-CO_2 intermediate compounds during liquid-solid contact in the pyrolysis process [26]. CaO can react with evolved CO_2 to form stable $CaCO_3$ species as shown in the following equation:

$$CaO\ (s) + CO_2\ \rightarrow CaCO_3(s), \Delta\mathring{H}_{923} = -170.5\ kJ\ (exothermic)$$

Mild acidic catalysts also achieved similar trends to acidic catalysts for pyrolytic products, bio-oil as the primary product with lower C/B ratios, and gases and bio-char as secondary and tertiary products with C/B of 2 and 3.

In two-stage pyrolysis mode, bio-oil was also the dominant product in all the experiments, resulting in varying yields from the combination of different types of catalysts. Noticeably, the combination of microporous acidic and mesoporous acidic or vice versa showed comparatively lower bio-oil yield than the combination of basic catalysts with either of microporous or mesoporous acidic catalysts. This is mainly because higher acidic sites showed enhanced cracking and carried out other several catalytic reactions to upgrade the pyrolytic vapors, which consequently increased the gas yield and decreased the bio-oil yield. On the other hand, the basic catalysts could not exhibit cracking activity and the availability of lower number of active sites

could not carry out efficiently the deoxygenation reactions. In addition, the CO_2 sorbent ability of CaO decreased the gas yield during pyrolysis, resulting in the higher bio-oil yield when CaO based catalysis were used.

Table 3. Product yield in one-stage *ex-situ* pyrolysis.

Catalyst	**C/B**	**Gas (wt%)**	**Bio-char (wt%)**	**Bio-oil (wt%)**
Control		14.65	18.43	66.92
ZSM-5	1	16.49	18.69	64.82
	2	21.5	19.73	58.77
	3	25.94	20.29	53.77
Al_2O_3	1	16.61	23.02	60.37
	2	22.64	20.20	57.16
	3	27.78	21.20	51.02
AlCaOMgO	1	18.81	19.64	61.55
	2	21.62	20.93	57.45
	3	27.81	17.76	54.43
CaO	1	1.65	22.36	75.99
	2	1.82	20.37	77.81
	3	2.51	19.69	77.80
Ni/ZSM-5	1	18.43	18.28	63.29
	2	25.67	18.50	55.83
	3	32.55	17.65	49.80
Ni/Al_2O_3	1	14.85	19.94	65.21
	2	21.5	19.67	58.83
	3	26.05	16.60	57.35
Ni/AlCaOMgO	1	13.86	16.54	69.60
	2	19.26	17.80	62.94
	3	25.82	16.02	58.16
Ni/CaO	1	3.38	18.33	78.29
	2	4.56	14.51	80.93
	3	5.31	16.72	77.97

Table 4. Product yield in two-stage *ex-situ* pyrolysis.

	Catalyst		**Gas (wt%)**	**Bio-char (wt%)**	**Bio-oil (wt%)**
Sample	Catalyst 1	Catalyst 2			
Control			14.65	18.43	66.92
Rxn1	Ni/ZSM-5	Al_2O_3	25.32	14.99	59.69
Rxn2	Ni/ZSM-5	AlCaOMgO	26.82	18.02	55.16
Rxn3	Ni/ZSM-5	CaO	12.91	17.61	69.48
Rxn4	Ni/ Al_2O_3	ZSM-5	21.08	19.47	59.45
Rxn5	Ni/ Al_2O_3	AlCaOMgO	21.33	20.21	58.46
Rxn6	Ni/ Al_2O_3	CaO	7.40	20.47	72.13
Rxn7	Ni/AlCaOMgO	ZSM-5	22.45	17.65	59.90
Rxn8	Ni/AlCaOMgO	Al_2O_3	20.89	18.37	60.74
Rxn9	Ni/AlCaOMgO	CaO	15.05	19.99	64.96
Rxn10	Ni/CaO	ZSM-5	9.85	16.76	73.39
Rxn11	Ni/CaO	Al_2O_3	11.97	21.88	66.15
Rxn12	Ni/CaO	AlCaOMgO	18.74	20.68	60.58
Rxn13	Al_2O_3	Ni/ZSM-5	26.58	17.67	55.75

Rxn14	Al_2O_3	Ni/AlCaOMgO	21.25	18.72	60.03
Rxn15	Al_2O_3	Ni/CaO	8.94	16.46	74.60
Rxn16	ZSM-5	Ni/ Al_2O_3	22.23	20.31	57.46
Rxn17	ZSM-5	Ni/AlCaOMgO	27.01	17.21	55.78
Rxn18	ZSM-5	Ni/CaO	6.73	21.50	71.77
Rxn19	AlCaOMgO	Ni/ZSM-5	21.53	21.47	57.00
Rxn20	AlCaOMgO	Ni/ Al_2O_3	25.44	21.61	52.95
Rxn21	AlCaOMgO	Ni/CaO	4.31	22.54	73.15
Rxn22	CaO	Ni/ZSM	8.14	18.04	73.82
Rxn23	CaO	Ni/ Al_2O_3	5.67	20.21	74.12
Rxn24	CaO	AlCaOMgO	8.59	18.16	73.25

Table 5. Gas composition produced during one-stage *ex-situ* pyrolysis.

Catalyst	**C/B**	**CH_4 (wt%)**	**CO_2 (wt%)**	**C_2H_4 (wt%)**	**C_2H_6 (wt%)**	**H_2 (wt%)**	**CO (wt%)**	**Total**
Control		1.70	7.79	0.11	0.17	0.00	4.88	14.65
ZSM-5	1	1.92	5.62	0.65	0.68	0.05	7.57	16.49
	2	2.42	7.82	0.75	0.59	0.12	9.80	21.50
	3	2.63	11.18	0.85	0.66	0.16	10.46	25.94
Al_2O_3	1	2.06	10.22	0.32	0.42	0.05	3.54	16.61
	2	3.39	13.42	0.48	0.52	0.11	4.72	22.64
	3	3.83	16.02	0.48	0.50	0.10	6.85	27.78
AlCaOMgO	1	3.04	11.82	0.30	0.42	0.05	3.18	18.81
	2	3.26	13.11	0.28	0.40	0.09	4.48	21.62
	3	4.20	17.44	0.22	0.26	0.19	5.50	27.81
CaO	1	0.63	0.42	0.00	0.03	0.57	0.00	1.65
	2	0.78	0.07	0.00	0.12	0.75	0.10	1.82
	3	1.18	0.15	0.06	0.06	1.06	0.00	2.51
Ni/ZSM-5	1	2.25	8.54	0.44	0.37	0.17	6.66	18.43
	2	2.37	13.97	0.56	0.37	0.18	8.22	25.67
	3	2.94	18.34	0.64	0.44	0.34	9.85	32.55
Ni/Al_2O_3	1	1.84	7.68	0.23	0.35	0.09	4.66	14.85
	2	2.20	10.83	0.32	0.46	0.13	7.56	21.50
	3	2.56	13.92	0.13	0.03	0.30	9.11	26.05
Ni/AlCaOMgO	1	1.66	8.06	0.07	0.04	0.18	3.85	13.86
	2	2.57	10.00	0.37	0.32	0.32	5.68	19.26
	3	2.90	13.68	0.47	0.54	0.40	7.83	25.82
Ni/CaO	1	2.29	0.37	0.11	0.28	0.11	0.22	3.38
	2	2.84	0.34	0.24	0.64	0.14	0.36	4.56
	3	3.95	0.16	0.09	0.23	0.19	0.70	5.32

The results of gas composition obtained during one-stage and two-stage pyrolysis are given in Table 5 and Table 6, respectively. In one-stage pyrolysis, sole ZSM-5 showed almost equal proportion of CO and CO_2, which indicates that it equally favoured the decarbonylation and decarboxylation reactions. The evolution of CO and CO_2 gases can be attributed to the release of CO and CO_2 by cracking of RR'CO or RCO_2H groups. All other catalysts with or without Ni except CaO-based catalysts showed higher proportions of CO_2 compared to CO, which indicates that they promoted more the decarboxylation reactions than decarbonylation. CH_4 was also produced in all catalytic pyrolysis reactions, owing to the demethylation of methoxy groups from

the lignin structure. In CaO catalysed pyrolysis, very low or negligible amount of CO_2 was found in the gas composition. It can be ascribed to the excellent CO_2 sorbent activity of CaO to fix CO_2 containing compounds and form active quasi-CO_2 intermediate compounds during the pyrolysis process [24]. The formation of active quasi-CO_2 intermediate compounds by CaO is well known and has been reported in the previous studies [24,38].

Another interesting finding was the increased H_2 yield in CaO catalysed pyrolysis. For example, CaO with C/B of 3 generated 1 wt% H_2 where CO_2 yield was 0.15 wt% and no CO was obtained. H_2 can be produced due to cracking of deformation of $C-H$ and $C=C$ bonds of the organic compounds. H_2 can also be generated via WGSR favoured by the catalysts by reacting CO and H_2O produced during pyrolysis [16].

Similar to one-stage, the dominant gases obtained in two-stage pyrolysis were CO, CO_2, and CH_4 with fraction of other gases like H_2, C_2H_4, C_2H_6 also found in the gas composition. However, the combination of different types of catalysts showed varying proportions of gases. For example, Ni/ZSM-5 with Al_2O_3 produced higher concentration of CO (13.71 wt%) and CO_2 (10.68 wt%) but Ni/ZSM-5 with CaO produced low amounts of CO (4.16 wt%) and CO_2 (5.76 wt%), indicating the former combination favoured decarbonylation and decarboxylation reactions effectively, but, in the latter combination, CO_2 and CO produced by Ni/ZSM-5 were absorbed by CaO to form active quasi-intermediates which decreased the total gas yield. The combination of Al_2O_3 with either Ni/ZSM-5 or Ni/AlCaOMgO generated more CO_2 than CO, suggesting the preference of decarboxylation reactions over decarbonylation by the catalysts. These catalysts also produced noticeable proportion of CH_4, demonstrating their ability to remove methoxy groups from oxygenated compounds, mainly from the lignin component. The combination of the catalysts containing CaO and Ni/CaO showed good activity to absorb CO_2 and, therefore, less amount of CO_2 was obtained from the pyrolysis, while the H_2 content was comparatively higher than other pyrolysis experiments.

3.3. Bio-oil composition in one and two-stage pyrolysis

The bio-oil composition obtained from both modes of pyrolysis was examined using GC-MS. The results were presented based on the peak area% that provides a qualitative analysis and suggests the formation of hydrocarbons and other organic compounds. Hence, possible pathways and deoxygenation reactions favoured by the catalysts in one-stage and two-stage pyrolysis can be predicted. Bio-oil composition obtained during one-stage pyrolysis is given in Table 7. The results showed that catalysts with increasing C/B ratio showed higher proportions of hydrocarbons. ZSM-5 and Al_2O_3 catalysts with and without Ni favoured the formation of aromatic hydrocarbons, while Ni/AlCaOMgO also showed significant generation of aliphatic hydrocarbons. The primary aromatics produced by ZSM-5 based catalysts were naphthalenes, fluorenes, phenanthrene,

biphenyl and benzene derived aromatics. Al_2O_3-based catalysts also promoted the formation of naphthalenes and benzene aromatics but additional aromatics like anthracene, retene and pyrene were also found in the bio-oils. Brønsted acid sites and Lewis acid sites in ZSM-5 and Al_2O_3 are well known to convert phenolic compounds directly into aromatics via deoxygenation and dehydration reactions, and also carry out the demethoxylation, dehydroxylation and methyl substitution reactions to produce monocyclic aromatics, like benzene and toluene [39]. Monocyclic aromatics further undergo secondary polymerization reactions to form polycyclic aromatics, like naphthalene and phenanthrene [20,33].

Table 6. Gas composition obtained during two-stage *ex-situ* pyrolysis at 500 ºC with C/B of 2.

	Catalyst		CH_4	CO_2	C_2H_4	C_2H_6	H_2	CO	Total
Sample	**Catalyst 1**	**Catalyst 2**	**(wt%)**	**(wt%)**	**(wt%)**	**(wt%)**	**(wt%)**	**(wt%)**	
Control			1.70	7.79	0.11	0.17	0.00	4.88	14.65
Rxn1	Ni/ZSM-5	Al_2O_3	0.37	10.68	0.39	0.01	0.16	13.71	25.32
Rxn2	Ni/ZSM-5	AlCaOMgO	2.55	12.07	0.08	0.04	0.27	11.81	26.82
Rxn3	Ni/ZSM-5	CaO	2.36	4.16	0.00	0.015	0.62	5.76	12.92
Rxn4	Ni/Al_2O_3	ZSM-5	2.66	10.85	0.39	0.51	0.09	6.58	21.08
Rxn5	Ni/Al_2O_3	AlCaOMgO	2.33	12.30	0.39	0.50	0.27	5.54	21.33
Rxn6	Ni/Al_2O_3	CaO	2.52	0.45	0.37	0.52	0.40	3.14	7.40
Rxn7	Ni/AlCaOMgO	ZSM-5	3.03	10.69	0.55	0.40	0.23	7.55	22.45
Rxn8	Ni/AlCaOMgO	Al_2O_3	2.22	10.81	0.51	0.58	0.22	6.55	20.89
Rxn9	Ni/AlCaOMgO	CaO	1.41	4.68	3.17	1.58	0.24	3.97	15.05
Rxn10	Ni/CaO	ZSM-5	2.52	1.05	0.61	0.60	0.87	4.20	9.85
Rxn11	Ni/CaO	Al_2O_3	1.67	4.33	1.53	1.04	0.79	2.61	11.97
Rxn12	Ni/CaO	AlCaOMgO	3.65	9.52	0.33	0.60	1.32	3.32	18.74
Rxn13	Al_2O_3	Ni/ZSM-5	4.57	13.73	0.03	0.44	0.29	7.52	26.59
Rxn14	Al_2O_3	Ni/AlCaOMgO	3.37	11.99	0.03	0.04	0.20	5.62	21.25
Rxn15	Al_2O_3	Ni/CaO	4.62	3.20	0.05	0.00	0.91	0.16	8.94
Rxn16	ZSM-5	Ni/Al_2O_3	2.27	11.91	0.10	0.09	0.28	7.58	22.23
Rxn17	ZSM-5	Ni/AlCaOMgO	2.66	13.29	0.25	0.35	0.35	10.11	27.01
Rxn18	ZSM-5	Ni/CaO	2.04	2.20	0.00	0.00	0.38	2.11	6.73
Rxn19	AlCaOMgO	Ni/ZSM-5	2.77	12.18	0.04	0.20	0.31	6.03	21.53
Rxn20	AlCaOMgO	Ni/Al_2O_3	3.15	14.47	0.02	0.01	0.27	7.52	25.44
Rxn21	AlCaOMgO	Ni/CaO	1.67	1.80	0.00	0.00	0.64	0.20	4.31
Rxn22	CaO	Ni/ZSM	1.76	4.54	0.00	0.00	0.65	1.19	8.14
Rxn23	CaO	Ni/Al_2O_3	1.90	1.87	0.06	0.12	0.80	0.92	5.67
Rxn24	CaO	AlCaOMgO	2.35	4.31	0.23	0.40	0.84	0.46	8.60

Al_2O_3CaOMgO converted the major oxygenated compounds into aromatic hydrocarbons like benzene, fluorene, phenanthrene, pyrene and retene. Interestingly, the catalyst favoured the formation of cyclic hydrocarbons like cyclopentene, ethyltetramethylcyclopentadiene, 1,3,5-cycloheptatriene, 2,5-diethyl-7,7-dimethyl, and heptamethyl-3-phenyl-1,4-cyclohexadiene.

On the other hand, CaO could not convert oxygenated compounds into hydrocarbons more efficiently and lower proportions of aromatic and aliphatic hydrocarbons were obtained, while promoted the formation of phenols. CaO is known to catalyze demethoxylation reactions to

convert lignin components into phenol and dehydration reactions to convert cellulose and hemicellulose components into furans, ketones and pyrans [26,27]. CaO exhibits cracking mechanism of aromatic ring side chains in five main steps, as shown in Scheme 1.

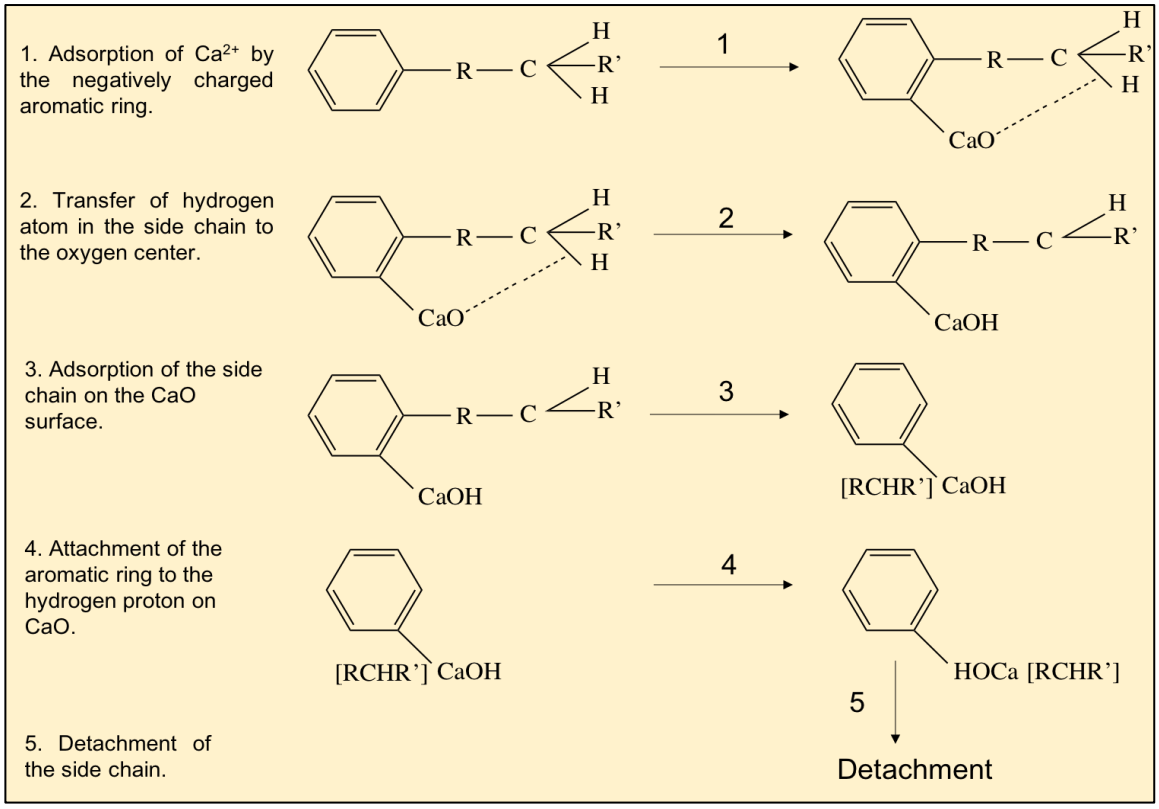

Scheme 1. Reaction mechanism of aromatic ring side chains by CaO.

Primary aromatics produced with CaO based catalysts were benzene, di-p-tolylacetylene, retene and naphthalene. In addition, Ni/CaO favored the formation of cyclic hydrocarbons like cyclohexene, cyclopentene and cycloheptatriene were found in the bio-oils.

Bio-oil composition obtained during two-stage pyrolysis is given in Table 8. The results revealed that the combination of catalysts in two-stage pyrolysis carried out additional deoxygenation reactions when compared to one-stage pyrolysis, owing to their diverse physicochemical properties and active sites, and thus produced a variety of hydrocarbons. For example, Ni/Al_2O_3 with ZSM-5 transformed all oxygenated compounds into aromatics like naphthalenes, fluorene, phenanthrene and anthracene. However, Ni/Al_2O_3 with AlCaOMgO produced extra aromatics, such as s-Indacene and annulene, and long chain alkanes like hexadecane and octadecane. On the other hand, the combination of Ni/Al_2O_3 with CaO catalyzed deoxygenation reactions to form long chain alkanes such as octadecane, 3-ethyl-5-(2-ethylbutyl), 5-ethyl-5-methylheptadecane, and hentriacontane and cyclic hydrocarbons such as ethylidenecyclobutane, cyclopropane and cyclopentene. Similarly, the other combinations of catalysts produced bio-oils with different composition involving a variety of hydrocarbons. Scheme 2 presents possible pathways involved in the conversion of oxygenated compounds into hydrocarbons.

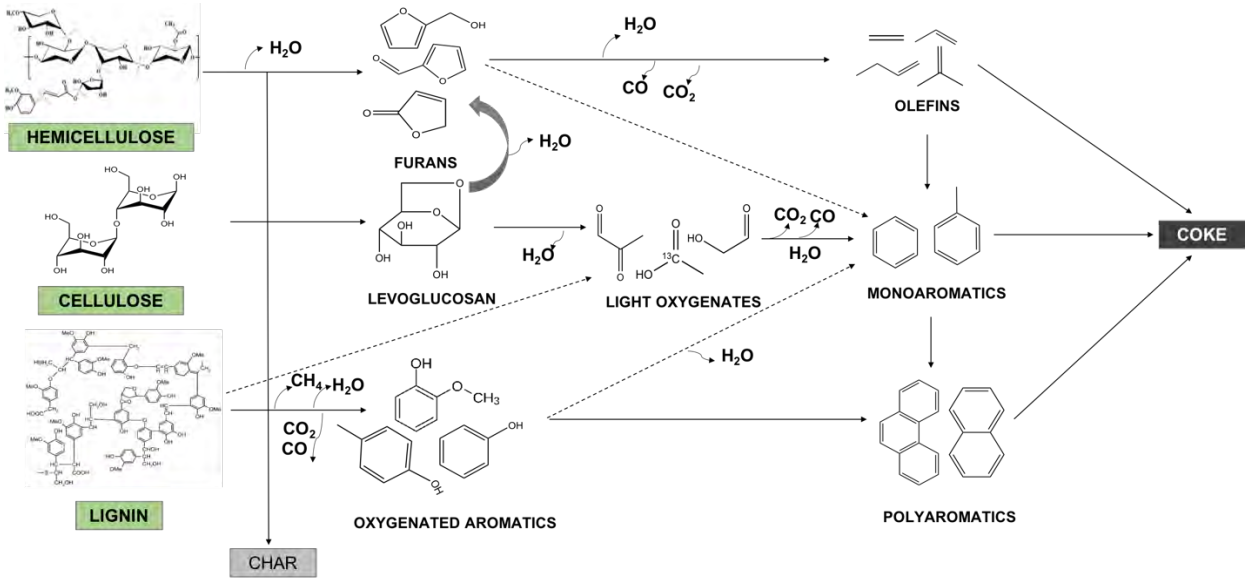

Scheme 2. Primary pathways involved in the production of hydrocarbons during catalytic pyrolysis of pinewood biomass.

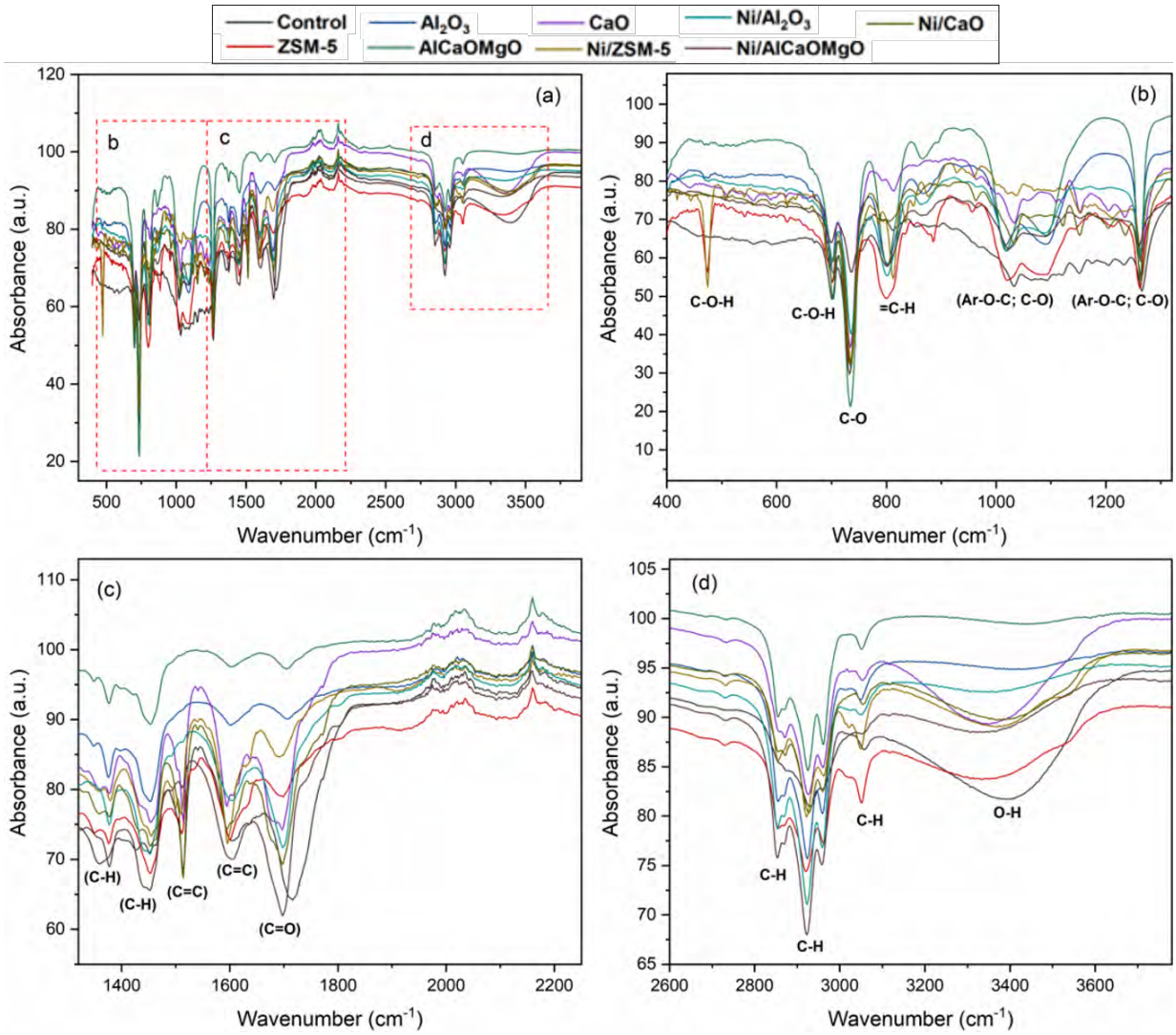

Figure 6. FTIR scans of bio-oil samples obtained during one-stage *ex-situ* pyrolysis at 500 °C, heating rate of 100 °C /min with C/B of 3.

Table 7. Bio-oil composition obtained from one-stage *ex-situ* pyrolysis.

	Bio-oil composition (peak area%)											
Catalyst	**Aromatic**	**Aliphatic**	**Phenol**	**Ketone**	**Ester**	**Aldehyde**	**Alcohol**	**Acid**	**Furan**	**Nitro**	**Sugar**	**Others**
Control	4.20	2.43	29.62	20.56	7.91	0.00	0.30	4.19	0.00	2.52	1.82	2.18
ZSM-5-1	34.22	0.85	31.76	6.86	0.93	0.00	0.81	0.00	0.68	3.18	0.00	1.84
ZSM-5-2	60.20	0.00	0.22	0.00	0.00	0.00	0.00	0.00	0.00	0.00	0.00	0.00
ZSM-5-3	87.15	0.00	0.22	0.00	0.00	0.00	0.57	0.00	0.35	0.00	0.00	0.00
Al_2O_3-1	6.59	3.33	23.99	11.16	4.90	0.00	2.97	1.37	1.37	4.32	0.00	0.65
Al_2O_3-2	41.31	1.80	1.88	1.45	0.00	0.00	3.13	0.00	0.00	0.00	0.00	0.00
Al_2O_3-3	33.13	6.40	0.00	1.00	0.00	0.62	0.91	0.00	0.00	1.95	0.00	0.00
AlCaOMgO-1	5.92	1.78	37.13	18.43	2.04	0.00	1.05	0.35	1.94	1.73	0.00	0.45
AlCaOMgO-2	29.19	5.81	2.24	0.80	2.74	0.00	3.00	1.74	0.00	1.09	0.00	0.56
AlCaOMgO-3	39.83	3.64	0.50	0.00	0.00	0.00	1.34	0.00	0.00	0.53	0.00	0.00
CaO-1	7.16	2.30	30.03	13.48	2.95	0.00	0.00	1.36	0.00	4.81	0.00	1.18
CaO-2	7.32	6.64	38.40	11.11	2.79	0.37	0.77	0.27	0.00	3.63	0.54	3.30
CaO-3	8.55	5.84	37.68	5.70	3.06	0.37	5.80	0.84	0.00	1.19	0.00	0.00
Ni/ZSM-5-1	60.31	0.38	13.58	1.93	0.00	0.00	1.39	0.00	0.91	0.35	0.00	0.00
Ni/ZSM-5-2	80.51	1.29	3.28	0.00	0.45	0.23	1.31	0.00	0.00	0.00	0.00	0.34
Ni/ZSM-5-3	86.56	5.92	1.60	0.00	0.00	0.00	0.00	0.22	0.00	0.00	0.00	0.00
Ni/Al_2O_3-1	21.82	9.21	10.34	3.52	2.80	0.63	2.06	0.00	0.00	0.00	0.00	0.00
Ni/Al_2O_3-2	41.40	8.89	2.17	0.00	0.57	0.76	1.88	0.00	0.00	0.00	0.00	0.00
Ni/Al_2O_3-3	36.83	17.39	0.41	1.89	0.97	0.00	0.40	0.00	1.53	0.00	0.00	0.00
Ni/AlCaOMgO-1	14.50	16.66	18.94	1.47	3.30	0.68	7.33	0.00	0.30	0.00	0.00	0.71
Ni/AlCaOMgO-2	27.25	6.35	4.04	7.16	1.22	0.92	0.00	0.00	0.00	0.00	0.00	1.81
Ni/AlCaOMgO-3	44.65	4.74	2.62	1.48	5.21	0.00	0.00	0.00	0.00	0.23	0.00	1.09
Ni/CaO-1	8.41	2.82	39.12	11.14	0.82	0.76	2.05	1.11	1.00	2.07	0.42	2.36
Ni/CaO-2	7.94	2.71	40.86	10.55	1.71	0.36	2.59	0.96	0.00	5.44	0.31	2.24
Ni/CaO-3	15.74	4.42	13.39	4.53	1.85	0.00	5.86	0.00	1.59	5.16	0.00	0.00

Table 8. Bio-oil composition obtained from two-stage *ex-situ* pyrolysis.

Catalysis run	Bio-oil composition (peak area %)											
	Aromatic	**Aliphatic**	**Phenol**	**Ketone**	**Ester**	**Aldehyde**	**Alcohol**	**Acid**	**Furan**	**Nitro**	**Sugar**	**Others**
Rxn1	51.81	0.00	0.58	0.00	5.49	0.00	6.12	0.00	0.00	0.56	0.00	3.34
Rxn2	97.06	0.00	0.00	0.38	0.56	0.00	0.86	0.00	0.00	0.12	0.00	0.00
Rxn3	65.92	0.41	11.12	0.86	0.40	0.00	4.82	0.00	0.00	0.00	0.00	0.19
Rxn4	56.50	0.00	0.00	0.00	0.00	0.00	0.16	0.23	0.00	0.43	0.00	0.08
Rxn5	27.59	12.87	0.47	0.00	3.05	0.00	5.05	1.40	0.00	0.52	0.00	0.00
Rxn6	9.07	13.10	22.16	6.78	3.31	0.00	3.23	1.56	0.43	0.00	0.00	2.39
Rxn7	35.41	0.59	0.00	0.00	0.00	0.00	5.86	0.00	0.00	3.44	0.00	0.00
Rxn8	77.63	0.44	0.44	0.00	0.42	0.00	0.27	0.00	0.00	0.27	0.00	0.00
Rxn9	12.30	7.52	2.86	4.43	5.05	0.00	2.73	1.91	1.02	0.00	0.00	4.44
Rxn10	82.21	0.00	0.00	0.00	1.09	0.00	0.54	0.00	0.00	0.00	0.00	0.32
Rxn11	38.93	0.00	0.91	0.00	4.60	0.00	2.71	0.00	0.00	0.74	0.00	0.65
Rxn12	35.21	2.70	0.00	0.69	4.71	0.00	1.47	0.00	0.00	1.39	0.00	0.00
Rxn13	55.74	1.64	0.36	0.00	0.00	0.00	3.43	0.00	0.00	0.00	0.00	1.29
Rxn14	26.21	5.48	2.28	0.00	3.44	0.00	4.65	0.00	0.00	0.63	0.00	0.58
Rxn15	17.99	7.64	7.13	1.48	3.60	0.82	2.79	1.64	0.00	0.00	0.00	0.79
Rxn16	88.14	0.00	0.00	0.00	1.12	0.00	0.27	0.00	0.00	0.00	0.00	0.00
Rxn17	91.02	0.39	0.82	0.21	0.87	0.00	0.00	0.48	0.28	0.00	0.00	0.32
Rxn18	66.91	0.59	6.73	1.52	1.19	0.00	2.27	0.82	0.00	0.85	0.00	0.45
Rxn19	24.95	13.18	0.53	1.22	5.28	0.00	8.27	0.00	0.00	0.00	0.00	4.16
Rxn20	84.34	0.31	0.40	0.00	1.05	0.00	0.56	0.00	0.00	0.00	0.00	0.36
Rxn21	15.53	6.21	4.48	3.10	3.63	1.02	2.15	1.20	0.00	0.00	0.00	2.21
Rxn22	67.64	1.65	6.82	1.41	1.07	0.00	5.47	1.30	0.61	0.00	0.00	2.39
Rxn23	30.44	3.80	5.87	3.93	1.64	0.00	4.59	0.00	0.00	0.68	0.00	1.95
Rxn24	26.50	3.01	1.08	3.28	6.13	0.75	3.95	0.00	0.00	0.00	0.00	2.02

3.4. FTIR of bio-oils

Figures 6 and 7 show FTIR scans of bio-oil samples obtained during one-stage and two-stage *ex-situ* pyrolysis using all catalysts, demonstrating intense IR absorbance at different wavelengths to confirm the presence of various functional groups-based organic compounds. As shown in the figures, all catalysts either in one-stage or two-stage *ex-situ* pyrolysis showed IR peaks for functional groups, such as $O-H,\ C-O,\ C=O,\ C-O-H$ that represent oxygenated compounds and also for the functional groups like $C-H, C=C,\ C-C$ that indicate the occurrence of numerous hydrocarbons in the bio-oils [40,41]. For one-stage pyrolysis, it can be clearly seen from the results that catalytic pyrolysis showed low intensity of peaks for the $O-H,\ C-O$ and $C=O$ functional groups, and high intensity vibrations for $C-H, C=C$ and $C-C$ stretches. For example, absorbance peaks at wavelengths of 2600-3100 cm^{-1} can be attributed to $C-H$ vibrations present in saturated and unsaturated aliphatic and aromatic compounds, while peaks at 1350-1500 cm^{-1} can be ascribed to other $C-H$ bound compounds, like aldehydes and ketones. Similarly, high intensity absorbance peaks achieved between 1514 and 1598 cm^{-1} can be assigned to $C=C$ functional groups of aromatic hydrocarbons and alkenes in the bio-oils. The Ni-modified catalysts Ni/ZSM-5 and Ni/Al_2O_3 showed higher intensity for these peaks compared to other catalysts and noncatalytic pyrolysis, which indicates that these catalysts promoted the formation of hydrocarbons. On the other hand, the peaks between 1000 and 1310 cm^{-1} are designated to $C-O$ and $C-C$ bonds which might be present in the family compounds of alkanes, alcohols, phenols and ethers. In addition, a broad band between 3100 and 3600 cm^{-1} is assigned to $O-H$ stretch of alcohols, phenols and water in the bio-oil. It was noticed that bio-oils obtained from catalytic pyrolysis showed low intensity peak for $O-H$ compared to noncatalytic pyrolysis, indicating a significant decrease in the concentration of $O-H$ associated oxygenated compounds.

Similar to one-stage pyrolysis, the combination of catalysts in two-stage pyrolysis showed enhanced intensity of absorbance peaks for $C-H, C=C$ and $C-C$ stretches, suggesting the presence of significant quantity of different hydrocarbons in the bio-oil samples. Furthermore, in two-stage pyrolysis, some samples showed very low intensity or no peak for $O-H$ between 3100 and 3600 cm^{-1}, indicating the presence of very low amount or absence of oxygenated compounds like alcohols, phenols and water in bio-oils.

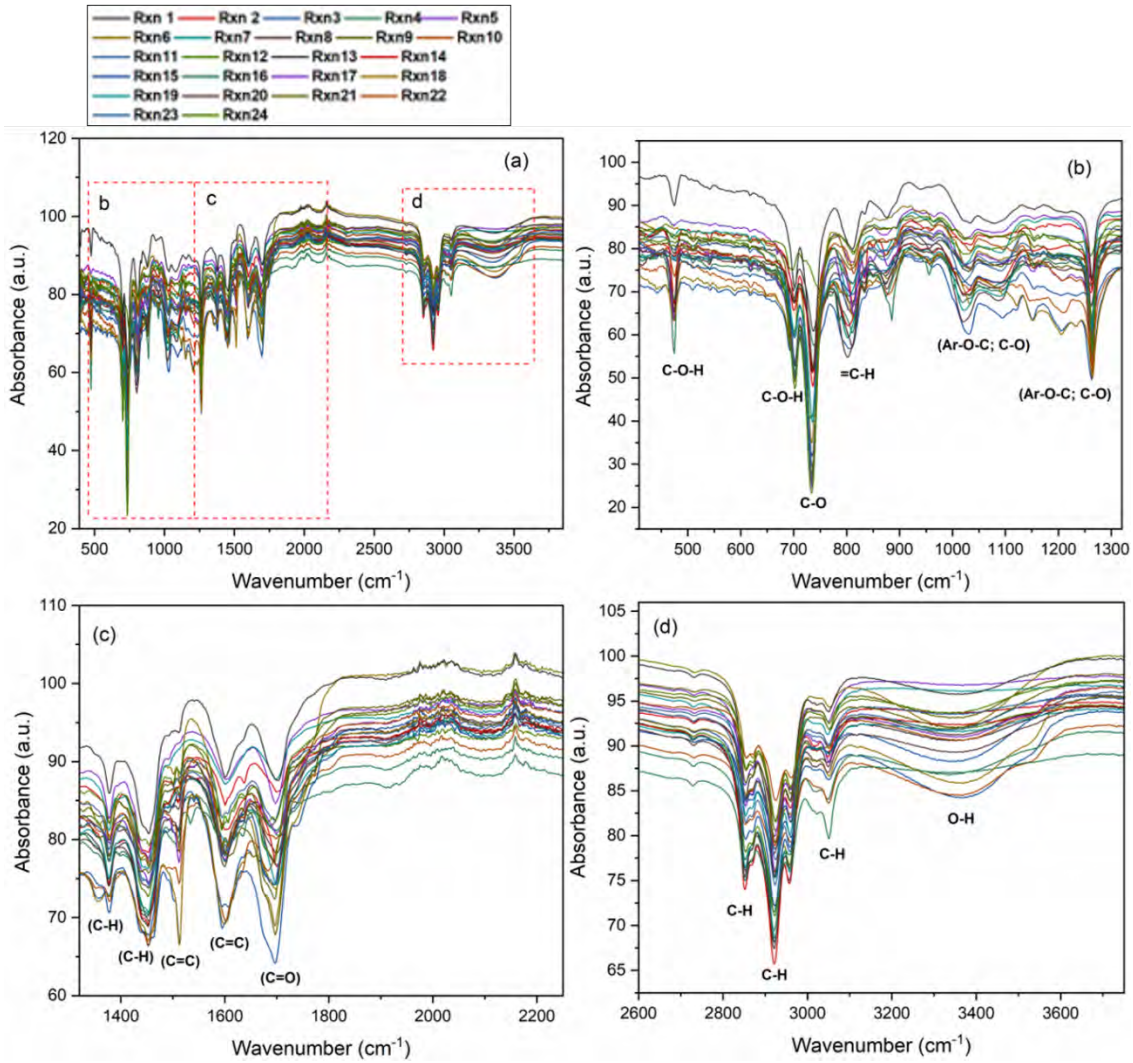

Figure 7. FTIR scans of bio-oil samples obtained during two-stage *ex-situ* pyrolysis at 500 °C, heating rate of 100 °C /min with C/B of 2.

3.5. Bio-oil deoxygenation and calorific values

The elemental composition of the bio-oils and bio-chars were determined and used to calculate their HHV [32], while the HHV of the produced gases were calculated as mentioned by Weldekidan et al. [31]. Results for elemental composition and calorific values of the bio-oils and bio-chars are given in Table 9-12. Oxygen distribution in bio-oils obtained from one and two-stage pyrolysis is also compared in Figure 8b and d. In one-stage pyrolysis, all catalysts showed noticeable reduction in the oxygen concentration, while the carbon content was significantly improved. It can be estimated from Table 9 that the catalytic supports (except CaO) produced better quality bio-oil with higher HHVs compared to noncatalytic pyrolysis. The addition of Ni enhanced the catalytic activity of supports and further produced the bio-oils with increased HHVs. For instance, the bio-oil obtained with ZSM-5 showed HHV of 21.73

MJ/kg that increased to 23.91 MJ/kg with Ni/ZSM-5. Similarly, Ni/Al_2O_3 generated the bio-oil with HHV of 20.61 MJ/kg which was higher than sole Al_2O_3 (17.83 MJ/kg). Overall, the best quality of bio-oil was obtained using Ni/ZSM-5, achieving the maximum HHV and lowest oxygen content of 29.54 wt%. This can be attributed to better physicochemical properties of Ni/ZSM-5, such as higher surface area that allowed better dispersion of Ni nanoparticles on catalyst, and presence of strong Brønsted active sites that carried out major deoxygenation reactions to transform low energy density oxygenated compounds into high energy density aromatics. Ni-modified mesoporous catalysts also produced bio-oils with improved calorific values, owing to their acidic character and larger pore volume that enhanced the mass transfer kinetics, and collectively, contributed to bio-oil upgrading.

In two-stage pyrolysis, some catalytic combinations that showed higher proportion of hydrocarbons in GC-MS analysis were further selected for elemental analysis and the results are shown in Table 10. After a comparative analysis, it can be estimated that the combination of two different catalysts of varying physicochemical properties could be more advantageous to achieve bio-oils with high energy content. The application of highly acidic-microporous and mild acidic-mesoporous or basic catalysts can carry out additional deoxygenation reactions and possess better mass transfer kinetics and selectivity for hydrocarbons and high value-added chemicals. One-stage pyrolysis that utilizes only catalyst can produce one dimensional products, while two-stage pyrolysis can produce a variety of hydrocarbons or sustainable chemicals. Evidently, some combinations of the catalysts in two-stage pyrolysis produced bio-oils with improved HHVs and low oxygen concentration. For instance, Ni/CaO with ZSM-5 and AlCaOMgO with Ni/Al_2O_3 produced bio-oil with higher HHVs of 24.4 and 23.57 MJ/kg, respectively. The production of high-quality bio-oil in two-stage pyrolysis by these catalysts can be attributed to their combined catalytic activities to convert the low-energy oxygenated compounds into high-energy hydrocarbons.

The bio-char samples obtained from either one-stage or two-stage pyrolysis showed significant calorific values with some samples achieving HHVs of more than 30 MJ/kg. The highest HHV of 34.77 MJ/kg for bio-char was obtained during one-stage pyrolysis with Ni/AlCaOMgO. Therefore, bio-chars obtained from the pyrolysis process can be regarded a valuable source of energy and, subsequently, can be used for energy production.

Table 9. Elemental composition of bio-oils obtained in one-stage *ex-situ* pyrolysis at 500 °C, heating rate of 100 °C/min with C/B of 2.

Catalyst	N (wt%)	C (wt%)	H (wt%)	O (wt%)	HHV (MJ/kg)
Control	0.00	44.79	5.59	49.62	17.09
ZSM-5	0.00	55.04	5.36	39.60	21.73
Al_2O_3	0.00	49.65	4.21	46.14	17.83
AlCaOMgO	0.00	47.45	6.00	46.55	19.14
CaO	0.00	43.57	3.48	52.95	14.16
Ni/ZSM-5	0.00	60.21	5.25	29.54	23.91
Ni/Al_2O_3	0.01	54.07	4.83	41.09	20.61
Ni/AlCaOMgO	0.06	51.19	5.34	43.41	19.98
Ni/CaO	0.00	46.84	4.09	49.07	16.41

Note: O (wt%) was calculated by the difference

Table 10. Elemental composition in bio-char samples obtained in one-stage *ex-situ* pyrolysis at 500 °C, heating rate of 100 °C/min with C/B of 2.

Catalyst	N (wt%)	C (wt%)	H (wt%)	O(wt%)	Ash (wt%)	HHV(MJ/kg)
Control	0.03	83.41	2.47	14.09	0.30	20.38
ZSM-5	0.02	84.09	3.09	12.80	8.01	31.64
Al_2O_3	0.01	79.03	2.84	18.12	3.12	29.14
AlCaOMgO	0.04	84.93	3.04	11.99	2.91	32.05
CaO	0.03	78.31	2.87	18.79	2.85	28.86
Ni/ZSM-5	0.02	74.83	2.66	22.49	5.48	26.97
Ni/Al_2O_3	0.01	78.26	2.77	18.96	4.47	28.67
Ni/AlCaOMgO	0.03	90.67	3.22	6.08	7.96	34.77
Ni/CaO	0.04	86.75	3.07	10.14	2.15	32.93

Note: O (wt%) was calculated by the difference

Table 11. Elemental composition in bio-oil samples obtained in two-stage *ex-situ* pyrolysis at 500 °C, heating rate of 100 °C/min with C/B of 2.

Sample	Catalyst 1	Catalyst 2	N (wt%)	C (wt%)	H (wt%)	O (wt%)	HHV (MJ/kg)
Rxn 1	Ni/ZSM	AlCaOMgO	0.00	47.03	4.06	48.91	16.36
Rxn 2	Ni/Al_2O_3	AlCaOMgO	0.08	49.81	4.18	45.93	17.77
Rxn 3	Ni/AlCaOMgO	Al_2O_3	0.00	52.60	4.23	43.17	19.08
Rxn 4	Ni/CaO	ZSM	0.00	59.24	6.05	34.71	24.40
Rxn 5	Al_2O_3	Ni/ZSM	0.02	64.84	2.27	32.87	22.09
Rxn 6	ZSM	Ni/Al_2O_3	0.03	54.68	4.87	40.42	20.84
Rxn 7	ZSM	Ni/AlCaOMgO	0.02	54.21	4.79	40.98	20.53
Rxn 8	AlCaOMgO	Ni/Al_2O_3	0.00	58.50	5.50	36.00	23.37

Note: O (wt%) was calculated by the difference

Table 12. Elemental composition in bio-char samples obtained in two-stage *ex-situ* pyrolysis at 500 °C, heating rate of 100 °C/min with C/B of 2.

Sample	Catalyst 1	Catalyst 2	N (wt%)	C(wt%)	H(wt%)	O(wt%)	Ash(wt%)	HHV (MJ/kg)
Rxn 1	Ni/ZSM	AlCaOMgO	0.02	84.99	2.99	12.00	3.16	32.01
Rxn 2	Ni/Al_2O_3	AlCaOMgO	0.05	87.70	3.00	9.25	0.07	33.31
Rxn 3	Ni/AlCaOMgO	Al_2O_3	0.04	81.24	2.72	16.00	2.85	29.99
Rxn 4	Ni/CaO	ZSM	0.00	79.47	2.94	17.59	2.69	29.47
Rxn 5	Al_2O_3	Ni/ZSM	0.03	54.68	4.87	40.42	1.35	20.82
Rxn 6	ZSM	Ni/Al_2O_3	0.03	86.26	3.15	10.56	2.63	32.80
Rxn 7	ZSM	Ni/AlCaOMgO	0.05	85.58	2.93	11.44	4.15	32.18
Rxn 8	AlCaOMgO	Ni/Al_2O_3	0.40	86.99	3.10	9.51	1.44	33.12

Note: O (wt%) was calculated by the difference

Energy yield (%) or energy conversion efficiency suggests the transfer of chemical energy present in the biomass into pyrolysis products. The results of one-stage and two-stage pyrolysis are shown in Figure 8a and c, respectively. In both modes of pyrolysis, bio-oil retained most of the chemical energy and showed the highest energy yield. For example, Ni/Al_2O_3 in one-stage pyrolysis attained 59.53% energy yield for bio-oil, while the combination of Al_2O_3 and Ni/ZSM-5 in two-stage pyrolysis achieved 61.69% energy yield for the bio-oil. Bio-char was the second pyrolytic product with high energy yield and gases reserved the least chemical energy. Results revealed that a range of energy yield between 23.50 and 32.80% was obtained for bio-char samples in one-stage pyrolysis and a similar range of energy yield was achieved in two-stage pyrolysis. Although the product yield could be lower for bio-chars compared to gases, they contain more chemical energy than gases and hence, are highly valuable pyrolytic product.

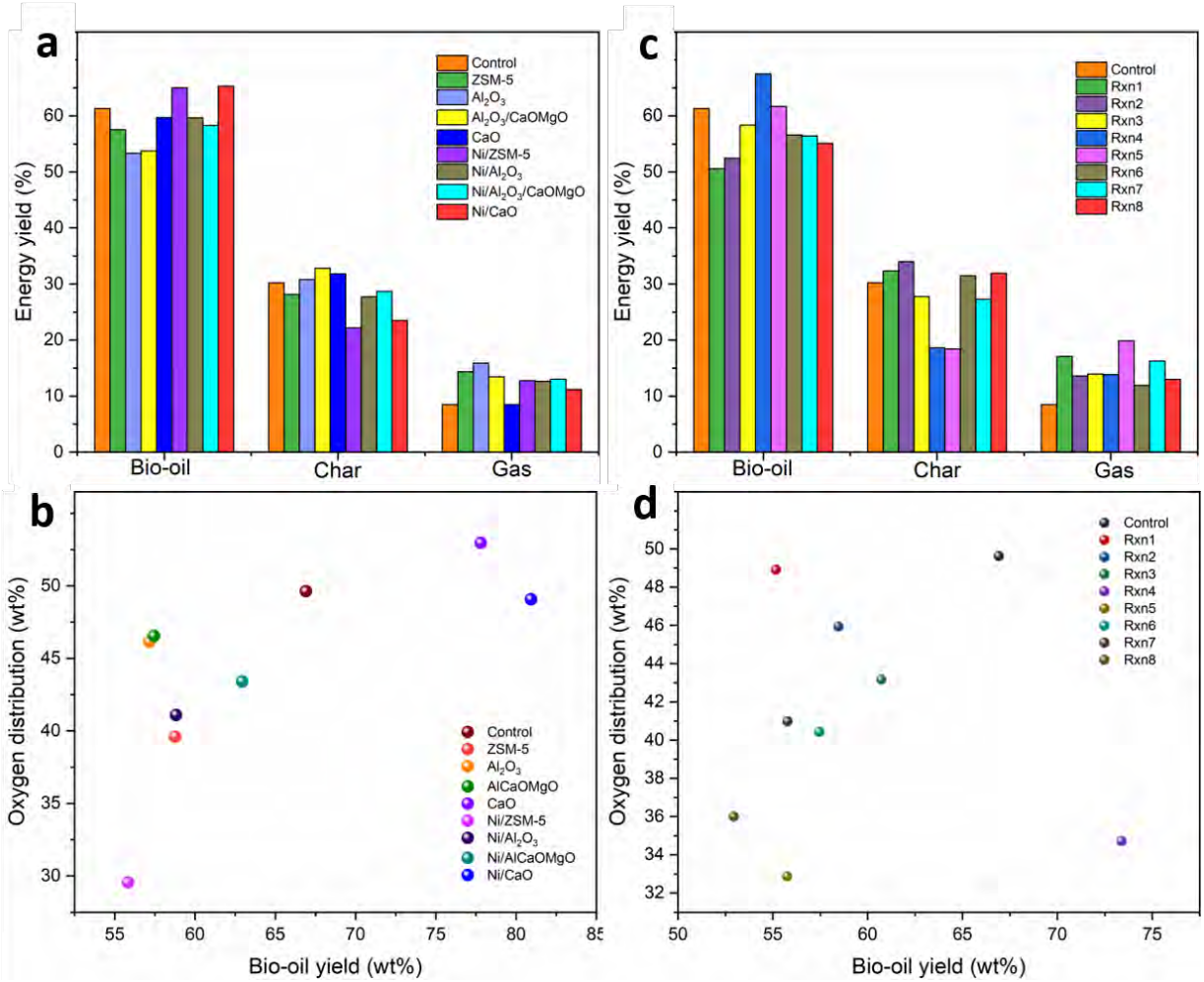

Figure 8. (a) Energy yield distribution in pyrolytic products obtained during one-stage and (c) two-stage pyrolysis, (b) oxygen distribution in bio-oils obtained from one-stage and (d) two-stage pyrolysis.

Note: Rxn1 utilized Ni/ZSM-5 and AlCaOMgO, Rxn2 utilized Ni/Al_2O_3 and AlCaOMgO, Rxn3 utilized Ni/AlCaOMgO and Al_2O_3, Rxn4 utilized Ni/CaO and ZSM-5, Rxn5 utilized Al_2O_3 and Ni/ZSM-5, Rxn6 utilized ZSM-5 and Ni/Al_2O_3, Rxn7 utilized ZSM-5, Rxn8 utilized AlCaOMgO and Ni/Al_2O_3.

3.6. Stability of Ni-modified catalysts

Stability or deactivation of all Ni-modified catalysts was examined, and four consecutive pyrolysis experiments were carried without regenerating the catalysts. The catalysts were characterized for coke deposition and other physicochemical properties. Figure 9 reports TPO results for Ni-modified catalysts during stability tests, showing the amount of coke deposition after every pyrolysis run. It can be clearly seen from the data that significant coke was deposited on the catalyst surfaces. Comparatively, acidic catalyst Ni/ZSM-5 showed less coke deposition compared to other catalysts, whereas Ni/CaO showed the highest coke deposition. For instance, Ni/ZSM-5 achieved coke deposition of 2.46 wt% at 1st pyrolysis run and 8.71wt% after 4th pyrolysis run, while Ni/CaO achieved a maximum coke deposition of 23.16 wt% after 4th pyrolysis run. On the other hand, Ni/Al_2O_3, and Ni/Al_2O_3/CaO/MgO

obtained 16.55 wt% of coke deposition. The results further revealed that each catalyst showed different types of interactions with the carbonaceous species, as weight loss in TPO scans was observed at varying temperatures. However, this may also be attributed to the presence of different types of carbon species after each pyrolysis run. Noticeably, Ni/ZSM-5 catalysts showed peaks between 500 and 550 °C, and Ni/Al_2O_3 between 450 and 550 °C, indicating presence of slightly varying types of carbon species. In contrast, Ni/CaO showed peaks at 400 °C, and between 700 and 750 °C, suggesting the occurrence of two types of carbon species where the former peaks could be ascribed to simple structured carbon species or might have weak interactions with the catalyst, while the latter peaks can be attributed to the presence of complex structured carbon species having strong interactions with the catalyst. Overall, it can be suggested that Ni/ZSM-5 showed greater stability and least deactivation, while Ni/CaO showed the highest deactivation with significant coke deposition.

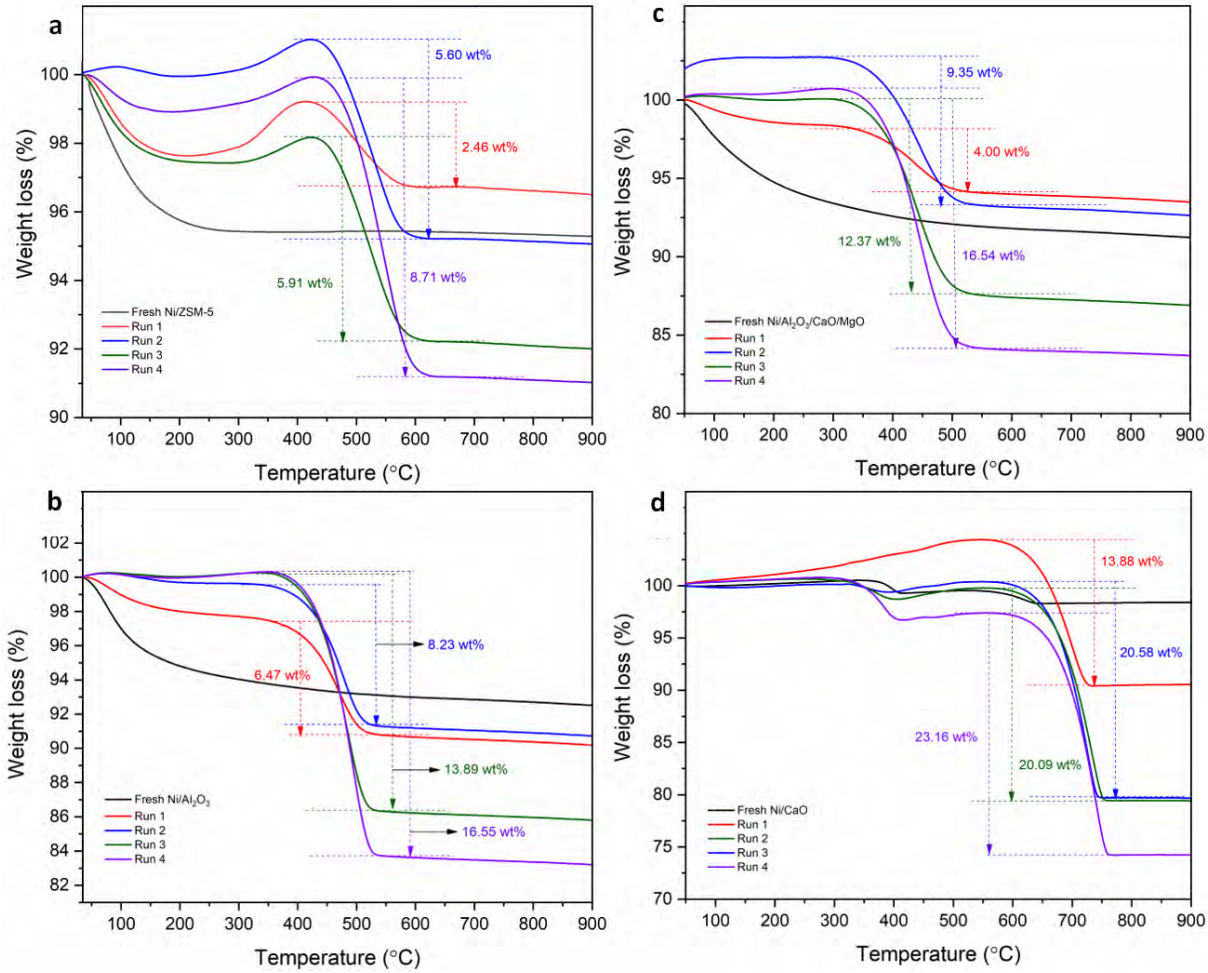

Figure 9. TPO results of catalysts after stability experiments (a) Ni/ZSM-5, (b) Ni/Al_2O_3, (c) Ni/Al_2O_3/CaO/MgO, and (d) Ni/CaO.

Figure 10 shows XRD patterns of all catalysts retrieved after each pyrolysis experiments. For Ni/ZSM-5 and Ni/CaO, it can be estimated from the results that compared to fresh catalysts where Ni was present in NiO form, it was completely changed to its metallic form as no diffraction peaks were found for NiO in the spent catalysts after the first run while intense crystalline peaks can be clearly seen for metallic Ni in each run. Noticeably, diffraction peaks at 2θ degree of 52.17 and 61.01 can be indexed to the 111 and 200 planes of crystalline Ni (reference code-00-004-0850). It is well known that NiO can react with H_2 produced during the pyrolysis process released from deoxygenation reactions carried out by the catalysts during upgrading of pyrolytic vapors and can be converted into Ni form [42]. On the other hand, for Ni/Al_2O_3 and Ni/Al_2O_3/CaO/MgO, NiO was partially converted to Ni form while the major content was in its original NiO form since a diffraction peak at 2θ degree of 43.23 (111 plane of NiO) can be clearly seen, while a small peak around 52.80 (111 plane of Ni) started to appear after the second run.

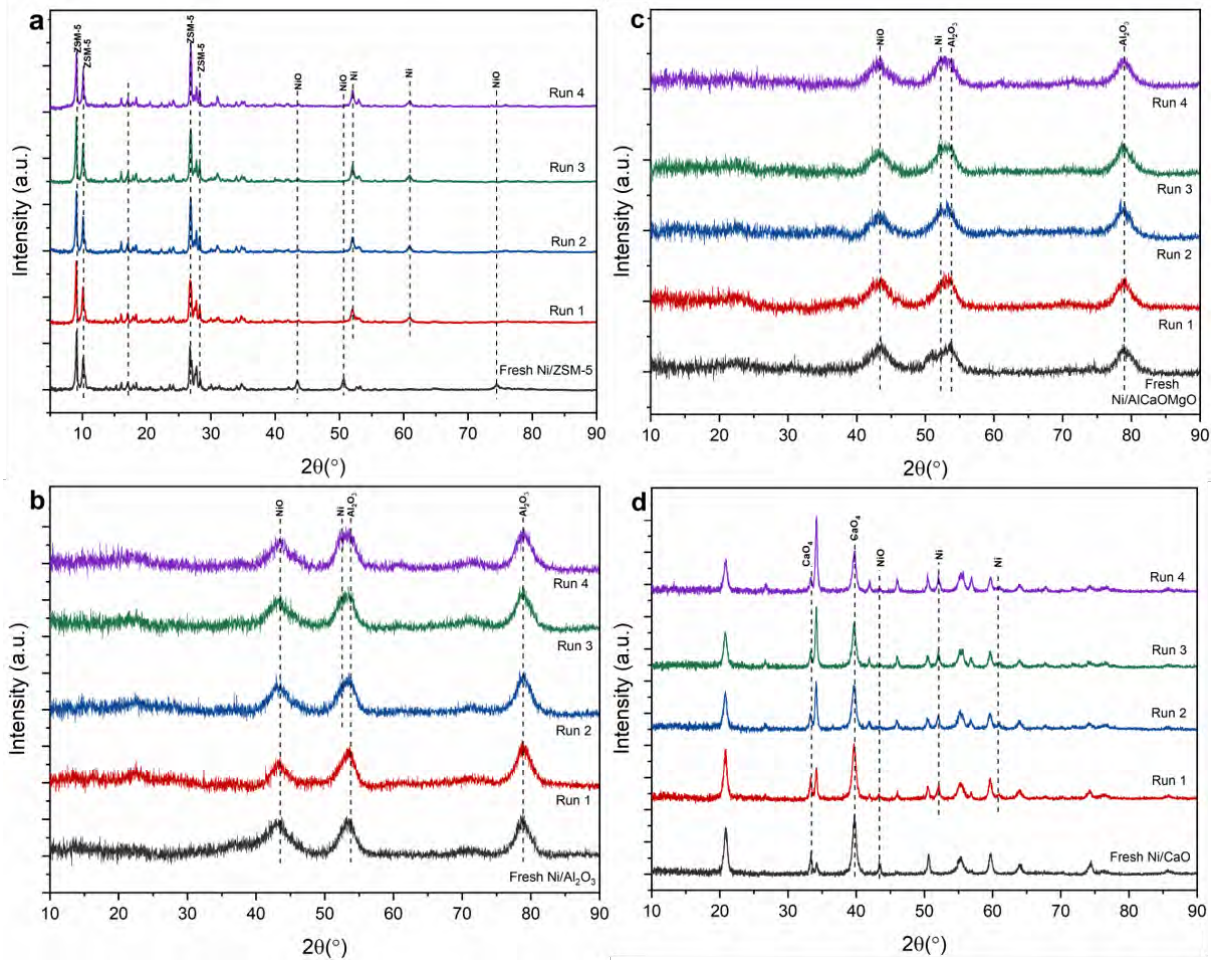

Figure 10. XRD patterns of catalysts after four consecutive runs. (a) Ni/ZSM-5, (b) Ni/Al_2O_3, (c) Ni/Al_2O_3/CaO/MgO, and (d) Ni/CaO.

Table 13. Textural properties of catalysts after stability experiments.

Catalyst	BET surface area (m^2/g)	External Surface area (m^2/g)	Micropore volume (cm^3/g)	Average Pore size (nm)
Fresh Ni/ZSM-5	403.23	135.64	0.249	1.16
Run 1	231.63	59.82	0.141	1.05
Run 2	215.73	56.51	0.130	1.02
Run 3	205.38	54.96	0.126	1.20
Run 4	141.63	38.76	0.088	1.02
Fresh Ni/Al_2O_3	199.39	192.80	0.476	15.89
Run 1	196.02	182.25	0.421	15.89
Run 2	194.74	169.39	0.394	15.89
Run 3	172.45	140.19	0.313	15.89
Run 4	90.40	72.12	0.267	15.89
Fresh Ni/AlCaOMgO	208.75	200.13	0.471	15.90
Run 1	177.96	163.49	0.379	15.90
Run 2	169.51	155.88	0.338	15.90
Run 3	162.92	152.09	0.310	15.90
Run 4	163.26	147.27	0.287	15.90
Fresh Ni/CaO	4.59	2.53	0.007	2.35
Run 1	8.04	3.57	0.012	1.88
Run 2	12.43	3.50	0.015	1.41
Run 3	12.47	5.65	0.015	1.55
Run 4	11.65	2.04	0.011	1.23

Supplementary Figures S2 and S3 show nitrogen sorption isotherms and pore distribution of the retrieved Ni-modified catalysts from each pyrolysis run. Table 13 shows the textural properties of the catalysts. As shown in the table, surface areas and micropore volumes considerably decreased after each pyrolysis run except Ni/CaO which showed a slight increase in the surface area and pore volume. The decrease in surface area can be attributed to the formation of carbonaceous species during pyrolysis and their accumulation on the catalytic pores. On the other hand, porous carbon deposition of Ni/CaO might enhance the N_2 adsorption of catalyst surface and contributed to the increase in surface area.

XPS analysis was carried out to confirm metallic states after pyrolysis. Figure 11 shows photoelectron spectra of Ni2p present in spent Ni-modified catalysts. Compared to the fresh catalysts, significant changes were observed for Ni2p spectra of the spent catalysts. For example, in Ni/ZSM-5, the binding energies for the two main peaks assigned to $Ni2p_{3/2}$ and $Ni2p_{1/2}$ slightly increased when compared to the fresh catalysts and also showed additional shake-up satellite, suggesting the evolution of new state of Ni metal. Hence, it can be assumed that Ni^{2+} present in the fresh Ni/ZSM-5 was reduced to Ni. In contrast, in Ni/CaO, intense peak at 849.45 eV was observed which was missing in the fresh Ni/CaO, indicating the presence of new state of Ni. Thus it can be assumed that NiO was reduced to Ni after reacting with

hydrogen and other gases released during the pyrolysis process or deoxygenation reactions catalyzed by Ni/CaO [35].

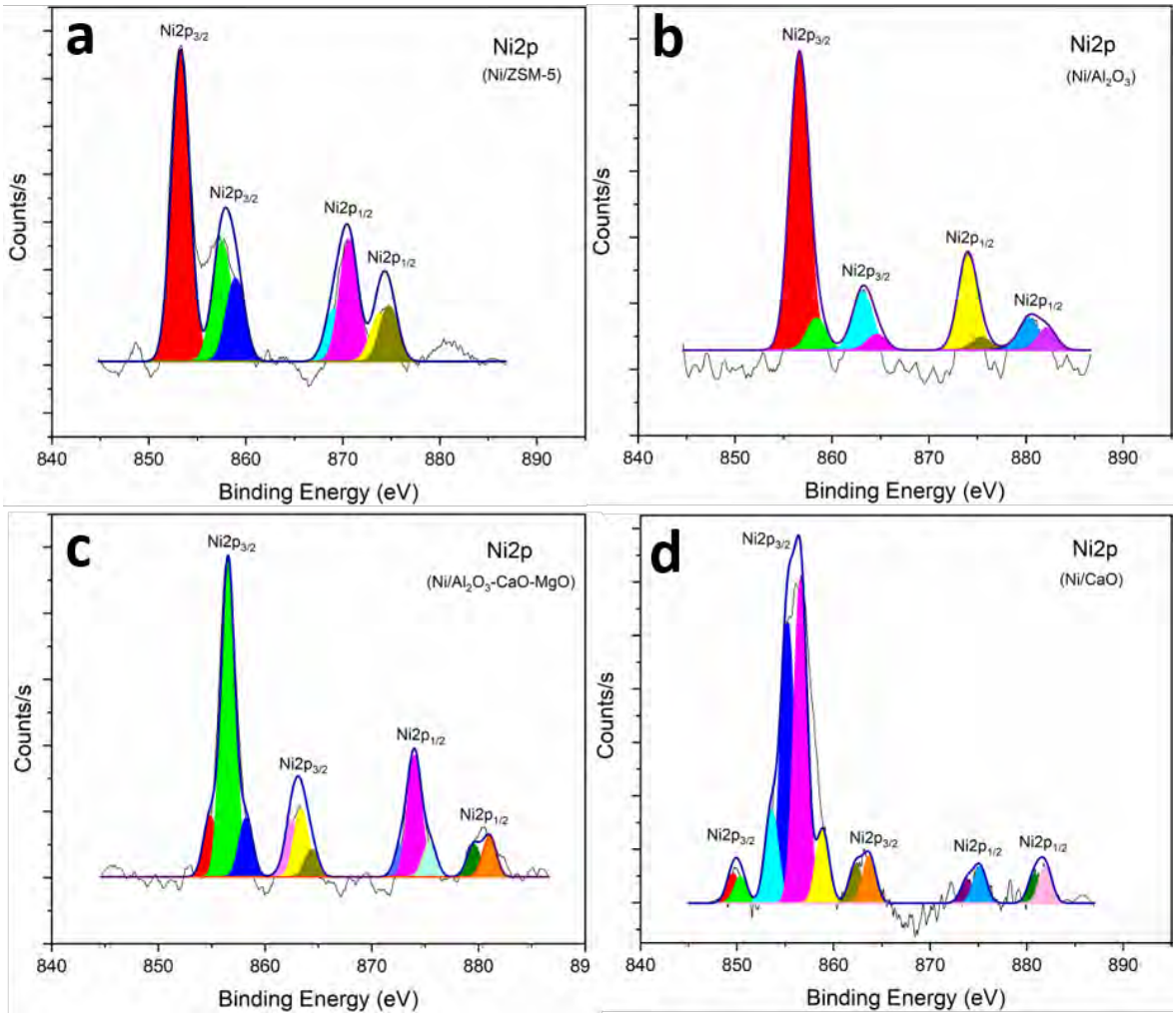

Figure 11. Photoelectron spectra of Ni2p in (a) Ni/ZSM-5 (b) Ni/Al_2O_3 (c) Ni/AlCaOMgO and (f) Ni/CaO.

Ni-impregnated catalysts were examined for their stability in one-stage *ex-situ* pyrolysis mode, and its effect on the distribution of pyrolysis products was observed. Tables S1 and S2 show the distribution for pyrolysis products and gas composition, respectively. It can be observed from the results that for acidic catalysts the bio-oil yield started to increase slightly compared to the fresh catalysts, while the gas yield decreased simultaneously after each pyrolysis experiment. This is probably due to the coke deposition on the catalyst surface that occupied the pores as well as active sites and thus decreased the catalytic activity of the catalysts. TPO analysis confirmed noticeable coke formation and BET results showed a decrease in pore volume and surface areas of the catalysts. In contrast, for Ni/CaO, a minor decrease in bio-oil yield and a subtle increase in gas yield was observed. This change in

pyrolytic products for Ni/CaO can be explained by the better activity for CO_2 absorption of the fresh Ni/CaO catalyst where coke deposition decreased its ability to absorb CO_2 compounds with the subsequent pyrolysis runs, thereby increasing the gas yield and decreasing the bio-oil yield.

Table 14. Elemental composition in bio-oil samples obtained in *ex-situ* pyrolysis during stability experiments at 500 °C, heating rate of 100 °C/min with C/B of 2.

	Catalyst	**N (wt%)**	**C(wt%)**	**H(wt%)**	**O(wt%)**	**HHV(MJ/kg)**
Run 1	Ni/ZSM-5	0.00	60.21	5.25	29.54	23.91
Run 1	Ni/Al_2O_3	0.01	54.07	4.83	41.09	20.61
Run 1	Ni/AlCaOMgO	0.06	51.19	5.34	43.41	19.98
Run 1	Ni/CaO	0.00	46.84	4.09	49.07	16.41
Run 4	Ni/ZSM-5	0.04	50.77	4.39	44.80	18.57
Run 4	Ni/Al_2O_3	0.00	46.94	3.53	49.53	15.74
Run 4	Ni/AlCaOMgO	0.42	49.67	3.11	46.80	16.47
Run 4	Ni/CaO	0.04	41.88	3.54	54.54	13.48

Note: O (wt%) was calculated by the difference

Coke deposition during the stability tests had significant effects on physicochemical properties of the catalysts such as decrease in pore volume and surface area, and reduction in the number of active sites. Therefore, the catalysts with reduced physicochemical properties impacted the bio-oil upgrading during the pyrolysis and resulted in bio-oil with comparatively lower calorific values. For example, fresh Ni/ZSM-5 produced bio-oil with HHV of 23.91 MJ/kg, while after the 4th pyrolysis, bio-oil with HHV of 18.57 MJ/kg was obtained. Table 14 and Table S3 show elemental composition of the bio-oil and biochar samples obtained in *ex-situ* pyrolysis during stability experiments, respectively.

Bio-oil composition obtained during stability tests after each pyrolysis run are given in Table 15. The results showed that despite coke deposition catalysts retained their catalytic activity and produced a variety of aromatic and aliphatic hydrocarbons. However, after the 3rd and 4th pyrolysis run, noticeable proportion of oxygenated compounds, like ketones and phenols, were also found in the bio-oils, indicating the adverse impact of coke deposition on catalytic activity. As shown in Figure S4, it can be observed the oxygen content was increased after the 4th pyrolysis run for all the catalysts, attributing to their diminished physicochemical properties due to coke deposition.

Table 15. Bio-oil composition obtained from *ex-situ* pyrolysis during stability tests.

Catalyst	Bio-oil composition (peak area %)											
	Aromatic	**Aliphatic**	**Phenol**	**Ketone**	**Ester**	**Aldehyde**	**Alcohol**	**Acid**	**Furan**	**Nitro**	**Sugar**	**Others**
Control	4.20	2.43	29.62	17.99	7.91	0.00	0.3	4.19	0.00	2.52	1.82	2.18
Ni/ZSM-5												
Fresh	86.56	5.92	1.60	0.00	0.00	0.00	0.00	0.22	0.00	0.00	0.00	0.00
Run 1	71.27	1.88	0.00	0.99	5.09	1.34	0.79	0.00	0.68	0.00	0.00	1.24
Run 2	73.72	0.46	2.99	1.06	0.59	0.49	0.61	0.00	0.00	0.91	0.00	0.38
Run 3	53.33	0.00	11.12	3.51	0.82	0.00	0.81	1.12	0.00	0.73	0.00	0.00
Run 4	59.35	0.00	9.40	4.45	0.33	0.00	0.49	0.00	1.11	0.33	0.00	0.00
Ni/Al_2O_3												
Fresh	36.83	17.39	0.41	1.89	0.97	0.00	0.4	0.00	1.53	0.00	0.00	0.00
Run 1	44.43	7.73	0.49	1.86	1.51	0.42	2.18	0.00	0.00	0.74	0.00	0.00
Run 2	56.56	2.65	0.00	0.00	0.99	0.00	0.42	0.00	0.00	0.00	0.00	0.51
Run 3	58.30	3.99	8.00	3.84	3.49	0.63	6.00	0.00	0.00	0.62	0.00	1.99
Run 4	18.46	11.39	13.95	6.88	5.96	0.56	1.48	0.80	0.00	1.35	0.00	0.00
Ni/AlCaOMgO												
Fresh	44.65	4.74	2.62	1.48	5.21	0.00	0.00	0.00	0.00	0.23	0.00	1.09
Run 1	33.37	10.61	1.46	1.6	1.54	0.00	1.69	0.00	0.00	2.82	0.00	0.30
Run 2	52.03	2.53	3.71	2.21	3.67	0.00	1.02	0.00	0.00	0.00	0.00	0.00
Run 3	23.33	0.00	24.61	7.94	10.54	0.00	0.00	3.4	0.79	4.3	0.00	0.00
Run 4	14.59	5.98	39.80	6.25	3.49	1.27	0.30	1.88	0.89	1.23	0.00	0.00
Ni/CaO												
Fresh	15.74	4.42	13.39	4.53	1.85	0.00	5.86	0.00	1.59	5.16	0.00	0.00
Run 1	9.96	6.61	43.58	1.88	7.79	0.2	7.69	0.00	1.55	0.00	0.00	0.29
Run 2	7.07	5.67	45.80	5.73	9.38	0.00	5.92	0.88	0.69	0.24	0.00	0.34
Run 3	10.38	1.85	51.31	6.11	2.83	0.00	0.95	0.00	1.64	0.00	0.00	0.00
Run 4	6.44	3.50	43.06	14.38	2.09	0.45	1.19	0.42	0.00	6.33	0.00	1.08

4. Conclusion

The present study investigated the effect of different types of catalytic support (ZSM-5, Al_2O_3, Al_2O_3/CaO/MgO, and CaO) with and without nickel impregnation for bio-oil deoxygenation in one-stage and two-stage *ex-situ* pyrolysis. Results revealed that efficient bio-oil deoxygenation could be achieved in both modes of pyrolysis. However, two-stage pyrolysis that employs two different catalysts of varying physicochemical properties possesses additional active sites to catalyse deoxygenation reactions, thus, leads to production of diverse range of hydrocarbons in the bio-oils. For example, Ni/Al_2O_3 in combination with ZSM-5 converted oxygenated compounds into aromatics, like naphthalenes, fluorene, phenanthrene and anthracene. In contrast, Ni/Al_2O_3 with AlCaOMgO produced extra aromatics, including s-Indacene and annulene and long-chain alkanes like hexadecane and octadecane, owing to the combined catalytic activity of both catalysts. The stability tests of Ni-modified catalysts further revealed that Ni/ZSM-5 showed the least coke deposition of 8.71 wt% after 4 successive pyrolysis run, while Ni/CaO achieved the highest coke deposition of 23.16 wt%. Consequently, coke deposition had a negative impact on the physicochemical properties of the catalysts and, therefore, on their catalytic activity for bio-oil deoxygenation.

References

[1] Hertzog J, Carré V, Jia L, Mackay CL, Pinard L, Dufour A, et al. Catalytic Fast Pyrolysis of Biomass over Microporous and Hierarchical Zeolites: Characterization of Heavy Products. ACS Sustainable Chemistry & Engineering 2018;6:4717–28. https://doi.org/10.1021/acssuschemeng.7b03837.

[2] Robinson AM, Hensley JE, Medlin JW. Bifunctional Catalysts for Upgrading of Biomass-Derived Oxygenates: A Review. ACS Catalysis 2016;6:5026–43. https://doi.org/10.1021/acscatal.6b00923.

[3] Ringer M, Putsche V, Scahill J. Large-Scale Pyrolysis Oil Production: A Technology Assessment and Economic Analysis. US: National Renewable Energy Laboratory (NREL), Golden, CO.; 2006. https://doi.org/10.2172/894989.

[4] Dai L, Wang Y, Liu Y, Ruan R, Duan D, Zhao Y, et al. Catalytic fast pyrolysis of torrefied corn cob to aromatic hydrocarbons over Ni-modified hierarchical ZSM-5 catalyst. Bioresource Technology 2019;272:407–14. https://doi.org/10.1016/j.biortech.2018.10.062.

[5] Ghorbannezhad P, Firouzabadi MD, Ghasemian A, de Wild PJ, Heeres HJ. Sugarcane bagasse ex-situ catalytic fast pyrolysis for the production of Benzene, Toluene and Xylenes (BTX). Journal of Analytical and Applied Pyrolysis 2018;131:1–8. https://doi.org/10.1016/j.jaap.2018.02.019.

[6] Kumar R, Strezov V. Thermochemical production of bio-oil: A review of downstream processing technologies for bio-oil upgrading, production of hydrogen and high value-added products. Renewable and Sustainable Energy Reviews 2021;135:110152. https://doi.org/10.1016/j.rser.2020.110152.

[7] Hu C, Zhang H, Xiao R. Effects of nascent char on ex-situ catalytic fast pyrolysis of wheat straw. Energy Conversion and Management 2018;177:765–72. https://doi.org/10.1016/j.enconman.2018.10.018.

[8] Kumar R, Strezov V, Lovell E, Kan T, Weldekidan H, He J, et al. Enhanced bio-oil deoxygenation activity by Cu/zeolite and Ni/zeolite catalysts in combined in-situ and ex-situ biomass pyrolysis. Journal of Analytical and Applied Pyrolysis 2019. https://doi.org/10.1016/j.jaap.2019.03.008.
[9] Ratnasari DK, Yang W, Jönsson PG. Two-stage ex-situ catalytic pyrolysis of lignocellulose for the production of gasoline-range chemicals. Journal of Analytical and Applied Pyrolysis 2018;134:454–64. https://doi.org/10.1016/j.jaap.2018.07.012.
[10] Hu C, Xiao R, Zhang H. Ex-situ catalytic fast pyrolysis of biomass over HZSM-5 in a two-stage fluidized-bed/fixed-bed combination reactor. Bioresource Technology 2017;243:1133–40. https://doi.org/10.1016/j.biortech.2017.07.011.
[11] Cheng Y-T, Huber GW. Chemistry of Furan Conversion into Aromatics and Olefins over HZSM-5: A Model Biomass Conversion Reaction. ACS Catalysis 2011;1:611–28. https://doi.org/10.1021/cs200103j.
[12] Corma A. State of the art and future challenges of zeolites as catalysts. Journal of Catalysis 2003;216:298–312. https://doi.org/10.1016/S0021-9517(02)00132-X.
[13] Wei Y, Parmentier TE, de Jong KP, Zečević J. Tailoring and visualizing the pore architecture of hierarchical zeolites. Chem Soc Rev 2015;44:7234–61. https://doi.org/10.1039/C5CS00155B.
[14] Busca G. Acidity and basicity of zeolites: A fundamental approach. Microporous and Mesoporous Materials 2017;254:3–16. https://doi.org/10.1016/j.micromeso.2017.04.007.
[15] Hu C, Zhang H, Wu S, Xiao R. Molecular shape selectivity of HZSM-5 in catalytic conversion of biomass pyrolysis vapors: The effective pore size. Energy Conversion and Management 2020;210:112678. https://doi.org/10.1016/j.enconman.2020.112678.
[16] Kumar R, Strezov V, Lovell E, Kan T, Weldekidan H, He J, et al. Bio-oil upgrading with catalytic pyrolysis of biomass using Copper/zeolite-Nickel/zeolite and Copper-Nickel/zeolite catalysts. Bioresource Technology 2019;279:404–9. https://doi.org/10.1016/j.biortech.2019.01.067.
[17] Gayubo AG, Aguayo AT, Atutxa A, Aguado R, Olazar M, Bilbao J. Transformation of Oxygenate Components of Biomass Pyrolysis Oil on a HZSM-5 Zeolite. II. Aldehydes, Ketones, and Acids. Industrial & Engineering Chemistry Research 2004;43:2619–26. https://doi.org/10.1021/ie030792g.
[18] Chen G, Zhang R, Ma W, Liu B, Li X, Yan B, et al. Catalytic cracking of model compounds of bio-oil over HZSM-5 and the catalyst deactivation. Science of The Total Environment 2018;631–632:1611–22. https://doi.org/10.1016/j.scitotenv.2018.03.147.
[19] Abu-Laban M. Ex-situ up-conversion of biomass pyrolysis bio-oil vapors using Pt/Al2O3 nanostructured catalyst synergistically heated with steel balls via induction. Catalysis Today 2017:10.
[20] Eschenbacher A, Saraeian A, Jensen PA, Shanks BH, Li C, Duus JØ, et al. Deoxygenation of wheat straw fast pyrolysis vapors over Na-Al2O3 catalyst for production of bio-oil with low acidity. Chemical Engineering Journal 2020;394:124878. https://doi.org/10.1016/j.cej.2020.124878.
[21] Mante OD, Dayton DC, Carpenter JR, Wang K, Peters JE. Pilot-scale catalytic fast pyrolysis of loblolly pine over γ-Al2O3 catalyst. Fuel 2018;214:569–79. https://doi.org/10.1016/j.fuel.2017.11.073.
[22] Che Q, Yang M, Wang X, Chen X, Chen W, Yang Q, et al. Aromatics production with metal oxides and ZSM-5 as catalysts in catalytic pyrolysis of wood sawdust. Fuel Processing Technology 2019;188:146–52. https://doi.org/10.1016/j.fuproc.2019.02.016.
[23] Kaewpengkrow P, Atong D, Sricharoenchaikul V. Catalytic upgrading of pyrolysis vapors from Jatropha wastes using alumina, zirconia and titania based catalysts. Bioresource Technology 2014;163:262–9. https://doi.org/10.1016/j.biortech.2014.04.035.
[24] Chen X, Li S, Liu Z, Chen Y, Yang H, Wang X, et al. Pyrolysis characteristics of lignocellulosic biomass components in the presence of CaO. Bioresource Technology 2019;287:121493. https://doi.org/10.1016/j.biortech.2019.121493.

[25] Pütün E. Catalytic pyrolysis of biomass: Effects of pyrolysis temperature, sweeping gas flow rate and MgO catalyst. Energy 2010;35:2761–6. https://doi.org/10.1016/j.energy.2010.02.024.
[26] Lin Y, Zhang C, Zhang M, Zhang J. Deoxygenation of Bio-oil during Pyrolysis of Biomass in the Presence of CaO in a Fluidized-Bed Reactor. Energy & Fuels 2010;24:5686–95. https://doi.org/10.1021/ef1009605.
[27] Veses A, Aznar M, Martínez I, Martínez JD, López JM, Navarro MV, et al. Catalytic pyrolysis of wood biomass in an auger reactor using calcium-based catalysts. Bioresource Technology 2014;162:250–8. https://doi.org/10.1016/j.biortech.2014.03.146.
[28] Stefanidis SD, Karakoulia SA, Kalogiannis KG, Iliopoulou EF, Delimitis A, Yiannoulakis H, et al. Natural magnesium oxide (MgO) catalysts: A cost-effective sustainable alternative to acid zeolites for the in situ upgrading of biomass fast pyrolysis oil. Applied Catalysis B: Environmental 2016;196:155–73. https://doi.org/10.1016/j.apcatb.2016.05.031.
[29] Fan L, Chen P, Zhang Y, Liu S, Liu Y, Wang Y, et al. Fast microwave-assisted catalytic co-pyrolysis of lignin and low-density polyethylene with HZSM-5 and MgO for improved bio-oil yield and quality. Bioresource Technology 2017;225:199–205. https://doi.org/10.1016/j.biortech.2016.11.072.
[30] Kumar R, Strezov V, Kan T, Weldekidan H, He J, Jahan S. Investigating the Effect of Mono- and Bimetallic/Zeolite Catalysts on Hydrocarbon Production during Bio-oil Upgrading from *Ex Situ* Pyrolysis of Biomass. Energy Fuels 2019:acs.energyfuels.9b02724. https://doi.org/10.1021/acs.energyfuels.9b02724.
[31] Weldekidan H, Strezov V, He J, Kumar R, Sarkodie SA, Doyi I, et al. Energy conversion efficiency of pyrolysis of chicken litter and rice husk biomass. Energy & Fuels 2019:acs.energyfuels.9b01264. https://doi.org/10.1021/acs.energyfuels.9b01264.
[32] Hernando H, Jiménez-Sánchez S, Fermoso J, Pizarro P, Coronado JM, Serrano DP. Assessing biomass catalytic pyrolysis in terms of deoxygenation pathways and energy yields for the efficient production of advanced biofuels. Catal Sci Technol 2016;6:2829–43. https://doi.org/10.1039/C6CY00522E.
[33] Yung MM, Starace AK, Mukarakate C, Crow AM, Leshnov MA, Magrini KA. Biomass Catalytic Pyrolysis on Ni/ZSM-5: Effects of Nickel Pretreatment and Loading. Energy & Fuels 2016;30:5259–68. https://doi.org/10.1021/acs.energyfuels.6b00239.
[34] Liu D, Li D, Yang D. Size-dependent magnetic properties of branchlike nickel oxide nanocrystals. AIP Advances 2017;7:015028. https://doi.org/10.1063/1.4974307.
[35] Grosvenor AP, Biesinger MC, Smart RStC, McIntyre NS. New interpretations of XPS spectra of nickel metal and oxides. Surface Science 2006;600:1771–9. https://doi.org/10.1016/j.susc.2006.01.041.
[36] Puértolas B, Veses A, Callén MS, Mitchell S, García T, Pérez-Ramírez J. Porosity-Acidity Interplay in Hierarchical ZSM-5 Zeolites for Pyrolysis Oil Valorization to Aromatics. ChemSusChem 2015;8:3283–93. https://doi.org/10.1002/cssc.201500685.
[37] Kumar M, Aberuagba F, Gupta JK, Rawat KS, Sharma LD, Murali Dhar G. Temperature-programmed reduction and acidic properties of molybdenum supported on MgO–Al2O3 and their correlation with catalytic activity. Journal of Molecular Catalysis A: Chemical 2004;213:217–23. https://doi.org/10.1016/j.molcata.2003.12.005.
[38] Asikin-Mijan N, Lee HV, Juan JC, Noorsaadah AR, Taufiq-Yap YH. Catalytic deoxygenation of triglycerides to green diesel over modified CaO-based catalysts. RSC Adv 2017;7:46445–60. https://doi.org/10.1039/C7RA08061A.
[39] Zheng Y, Chen D, Zhu X. Aromatic hydrocarbon production by the online catalytic cracking of lignin fast pyrolysis vapors using Mo2N/γ-Al2O3. Journal of Analytical and Applied Pyrolysis 2013;104:514–20. https://doi.org/10.1016/j.jaap.2013.05.018.
[40] Li B, Lv W, Zhang Q, Wang T, Ma L. Pyrolysis and catalytic pyrolysis of industrial lignins by TG-FTIR: Kinetics and products. Journal of Analytical and Applied Pyrolysis 2014;108:295–300. https://doi.org/10.1016/j.jaap.2014.04.002.

[41] Wang D, Xiao R, Zhang H, He G. Comparison of catalytic pyrolysis of biomass with MCM-41 and CaO catalysts by using TGA–FTIR analysis. Journal of Analytical and Applied Pyrolysis 2010;89:171–7. https://doi.org/10.1016/j.jaap.2010.07.008.
[42] Heracleous E, Pachatouridou E, Hernández-Giménez AM, Hernando H, Fakin T, Paioni AL, et al. Characterization of deactivated and regenerated zeolite ZSM-5-based catalyst extrudates used in catalytic pyrolysis of biomass. Journal of Catalysis 2019;380:108–22. https://doi.org/10.1016/j.jcat.2019.10.019.

Supporting information

Effect of catalyst supports with and without nickel on bio-oil upgrading and energy distribution in pyrolytic products during one and two-stage *ex-situ* biomass pyrolysis

Ravinder Kumar[a*], Vladimir Strezov[a], Jing He[a], Yutong Zhao[b], Behnam Dastjerdi[a], Tao Kan[a] Haimei Xu[b], Yijiao Jiang[b]

[a]*Department of Earth and Environmental Sciences, Faculty of Science & Engineering, Macquarie University, Sydney, NSW 2109, Australia*

[b]*School of Engineering, Macquarie University, North Ryde, NSW 2109, Australia*

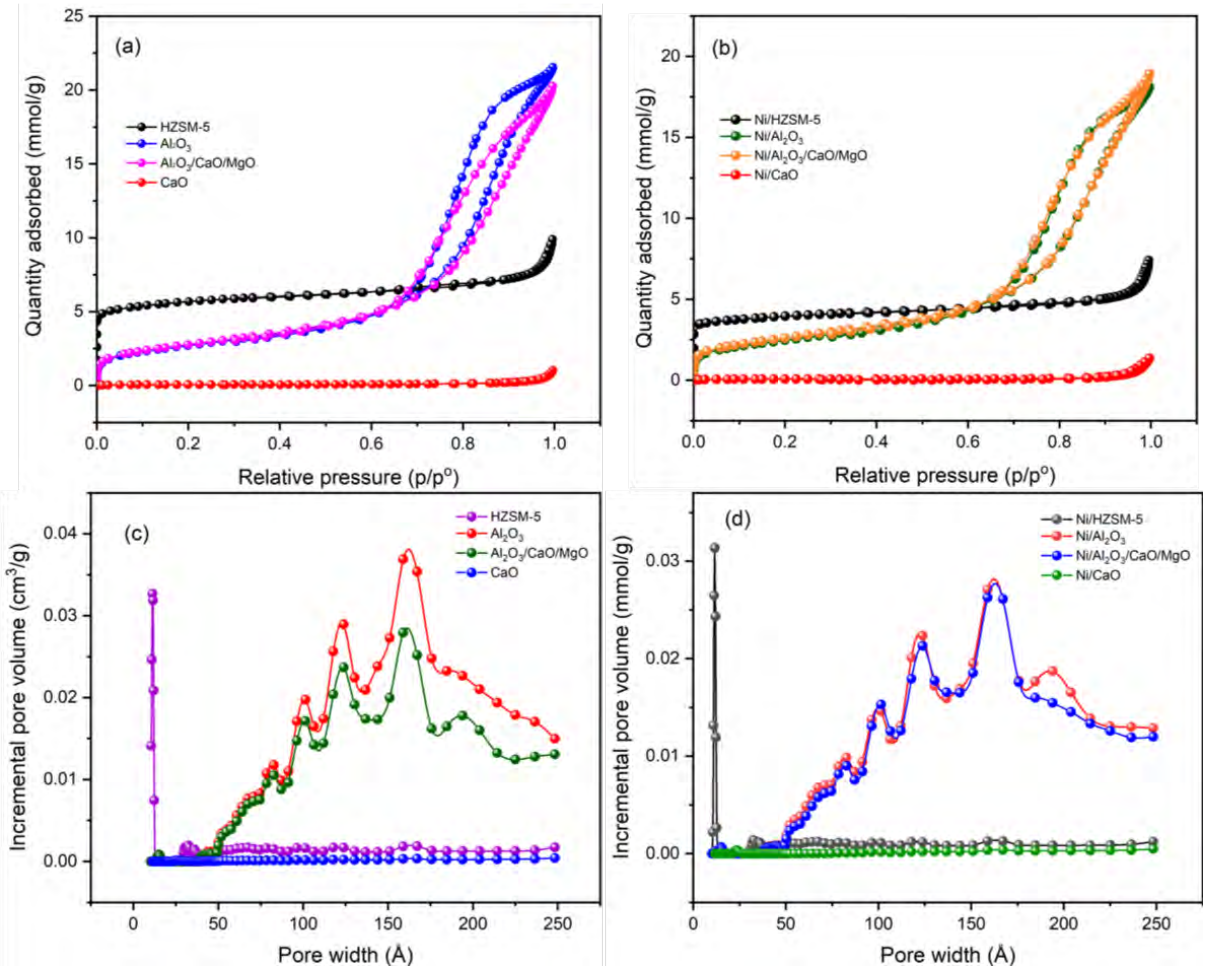

Figure S1. Nitrogen sorption isotherms for (a) catalytic supports (b)Ni-modified catalysts and pore distribution in (c) catalytic supports (d) Ni-modified catalysts.

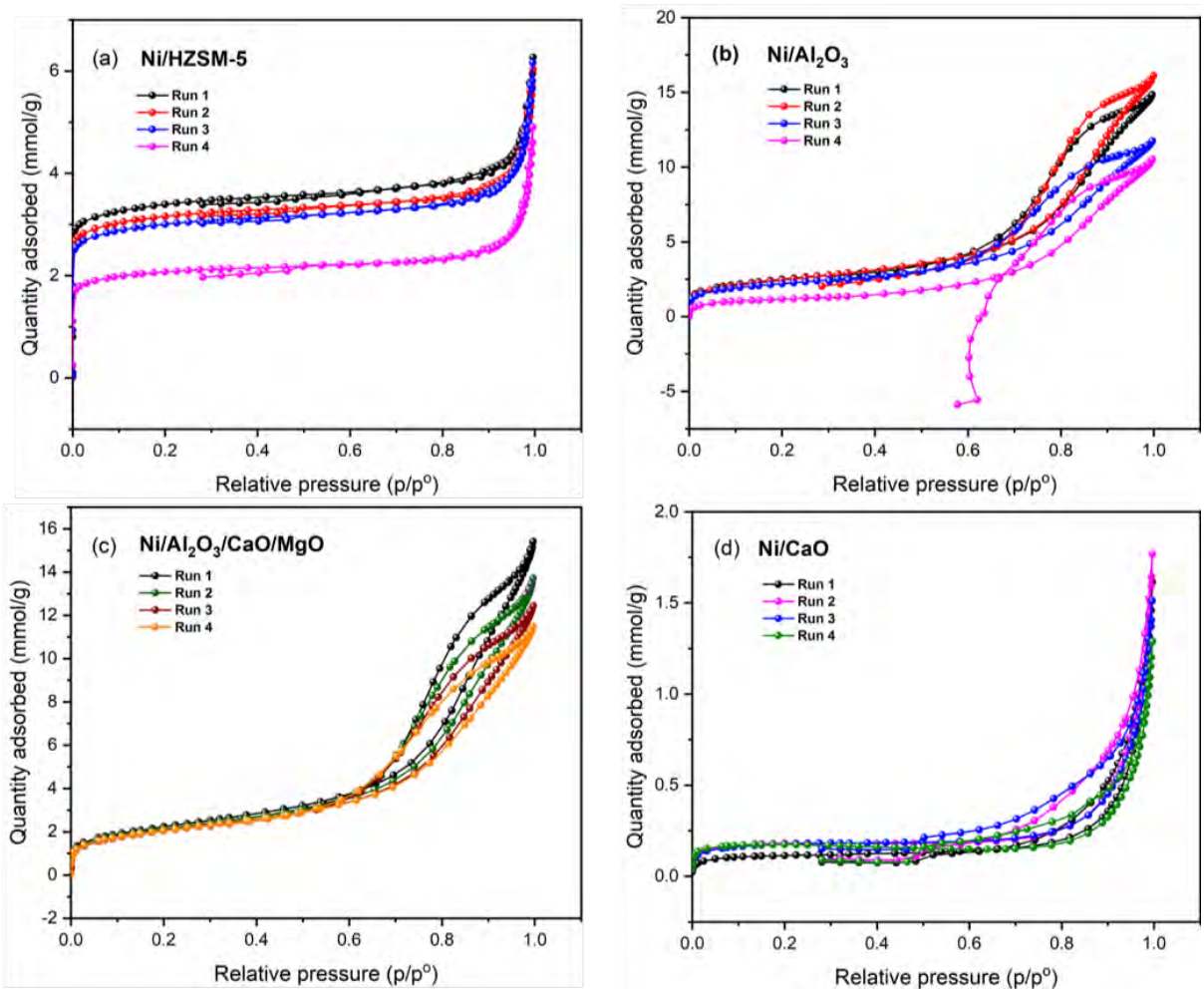

Figure S2. Nitrogen sorption isotherms of Ni-modified catalysts after stability tests: (a) Ni/ZSM-5, (b) Ni/Al_2O_3, (c) $Ni/Al_2O_3/CaO/MgO$ and (d) Ni/CaO.

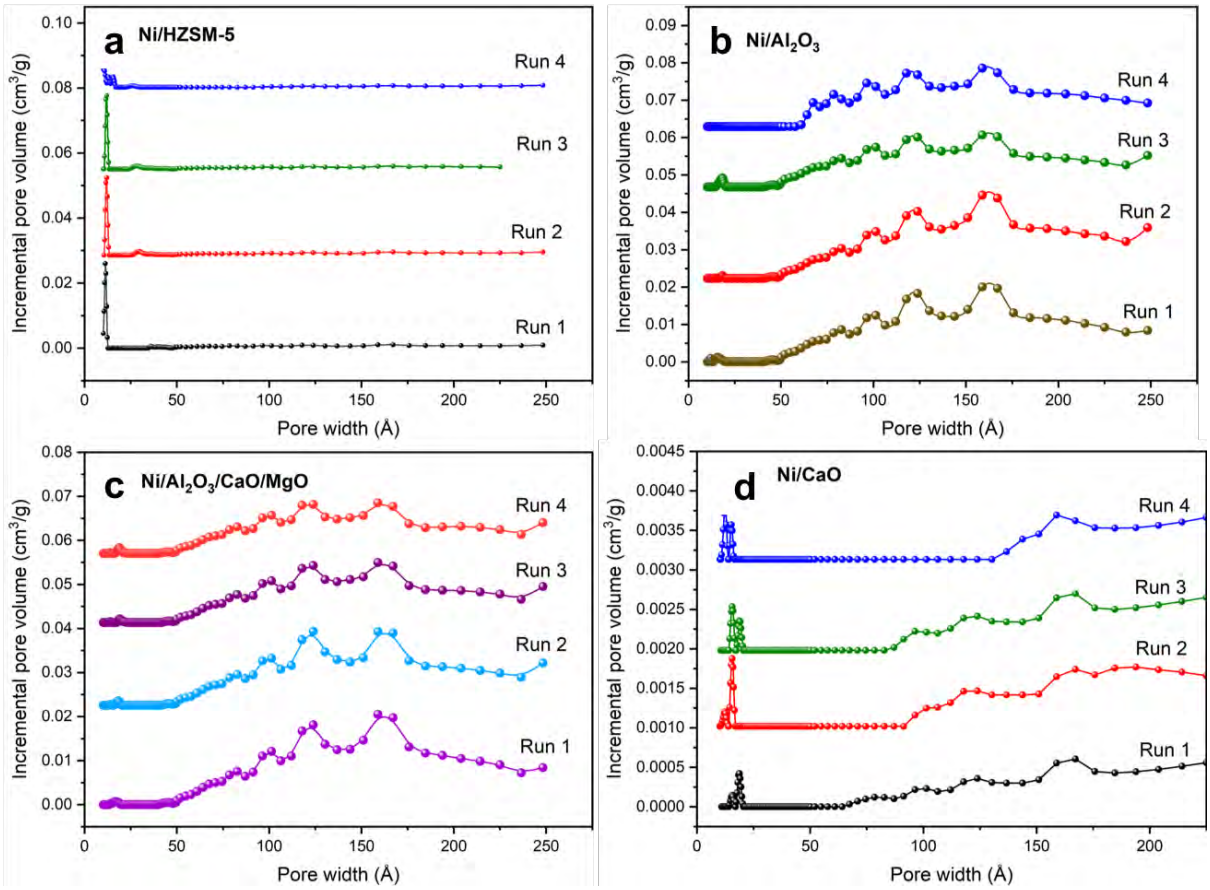

Figure S3. Pore distribution in Ni-modified catalysts after stability tests: (a) Ni/ZSM-5, (b) Ni/Al_2O_3, (c) $Ni/Al_2O_3/CaO/MgO$ and (d) Ni/CaO.

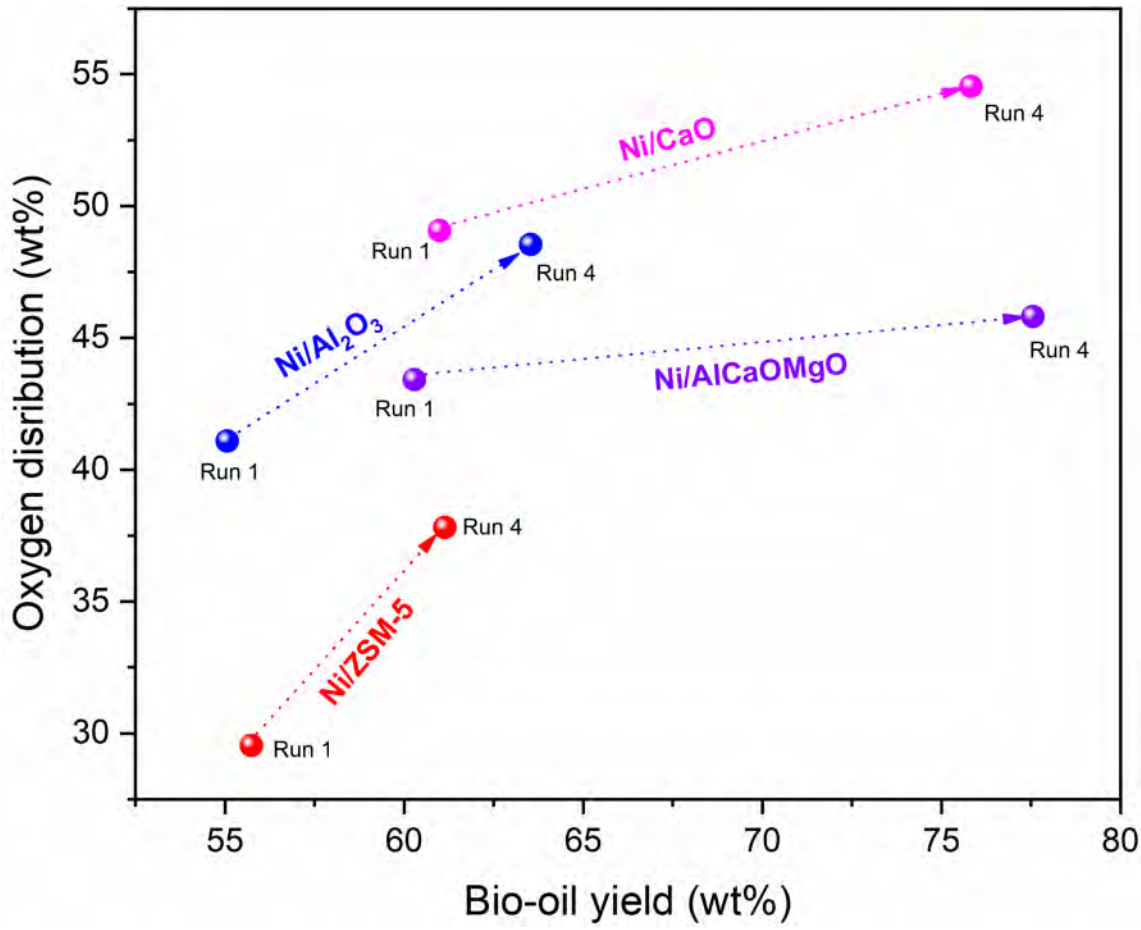

Figure S4. Change in oxygen concentration of bio-oils after Run 1 and Run 4 using Ni-modified catalysts.

Table S1. Product yield during stability tests.

Catalyst	Sample	Gas (wt%)	Char (wt%)	Bio-oil (wt%)
Ni/ZSM	Fresh	32.55	17.65	49.80
	Run 1	28.08	16.18	55.74
	Run 2	27.54	19.41	53.05
	Run 3	25.14	19.46	55.40
	Run 4	25.82	19.11	55.07
Ni/Al_2O_3	Fresh	26.05	16.60	57.35
	Run 1	22.02	17.69	60.29
	Run 2	23.44	22.27	54.29
	Run 3	22.79	16.73	60.48
	Run 4	21.07	17.94	60.99
Ni/AlCaOMgO	Fresh	25.82	16.02	58.16
	Run 1	21.88	16.97	61.15
	Run 2	21.03	21.14	57.83
	Run 3	19.00	19.87	61.13
	Run 4	17.52	18.95	63.53
Ni/CaO	Fresh	5.31	16.72	77.97
	Run 1	4.59	17.85	77.56
	Run 2	5.42	17.30	77.28
	Run 3	5.68	16.13	78.19
	Run 4	6.54	17.63	75.83

Table S2. Gas composition during stability runs.

Catalyst	Sample	CH_4 (wt%)	CO_2 (wt%)	C_2H_4 (wt%)	C_2H_6 (wt%)	H_2 (wt%)	CO (wt%)	Total
Ni/ZSM	Fresh	2.94	18.34	0.64	0.44	0.34	9.85	32.55
	Run 1	2.25	16.70	0.17	0.16	0.65	8.15	28.08
	Run 2	2.43	13.81	0.14	0.05	0.70	10.41	27.54
	Run 3	2.89	13.76	0.22	0.25	0.57	7.45	25.14
	Run 4	2.18	12.68	0.93	0.38	0.66	8.99	25.82
Ni/Al_2O_3	Fresh	2.56	13.92	0.13	0.03	0.30	9.11	26.05
	Run 1	2.04	12.66	0.08	0.02	0.37	6.85	22.02
	Run 2	2.45	11.49	0.31	0.37	0.51	8.31	23.44
	Run 3	2.01	11.64	0.05	0.04	0.79	8.26	22.79
	Run 4	2.85	10.20	0.13	0.23	0.5	7.16	21.07
Ni/AlCaOMgO	Fresh	2.90	13.68	0.47	0.54	0.40	7.83	25.82
	Run 1	2.24	10.57	0.37	0.37	0.41	7.92	21.88
	Rin 2	2.69	9.05	0.09	0.21	0.94	8.05	21.03
	Run 3	1.93	8.60	0.03	0.15	1.17	7.12	19.00
	Run 4	1.21	7.26	0.03	0.18	0.94	7.90	17.52
Ni/CaO	Fresh	3.95	0.16	0.09	0.23	0.19	0.70	5.32
	Run 1	2.26	0.13	0.03	0.07	2.06	0.04	4.59
	Run 2	1.73	0.07	0.25	0.36	2.14	0.87	5.42
	Run 3	2.53	0.15	0.07	0.05	1.68	1.20	5.68
	Run 4	1.93	1.30	0.10	0.16	1.68	1.37	6.54

Table S3. Elemental composition in biochar samples obtained in *ex-situ* pyrolysis during stability experiments at 500 °C, heating rate of 100 °C/min with C/B of 2.

	Catalyst	N (wt%)	C(wt%)	H(wt%)	O(wt%)	Ash(wt%)	HHV (MJ/kg)
Run 1	Ni/ZSM-5	0.02	74.83	2.66	22.49	5.48	26.97
Run 1	Ni/Al_2O_3	0.01	78.26	2.77	18.96	4.47	28.67
Run 1	Ni/AlCaOMgO	0.03	90.67	3.22	6.08	7.96	34.77
Run 1	Ni/CaO	0.04	86.75	3.07	10.14	2.15	32.93
Run 4	Ni/ZSM-5	0.01	86.11	3.02	10.86	4.13	32.53
Run 4	Ni/Al_2O_3	0.03	86.11	3.02	10.84	3.71	32.54
Run 4	Ni/AlCaOMgO	0.00	76.05	2.77	21.18	5.44	27.66
Run 4	Ni/CaO	0.00	79.40	2.95	17.65	3.19	29.44

Note: O (wt%) was calculated by the difference

Chapter 10

Conclusions and future outlook

1. Conclusions

This thesis studied the application of diverse types of catalysts (mesoporous, microporous, acidic and basic catalysts) primarily for *ex-situ* catalytic biomass pyrolysis (CBP) modes and the combined *in-situ* and *ex-situ* mode using pinewood sawdust as the feedstock. The results found in the thesis may enhance the fundamental understandings of *ex-situ* CBP and help in designing catalysts for two-stage *ex-situ* CBP for efficient bio-oil deoxygenation or production of other sustainable chemicals.

Firstly, this thesis compared the potential of Cu/zeolite and Ni/zeolite catalysts for bio-oil deoxygenation in *in-situ*, *ex-situ* and combined *in-situ* and *ex-situ* pyrolysis. Competitive results were obtained in *ex-situ* and combined pyrolysis modes, while the *in-situ* mode could not achieve desirable bio-oil deoxygenation. The study showed that the combined pyrolysis with highest catalyst to biomass ratio of 5 achieved the maximum proportion of total hydrocarbons (73%) in the bio-oil, compared to *ex-situ* and *in-situ* pyrolysis mode. After comparing the bio-oil quality with petroleum crude oil (naphthenes-49%, paraffins- 30%, aromatic hydrocarbons-15%), it can be suggested that the combined pyrolysis approach obtained a competitive proportion of aromatic hydrocarbons (˜15%) and naphthenes (˜48%) but could not produce sufficient paraffins in the bio-oil. The major aliphatic hydrocarbons detected in all bio-oil samples was ethylidenecyclobutane, while retene, fluorene, phenanthrene, and pyrene were the primary aromatic hydrocarbons in all the bio-oil samples. The enhanced deoxygenation activity and hydrocarbon production by the catalysts can be attributed to abundant acidic sites insides the pores or on the surface of the catalysts that carried out major deoxygenation reactions, such as dehydration, decarboxylation, decarbonylation, aldol condensation and aromatization. Although combined catalytic pyrolysis process could be advantageous to obtain higher deoxygenation of bio-oil compared to either *in-situ* or *ex-situ* catalytic pyrolysis, *ex-situ* pyrolysis proved more viable since the catalyst can be easily recovered from the reactor. Subsequently, the catalyst can be used multiple times in further pyrolysis experiments. Thus, *ex-situ* pyrolysis was further explored for bio-oil upgrading using different types of catalysts.

The activity of monometallic catalysts (Ni/zeolite and Cu/zeolite) was compared with a bimetallic catalyst (CuNi/zeolite) in one-stage and two-stage *ex-situ* pyrolysis modes. In one-stage pyrolysis, Cu/zeolite promoted only aliphatic hydrocarbons, while Ni/zeolite also facilitated the formation of aromatic hydrocarbons. In contrast, CuNi/zeolite showed better deoxygenation efficiency than Cu/zeolite or Ni/zeolite and also produced comparatively a variety of aromatic hydrocarbons (14.53%) and aliphatic hydrocarbons (39.94%), attributing to its higher acidity that created a higher number of active sites for deoxygenation reactions. The main deoxygenation pathway for monometallic catalysts was decarboxylation, while the bimetallic catalyst favoured decarboxylation and decarbonylation reactions as the main deoxygenation pathways. On the other hand, compared to combined monometallic catalysts (in two-stage pyrolysis mode), the sole bimetallic catalyst (in one-stage mode) showed better deoxygenation activity as only 0.11% of phenols, and 0.33% of acids were obtained in the bio-oil samples. At the same time, ketones and aldehydes were converted entirely to liquid and gaseous products. It was observed that sole bimetallic catalyst preferred the production of aliphatic hydrocarbons, with CuNi/zeolite generating 49.34% of aliphatic hydrocarbons, whereas the combination of monometallic catalysts favoured the production of aromatic hydrocarbons, with Cu/zeolite: Ni/zeolite producing 18.87% of aromatics in the bio-oil. The major deoxygenation reactions promoted by the catalysts were found to be cracking, aromatization, dehydration, decarboxylation and decarbonylation.

Since bimetallic catalyst showed significant results for hydrocarbon production in *ex-situ* pyrolysis, the synergistic effect of different transition metals as bimetallic catalysts was explored for bio-oil deoxygenation, hydrocarbon selectivity and energy distribution in pyrolytic products. Among all the catalysts studied, it can be concluded the synergistic effect of Ni and Cu on ZSM-5 was found advantageous, owing to their better physicochemical properties, such as higher surface area and a large number of acidic sites, and the combined catalytic activity of Ni^{3+}/Cu^{2+}/ZSM-5 that paved the way to convert the oxygenated compounds into hydrocarbons. Evidently, NiCu/ZSM-5 produced bio-oil with the least amount of oxygen (31.90 wt%) and maximum carbon content (63.51wt%), resulting in HHV of 24.28 MJ/kg. The synergistic effect of other metal combinations was also found useful for bio-oil deoxygenation and achieving the bio-oil with improved calorific values. For instance, NiFe/ZSM-5 and CuFe/ZSM-5 produced bio-oils with HHVs of 23.06 and 18.64 MJ/kg, respectively. The bio-oil compositions obtained indicate the formation of varying types of hydrocarbons, ascribed to the synergistic effect of bi-metals.

Lastly, the diverse nature of catalytic supports like ZSM-5, Al_2O_3, Al_2O_3/CaO/MgO, and CaO were impregnated with nickel metal and explored in one-stage and two-stage *ex-situ* CBP for bio-oil deoxygenation, hydrocarbon production and energy distribution in pyrolytic products. The results revealed that efficient bio-oil deoxygenation could be achieved in both modes of pyrolysis. However, two-stage pyrolysis that employs two different catalysts of varying physicochemical

properties possesses additional active sites to catalyse deoxygenation reactions producing diverse hydrocarbons in the bio-oils. For example, Ni/Al_2O_3 in combination with ZSM-5 converted oxygenated compounds into aromatics like naphthalenes, fluorene, phenanthrene and anthracene. In contrast, Ni/Al_2O_3 with AlCaOMgO produced extra aromatics like s-Indacene and annulene and long-chain alkanes like hexadecane and octadecane, owing to the combined catalytic activity of both catalysts. The stability tests of Ni-modified catalysts further revealed that Ni/ZSM-5 showed the least coke deposition of 8.71 wt% after 4 successive pyrolysis run, while Ni/CaO achieved the highest coke deposition of 23.16 wt%. Consequently, coke deposition had a negative impact on the physicochemical properties of the catalysts and, therefore, on their catalytic activity for bio-oil deoxygenation.

2. Limitations and future outlook

Although this work enhanced the understanding of CBP in one and two-stage pyrolysis modes for bio-oil deoxygenation and hydrocarbon production, there are substantial limitations to this work which could be taken as opportunities for future work.

This study utilized *in-situ* pyrolysis mode sole (and in combined pyrolysis mode) in a fixed-bed pyrolysis reactor where the biomass and catalyst were mixed. After the pyrolysis, it was impossible to separate the catalysts, and thus the mass yield of pyrolytic products and coke deposition could not be determined. Besides, the loss of catalyst in the process could prove the process expensive compared to the *ex-situ* mode. A continuous type of pyrolysis reactor that allows catalyst's recovery from the mixture can be used to recover the catalyst. After the oxidative regeneration process, the catalyst can be used for successive experiments for bio-oil upgrading. To make the combined pyrolysis mode significant, an optimization study of other parameters like amount of catalyst, temperature for *in-situ* and *ex-situ* catalyst bed can be organized to determine favorable pyrolysis conditions for enhanced bio-oil deoxygenation. In addition, similar to two-stage pyrolysis that was employed with different types of catalysts in this study, combined *in-situ* and *ex-situ* can also be explored with a variety of catalysts, and possible reaction pathways can be studied for hydrocarbon production.

Another major limitation of the work was that the study (especially in chapters 5-7) employed qualitative analyses to examine bio-oil deoxygenation. Therefore, quantitative methods should be used for bio-oil characterization to compare the catalytic activity of catalysts with more accuracy.

This study utilized real biomass in all pyrolysis modes, so it was difficult to determine the accurate reaction pathways for hydrocarbon production. Particularly, in combined pyrolysis and two-stage pyrolysis modes. Thus, it would be highly interesting to know the chemical reactions taking place at the first stage, production of intermediate compounds and reaction pathways taking

place at the second stage. Therefore, utilizing a model compound like *m*-cresol or guaiacol and two catalysts such as ZSM-5 and Al_2O_3 employed either in combined pyrolysis or two-stage pyrolysis modes can be carried out, and reaction pathways for selective hydrocarbons can be studied. Furthermore, the effects of varying the pyrolysis parameters and catalyst physicochemical properties, altering active sites on the selectivity of hydrocarbons and bio-oil deoxygenation can be investigated. A comparative study to examine the effect of pore size (micro, meso and macroporous catalyst) on bio-oil upgrading can also be carried out in all three pyrolysis modes.

In the last chapter, CaO based catalysts showed the ability to enhance hydrogen production. The *in-situ* produced hydrogen can be utilized for partial hydrodeoxygenation reactions, which is considered a highly efficient way for bio-oil deoxygenation. Therefore, more catalysts can be explored for *in-situ* hydrogen production. Such catalysts could be highly advantageous in combined and two-stage *ex-situ* pyrolysis, where the hydrogen produced at the first stage can be utilized at the second stage. This approach may require more research insights to prove the hypothesis.

Catalyst deactivation due to the deposition of carbonaceous species during the pyrolysis is a major concern for commercializing the technique. Results of this study also showed considerable coke deposition on the catalyst. Therefore, coke deposition should be reduced to enhance the stability of catalysts for the successful commercialization of CBP. This study also conducted stability tests for the catalysts. However, the catalysts were used in the pyrolysis without regenerating them. The regenerated catalysts would exhibit different physicochemical properties and thus would show varying results for bio-oil upgrading. Hence, a separate study can be carried out to compare their bio-oil deoxygenation activity with regenerated catalysts.

It is crucial to produce the bio-oil at a competitive price to already commercialized biofuels. Hence, a techno-economic study considering all the CBP steps should be conducted to examine the total cost required to produce upgraded bio-oil.